



Rapid qualitative and quantitative analysis of novel drug analogues via Desorption Electrospray Ionisation - Mass Spectrometry (DESI-MS)

By: Natasha Stojanovska

A thesis submitted for the
Degree of Doctor of Philosophy (Science),

Centre for Forensic Science,
University of Technology, Sydney,

2013

“Learn from yesterday, live for today, hope for tomorrow. The important thing is not to stop questioning.” - Albert Einstein.

“To be yourself in a world that is constantly trying to make you something else is the greatest accomplishment.” - Ralph Waldo Emerson.

Certificate of authorship and originality

I certify that the work in this thesis has not previously been submitted for a degree nor has it been submitted as part of the requirements for a degree except as fully acknowledged within the text.

I also certify that the thesis has been written by me. Any help that I have received in my research work and the preparation of the thesis itself has been acknowledged. In addition, I certify that all the information sources and literature used are indicated in the thesis.

NAME: Natasha Stojanovska

DATE:

Acknowledgements

I would like to express my deepest gratitude to my supervisors Dr. Shanlin Fu, Dr. Mark Tahtouh and Dr. Tamsin Kelly for the continual support and effort throughout the project. I could not have asked for a better group of people to be my mentors.

Dr. Shanlin Fu, I admire your patience, your wisdom and your positive attitude. You have been very supportive along the entire journey and I thank you very much for that. I hope you continue to be the great supervisor that you are and I wish you all the best in your future research endeavours.

Dr. Mark Tahtouh, thank you for your insight, guidance and pure intelligence. You have been a fundamental part of this research and I appreciate all the thought and effort you put into the project.

Dr. Tamsin Kelly, thank you for all your mass spec expertise. Your insight has been invaluable and you have assisted greatly in all aspects of the project. Thank you for putting in the effort to come up from Canberra for meetings and presentations. Your commitment has been second to none and I thank you for that.

I would like to thank Dr. Alison Beavis for assisting greatly in the editing process and for providing thoughtful insight into issues at hand. Thank you for all the DESI/LC/QTOF-MS training. You have been an essential part of this project.

I would like to thank Dr. Ronald Shimmon for all his invaluable assistance in organic synthesis. Thank you to Dr. David Bishop for your technical assistance with the GC-MS and especially the QTOF-MS which proved to be a challenging instrument over the years.

I would like to acknowledge the Australian Federal Police (AFP) for funding and for the samples that were provided for this project. In addition, I acknowledge the AFP for providing the Prosolia™ DESI source for use at the University of Technology, Sydney, for the duration of this project. I would also like to thank Agilent Technologies® for their technical support with the instruments.

I would also like to acknowledge Rochelle Seneviratne from the Science Faculty for all her administrative assistance and for answering all our questions no matter how trivial they

were. I would like to thank everyone in the Centre for Forensic Science for their support and interest in the project and the University of Technology, Sydney, for providing me the opportunity to do my PhD.

I would like to thank my fellow PhD and post-doctoral students: Susan Luong, Anna Molnar, Scott Chadwick, Michael Wood, Marie Morelato, Aimee Lloyd, Joyce Chan, Adrian De Grazia, Regina Verena Taudte, Katelynn Perrault, Maiken Ueland, Kate Grimwood, Unni Kuzhiumparambil and Nathan Charlton and all the other students I had contact with during the years for all the fun times and the amazing support along the way. Finally, a very special thank you goes out to my family and my husband for putting up with me through the hard times and for the unconditional love.

Table of contents

Certificate of authorship and originality.....	iii
Acknowledgements.....	iv
List of figures.....	xiii
List of tables.....	xxx
Abbreviations.....	xxxii
Abstract.....	xxxvi
CHAPTER 1: INTRODUCTION.....	2
1.1 PREVALENT ILLICIT DRUGS AND NOVEL ANALOGUES.....	2
1.1.1 <i>Amphetamine</i>	4
1.1.2 <i>Methylamphetamine</i>	5
1.1.3 <i>3,4-Methylenedioxyamphetamine</i>	5
1.1.4 <i>3,4-Methylenedioxyamphetamine</i>	6
1.1.5 <i>N,N-Dimethylamphetamine</i>	6
1.1.6 <i>4-Methoxyamphetamine</i>	7
1.1.7 <i>Cocaine</i>	7
1.1.8 <i>Drug analogues</i>	8
1.1.8.1 Piperazine analogues.....	8
1.1.8.2 Cathinone analogues.....	9
1.2 DRUG INTELLIGENCE/PROFILING.....	11
1.3 DRUG ANALYSIS TECHNIQUES.....	14
1.3.1 <i>Current preliminary identification techniques</i>	14
1.3.2 <i>Current confirmatory analysis techniques</i>	14
1.3.3 <i>Quantification of drug compounds</i>	15
1.3.4 <i>Atmospheric pressure ionisation techniques</i>	16
1.4 DATABASE AND LIBRARY COMPOUND MATCHING.....	18

1.5	DESORPTION ELECTROSPRAY IONISATION – MASS SPECTROMETRY.....	18
1.5.1	<i>Mechanisms involved in DESI-MS</i>	20
1.5.2	<i>Important parameters</i>	21
1.5.3	<i>Applications of DESI-MS</i>	24
1.5.4	<i>Time-of-Flight - Mass Spectrometry</i>	28
1.6	EXPERIMENTAL DESIGN	29
1.6.1	<i>Types of experimental design</i>	30
1.6.1.1	Full-factorial design.....	30
1.6.1.2	Central composite design	31
1.7	AIMS.....	32
CHAPTER 2:	SYNTHESIS.....	34
2.1	INTRODUCTION	34
2.2	MATERIALS AND METHODS	34
2.2.1	<i>4-Methylmethcathinone (M1 – M4)</i>	36
2.2.2	<i>1-Benzylpiperazine (BZP 1 - BZP 4)</i>	39
2.2.3	<i>3-Trifluoromethylphenylpiperazine (TFMPP 1 – TFMPP 4)</i>	41
2.2.4	<i>3-Chlorophenylpiperazine (mCPP 1)</i>	43
2.2.5	<i>4-Methoxyphenylpiperazine (MeOPP 1)</i>	44
2.3	RESULTS AND DISCUSSION	45
2.3.1	<i>4-Methylmethcathinone</i>	45
2.3.1.1	Yield of 4-methylmethcathinone	45
2.3.1.2	Purity of 4-methylmethcathinone	45
2.3.1.3	2-Chloro-4-methylpropiophenone as intermediate to 4-MMC	47
2.3.1.4	2-Bromo-4-methylpropiophenone as intermediate to 4-MMC	49
2.3.2	<i>1-Benzylpiperazine</i>	51
2.3.3	<i>3-Trifluoromethylphenylpiperazine</i>	61
2.3.4	<i>3-Chlorophenylpiperazine</i>	68

2.3.5	<i>4-Methoxyphenylpiperazine</i>	71
2.4	CONCLUSIONS.....	75
CHAPTER 3: METHOD DEVELOPMENT AND VALIDATION.....		77
3.1	INTRODUCTION	77
3.2	MATERIALS AND METHODS	78
3.2.1	<i>Sample preparation</i>	79
3.2.2	<i>Experimental design</i>	79
3.2.2.1	Experimental space.....	80
3.2.2.2	Factor levels.....	81
3.2.2.3	Data analysis	81
3.3	RESULTS AND DISCUSSION	82
3.3.1	<i>Optimising DESI-MS parameters</i>	82
3.3.1.1	Experimental design	85
3.3.1.2	One-factor-at-a-time optimisation	91
3.3.1.3	Sampling method.....	96
3.3.2	<i>Pharmaceuticals analysis</i>	102
3.3.3	<i>Optimising GC-MS parameters</i>	103
3.3.3.1	GC-MS conditions	104
3.3.3.2	Temperature program	104
3.3.4	<i>Optimising LC-MS parameters</i>	109
3.3.4.1	LC-MS conditions	109
3.3.4.2	Mobile phase gradient development.....	110
3.4	CONCLUSIONS.....	112
CHAPTER 4: ANALYSIS OF AMPHETAMINE-TYPE SUBSTANCES		114
4.1	INTRODUCTION	114
4.2	MATERIALS AND METHODS	114
4.3	RESULTS AND DISCUSSION	115

4.3.1	<i>Adulteration and LOD</i>	115
4.3.1.1	Methylamphetamine	115
4.3.1.2	4-Methoxyamphetamine	119
4.3.1.3	Amphetamine	120
4.3.1.4	N,N-Dimethylamphetamine.....	122
4.3.1.5	3,4-Methylenedioxymethylamphetamine	124
4.3.1.6	Limit of Detection summary	127
4.3.2	<i>Analysis of 3,4-methylenedioxymethylamphetamine</i>	127
4.3.2.1	Desorption electrospray ionisation – mass spectrometry	127
4.3.2.2	Gas chromatography – mass spectrometry	133
4.3.2.3	Liquid chromatography – mass spectrometry	137
4.3.3	<i>Analysis of 4-methoxymethylamphetamine</i>	140
4.3.3.1	Desorption electrospray ionisation – mass spectrometry	140
4.3.3.2	Gas chromatography – mass spectrometry	143
4.3.3.3	Liquid chromatography – mass spectrometry	146
4.3.4	<i>Analysis of dimethylamylamine</i>	147
4.3.4.1	Desorption electrospray ionisation – mass spectrometry	147
4.3.4.2	Gas chromatography – mass spectrometry	150
4.3.4.3	Liquid chromatography – mass spectrometry	151
4.3.5	<i>Mass accuracy</i>	152
4.4	CONCLUSIONS.....	155
CHAPTER 5:	ANALYSIS OF COCAINE	157
5.1	INTRODUCTION	157
5.2	MATERIALS AND METHODS	157
5.3	RESULTS AND DISCUSSION	158
5.3.1	<i>Adulteration and LOD</i>	158
5.3.2	<i>Analysis of seized cocaine samples</i>	163

5.3.2.1	Desorption electrospray ionisation – mass spectrometry	163
5.3.2.2	Gas chromatography – mass spectrometry	171
5.3.2.3	Liquid chromatography – mass spectrometry	178
5.3.3	<i>Mass accuracy</i>	184
5.4	CONCLUSIONS.....	187
CHAPTER 6: ANALYSIS OF PIPERAZINE ANALOGUES		189
6.1	INTRODUCTION	189
6.2	MATERIALS AND METHODS	189
6.3	RESULTS AND DISCUSSION	190
6.3.1	<i>Adulteration and LOD</i>	190
6.3.1.1	1-Benzylpiperazine.....	190
6.3.1.2	3-Trifluoromethylphenylpiperazine	193
6.3.1.3	3-Chlorophenylpiperazine	194
6.3.1.4	4-Methoxyphenylpiperazine.....	196
6.3.1.5	Piperazine mixtures	198
6.3.2	<i>Analysis of 1-benzylpiperazine</i>	200
6.3.2.1	Desorption electrospray ionisation – mass spectrometry	200
6.3.2.2	Gas chromatography – mass spectrometry	205
6.3.2.3	Liquid chromatography – mass spectrometry	209
6.3.3	<i>Analysis of 3-trifluoromethylphenylpiperazine</i>	212
6.3.3.1	Desorption electrospray ionisation – mass spectrometry	212
6.3.3.2	Gas chromatography – mass spectrometry	217
6.3.3.3	Liquid chromatography – mass spectrometry	220
6.3.4	<i>Analysis of 3-chlorophenylpiperazine</i>	222
6.3.4.1	Desorption electrospray ionisation – mass spectrometry	222
6.3.4.2	Gas chromatography – mass spectrometry	224
6.3.4.3	Liquid chromatography – mass spectrometry	226

6.3.5	<i>Analysis of 4-methoxyphenylpiperazine</i>	227
6.3.5.1	Desorption electrospray ionisation – mass spectrometry	227
6.3.5.2	Gas chromatography – mass spectrometry	229
6.3.5.3	Liquid chromatography – mass spectrometry	231
6.3.6	<i>Mass accuracy</i>	232
6.4	CONCLUSIONS.....	236
CHAPTER 7: ANALYSIS OF CATHINONE ANALOGUES.....		238
7.1	INTRODUCTION	238
7.2	MATERIALS AND METHODS	238
7.2.1	<i>Selectivity study</i>	238
7.2.2	<i>DESI-MS method validation</i>	238
7.2.3	<i>GC-MS method validation</i>	241
7.2.4	<i>LC-MS method validation</i>	242
7.3	RESULTS AND DISCUSSION	243
7.3.1	<i>Qualitative analysis</i>	243
7.3.1.1	Desorption electrospray ionisation – mass spectrometry	243
7.3.1.2	Gas chromatography – mass spectrometry	248
7.3.1.3	Liquid chromatography – mass spectrometry	250
7.3.2	<i>Selectivity study</i>	250
7.3.2.1	4-Methylmethcathinone and methylon.....	256
7.3.2.2	Differentiating compounds based on MS/MS spectra	258
7.3.3	<i>Quantitative analysis</i>	261
7.3.3.1	Internal standard	261
7.3.3.2	Quantification	263
7.3.4	<i>Mass accuracy</i>	264
7.4	CONCLUSIONS.....	266
CHAPTER 8: COMPARING DESI-MS TO CURRENT DRUG DETECTION/ANALYSIS TECHNIQUES		268

8.1	INTRODUCTION	268
8.2	MARQUIS REAGENT	268
8.3	CONFIRMATORY ANALYSIS TECHNIQUES.....	268
8.4	COMPARING DESI-MS TO PRELIMINARY IDENTIFICATION TECHNIQUES.....	269
8.5	COMPARING DESI-MS TO QUANTITATIVE ANALYSIS TECHNIQUES.....	270
8.5.1	<i>Gas chromatography – mass spectrometry.....</i>	<i>270</i>
8.5.2	<i>Liquid chromatography – mass spectrometry.....</i>	<i>271</i>
8.5.3	<i>Desorption electrospray ionisation - mass spectrometry</i>	<i>272</i>
8.6	FALSE POSITIVE AND FALSE NEGATIVE RESULTS	275
8.7	CONCLUSIONS.....	276
CHAPTER 9:	CONCLUSIONS AND FUTURE WORK	278
9.1	CONCLUSIONS.....	278
9.2	FUTURE WORK.....	281
Appendix.....	282
References.....	298

List of figures

Figure 1-1 Molecular structures of AP, MA, MDMA, MDA, DMA and PMA.	4
Figure 1-2 Molecular structure of cocaine.....	7
Figure 1-3 Molecular structures of BZP, TFMPP, mCPP, MeOPP, and FPP.....	9
Figure 1-4 Molecular structure of cathinone, methcathinone and 4-MMC.....	10
Figure 1-5 Generic sites for structural variation of cathinone ⁶	10
Figure 1-6 DESI source and moving stage used to position the source ⁷²	19
Figure 1-7 Simulation of the DESI process showing the formation of dozens of microdroplets resulting from a single droplet-thin film collision event ⁷³	21
Figure 1-8 Schematic showing DESI parameters requiring optimisation ⁷⁹	22
Figure 1-9 Dependence of signal intensity on the spray position at various impact angles from normal ⁷⁸	23
Figure 1-10 The Agilent QTOF schematic, showing ion source, ion transfer, optics, beam shaping optics, ion pulsar, flight tube, and detector ⁹³	29
Figure 1-11 The points of a CCD with three input parameters ⁹⁴	31
Figure 2-1 Reaction scheme for the synthesis of 4-methylmethcathinone (M1 – M2) via an α -bromination reaction ⁹⁵	36
Figure 2-2 Reaction scheme for the synthesis of 4-methylmethcathinone (M3) via an α -bromination reaction using N-bromosuccinimide ¹⁰²	37
Figure 2-3 Reaction scheme for the synthesis of 4-methylmethcathinone (M4) via an α -bromination reaction.	38
Figure 2-4 Reaction scheme for the synthesis of 1-benzylpiperazine (BZP 1 - BZP 3) ⁹⁶	39
Figure 2-5 Reaction scheme for the synthesis of 1-benzylpiperazine (BZP 4) ⁹⁷	40

Figure 2-6 Reaction scheme for the synthesis of 3-trifluoromethylphenylpiperazine (TFMPP 1 – TFMPP 3) ⁹⁶	41
Figure 2-7 Reaction scheme for the synthesis of 3-trifluoromethylphenylpiperazine (TFMPP 4) ¹⁰⁴	42
Figure 2-8 Reaction scheme for the synthesis of 3-chlorophenylpiperazine (mCPP 1) ¹⁰⁴	43
Figure 2-9 Reaction scheme for the synthesis of 4-methoxyphenylpiperazine (MeOPP 1).	44
Figure 2-10 Calibration curve for 4-MMC standard analysed using GC-MS, codeine-D ₆ as IS, n=3 (GC method 1).....	45
Figure 2-11 ¹ H NMR of 4-MMC (M1) before vacuum drying.....	46
Figure 2-12 ¹ H NMR of 4-MMC (M1) after vacuum drying.....	47
Figure 2-13 Reaction scheme for the synthesis of 4-methylmethcathinone using sulfuryl chloride.....	48
Figure 2-14 GC-MS chromatogram of extract 1; 4-methylpropiofenone at 8.9 minutes, 2-chloro-4-methylpropiofenone at 10.3 minutes (GC method 1).....	48
Figure 2-15 EI mass spectrum of extract 1; 4-methylpropiofenone (GC method 1).	48
Figure 2-16 EI mass spectrum of extract 1; 2-chloro-4-methylpropiofenone (GC method 1).	49
Figure 2-17 GC-MS chromatogram of 2-bromo-4-methylpropiofenone (Br-M4) at 11.2 minutes, 4-methylpropiofenone at 9.1 minutes (GC method 1).....	50
Figure 2-18 EI mass spectrum of 2-bromo-4-methylpropiofenone (Br-M4) (GC method 1).	51
Figure 2-19 GC-MS chromatogram of BZP 1.HCl at 4.9 minutes, DBZP at 7.7 minutes (GC method 1).....	53
Figure 2-20 EI mass spectrum of BZP 1.HCl (GC method 1).....	53
Figure 2-21 EI mass spectrum of DBZP (GC method 1).....	54

Figure 2-22 ^1H NMR of BZP 1.	54
Figure 2-23 Molecular structure of DBZP.	55
Figure 2-24 ^{13}C NMR of BZP 1.	55
Figure 2-25 ^{13}C DEPT NMR of BZP 1.	56
Figure 2-26 ^1H -NMR of BZP 2 showing ratio of DBZP to BZP signals.	57
Figure 2-27 GC-MS chromatogram of BZP 3.HCl at 6.1 minutes, DBZP at 8.5 minutes (GC method 2).....	58
Figure 2-28 GC-MS chromatogram of BZP 4.HCl at 5.0 minutes, MBCP at 6.6 minutes, EBCP at 6.8 minutes, DBZP at 7.7 minutes (GC method 1).	59
Figure 2-29 EI mass spectrum of MBCP (GC method 1).....	59
Figure 2-30 EI mass spectrum of EBCP (GC method 1).	60
Figure 2-31 Proposed reaction scheme for the formation of ethyl 1-benzyl-4-carboxypiperazine and methyl 1-benzyl-4-carboxypiperazine.....	60
Figure 2-32 Reaction mechanism for the formation of 3-trifluoromethylphenylpiperazine (TFMPP), 2-trifluoromethylphenylpiperazine and 4-trifluoromethylphenylpiperazine.	62
Figure 2-33 GC-MS chromatogram of TFMPP 1 at 5.1 minutes (GC method 1).	63
Figure 2-34 EI mass spectrum of TFMPP (GC method 1).	64
Figure 2-35 A: GC-MS chromatogram of TFMPP 2.HCl at 5.7 minutes and 6.2 minutes, 3-chlorobenzotrifluoride at 3.2 minutes, 3-trifluoromethylphenol at 4.0 minutes; B: EI mass spectrum of 3-trifluoromethylphenol (GC method 2).	65
Figure 2-36 A: GC-MS chromatogram of TFMPP 3.HCl at 4.5 minutes, 5.0 minutes, 5.3 minutes; piperazine at 2.5 minutes; B: EI mass spectrum of piperazine (GC method 1).	66
Figure 2-37 EI mass spectrum of TFMPP at 4.5 minutes (GC method 1).	67

Figure 2-38 EI mass spectrum of TFMPP at 5.0 minutes (GC method 1).....	67
Figure 2-39 EI mass spectrum of TFMPP at 5.3 minutes (GC method 1).....	67
Figure 2-40 A: GC-MS chromatogram of TFMPP 4.HCl at 6.2 minutes, 3-(trifluoromethyl)aniline at 3.8 minutes; B: EI mass spectrum of 3-(trifluoromethyl)aniline (GC method 2).....	68
Figure 2-41 A: GC-MS chromatogram of 1,3-dichlorobenzene at 2.3 minutes; B: EI mass spectrum of 1,3-dichlorobenzene (GC method 1).....	69
Figure 2-42 A: GC-MS chromatogram of mCPP 1.HCl at 7.2 minutes, 3-chloroaniline at 4.5 minutes; B: EI mass spectrum of mCPP (GC method 2).....	70
Figure 2-43 EI mass spectrum of 3-chloroaniline (GC method 2).....	71
Figure 2-44 Structure of 2-chloroanisole starting material.	72
Figure 2-45 Proposed reaction mechanism for the formation of 2-methoxyphenylpiperazine and 3-methoxyphenylpiperazine.	72
Figure 2-46 A: GC-MS chromatogram of MeOPP 1.HCl at 7.1 minutes, bis(2-chloroethyl)amine at 3.5 minutes, 4-anisidine at 4.3 minutes; B: EI mass spectrum of MeOPP (GC method 2). ..	73
Figure 2-47 EI mass spectrum of 4-anisidine (GC method 2).....	74
Figure 2-48 EI mass spectrum of bis(2-chloroethyl)amine (GC method 2).	74
Figure 3-1 NoDoz repeat injection in standard trial.	83
Figure 3-2 Codral repeat injection in standard trial.....	83
Figure 3-3 Caffeine KBr (100 mg/g) repeat injection in standard trial.	84
Figure 3-4 Depletion of morphine signal over time.....	85
Figure 3-5 Main effects plot for 100 mg/g caffeine KBr disc.	86
Figure 3-6 Interaction plot for 100 mg/g caffeine KBr disc.....	87

Figure 3-7 Effects plot for 100mg/g caffeine in KBr disc.	88
Figure 3-8 Residual plots for 100 mg/g caffeine KBr disc.	89
Figure 3-9 Response surface plots for 100 mg/g caffeine KBr disc.....	90
Figure 3-10 Contour plot for 100 mg/g caffeine KBr disc.	90
Figure 3-11 Optimisation plot for 100 mg/g caffeine KBr disc.	91
Figure 3-12 Optimising solvent flow rate (mL/hr) for 100 mg/g caffeine KBr disc, n=5.	93
Figure 3-13 Optimising gas pressure for 100 mg/g caffeine KBr disc, n=5.	93
Figure 3-14 Optimising spray high voltage for 100 mg/g caffeine KBr disc, n=5.	94
Figure 3-15 Optimising solvent composition for 100 mg/g caffeine KBr disc, n=5.....	95
Figure 3-16 Optimising fragmentor voltage for 100 mg/g caffeine KBr disc, n=5.	96
Figure 3-17 Paracetamol tablet being analysed by DESI-MS.	97
Figure 3-18 DESI-MS spectra of 4-MMC; A: M1, B: M2, C: M3, D: M4 in KBr disc.....	98
Figure 3-19 DESI-MS spectra of 4-MMC; A: M1, B: M2, C: M3, D: M4 on PVC plate.....	99
Figure 3-20 DESI-MS spectra of 4-MMC; A: M1, B: M2, C: M3, D: M4 powder on PVC plate.	100
Figure 3-21 Double sided tape with sample powders for DESI-MS analysis. 0=blank, 1=M1, 2=M2, 5=M3, 6=M4, C=Caffeine.	100
Figure 3-22 DESI-MS spectra of 4-MMC; A: M1, B: M2, C: M3, D: M4 on double sided tape.	101
Figure 3-23 A: Polyvinyl chloride (PVC); B: Polymethyl methacrylate (pMMA); C: Polytetrafluoroethylene (PTFE).	101
Figure 3-24 GC-MS chromatogram of codeine-D ₆ using gradient A.	105
Figure 3-25 GC-MS chromatogram of codeine-D ₆ using gradient B.	106

Figure 3-26 GC-MS chromatogram of codeine-D ₆ using gradient C.	106
Figure 3-27 GC-MS chromatogram of codeine-D ₆ using gradient D.	107
Figure 3-28 GC-MS chromatogram of 4-MMC; 2 µL injection, splitless mode.	108
Figure 3-29 GC-MS chromatogram of 4-MMC and codeine-D ₆ using gradient D; 2 µL injection, splitless mode.	109
Figure 3-30 LC-MS EIC of 4-MMC and codeine-D ₆ , gradient 1, resolution = 1.1.	111
Figure 3-31 LC-MS EIC of 4-MMC and codeine-D ₆ , gradient 2, resolution = 2.3.	111
Figure 3-32 LC-MS EIC of 4-MMC and codeine-D ₆ , gradient 3, resolution = 2.6.	111
Figure 4-1 Chemical structures of common adulterants in ATS preparations.	116
Figure 4-2 Intra-day study of the effects of different adulterants on the detection of MA (0.36 µg), 1:1 ratio, n=3.	116
Figure 4-3 Inter-day study of the effect of different adulterants on the detection of MA (0.36 µg), 1:1 ratio, n=3.	117
Figure 4-4 Adulterating MA standard with caffeine at varying amounts caffeine added (0 %, 20 %, 50 %, 90 %, 95 % w/w), n=3, 2 µL of 74.5 µg/mL, equivalent to 0.14 µg MA.	118
Figure 4-5 A: DESI-MS of MA, B: MS/MS of MA at 20 eV.	118
Figure 4-6 Proposed collision induced dissociation of the [M+H] ⁺ ion of MA.	118
Figure 4-7 Adulterating PMA standard with caffeine at varying amounts of caffeine added (0 %, 20 %, 50 %, 90 %, 95 % w/w), n=3, 2 µL 826 µg/mL, equivalent to 1.65 µg PMA.	119
Figure 4-8 A: DESI-MS of PMA, B: MS/MS of PMA at 20 eV.	120
Figure 4-9 Proposed collision induced dissociation of the [M+H] ⁺ ion of PMA.	120
Figure 4-10 Adulterating AP standard with caffeine at varying amounts of caffeine added (0 %, 20 %, 50 %, 90 %, 95 % w/w), n=3, 2 µL of 67.6 µg/mL, equivalent to 0.14 µg AP.	121

Figure 4-11 A: DESI-MS of AP, B: MS/MS of AP at 20 eV.	121
Figure 4-12 Proposed collision induced dissociation of the $[M+H]^+$ ion of AP.	122
Figure 4-13 Inter-day study of AP adulterated with caffeine (0 %, 20 %, 50 %, 90 %, 95 % w/w); n=3, (2 μ L of 67.6 μ g/mL, equivalent to 0.14 μ g AP).....	122
Figure 4-14 Adulterating DMA standard with caffeine at varying amounts of caffeine added (0 %, 20 %, 50 %, 90 %, 95 % w/w), n=3, 2 μ L of 80 μ g/mL, equivalent to 0.16 μ g DMA.	123
Figure 4-15 A: DESI-MS of DMA, B: MS/MS of DMA at 20 eV.	124
Figure 4-16 Proposed collision induced dissociation of the $[M+H]^+$ ion of DMA.	124
Figure 4-17 Adulterating MDMA standard with caffeine at varying amounts of caffeine added (0 %, 20 %, 50 %, 90 %, 95 % w/w), n=3, 2 μ L of 9660 μ g/mL, equivalent to 19.4 μ g MDMA.	125
Figure 4-18 A: DESI-MS of MDMA; B: MS/MS of MDMA; C: MS/MS of caffeine at 20 eV.	126
Figure 4-19 Proposed collision induced dissociation of the $[M+H]^+$ ion of MDMA.	126
Figure 4-20 Data on MDMA sample provided by AFP (analysis conducted by NMI).....	128
Figure 4-21 DESI-MS spectra of MDMA tablet.....	129
Figure 4-22 A: DESI-MS of MDMA tablet, B: MS/MS of MDMA, C: MS/MS of 3,4-methylenedioxyphenyl-2-propanol (MDP-2-POH), D: MS/MS of 3,4-methylenedioxydimethylamphetamine (MDDMA).	129
Figure 4-23 Proposed collision induced dissociation of the $[M+H]^+$ ion of MDMA (- - >), MDP-2-POH (→) and MDDMA (→).	130
Figure 4-24 A: DESI-MS of MDMA sample, B: MS/MS of MDMA, C: MS/MS of MDP-2-P, D: MS/MS of PN.....	131
Figure 4-25 Proposed collision induced dissociation of the $[M+H]^+$ ion of MDP-2-P (- - >) and PN (→).....	131

Figure 4-26 PCDL library match to MDMA.....	132
Figure 4-27 GC-MS chromatogram of MDMA tablet; MDP-2-POH at 6.1 minutes, MDMA at 6.3 minutes, MDDMA at 6.5 minutes (GC method 2).....	133
Figure 4-28 EI mass spectrum of MDMA (GC method 2).....	134
Figure 4-29 EI mass spectrum of MDP-2-POH (GC method 2).....	134
Figure 4-30 EI mass spectrum of MDDMA (GC method 2).	135
Figure 4-31 Proposed EI fragmentation of MDMA tablet.....	135
Figure 4-32 GC-MS chromatogram of synthesised MDMA base; PN at 5.4 minutes, MDMA at 6.2 minutes, MDP-2-P at 6.6 minutes, N-formyl-MDMA at 7.7 minutes (GC method 2).	136
Figure 4-33 EI mass spectrum of PN (GC method 2).....	136
Figure 4-34 EI mass spectrum of MDP-2-P (GC method 2).....	137
Figure 4-35 EI mass spectrum of N-formyl-MDMA (GC method 2).	137
Figure 4-36 LC-MS chromatogram of MDMA tablet; A: EIC of MDMA at 4.9 minutes, m/z 194; B: EIC of MDP-2-POH (trace) at 1.3 minutes, m/z 181; C: EIC of MDDMA at 5.1 minutes, m/z 208.	138
Figure 4-37 LC-MS spectra of MDMA tablet; A: MDMA, B: MDP-2-POH, C: MDDMA.....	139
Figure 4-38 LC-MS chromatogram of MDMA base; A: EIC of MDMA at 4.8 minutes, m/z 194; B: EIC of MDP-2-P at 1.8 minutes, m/z 179; C: EIC of N-formylMDMA at 10.2 minutes, m/z 222.	139
Figure 4-39 LC-MS/MS spectra of MDMA base; A: MDMA; B: MDP-2-P; C: N-formyl-MDMA.	140
Figure 4-40 A: DESI-MS spectra of PMMA; B: MS/MS of PMMA.....	141
Figure 4-41 Proposed collision induced dissociation of the $[M+H]^+$ ion of PMMA.	141

Figure 4-42 PCDL library match to PMMA.	142
Figure 4-43 A: GC-MS chromatogram of synthesised PMMA, anethole at 4.9 minutes, PMMA at 5.8 minutes, PMP-2-P at 6.4 minutes; B: EI mass spectrum of PMMA (GC method 2).	144
Figure 4-44 EI mass spectrum of anethole (GC method 2).	145
Figure 4-45 EI mass spectrum of PMP-2-P (GC method 2).	145
Figure 4-46 Proposed EI fragmentation of PMMA base.	146
Figure 4-47 LC-MS chromatogram of PMMA base; A: EIC of PMMA at 10.3 minutes, m/z 180; B: EIC of anethole at 5.1 minutes, m/z 149; C: EIC of PMP-2-P at 19.8 minutes, m/z 165.	146
Figure 4-48 LC-MS/MS of PMMA base; A: PMMA; B: anethole; C: PMP-2-P.	147
Figure 4-49 A: DESI-MS spectra of "Jack3d" containing DMAA and caffeine, B: MS/MS of DMAA, C: MS/MS of caffeine.	148
Figure 4-50 Proposed collision induced dissociation of the $[M+H]^+$ ion of DMAA.	148
Figure 4-51 Proposed collision induced dissociation of the $[M+H]^+$ ion of caffeine.	148
Figure 4-52 PCDL library match to DMAA.	149
Figure 4-53 A: GC-MS chromatogram of "Jack3d", caffeine at 7.5 minutes; B: EI mass spectrum of caffeine (GC method 2).	150
Figure 4-54 LC-MS chromatogram of "Jack3d"; A: EIC of caffeine at 4.1 minutes, m/z 195; B: EIC of creatine monohydrate at 1.2 minutes, m/z 132; C: EIC of DMAA at 4.9 minutes, m/z 116.	151
Figure 4-55 LC-MS/MS spectra of "Jack3d"; A: caffeine, B: creatine monohydrate, C: DMAA.	151
Figure 5-1 Chemical structures of common adulterants in illicit cocaine preparations.	159
Figure 5-2 Intra-day study of the effects of different adulterants on the detection of cocaine, n=3.	159

Figure 5-3 Inter-day study of the effect of different adulterants on the detection of cocaine, n=3.	160
Figure 5-4 Adulterating cocaine standard with varying amounts of caffeine added (i.e. 0 %, 20 %, 50 %, 90 %, 95 % w/w), n=3, 2 µL of 12130 µg/mL, equivalent to 24.3 µg cocaine.	161
Figure 5-5 A: DESI-MS spectra of cocaine; B: MS/MS spectra of cocaine at 20 eV.	161
Figure 5-6 Proposed collision induced dissociation of the $[M+H]^+$ ion of cocaine ¹²⁶	162
Figure 5-7 Data on cocaine samples provided by AFP (analysis conducted by NMI).	165
Figure 5-8 DESI-MS spectra of AFP cocaine samples; A: Item 1, B: Item 1/2, C: Item 5/2.	166
Figure 5-9 DESI-MS/MS spectra of cocaine item 5/2; A: cocaine, B: CC, C: truxilline, D: hydroxyzine, E: EME, F: levamisole.	166
Figure 5-10 Proposed collision induced dissociation of the $[M+H]^+$ ion of CC.	167
Figure 5-11 Proposed collision induced dissociation of the $[M+H]^+$ ion of α -truxilline.	167
Figure 5-12 Proposed collision induced dissociation of the $[M+H]^+$ ion of hydroxyzine.	168
Figure 5-13 Proposed collision induced dissociation of the $[M+H]^+$ ion of EME.	168
Figure 5-14 Proposed collision induced dissociation of the $[M+H]^+$ ion of levamisole.	168
Figure 5-15 Proposed collision induced dissociation of the $[M+H]^+$ ion of 3,4,5-trimethoxycocaine.	169
Figure 5-16 PCDL library match to cocaine.	170
Figure 5-17 A: GC-MS chromatogram of cocaine Item 1, benzoic acid at 4.6 minutes, ecgonidine methyl ester at 5.7 minutes, EME at 6.1 minutes, caffeine at 7.6 minutes, tropacocaine at 7.9 minutes, cocaine at 8.8 minutes, 3,4,5-trimethoxycocaine at 9.1 minutes, CC at 9.7 minutes; B: EI mass spectrum of cocaine (GC method 2).	171
Figure 5-18 EI mass spectrum of ecgonidine methyl ester (GC method 2).	172

Figure 5-19 EI mass spectrum of EME (GC method 2).	172
Figure 5-20 EI mass spectrum of caffeine (GC method 2).	173
Figure 5-21 EI mass spectrum of tropacocaine (GC method 2).	173
Figure 5-22 EI mass spectrum of 3,4,5-trimethoxycocaine (GC method 2).	174
Figure 5-23 EI mass spectrum of CC (GC method 2).	174
Figure 5-24 GC-MS chromatogram of cocaine standard; benzoic acid methyl ester at 4.2 minutes, ecgonidine methyl ester at 5.7 minutes, EME at 6.1 minutes, cocaine at 8.7 minutes (GC method 2).	175
Figure 5-25 GC-MS chromatogram of cocaine Item 1/2; benzoic acid at 4.7 minutes, ecgonidine methyl ester at 5.7 minutes, EME at 6.2 minutes, caffeine at 7.6 minutes, cocaine at 8.8 minutes, CC at 9.4 minutes, BE at 10.1 minutes (GC method 2).	175
Figure 5-26 EI mass spectrum of BE (GC method 2).	176
Figure 5-27 Chemical structures of benzoic acid, ecgonidine methyl ester and benzoylecgonine.	176
Figure 5-28 GC-MS chromatogram of cocaine Item 5/2; benzoic acid at 4.7 minutes, ecgonidine methyl ester at 5.7 minutes, EME at 6.1 minutes, caffeine at 7.6 minutes, levamisole at 8.1 minutes, cocaine at 8.8 minutes, CC at 9.7 minutes, BE at 10.1 minutes (GC method 2).	177
Figure 5-29 EI mass spectrum of levamisole (GC method 2).	177
Figure 5-30 Proposed EI fragmentation pathway for cocaine.	178
Figure 5-31 LC-MS chromatogram of cocaine Item 1; A: EIC of cocaine at 7.2 minutes, m/z 304; B: EIC of truxillines at 9.2 minutes, m/z 659; C: EIC of 3,4,5-trimethoxycocaine at 8.1 minutes, m/z 394; D: EIC of tropacocaine at 6.3 minutes, m/z 246; E: EIC of caffeine at 4.2 minutes, m/z 195; F: EIC of EME at 1.5 minutes, m/z 200; G: EIC of CC at 9.6 minutes, m/z 330.	179

Figure 5-32 LC-MS/MS spectra of cocaine Item 1; A: cocaine, B: truxilline, C: 3,4,5-trimethoxycocaine, D: tropacocaine, E: caffeine, F: EME, G: CC at 20 eV.	180
Figure 5-33 LC-MS chromatogram of cocaine Item 1/2; A: EIC of cocaine at 7.2 minutes, m/z 304; B: EIC of truxillines at 10.2 minutes, m/z 659; C: EIC of 3,4,5-trimethoxycocaine at 8.1 minutes, m/z 394; D: EIC of caffeine at 4.2 minutes, m/z 195; E: EIC of EME at 1.5 minutes, m/z 200; F: EIC of CC at 9.4 minutes, m/z 330.	181
Figure 5-34 LC-MS/MS spectra of cocaine Item 1/2; A: cocaine, B: truxilline, C: 3,4,5-trimethoxycocaine, D: caffeine, E: EME, F: CC at 20 eV.	181
Figure 5-35 LC-MS chromatogram of cocaine Item 5/2; A: EIC of cocaine at 7.3 minutes, m/z 304; B: EIC of truxillines at 9.2 minutes, m/z 659; C: EIC of 3,4,5-trimethoxycocaine at 8.1 minutes, m/z 394; D: EIC of levamisole at 5.0 minutes, m/z 205; E: EIC of hydroxyzine at 12.1 minutes, m/z 375; F: EIC of caffeine at 4.2 minutes, m/z 195; G: EIC of EME at 1.5 minutes, m/z 200; H: EIC of CC at 9.6 minutes, m/z 330.	182
Figure 5-36 LC-MS/MS spectra of cocaine Item 5/2; A: cocaine, B: truxilline, C: 3,4,5-trimethoxycocaine, D: levamisole, E: hydroxyzine, F: caffeine, G: EME, H: CC at 20 eV.	183
Figure 5-37 LC-MS/MS spectra of cocaine standard; A: EME at m/z 200, B: cocaine at m/z 304.	183
Figure 6-1 Adulterating BZP 2 with caffeine at varying amounts of caffeine added (0 %, 20 %, 50 %, 90 %, 95 % w/w), n=3, 2 μ L of 7050 μ g/mL, equivalent to 14.10 μ g BZP.	191
Figure 6-2 A: DESI-MS spectra of BZP 2; B: MS/MS spectra of BZP at 20 eV.	191
Figure 6-3 Proposed collision induced dissociation of the $[M+H]^+$ ion of BZP.	192
Figure 6-4 Inter-day study of BZP adulterated with caffeine (0 %, 20 %, 50 %, 90 %, 95 % w/w); n=3, (2 μ L of 7050 μ g/mL, equivalent to 14.10 μ g BZP).	192
Figure 6-5 Adulterating TFMPP standard with caffeine at varying amounts of caffeine added (0 %, 20 %, 50 %, 90 %, 95 % w/w), n=3, 2 μ L of 920 μ g/mL, equivalent to 1.84 μ g TFMPP.	193
Figure 6-6 A: DESI-MS spectra of TFMPP; B: MS/MS spectra of TFMPP at 20 eV.	194

Figure 6-7 Proposed collision induced dissociation of the $[M+H]^+$ ion of TFMPP.	194
Figure 6-8 Adulterating mCPP standard with caffeine at varying amounts of caffeine added (0 %, 20 %, 50 %, 90 %, 95 % w/w), n=3, 2 μ L of 8000 μ g/mL, equivalent to 16.0 μ g mCPP.....	195
Figure 6-9 A: DESI-MS spectra of mCPP; B: MS/MS spectra of mCPP at 20 eV.	196
Figure 6-10 Proposed collision induced dissociation of the $[M+H]^+$ ion of mCPP.	196
Figure 6-11 Adulterating MeOPP 1 with caffeine at varying amounts of caffeine added (0 %, 20 %, 50 %, 90 %, 95 % w/w), n=3, 2 μ L of 1560 μ g/mL, equivalent to 3.10 μ g MeOPP.....	197
Figure 6-12 A: DESI-MS spectra of MeOPP 1; B: MS/MS spectra of MeOPP at 20 eV.....	198
Figure 6-13 Proposed collision induced dissociation of the $[M+H]^+$ ion of MeOPP.....	198
Figure 6-14 Adulterating a mixture of BZP 1 HCl and TFMPP 2 base (1:1) with varying amounts of caffeine, n=3.	199
Figure 6-15 DESI-MS spectra of A: BZP 1, B: BZP 2, C: BZP 3.	201
Figure 6-16 DESI-MS/MS of A: BZP 1 and B: DBZP.....	201
Figure 6-17 Proposed collision induced dissociation of the $[M+H]^+$ ion of BZP (- - \rightarrow) and DBZP (\rightarrow).	202
Figure 6-18 PCDL library match to BZP.	203
Figure 6-19 DESI-MS spectra of A: BZP 4, B: MS/MS of BZP, C: MS/MS of DBZP, D: MS/MS of MBCP, E: MS/MS of MS/MS of EBCP, F: MS/MS of benzyl chloride.....	204
Figure 6-20 Proposed collision induced dissociation of the $[M+H]^+$ ion of MBCP (by-product, \rightarrow), EBCP (intermediate, \Rightarrow) and benzyl chloride (- - \rightarrow).....	205
Figure 6-21 GC-MS chromatogram of BZP 1.HCl at 6.1 minutes, DBZP at 8.5 minutes (GC method 2).....	206
Figure 6-22 EI mass spectra of BZP 1.HCl (GC method 2).	206

Figure 6-23 Proposed EI fragmentation pathway for BZP.	207
Figure 6-24 GC-MS chromatogram of BZP 2.HCl at 6.1 minutes, DBZP at 8.5 minutes (GC method 2).....	207
Figure 6-25 GC-MS chromatogram of BZP 3.HCl at 6.1 minutes, DBZP at 8.5 minutes (GC method 2).....	208
Figure 6-26 GC-MS chromatogram of BZP 4.HCl at 5.0 minutes, MDCP at 6.6 minutes, EBCP, 6.8 minutes, DBZP at 7.7 minutes (GC method 1).	208
Figure 6-27 LC-MS chromatogram of BZP 1.HCl; A: EIC of BZP at 4.3 minutes, m/z 177; B: EIC of DBZP at 11.3 minutes, m/z 267.	209
Figure 6-28 LC-MS chromatogram of BZP 2.HCl; A: EIC of BZP at 4.3 minutes, m/z 177; B: EIC of DBZP at 11.3 minutes, m/z 267.	209
Figure 6-29 LC-MS chromatogram of BZP 3.HCl; A: EIC of BZP at 4.3 minutes, m/z 177; B: EIC of DBZP at 11.3 minutes, m/z 267.	210
Figure 6-30 LC-MS/MS spectra of A: BZP, B: DBZP.	210
Figure 6-31 LC-MS chromatogram of BZP 4.HCl A: EIC of BZP at 4.3 minutes, m/z 177; B: EIC of MBCP at 11.1 minutes, m/z 235; C: EIC of DBZP at 11.8 minutes, m/z 267; D: EIC of EBCP at 13.0 minutes, m/z 249.	211
Figure 6-32 LC-MS/MS of A: BZP, B: MBCP, C: DBZP, D: EBCP.....	211
Figure 6-33 DESI-MS spectra of A: TFMPP 1, B: TFMPP 2, C: TFMPP 3, D: TFMPP 4.	212
Figure 6-34 DESI-MS/MS of TFMPP 2 and TFMPP 3; A: TFMPP, B: 3-trifluoromethylphenol, C: piperazine, D: 3-(trifluoromethyl)aniline.	214
Figure 6-35 PCDL library match to TFMPP.	215
Figure 6-36 Proposed collision induced dissociation of the $[M+H]^+$ ion of TFMPP, TFMPP (\rightarrow), 3-(trifluoromethyl)aniline ($-->$) and piperazine.	216
Figure 6-37 GC-MS chromatogram of TFMPP 1.HCl at 5.1 minutes (GC method 1).....	217

Figure 6-38 EI mass spectra for TFMPP 1 (GC method 1).	218
Figure 6-39 Proposed EI fragmentation pathway for TFMPP.	218
Figure 6-40 GC-MS chromatogram of TFMPP 2.HCl at 5.7 minutes and 6.2 minutes, 3-chlorobenzotrifluoride at 3.3 minutes, 3-trifluoromethylphenol at 4.0 minutes (GC method 2).	219
Figure 6-41 GC-MS chromatogram of TFMPP 3.HCl at 4.5 minutes, 5.0 minutes, 5.3 minutes; piperazine at 2.5 minutes (GC method 1).....	219
Figure 6-42 GC-MS chromatogram of TFMPP 4.HCl at 6.2 minutes, 3-(trifluoromethyl)aniline at 3.8 minutes (GC method 2).....	220
Figure 6-43 LC-MS chromatogram of TFMPP; A: EIC of TFMPP 1 at 8.0 minutes, m/z 231; B: EIC of TFMPP 2; C: EIC of TFMPP 3; D: EIC of TFMPP 4; E: EIC of 3-(trifluoromethyl)aniline at 3.9 minutes, m/z 162; F: MS/MS of TFMPP.	221
Figure 6-44 DESI-MS spectra of A: mCPP 1, B: MS/MS spectra of mCPP, C: MS/MS spectra of 3-chloroaniline.	222
Figure 6-45 PCDL library match to mCPP.	223
Figure 6-46 Proposed collision induced dissociation of the $[M+H]^+$ ion of mCPP and 3-chloroaniline.	224
Figure 6-47 GC-MS chromatogram of mCPP 1.HCl at 7.2 minutes, 3-chloroaniline at 4.5 minutes (GC method 2).....	225
Figure 6-48 EI mass spectrum of mCPP 1 (GC method 2).	225
Figure 6-49 Proposed EI fragmentation pathway for mCPP.	226
Figure 6-50 LC-MS chromatogram of mCPP 1; A: EIC of mCPP at 6.4 minutes, m/z 197; B: MS/MS of mCPP.	226
Figure 6-51 DESI-MS spectra of A: MeOPP 1, B: MS/MS spectra of MeOPP, C: MS/MS spectra of 4-anisidine.	227

Figure 6-52 PCDL library match to MeOPP.	228
Figure 6-53 Proposed collision induced dissociation of the $[M+H]^+$ ion of MeOPP and 4-anisidine.	229
Figure 6-54 GC-MS chromatogram of MeOPP 1.HCl at 7.2 minutes, bis(2-chloroethyl)amine at 3.5 minutes, 4-anisidine at 4.3 minutes (GC method 2).	230
Figure 6-55 EI mass spectra of MeOPP 1 (GC method 2).	230
Figure 6-56 Proposed EI fragmentation pathway for MeOPP.	231
Figure 6-57 LC-MS chromatogram of MeOPP; A: EIC of MeOPP 1 at 4.2 minutes, m/z 193; B: EIC of 4-anisidine at 5.8 minutes, m/z 124; C: MS/MS of MeOPP 1	232
Figure 7-1 DESI-MS calibration curve for 4-MMC, n=3.	239
Figure 7-2 GC-MS calibration curve for 4-MMC, n=3 (GC method 1).	241
Figure 7-3 LC-MS calibration curve for 4-MMC, n=3.	242
Figure 7-4 DESI-MS of 4-MMC (M1, M2, M3 and M4) in positive ion mode.	244
Figure 7-5 A: MS of 4-MMC, B: MS/MS spectra of triethylamine, C: MS/MS spectra of 4-MMC product ion at m/z 178 in positive ion mode at 30 eV.	245
Figure 7-6 Proposed collision induced dissociation of the $[M+H]^+$ ion of 4-MMC.	246
Figure 7-7 Proposed collision induced dissociation of the $[M+H]^+$ ion of triethylamine.	246
Figure 7-8 PCDL library match to 4-MMC.	247
Figure 7-9 GC-MS chromatogram of 4-MMC (M4) at 4.4 minutes, 2-methylpropiofenone at 3.6 minutes, 2-bromo-4-methylpropiofenone at 4.1 minutes (GC method 1).	248
Figure 7-10 EI mass spectra of 4-MMC (GC method 1).	249
Figure 7-11 Proposed EI fragmentation pathway of 4-MMC.	249

Figure 7-12 LC-MS chromatogram of 4-MMC A: EIC of M1 at 5.7 minutes, m/z 178; B: EIC of M2; C: EIC of M3; D: EIC of M4; E: LC-MS/MS of 4-MMC at 20 eV.	250
Figure 7-13 DESI-MS spectra of A: 4-MMC, caffeine and paracetamol as a mixture; B: 4-MMC, caffeine, paracetamol and. codeine-D ₆ as a mixture.	252
Figure 7-14 Structure of drug compounds used in selectivity study.	253
Figure 7-15 Ion suppression/enhancement present in different mixtures analysed using DESI-MS.	254
Figure 7-16 Calibration curve for 4-MMC in a mixture of caffeine and MA.	255
Figure 7-17 Molecular structure of methylone.	256
Figure 7-18 DESI-MS spectra of 4-MMC and methylone (with codeine-D ₆ IS).	257
Figure 7-19 DESI-MS/MS spectra of A: methylone, B: 4-MMC at 20 eV.	257
Figure 7-20 Proposed collision induced dissociation of the [M+H] ⁺ ion of methylone.	258
Figure 7-21 DESI-MS/MS spectra for A: 4-MMC, B: 4-DEAB, C: mixture of 4-MMC and 4-DEAB at 20 eV.	259
Figure 7-22 Proposed collision induced dissociation of the [M+H] ⁺ ion of 4-DEAB.	259
Figure 7-23 DESI-MS/MS spectra for A: 1B3P, B: 4-MMC, C: mixture of 4-MMC and 1B3P at 20 eV.	260
Figure 7-24 Proposed collision induced dissociation of the [M+H] ⁺ ion of 1B3P.	260
Figure 7-25 DESI-MS spectra of 4-MMC.	264
Figure 8-1 A: DESI-MS/MS spectra of MA, B: DESI-MS/MS spectra of phentermine.	274

List of tables

Table 3-1 List of mixtures tested for optimal solvent composition.....	78
Table 3-2 Design layout for 2 ³ design.	80
Table 3-3 Factor levels for drug analysis using DESI-MS.....	81
Table 3-4 Optimal parameters for caffeine.	91
Table 3-5 Comparison of the reproducibility of signal intensity of 4-MMC on three different plates, n=5.....	102
Table 3-6 Summary of optimised values for drug compounds; set values: d ₁ =3 mm, d ₃ =5 mm, β=15°, α=55°, solvent flow rate=0.21 mL/hr, high voltage=4 kV, gas flow rate=100 psi.	103
Table 4-1 Limit of detection of different ATS, n=3.....	127
Table 4-2 Mass accuracy of ATS, using positive ion mode.....	152
Table 4-3 Mass accuracy of MS/MS ions using positive ion mode at 20 eV.....	153
Table 4-4 Compounds detected in “Jack3d”, MDMA (tablet and synthesised base), and PMMA (synthesised base) using DESI-MS, GC-MS, and LC-MS.	154
Table 5-1 Limit of detection, intra-day and inter-day precision of cocaine, n=3.....	162
Table 5-2 Mass accuracy of cocaine and related compounds using positive ion mode.....	184
Table 5-3 Mass accuracy of MS/MS ions using positive ion mode at 20 eV.....	185
Table 5-4 Compounds detected in cocaine samples using DESI-MS, GC-MS, and LC-MS.	186
Table 6-1 Limit of detection of piperazine analogues, n=3.	199
Table 6-2 Mass accuracy of piperazine and related compounds using positive ion mode. ...	233
Table 6-3 Mass accuracy of MS/MS ions using positive ion mode at 20 eV.....	233

Table 6-4 Compounds detected in piperazine analogues using DESI-MS, GC-MS, and LC-MS.	235
Table 7-1 Statistical comparison of DESI-MS, GC-MS, and LC-MS in the analysis of 4-MMC.	240
Table 7-2 List of by-products found in synthesised 4-MMC samples with corresponding m/z values.	243
Table 7-3 Calculated concentrations of M1 using pure and mixed calibrator calibration curves.	256
Table 7-4 Comparison of codeine-D ₆ and 4-MMC-D ₃ , as internal standards.	262
Table 7-5 Optimising codeine-D ₆ IS concentration, n=3.	262
Table 7-6 Purity of M1, M2, M3, M4 as determined using DESI-MS, GC-MS, and LC-MS.	263
Table 7-7 Mass accuracy of 4-MMC and related compounds using positive ion mode.	264
Table 7-8 Mass accuracy of MS/MS fragments using positive ion mode at 20 eV.	265
Table 7-9 Compounds detected in 4-MMC samples using DESI-MS, GC-MS and LC-MS.	266
Table 8-1 Results of Marquis reagent with BZP.	270
Table A-1 International seizures classified by drug type.	285

Abbreviations

- 1B3P – 1-Benzyl-3-pyrrolidinol
2C-I – 4-Iodo-2,5-dimethoxyphenethylamine
4-DEAB – 4-(Diethylamino)benzaldehyde
4-F-AP – 4-Fluoroamphetamine
4-MMC – 4-Methylmethcathinone
4-MTA – 4-Methylthioamphetamine
4-OH-AP – 4-Hydroxyamphetamine
5-HT – Serotonin
ABDF – Bromobenzodifuranylisopropylamine
AccuTOF – Accurate time-of-flight
AF – Ammonium formate
AFP – Australian Federal Police
AGAL – Australian Government Analytical Laboratories
AIDIP – Australian Illicit Drug Intelligence Program
AP – Amphetamine
API – Atmospheric pressure ionisation
APPI – Atmospheric pressure photoionisation
AP-MALDI – Atmospheric pressure – matrix assisted laser desorption ionisation
ASAP – Atmospheric-pressure solids analysis probe
ATR – Attenuated total reflection
ATS – Amphetamine-type substances
BE – Benzoyllecgonine
BZP – *N*-Benzylpiperazine or 1-benzylpiperazine
CC – Cinnamoyl cocaine
CCD – Central composite design
cps – Counts per second
 C_{the} – Theoretical concentration
DAPPI – Desorption atmospheric pressure photoionisation
DART – Direct analysis in real time
DBZP – 1,4-Dibenzylpiperazine
DESI – Desorption electrospray ionisation
DMA – *N,N*-Dimethylamphetamine

DMAA – Dimethylamylamine
DMMP – Dimethyl methylphosphonate
DMS – Dimethyl sulfone
EBCP – Ethyl 1-benzyl-4-carboxypiperazine
EC – Ethyl centralite
EI – Electron ionisation
EIC – Extracted ion chromatogram
ELDI – Electrospray-assisted laser desorption ionisation
EME – Ecgonine methyl ester
EP – Ephedrine
ESI – Electrospray ionisation
FA – Formic acid
FFD – Full factorial design
FI – Flow injection
FTIR – Fourier transform infrared
GC-FID – Gas chromatography - flame ionisation detector
GC-MS – Gas chromatography - mass spectrometry
GSR – Gun-shot residue
H₂O – Water
HCl – Hydrochloride
HPLC – High performance-liquid chromatography
HS-GC – Head space - gas chromatography
IRMS – Isotope ratio - mass spectrometry
IS – Internal standard
IT – Ion trap
KBr – Potassium bromide
K-tBuO – Potassium tert-butoxide
LC – Liquid chromatography
LC-MS – Liquid chromatography-mass spectrometry
LOD – Limit of detection
LOL – Limit of linearity
LOQ – Limit of quantitation
LSD – Lysergic acid diethylamide
M – Mean of the experimentally determined concentrations

MA – Methylamphetamine
MALDESI – Matrix-assisted laser desorption electrospray ionisation
MBCP – Methyl 1-benzyl-4-carboxypiperazine
MC – Methyl centralite
mCPP – 3-Chlorophenylpiperazine
MDA – 3,4-Methylenedioxyamphetamine
MDDMA – 3,4-Methylenedioxydimethylamphetamine
MDEA – 3,4-Methylenedioxyethylamphetamine
MDHOET – 3,4-Methylenedioxy-*N*-(2-hydroxyethyl)amphetamine
MDMA – Methylenedioxymethylamphetamine ('Ecstasy')
MDP-2-P – 3,4-Methylenedioxyphenyl-2-propanone
MDP-2-POH – 3,4-Methylenedioxyphenyl-2-propanonol
MeOH – Methanol
MeOPP – 4-Methoxyphenylpiperazine
MS – Mass spectrometry/Mass spectrometer
MS/MS – Tandem mass spectrometry
MUX – Multiplexed
NHSP – National Heroin Signature Program
NMI – National Measurement Institute
NMR – Nuclear magnetic resonance
OFAT – One-factor-at-a-time
OMPP – 2-Methoxyphenylpiperazine
P2P – Phenyl-2-propanone
PCDL – Personal Compound Database and Library
pEP – Pseudoephedrine
PMA – 4-Methoxyamphetamine
PMMA – 4-Methoxymethylamphetamine
pMMA – Polymethyl methacrylate
PMP-2-P – 4-Methoxyphenyl-2-propanone
PN – Piperonyl nitrile
PTFE – Polytetra fluoroethylene (Teflon)
PVC – Polyvinyl chloride
QC – Quality check samples
QTOF – Quadrupole time-of-flight

IR – Infrared

RDX – Trinitrohexahydro-1,3,5-triazine

RE – Relative error

RSD – Relative standard deviation

SEM-EDX - Scanning electron microscopy – energy dispersive X-ray

SD – Standard Deviation

SNR – Signal-to-noise ratio

TFMPP – 3-Trifluoromethylphenylpiperazine

THC – Δ^9 -Tetrahydrocannabinol

TLC – Thin-layer chromatography

TOF – Time-of-flight

UNODC – United Nations Office on Drugs and Crime

US – United States

UV – Ultraviolet

UV-DAD – Ultraviolet diode array detector

Abstract

Desorption electrospray ionisation - mass spectrometry (DESI-MS) is an ambient ionisation technique that can be applied to the analysis of illicit drugs and novel drug analogues in seized drug material. Currently used preliminary identification techniques lack sensitivity and selectivity and are prone to false positive and false negative results. Therefore, it was important to investigate the use of DESI-MS as a novel preliminary identification technique in the analysis of a range of compounds with the potential for future automated library matching aiding in the rapid identification of unknowns.

In this research, 4-methylmethcathinone (mephedrone or 4-MMC), cocaine, 1-benzylpiperazine (BZP), 3-trifluoromethylphenylpiperazine (TFMPP), 3-chlorophenylpiperazine (mCPP), 4-methoxyphenylpiperazine (MeOPP) and other amphetamine-type substances (ATS) such as amphetamine (AP), methylamphetamine (MA), 3,4-methylenedioxymethylamphetamine (MDMA), *N,N*-dimethylamphetamine (DMA), 4-methoxyamphetamine (PMA), and 4-methoxymethylamphetamine (PMMA) were the drugs of interest since they are increasingly prevalent drugs of abuse globally.

The optimisation of the technique and the application of DESI-MS to the analysis of these compounds were demonstrated. A particularly suitable surface, semi-porous polytetrafluoroethylene (PTFE, Teflon) was utilised, as it gave superior signal stability and reproducibility as compared to other surfaces (polymethyl methacrylate (PMMA) and polyvinyl chloride (PVC)).

The limits of detection (LOD) of 4-MMC and the piperazine analogues were determined to range between 0.0023 - 2.30 $\mu\text{g}/\text{mm}^2$. The LOD of the ATS was determined to be in the range 0.02 - 2.80 $\mu\text{g}/\text{mm}^2$. DESI-MS was also utilised in the preliminary analysis of illicit cocaine samples. The LOD of cocaine was determined to be 3.47 $\mu\text{g}/\text{mm}^2$. The chemical profiles obtained using DESI-MS were also compared to two current confirmatory analysis techniques, gas chromatography – mass spectrometry (GC-MS) and liquid chromatography – mass spectrometry (LC-MS). The by-products and impurities detected were used to link samples to their synthetic route of manufacture and to the precursors used. The detection of truxillines in the seized cocaine samples aided in determining their geographical origin.

Selectivity and matrix effects were evaluated for the compounds of interest in each study. The effect of adulterants including caffeine, procaine, levamisole, lignocaine, paracetamol, and atropine on the detectability of cocaine were investigated. The detectability of ATS were evaluated by adding caffeine, paracetamol, magnesium stearate, and dimethyl sulfone. Piperazine compounds were adulterated using caffeine and a mixture of piperazines (TFMPP and BZP) was also evaluated since these are commonly found in combination. 4-MMC was adulterated with caffeine, paracetamol, MA, phentermine, AP, MDMA, 4-hydroxyamphetamine, 4-fluoroamphetamine, nordiazepam, diazepam, oxazepam, cocaine, heroin, methadone, cathine, cathinone, 4-diethylaminobenzaldehyde, 1-benzyl-3-pyrrolidinol, and methylone. In most cases, despite the presence of ion enhancement or suppression due to the addition of adulterant, the analytes remained detectable.

Quantitative experiments for 2 μL spotted solutions of 4-MMC, using codeine- D_6 as an internal standard, introduced in the desorption spray solvent, showed a linear correlation ($R^2 > 0.9840$) over the range 50 – 800 $\mu\text{g}/\text{mL}$. The precision for triplicates analysed on five different days ($n = 15$) was $<38\%$ RSD. The accuracy, expressed as relative error, was $<13\%$. Identification based on accurate mass and MS/MS spectra aided in discriminating compounds with the same molecular formula. The results obtained using DESI-MS demonstrate its applicability in the rapid qualitative analysis (and preliminary quantitative analysis of 4-MMC) of cocaine, 4-MMC, BZP, TFMPP, mCPP, MeOPP and ATS.

Chapter 1:

Introduction

Chapter 1: Introduction

1.1 Prevalent illicit drugs and novel analogues

Recreational use of illicit drugs is a phenomenon that has been apparent for many years. The amphetamine-type substances (ATS) such as amphetamine (AP), methylamphetamine (MA), 3,4-methylenedioxyamphetamine (MDA), and 3,4-methylenedioxymethylamphetamine (MDMA) are particularly popular drugs of abuse^{1,2}. ATS are sometimes collectively referred to as phenethylamines due to their common structural features. According to the United Nations Office on Drugs and Crime (UNODC), ATS are firmly established on the global illicit drug market, with use continuing to exceed that of cocaine and heroin combined³. In Australia, ATS are the second most commonly used illicit drugs, only after cannabis. In East and South-East Asia, as well as in the Middle East, consumption of ATS, particularly MA, is increasing⁴.

The increased demand for ATS continues to drive a highly profitable trade in clandestine ATS production and trafficking. According to the International Narcotics Control Board (INCB), the manufacture and trafficking of ATS is increasing globally, especially throughout the region of South-East Asia, including Myanmar, Cambodia and China³. Compared with other regions in the world such as the United States (US), the number of clandestine laboratory detections in South-East Asia is small. However, most of the detected mega-laboratories have been located in this region, i.e. laboratories producing 1,000 kg or more of drug per production cycle³. Large seizures of ATS products are also prevalent in South-East Asia, including a 745 kg seizure of crystal MA in the Philippines during May 2008 among many other seizures as shown in Appendix 2, Table A-1. The table compiles some of the most significant drug seizure data gathered from various official reports and publications.

The production and use of unusual phenethylamines is sometimes accidental, but is often an intentional response to laws controlling illicit drugs of abuse and/or their precursors⁴. Most of the common phenethylamine drugs – and most of the more popular ones – are illegal, which leads to clandestine laboratories producing these compounds. However, because the laws of many countries that control illicit drugs are specific, new and/or non-regulated drugs occasionally appear on underground markets. As these substances are often specifically

synthesised due to their non-regulated status, they are commonly known as 'designer drugs' or novel drug analogues. However, Australian laws dictate that a substance is a controlled drug if the substance (the drug analogue) is, in relation to a controlled drug a stereoisomer, or a structural isomer (with the same constituent groups) or an alkaloid of such a controlled drug, according to the *Criminal Code Act 1995*, Section 301.9⁵. This suggests that analogues of existing illegal drugs are also considered controlled substances making it difficult to circumvent such laws controlling the production of novel analogues in Australia. In Europe, some examples of novel drug analogues include 4-methylthioamphetamine (4-MTA) and 4-iodo-2,5-dimethoxyphenethylamine (2C-I)⁴.

In addition to ATS and their related novel analogues, piperazine drugs are another group of compounds of high prevalence based on the survey data shown in Appendix 2, Table A-1. Amongst others, the most popular drugs encountered include MA, MDMA, ketamine, pseudoephedrine/ephedrine, and piperazine analogues such as 1- benzylpiperazine (BZP), 3-trifluoromethylphenylpiperazine (TFMPP), 3-chlorophenylpiperazine (mCPP) and 4-methoxyphenylpiperazine (MeOPP).

The misuse of selected synthetic cathinones is also evident from the compiled drug seizure data (Appendix 2, Table A-1). The emergence of six synthetic cathinones in Germany was reported between 1997 and 2004⁶. All six substances bear an α -pyrrolidino functionality and are therefore closely related to pyrovalerone⁶. More recently, there has been an increase in the number of reports of other synthetic cathinones encountered within the European Union. Many of these compounds are simply β -keto analogues of AP, in which the presence of the ketone functionality often circumvents any legislative control measures which may already be in place for the related APs. Of the total number of cathinone derivatives encountered by UK forensic providers, the most commonly encountered is 4-methylmethcathinone (mephedrone or 4-MMC) (89 % of seizures). Intelligence from Australian Customs and Border Protection Service has identified China and the UK as being the principal sources of 4-MMC⁶.

Given the expanding production and use of ATS and other synthetic drugs including piperazines and cathinones globally, illicit use presents a major social problem and health concern. Their availability and potential toxicity illustrates the importance of detecting these compounds and preventing them from being distributed around the globe. One of the more worrying developments in the recent history of clandestine synthetic drugs is that their

production and distribution are increasingly becoming structured, and integrated into international organised criminal activities⁷. This places more importance on the need to police these activities which can be done through a drug intelligence network. Drug profiling is considered the key constituent in drug intelligence. Profiling of drugs provides physical and chemical information that can in turn provide information of the geographical origin or the synthetic pathway of manufacture of the drug. Such information is essential as it can lead to dismantling well-established clandestine laboratories and/or large drug syndicates. Rapid and accurate identification of a large number of drug compounds by modern analytical techniques is becoming increasingly important in assisting law enforcement authorities in fighting drug-related crime.

1.1.1 Amphetamine

Amphetamine (Figure 1-1) is a chiral compound. The racemic mixture can be divided into its optical isomers: *levo*- and *dextro*-AP³. The compound AP is synthetically derived from β -phenethylamine to produce a substance which is similar to both the hormone adrenaline and the naturally occurring stimulant ephedrine (EP). Commercially manufactured varieties of AP are commonly used for therapeutic treatment of conditions such as attention deficit disorder, narcolepsy and obesity. APs are also commonly manufactured in clandestine laboratories for illicit distribution and use³.

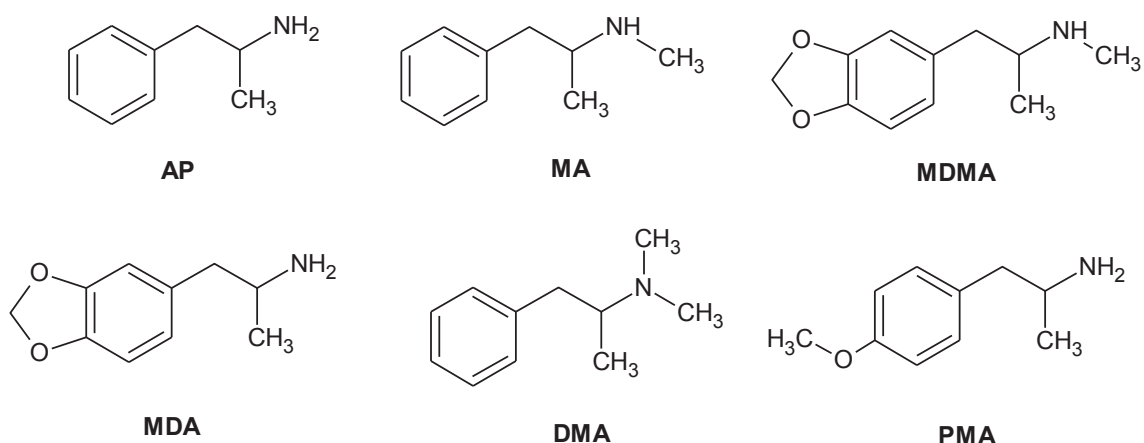


Figure 1-1 Molecular structures of AP, MA, MDMA, MDA, DMA and PMA.

1.1.2 Methylamphetamine

Methylamphetamine is also a chiral compound with two isomeric forms, the *levo*- and *dextro*-MA. MA is structurally similar to AP, through the inclusion of a methyl group to the terminal amine (Figure 1-1), although comparable doses produce more potent and longer lasting effects³. Clandestine laboratories produce two chemical forms of MA, the free base ('MA base') and the hydrochloride salt ('MA HCl'). The free base, which is the initial product of clandestine synthesis, is a liquid at room temperature. The hydrochloride (HCl) salt is produced from the free base by bubbling hydrogen chloride gas through a solution of the free base⁸. Pure MA HCl is a colourless crystalline solid. A common misconception is that MA ('ice') found on the street is pure; however, it is commonly diluted/adulterated with other chemicals.

In Australia, MA is commonly sold in four forms: tablet, powder (also referred to as 'speed'), base (also referred to as 'paste') and crystal (also referred to as 'ice'). While a liquid form of the free base (also referred to as 'oxblood') has been identified, its use and prevalence is uncommon. Methods of administration vary depending on the form consumed, with users able to swallow, snort, inject or smoke the drug. The crystal form of MA is generally considered to be the most potent; in which users typically heat the crystals in a small glass pipe and inhale the vapours³.

1.1.3 3,4-Methylenedioxymethylamphetamine

The most widely known phenethylamine is MDMA, commonly referred to as 'Ecstasy'. MDMA is chemically derived from the addition of a methylenedioxy group at the 3 and 4 positions on the benzene ring of MA (Figure 1-1). Although chemically similar to AP, MDMA is not a derivative of AP and is produced by a distinct chemical process using different precursor compounds. MDMA tablets are usually inscribed and marketed by a symbol/logo from popular culture, such as those from fashion labels (such as Louis Vuitton 'LV') or car manufacturers (such as Mercedes)³.

Drugs marketed as 'Ecstasy' may contain a variety of drugs mixed with MDMA, or may contain no MDMA at all. Tablets have been detected containing various combinations of substances including EP, ketamine, MDA and MA (Appendix 2, Table A-1). This leads to

unpredictable toxicity and effects of these drugs. Associated health risks are further increased when combined with alcohol or other illicit drugs as synergistic effects may be present.

1.1.4 3,4-Methylenedioxyamphetamine

3,4-Methylenedioxyamphetamine is a minor metabolite of the more widely used MDMA but has its own long history as an independently used drug. MDA is chemically derived from the addition of a methylenedioxy group at the 3 and 4 positions on the benzene ring of AP (Figure 1-1). MDA was first synthesised in 1910 and became popular for recreational use in the 1960s. MDA may be incorrectly sold as 'Ecstasy' in tablet form. Some reports indicate that MDA may have more potent effects than MDMA³.

3,4-Methylenedioxyamphetamine is rather unique in that it produces effects that are both AP-like and hallucinogen-like. The AP-like properties of MDA appear to be associated primarily with the *S*-(+)-isomer whereas the *R*-(-)-isomer seems to be more responsible for the hallucinogen-like properties. Distinct structure-activity relationships have been formulated for phenylisopropylamine substances and phenylisopropylamine hallucinogens, for example, for those phenylisopropylamines with central stimulant activity, the *S*-isomers are several times more potent than their *R*-enantiomers. Also, the presence of small alkyl groups on the terminal amine function has relatively little effect on AP-like action but suppresses hallucinogen-like activity⁹.

1.1.5 *N,N*-Dimethylamphetamine

N,N-Dimethylamphetamine (DMA) is an analogue of MA that first appeared in the illicit drug market in the late 1980s¹⁰ (Figure 1-1). DMA is derived from the addition of two methyl groups to the terminal amine of the compound AP. Witkin *et al.*¹¹ established that DMA possesses 10 % the potency of MA. Even when given at behaviourally equivalent doses as MA, DMA lacks both dopamine and serotonin (5-HT) neurotoxic activity¹⁰. This strongly suggests that the neurotoxic and pharmacologic effects of MA and related drugs are independent.

Since the crystalline forms of DMA and MA share similar physical appearance, DMA may be sold to users of MA. Most of the seized DMA samples in Hong Kong were crystalline solids

that were either in the pure form or mixed with MA. Apart from its presence in crystalline solid samples, DMA has also been found in tablets, sold as 'Ecstasy'. Like 'Ecstasy', these tablets were different in colour and markings and usually mixed with various abused drugs including MDMA, MDA, MA and ketamine¹².

1.1.6 4-Methoxyamphetamine

4-Methoxyamphetamine (PMA) is an analogue of AP that first appeared in the early 1970s (Figure 1-1). It is occasionally identified in tablets marketed as 'Ecstasy'. It is commonly synthesised from anethole (from anise and fennel), mainly due to the limited availability of safrole due to tighter restrictions on its distribution. PMA was intentionally used as a substitute for the hallucinogen lysergic acid diethylamide (LSD). There have been a number of deaths around the world associated with PMA, several of which occurred in Australia in the mid-1990s¹³⁻¹⁸.

1.1.7 Cocaine

Cocaine, also known as benzoylecgonine, is a crystalline tropane alkaloid that is extracted from the leaves of the coca plant (naturally derived as opposed to synthesised ATS). Most research suggests that cocaine is the second most problematic drug world-wide in terms of negative health effects and the most problematic in terms of trafficking-related violence¹⁹. There are three main regions worldwide for cocaine cultivation namely Bolivia, Peru and Colombia¹⁹. Cocaine differs from common synthetic ATS in that it is a naturally derived compound. Profiling cocaine commonly involves chemical and physical profiling which is used to determine the geographical origin of the drug (Figure 1-2).

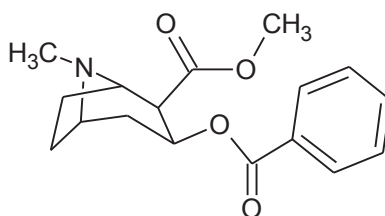


Figure 1-2 Molecular structure of cocaine.

1.1.8 Drug analogues

The principle of modifying the chemical structure of a well-characterised parent molecule is a basic concept in modern pharmaceutical research and industrial manufacture which could potentially be replicated by ‘cooks’ in clandestine laboratories⁷.

The most common way for the construction of a modified ‘designer drug’ is the introduction of a *N*-alkyl substituent of a different size into the molecule of a parent drug of known activity^{20, 21}. Consequently, a number of MDA homologues, such as MDMA, methylenedioxyethylamphetamine (MDEA), *N,N*-dimethyl-4,5-methylenedioxyamphetamine, *N*-propyl-3,4-methylenedioxyamphetamine and *N*-isopropyl-3,4-methylenedioxyamphetamine were synthesised and introduced into the illicit drug market. In addition, the modification of PMA to its *N*-methyl-homologue, 4-methoxymethylamphetamine (PMMA), has been performed several years ago. The presence of *N*-ethyl-4-methoxyamphetamine has also been identified in illicit samples in the US²⁰.

An *N*-hydroxy analogue of MDMA, *N*-hydroxy MDMA, has recently been distributed as a new drug analogue in some drug markets²². The *N*-hydroxy group has been found to have unique analytical properties in similar compounds such as *N*-hydroxy-3,4-methylenedioxyamphetamine.

Although not specifically related to the more common ATS, dimethylamylamine (DMAA, methylhexanamine) is a stimulant that functions very similar to caffeine. DMAA is commonly found in pre-workout supplements such as “Jack3d” and has been abused by many professional athletes. In 2012, DMAA was classified as a “highly dangerous substance” in the *NSW Poisons List* and was banned from use²³. Other products that have been found to contain DMAA include Noxpump, Presurge, OxyELITE Pro, 3-D Explosion, 1 MR, Mesomorph, Hemo Rage Black, Beta-Cret, Cryoschock, Neurocore and White Lightning.

1.1.8.1 Piperazine analogues

1-Benzylpiperazine (BZP) and related active ingredients of some recently encountered ‘party pills’ such as TFMPP, mCPP, 4-methoxyphenylpiperazine (MeOPP), and 3-fluorophenylpiperazine (FPP), are used extensively as recreational drugs globally despite their prohibition in several countries²⁴ (Figure 1-3).

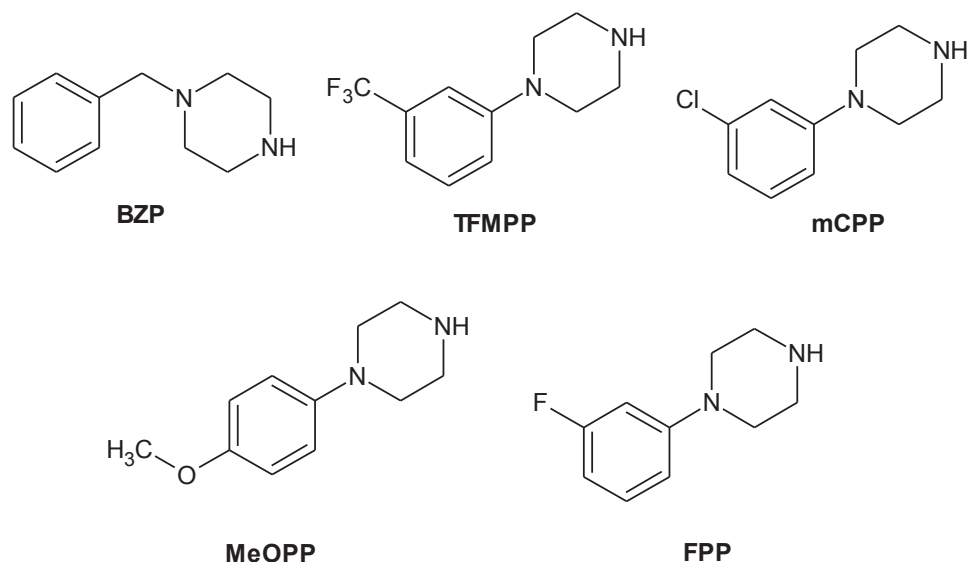


Figure 1-3 Molecular structures of BZP, TFMP, mCPP, MeOPP, and FPP.

These piperazines became known as drugs of abuse in the UK during early 2008. A few non-fatal and fatal cases where BZP has been reported, typically involve other drugs. However, toxicity involving BZP alone has also been reported²⁵. In the UK, the presence of BZP and TFMP have been confirmed in three fatalities (road traffic deaths and a fatal fall off a building), with two of these involving both drugs^{25, 26}.

Research has shown that drug users are ingesting piperazine analogues, like BZP and TFMP, in order to mimic the psychoactive effects of MDMA²⁷. In a study conducted by Baumann *et al.*²⁷, it was demonstrated that BZP/TFMP and MDMA share the ability to evoke monoamine release, but dangerous drug synergism may occur when piperazines are co-administered in high doses.

3-Trifluoromethylphenylpiperazine, mCPP, and MeOPP have structural isomers relating to substitution at the 2-, 3-, and 4- positions relating to *ortho*-, *meta*-, and *para*- respectively. The existence of structural isomers of TFMP and mCPP can complicate identification of these piperazines²⁸.

1.1.8.2 Cathinone analogues

The misuse of selected synthetic cathinones is not new; methcathinone (ephedrone), originally used as an antidepressant in the 1930s, went on to be used recreationally in the

Netherlands and in the US during the period 1970s to 1990s⁶. Methylone was found in street drugs in the Netherlands in 2004²⁹. Methylone (3,4-methylenedioxyamfetamine) is the main ingredient of a new liquid drug analogue that appeared on the Dutch drug market, called 'Explosion'. The subjective effects of methylone exhibit subtle differences with those of MDMA.

Cathinone is structurally related to methcathinone, in much the same way as AP is related to MA. Cathinone differs from AP by possessing a ketone oxygen atom (C=O) on the β (beta) position of the side chain (Figure 1-4).

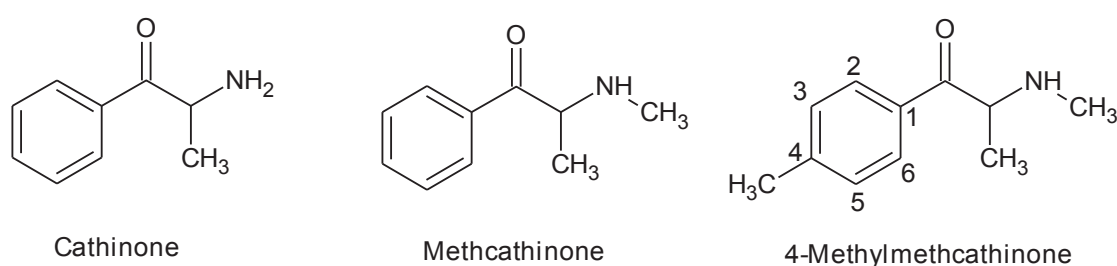


Figure 1-4 Molecular structure of cathinone, methcathinone and 4-MMC.

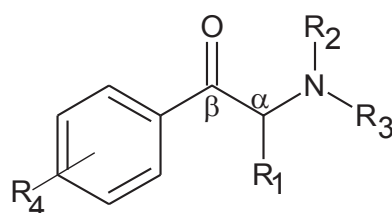


Figure 1-5 Generic sites for structural variation of cathinone⁶.

The molecular structure of cathinone can be altered to produce a series of analogues⁶ (Figure 1-5). The inclusion of additional functionality on the aromatic ring (ring substitution, R^4), *N*-alkylation (or inclusion of the nitrogen atom in a ring structure, R^2 and R^3), and variation of the (typically alkyl) α -carbon substituent (R^1) is one such example. More recently, there has been an increase in the number of reports of other synthetic cathinones encountered globally. Many of these compounds are simply β -keto analogues of APs, in which the presence of the ketone functionality often circumvents any legislative control measures which may already be in place for the related APs^{6, 30-47}.

Cathinone can be extracted from *Catha edulis*, or synthesised from α -bromopropiophenone (which is easily made from propiophenone; section 2.2.2). The synthesis of these materials is relatively simple. Even the chiral synthesis of these materials has been reported using amino acids as precursors which does not appear to be a challenge to someone with a basic chemistry knowledge⁴⁸. The ease of preparation has contributed to the increasing reports of cathinone analogue synthesis. Despite being a restricted substance, methcathinone seems to be quite popular due to its ease of synthesis from ephedrine via an oxidation reaction⁶.

Dal Cason *et al.*⁴⁹ conducted a study on several *N*-alkyl and methylenedioxy-substituted analogues and found that both optical isomers of methcathinone are active but that *S*-(-)-methcathinone is three to five times more potent than *R*-(+)-methcathinone.

Cathinones are usually advertised as being of 'high purity', typically >95 %. Some adulterants, including benzocaine, lignocaine, caffeine and paracetamol, have been detected in a small proportion of seizures of the cathinones⁶. Some have also been adulterated with controlled drugs such as cocaine, ketamine, AP and BZP, although these are rarely encountered. The compound 3-fluoromethcathinone has also been identified in capsules marketed as plant food available from internet suppliers in the UK⁴⁸.

1.2 Drug intelligence/profiling

A term frequently used in the context of law enforcement is 'intelligence' which, in a forensic perspective, is taken to refer to the timely, accurate and usable product of logically processed forensic case data⁵⁰. The purpose of such an exercise is to learn as much as possible about the subject being 'profiled' and then use that information for intelligence. In the case of drug profiling, chemical and physical information about the drug is collected in order to assist law enforcement agencies by identifying drug trafficking organisations, and disrupting or eliminating their activities⁵¹.

In drug-related criminal proceedings, evidence is commonly given as to the identity of the drug and its purity. Determining whether a suspect sample contains illicit substances is well established⁵¹. However, this provides little source information such as where the drug originated from and which drug-trafficking organisation transported the drug to its current state of possession.

In most cases, synthetic drugs possess an individual chemical make-up (batch-to-batch variation may occur). Unlike legitimate drug production, clandestine facilities in which drugs are manufactured have no quality control, suggesting that the quality of the product is highly variable. Chemical analysis of AP, MA and 'Ecstasy' produced in clandestine laboratories will generally identify by-products and/or impurities indicative of the synthetic route and precursors used. This provides useful information for government agencies attempting to control industrial chemicals that may be diverted to illicit drug production⁵¹. In addition, seized drugs often contain adulterants (or diluents), which may be added at various stages during the distribution chain, subsequent to drug manufacture. These also may be characteristic of individual drug seizures.

More recently, trace element analyses and stable isotope analyses have increased the confidence of geographical sourcing. Increasingly, sophisticated pattern recognition techniques have been employed to process the enormous databases generated by source determination programs. In the past, processing origin could be reasonably correlated with geographical origin by employing analysis techniques; however, the expansion of drug producing regions and the concomitant convergence of processing techniques, have mandated more sophisticated analyses^{50, 52}.

With the increased interest from law enforcement in the trade and distribution of precursor materials, it should be expected that clandestine drug laboratory 'cooks' will look for manufacturing methods that utilise chemicals that are not regulated by legislation⁵³. Clandestine drug laboratories involved in the production of illicit drugs pose a significant social challenge in most societies. Many clandestine drug laboratories are temporary and are capable of producing large quantities of prohibited drugs in production cycles that can often span less than 48 hours, making timely discovery essential. Different manufacturing processes are said to have unique temporal chemical signatures and it is possible that this signature can be used to distinguish a MA laboratory from other legitimate sources of chemical production.

A few limitations with profiling illicit drugs may arise as a result of their manufacture. Clandestine laboratories may produce substances of high purity such that very few (if any) impurities remain. Further, comparisons based on impurity profiling are often not sufficiently

conclusive due to difficulty in achieving reproducible chromatograms as a result of low level impurities⁵⁴.

Australian efforts in drug profiling are comparatively recent. Following research and development work between 1991 and 1995 the National Heroin Signature Program (NHSP) was established in 1997⁵¹ as a collaborative project between the Australian Federal Police (AFP) and the Australian Government Analytical Laboratories (AGAL). The NHSP was born of the Prime Minister's 'Tough on Drugs' policy and was the country's first attempt at drug profiling. Heroin was the focus of the program due to its contribution to health issues and drug related crime.

In 2003, the NHSP was expanded to become the Australian Illicit Drug Intelligence Program (AIDIP)⁵¹. The objective of the AIDIP was to consolidate work completed on heroin and expand into other major drug types. The AIDIP developed signature programmes for heroin, cocaine and the ATS such as MA and MDMA. The AIDIP has two major arms to it: chemical profiling and physical profiling, which are designed to complement each other. Chemical profiling involves an in depth chemical analysis of the drugs to provide information that may complement intelligence previously acquired by law enforcement. To chemically profile illicit drugs, AIDIP utilises the National Measurement Institute (NMI), and while it remains the only routine drug profiling program within Australia, it networks with other similar initiatives in overseas jurisdictions to track and comprehend trends.

Strategic intelligence relates to information of the geographical origin of cultivated or semi-cultivated drugs and the methods of preparation of the fully synthetic drugs. Tactical intelligence relates to information which can be provided to law enforcement agencies to assist in creating or confirming links between drug seizures or drug syndicates. Chemical profiling attempts to provide strategic and tactical intelligence. Physical profiling refers to the physical properties of a drug (tablet) including characteristics such as diameter, thickness and weight⁵¹.

1.3 Drug analysis techniques

1.3.1 Current preliminary identification techniques

There is a definite need for a simple, rapid and reliable means of drug detection and analysis. Traditional colour tests with specific reagents are still predominately used as a first step for screening of suspected seizures⁵⁵. The Marquis and Simon's tests are widely used for on-site testing of 'Ecstasy'. Although the test is very simple and inexpensive, the diversity of drugs makes it difficult to evaluate the results leading to false positive and false negative results, i.e. they lack selectivity⁵⁶. In addition, the actual colours observed by an analyst depend on many factors, such as drug concentration, the presence of contaminants in the tablets and the subjective colour discrimination of the analyst.

Portable Fourier Transform Infrared (FTIR) spectrometers have also been developed for on-site screening of hazardous materials and drugs. These instruments generate attenuated total reflection (ATR) infrared (IR) spectra simply by bringing the sample into contact with the diamond internal reflection element⁵⁷. There have been reports that suggest that IR spectroscopy provides a higher level of discriminating power than does a colour test⁵⁷. However, built-in spectral libraries for pure compounds may not be useful for the identification of 'Ecstasy' tablets (and other drug mixtures), which usually contain diluents and adulterants, in addition to controlled drugs.

Current methods for the preliminary identification of suspected border controlled substances suffer from one or more problems including a potential for false positives, poor sensitivity, poor specificity and limitations in identifying novel substances. Furthermore analysis can be time consuming and often performs poorly with samples that contain mixtures of compounds (e.g. tablets or powders with diluents, adulterants and cutting agents).

1.3.2 Current confirmatory analysis techniques

Some techniques which are currently used for high-throughput analysis and also help to prevent false positives and false negative results include near-infrared reflectance spectroscopy, ultraviolet (UV)-visible absorption spectroscopy, fluorescence spectroscopy, and to a lesser extent, mass spectrometry (MS)⁵⁸. Raman, FTIR, and near-IR spectroscopies

have the ability to provide high-throughput analysis without the need for prior sample preparation⁵⁸. These techniques provide useful, however somewhat limited information on the chemical composition of pharmaceuticals in a non-destructive fashion as they are best suited for uncut or pure samples⁵⁸. Thin-layer chromatography (TLC) has also been used in the past for the separation and identification of reaction components or drug mixtures. Unfortunately, TLC is temperature dependant with changes in selectivity observed with temperature fluctuations. Other techniques like nuclear quadrupole resonance also show promise as a non-destructive analysis technique⁵⁹.

In the past, impurity profiling of synthetic drugs has mainly utilised gas chromatography (GC), with a range of detectors used including flame ionisation detector and mass spectrometers. For gas chromatography – mass spectrometry (GC-MS), large spectral libraries have been developed, making the method suitable for the analysis of unknown samples. Alternative methods such as high-performance liquid chromatography (HPLC) have also been applied⁶⁰.

The GC-MS technique has been the method of choice for the analysis of drug impurities in forensic science but only volatile components can be successfully analysed⁶⁰. In addition, lengthy derivitisation procedures might be required to increase the selectivity of the technique. Since some impurities are non-volatile, they will not be detected using GC-MS in which case liquid chromatography (LC) coupled to ultraviolet-diode array detector (UV-DAD) or a MS detector can be used. The use of liquid chromatography-mass spectrometry (LC-MS) techniques has made it possible for laboratories to include more substances in routine testing than was possible with GC-MS alone.

1.3.3 Quantification of drug compounds

In the past, high-throughput applications have not been well developed using MS techniques since they have traditionally involved considerable sample manipulation including extraction and chromatographic separation. However, this is changing with the use of automated sample-handling equipment and the beginning of multiplexed (MUX) instruments⁵⁸. The MUX technology meets these demands by multiplexing four sample streams into a single MS. By coupling parallel LC analyses with electrospray MS, accelerated compound screening is made possible⁵⁸. This technique works by multiplexing the separation phase but not the mass analysis step. This approach works well when analysis rates are limited, not by the MS, but by

either the chromatography step or the sample introduction process. Multiple nano LC columns have been combined with an electrospray chip in an attempt to combat current demands for MS and lab-on-a-chip technologies. A high-density electrospray ionisation (ESI) chip with 400 nanoelectrospray nozzles has been shown to provide high-throughput analysis of protein samples⁵⁸. ESI or atmospheric pressure photoionisation (APPI) are employed to transfer analytes from the liquid phase into the form of gas-phase ions which can be analysed and detected. Selectivity and sensitivity can be improved by tandem mass spectrometry (MS/MS). Mass spectrometers such as ion traps (IT) or triple quadrupoles (QqQ) can quantify levels down to a few picograms per millilitre. Mass analysis and detection is achieved in milliseconds, so the limiting factor in terms of analysis time is the slower process of LC separation. In an attempt to decrease or eliminate separation times, non-chromatographic techniques have increasingly received attention, evident in the increasing use of matrix-assisted laser desorption ionisation (MALDI) systems to perform quantification. Two limitations of this technique, strong matrix interference in the low molecular mass range ($m/z < 500$) and poor reproducibility of signal intensities, appear to be resolved by the use of MS/MS and averaging multiple analyses of the same spot using appropriate internal standards (IS)⁶¹. Quantitative analysis requires method validation which includes evaluating linearity, precision, and accuracy (both intra-day and inter-day)⁶².

1.3.4 Atmospheric pressure ionisation techniques

Mass spectrometry has many advantages of sensitivity, specificity, and general applicability, but is limited by requirements for sample preparation, principally those associated with the fact that the samples must be introduced into a vacuum system for analysis. A significant advance was provided by the introduction of atmospheric pressure ionisation (API) methods, such as AP-MALDI, and the more recent method matrix-assisted laser desorption electrospray ionisation (MALDESI)⁶³. These techniques allow for the direct analysis of condensed phase samples, although there are some sample preparation requirements. Desorption electrospray ionisation (DESI) and the related methods of direct analysis in real time (DART), desorption atmospheric pressure chemical ionisation, atmospheric solids analysis probe (ASAP), and electrospray-assisted laser desorption ionisation (ELDI), remove the requirements for sample preparation^{63, 64}.

Steiner *et al.* validated the use of DART coupled to a quadrupole time-of-flight mass spectrometer (QTOF)-MS for the rapid screening of forensic evidence for drugs of abuse⁶⁵. With respect to using the accurate time-of-flight (AccuTOF)-DART as a screening tool, the spectra generated with this instrument were much richer in detail than the information typically obtained from a GC-MS instrument. The AccuTOF-DART and other similar ionisation techniques, such as DESI, are able to simultaneously detect many more compounds than GC-MS since ionisation is of entire mixtures and is not encumbered by the limitations caused by temperature and time constraints on the GC-MS instrument runs. GC-MS runs are typically limited to specific oven temperature ranges in order to reduce the amount of time per run and thereby increase sample throughput. In addition, some minor compounds which were able to be seen using the AccuTOF-DART were not seen at all in the GC-MS analysis conducted by Steiner *et al.*⁶⁵

Desorption atmospheric pressure photoionisation (DAPPI) is a new technique that has recently joined the group of direct ionisation techniques. The sensitivity of DAPPI has shown to be similar to that of DESI when analysing polar analytes and better when analysing non-polar analytes⁶⁶. The feasibility of DAPPI in the direct analysis of illicit drugs was demonstrated by Kauppila *et al.*⁶⁶ MDMA, AP, phenazepam, and buprenorphine were detected from the analysed tablets, LSD and bromobenzodifuranylisopropylamine (bromo-Dragonfly, ABDF) from blotter paper, and Δ^9 -tetrahydrocannabinol (THC) from *Cannabis Sativa* bloom and resin.

Ion mobility spectrometry has also been used for the detection of illicit drugs in seized samples. The use of flow-injection (FI) data-dependent MS/MS combined with an automated library search has been reported for the identification of pharmacologically active compounds in tablets and tablet residues⁶⁷. FI is one of the simplest forms of rapid sample introduction into the MS, and is widely used for the analysis of new chemical entities for pharmaceutical discovery. One major disadvantage of FI-MS is ion suppression due to co-eluting sample components. Twelve samples contained compounds only detectable in positive ion mode (sildenafil, dihydrocodeine, diphenhydramine, oxprenolol, *N*-methyl-3,4-methylenedioxyamphetamine, morphine, amphetamine, caffeine, pemoline, orphenadrine, mCPP and tramadol), six samples contained species exclusively detectable in negative ion mode (salicylic acid, acetylsalicylic acid, ibuprofen, ketorolac, valproic acid and phenobarbital), and three samples contained diclofenac detectable in both ionisation

modes⁶⁷. A total of 22 casework samples were screened with the technique enabling the detection of specific substances of diverse chemical properties.

It is apparent that over the past twenty years, the commercial availability of atmospheric pressure ionisation sources, such as ESI, has given greater flexibility within MS analysis, and has overcome a number of limitations related to the prepared sample and its introduction into the MS vacuum system⁶⁸. The introduction of such techniques is a significant step forward in the development of high-throughput analysis protocols. Their application to the analysis of forensic samples could have a great impact on the quantity and quality of data generated by forensic chemists, especially during the rapid screening of illicit substances.

1.4 Database and library compound matching

Compound databases allow screening of compounds via the use of accurate masses. While accurate mass is a good indicator of the presence of a compound, it is prone to false positives. For this reason, accurate-mass databases should include a MS/MS library that provides more certainty in the compound match. For screening analyses, the MS/MS spectra can reduce or eliminate false positives and give much greater confidence in the identification of a drug. However, to make practical use of these spectra, a large, searchable library of quality spectra collected under well-defined and reproducible conditions is required.

The Agilent MassHunter Personal Compound Database and Library (PCDL) software allows the user to create, edit, and search accurate-mass databases and MS/MS libraries. The software enables MS/MS matching (score out of 100) based on the spectra in the database (over 6700 compounds). This database facilitated the identification of novel and illicit drug compounds in this study.

1.5 Desorption electrospray ionisation – mass spectrometry

Desorption electrospray ionisation, developed in the laboratory of Professor R. Graham Cooks at Purdue University and now commercialised by Prosolia™, Inc., is considered one of the principal methods amongst the family of API techniques.

Desorption electrospray ionisation is a very useful technique as it allows MS to be used for on-line high-throughput monitoring of pharmaceutical and illicit drug samples in the ambient environment, without the need for prior sample preparation^{58, 69}. Using this technique, ions can be generated directly from solid surfaces of various types. The pneumatically assisted electrospray is used to direct ionised solvent droplets and molecules onto a surface bearing the sample (Figure 1-6). The application area of DESI mirrors that of MALDI⁵⁸; however, DESI does not require prior surface modification such as application of matrix compounds, hence it can be applied to the interrogation of ordinary surfaces. The samples can be analysed either directly or after deposition onto a surface⁷⁰. The interface of the DESI with a MS detector allows for the identification of charged species, providing molecular mass and structural information⁷⁰.

Desorption electrospray ionisation – mass spectrometry can be used first as a rapid qualitative screening tool, before complementary analyses are undertaken, if needed. It must be pointed out that a consequence of ‘rapid’ can be that no desorption occurs or it can cause lower concentration analytes to be missed. A longer desorption is in some cases required to perform an exhaustive desorption^{56, 71}.

THIS FIGURE IS EXCLUDED DUE TO COPY RIGHT

Figure 1-6 DESI source and moving stage used to position the source⁷².

1.5.1 Mechanisms involved in DESI-MS

The ion formation process during DESI-MS has been suggested to consist of at least three possible mechanisms⁷⁰. The first involves charge transfer between gaseous ions formed from the electrospray source and the analyte compound on the surface. Desorption of the analyte ions from the surface is thought to occur by a type of chemical sputtering⁷². The second mechanism (droplet pickup) involves impact of the electrosprayed droplets on the surface, dissolution of the analyte into the liquid deposited in the region of the surface impacted by the electrospray, followed by subsequent splashing of the liquid film by incoming droplets generating secondary droplets that carry the analyte. Subsequent evaporation of the solvent and Coulomb fission generates ions by processes that parallel those that occur in conventional ESI. The third mechanism of ion formation involves volatilisation/desorption of neutral species from the surface followed by gas-phase ionisation through proton/electron transfer or other ion/molecule reactions at atmospheric pressure. Transport of these analyte ions to the MS may be facilitated by momentum transfer in the course of the gaseous ion/charged microdroplet impact on the molecular species on the surface, or suction of the vacuum at the inlet of the transfer capillary⁷².

Weston *et al.*⁶⁸ recently performed a number of experiments and simulations to elucidate how the resulting droplets are formed by DESI and transported to the MS. Their study showed that surface wetting by the spray plume led to the formation of a thin film on the sample surface, affecting extraction of the condensed-phase analyte into the surface film, a process which has been shown to be subject to a 'solvation delay', which is the time taken to wet and then extract from the sample surface⁶⁸. Subsequent momentum transfer from impacting droplets and nebulisation gas provided the energy needed to form product droplets and transport them towards the MS inlet (Figure 1-7), with some selectivity being offered by manipulation of spray angles and distances. In addition, this study largely ruled out significant contribution to droplet formation and transport by electrostatic forces or spray voltage⁶⁸.

THIS FIGURE IS EXCLUDED DUE TO COPY RIGHT

Figure 1-7 Simulation of the DESI process showing the formation of dozens of microdroplets resulting from a single droplet-thin film collision event⁷³.

1.5.2 Important parameters

A unique feature of DESI-MS compared to other ambient MS ionisation methods is the ability to tailor the spray solvent for specific analytes as this can dramatically affect the signal intensity of some compounds. For trace analysis of agrochemicals, several spray solvent systems have been investigated⁷⁴. They included different ratios of methanol, water, and acetonitrile including the addition of formic acid to promote the protonation of the target compounds, all used in the positive ion mode. Optimisation of the solvent spray led to the use of acetonitrile/water (80:20) (v/v), with 1 % formic acid in a study conducted by Gracia-Reyes *et al.*^{58, 74, 75}

Badu-Tawiah *et al.*⁷⁵ have demonstrated the use of non-aqueous solvents in DESI-MS by analysing a set of 43 compounds using binary mixtures of chloroform, tetrahydrofuran, and acetonitrile as the spray solvent. From the data obtained it was evident that non-aqueous solvent systems have practical value for DESI, especially in the analysis of hydrophobic compounds. Non-aqueous mixtures include chloroform: tetrahydrofuran (50:50) and chloroform: acetonitrile (50:50) as spray solvents.

Solvent choice greatly affects the DESI ionisation efficiency, which is expected given that the solvent is responsible for dissolution. A few important factors have been well developed including the fact that methanol/water is a standard solvent for many polar molecules, both in the positive and negative ion modes; the fact that addition of small amounts of acid favours positive ion formation and the fact that a correlation exists between the solubility of a compound in a particular solvent and the success of that solvent in DESI⁷³. In the negative

ion mode ammonium hydroxide (0.1 %) has been used to favour deprotonation reactions⁷⁶. The use of an entirely aqueous solvent has been observed to enhance the signal of polar analytes, such as benzodiazepines, while the use of a spray solvent with a high organic content increases the signal of less polar analytes such as codeine and morphine⁷⁵.

A large number of parameters can affect DESI-MS performance⁷⁷. The geometric parameters of most importance include (α , β , d_1 , d_2 , d_3)⁶⁸ (Figure 1-8), spray parameters (gas and liquid flow rates, spray high voltage), chemical parameters (sprayed solvent, solvent used for deposition of sample), and surface parameters (composition, temperature, potential)⁷⁸. With regard to geometric parameters, α and d_1 have direct effects on the ionisation process, while the remaining parameters have important effects on the collection efficiency and, hence on the sensitivity of the method. The optimal setting is approximately 60° for α , $5 - 10^\circ$ for β , $1.5 - 2$ mm for d_1 , $1 - 2$ mm for d_2 , and ~ 5 mm for d_3 ⁷⁸. The dependence of signal intensity on the parameters α and d_1 is shown in Figure 1-9.

THIS FIGURE IS EXCLUDED DUE TO COPY RIGHT

Figure 1-8 Schematic showing DESI parameters requiring optimisation⁷⁹.

THIS FIGURE IS EXCLUDED DUE TO COPY RIGHT

Figure 1-9 Dependence of signal intensity on the spray position at various impact angles from normal⁷⁸.

Spray parameters also influence the spectral characteristics of DESI-MS. These parameters determine the size distribution, average charging, and velocity of impacting droplets and ions⁷⁸. Interestingly, the signal intensity does not drop to zero in the absence of an electrospray high voltage. Analytes that are ionised by different mechanisms of ionisation in DESI appear to have different optimal geometric parameter values. As a general guide, small drug molecules (such as caffeine and steroids) exhibit one set of optimal conditions, i.e. larger d_2 and smaller α value; whereas large compounds (such as proteins and peptides) require a different set of optimal conditions for ionisation, i.e. smaller d_2 and larger α value⁷⁸.

The gas flow rate has a dual role in DESI as reported by Takats *et al.*⁷⁸ High gas flow rates decrease the initial droplet size and increase the velocity of impacting droplets. These phenomena are advantageous up to a point because smaller droplet sizes favour enhanced desolvation efficiency and droplets having higher velocity produce more offspring droplets upon impact⁷⁸. However, above a certain limit the small size and high velocity will cause droplet evaporation before impact with the surface, a result that happens to correlate with the lack of ion formation in the case of peptides and proteins.

Solvent flow rate is also expected to have an effect on droplet size distribution and on the average charge carried by the droplets. At low solvent flow rates, the droplet size may be too small for survival of the droplets from the spray tip to the surface, a phenomenon similar to that described in the case of high gas flow rates. High solvent flow rates result in the formation of larger droplets, which might cause inefficient desolvation and accumulation of liquid on the surface. These constraints define a clear optimal working range of solvent flow rates⁷⁸.

Increased signal intensity has been observed at increased capillary temperatures⁵⁸. Increased signal at higher temperatures may be due to more efficient desolvation. However, higher temperatures also increase the chance of thermal degradation and gas-phase ion fragmentation. The use of high capillary temperatures contributes toward eliminating memory effects. However, at very high temperature, fragmentation takes place and some signal intensity is lost for the molecular ion, thereby reducing sensitivity. It is important to note that the optimum conditions for low carryover are not the same as those that are optimal for high sensitivity and a balance has to be maintained between these two conditions. If the DESI-MS mechanism responsible for carryover involves a droplet-surface interaction, the problem can be reduced by avoiding the introduction of droplets into the heated capillary⁵⁸. Optimally, the DESI-MS ion source should produce droplets that are large enough to hit the surface, but the droplets leaving the surface should be sufficiently small in order to undergo complete evaporation before entering the heated capillary. Parameters determining droplet size (solvent flow rate, gas inlet pressure) are thus optimum (to avoid carryover) when the droplets are just large enough to cause ionisation⁵⁸.

1.5.3 Applications of DESI-MS

An assessment of the papers published since the development of DESI by the Cooks group⁸⁰⁻⁸² demonstrates the broad utilisation and applicability of this technique. A diverse range of analytes, from small drug molecules to large protein molecules have been analysed using this technique. DESI is inherently easy to incorporate into any MS system, where often little modification of existing MS hardware is required. The appearance of commercial DESI sources, made this technique amenable to incorporation into industrial settings. Due to its speed, and ease of use, DESI-MS is becoming a useful tool in a wide variety of applications such as the analysis of pharmaceuticals, intact bacteria, tissues, lipids, urine, drugs of abuse,

steroids, explosives, chemical warfare agents, and agricultural chemicals^{74, 83}. DESI-MS seems to be particularly promising for forensic and public-safety applications, including the analysis of dried blood, detection of explosives, and monitoring chemical warfare agents as illustrated by Takats *et al.*⁷⁷

Illicit substances such as marijuana, opium, gamma-hydroxybutyric acid (GHB)/ gamma-butyrolactone mixtures and other licit substances have successfully been analysed using DESI-MS to produce characteristic ions confirming the presence of licit or illicit substance⁷¹. Leuthold *et al.* demonstrated the use of a home-made DESI source coupled to a triple quadrupole MS. Twenty-one commercial drugs as well as some illicit 'Ecstasy' tablets and powders were analysed⁶⁰. Mass spectra commonly showed the protonated (positive ion mode) or deprotonated (negative ion mode) ion of the drug after directing the pneumatically assisted electrospray onto the tablet's surface. Directly triggered MS/MS spectra were used for confirmatory analysis, with analysis times often below 10 s per tablet⁶⁰. For the analysis of 'Ecstasy' tablets, DESI-MS, GC-MS and LC-MS provided similar qualitative results for the main analytes⁶⁰.

Nyadong *et al.*⁸⁴ presented competitive host-guest chemistry on a DESI-MS platform as the basis for a rapid and quantitative screening method for assessing the quality of Tamiflu[®] capsules with minimal sample preparation. Oseltamivir, the active ingredient in Tamiflu[®] is an orally active neuraminidase inhibitor antiviral⁸⁴. The high cost and demand for this drug has made it a target for counterfeiters, prompting the development of a rapid and sensitive tool for Tamiflu[®] authentication. The method applied in this study focused on the selective recognition of oseltamivir by crown ethers added to the DESI-MS spray solvent. Competitive experiments with various pairs of crown ethers were used to assess the relative binding selectivities for oseltamivir. These competitive reactions formed the basis for rapid quantification of oseltamivir by reactive DESI-MS without the need for an IS.

Kaupila *et al.*⁷⁶ used DESI-MS for the screening of urine samples, obtained from drug abusers, for the presence of drugs of abuse and their metabolites. The detected analyte classes included APs, opiates, cannabinoids and benzodiazepines.

The DESI-MS technique has been successfully applied to the rapid, in situ, direct qualitative and quantitative (ultra)trace analysis of agrochemicals in foodstuffs such as fruits and

vegetables^{74, 85}. The results obtained correlated well with those obtained by LC-MS, and the sensitivity achieved using DESI-MS was adequate for the analysis of 16 representative agrochemicals in a variety of types of samples. Ion suppression due to matrix effects, which are common in electrospray MS, were observed but were circumvented with appropriate dilutions⁷⁴.

In an experiment conducted by Takats *et al.*⁷⁷, the explosive trinitrohexahydro-1,3,5-triazine (RDX) was desorbed from an insulating tanned leather surface, in negative ion mode, to give a characteristic collision induced dissociation of $[\text{RDX} + \text{TFA}]^-$ ($334 > 112$). In the second experiment, nitrile gloves were exposed for less than 1 s to dimethyl methylphosphonate (DMMP) vapours and gave a mass spectrum that distinctly indicated the presence of trace levels of DMMP⁷⁷.

The DESI-MS technique can be applied to the spatial analysis of native surfaces, such as plant or animal tissues⁷⁷. The potential for this type of application is illustrated by the DESI analysis of a seed section of the poison hemlock. A peak was observed indicative of coniceine, which is known to be present in this particular plant species. Similarly, DESI-MS was applied to the analysis of tomato skin, which also indicates the localisation of characteristic compounds, including lycopene. DESI-MS has also been applied to the *in vivo* sampling of living tissue surfaces. An aqueous-alcohol spray was directed onto the finger of a person who had taken 10 mg of the over-the-counter antihistamine Loratadine. Approximately 40 minutes after ingestion, the molecule was detected directly on the skin or in saliva with surface concentrations remaining above the limit of detection (LOD) for a subsequent 50 minutes⁷⁷.

The DESI-MS has also been employed in the forensic analysis of documents⁸⁶, allowing the examination of blue ballpoint pen inks applied to ordinary writing paper under ambient conditions without any prior sample preparation. The recent development of chemical imaging methods based on DESI (imaging DESI) has allowed two-dimensional chemical mapping of samples⁸⁶. Van Berkel and Kertesz reported a practical application of DESI imaging for rhodamine dyes separated on a TLC plate⁸⁷. Their studies found a spatial resolution of at least 400 μm and similar lateral resolution. Successful mapping of lipid distributions in microtome sections of rat brain represent another application of DESI chemical imaging⁸⁸.

Zhao *et al.*⁸⁹ reported a direct and sensitive DESI-MS/MS method for the detection of methyl centralite (MC) and ethyl centralite (EC) in gunshot residues (GSRs). The most commonly detected organic GSRs include propellants such as nitrocellulose and nitroglycerine, and the stabilisers include EC and MC as well as diphenylamine and its nitrated products. One crucial requirement of the analytical method for detecting organic GSRs is high sensitivity. To decrease the detection limits of DESI-MS for the detection of organic GSRs, MS/MS is employed, not only for structure analysis, but also to enhance signal to noise ratio (SNR). Tandem mass spectral methods can significantly reduce interferences and the level of noise⁸⁹. It has been shown that MC and EC can be detected on various surfaces, with detection limits of 5 - 70 pg/cm². In more recent work conducted by Morelato *et al.*⁹⁰, the application of DESI-MS to the detection of MC, EC and diphenylamine on adhesive tape GSR stubs is documented. Their work suggested that subjecting GSR stubs to DESI-MS analysis did not interfere with subsequent scanning electron microscopy – energy dispersive X-ray (SEM-EDX) analysis of primer residues allowing for possible sequencing of techniques.

Hartmanova *et al.*⁹¹ reported the use of desorption nano-electrospray ionisation as a useful tool for the fast recording of profiles of main anthocyanins in wine. The findings suggested that acidification of samples and the addition of formic acid to spray liquid had crucial effects on the improvement of mass spectra by increasing signal intensities. Nano-DESI can be applied to the detection of adulteration of wine by the presence of the unnatural anthocyanins or unusually high amount of some anthocyanin⁹¹. It can also be used for the determination of a ratio of cultivars in their mixture.

Tablets and cream formulations can be analysed using DESI-MS or DAPPI-MS; however, due to the nature of desorption/ionisation methods, powdered samples must be compressed prior to analysis to prevent spreading of the sample⁶⁴. Alternatively, the drug samples can be dissolved in solvent prior to analysis, and analysed both by DESI-MS and DAPPI-MS. Both methods are feasible for the rapid detection of drug compounds and are faster than conventional infusion studies with APPI-MS or ESI-MS. Luosujarvi describes the rapid screening applications for powdered samples of drugs of abuse⁶⁴. The samples analysed include powders of AP, cocaine, heroin, MA, and MDMA, some of which may also contain cutting agents.

Confiscated drugs typically contain varying amounts of cutting agents that may hinder droplet pick-up in DESI-MS; the matrix species may also compete with the analytes for the charge and thus reduce the sensitivity. The general trend is that DESI-MS is better suited for polar and high-proton affinity compounds⁶⁴. Since all the analytes were salts in this study (sulfates or hydrochlorides), it appears that sufficiently high sensitivity is obtained even for analytes in salt form with DESI-MS⁶⁴.

1.5.4 Time-of-Flight - Mass Spectrometry

Time-of-flight - mass spectrometry (TOF-MS) is a method of MS in which ions are accelerated by an electric field of known strength⁹². This acceleration results in an ion having the same kinetic energy as any other ion that has the same charge. The velocity of the ion depends on the m/z ratio. The time that it subsequently takes for the particle to reach a detector at a known distance is measured. This time will depend on the m/z ratio of the particle (heavier particles reach lower speeds). From this time and the known experimental parameters the m/z ratio of the ion is calculated, in turn identifying the compound under analysis⁹².

The Agilent 6500 Series QTOF is a MS that performs MS/MS using a quadrupole, a hexapole collision cell and a time-of-flight portion to produce spectra (Figure 1-10). The quadrupole selects precursor ions that are fragmented in the collision cell into product ions, which are then impelled to the detector, at an angle perpendicular to the original path. The Agilent 6500 Series QTOF LC-MS supports several API sources, including DESI. A common atmospheric sampling interface introduces ions from these various sources into the MS vacuum system.

THIS FIGURE IS EXCLUDED DUE TO COPY RIGHT

Figure 1-10 The Agilent QTOF schematic, showing ion source, ion transfer, optics, beam shaping optics, ion pulsar, flight tube, and detector⁹³.

1.6 Experimental design

Experimental design is a term used to describe the stages of identifying factors that may affect the result of an experiment; designing the experiment so as to minimise the effects of uncontrolled factors and using statistical analysis to separate and evaluate the effects of each of the different factors involved⁹⁴.

Experimentation is an important aspect of many fields and areas of inquiry, especially in scientific research. Poorly designed experiments can result in erroneous or misleading conclusions. The principles of experimental design are extremely useful in developing effective and useful experiments.

Experiments using statistical principles are known to be more effective and thus desirable; however, they are not generally used in the majority of experiments performed. Most experimentation is of the trial-and-error category. Many other experiments fall into the one-factor-at-a-time (OFAT) category. OFAT designs involve varying one or two factors at a time while the other factors are held at a particular level. This can lead to misleading information, although there are some situations where OFAT designs can be beneficial⁹⁴.

1.6.1 Types of experimental design

There are many different types of experimental designs that can be employed depending on the circumstances of the design. Two of the most common are full factorial designs (FFD) and central composite designs (CCD). These are useful for determining the significance of the effects of different factors on the response variable and for modelling the response at different factor levels.

1.6.1.1 Full-factorial design

Full-factorial designs are the most commonly used designs for experiments involving multiple factors⁹⁴. A factorial design involves choosing a number of levels for each factor. A series of experiments are then set up so that every possible combination of factor levels is run. A factorial design is usually represented in the form s^k , with s representing the number of factor levels and k representing the number of factors. For example, a design involving four factors at two levels would be written as 2^4 . For a two level design, the two factor levels are set as 'high' and 'low' if the factors are quantitative and these define the experimental space.

From the experimental results, the effects of the factors on the response variable can be determined. The other effects that can be determined from the results of the factorial design are known as interaction effects. This refers to the effect of one factor on the levels of other factors. The identification and estimation of interaction effects is the greatest strength of factorial design over OFAT designs. This is because the presence of interaction, and in particular extreme interaction, can cause erroneous conclusions to be drawn from the results. If the interaction effect is greater than the main effects the interaction can negate the main effects, making main effects analysis extremely misleading.

When the effects have been computed from the experimental results they can be processed in a number of ways. This can be achieved using software programs such as Minitab™. Using such programs enables main effects and interaction plots to be constructed in order to visually represent the significance of the effects on the response. This can also be used to construct effects plots to compare the effects to a normal distribution and determine which effects are significant. From this, the best combination of factors can be determined or further experimental designs can be constructed.

1.6.1.2 Central composite design

Central composite designs are very similar to factorial designs, the difference being the number of data points used to investigate the experimental space⁹⁴. A CCD is essentially made up of a full factorial design with axial points and some experiments in the centre of the experimental space (Figure 1-11). From these points, a response surface can be constructed. The effect of having the extra data points is that a CCD can detect curvature in the response. Using a CCD a response surface can be constructed for the factor combinations. Using this and the results from the design, a model can be constructed for the response within the experimental space. This can be used to maximise the response.

THIS FIGURE IS EXCLUDED DUE TO COPY RIGHT

Figure 1-11 The points of a CCD with three input parameters⁹⁴.

1.7 Aims

The objectives of the project were to optimise the DESI-MS parameters for the analysis of licit and illicit drug compounds (including the implementation of FFD and CCD to optimise inter-dependent parameters), synthesise novel controlled substances which are not readily available from seizures for DESI-MS analysis, investigate the potential use of DESI-MS for the rapid qualitative identification of pharmaceutical samples and multiple novel substances within a single sample. In addition, to explore the application of MS and MS/MS data for the fast analysis and profiling of novel and illicit drug analogues, and compile MS/MS spectral data obtained for future automated library matching, develop a method for the quantitative analysis of novel substances (i.e. 4-MMC) via DESI-MS, and compare the results obtained with DESI-MS to those obtained with currently used drug detection/analysis techniques, i.e. preliminary and confirmatory analysis techniques (such as colour tests, GC-MS and LC-MS, respectively).

Chapter 2: Synthesis

Chapter 2: Synthesis

2.1 Introduction

Drug analogues are made to avoid the provisions of existing legislative control, by modifying the structure of existing drugs or by finding chemicals with entirely different chemical structures that produce similar effects to existing illicit drugs. As previously discussed, piperazine and cathinone analogues are prevalent drug analogues of abuse globally despite their control in several countries^{6, 24-27}. The use of these drugs has been reported as early as the 1930s; however, they have only recently become recreational drugs of abuse⁶. The synthesis of 4-MMC, BZP, TFMPP, MeOPP and mCPP is detailed in this chapter. Syntheses have previously been reported for 4-MMC by Camilleri *et al.*⁹⁵, and BZP by Cymerman and Young⁹⁶, and Baltzly *et al.*⁹⁷ The objective of synthesising these compounds was to obtain samples that contain potential by-products/impurities from synthesis that would mimic those observed in a clandestine laboratory. For this reason, no attempts were made to purify the products obtained. Once the piperazine analogues and 4-MMC were synthesised they were analysed by the developed DESI-MS method as well as GC-MS and LC-MS.

2.2 Materials and methods

Where mentioned throughout this thesis, the chemicals used were sourced from the following manufacturers:

1,3-Dichlorobenzene, 1-benzyl-3-pyrrolidinol, 1-piperazinecarboxylate, 2-chloroanisole, sulfuryl chloride, bromine, *N*-bromosuccinimide, bis(2-chloroethyl)amine, 4-anisidine, 3-(trifluoromethyl)aniline, 3-chloroaniline, 4-diethylaminobenzaldehyde, 4-methylpropiofenone, acetonitrile, atropine sulfate, benzoic acid, benzyl chloride, caffeine, formic acid, levamisole hydrochloride, lignocaine hydrochloride, magnesium stearate, 3-chlorobenzotrifluoride, methanol, methylamine hydrochloride, piperazine hexahydrate, potassium bromide (KBr), potassium tert-butoxide, procaine hydrochloride, sodium carbonate, sodium hydride and triethylamine were purchased from Sigma Aldrich (Castle Hill, NSW, Australia). IS codeine-D₆ was purchased from Lipomed, Inc. (Cambridge, MA, USA). (±)-

4-MMC HCl, mCPP HCl, TFMPP HCl, *d*-(±)-AP SO₄, (±)-MA HCl, (-)-*N,N*-DMA, (±)-PMA, (±)-MDMA standards, phentermine, 4-hydroxyamphetamine (4-OH-AP), 4-fluoroamphetamine (4-F-AP), nordiazepam, diazepam, oxazepam, cocaine, heroin, methadone, cathinone and 4-MMC-D₃ were obtained from National Measurement Institute (NMI, North Ryde, NSW, Australia). Seized samples which were obtained from the AFP include: cocaine (Item 1, Item 1/2, and Item 5/2) and a yellow MDMA tablet. Pharmaceutical samples including Aspirin tablets, Centrum tablets, Clarityne tablets, NoDoz tablets, Panadol tablets were sourced from local pharmacies. "Jack3d" was purchased from Vitamin King (Rockdale, NSW, Australia). MDMA base and PMMA base were synthesised at the University of Technology, Sydney^{98, 99}. Double sided tape (3M Scotch Mounting Tape) was obtained from Bunnings Warehouse, (Rockdale, Australia). Polyvinyl chloride (PVC) and polytetra fluoroethylene (PTFE or Teflon) were purchased from the Plastix Centre, (Arncliffe, NSW, Australia). Polymethyl methacrylate (pMMA) and HTC-printed slides were purchased from Prosolia™, Inc. (Indianapolis, IN, US). Ace pressure tube (100 mL) was purchased from Sigma Aldrich – Specifications: 17.8 cm L x 38.1 mm O.D., 150 psi, 15 mm Teflon plug.

A commercially available DESI interface was purchased from Prosolia™, Inc. This DESI source was utilised throughout the project by coupling it to the Agilent 6510 Series QTOF mass spectrometer. ¹H and ¹³C nuclear magnetic resonance (NMR) spectra were recorded using a Bruker DRX NMR spectrometer operating at 300 MHz and 75 MHz, respectively or an Agilent Technology 500/54 Premium Shielded NMR with 7510-AS operating at 500 MHz and 125 MHz, respectively. Spectra were calibrated using residual protic solvent, which included methanol and chloroform. ¹H NMR chemical shifts are quoted on the δ scale, followed by proton integration, multiplicity, coupling in Hertz and proton assignment. Infrared spectra were recorded using a Nicolet Magna IR-760 spectrometer with sample incorporated into KBr discs and spectra collected in transmission mode (resolution 4 cm⁻¹, 16 scans). GC-MS was performed on the HP 5890 gas chromatograph coupled to a 5970 mass spectrometer (GC method 1) or an Agilent Technologies 7890A gas chromatograph coupled to a 5975C electron ionisation (EI) mass spectrometer (GC method 2). The column used was an Agilent Technology HP-5MS (30 m x 0.25 mm ID x 0.25 μm). The GC conditions were optimised as follows: injector temperature, 250 °C; oven temperature program, 100 °C (hold 1 min), increase 30 °C/min to 300 °C (hold 3 min). The fragmentation peaks reported in this thesis are greater than 10 % in abundance relative to the base peak. LC-MS was performed on an

Agilent Technologies 1200 series liquid chromatograph coupled to an Agilent 6510 series QTOF mass spectrometer. The column utilised in LC-MS analysis was a Phenomenex C18 column with dimensions 150 x 3 mm x 5 micron. All experiments were run in full scan mode and MS/MS mode for DESI-MS and LC-MS analysis. Melting points were obtained on a John Morris Electro Thermal melting point apparatus and were calibrated using benzoic acid (MP: 122.4 °C¹⁰⁰).

GC-MS samples were dissolved in methanol and the linear calibration range was 5 - 400 µg/mL. Four synthesised samples (M1 – M4) of 4-MMC were prepared in methanol (80 µg/mL), and analysed using GC-MS for purity determination. It is important to note that minimal purification of the synthesised samples was conducted due to the desire to retain as many by-products/impurities in the synthesised samples for analysis via DESI-MS, GC-MS and LC-MS. The presence of these by-products and impurities in the synthesised samples would assist greatly in linking the samples to the route of manufacture and also in providing information for future chemical profiling work.

2.2.1 4-Methylmethcathinone (M1 – M4)

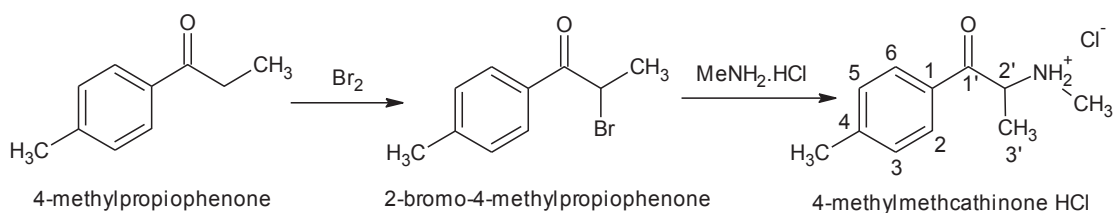


Figure 2-1 Reaction scheme for the synthesis of 4-methylmethcathinone (M1 – M2) via an α -bromination reaction⁹⁵.

4-Methylmethcathinone was synthesised in four separate batches (M1-M4). M1 and M2 were synthesised following the published procedure by Camilleri *et al.*⁹⁵ in which triethylamine was utilised as a catalyst. M1 yielded 0.39 g (35 %) crude 4-MMC.HCl, MP: 185 - 206 °C (literature¹⁰¹ 246 - 248 °C). M2 yielded 0.41 g (25 %) crude 4-MMC.HCl, MP: 188 - 198 °C.

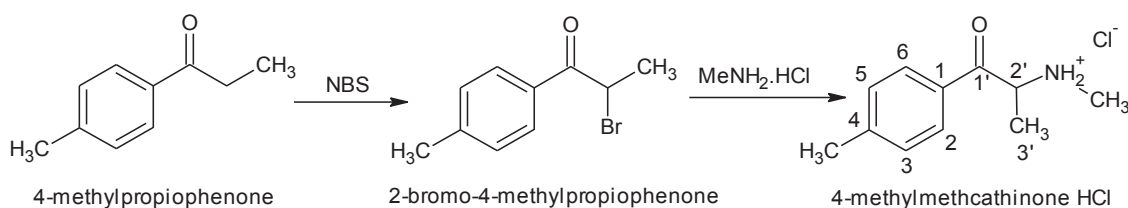


Figure 2-2 Reaction scheme for the synthesis of 4-methylmethcathinone (M3) via an α -bromination reaction using *N*-bromosuccinimide¹⁰².

M3 was synthesised via the α -bromination of 4-methylpropiophenone using *N*-bromosuccinimide followed by its amination to form 4-MMC. In a flask 2.0 g (2.02 mL) of 4-methylpropiophenone (13.5 mmol) was added to 3.9 g of *p*-toluene sulfonic acid (20.3 mmol) in acetonitrile (50 mL). To this solution 2.4 g of *N*-bromosuccinimide (13.5 mmol) was slowly added and the solution was refluxed for 2 hours. Once the reaction mixture was cooled it was poured into 100 mL of ice-cold water and the 2-bromo-4-methylpropiophenone oil layer was extracted twice with 50 mL dichloromethane. The oil layer was then washed with a solution of saturated sodium carbonate. The solvent was removed *in vacuo*. A solution containing 1.4 g of sodium hydroxide (35.2 mmol) and 2.4 g methylamine HCl (35.2 mmol) in 25 mL cold water was added to a stirred solution containing 2.0 g of the crude 2-bromo-4-methylpropiophenone (8.8 mmol) in 15 mL toluene, over 5 minutes. The mixture was allowed to stir for a further 24 hours at 20 - 25 °C, then was poured into 100 mL ice-cold water. The toluene layer was separated off, and the remaining free base extracted with 2 x 20 mL toluene. The combined toluene extracts were washed with 2 x 20 mL water and then acidified with 2 x 15 mL dilute HCl. The combined acidic extracts were then washed with 2 x 20 mL toluene and evaporated *in vacuo*, allowing an off-white solid to form. The yield of M3 was 0.51 g (47 % yield) crude 4-MMC.HCl, MP: 208 - 210 °C (literature¹⁰¹ 246 - 248 °C).

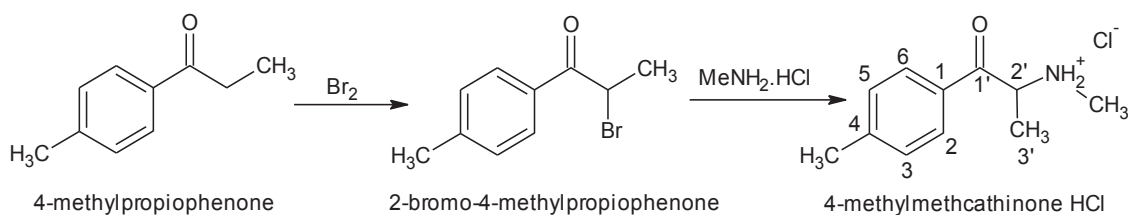


Figure 2-3 Reaction scheme for the synthesis of 4-methylmethcathione (M4) via an α -bromination reaction.

The synthesis of M4 followed the α -bromination of 4-methylpropiophenone using bromine and its subsequent amination to form 4-MMC. In a flask 2.3 g (2.32 mL) of 4-methylpropiophenone (13.5 mmol) was added to 44 mL of glacial acetic acid. Bromine (0.7 mL, 13.5 mmol) was added drop-wise to the flask kept at 20 - 25 °C and stirred over a period of 1 hour. The reaction mixture was poured into 100 mL of ice-cold water and the 2-bromo-4-methylpropiophenone oil layer was extracted with 2 x 50 mL dichloromethane. The oil layer was then washed with a 50 mL solution of saturated sodium carbonate. The solvent was removed *in vacuo*. A solution containing 1.4 g of sodium hydroxide (35.2 mmol) and 2.4 g methylamine HCl (35.2 mmol) in 25 mL cold water was added to a stirred solution containing 2.0 g of the crude 2-bromo-4-methylpropiophenone in toluene, over 5 minutes. The mixture was allowed to stir for a further 24 hours at 20 - 25 °C, then was poured into 100 mL ice-cold water. The toluene layer was separated off, and the remaining free base extracted with 2 x 20 mL toluene. The combined toluene extracts were washed with 2 x 20 mL water and then acidified with 2 x 15 mL dilute HCl. The combined acidic extracts were then washed with 2 x 20 mL toluene and evaporated *in vacuo*, allowing an off-white solid to form. Crude M4 yielded 0.38 g (36 % yield), MP: 201 - 205 °C (literature¹⁰¹ 246 - 248 °C).

M1.HCl: ¹H NMR (300 MHz, MeOH-D₄): δ 7.96 (2H, d, J = 8.2 Hz, H2 and H6), 7.41 (2H, d, J = 8.2 Hz, H3 and H5), 5.11 (1H, q, J = 7.2 Hz, H2'), 2.77 (3H, s, N-Me), 2.45 (3H, s, Ar-Me), 2.15 (1H, s, N-H), 1.58 (3H, d, J = 7.2 Hz, H3'). ¹³C NMR (75 MHz, MeOH-D₄): 196.57 (C1'), 147.54 (C4), 131.69 (C1), 130.95 (C3), 130.13 (C2), 60.51 (C2'), 31.74 (N-Me), 21.77 (Ar-Me), 18.38 (C3'). IR ν_{max} (cm⁻¹): 2975 and 2939 (CH aliphatic stretching), 1684 (C=O), 1605 and 1475 (C=C aromatic), 1398 (CH bending), 1189 (CN). EI: m/z 177 (M⁺, 2 %), 91 (12), 65 (10), 58 (100). M2 - M4 resulted in comparable characteristic data.

2.2.2 1-Benzylpiperazine (BZP 1 - BZP 4)

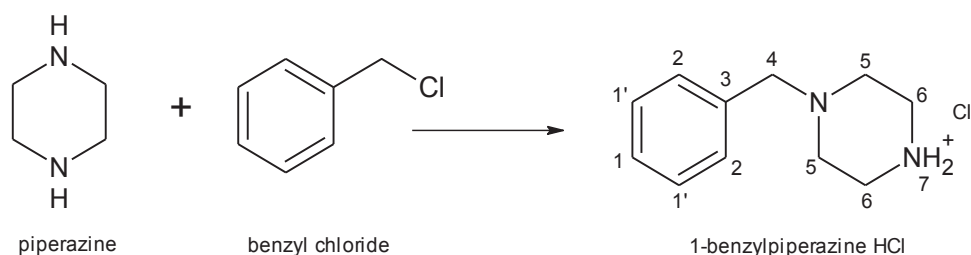


Figure 2-4 Reaction scheme for the synthesis of 1-benzylpiperazine (BZP 1 - BZP 3)⁹⁶.

1-Benzylpiperazine was synthesised in four batches (BZP 1 – BZP 4). BZP 1 – BZP 3 were synthesised via a common synthetic pathway as described by Cymerman and Young⁹⁶. In a 250-mL round bottom flask, a solution of 4.86 g (25 mmol) of piperazine hexahydrate in 50 mL of absolute ethanol was warmed at 65 °C as there was dissolved in the solution by swirling, 4.42 g (25 mmol) of piperazine dihydrochloride monohydrate (Note 1). As warming in the bath continued, there was added during 5 minutes, 3.16 g (2.87 mL, 25 mmol) of benzyl chloride. The separation of white needle commenced almost immediately. After the solution had been stirred for an additional 25 minutes at 65 °C, it was cooled, and the unstirred solution kept in an ice bath for about 30 minutes. The crystals of the recovered piperazine dihydrochloride monohydrate were collected by suction filtration, washed with 3 x 10 mL portions of ice-cold absolute ethanol, and then dried. Recovery of the dihydrochloride was 97 - 99 %. The combined filtrate and washings from the piperazine dihydrochloride were cooled in an ice-bath and treated with 25 mL of ethanolic HCl. After the solution had been well mixed, it was cooled for 10 - 15 minutes in an ice-bath. The precipitated white plates of 1-benzylpiperazine dihydrochloride were collected by suction filtration, washed with 2 x 10 mL dry benzene and dried. The free base was obtained by dissolving 2.00 g of the salt in 50 mL of water and making alkaline (pH>12) with 60 mL of 5 M sodium hydroxide, then extracted twelve times with 20 mL portions of chloroform. The combined extracts were dried over calcium sulfate and the oil remaining after removal of solvent *in vacuo* was the free base of 1-benzylpiperazine.

Note 1 = Piperazine dihydrochloride monohydrate was prepared by passing a stream of HCl gas over 5 - 10 minutes into a solution of 5 g of piperazine hexahydrate in 50 mL absolute ethanol in a 250-mL round bottom flask¹⁰³. The flask was cooled in an ice-bath to keep the

reaction temperature at about 25 °C. After this the contents were cooled to about 0 °C, and the crystalline product was collected by suction filtration and washed with two 25 mL portions of ice-cold absolute ethanol. The yield was 95 %.

BZP 1.HCl yielded 4.34 g (98 %). MP: 253 °C (decomposes at 287 °C) (literature⁹⁷ 253 °C). In the synthesis of BZP 2, 0.017 mole of benzyl chloride was used. BZP 2.HCl yielded 2.74 g (92 %). In the synthesis of BZP 3, 0.039 mole of benzyl chloride and 0.013 mole of piperazine were used. BZP 3.HCl yielded 2.08 g (91 %). BZP 4 was synthesised via the method published by Baltzly *et al.*⁹⁷ BZP 4.HCl yielded 0.81 g (58 %). MP: 260 °C (decomposes at 310 °C) (Figure 2-5).

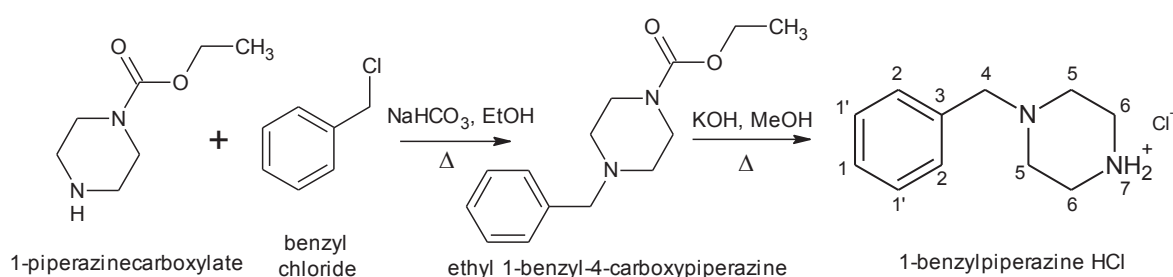


Figure 2-5 Reaction scheme for the synthesis of 1-benzylpiperazine (BZP 4)⁹⁷.

BZP 1.base: ¹H NMR (300 MHz, CDCl₃): δ 1.52 (1H, s, H7), 2.31 - 2.51 (4H, broad t, H6), 2.85 (4H, t, J = 4.8 Hz, H5), 3.49 (2H, s, H4), 7.26 (5H, Ar, H2, H1' & H1). ¹³C NMR (75 MHz, CDCl₃): 46.12 (C6), 54.54 (C5), 63.68 (C4), 126.94 (C1), 128.13 (C1'), 129.17 (C2), 138.10 (C3). IR ν_{max} (cm⁻¹): 3241 (NH stretching), 3128 (CH aromatic stretching), 2993 and 2759 (CH aliphatic stretching), 1631 (NH bending), 1557 and 1443 (C=C aromatic), 1421 (CH bending), 1063 (CN). BZP 1.HCl: EI: *m/z* 176 (M⁺, 16 %), 176 (16), 134 (60), 91 (100), 85 (10), 65 (14), 56 (23). BZP 2 – BZP 4 resulted in comparable characteristic data.

2.2.3 3-Trifluoromethylphenylpiperazine (TFMPP 1 – TFMPP 4)

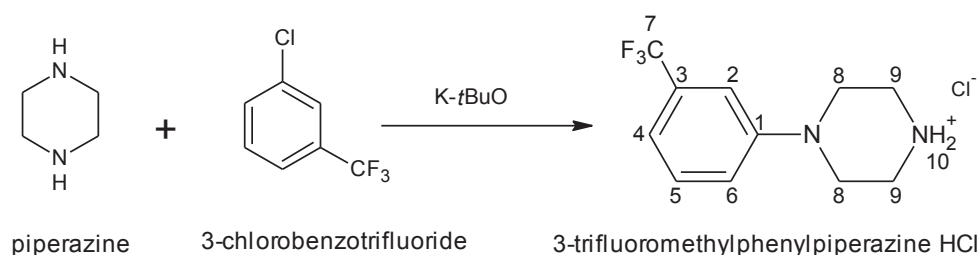


Figure 2-6 Reaction scheme for the synthesis of 3-trifluoromethylphenylpiperazine (TFMPP 1 – TFMPP 3)⁹⁶.

3-Trifluoromethylphenylpiperazine was synthesised in four batches (TFMPP 1 - TFMPP 4). The first three batches follow a common synthetic pathway adapted from Cymerman and Young⁹⁶. A solution of 3.92 g (20 mmol) of piperazine hexahydrate in 50 mL of toluene, contained in a 250-mL round bottom flask, was warmed at 70 °C. As warming was continued, there was added during 5 minutes, with vigorous stirring, 3.37 g (30 mmol) of potassium tert-butoxide. Following this, 1.81 g (1.36 mL, 10 mmol) of 3-chlorobenzotrifluoride was added. After the solution had been stirred and refluxed for an additional 36 hours at 135 °C, it was cooled, and the unstirred solution was kept in an ice bath for 30 minutes. The solution was treated with 25 mL of ethanolic HCl. After the solution has been well mixed, it was cooled for 10 - 15 minutes in an ice-bath. The precipitated white plates of TFMPP.HCl were collected by suction filtration, washed with 2 x 20 mL dry benzene and dried. The base was extracted when a solution of this salt, was made alkaline (pH>12) with about 60 mL of 5 M sodium hydroxide, then extracted with 12 x 20 mL portions of dichloromethane. The combined extracts were dried over sodium sulfate and the oil remaining after removal of solvent *in vacuo* amounted to 1.10 g (49 % yield). In the synthesis of TFMPP 2, the temperature was increased from 135 °C to 140 °C. TFMPP 2.base yielded 1.27 g (55 %). In the synthesis of TFMPP 3, the reaction temperature was kept at 135 °C; however, reaction time was increased from 36 to 72 hours. TFMPP 3.base yielded 1.11 g (48 %).

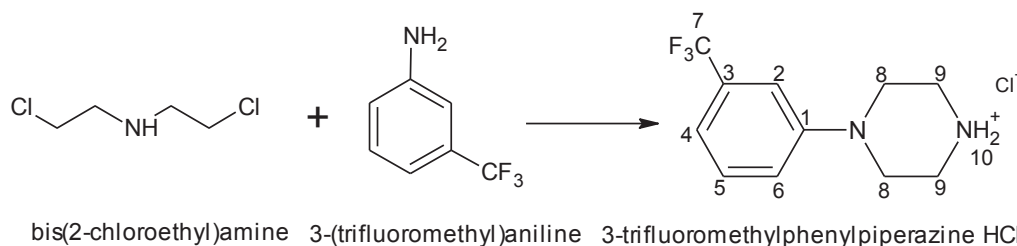


Figure 2-7 Reaction scheme for the synthesis of 3-trifluoromethylphenylpiperazine (TFMPP 4)¹⁰⁴.

3-Trifluoromethylphenylpiperazine (TFMPP 4) was synthesised via the general method reported by Liu and Robichaud¹⁰⁴. To a round bottom flask containing bis(2-chloroethyl)amine (7.05 g, 50 mmol), dissolved in n-butanol (40 mL), 3-(trifluoromethyl)aniline (8.05 g, 50 mmol) in n-butanol (10 mL) was added. The reaction mixture was heated to 130 °C with constant stirring and allowed to reflux for 14 hours. After 14 hours, potassium carbonate (2.61 g) was added portion wise to the reaction and allowed to react for a further 48 hours until reaction completion. The potassium carbonate was collected by suction filtration using a Buchner funnel. The filtrate solidified at room temperature and was filtered through glass sinter and washed with ice cold ethanol and then dried under high vacuum. TFMPP 4.HCl yielded 3.80 g (42 % yield). A solution of the synthesised TFMPP.HCl in water was made alkaline (pH>12) with 5 M potassium hydroxide extracted with 3 x 20 mL portions of diethyl ether. The combined extracts were dried over anhydrous sodium sulfate, filtered and concentrated *in vacuo*. The oil remaining after removal of solvent yielded 2.00 g (95 %). TFMPP 4.HCl MP: 238 °C (decomposes at 251 °C) (literature¹⁰⁵ 240 °C).

TFMPP 1.base: ¹H NMR (500 MHz, CDCl₃): δ 1.58 (1H, s, H10), 2.86 (4H, s, H9), 3.48 (4H, s, H8), 7.27 - 7.62 (4H, Ar, H2, H4, H5, H6). ¹³C NMR (125 MHz, CDCl₃): 46.87 (C9), 50.69 (C8), 109.97 (C2), 130.12 (C4), 130.55 (C6), 131.54 (C7), 132.54 (C5), 134.04 (C3), 145.68 (C1). IR ν_{\max} (cm⁻¹): 3087 (NH stretching), 3063 (CH aromatic stretching), 2922 and 2873 (CH aliphatic stretching), 1605 (NH bending), 1524 and 1496 (C=C aromatic), 1433 (CH bending), 1323 (CN), 1299 and 1134 (C-F stretching). TFMPP.HCl: EI: *m/z* 230 (M⁺, 26 %), 188 (100), 172 (15), 145 (17), 56 (15). TFMPP 2 – TFMPP 4 resulted in comparable characteristic data.

2.2.4 3-Chlorophenylpiperazine (mCPP 1)

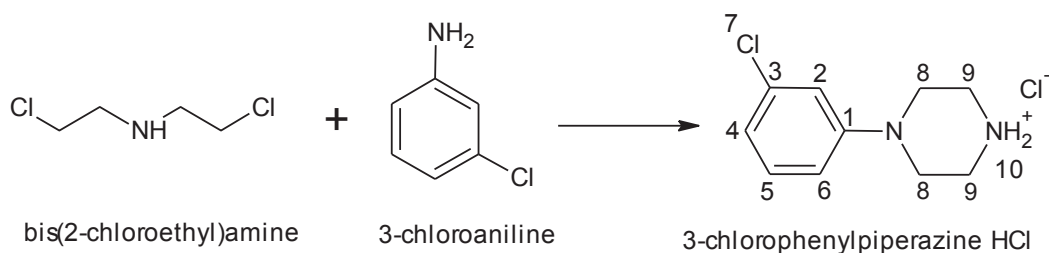


Figure 2-8 Reaction scheme for the synthesis of 3-chlorophenylpiperazine (mCPP 1)¹⁰⁴.

3-Chlorophenylpiperazine (mCPP 1) was synthesised via a similar approach to the method reported by Liu and Robichaud¹⁰⁴. To a round bottom flask containing bis(2-chloroethyl)amine (7.05 g, 50 mmol), dissolved in n-butanol (40 mL), 3-chloroaniline (6.35 g, 50 mmol) in n-butanol (10 mL) was added. The reaction mixture was heated to 130 °C with constant stirring and allowed to reflux for 14 hours. After 14 hours, potassium carbonate (2.61 g) was added portion wise to the reaction and allowed to react for a further 48 hours. The potassium carbonate was collected by suction filtration using a Buchner funnel. The filtrate solidified at room temperature and was filtered through glass sinter and washed with ice cold ethanol and then dried under high vacuum yielding 4.80 g mCPP 1.HCl (62 % yield). A solution of the synthesised mCPP.HCl in water was made alkaline (pH>12) with 5 M potassium hydroxide and extracted three times with 20 mL portions of diethyl ether. The combined extracts were dried over anhydrous sodium sulfate, filtered and concentrated *in vacuo*. The oil remaining after removal of solvent yielded 2.30 g (92 % yield). mCPP 1.HCl: MP: 214 - 217 °C (decomposes at 240 °C) (literature¹⁰⁶ 210 - 214 °C).

mCPP 1.base: ¹H NMR (500 MHz, CDCl₃): δ 1.22 (1H, s, H10), 2.98 (4H, s, H9), 3.13 (4H, s, H8), 6.76 - 7.18 (4H, Ar, H2, H4, H5, H6). ¹³C NMR (125 MHz, CDCl₃): 45.49 (C9), 49.50 (C8), 113.84 (C7), 115.63 (C4) 119.20 (C6), 129.20 (C5), 134.67 (C3), 152.51 (C1). IR ν_{\max} (cm⁻¹): 3100 (NH stretching), 3050 (CH aromatic stretching), 2909 (CH aliphatic stretching), 1595 (NH bending), 1568 and 1487 (C=C aromatic), 1399 (CH bending), 1256 (CN), 750 (Cl). mCPP 1.HCl: EI: *m/z* 196 (M⁺, 30 %), 154 (100), 56 (17), 138 (13), 111 (12).

2.2.5 4-Methoxyphenylpiperazine (MeOPP 1)

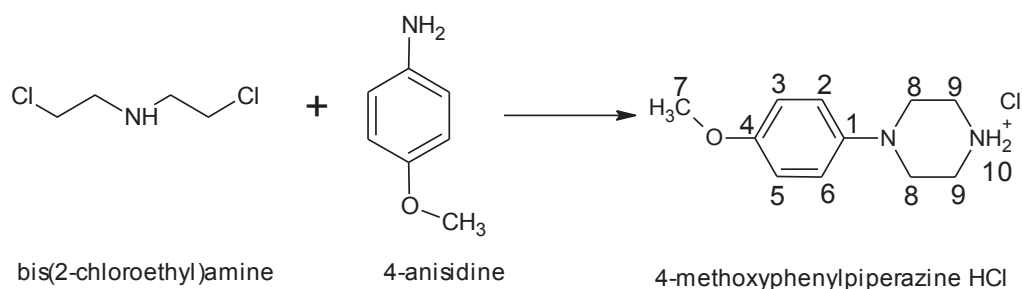


Figure 2-9 Reaction scheme for the synthesis of 4-methoxyphenylpiperazine (MeOPP 1).

4-Methoxyphenylpiperazine (MeOPP 1) was synthesised via a similar approach to the method reported by Liu and Robichaud¹⁰⁴. Bis(2-chloroethyl)amine (7.05 g, 50 mmol), dissolved in *n*-butanol (40 mL), was added to 4-anisidine (6.15 g, 50 mmol) in *n*-butanol (10 mL). The reaction mixture was heated to 130 °C with constant stirring and allowed to reflux for 14 hours. Following this, potassium carbonate (2.61 g) was added portion wise to the reaction and allowed to react for a further 48 hours. The observed solid was collected by suction filtration using a Buchner funnel. The filtrate solidified at room temperature and was filtered through glass sinter and washed with ice cold ethanol and then dried under high vacuum. MeOPP 1.HCl yielded 6.30 g (83 %). A solution of the synthesised MeOPP.HCl in water was made alkaline (pH>12) with 5 M potassium hydroxide and extracted with 3 x 20 mL of diethyl ether. The combined extracts are dried over anhydrous sodium sulfate, filtered and concentrated *in vacuo*. The oil (MeOPP.base) remaining after removal of solvent yielded 2.20 g (89 %).

MeOPP.HCl: MP: 220 °C (decomposes at 261 °C) (literature⁹⁷ 261 - 262 °C). MeOPP.base: ¹H NMR (500 MHz, CDCl₃): δ 1.67 (1H, s, H10), 3.04 (4H, s, H9), 3.48 (4H, s, H8), 3.77 (3H, s H7), 6.84 – 6.92 (4H, Ar, H2, H3, H5, H6). ¹³C NMR (125 MHz, CDCl₃): 48.13 (C9), 52.72 (C8), 57.54 (C7), 116.41 (C6, C2), 120.20 (C3, C5), 148.17 (C1), 155.87 (C4). IR ν_{\max} (cm⁻¹): 3379 (NH stretching), 3000 (CH aromatic stretching), 2936 (CH aliphatic stretching), 1646 (NH bending), 1601 and 1515 (C=C aromatic), 1467 (CH bending), 1027 (CN), 1250 (CO). MeOPP.HCl: EI: *m/z* 192 (M⁺, 62 %), 150 (100), 120 (28), 135 (25), 56 (21).

2.3 Results and discussion

2.3.1 4-Methylmethcathinone

2.3.1.1 Yield of 4-methylmethcathinone

A low yield resulted for the synthesis of 4-MMC.HCl (M1 and M2) from 2-bromo-4-methylpropiofenone, due to side reactions indicated by the presence of di-bromo substituted by-products¹⁰⁷ (via α -bromination with Br_2 – section 2.2.1). Pyrazine formation during synthesis is extremely common and also extremely difficult to prevent¹⁰⁸. In addition, the presence of residual triethylamine.HCl as catalyst, further reduced the purity of 4-MMC. An alternate reaction was employed in latter syntheses of 4-MMC (i.e. M3 and M4), where no triethylamine was employed, leading to slightly increased yields (47%).

2.3.1.2 Purity of 4-methylmethcathinone

A standard calibration curve was constructed using GC-MS analysis in order to evaluate the purity of the synthesised products (section 2.2).

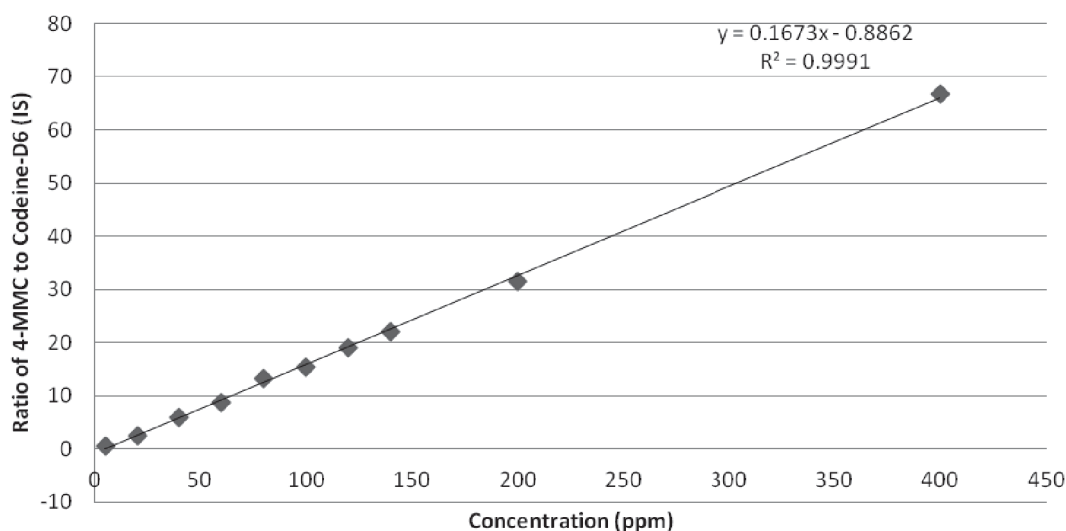


Figure 2-10 Calibration curve for 4-MMC standard analysed using GC-MS, codeine-D₆ as IS, n=3 (GC method 1).

Four samples were prepared M1 – M4 (80 µg/mL), and analysed using GC-MS (section 7.2.3). The GC-MS results revealed samples of low purity; i.e. 23.6 % and 19.3 % 4-MMC.HCl in M1 and M2, respectively. This low purity can be attributed to the presence of triethylamine.HCl, diethyl ether and water.

M1.HCl was dried under vacuum, successfully removing the diethyl ether solvent (Figure 2-11 and Figure 2-12). M3 and M4 were found to have a purity of 43.6 % and 39.4 %, respectively, and were found to contain the starting materials methylamine, 4-methylpropiophenone, and the intermediate 2-bromo-4-methylpropiophenone.

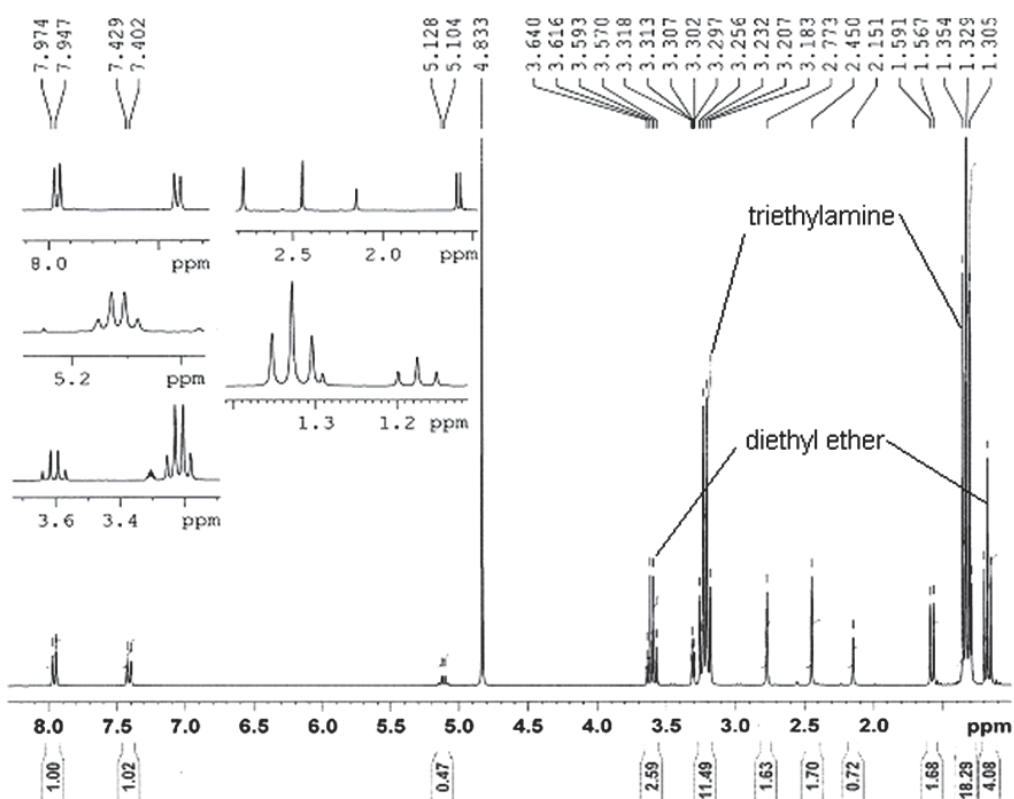


Figure 2-11 ^1H NMR of 4-MMC (M1) before vacuum drying.

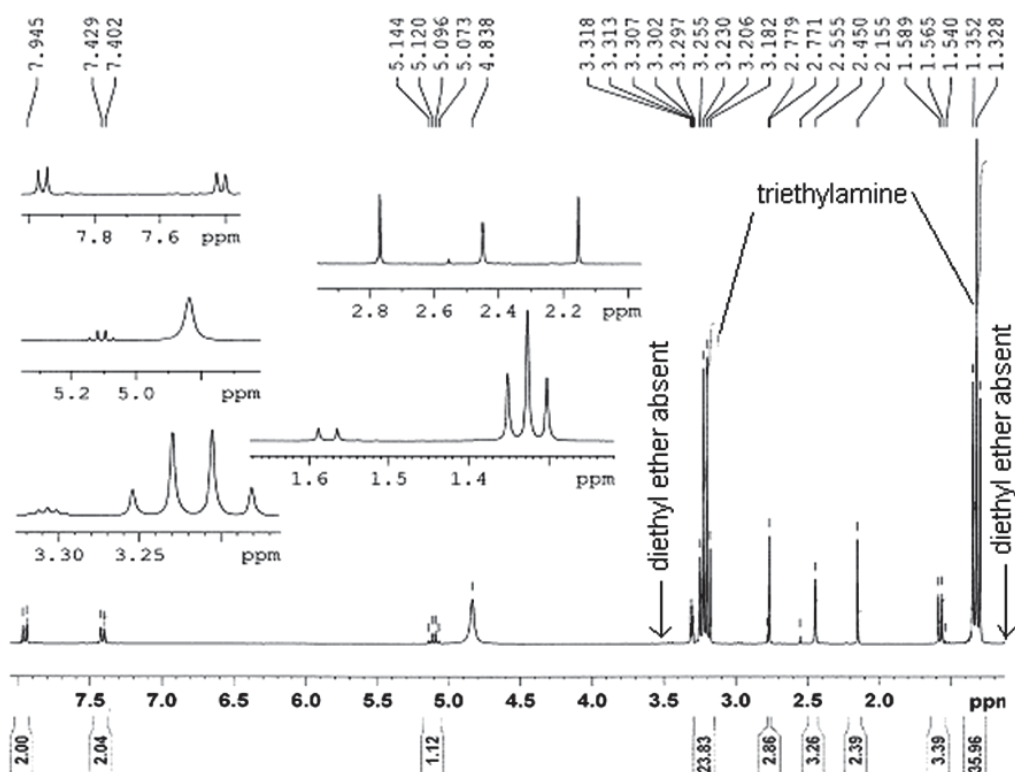


Figure 2-12 ^1H NMR of 4-MMC (M1) after vacuum drying.

2.3.1.3 2-Chloro-4-methylpropiophenone as intermediate to 4-MMC

Alternate reaction schemes were explored as it is common for a range of synthetic procedures to be employed in different clandestine settings. This enabled an evaluation of the range of chemical profiles that may be encountered in clandestinely prepared 4-MMC samples. The alternate reaction involved synthesising the 2-chloro-4-methylpropiophenone intermediate using suluryl chloride as one of the reactants (Figure 2-13). This reaction resulted in a high yield for the intermediate (95.5 %); however, did not produce the desired end-product. GC-MS analysis suggests that no product was formed; however, 4-methylpropiophenone and 2-chloro-4-methylpropiophenone remain in the extract (Figure 2-14 - Figure 2-16).

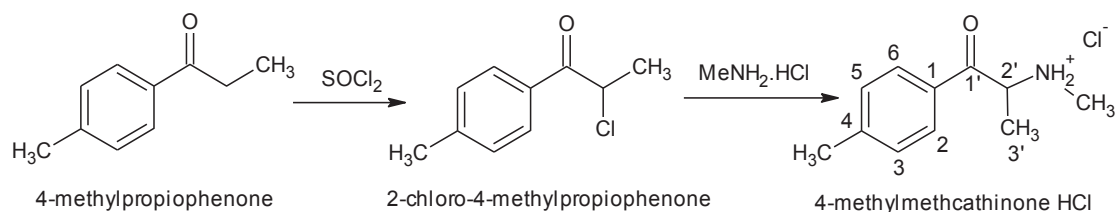


Figure 2-13 Reaction scheme for the synthesis of 4-methylmethcathinone using sulfuryl chloride.

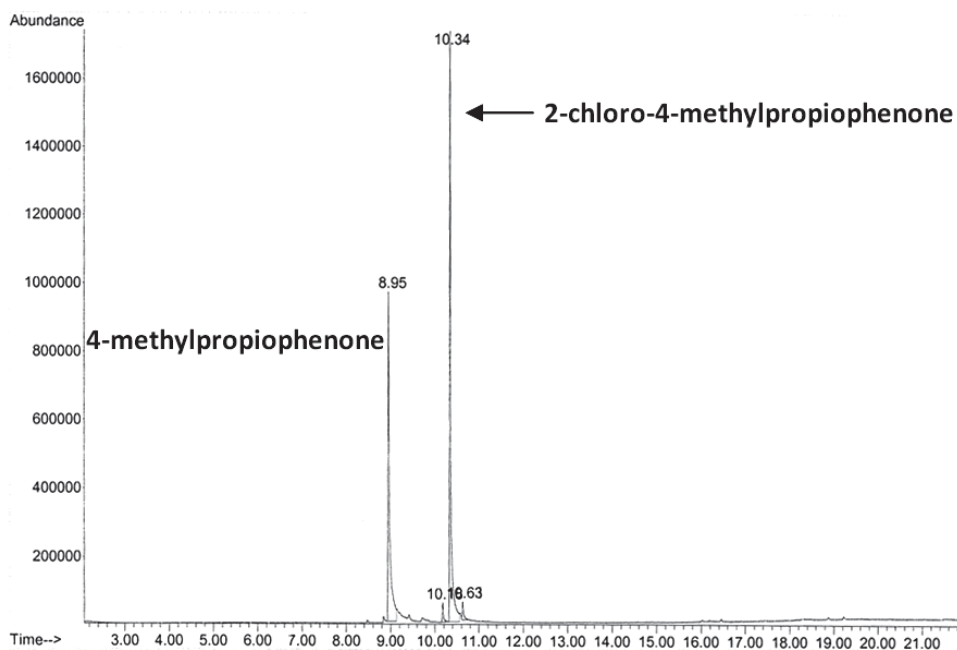


Figure 2-14 GC-MS chromatogram of extract 1; 4-methylpropiophenone at 8.9 minutes, 2-chloro-4-methylpropiophenone at 10.3 minutes (GC method 1).

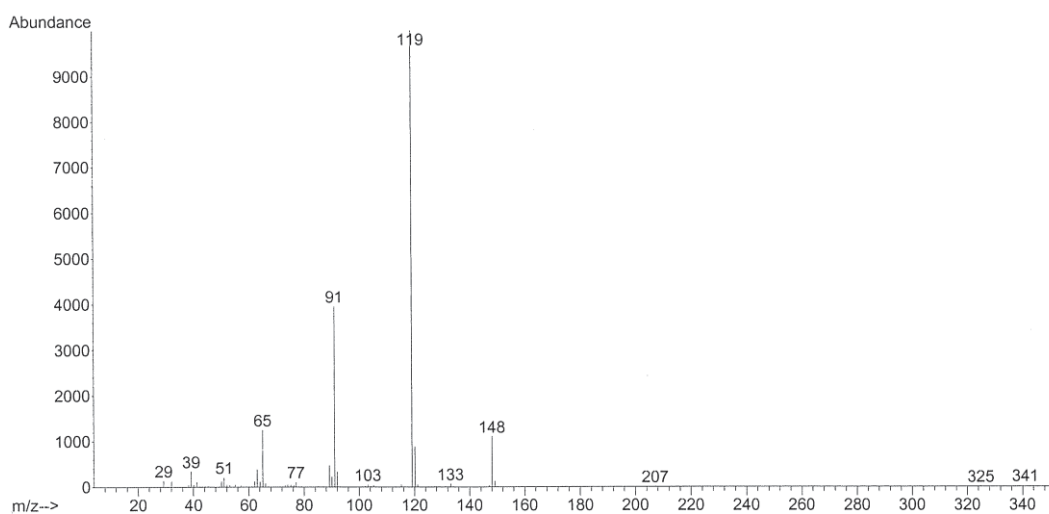


Figure 2-15 EI mass spectrum of extract 1; 4-methylpropiophenone (GC method 1).

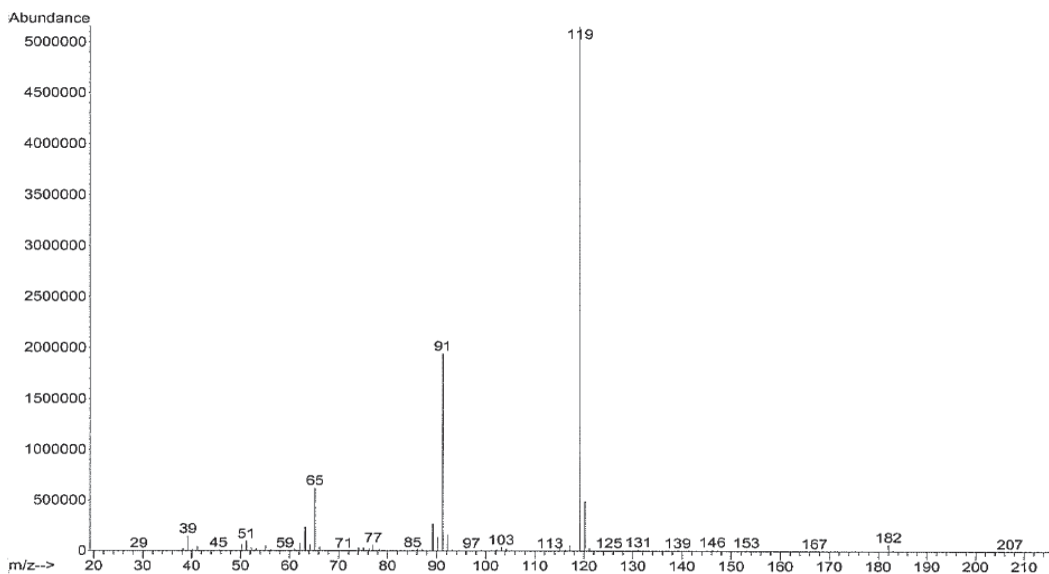


Figure 2-16 EI mass spectrum of extract 1; 2-chloro-4-methylpropiophenone (GC method 1).

The lack of product formation is hypothesised to be due to an absence of conditions required for an S_N2 reaction to be successful. The first requirement is that the nucleophile is relatively basic in order to possess a high nucleophilicity (affinity of Lewis base to a carbon atom). The nucleophile in this reaction is methylamine. This nucleophile possesses little basicity and thus little nucleophilicity for the alpha carbon atom. This poses a problem as the attraction toward the carbon atom is minimised¹⁰⁸.

In addition, the leaving group plays an important role in the overall rate and success of the reaction. The best leaving groups are weak bases¹⁰⁸. This suggests that a $-Br$ leaving group is better than a $-Cl$ leaving group. By having $-Cl$ as the leaving group in this reaction, the energy of the transition state is much higher and this makes the reaction rate much lower, inhibiting product formation. A careful consideration of the properties required for an S_N2 reaction indicates that a product would not be obtained using this reaction.

2.3.1.4 2-Bromo-4-methylpropiophenone as intermediate to 4-MMC

The attempted conversion of the intermediate Br-M4 to the corresponding 4-MMC at 0°C was unsuccessful (refer reaction scheme Figure 2-1). The intermediate was a liquid at room temperature which suggested that a large portion of the synthesised sample contained methylamine and the resulting conversion to the 4-MMC product would not be viable with

the low purity intermediate available for the conversion. The reaction was kept at 0 °C throughout in an attempt to prevent di-substituted products from occurring. In addition, care was taken so that the two reactants; i.e. 4-methylpropiophenone and bromine; were kept at equal mole ratios in order to prevent side-products from occurring as a result of excess reactants.

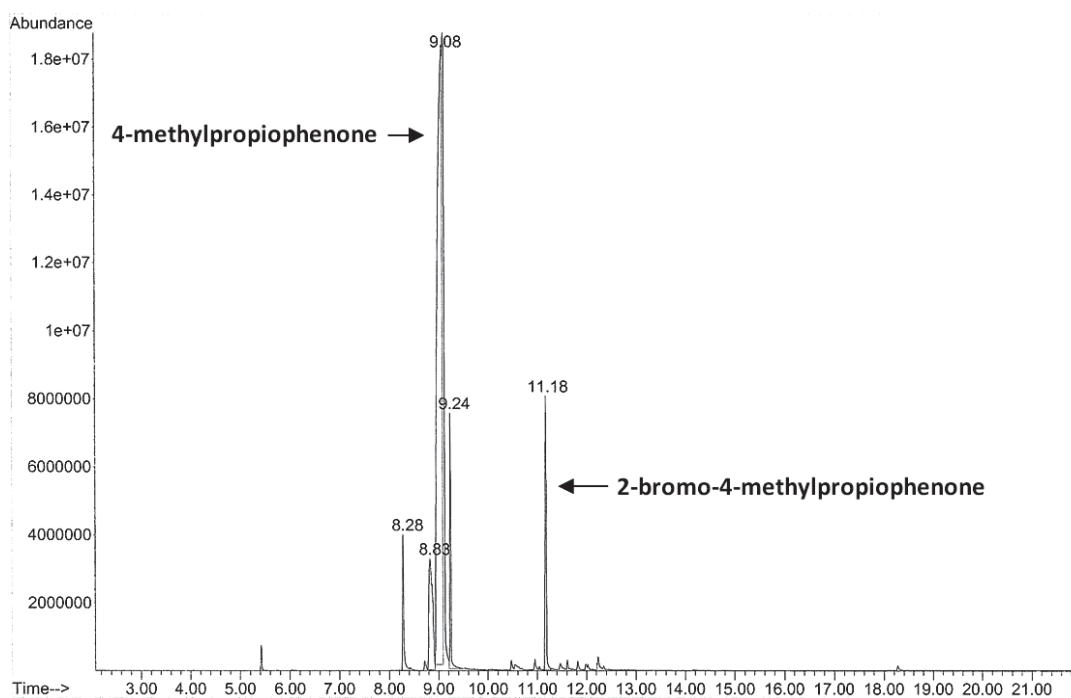


Figure 2-17 GC-MS chromatogram of 2-bromo-4-methylpropiophenone (Br-M4) at 11.2 minutes, 4-methylpropiophenone at 9.1 minutes (GC method 1).

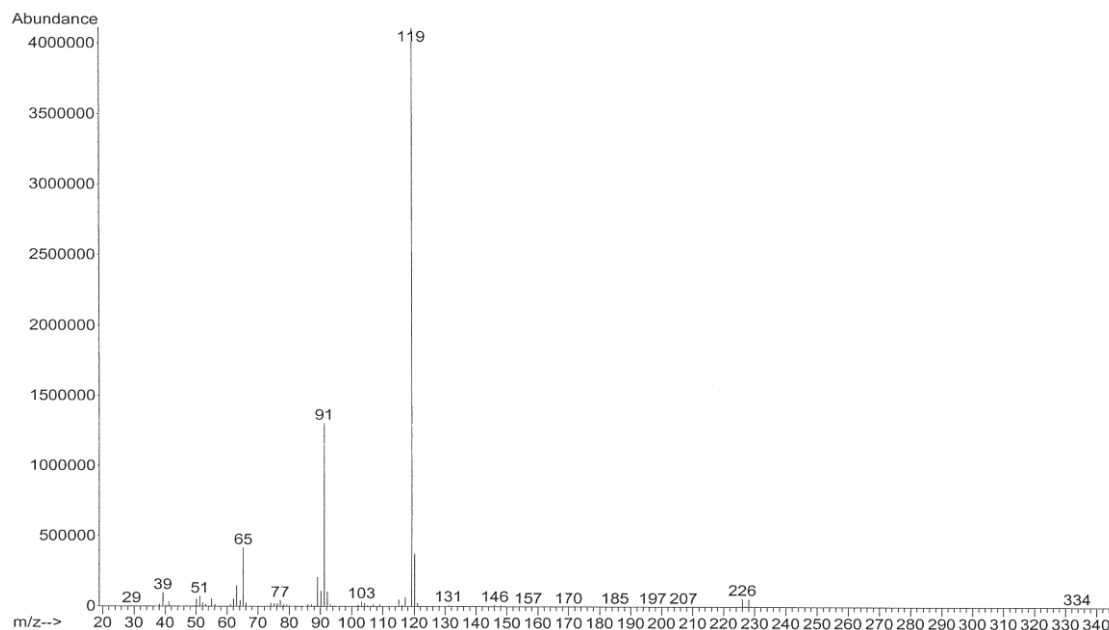


Figure 2-18 EI mass spectrum of 2-bromo-4-methylpropiophenone (Br-M4) (GC method 1).

The GC-MS chromatogram (Figure 2-17) exhibited a peak at 9.1 minutes indicating that there was still a large amount of the 4-methylpropiophenone starting material remaining (Figure 2-15 for 4-methylpropiophenone spectra and Figure 2-18). In addition there was a smaller peak of the intermediate 2-bromo-4-methylpropiophenone at 11.2 minutes which was supported by mass spectra. From the GC-MS results it was clear that the reaction did not go to completion and this suggests that the modifications made to the synthetic method were not successful. By keeping the mixture at 0 °C the α -bromination reaction was inhibited.

An alternate bromination reaction employing *N*-bromosuccinimide (section 2.2.1) showed promising results (98.9 % yield was obtained for the intermediate product 2-bromo-4-methylpropiophenone). Very little starting material (i.e. 4-methylpropiophenone) remained after the conversion.

2.3.2 1-Benzylpiperazine

The synthesised product BZP 1 was analysed by GC-MS (Figure 2-19 - Figure 2-21) and NMR (section 2.2.2). The by-product of the reaction was confirmed to be 1,4-dibenzylpiperazine (DBZP) and is commonly found in illicit BZP samples. The GC-MS chromatogram exhibited a peak at 4.9 minutes with m/z 176 corresponding to the product BZP, and another peak at 7.7

minutes with m/z 266 corresponding to the parent ion of DBZP (consistent with the literature^{109, 110}). In this reaction the two precursors, piperazine hexahydrate and benzyl chloride, were reacted in a 1:1 mole ratio. The ratio of DBZP to BZP 1 was ~1:8 as was evident in the ¹H-NMR spectra (Figure 2-22). The integrated proton values that are circled represent the DBZP product at 3.51 ppm (integration 0.26) and the major product BZP at 3.49 ppm (integration 2.09). The additional benzyl group (aromatic) in DBZP deshields the -CH₂ group resulting in a slight downfield shift. Further to this there are two additional peaks at 2.84 ppm and 2.50 ppm that correspond to the H5 and H6 proton environments on the piperazine ring of DBZP further confirming the presence of this by-product (Figure 2-23).

Further confirmation of this by-product was obtained using ¹³C-NMR (Figure 2-24). The three carbon signals circled correspond to C4₂ at 63.04 ppm, C5 at 53.06 ppm, and C6 at 47.32 ppm. The downfield shift of C6 can be explained due to the addition of the benzyl group acting to deshield this carbon environment. The very slight upfield shift observed for C4₂ and C5 may be attributable to the increased symmetry of the DBZP molecule, in which the deshielding effect of the two aromatic rings become evenly distributed across the molecule (having less effect on C4₂ and C5). Similarly in the ¹³C DEPT 135 experiment, the carbon environments circled also represent C4₂ at 63.09 ppm, C5 at 53.10 ppm, and C6 at 47.37 ppm respectively, (Figure 2-25) reiterating the fact that the impurity was in fact DBZP. These three carbon environments are in the negative segment of the spectra representing -CH₂ groups.

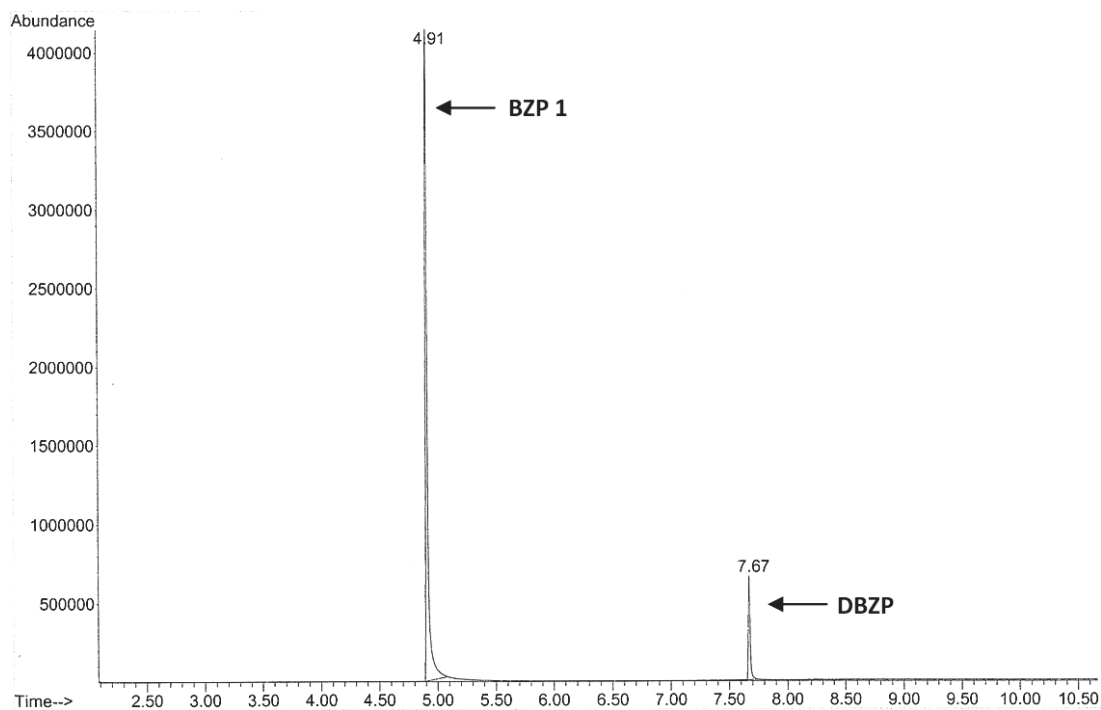


Figure 2-19 GC-MS chromatogram of BZP 1.HCl at 4.9 minutes, DBZP at 7.7 minutes (GC method 1).

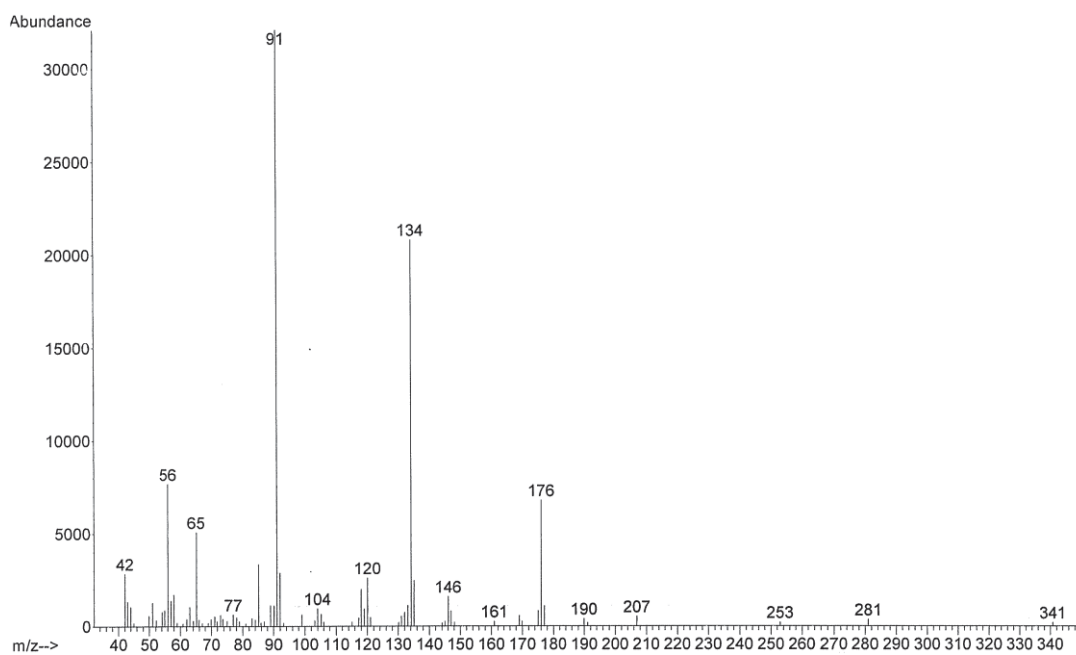


Figure 2-20 EI mass spectrum of BZP 1.HCl (GC method 1).

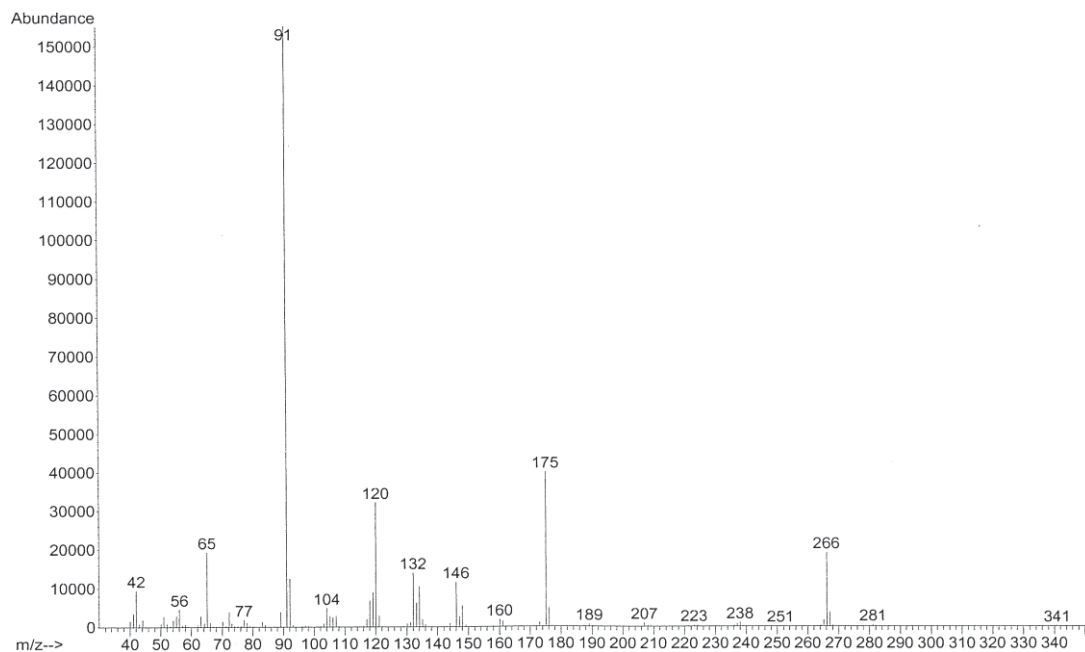
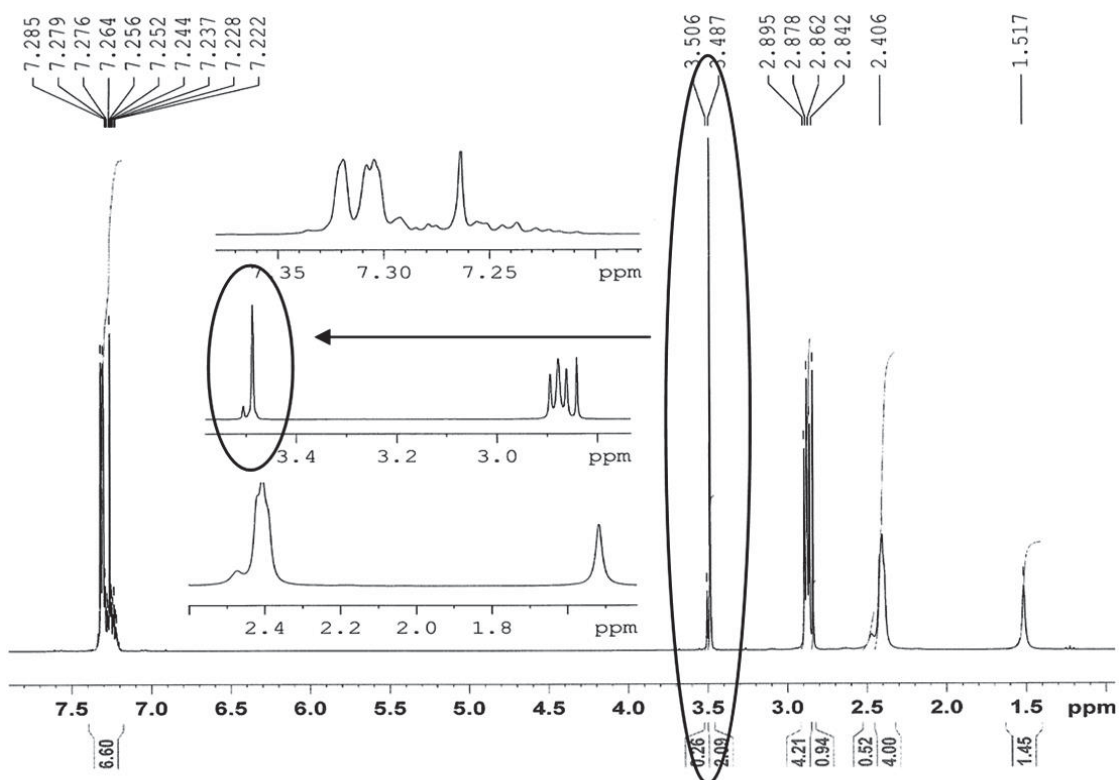


Figure 2-21 EI mass spectrum of DBZP (GC method 1).

Figure 2-22 ^1H NMR of BZP 1.

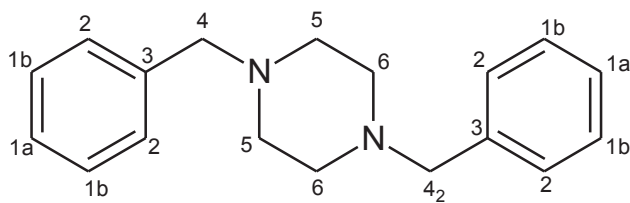
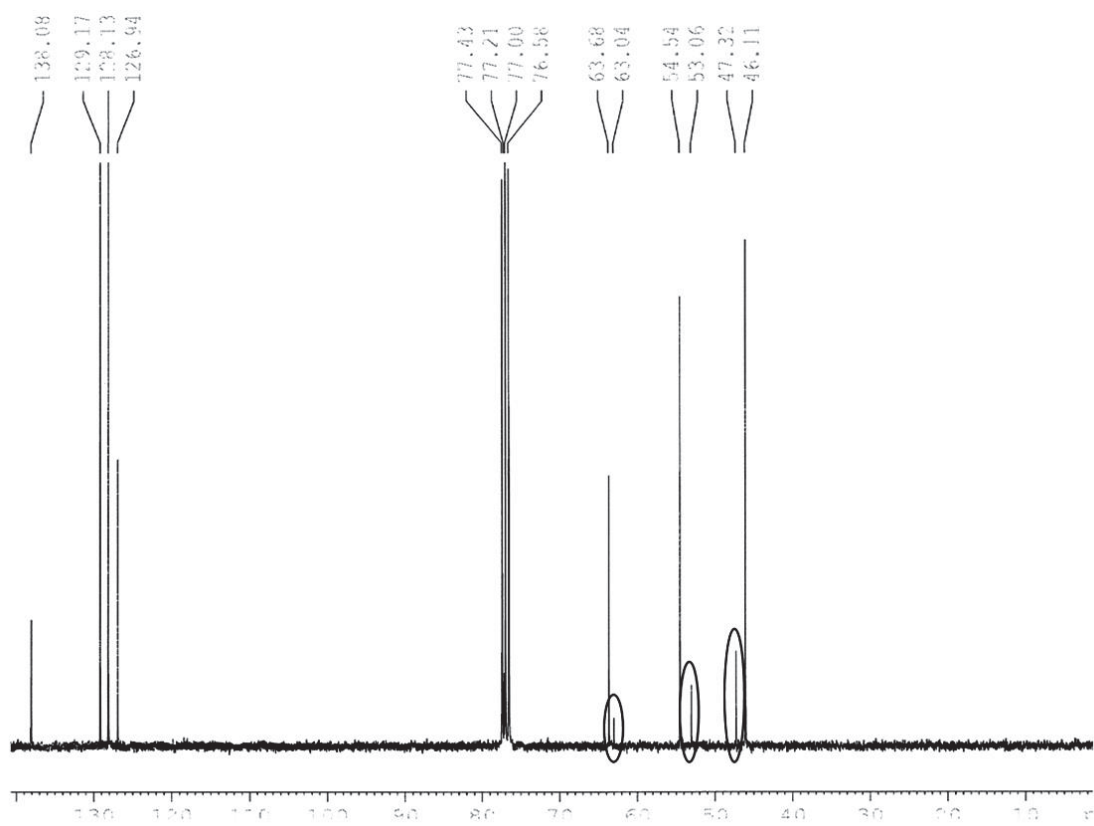


Figure 2-23 Molecular structure of DBZP.

Figure 2-24 ¹³C NMR of BZP 1.

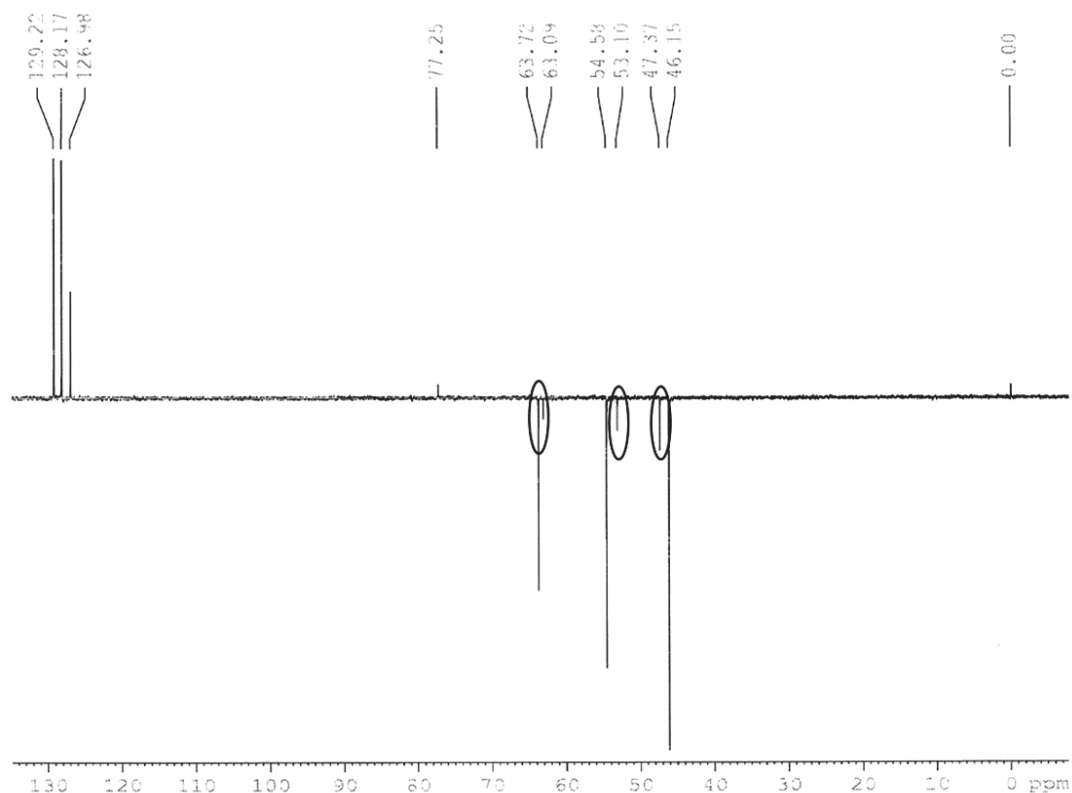


Figure 2-25 ^{13}C DEPT NMR of BZP 1.

The synthetic method (in the synthesis of BZP 1 – BZP 3) was altered in an attempt to minimise the amount of by-product formation. In the synthesis of BZP 2, the mole ratio of the reactants was 1:0.8 for piperazine hexahydrate to benzyl chloride, respectively. Based on the ^1H -NMR data obtained for this product it was evident that the ratio of DBZP:BZP had decreased to 1:16 (Figure 2-26) as the integration of the respective $-\text{CH}_2$ groups was 0.10: 1.64. This suggests that limiting the moles of the benzyl chloride starting material will in turn limit the amount of by-product formed in the reaction. It was hypothesised that the use of a large excess of piperazine (i.e. 10:1 mole ratio) would further aid in limiting the amount of by-product formation.

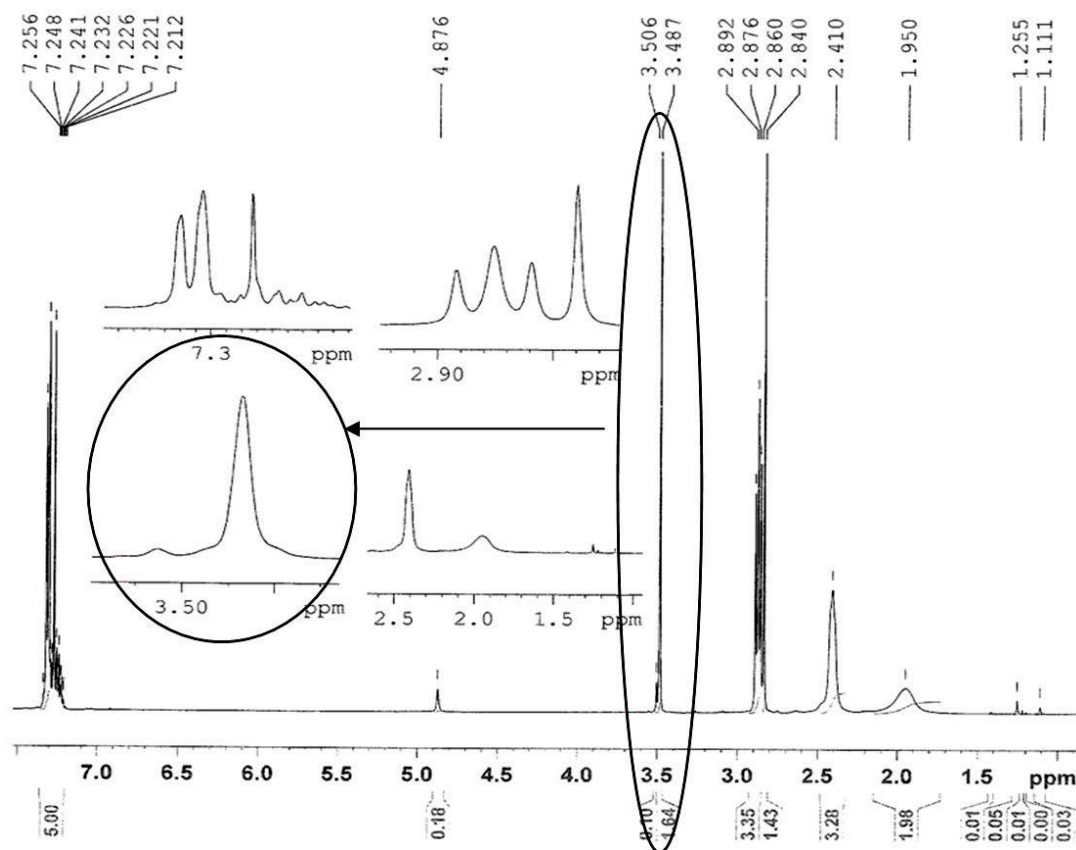


Figure 2-26 $^1\text{H-NMR}$ of BZP 2 showing ratio of DBZP to BZP signals.

In an attempt to maximise by-product formation in the synthesis of BZP 3, a large excess of the benzyl chloride starting material was used (1:3 mole ratio of piperazine hexahydrate to benzyl chloride). Increasing the amount of by-product was desirable in order to have samples with varying amounts of by-product for comparison using DESI-MS, GC-MS and LC-MS (i.e. for chemical profiling work, section 6.3.2). The reaction was conducted over 18 hours (instead of 30 minutes) and the reaction temperature was increased to 70 °C. All of these factors contributed to increasing the by-product formation dramatically. As was seen in the GC-MS chromatogram of BZP 3 (Figure 2-27, see Figure 2-20 and Figure 2-21 for BZP and DBZP spectra, respectively), the large peak at 8.5 minutes represented the by-product DBZP and the peak at 6.1 minutes was found to be BZP. Slight variations in retention times were observed for BZP and other compounds analysed using GC-MS, mainly due to two instruments being utilised throughout the study, i.e. GC method 1 and 2, and these are specified in the spectra provided.

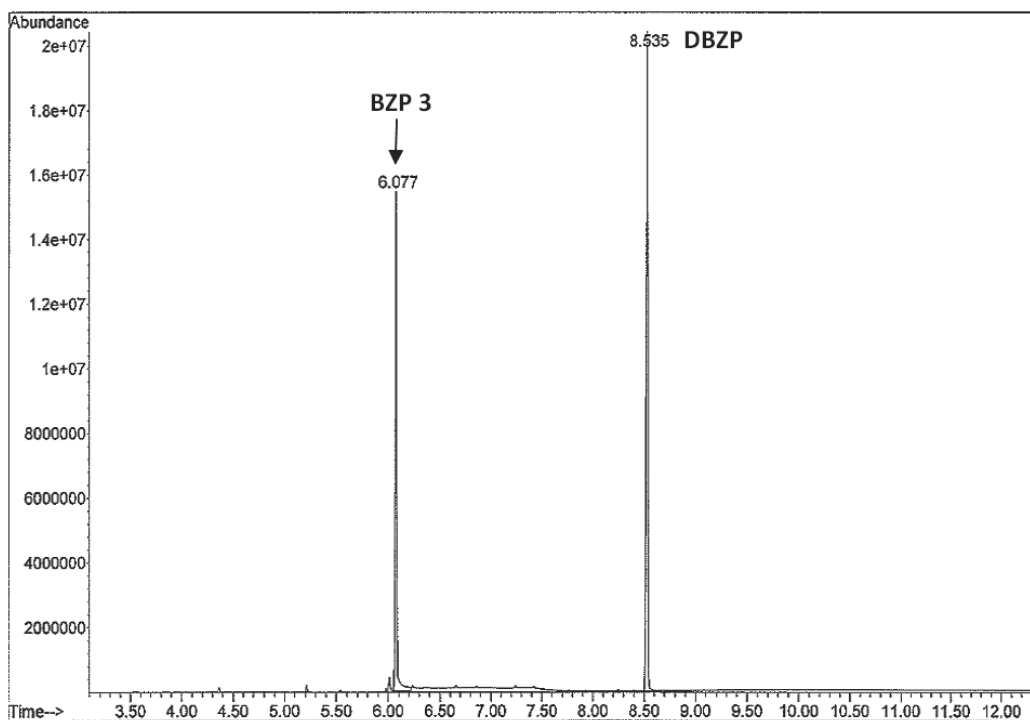


Figure 2-27 GC-MS chromatogram of BZP 3.HCl at 6.1 minutes, DBZP at 8.5 minutes (GC method 2).

During the synthesis of BZP 4 an alternate reaction scheme was utilised (section 2.2.2). This resulted in a mixture of by-products and impurities. From the GC-MS chromatogram, BZP 4 was identified as one of the major products at 5.0 minutes. Ethyl 1-benzyl-4-carboxypiperazine (EBCP) was identified at 6.8 minutes. This compound was present as unreacted intermediate. In addition, methyl 1-benzyl-4-carboxypiperazine (MBCP) and DBZP were identified at 6.6 minutes and 7.7 minutes, respectively (Figure 2-28 - Figure 2-30, see Figure 2-20 and Figure 2-21 for BZP and DBZP spectra, respectively). It was hypothesised that the by-product MBCP was formed as a result of transesterification between methanol and EBCP¹¹¹ (Figure 2-31).

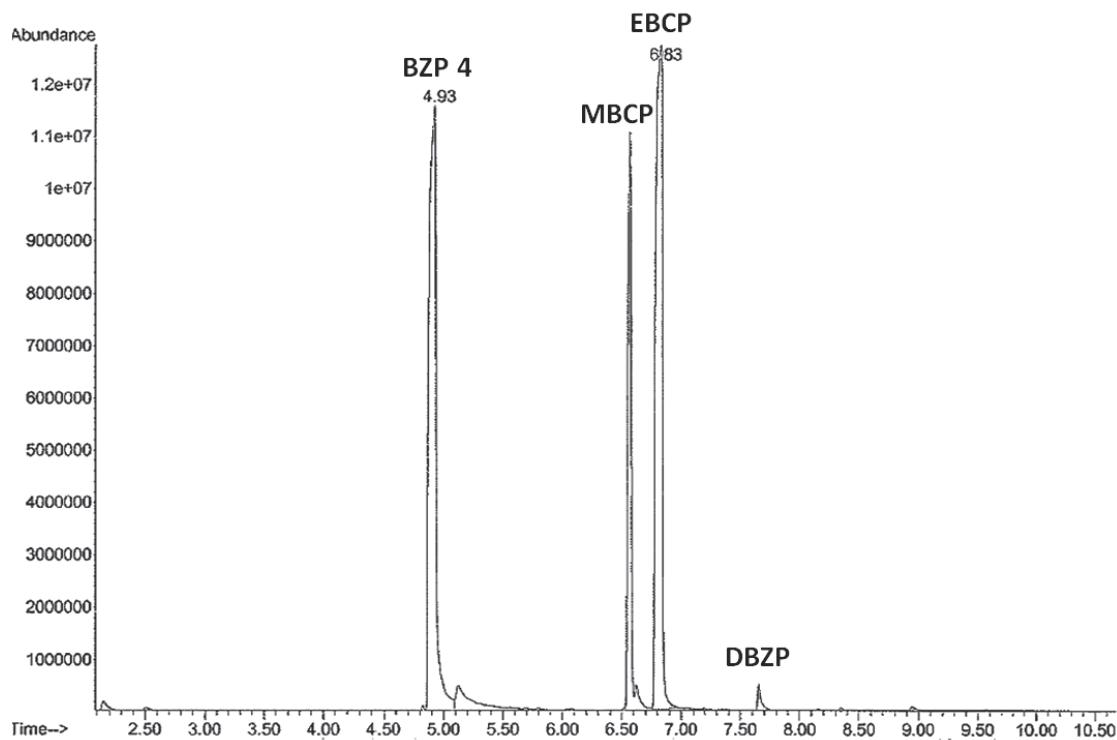


Figure 2-28 GC-MS chromatogram of BZP 4.HCl at 5.0 minutes, MBCP at 6.6 minutes, EBCP at 6.8 minutes, DBZP at 7.7 minutes (GC method 1).

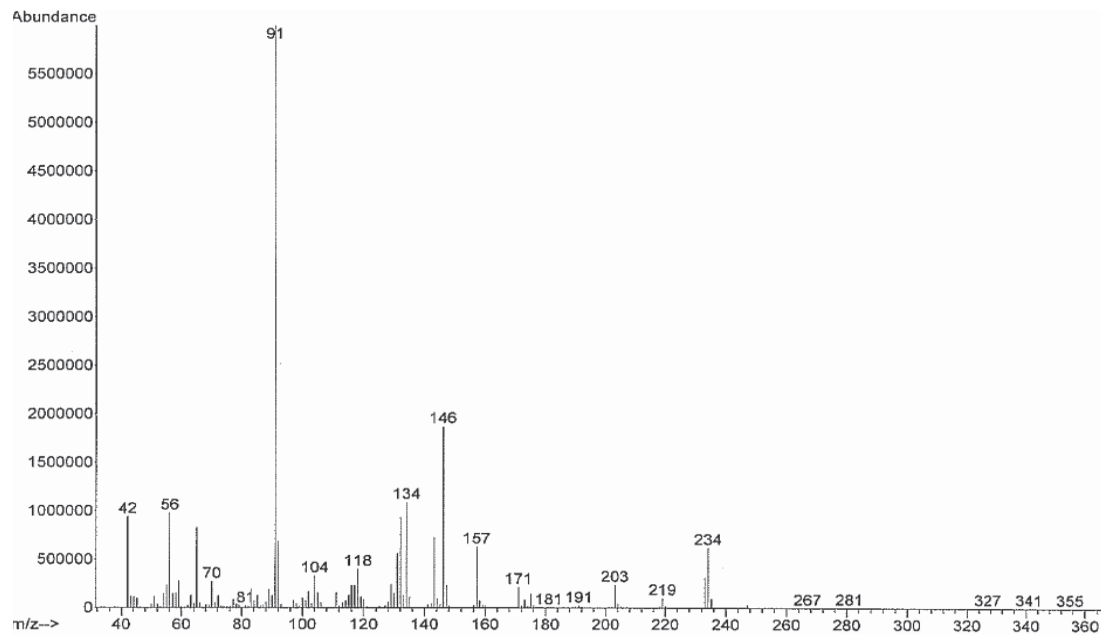


Figure 2-29 EI mass spectrum of MBCP (GC method 1).

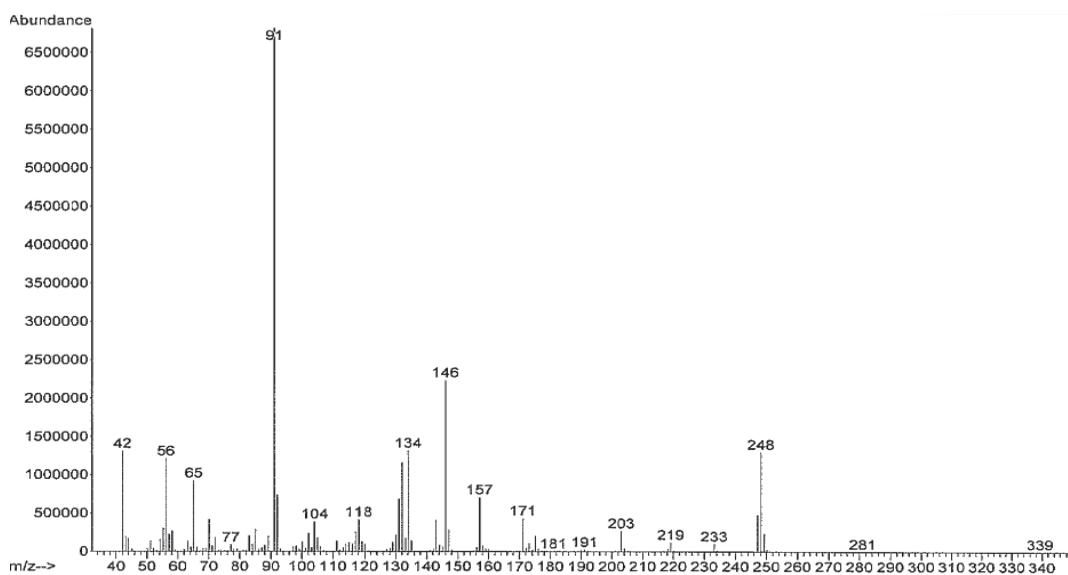


Figure 2-30 EI mass spectrum of EBCP (GC method 1).

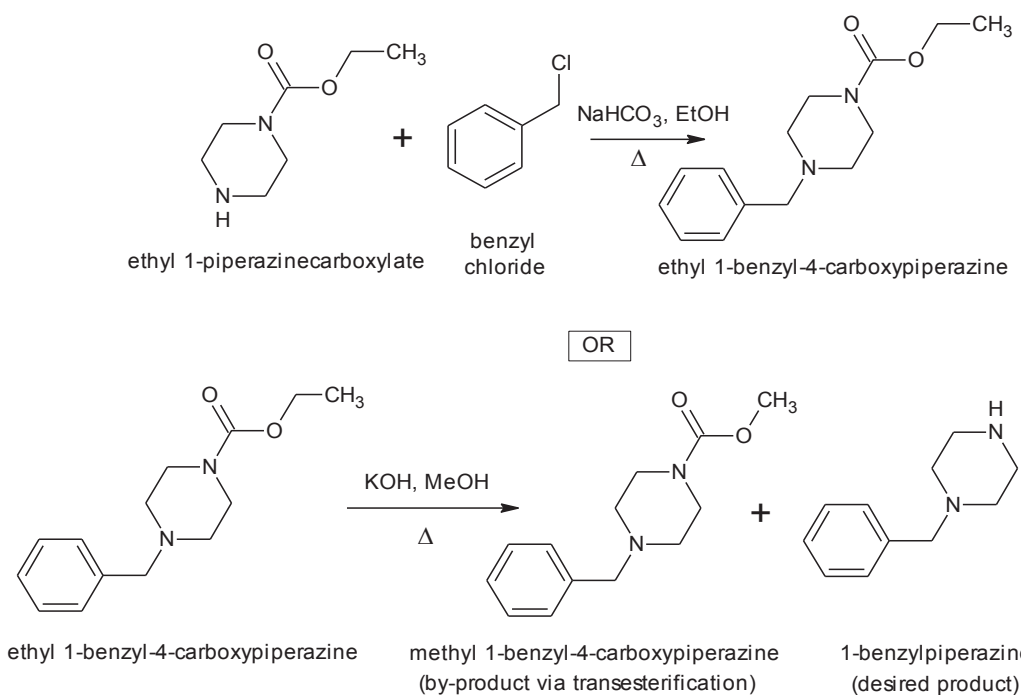


Figure 2-31 Proposed reaction scheme for the formation of ethyl 1-benzyl-4-carboxypiperazine and methyl 1-benzyl-4-carboxypiperazine.

2.3.3 3-Trifluoromethylphenylpiperazine

The reaction employed in the synthesis of 3-trifluoromethylphenylpiperazine (TFMPP 1 - TFMPP 3) is hypothesised to follow the “benzyne mechanism” (Figure 2-32, section 2.2.3). The starting material 3-chlorobenzotrifluoride contains a trifluoromethyl group at the 1-position and a chloro group at the 3-position. The trifluoromethyl group is electron-withdrawing which destabilises the benzene ring allowing the substitution of the chloro group to occur more readily. This speeds up the reaction and allows for the formation of the “benzyne” intermediate and subsequent product formation. The three TFMPP products were synthesised using different reaction conditions (section 2.2.3). The major product according to the proposed mechanism was TFMPP and the two minor products being 2-trifluoromethylphenylpiperazine and 4-trifluoromethylphenylpiperazine. A mixed product is observed due to the formation of two “benzyne” intermediates as illustrated in Figure 2-32 allowing for substitution at the *-ortho*, *-meta* and *-para* positions. The multiple peaks present in the GC-MS chromatograms of TFMPP 2 - TFMPP 3 are hypothesised to correspond to isomers of the product, i.e. 1-trifluoromethylphenylpiperazine, 2-trifluoromethylphenylpiperazine, 3-trifluoromethylphenylpiperazine; indicative of the *ortho*-, *meta*- and *para*- substituted TFMPP, respectively (Figure 2-37 - Figure 2-39).

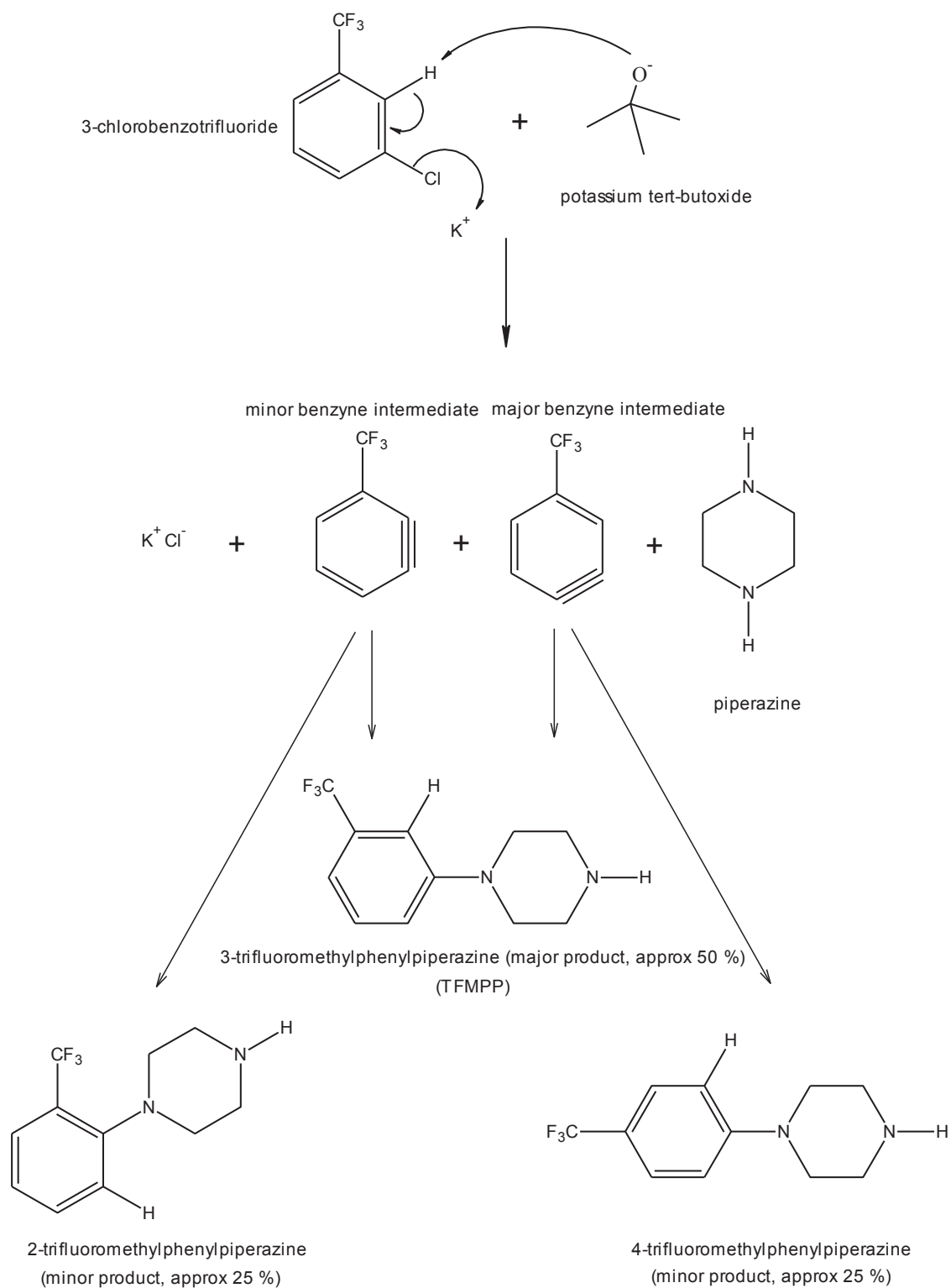


Figure 2-32 Reaction mechanism for the formation of 3-trifluoromethylphenylpiperazine (TFMPP), 2-trifluoromethylphenylpiperazine and 4-trifluoromethylphenylpiperazine.

TFMPP 1 – TFMPP 3 resulted in different by-products/impurities due to different reaction conditions utilised. The respective yields were 49 %, 55 % and 48 %. Higher yields were limited by the equipment used as the solution temperature could not be increased in excess of 140 °C. The third synthesis was conducted in an ace pressure tube; however, this did not result in increased yields.

TFMPP 1 exhibited no impurities in the GC-MS chromatogram (Figure 2-33 - Figure 2-34). The impurities resulting from the synthesis of TFMPP 2 include 3-chlorobenzotrifluoride at 3.2 minutes, 3-trifluoromethylphenol at 4.0 minutes, and 2,4-bis(1,1-dimethylethyl)phenol at 6.1 minutes (Figure 2-35). 2,4-Bis(1,1-dimethylethyl)phenol was thought to be present due to column bleeding effects at high temperatures. The presence of the impurity, 3-trifluoromethylphenol, was thought to be due to a minor side-reaction between 3-chlorobenzotrifluoride and water (moisture in solvent toluene) in which the –Cl group is substituted with a hydroxy group. Interestingly, this side-reaction did not occur in TFMPP 1 or TFMPP 3 possibly due to lower moisture levels. The synthesis of TFMPP 3 resulted in fewer by-products (Figure 2-36), however the presence of isomers is apparent (Figure 2-37 - Figure 2-39). Piperazine was detected at 2.9 minutes and this was carried through as unreacted starting material.

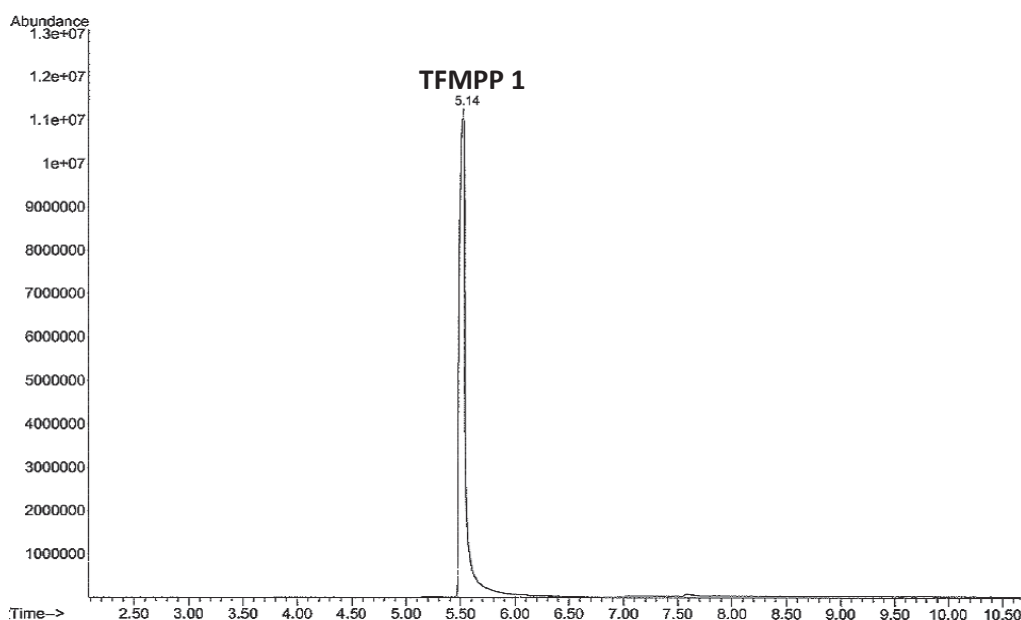


Figure 2-33 GC-MS chromatogram of TFMPP 1 at 5.1 minutes (GC method 1).

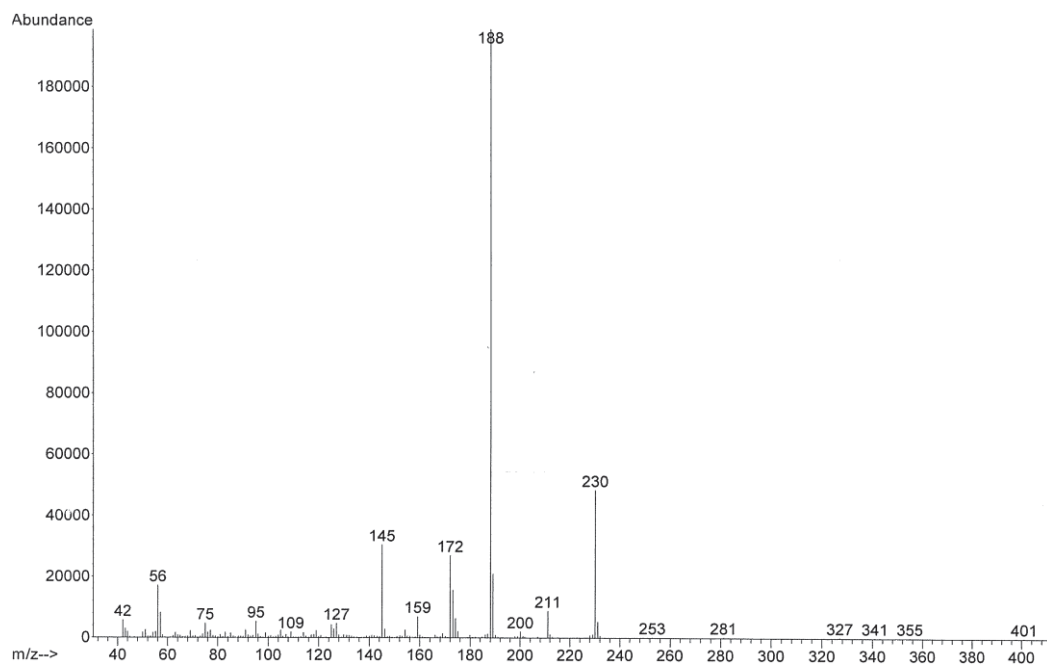


Figure 2-34 EI mass spectrum of FMPP (GC method 1).

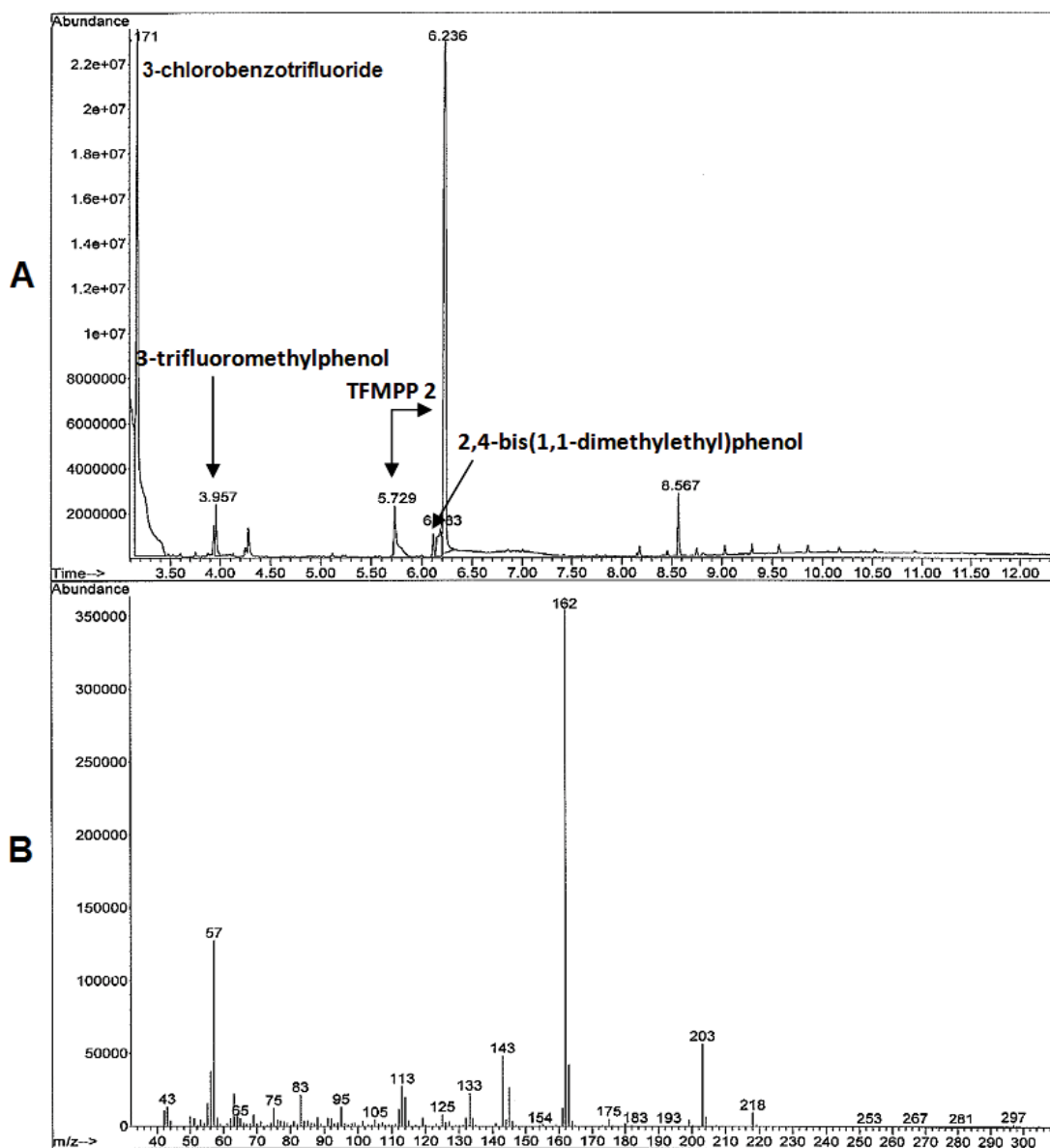


Figure 2-35 A: GC-MS chromatogram of TFMPP 2.HCl at 5.7 minutes and 6.2 minutes, 3-chlorobenzotrifluoride at 3.2 minutes, 3-trifluoromethylphenol at 4.0 minutes; B: EI mass spectrum of 3-trifluoromethylphenol (GC method 2).

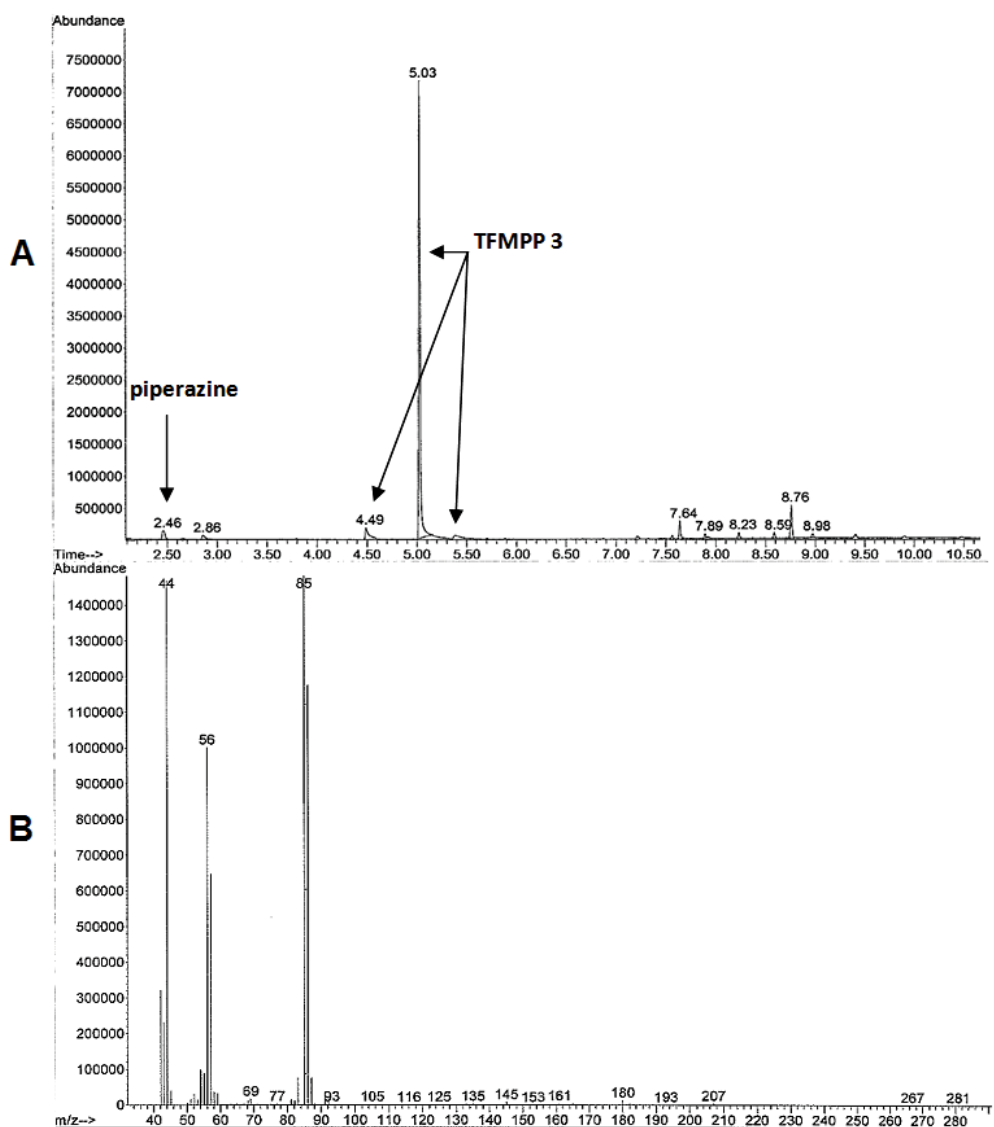


Figure 2-36 A: GC-MS chromatogram of TFMPP 3.HCl at 4.5 minutes, 5.0 minutes, 5.3 minutes; piperazine at 2.5 minutes; **B:** EI mass spectrum of piperazine (GC method 1).

An alternate reaction was utilised in the synthesis of TFMPP 4 that involved bis(2-chloroethyl)amine and 3-(trifluoromethyl)aniline. The desired end-product was obtained with high purity. Only trace amounts of unreacted 3-(trifluoromethyl)aniline were detected in the GC-MS chromatogram (Figure 2-40). No other by-products or impurities were found.

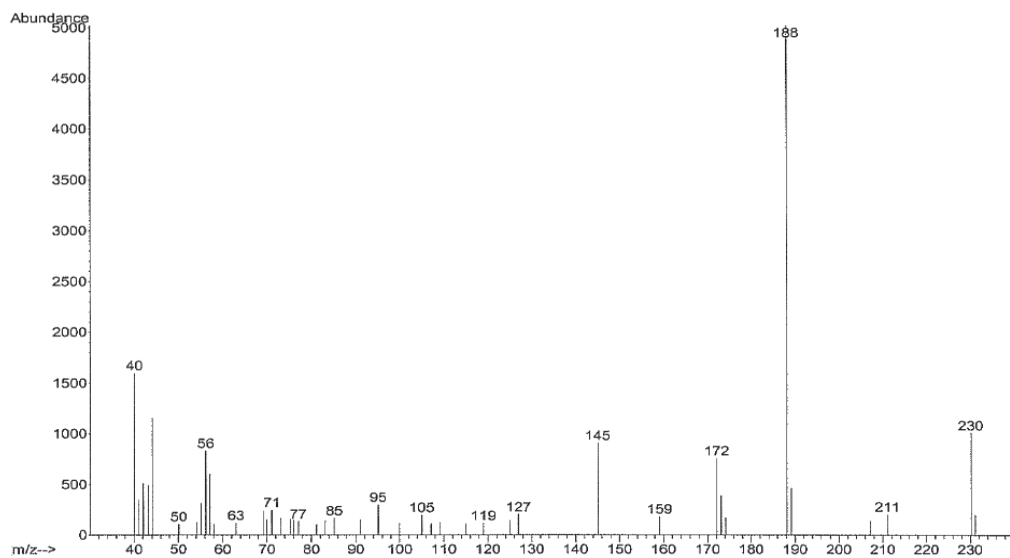


Figure 2-37 EI mass spectrum of TFMPP at 4.5 minutes (GC method 1).

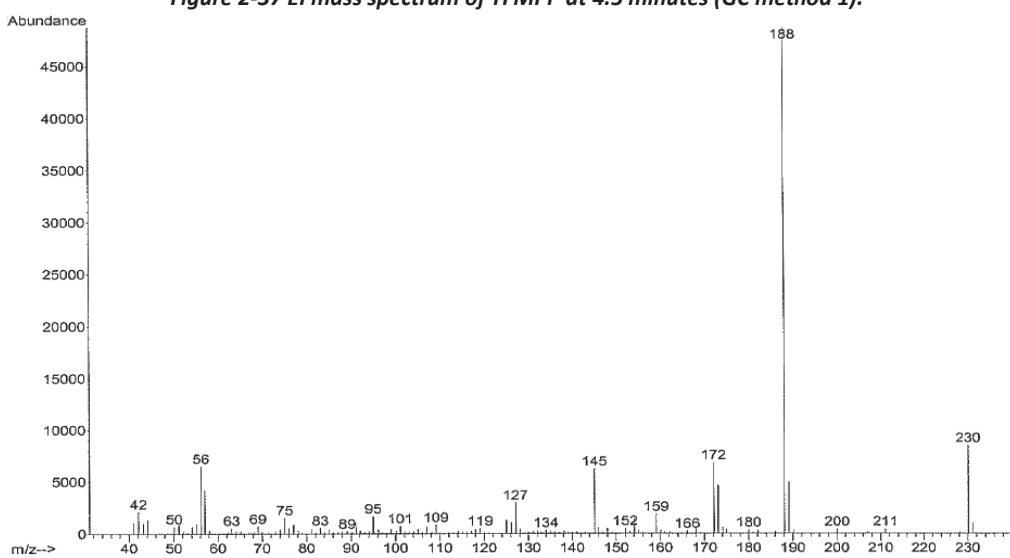


Figure 2-38 EI mass spectrum of TFMPP at 5.0 minutes (GC method 1).

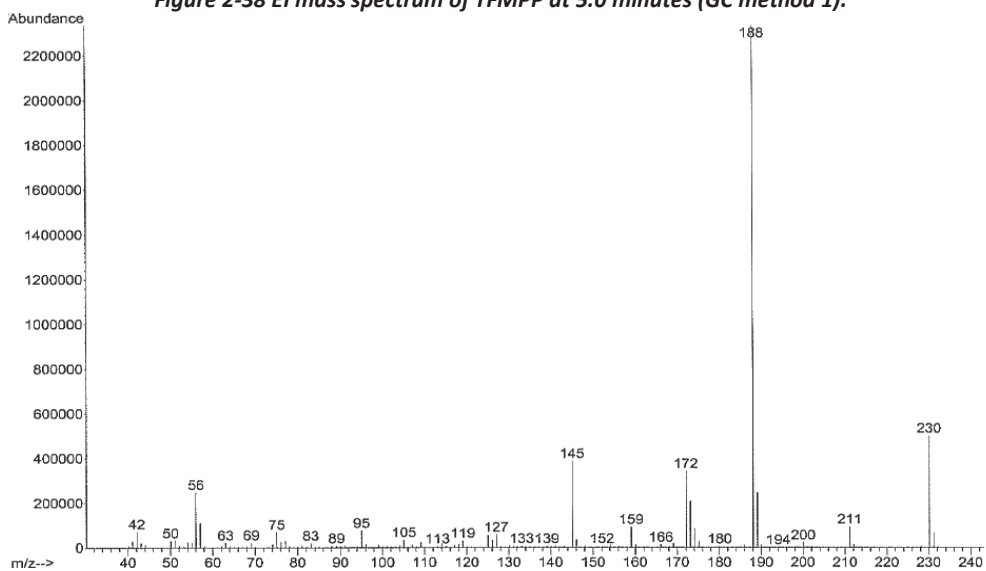


Figure 2-39 EI mass spectrum of TFMPP at 5.3 minutes (GC method 1).

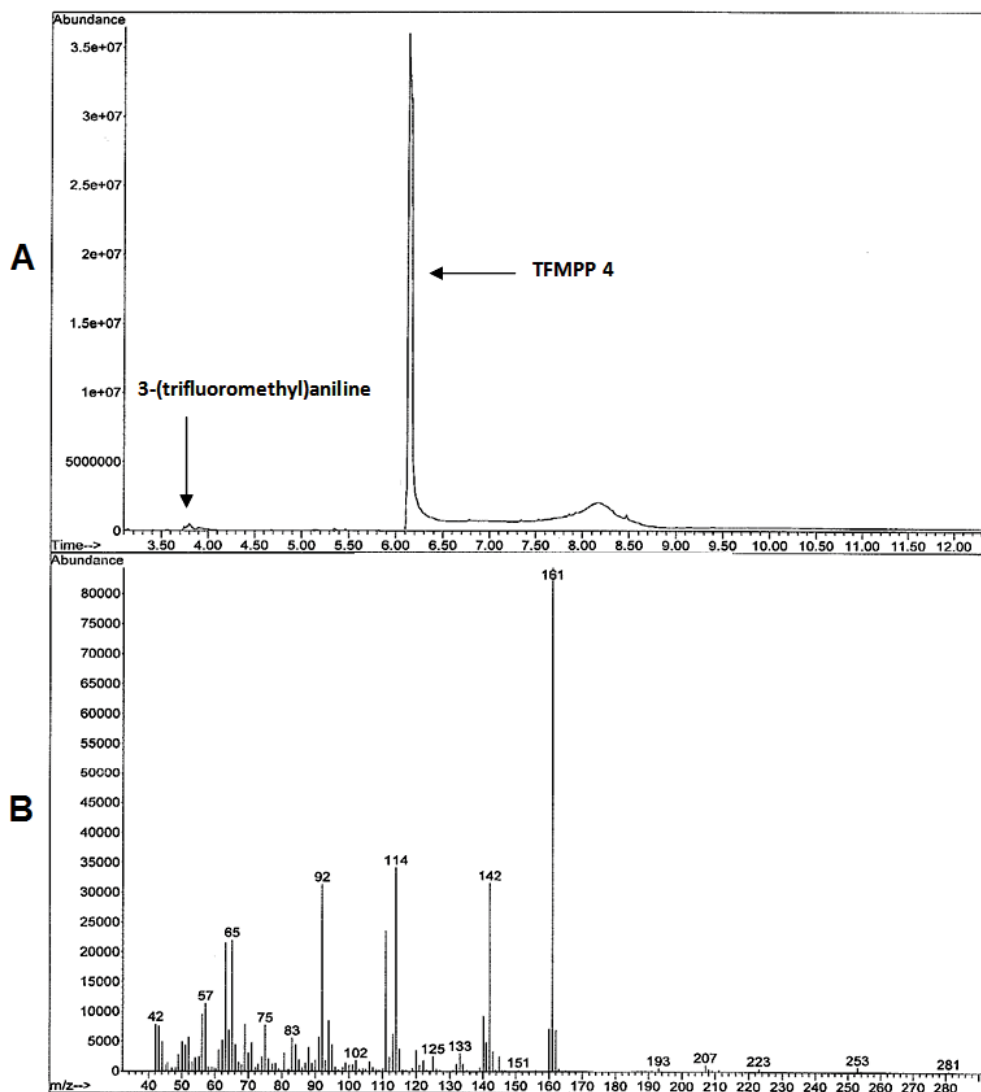


Figure 2-40 A: GC-MS chromatogram of TFMPP 4.HCl at 6.2 minutes, 3-(trifluoromethyl)aniline at 3.8 minutes; B: EI mass spectrum of 3-(trifluoromethyl)aniline (GC method 2).

2.3.4 3-Chlorophenylpiperazine

Despite attempts at synthesising mCPP via two reaction schemes no product was obtained. A number of limitations have been associated with the formation of mCPP via the reaction between 1,2-dichlorobenzene or 1,3-dichlorobenzene and piperazine hexahydrate in the presence of potassium tert-butoxide base. The first being the starting materials themselves; i.e. 1,2- and 1,3-dichlorobenzene have two chlorine atoms attached to the benzene ring. In order for this reaction to proceed, one of the chlorine atoms must undergo substitution with piperazine. Chlorine being an electron-withdrawing group suggests that it is a good leaving

group; however, competition between the two chlorine atoms makes this an unlikely event (benzyne intermediate will be unstable; therefore, equilibrium lies to the reactants side). Other factors including the reaction being extremely sensitive to water will also inhibit product formation. It was evident from the GC-MS chromatogram below that a majority of the starting material remained, suggesting the lack of product formation (Figure 2-41). Alternate metal-catalysed reactions utilising Pd or Pt, instead of potassium tert-butoxide base, may be more successful in producing mCPP; however, this was beyond the scope of this study.

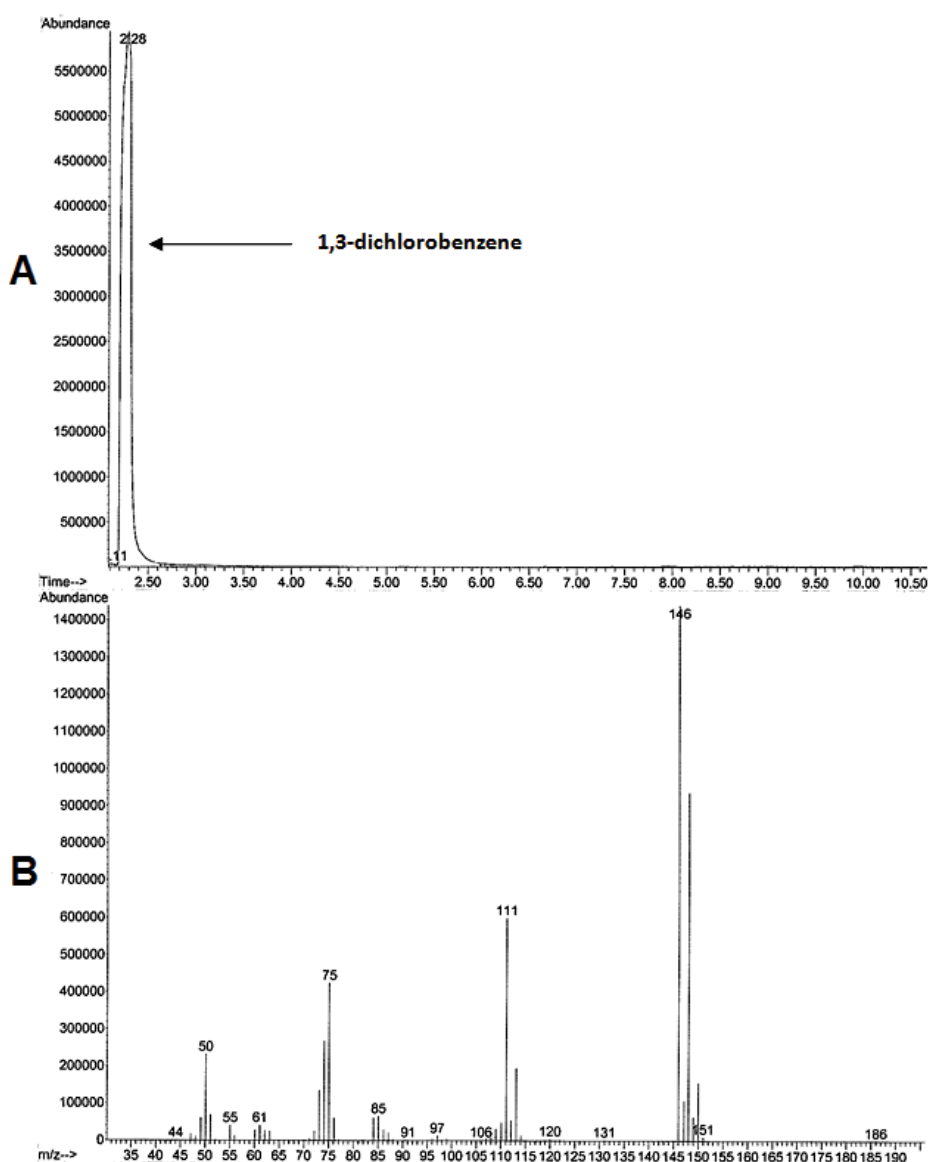


Figure 2-41 A: GC-MS chromatogram of 1,3-dichlorobenzene at 2.3 minutes; B: EI mass spectrum of 1,3-dichlorobenzene (GC method 1).

An alternate reaction was utilised in the synthesis of mCPP 1 that involved bis(2-chloroethyl)amine and 3-chloroaniline (section 2.2.4). The desired end-product was obtained with high purity. Only trace amounts of unreacted 3-chloroaniline were detected in the GC-MS chromatogram (Figure 2-42 - Figure 2-43). No other by-products or impurities were found.

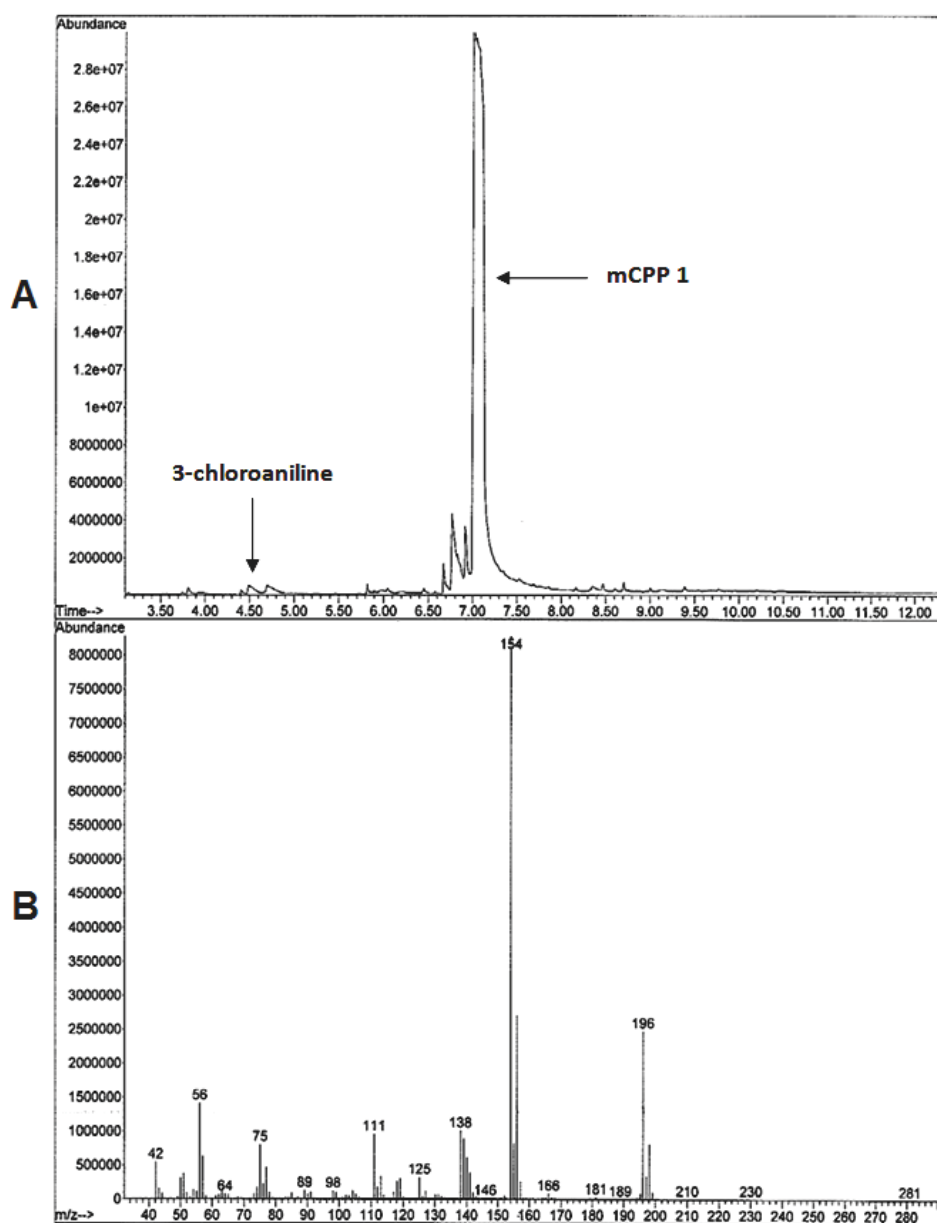


Figure 2-42 A: GC-MS chromatogram of mCPP 1.HCl at 7.2 minutes, 3-chloroaniline at 4.5 minutes; B: EI mass spectrum of mCPP (GC method 2).

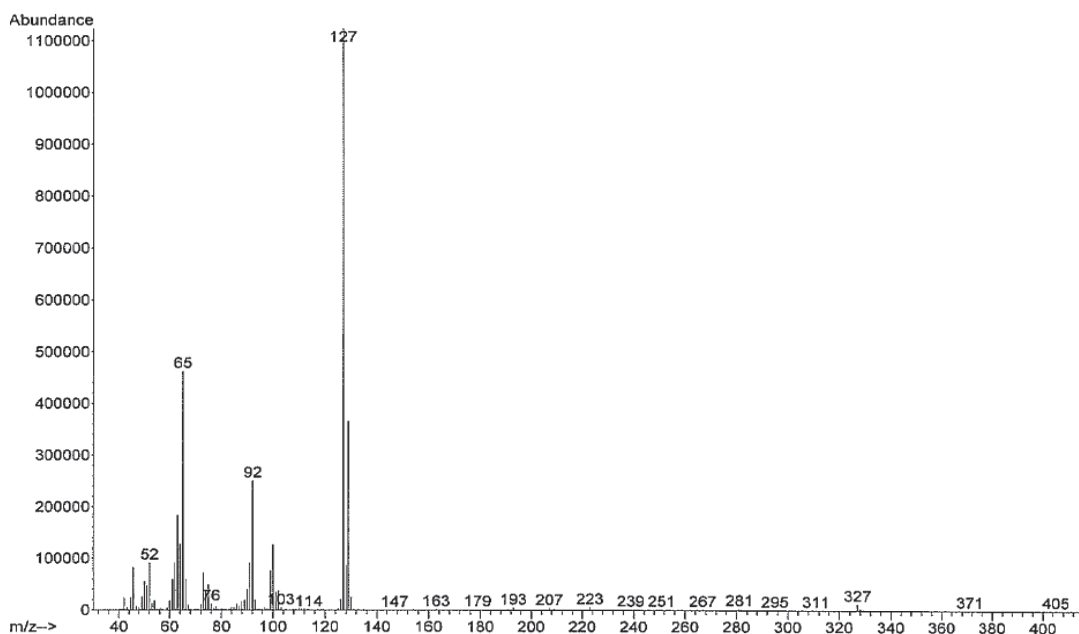


Figure 2-43 EI mass spectrum of 3-chloroaniline (GC method 2).

2.3.5 4-Methoxyphenylpiperazine

Despite numerous attempts at synthesising 4-methoxyphenylpiperazine according to the synthesis reaction adapted from Beller *et al.*¹¹² (section 2.2.5) no product was obtained. Various limitations were associated with the formation of this product, mostly due to the type of reaction involved (“benzyne mechanism”). The starting material 2-chloroanisole (Figure 2-44) contains a methoxy group and a chloro group at the 2-position, the leaving group in this reaction (Figure 2-45 shows the proposed reaction mechanism). In order for the reaction to proceed, the chloro group must be removed via a strong base (slow step in reaction) in order for the substitution of the piperazine ring to commence. However, this substitution was greatly hindered by the electron-donating methoxy group present on the benzene ring stabilising the ring and in turn deeming the ‘slow step’ of this reaction an unlikely event¹¹³. Further to this, if the proposed benzyne intermediate formed, then the end-product resulting from this reaction would be directed to the *-meta* position and not the *-para* position¹¹³.

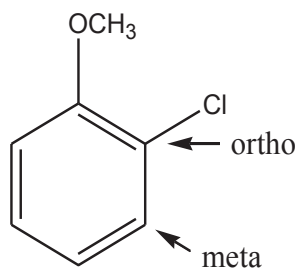


Figure 2-44 Structure of 2-chloroanisole starting material.

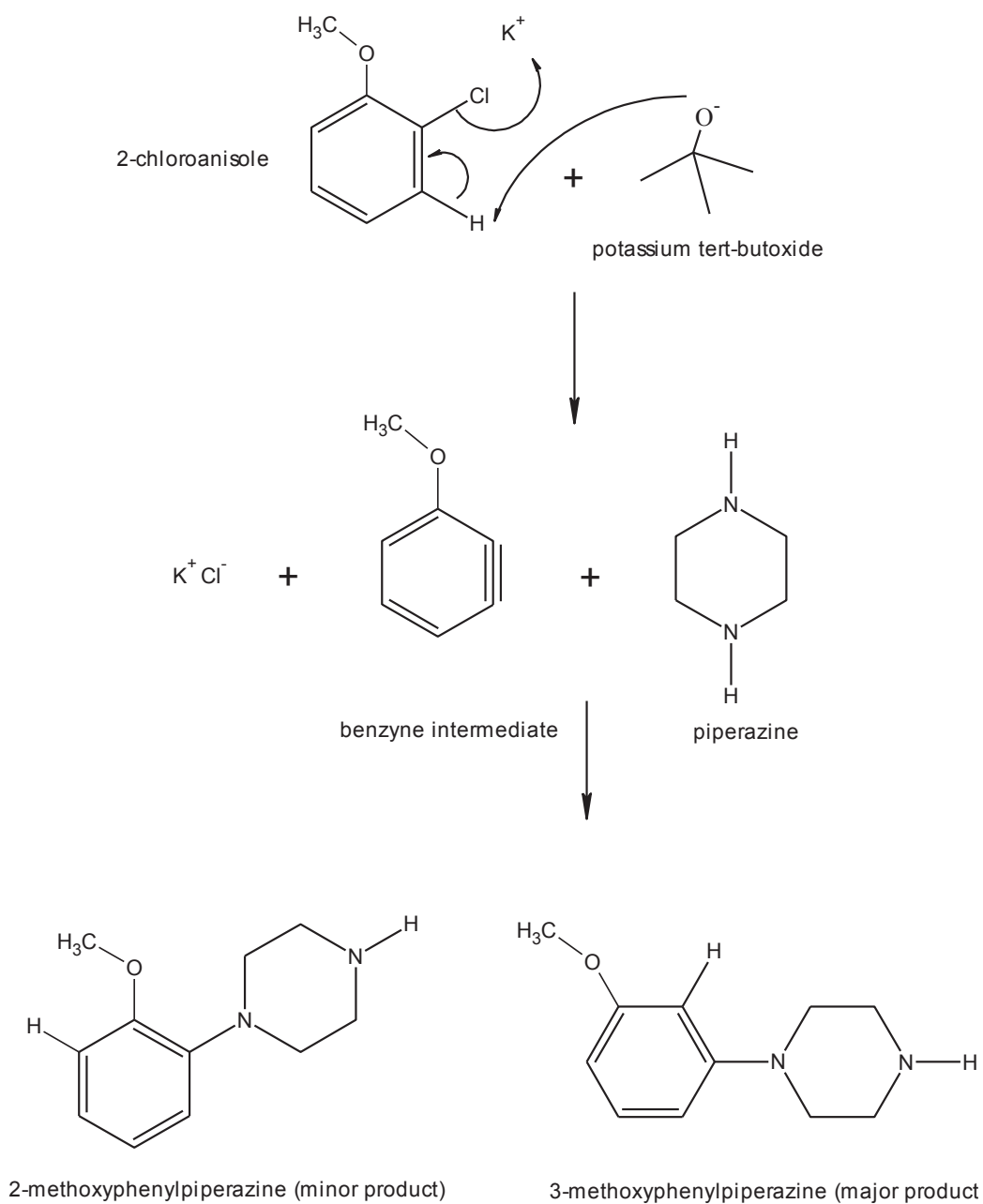


Figure 2-45 Proposed reaction mechanism for the formation of 2-methoxyphenylpiperazine and 3-methoxyphenylpiperazine.

An alternate reaction involving bis(2-chloroethyl)amine and 4-anisidine was successful in obtaining the desired end-product (MeOPP 1, Figure 2-46 - Figure 2-48). The resulting chromatogram suggests low levels of impurities with trace amount of unreacted starting material remaining. No other by-products resulted in this reaction.

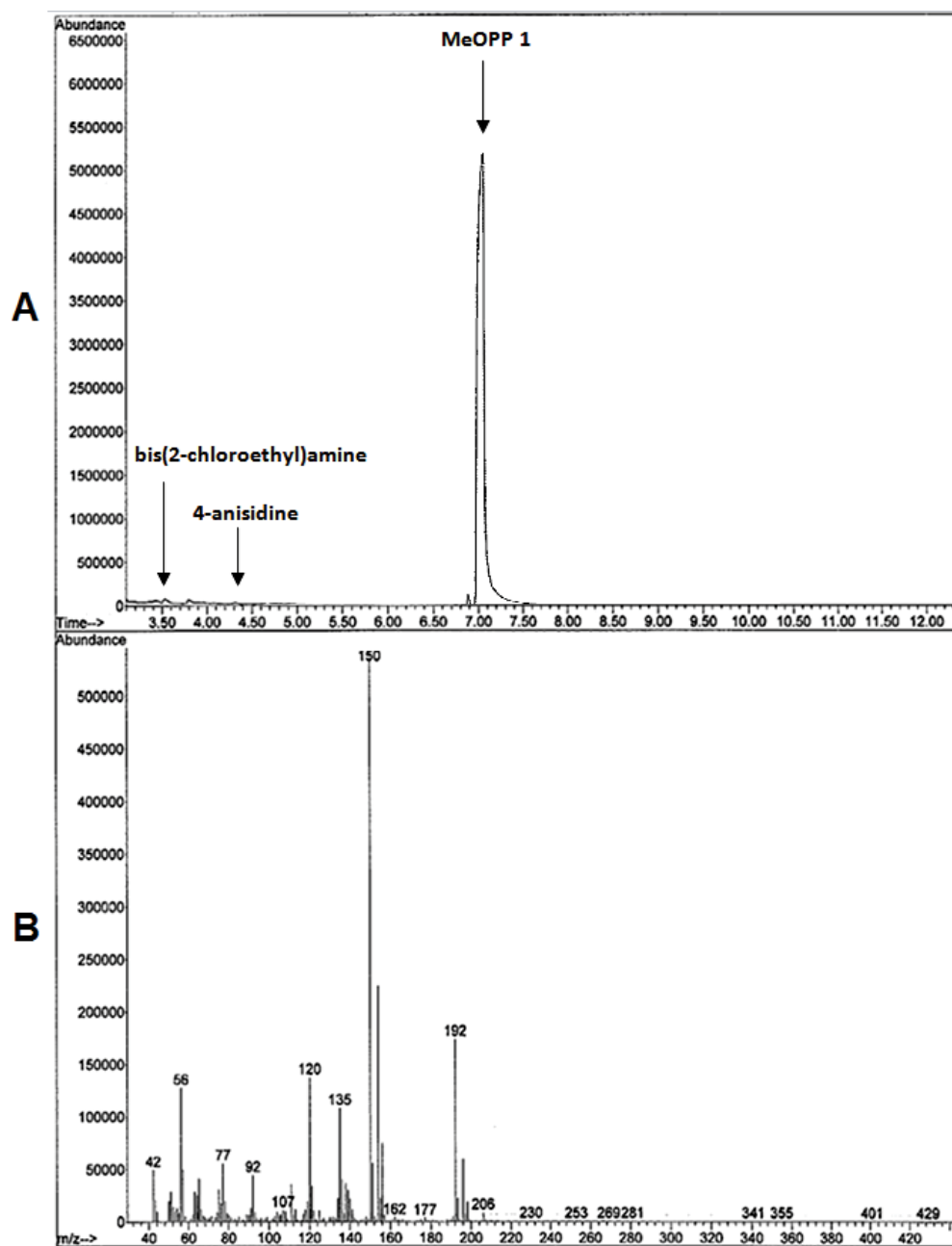


Figure 2-46 A: GC-MS chromatogram of MeOPP 1.HCl at 7.1 minutes, bis(2-chloroethyl)amine at 3.5 minutes, 4-anisidine at 4.3 minutes; B: EI mass spectrum of MeOPP (GC method 2).

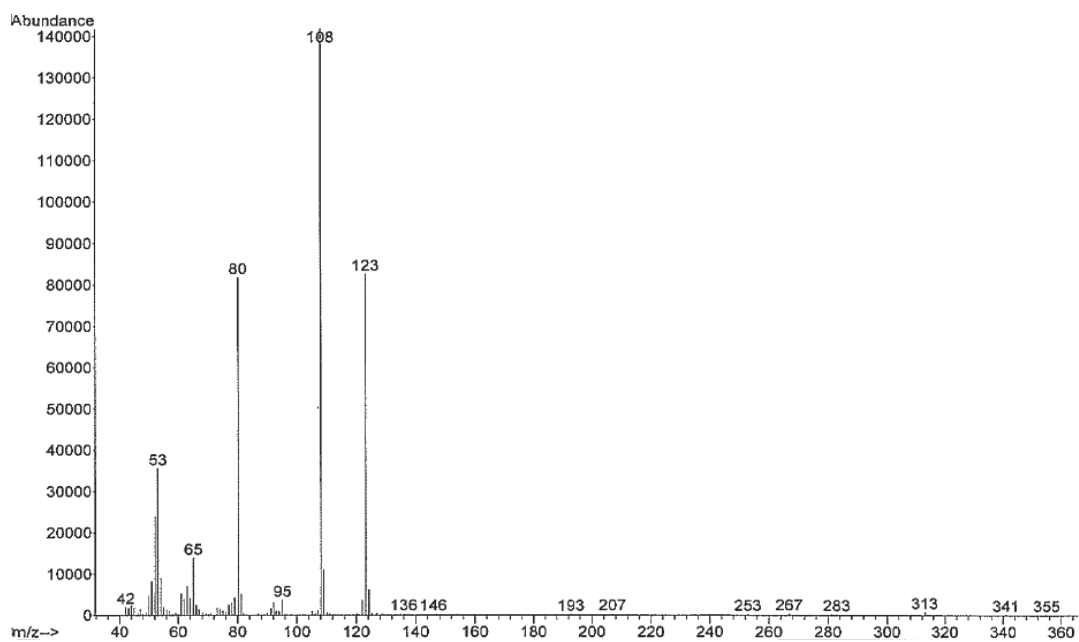


Figure 2-47 EI mass spectrum of 4-anisidine (GC method 2).

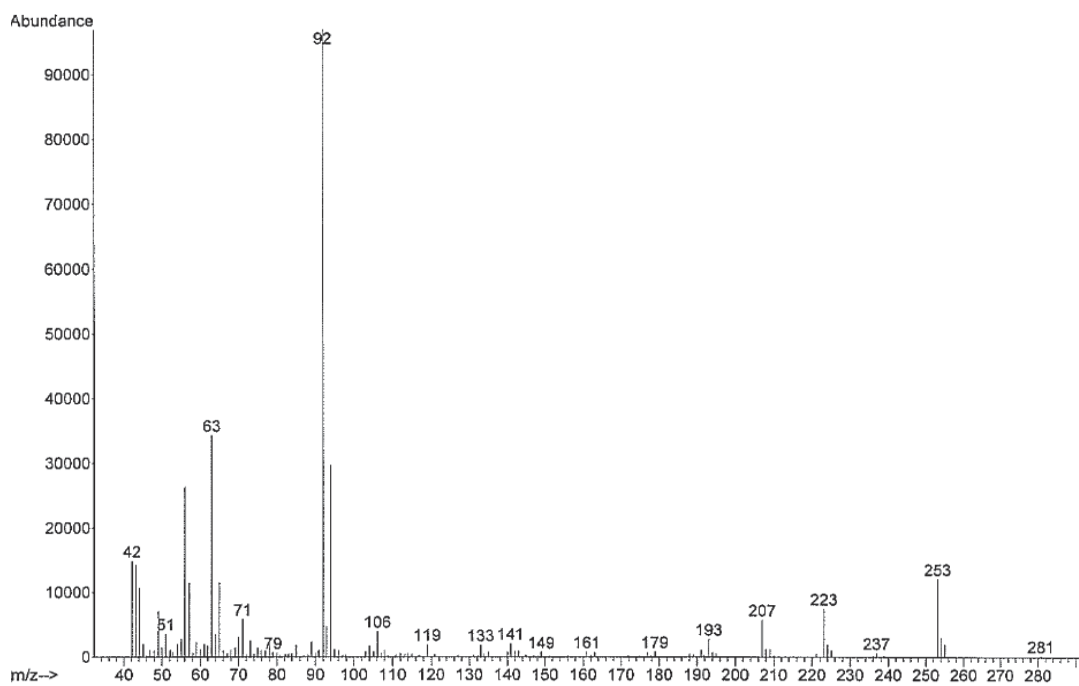


Figure 2-48 EI mass spectrum of bis(2-chloroethyl)amine (GC method 2).

2.4 Conclusions

Using the synthetic methods above, 4-MMC, BZP, TFMPP, mCPP and MeOPP were successfully synthesised. These compounds were subsequently analysed by DESI-MS, GC-MS and LC-MS (section 6.3.2 - 6.3.4 and 7.3.1 - 7.3.2). The by-products and impurities present were consistent with the synthetic routes of manufacture employed and aided in providing information that may be useful in linking synthetic batches in future chemical profiling work.

Chapter 3: Method development and validation

Chapter 3: Method development and validation

3.1 Introduction

A significant number of parameters have an effect on DESI-MS performance. The parameters of most importance include geometric parameters (α , β , d_1 , d_3 , Figure 1-8), spray parameters (gas and solvent flow rates, high voltage), chemical parameters (sprayed solvent, solvent used for deposition of sample), and surface parameters (composition, temperature, potential)⁷⁸. With regard to geometric parameters, α and d_1 have direct effects on the desorption and ionisation processes, while the other two parameters have important effects on the collection efficiency and, hence, on the sensitivity of the method. The optimal setting is generally 5 - 10° for β and 0 - 2 mm for d_3 . Previous reports suggest that high α values are preferred (angle measured from the sample surface), although considerable increases in chemical noise are observed above 80°⁷⁸. The position of the spray tip, both within the spray head and relative to the surface to be analysed, is critical for the success of DESI-MS. Green *et al.*⁷⁹ have recommended that the tip is positioned centrally within the gas flow, the tip protrusion is optimised, the tip position relative to the surface is optimised, and the tip position relative to the sniffer is optimised.

Additionally, the electrospray voltage, which is typically applied directly to the ESI spray tip, affects the amount of charge on the electrospray droplets and hence will affect the signal intensity. Experiments have revealed that the signal intensity rises with electrospray voltage, since more charge is available to create ions⁷⁹. However, it should be noted that a voltage greater than 5000 V causes unstable signal intensity, perhaps due to the build-up of charge at the surface of the sample.

Interestingly, Takats *et al.*⁷⁸ have shown that some of the geometrical parameters (such as d_1 and d_3) may have different optimal values for different analytes. Additionally, even using the same analyte small variations in the optimal values from day to day can be observed. This may be due to small differences in humidity or nebulising gas and solvent flow rates.

This chapter details the optimisation of a number of parameters essential for the DESI-MS analysis of small drug compounds. Inter-dependent parameters were first identified using a FFD followed by their optimisation using a CCD. All other parameters were optimised OFAT. In addition, GC-MS and LC-MS methods were optimised for the analysis and comparison of compounds analysed using DESI-MS.

3.2 Materials and methods

A range of solvents were utilised throughout this project in order to obtain the optimal solvent for the analysis of small drug molecules (Table 3-1).

Table 3-1 List of mixtures tested for optimal solvent composition.

Solvent	Mixture
1	methanol
2	methanol/water (1:1)
3	methanol/water (1:1) + 1 % formic acid
4	methanol/water (1:1) + 1 % ammonium formate
5	methanol/water (1:1) + 1 % acetic acid
6	water + 1 % formic acid
7	methanol + 1 % formic acid
8	methanol/water (1:3) + 1 % formic acid
9	methanol/water (3:1) + 1 % formic acid
10	acetonitrile/water (1:1) + 1 % formic acid
11	acetonitrile + 1 % formic acid
12	acetonitrile/water (1:3) + 1 % formic acid
13	acetonitrile/water (3:1) + 1 % formic acid

It was essential to choose an appropriate standard which would deliver consistent results throughout the optimisation of the DESI-MS parameters. The standards that were compared, were chosen to resemble as closely as possible, the shape and size of the drug molecules under analysis. The three standards were a NoDoz tablet, a Codral tablet and an in-house manufactured 100 mg/g caffeine/KBr disc. NoDoz and Codral tablets were obtained from a local pharmacy and caffeine and KBr were purchased from Sigma Aldrich (Castle Hill, NSW, Australia).

The KBr discs were prepared by mixing 100 mg of caffeine in 1 g of KBr powder. This mixture was then ground with a mortar and pestle for 5 minutes until well combined and to ensure

small particle size. The powder was then pressed into KBr discs (approximately 5 discs, 2 mm in thickness).

The NoDoz tablet, Codral tablet and caffeine KBr disc were then subjected to five repeated readings ($n=5$) using DESI-MS. The solvent which was employed was 1:1 water:methanol ($H_2O:MeOH$) + 1 % formic acid mixture. The DESI-MS parameters were as follows: spray tip-to-surface distance (d_1) = 3 mm; spray tip-to-sniffer distance (d_3) = 5 mm; spray impact angle (α) = 50° ; capillary inlet angle (β) = 10° ; solvent flow rate = 0.5 mL/hr; gas flow rate = 100 psi; spray high voltage = 4 kV; fragmentor voltage = 175 V.

In addition to the above experimentation, a signal depletion series was conducted in order to assess the signal stability in DESI-MS experiments. Morphine was used as a representative sample for small drug molecules due to its basic nature and was purchased from Sigma Aldrich (Castle Hill, NSW, Australia). This experiment was conducted over a period of 30 minutes (section 3.3.1).

3.2.1 Sample preparation

All pharmaceutical samples that were tested using DESI-MS had tablet coatings removed by way of scraping using a scalpel. This was necessary in order to avoid interference from tablet coatings and to circumvent the lack of active ingredient on the surface of the tablet. All other powder samples were dissolved in methanol at the specified concentration.

3.2.2 Experimental design

It was decided that experimental design principles would be utilised throughout this project in order to optimise appropriate parameters for DESI-MS, conducted using a caffeine standard (100 mg/g KBr disc). This involved two stages, the first being a FFD used as a type of screening test to determine which factors had a significant effect of the detection of drug compounds. This was followed by a response surface design using only the factors identified as important to maximise the response. From this design the optimum settings for each factor were determined in order to achieve the greatest signal response for the substances tested.

Three factors were identified to be the most important in the detection of licit and illicit drugs. These were the spray tip-to-surface distance (d_1), spray tip-to-sniffer distance (d_3), and the spray impact angle (α). These were selected based on the fact that these parameters determine the experimental space and are most likely to influence signal response⁷⁸. These three parameters were applied in the context of a FFD experiment, i.e. 2^3 factorial design.

The remaining parameters requiring optimisation (i.e. solvent flow rate, gas pressure, spray high voltage, solvent composition, fragmentor voltage, and collision energy) were conducted OFAT.

3.2.2.1 Experimental space

For a two level design such as the one used in this project, the two levels set for the factors were 'high' and 'low' which define the experimental space. When referring to different factor treatment combinations the high and low levels are designated using the presence and absence of lowercase letters. For example, in a design with two factors, A and B, the treatment combination of the high level of A and the low level of B would be written as 'a'. For the situation where all the factors are set at the low level this would result in a blank space. To avoid this, that treatment combination is generally written as (1). The design layout for the experiments is shown in Table 3-2 below. In this table the high level of the factor is designated by +1 and the low level by -1. The factor levels were set for the drug samples analysed and the runs were randomised as much as possible.

Table 3-2 Design layout for 2^3 design.

Treatment Combination	A (Spray tip-to-surface distance) (d_1)	B (Spray tip-to-sniffer distance) (d_3)	C (Spray impact angle) (α)
(1)	-1	-1	-1
a	+1	-1	-1
b	-1	+1	-1
c	-1	-1	+1
ab	+1	+1	-1
ac	+1	-1	+1
bc	-1	+1	+1
abc	+1	+1	+1

3.2.2.2 Factor levels

The factor settings chosen were based on reported values from the literature^{58, 70, 71} and were as follows:

Table 3-3 Factor levels for drug analysis using DESI-MS.

Factor	Low	High
Spray tip-to-surface distance (d_1)	1 mm	3 mm
Spray tip-to-sniffer distance (d_3)	3 mm	5 mm
Spray impact angle (α)	40°	55°

3.2.2.3 Data analysis

Once the experiments were completed, data analysis for the factorial design was undertaken. This involved the construction and interpretation of a number of different graphs to determine the effects of each factor and the significance of these effects.

The first plot constructed for the factorial design was a main effects plot. This was constructed by plotting the mean response at each level for each factor. This shows the effect that the factor has on the response. The magnitude of the effect is represented visually as the vertical distance between the two points and by the slope of the line joining them.

The second plot constructed for the factorial design was an interaction plot. This plot is used to examine the interaction between the various factors and to determine the effect that the interaction has on the response variable. For each pair of factors, the response is plotted for each combination of factor levels. The parallelism of the lines produced gives a visual indication of the interaction between the pair of factors. If the lines are parallel then there is no interaction between the factors. The further the lines deviate from parallelism the greater the interaction, with the greatest possible interaction resulting in the lines intersecting each other⁹⁴.

The third plot constructed for each design was a normal probability plot of the effects, or an effects plot. An effects plot shows the normal distribution of effects as a straight line with the experimentally determined effects plotted on the same graph. Any effects that are normally distributed will lie close to the line and are not considered significant. Conversely, points that

lie far from the line are not normally distributed and are thus deemed significant. The criterion for determining significance is based on the error term and uses an α value of 0.05⁹⁴.

From the results of these designs, important factors and factor interactions were identified. Using the factors that were identified as significant, the second stage of the experimental design was undertaken. The second design stage of this project involved a CCD. Using response surface designs the optimum parameter settings were determined for the caffeine standard.

3.3 Results and discussion

3.3.1 Optimising DESI-MS parameters

Three standards, i.e. NoDoz tablet (containing 100 mg caffeine), Codral tablet (containing 500 mg paracetamol) and 100 mg/g caffeine KBr disc were subject to DESI-MS analysis.

The results of the repeat analysis suggested that the 100 mg/g caffeine KBr disc was the best standard to use since the best linearity was achieved over the five repeat injections (Figure 3-1 - Figure 3-3). In the absence of caffeine-KBr discs, optimisation could also be conducted using other substrates with similar optimal conditions resulting; however, larger standard deviations would be expected due to the variable signal responses observed on substrates such as NoDoz and Codral tablets, most likely due to the inhomogeneity of the preparations themselves.

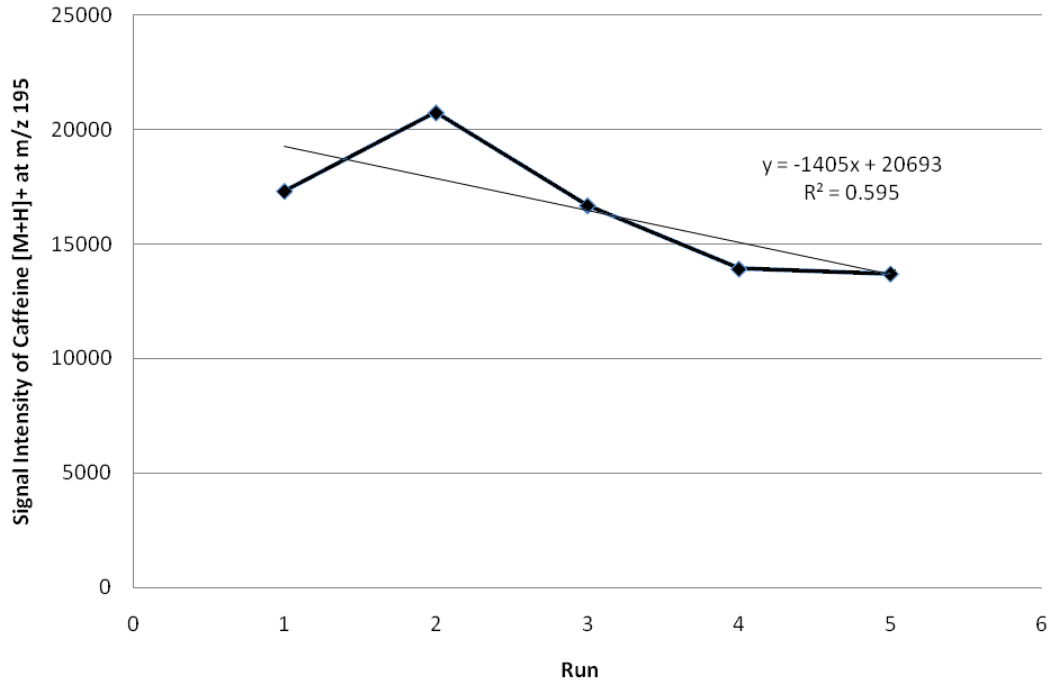


Figure 3-1 NoDoz repeat injection in standard trial.

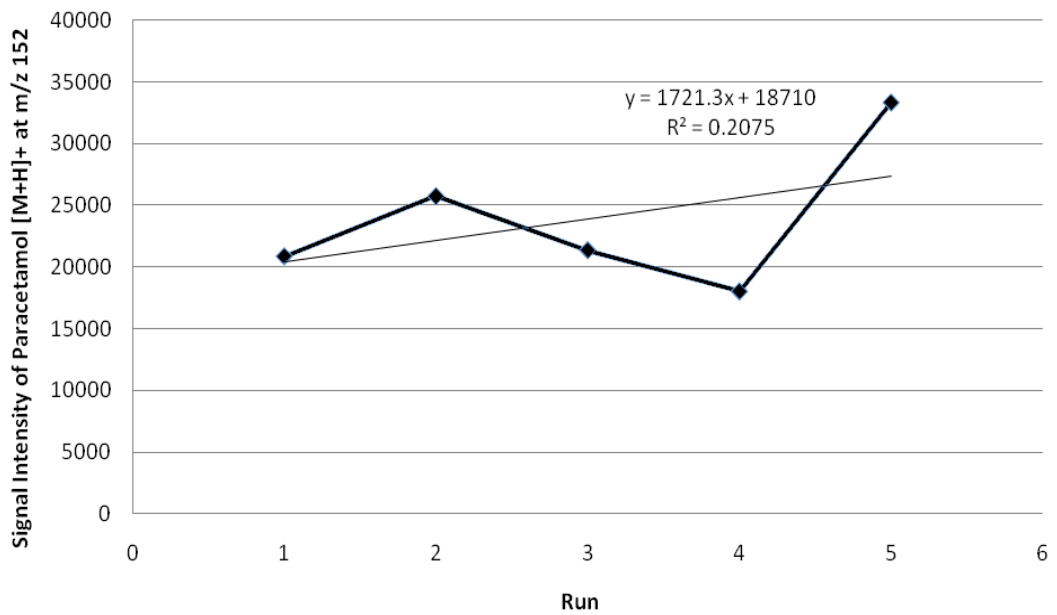


Figure 3-2 Codral repeat injection in standard trial.

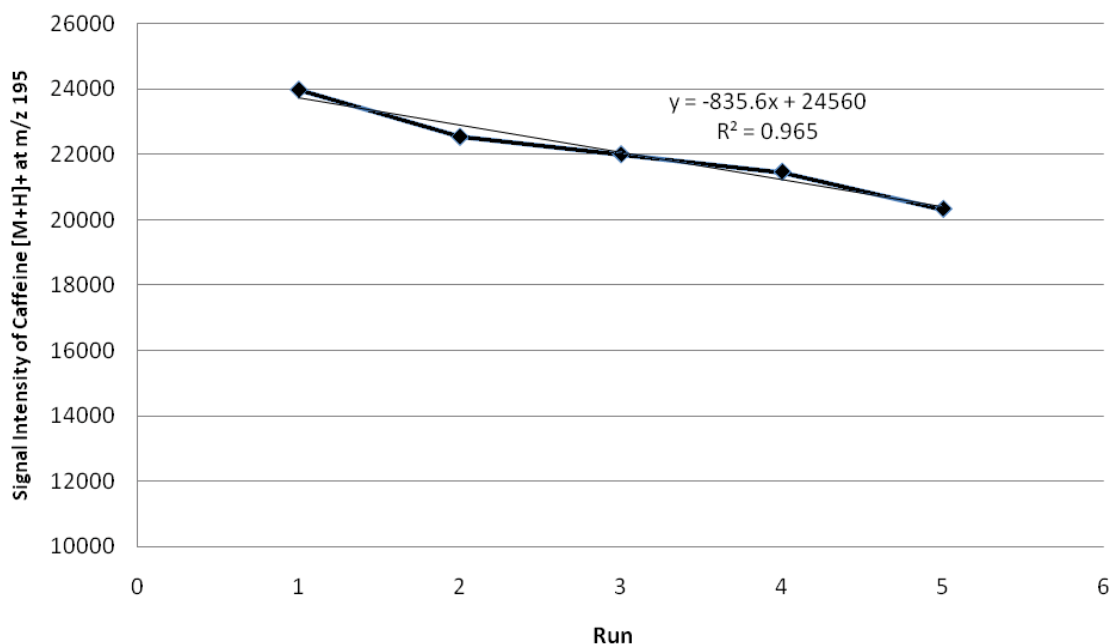


Figure 3-3 Caffeine KBr (100 mg/g) repeat injection in standard trial.

A depletion study was conducted on morphine to determine whether factors such as capillary inlet temperature have an effect on signal intensity. Morphine was used here so as to differentiate it from the caffeine standard being used for initial optimisations. This experiment was the first run of the day, suggesting that the capillary inlet was cold prior to turning on the instrument. It is evident in Figure 3-4, by the circle-point trendline, that the signal intensity decreases steadily over the first 15 - 16 minutes. This suggests that in the time taken for the capillary inlet (sniffer) to heat up (i.e. approximately 15 minutes) the signal intensity of the analyte ion will continue to decrease until a stable capillary temperature is reached. This observation was further confirmed by the second diamond-point trendline in which the signal intensity was relatively stable over the 30 minute period. The initial drop in signal in morphine depletion 2 was hypothesised to be due to stabilisation of the flow of solvent (containing analyte) or due to charge buildup inside the detector at the beginning of the second run, resulting in a slightly higher reading prior to the signal leveling out.

The morphine depletion experiment was conducted with the analyte infused in the solvent line thereby allowing for a consistent flow of ions into the mass spectrometer. This limited the number of variables, attributing the observed signal response to the temperature of the capillary inlet alone. In other DESI-MS experiments the analyte is spotted onto the surface of the plate in which there is observed reductions in signal response over time during analysis.

This occurs due to depletion of the analyte by the spray solvent. In this study, analyte signals were averaged over 1 minute as it was observed that significant signal reduction and analyte depletion occurred after 1 minute of desorption and analysis.

The apparent decrease in signal intensity as the capillary inlet heats up can be explained by the increasing rate of vaporisation of solvent close to the sniffer. Less solvent will impact the sample surface, in turn resulting in less ionisation and desorption of the analyte. The decrease in signal intensity with increasing capillary inlet temperatures may also be explained due to ions undergoing thermal degradation at capillary temperatures in excess of 200 °C as has been suggested in the literature⁵⁸. In general, 15 - 20 minutes must be allowed for the capillary inlet to reach a stable temperature in order to obtain stable signal responses in subsequent experiments.

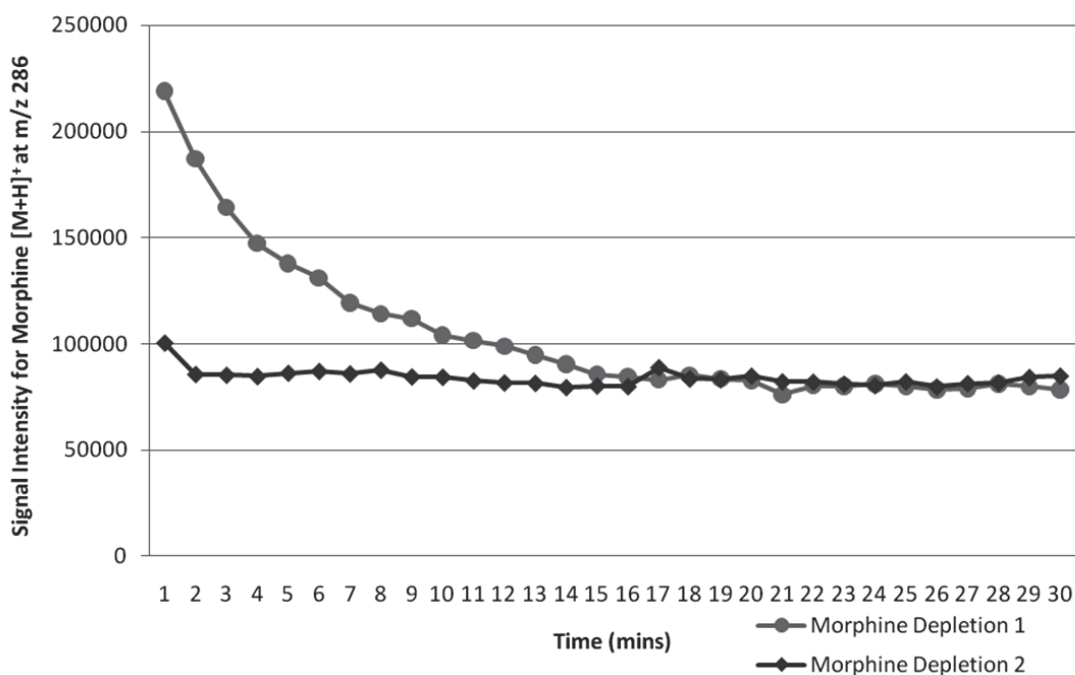


Figure 3-4 Depletion of morphine signal over time.

3.3.1.1 Experimental design

As detailed (section 1.6.1), a 2^3 factorial design was constructed to determine which, if any, of the three factors had a significant effect on the detection of caffeine in the standard. In order to determine the effect of detection, signal intensity at m/z 195 was used as the response indicator. From this analysis the main effects plot and an interaction plot were constructed.

These demonstrated the effects of each of the factors on the response, as well as the effects of interactions between the factors.

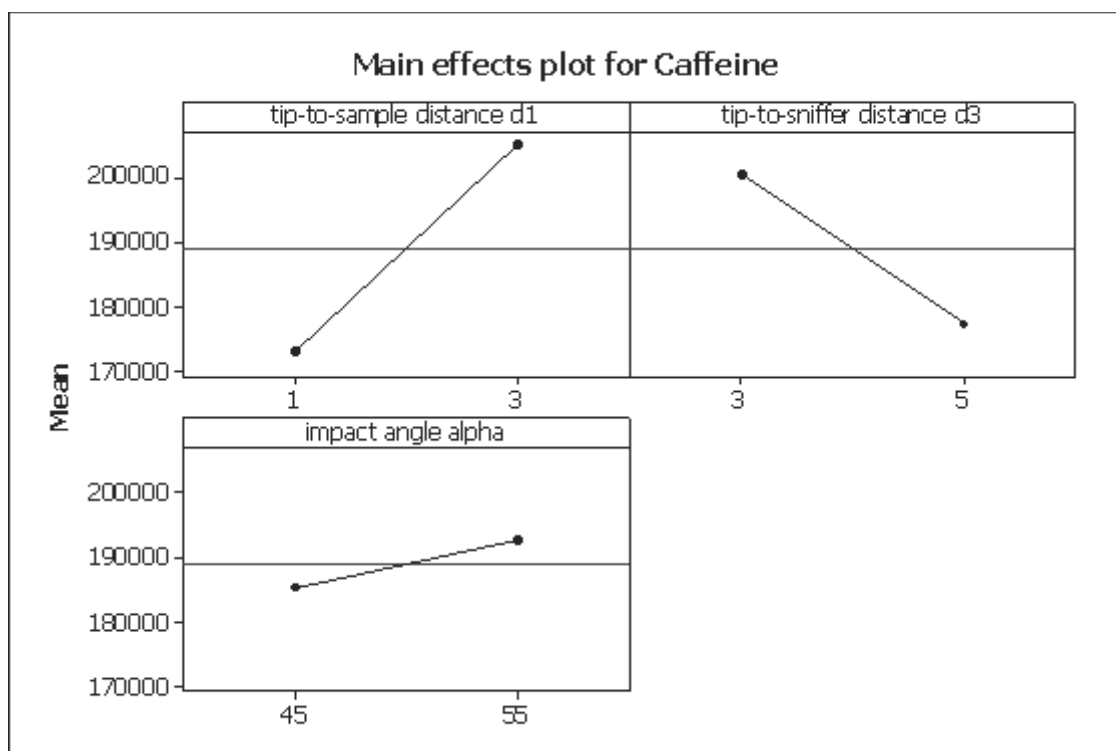


Figure 3-5 Main effects plot for 100 mg/g caffeine KBr disc.

The main effects plot indicates that signal intensity is influenced by each of the factors, in particular spray tip-to-sample distance. This can be seen from the slope of the line for each plot and the difference between the mean responses at each parameter.

The interaction plot shows the interactions between the various factors. For each pair of factors the response was plotted for each combination of factor levels. The parallelism of the lines produced gives a visual indication of the interaction between the pair of factors. If the lines are parallel then there was no interaction between the factors. The further the lines deviate from parallelism the greater the interaction, with the greatest possible interaction resulting in an 'X' with the lines intersecting each other⁹⁴.

From the interaction plot for caffeine (Figure 3-6), it is clear that there are some significant interaction effects as well as some main effects. Of particular interest is the interaction between the spray tip-to-sample distance and the impact angle. In the interaction plot for this pair of factors the lines are intersecting each other. This indicates a significant

interaction. These need to be considered when determining the optimal conditions. The interaction between the spray tip-to-sample distance and the spray tip-to-sniffer distance as well as the interaction between the spray tip-to-sniffer distance and the impact angle show less interaction as the lines do not intersect each other; however, this interaction cannot be over-looked since some interaction still exists as the lines do not exhibit complete parallelism.

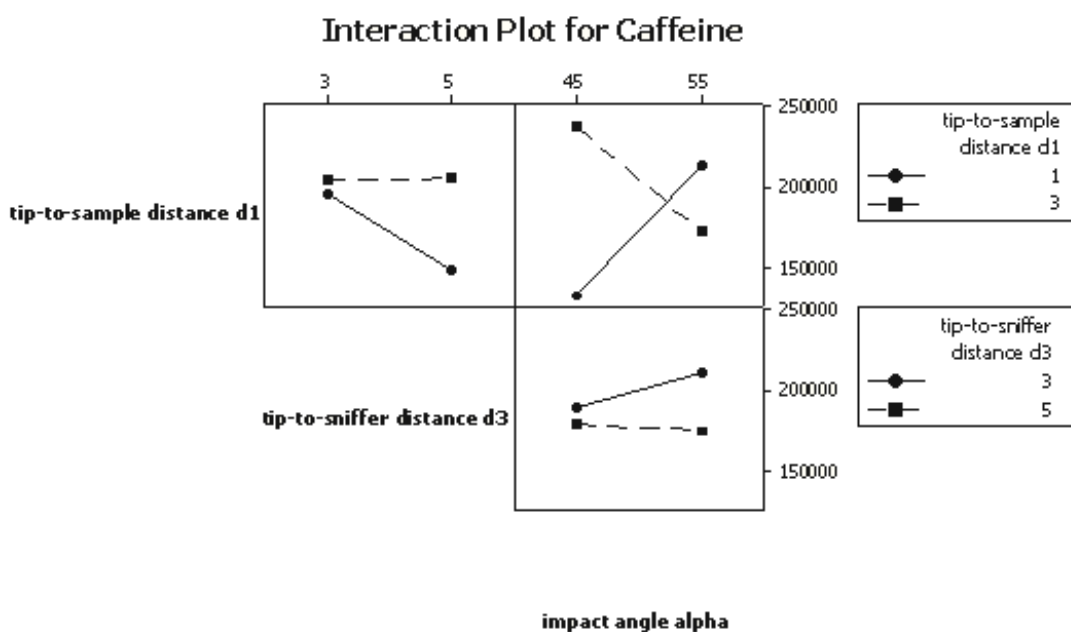
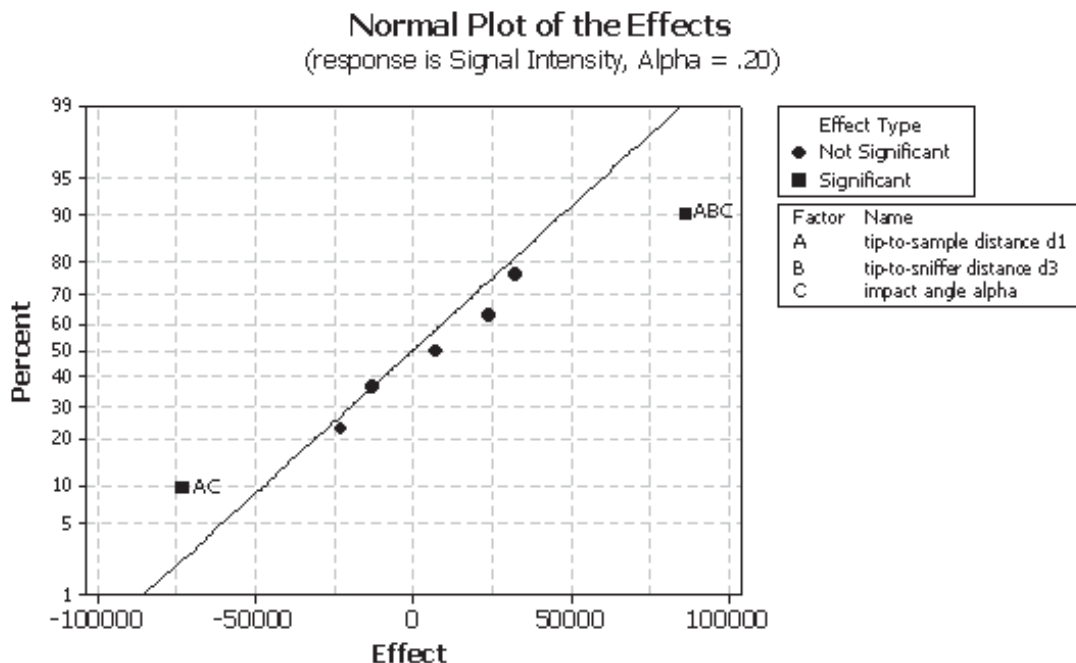


Figure 3-6 Interaction plot for 100 mg/g caffeine KBr disc.

In order to further confirm which of the main and interaction effects were significant an effects plot was constructed. This allows statistically significant effects to be identified. An effects plot shows the normal distribution of effects as a straight line with the experimentally determined effects plotted on the same graph. Any effects that are normally distributed will lie close to the line and are not considered significant. Conversely, points that lie further away from the line are not normally distributed and are thus deemed significant. In conventional experimental design the criteria for determining significance is based on the error term and uses an α value of 0.05⁹⁴. However, due to the transient nature of DESI-MS analysis an α value of 0.2 had to be applied as greater discrimination was necessary to determine the significant parameters.

From the effects plot three significant effects were identified. These were the AC and ABC effects (Figure 3-7). This means that there were significant interaction effects between the spray tip-to-sample distance, spray tip-to-sniffer distance and the impact angle.



Lenth's PSE = 36611.8

Figure 3-7 Effects plot for 100mg/g caffeine in KBr disc.

A reduced factorial model was fitted to the results using only the significant factors. This was tested to see if the model was satisfactory and that the factors chosen were in fact important. To test the model, residuals plots were constructed. The normal probability plot compares residuals to a normal distribution. The points form a straight line, indicating the data is normally distributed. The residual values versus fitted values plot shows a random distribution of points with no discernible pattern. The histogram does not exhibit any tailing patterns, indicating that there is no skewness to the data. Finally, the residuals versus observation order plot does not exhibit any pattern that would suggest non-random errors (Figure 3-8)⁹⁴. These were all acceptable and thus the model was deemed fit for the CCD.

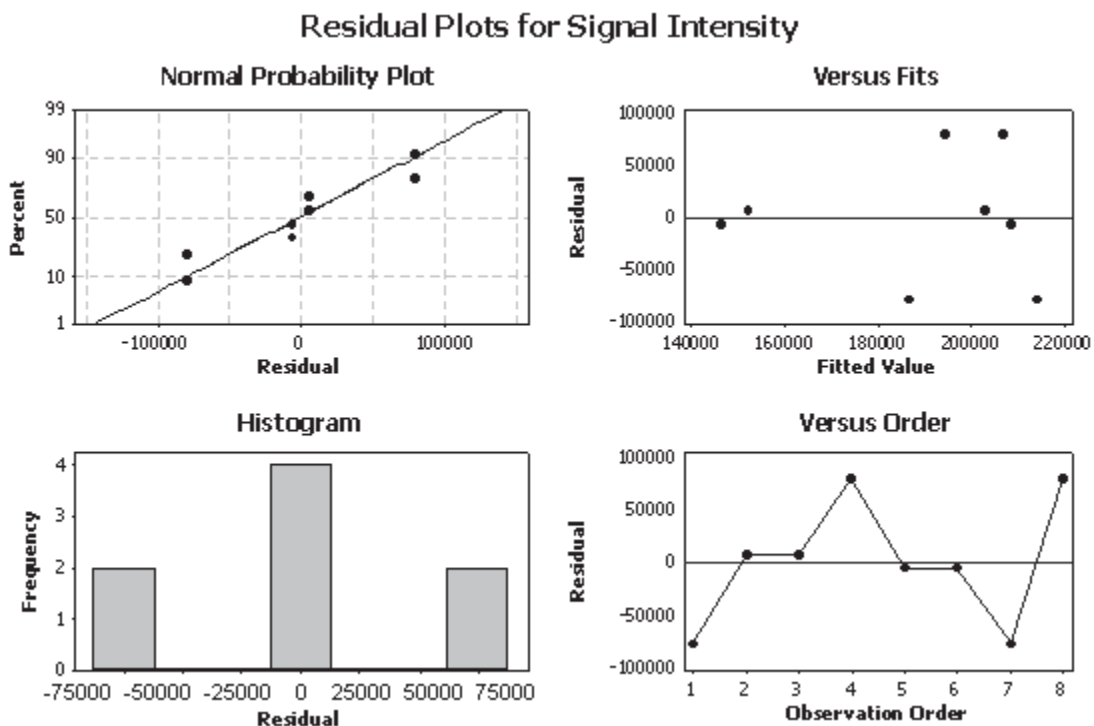


Figure 3-8 Residual plots for 100 mg/g caffeine KBr disc.

Using the important factors identified through the FFD, a CCD was constructed. This design involves a greater number of data points than a factorial design with the same number of factors but allows for the identification of trends and for signal (response) optimisation. The results of this analysis facilitated the generation of contour plots and response surfaces were constructed. These indicate the trends in the response associated with the various factors. The plots for caffeine show a curved response trend, with the optimal signal intensity found to be towards the edges of the experimental space (Figure 3-9 and Figure 3-10). This experiment was unable to deliver optimal signal intensities in the middle of the experimental space due to the nature of the DESI set-up. Values outside the specified 'high' and 'low' values would give experimental results which were unviable and outside the capabilities of the DESI source.

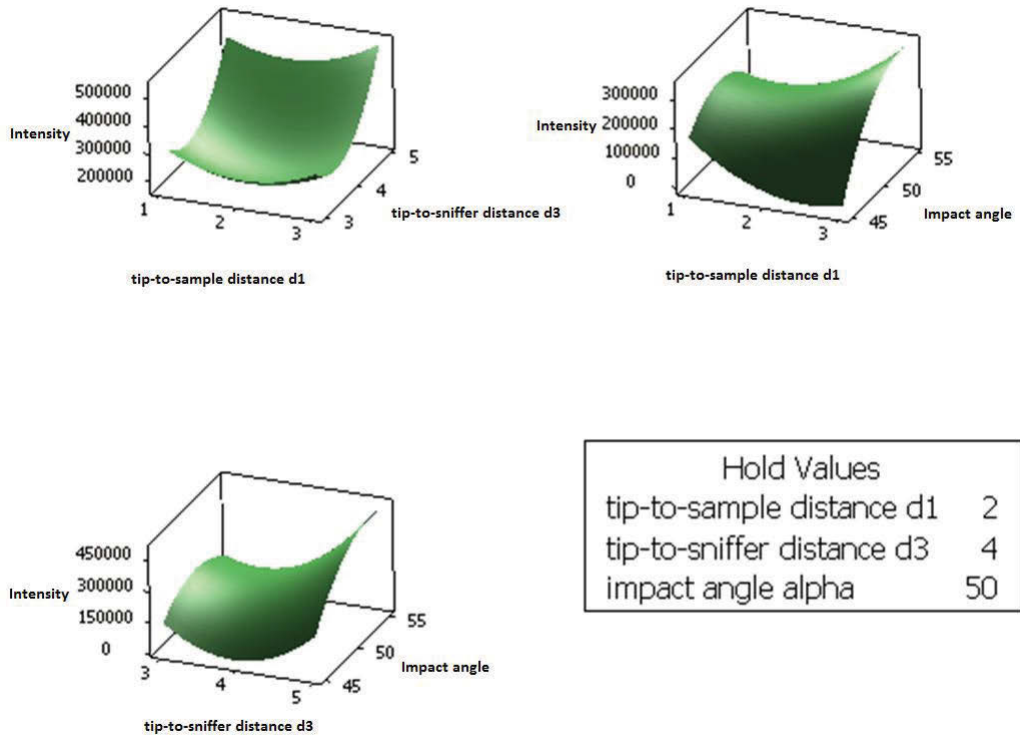


Figure 3-9 Response surface plots for 100 mg/g caffeine KBr disc.

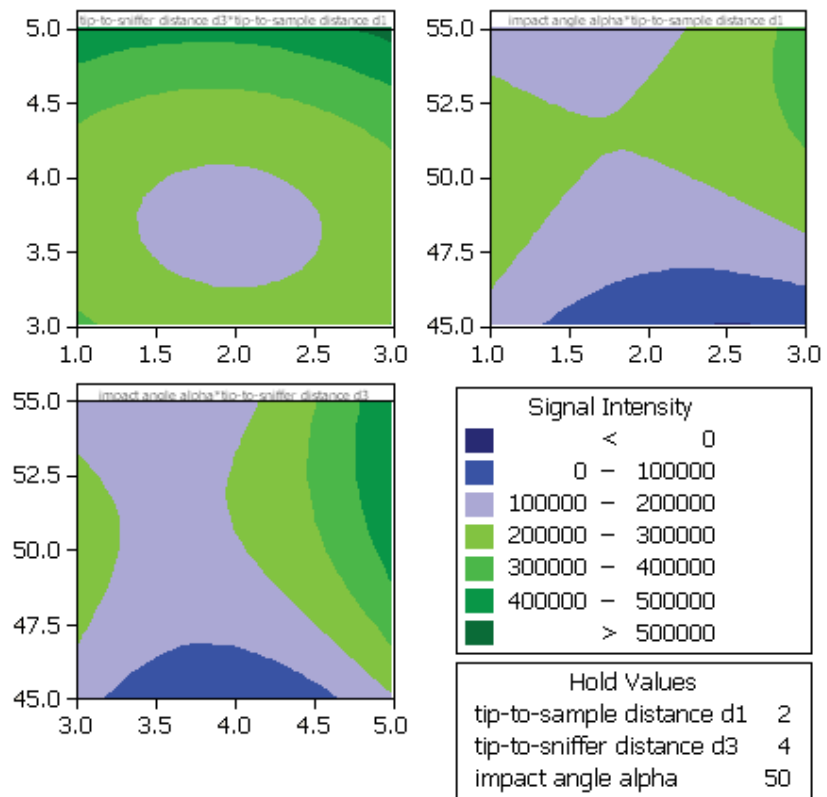


Figure 3-10 Contour plot for 100 mg/g caffeine KBr disc.

The response surface plots give an approximation of the optimal conditions for maximum peak height. In order to determine these conditions exactly, a response optimisation plot was used. This takes into account all of the factors and identifies the factor levels that will give the optimal response (Figure 3-11).

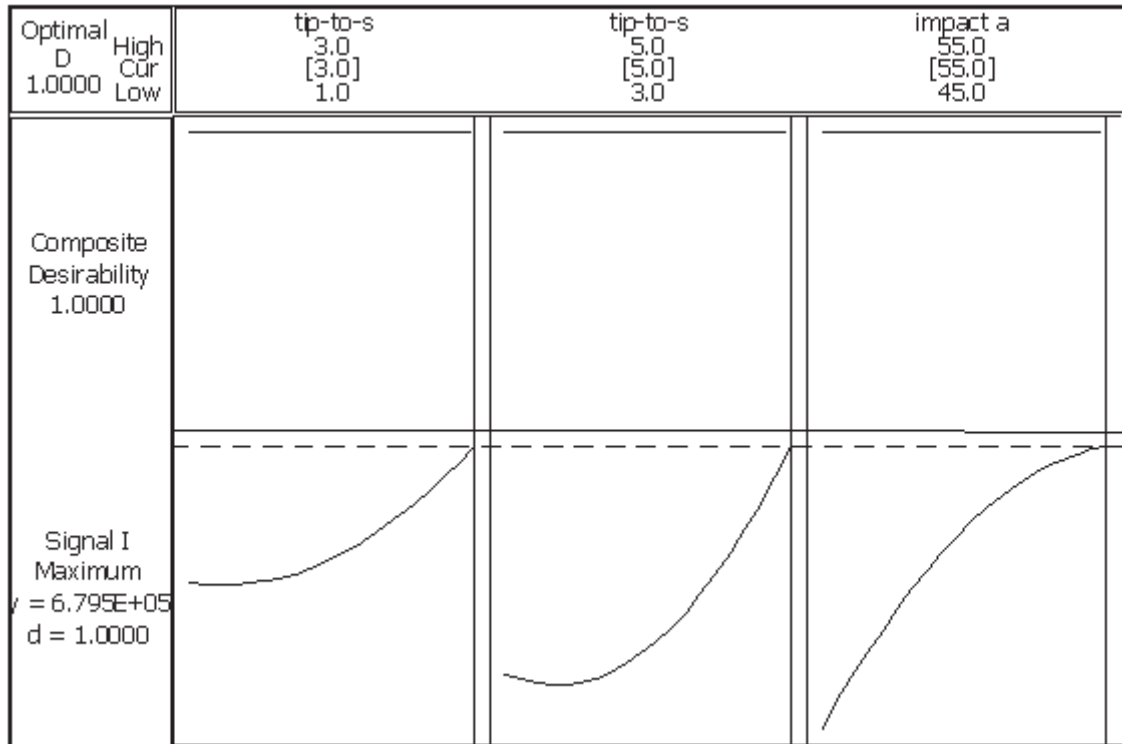


Figure 3-11 Optimisation plot for 100 mg/g caffeine KBr disc.

From the optimisation plot, the optimal conditions determined for caffeine were:

Table 3-4 Optimal parameters for caffeine.

Factor	Optimal
Spray tip-to-surface distance (d_1)	3 mm
Spray tip-to-sniffer distance (d_3)	5 mm
Spray impact angle (α)	55°

The three optimised conditions were used in the following OFAT experiments.

3.3.1.2 One-factor-at-a-time optimisation

The remaining parameters which required optimisation were conducted on an OFAT basis. These parameters were determined to have minimal interaction with other parameters and

did not affect desorption and ionisation to the same extent as the previously optimised parameters, i.e. d_1 , d_3 and α . This is partly due to the fact that these parameters do not determine the experimental space where the spatial orientation of d_1 , d_3 and α plays a major role in determining signal intensity/response⁷⁸. In addition, a FFD was conducted on these parameters and no significant interactions were noted.

The parameters which required optimisation via the OFAT experimental design include: solvent flow rate, gas pressure, spray high voltage, solvent composition and fragmentor voltage.

The OFAT experiments were conducted using the same 100 mg/g caffeine KBr standard as was used in the FFD and CCD experiments above. The hold values (excluding parameters being optimised) were: spray tip-to-surface distance (d_1) = 3 mm, spray tip-to-sniffer distance (d_3) = 5 mm, spray impact angle (α) = 55°, sniffer-to-surface distance (β) = 15° (fixed), solvent flow rate = 0.21 mL/hr, gas pressure = 100 psi, fragmentor voltage = 175 V, spray high voltage = 4 kV.

The optimised solvent flow rate was chosen to be 0.21 mL/hr. Despite the fact that the graph trends upward at higher flow rates (Figure 3-12), this value was chosen since higher flow rates disrupted the sample surface significantly. This caused large craters in the sample surface and resulted in an increase in the level of carry-over as sample began to 'splash' onto the sniffer inlet. Solvent 'splashing' was kept at a minimum at 0.21 mL/hr, while generating adequate signal response.

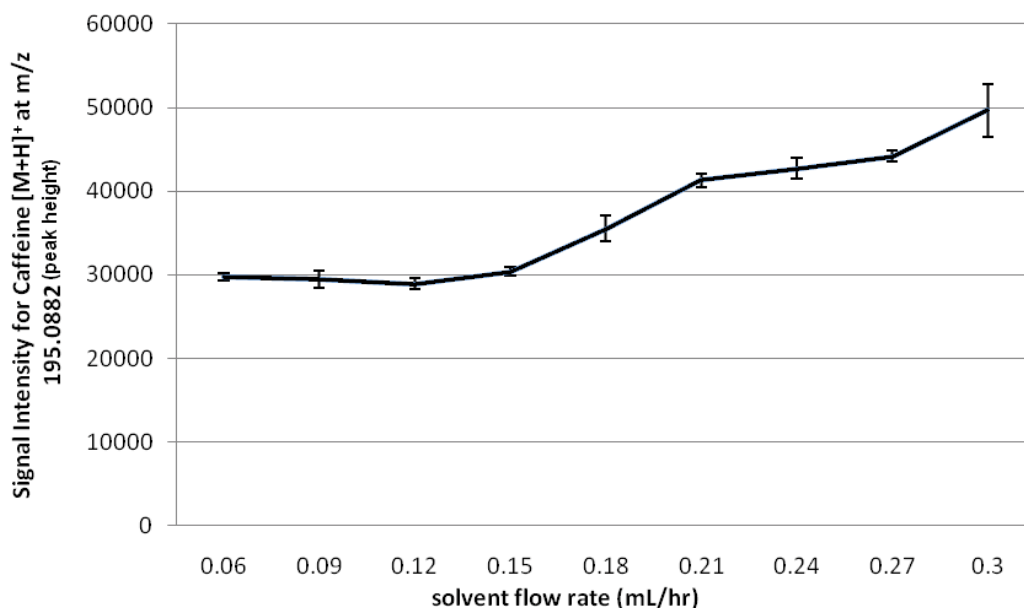


Figure 3-12 Optimising solvent flow rate (mL/hr) for 100 mg/g caffeine KBr disc, n=5.

The optimal gas pressure was chosen to be 100 psi. Despite 200 psi resulting in a slightly higher signal (Figure 3-13), significant erosion of the sample surface was observed at the elevated pressure and resulted in high carry-over due to sample ‘splashing’ onto the sniffer. The lack of fine pressure control may have resulted in the variation of signal response observed at 150 psi. Other effects such as inefficient desolvation and the lack of surface wetting may also have contributed to the decrease in response at this pressure; however, this was not further investigated.

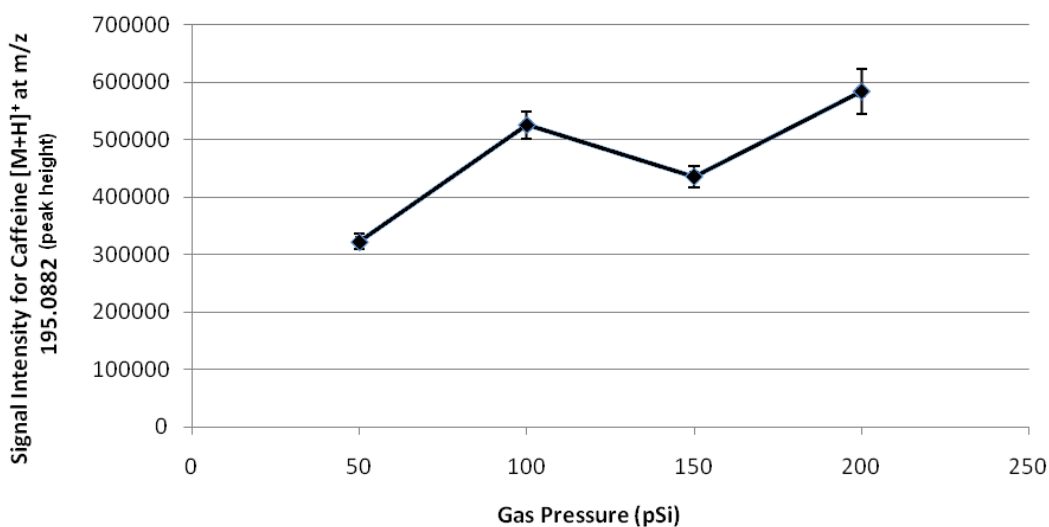


Figure 3-13 Optimising gas pressure for 100 mg/g caffeine KBr disc, n=5.

The optimal spray high voltage value was chosen to be 4 kV as this value gave a higher signal intensity for the protonated molecular ion $[M+H]^+$ of caffeine at m/z 195 (Figure 3-14). Overall, the observed signal intensity did not change dramatically as the spray high voltage was varied; therefore, a lower high voltage was advantageous since a more stable ion count is achievable at lower voltages.

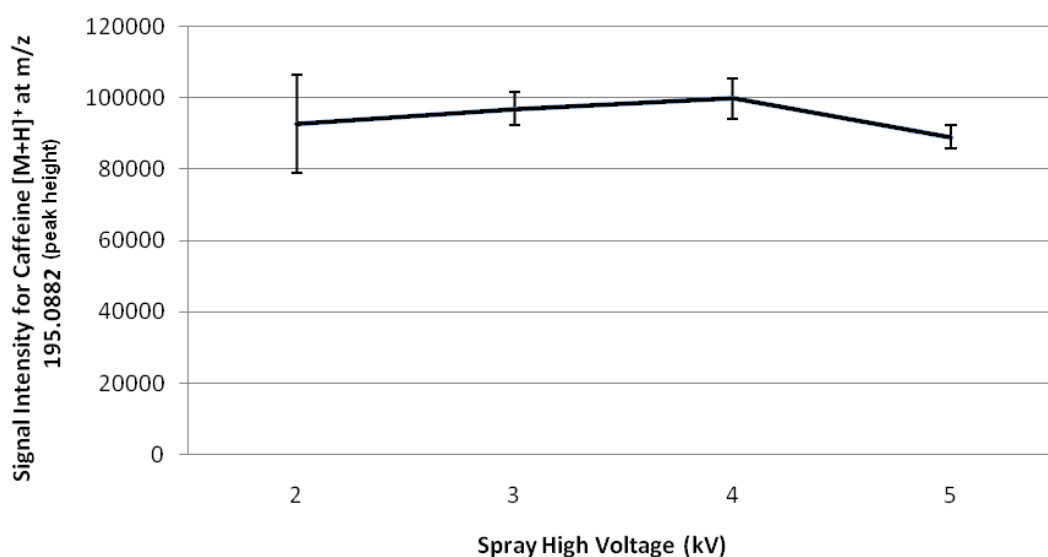


Figure 3-14 Optimising spray high voltage for 100 mg/g caffeine KBr disc, $n=5$.

The optimal solvent composition was a 1:1 mixture of water and methanol with 1 % formic acid additive as this mixture gave the highest signal response for the 100 mg/g caffeine standard. Solvent composition is an important parameter in DESI-MS analysis and requires careful attention since different compounds will respond differently to a range of solvent mixtures. The addition of formic acid facilitated protonation and thus ionisation of the solvated molecules prior to entering the MS, while the addition of methanol aided in volatilisation.

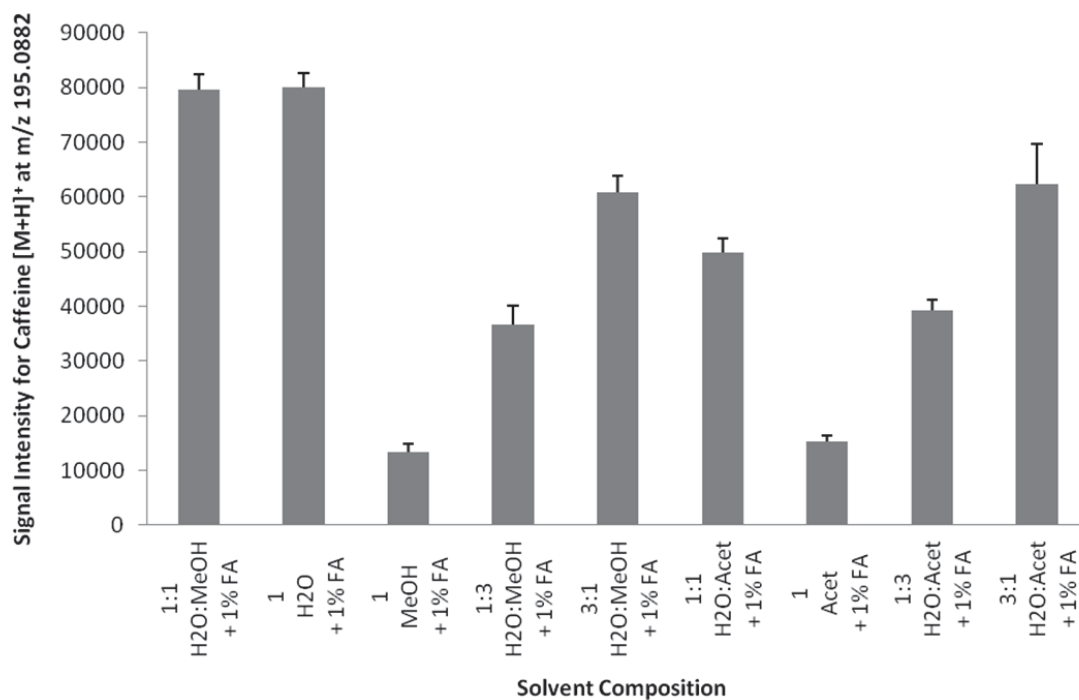


Figure 3-15 Optimising solvent composition for 100 mg/g caffeine KBr disc, n=5.

The optimal fragmentor voltage value for caffeine was found to be 195 V as this setting gave the most intense signal response for the caffeine standard tested (Figure 3-16). Similar to solvent composition, fragmentor voltage values vary amongst different drug samples. This necessitates the need to take special care when selecting a fixed fragmentor voltage value for analysing a variety of drug samples.

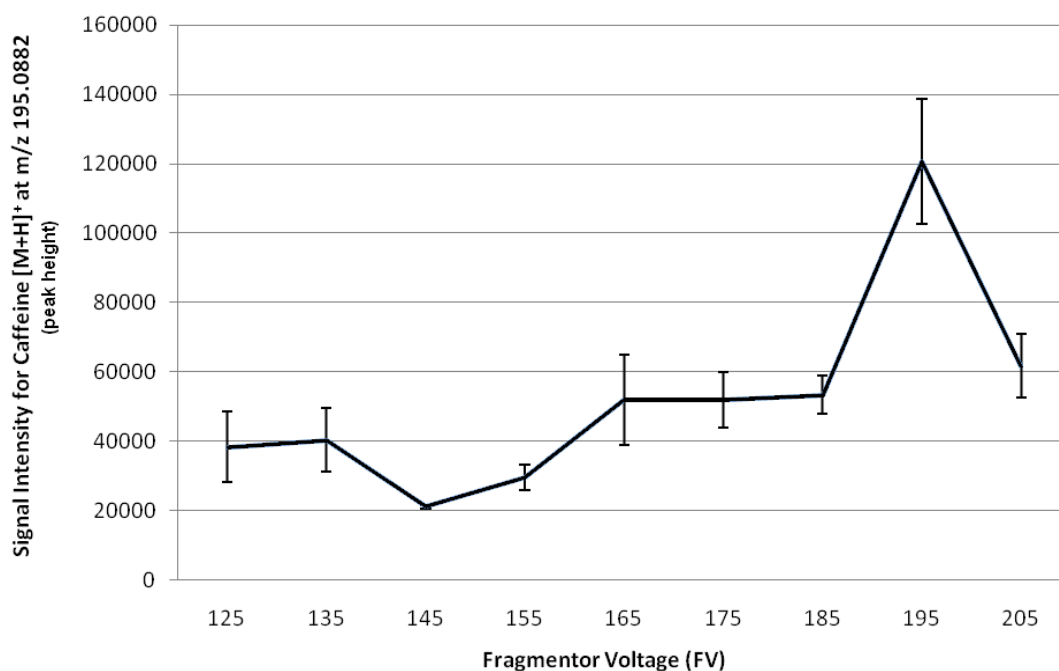


Figure 3-16 Optimising fragmentor voltage for 100 mg/g caffeine KBr disc, n=5.

3.3.1.3 Sampling method

In order to assess the best and most rapid way to sample compounds for drug analysis, four techniques were compared: preparing KBr discs with the drug powder of interest, spotting the dissolved solution onto well plates, spotting powder and then dissolving in methanol and spotting powder on double sided tape. Samples in tablet form required no sample preparation (coatings needed to be removed in some cases) and were directly analysed using DESI-MS (Figure 3-17).



Figure 3-17 Paracetamol tablet being analysed by DESI-MS.

KBr discs were prepared using the four synthesised 4-MMC samples (i.e. M1 – M4) to approximately 100 mg/g. These KBr discs were then subject to DESI-MS analysis. The main analyte of interest ($m/z = 178 [M+H]^+$) for 4-MMC was detected in all four of the samples tested with good intensity, ranging from $10.9 \times 10^4 - 36.5 \times 10^4$ cps (Figure 3-18).

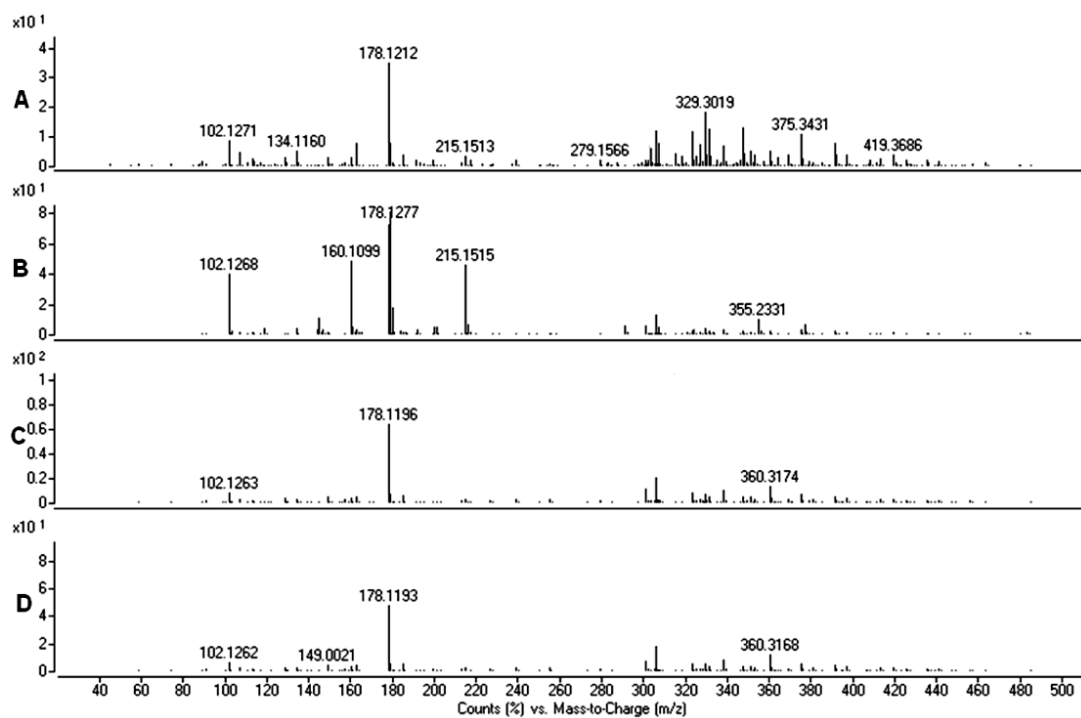


Figure 3-18 DESI-MS spectra of 4-MMC; A: M1, B: M2, C: M3, D: M4 in KBr disc.

Overall, the analysis of the four samples was very promising as the peak intensity of the analyte of interest was detectable in all trials. One major disadvantage of this method of sample preparation is the time and expertise needed to prepare KBr discs. In the overall context of this study, DESI-MS should be a fast and easy technique for analysing novel drug compounds and the method of KBr discs was too time consuming.

Solutions of the four synthesised samples (M1, M2, M3 and M4) were prepared to a concentration of 1 mg/mL. These solutions were then spotted (3 x 2 μ L spots) on a PVC well plate where the solvent was left to evaporate and then analysed by DESI-MS. The main analyte of interest ($m/z = 178$ $[M+H]^+$) for 4-MMC was detected in all four of the samples tested with good intensity, ranging from 5.3×10^4 – 11.2×10^4 cps (Figure 3-19).

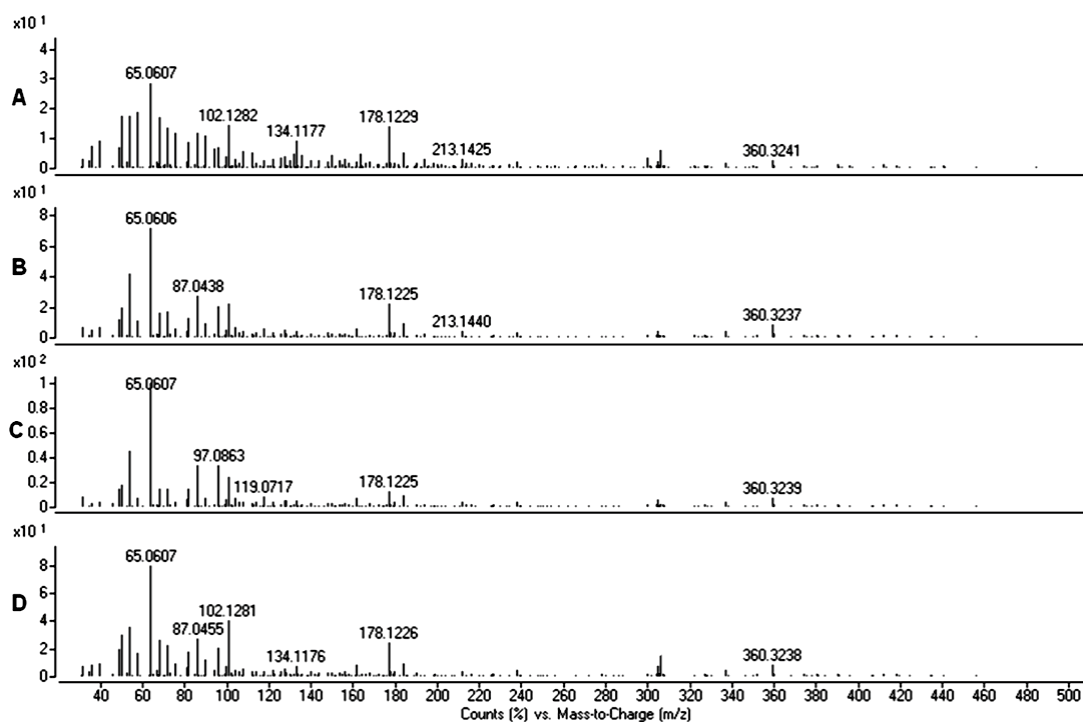


Figure 3-19 DESI-MS spectra of 4-MMC; A: M1, B: M2, C: M3, D: M4 on PVC plate.

This method of sample preparation has shown to be a faster alternative to preparing KBr discs and was a viable alternative in the analysis of novel drug compounds.

Approximately 1 mg of each of the four synthesised sample powders (M1, M2, M3 and M4) were placed onto a PVC wellled slide and dissolved in 2 μL of methanol and the solvent was allowed to evaporate. These samples were then analysed using DESI-MS. The main analyte of interest ($m/z = 178$ $[\text{M}+\text{H}]^+$) for 4-MMC was detected in all four of the samples tested with good intensity, ranging from 12.4×10^4 – 23.1×10^4 cps (Figure 3-20).

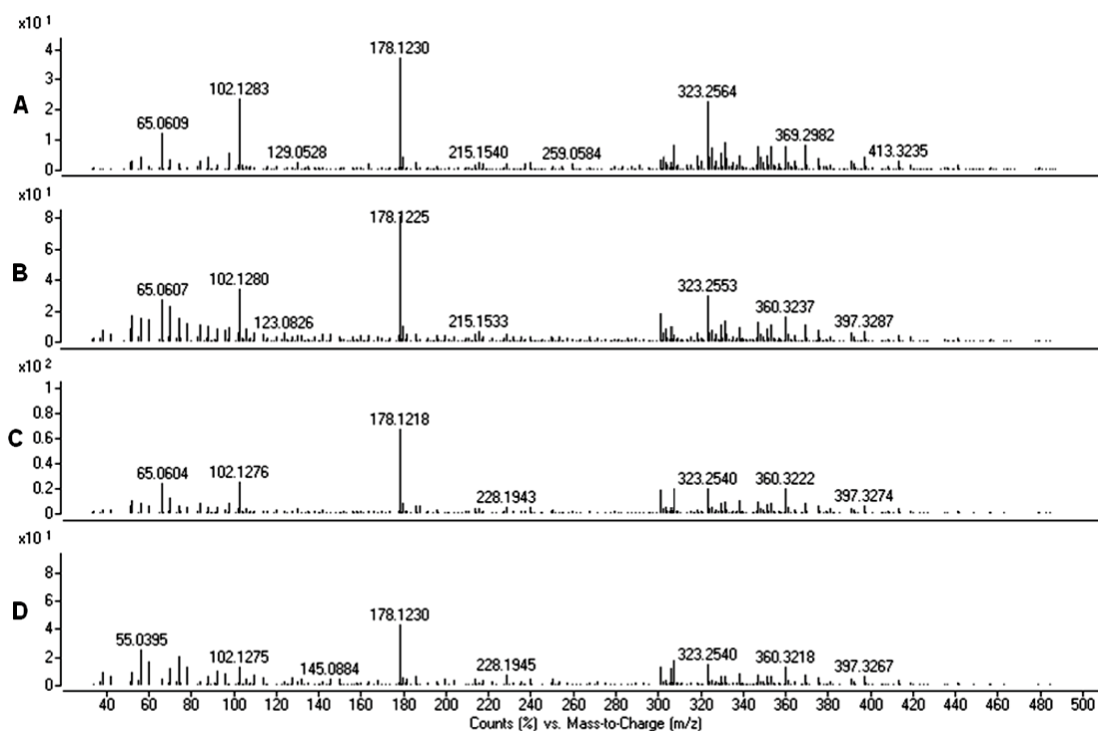


Figure 3-20 DESI-MS spectra of 4-MMC; A: M1, B: M2, C: M3, D: M4 powder on PVC plate.

Another similar technique of preparing powders for DESI-MS analysis was to spot approximately 1 mg of the sample onto double sided tape that has been stuck to a glass slide (Figure 3-21).



Figure 3-21 Double sided tape with sample powders for DESI-MS analysis. 0=blank, 1=M1, 2= M2, 5=M3, 6=M4, C=Caffeine.

The main analyte of interest ($m/z = 178 [M+H]^+$) for 4-MMC was detected in all four of the samples tested with good intensity, ranging from $2.9 \times 10^3 - 443 \times 10^3$ cps (Figure 3-22).

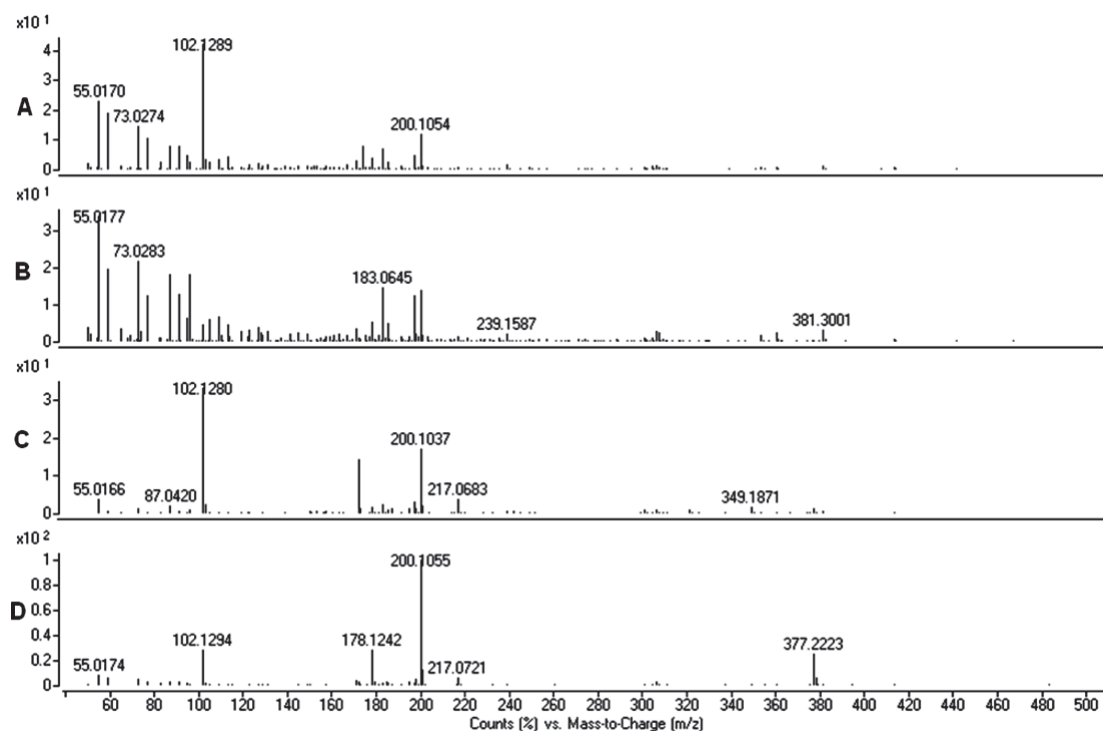


Figure 3-22 DESI-MS spectra of 4-MMC; A: M1, B: M2, C: M3, D: M4 on double sided tape.

The method of spotting powder onto double sided tape required the least sample preparation of the three techniques tested. However, higher signal responses were obtained when samples were deposited from solution; therefore this method was used in subsequent analyses. The sticky surface of the double sided tape may have contributed to a weaker signal being observed as was reported in GSR work using adhesive stubs⁹⁰.

In order to directly compare the pMMA slide to the PVC and PTFE slides (Figure 3-23), the same technique was used for creating wells on these slides as was used on the PVC slides. The wells were 3 mm in diameter (7 mm²) and were spotted with 2 μ L aliquots of the sample solution to be analysed.

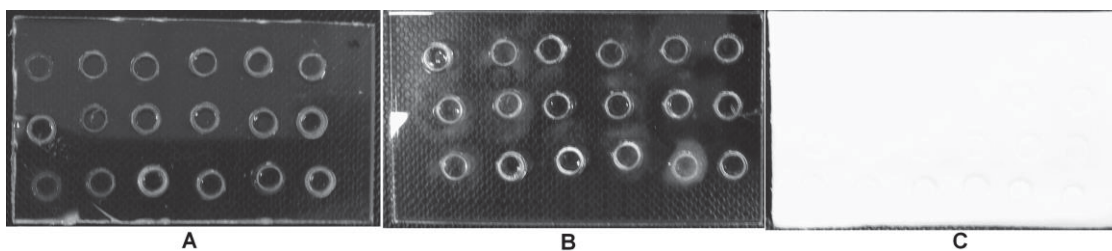


Figure 3-23 A: Polyvinyl chloride (PVC); B: Polymethyl methacrylate (pMMA); C: Polytetra fluoroethylene (PTFE).

Table 3-5 Comparison of the reproducibility of signal intensity of 4-MMC on three different plates, n=5.

Plate	Mean 4-MMC signal response (cps) ^a	SD	% RSD
pMMA	29845	18920	63
PVC	47231	26261	55
PTFE	9853	2418	24

^a Concentration of 4-MMC used = 400 µg/mL, 2 µL spotted on plate.

A 400 µg/mL solution of 4-MMC was analysed using DESI-MS and the average signal intensity of five runs (n=5) was compared for the three surfaces. The standard deviation (SD) obtained for the three different surfaces was used as a means to illustrate the reproducibility of the signal response on the different surfaces. pMMA, PVC and PTFE resulted in 63 %, 55 %, 24 % relative standard deviation (% RSD), respectively. PTFE was chosen as the best surface due to the lowest % RSD, reflecting its superior signal stability (Table 3-5). Despite a much reduced RSD, PTFE also resulted in a reduction in signal response. This is hypothesised to be due to the increased interaction between the semi-porous PTFE surface and the analyte being desorbed in the DESI-MS experiment. This suggests that desorption is taking place at a slower rate resulting in a sustainable flow of ions into the mass spectrometer, and thus better RSD.

3.3.2 Pharmaceuticals analysis

An important stage of this research was to develop a suitable method to analyse novel and controlled drugs that commonly contain impurities and by-products from synthesis. The approach that was taken was to analyse a range of pharmaceutical samples and optimise the parameters for each sample separately. The three parameters that were sample dependent and therefore required optimisation were solvent composition, fragmentor voltage, and collision energy. The values were then tabulated and the optimal factors were chosen as a method for running all drug compounds. The pharmaceutical samples tested included: NoDoz, Clarityne (loratadine), Centrum, Panadol (paracetamol), Aspirin, and Neurofen (ibuprofen) tablets. Most samples were run in positive ionisation mode; however, a select few were also run in negative ionisation mode due to the main ingredients being acidic in nature (ionising more efficiently in negative mode). The optimised conditions for each of the pharmaceuticals discussed above have been collated in Table 3-6. Caffeine, morphine, codeine and benzoic acid, have also been optimised and added to the table in order to obtain a broader view of the optimal settings for a range of compounds (acidic to basic).

Table 3-6 Summary of optimised values for drug compounds; set values: $d_1=3$ mm, $d_3=5$ mm, $\theta=15^\circ$, $\alpha=55^\circ$, solvent flow rate=0.21 mL/hr, high voltage=4 kV, gas flow rate=100 psi.

Compound	Solvent composition	Positive/negative ionisation mode	FV (V)	CE (eV) MS/MS
Caffeine	1:1 H ₂ O:MeOH + 1 % FA	Positive	195	35
Benzoic Acid	MeOH	Negative	195	10 or 15
Paracetamol	1:1 H ₂ O:MeOH + 1 % FA	Positive	125	20
Paracetamol (2)	1:1 H ₂ O:MeOH + 1 % AF	Negative	165	16
Codeine	1:1 H ₂ O:MeOH + 1 % FA	Positive	175	35
Morphine	1:1 H ₂ O:MeOH + 1 % FA	Positive	175	35
Aspirin	MeOH	Positive	165	5
Aspirin (2)	1:1 H ₂ O:MeOH + 1 % FA	Negative	205	15
NoDoz-Caffeine	1:1 H ₂ O:MeOH + 1 % FA	Positive	195	30
Centrum	MeOH	Positive	205	30
Neurofen	MeOH	Negative	185	8
Loratadine	1:1 H ₂ O:MeOH	Positive	175	30

FA = Formic acid, AF = Ammonium formate

Based on optimised values a method was developed for the analysis of drug compounds. The method consisted of the following set parameters: spray tip-to-surface distance (d_1) = 3 mm; spray tip-to-sniffer distance (d_3) = 5 mm; spray impact angle (α) = 55° ; capillary inlet angle (β) = 10° ; solvent flow rate = 0.21 mL/hr; gas flow rate = 100 psi; spray high voltage = 4 kV; fragmentor voltage = 175 V; collision energy = 20 and 30 eV; solvent composition = methanol/water (1:1) + 1 % formic acid.

3.3.3 Optimising GC-MS parameters

Gas chromatography – mass spectrometry was chosen as one of the comparison techniques in this study due to its history as one of the principle drug analysis techniques. Methods have been well-established and routine analyses are commonly conducted using GC-MS¹¹⁴⁻¹¹⁹ (section 1.3.2).

3.3.3.1 GC-MS conditions

A 2 μ L splitless sample injection volume was used for GC-MS experiments in full scan mode. Injector temperature was 250 °C, with oven temperature program 100 °C (hold 1 minute), 30 °C/minute to 300 °C (hold 3 minutes).

Once samples were run, extracted ion chromatograms (EIC) were used to obtain peak areas, i.e. extracted ion chromatograms at m/z 58 as this was the base peak for 4-MMC, and m/z 305 for codeine-D₆ as this was the most abundant ion encountered.

3.3.3.2 Temperature program

In order to obtain workable spectra for our compounds of interest, the temperature gradient was optimised for GC-MS analysis (using GC method 1). The analyte of interest and the IS (codeine-D₆) were optimised individually and were then analysed in combination to avoid co-eluting peaks. Codeine-D₆ was chosen as the internal standard since the undeuterated form may be encountered in some mixtures under examination. Other deuterated standards that are similar in size to the small drug molecules in question would also be suitable for this application. Despite thoughts that the deuterated form of 4-MMC would be a better choice, it was found to be unsuitable in this application since increased matrix effects were observed in mixtures analysed (section 7.3.3.1). Four temperature programs were trialled: Gradient A: 60 °C (1 minute), 20 °C/minute to 140 °C (hold 4 minutes), 30 °C/minute to 300 °C (hold 3 minutes); Gradient B: 100 °C (1 minute), 10 °C/minute to 140 °C (no hold), 30 °C/minute to 300 °C (hold 3 minutes); Gradient C: 100 °C (1 minute), 25 °C/minute to 140 °C (no hold), 30 °C/minute to 300 °C (hold 3 minutes); and Gradient D: 100°C (1 minute), 30°C/minute to 300°C (hold 3 minutes).

Gradient A was undesirable as the codeine-D₆ eluted too late (14.3 minutes) (Figure 3-24). Gradient B produced a superior chromatographic peak for codeine-D₆ as it eluted earlier (11.3 minutes); however, the elution still appeared to be towards the end of the run where the baseline tended upwards (Figure 3-25). Gradient C also improved the results for codeine-D₆ as it eluted even earlier once again (8.9 minutes, Figure 3-26). Gradient D produced the best chromatogram for the analysis of codeine-D₆. Elution time was reduced to 8.6 minutes; the peak shape was highly symmetrical and the increasing baseline did not affect peak shape

(Figure 3-27). This was the best gradient for the elution of codeine-D₆; therefore, gradient D was used in subsequent analyses.

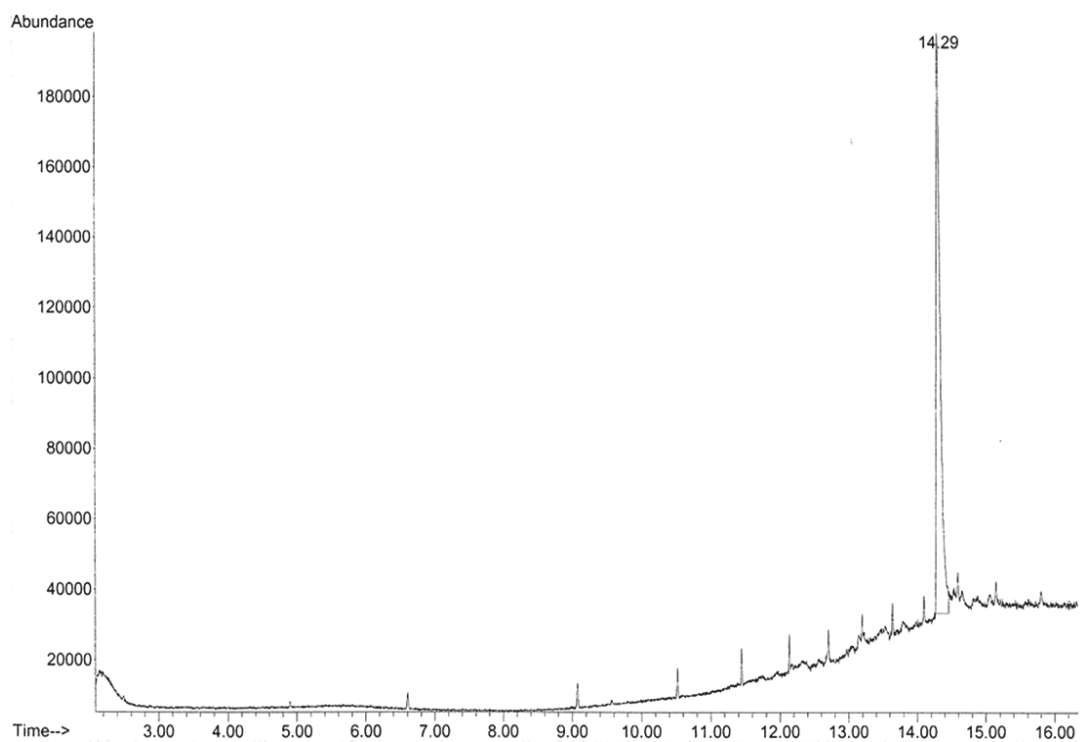


Figure 3-24 GC-MS chromatogram of codeine-D₆ using gradient A.

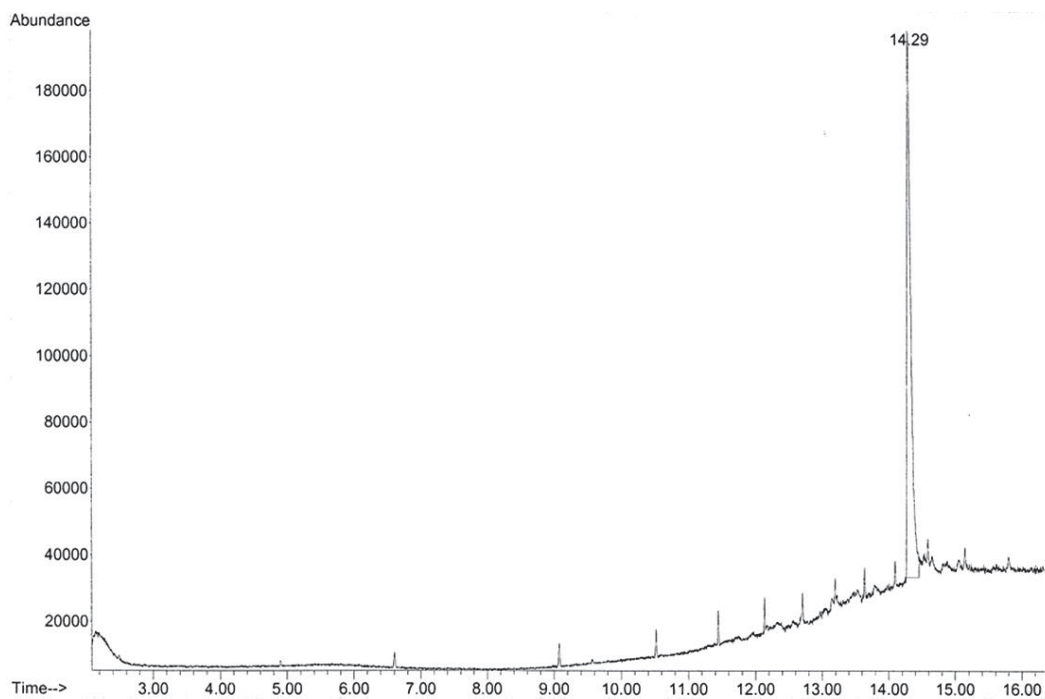


Figure 3-25 GC-MS chromatogram of codeine-D₆ using gradient B.

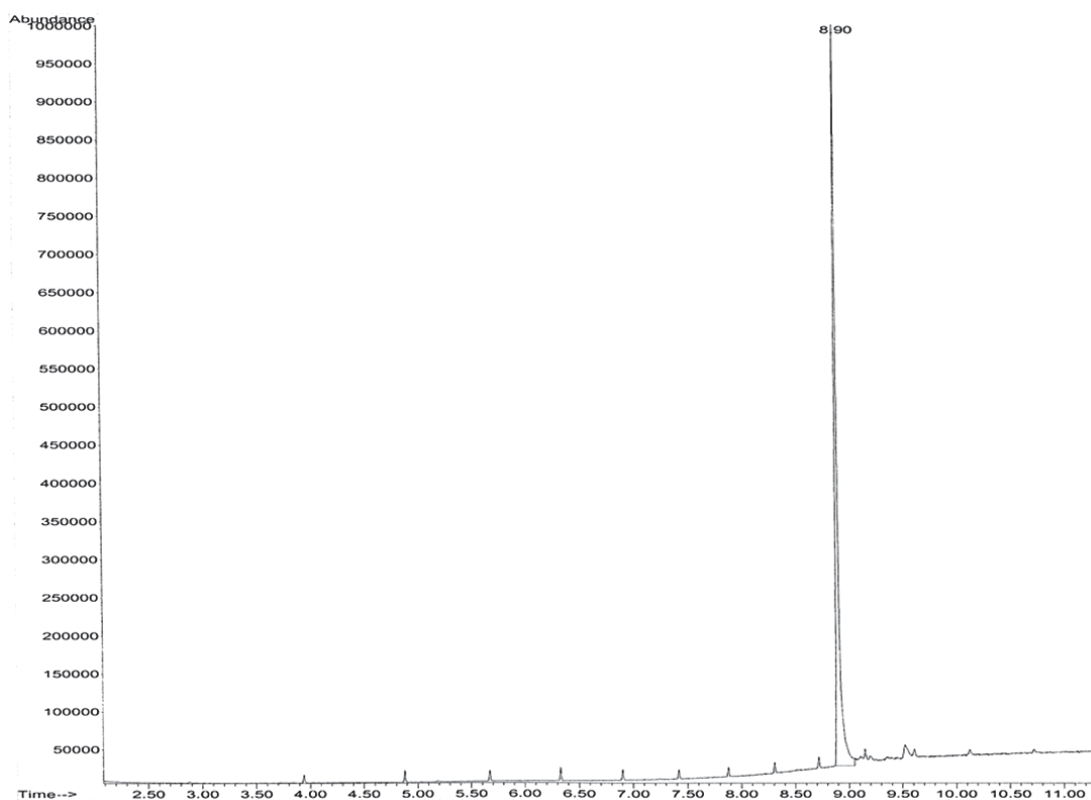


Figure 3-26 GC-MS chromatogram of codeine-D₆ using gradient C.

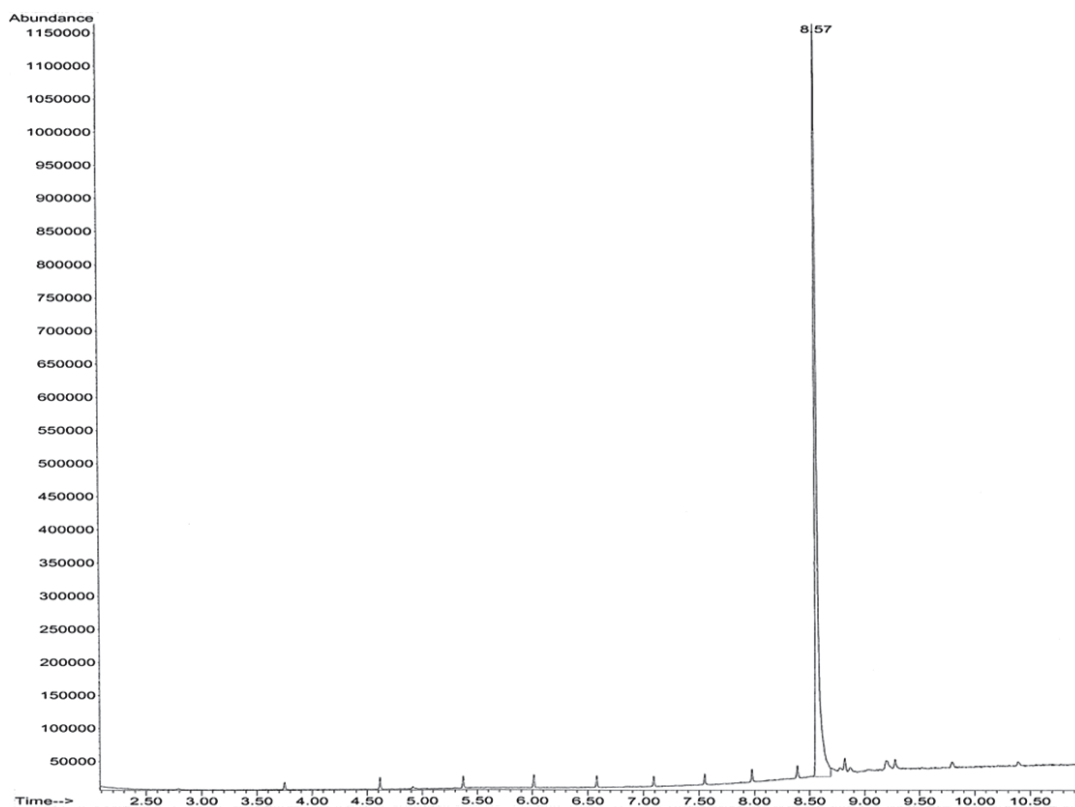


Figure 3-27 GC-MS chromatogram of codeine-D₆ using gradient D.

In addition to optimising the gradient temperature in the GC-MS analysis of codeine-D₆, the injection volume was increased to 2 μ L and samples were run in splitless mode in order to increase signal response, in particular for very dilute samples. The benefit of using a 2 μ L injection and splitless mode with gradient D was highly apparent in the increase in the signal response for 4-MMC (Figure 3-28).

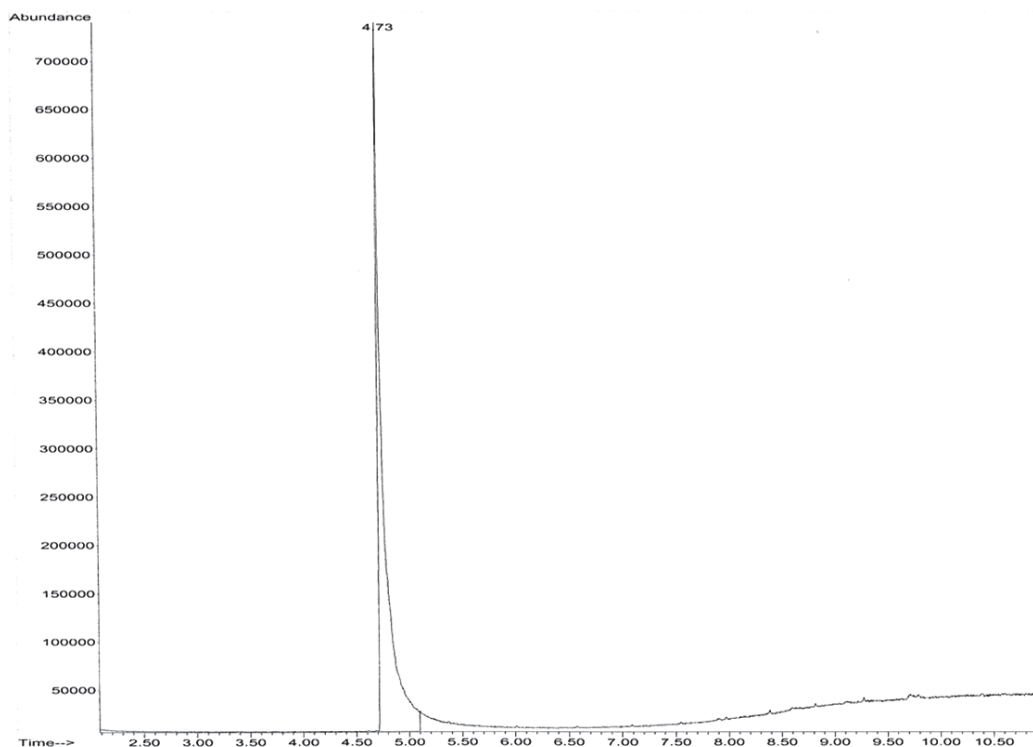


Figure 3-28 GC-MS chromatogram of 4-MMC; 2 μ L injection, splitless mode.

In order to confirm the success of gradient D, a mixture of 4-MMC and codeine-D₆ was subject to GC-MS analysis. The results revealed that both compounds eluted separately as they had significantly different retention times (Figure 3-29). The selectivity factor (defining the separation of two compounds) for codeine-D₆ and 4-MMC was found to be $\alpha = 1.91$.

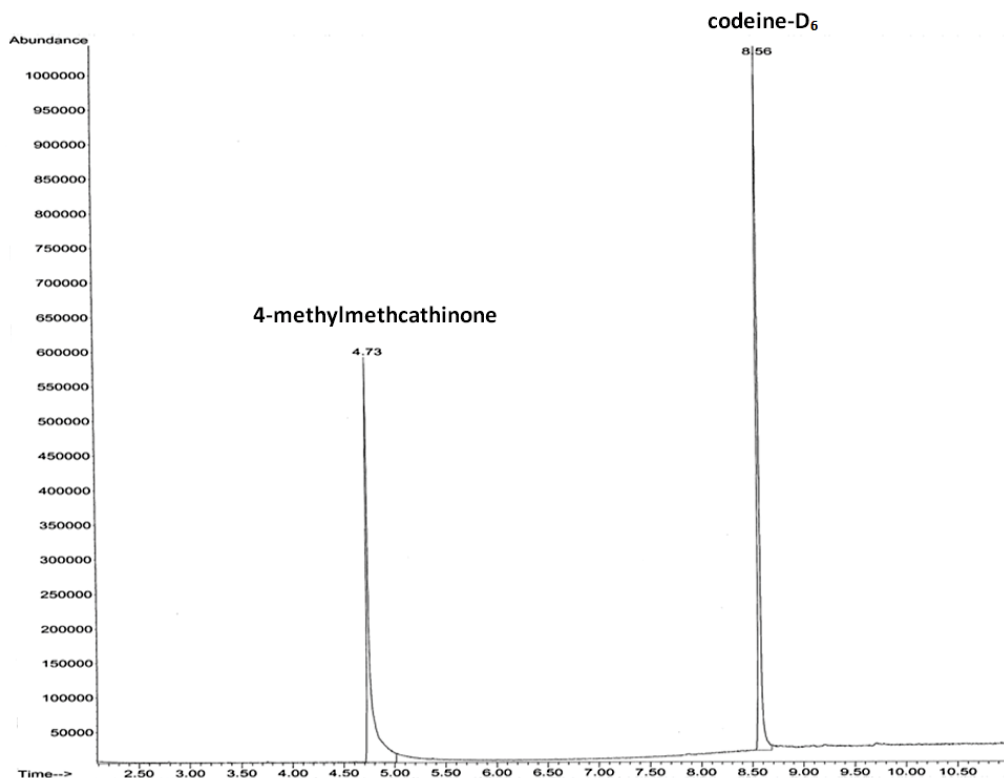


Figure 3-29 GC-MS chromatogram of 4-MMC and codeine-D₆ using gradient D; 2 μ L injection, splitless mode.

3.3.4 Optimising LC-MS parameters

Liquid chromatography – mass spectrometry was chosen as another comparison technique in this study due to its applications in drug analysis. Methods have been well-established using this technique and routine analyses are commonly conducted^{15, 47, 120-122} (section 1.3.2).

3.3.4.1 LC-MS conditions

A 10 μ L sample injection volume was used in LC-MS experiments at a flow rate of 0.5 mL/min. The column temperature was set to 35 °C, and the buffer solution was a mixture of A: 10 mM ammonium formate, B: acetonitrile (+ 5 % water to prevent polymerisation). The gradient was as follows: 0 minutes 10 % B, 20 minutes 90 % B, 20.1 minutes 10 % B, 25 minutes 10 % B.

3.3.4.2 Mobile phase gradient development

The two buffer solutions used during LC-MS method development were aqueous: A: 10 mM ammonium formate and organic: B: 100 % acetonitrile.

Varying concentrations of organic content were evaluated in order to obtain good peak shape and separation for both 4-MMC and the IS codeine-D₆. Three different gradients were applied as follows: gradient 1: 0 minutes 10 % B, 10 minutes 90 % B, 10.1 minutes 10 % B, 15 minutes 10 % B; gradient 2: 0 minutes 10 % B, 15 minutes 90 % B, 15.1 minutes 10 % B, 20 minutes 10 % B; gradient 3: 0 minutes 10 % B, 20 minutes 90 % B, 20.1 minutes 10 % B, 25 minutes 10 % B.

Gradient 1 resulted in the separation of 4-MMC and codeine-D₆; however, the two compounds eluted very close together, 0.3 minutes apart (resolution 1.1, i.e. not baseline resolved); therefore; this gradient was not desirable for the separation of the two compounds of interest (Figure 3-30). Gradient 2 resulted in a better separation of the two compounds of interest with a separation of 0.6 minutes, i.e. resolution = 2.3 (baseline resolution = 1.5) (Figure 3-31). Gradient 3 resulted in the best separation of 4-MMC and codeine-D₆ with the compounds eluting 0.7 minutes apart (resolution = 2.6) (Figure 3-32). Therefore, gradient 3 was used in future analyses. Despite gradient 2 being baseline resolved, Gradient 3 was chosen as optimal due to potential analyses involving mixed compounds (complex matrices) where overlapping peaks may result, a higher resolution is desirable.

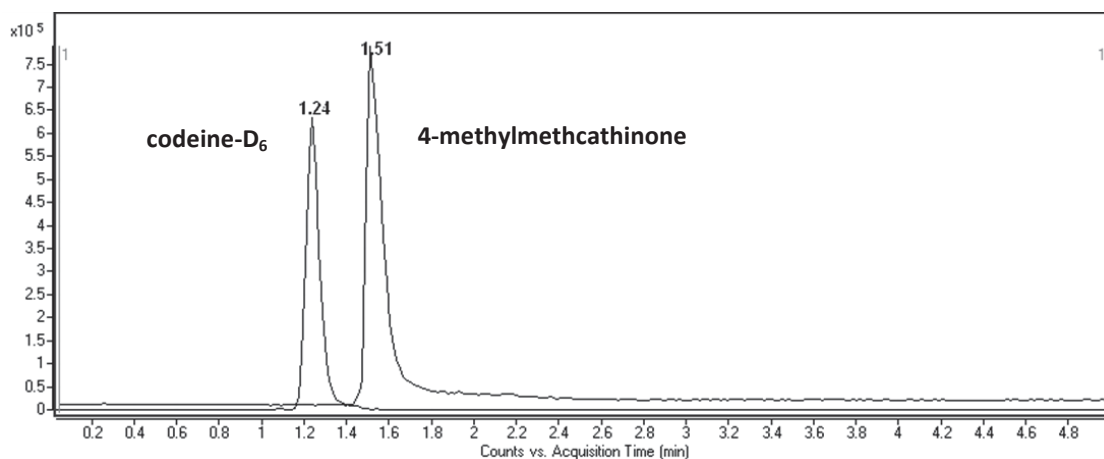


Figure 3-30 LC-MS EIC of 4-MMC and codeine- D_6 , gradient 1, resolution = 1.1.

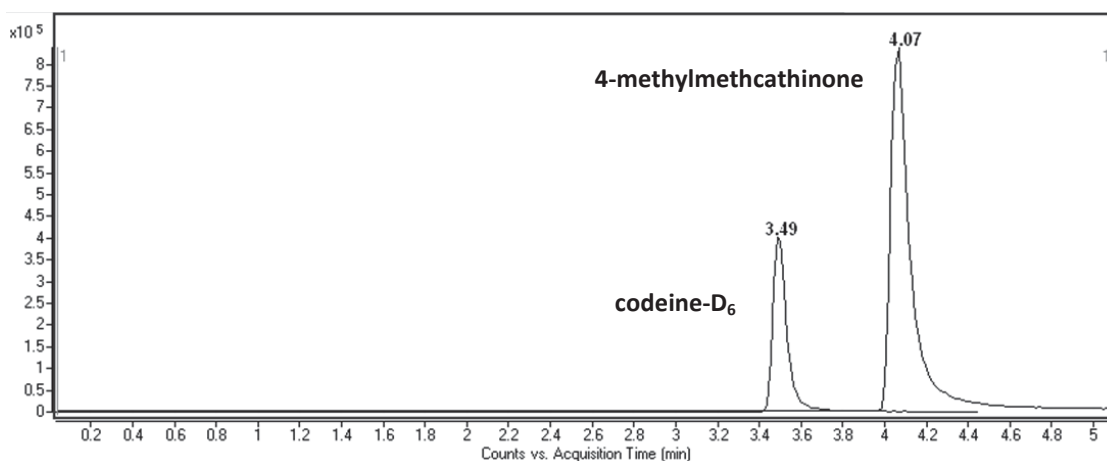


Figure 3-31 LC-MS EIC of 4-MMC and codeine- D_6 , gradient 2, resolution = 2.3.

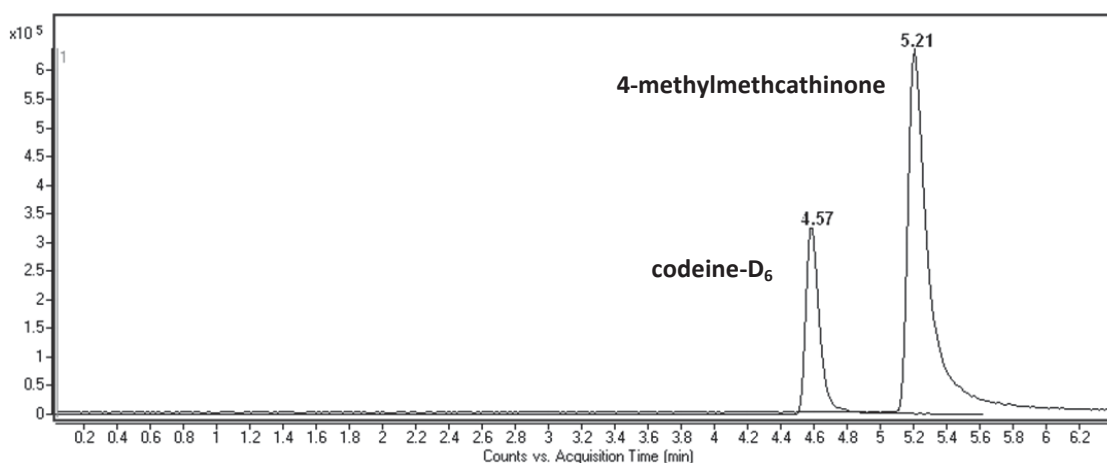


Figure 3-32 LC-MS EIC of 4-MMC and codeine- D_6 , gradient 3, resolution = 2.6.

3.4 Conclusions

Based on these results, a DESI-MS method was developed to suit a range of compounds for the analysis of novel and controlled substances. The solvent composition that was selected for general sample analysis was methanol/water (1:1) + 1 % formic acid since this solvent was used for the majority of compounds tested. The fragmentor voltage was set at 175 V since this represented the average of the optimised fragmentor voltages. In addition, some mixtures were analysed at two or three collision energies, i.e. 5, 20, and 30 eV in order to obtain appropriate collision induced dissociation data where necessary. The optimised GC-MS method was as follows: 2 μ L, splitless sample injection, full scan mode, injector temperature: 250 °C, oven temperature: 100 °C (hold 1 minute), 30 °C/minute to 300 °C (hold 3 minutes). The optimised LC-MS method was as follows: 10 μ L sample injection, flow rate: 0.5 mL/min, column temperature: 35 °C, mobile phase: A: 10 mM ammonium formate, B: acetonitrile (+ 5 % water), 0 minutes 10 % B, 20 minutes 90 % B, 20.1 minutes 10 % B, 25 minutes 10 % B. These optimised methods were applied in subsequent analyses in this research.

Chapter 4: Analysis of amphetamine-type substances

Chapter 4: Analysis of amphetamine-type substances

4.1 Introduction

The developed DESI-MS method was applied to the chemical analysis of ATS in this chapter. The LOD and effect of common adulterants, on the detectability of ATS was also evaluated. Illicit MDMA, PMMA, and DMAA (“Jack3d”) were analysed using DESI-MS and any by-products/impurities were identified. The results obtained from DESI-MS were also compared to GC-MS and LC-MS.

4.2 Materials and methods

Amphetamine, MA, MDMA, DMA and PMA standards were obtained from NMI (North Ryde, NSW, Australia). An MDMA tablet was obtained from the AFP. MDMA base and PMMA base were synthesised at the University of Technology, Sydney (UTS)^{98, 99}. “Jack3d” was purchased from Vitamin King, (Rockdale, NSW, Australia).

The methods developed using DESI-MS, GC-MS and LC-MS in section 3.3.1 - 3.3.4 were applied to the analysis of ATS in this chapter. The DESI-MS operating parameters were as optimised with experiments run in full scan mode (m/z 50 - 500) and MS/MS experiments conducted in the targeted product ion scan mode with collision energy of 20 eV. Samples were dissolved in methanol (10 mg/mL) unless otherwise specified. Sample aliquots (2 μ L) were deposited onto the PTFE sample plate. Analyte identity was supported by MS/MS experiments. Data analysis was conducted using Agilent MassHunter Workstation software, Qualitative Analysis, Version B.03.01 (Agilent Technologies). GC-MS was conducted in full scan mode (m/z 50 - 500). Samples were dissolved in methanol (1 mg/mL). Injection was done in splitless mode with an injection volume of 2 μ L. LC-MS was conducted in full scan mode (m/z 50 - 500) and MS/MS experiments were conducted in the product ion scan mode (auto MS/MS) with collision energy of 20 eV and injection volume of 10 μ L. Samples were dissolved in methanol (0.1 mg/mL). See section 2.2 for more method details.

The ATS standards were adulterated with caffeine, paracetamol (acetaminophen), magnesium stearate, and dimethyl sulfone (DMS), in order to evaluate the effects of adulterating the compound of interest. Adulteration involving caffeine was conducted with varying amounts of caffeine added (i.e. 20 %, 50 %, 90 %, 95 % w/w, respectively).

In DESI-MS analysis, the LOD was defined to be the lowest concentration required to give a signal equal or greater than the average intensity of the blank signal plus three times the SD of the blank⁹. In the GC-MS and LC-MS analysis, the LOD was defined to be the lowest peak concentration to exhibit a peak height three times the noise level (SNR 3:1). The ANOVA test was utilised as a means to determine whether the observed ion enhancement or suppression in adulteration experiments was significantly different to the unadulterated signal response (i.e. $p < 0.05$).

4.3 Results and discussion

4.3.1 Adulteration and LOD

4.3.1.1 *Methylamphetamine*

An intra-day study assessing the effects of adulterants on the detectability of MA was conducted (Figure 4-1 and Figure 4-2). The adulterants used were magnesium stearate, paracetamol, caffeine and DMS as these were a selection of the most common adulterants used in ATS manufacture. The adulterants presented herein are commonly found in a variety of ATS; however, MA was the focus of this study as it is one of the more prevalent ATS. It was found that the addition of magnesium stearate to a MA sample significantly enhanced the signal response of the protonated molecular ion $[M+H]^+$ ($p < 0.05$). This was thought to be due to the hydrophobic properties of magnesium stearate itself aiding in the initial wetting of the surface and subsequent splashing of the secondary droplets carrying the more hydrophilic components, i.e. the MA ions. On the contrary, paracetamol, caffeine and dimethyl sulfone did not result in significant enhancement effects ($p > 0.05$, Figure 4-2).

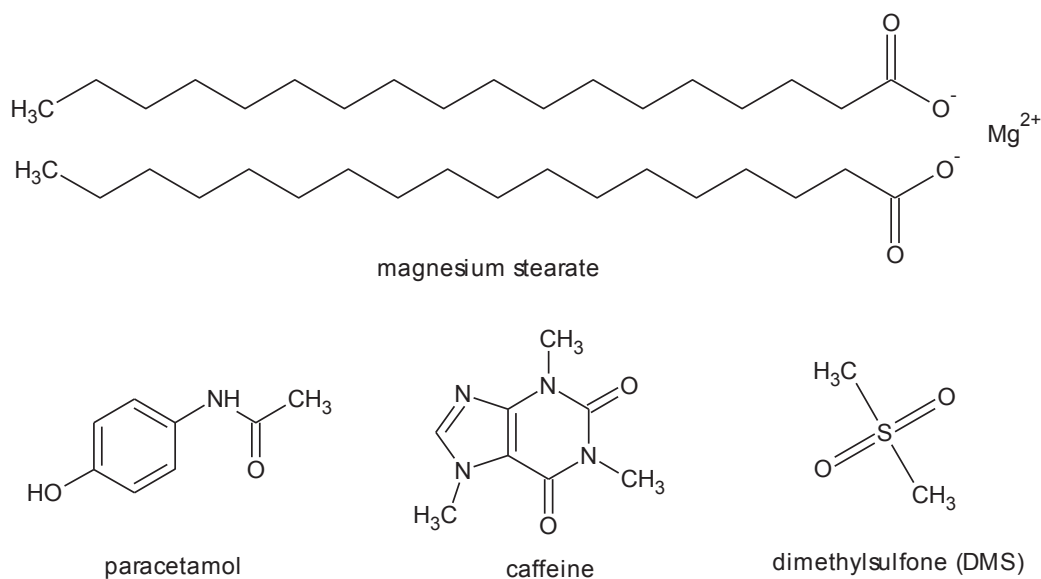


Figure 4-1 Chemical structures of common adulterants in ATS preparations.

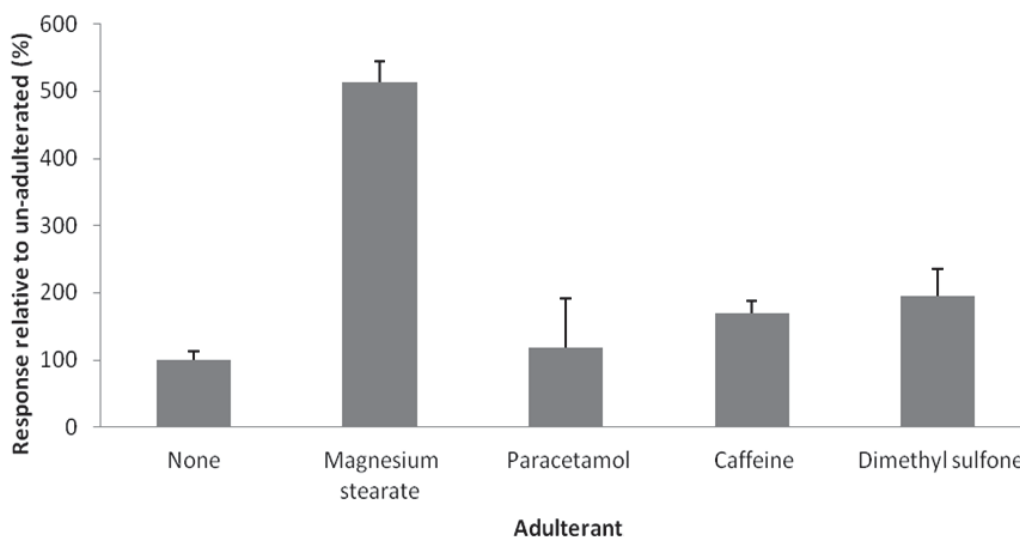


Figure 4-2 Intra-day study of the effects of different adulterants on the detection of MA (0.36 μ g), 1:1 ratio, n=3.

This experiment was repeated over three days in order to evaluate the repeatability of this study. The same trend was observed over the three days tested; with magnesium stearate resulting in the largest enhancement of the MA signal ($p < 0.05$) and paracetamol, caffeine and dimethyl sulfone resulting in indifferent responses to the unadulterated MA response ($p > 0.05$, Figure 4-3). The intra-day and inter-day precision for unadulterated MA was 14 % RSD and 58 % RSD, n=3, respectively. The changes in instrument response over time and the transient signal in the DESI source were contributing factors in the precision values obtained.

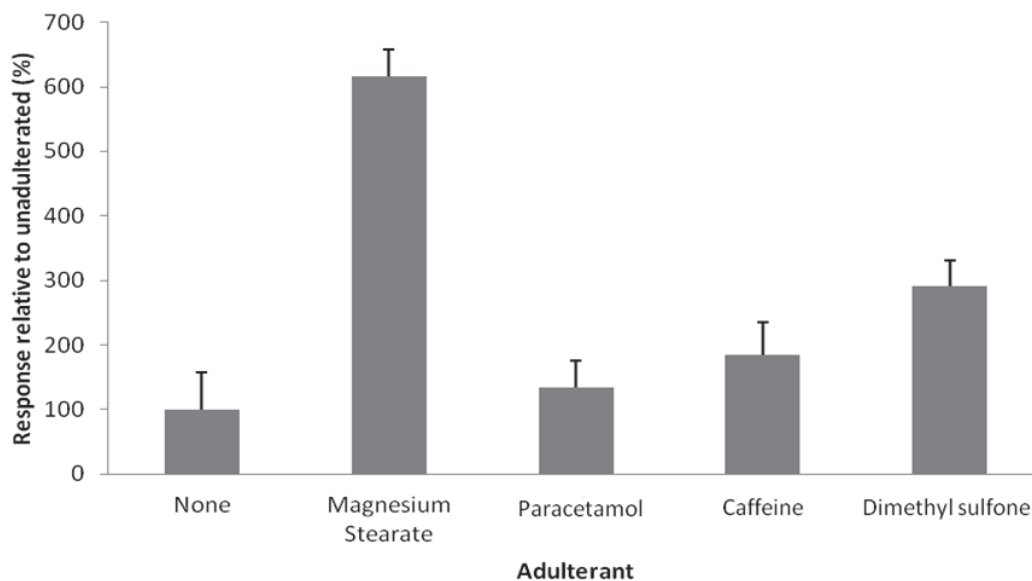


Figure 4-3 Inter-day study of the effect of different adulterants on the detection of MA (0.36 μg), 1:1 ratio, $n=3$.

A MA standard was adulterated with various amounts of caffeine. Based on the data obtained, it was determined that the LOD for MA using DESI-MS was 0.14 μg (equivalent to 0.02 $\mu\text{g}/\text{mm}^2$, spot size 7 mm^2). The average signal response (peak height) of MA at this concentration (with 0 % caffeine) was 3404 cps which was greater than the LOD determined from the solvent blank plus 3 x SD (i.e. average + 3SD = 1487 cps, m/z 100 - 200), allowing MA to be distinguished unambiguously amongst the background noise peaks. It was evident that at 0.14 μg of MA, increasing the amount of caffeine (20 % to 95 % w/w) had significant enhancement effects on the MA being detected in the DESI source ($p < 0.05$, Figure 4-4). The presence of MA in these samples was supported by MS/MS data (Figure 4-5); the proposed collision induced dissociation of the $[\text{M}+\text{H}]^+$ ion¹²³ is illustrated in Figure 4-6.

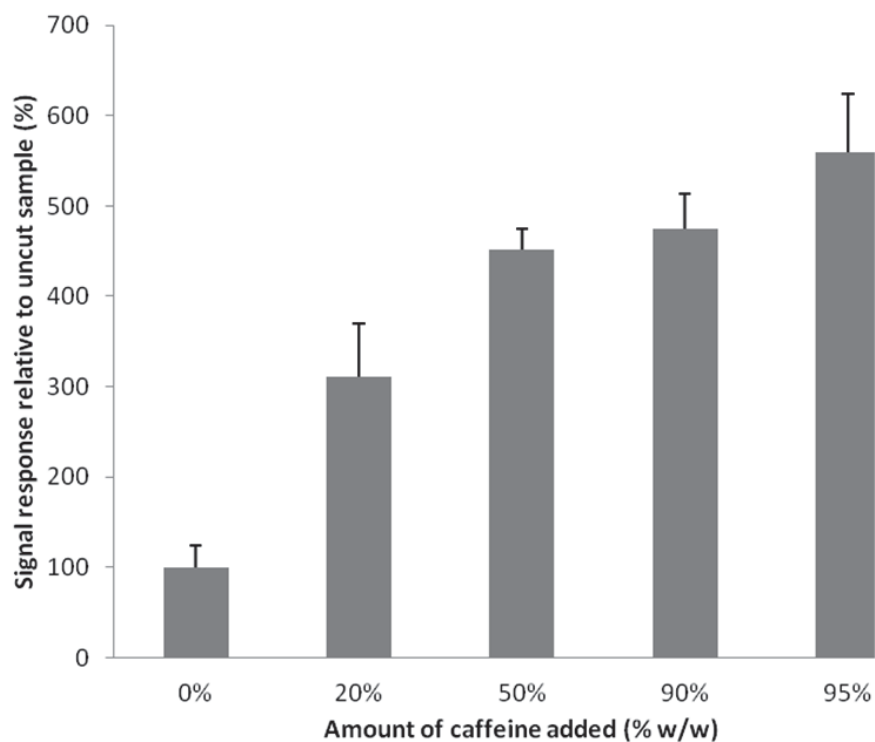


Figure 4-4 Adulterating MA standard with caffeine at varying amounts caffeine added (0 %, 20 %, 50 %, 90 %, 95 % w/w), $n=3$, 2 μL of 74.5 $\mu\text{g/mL}$, equivalent to 0.14 μg MA.

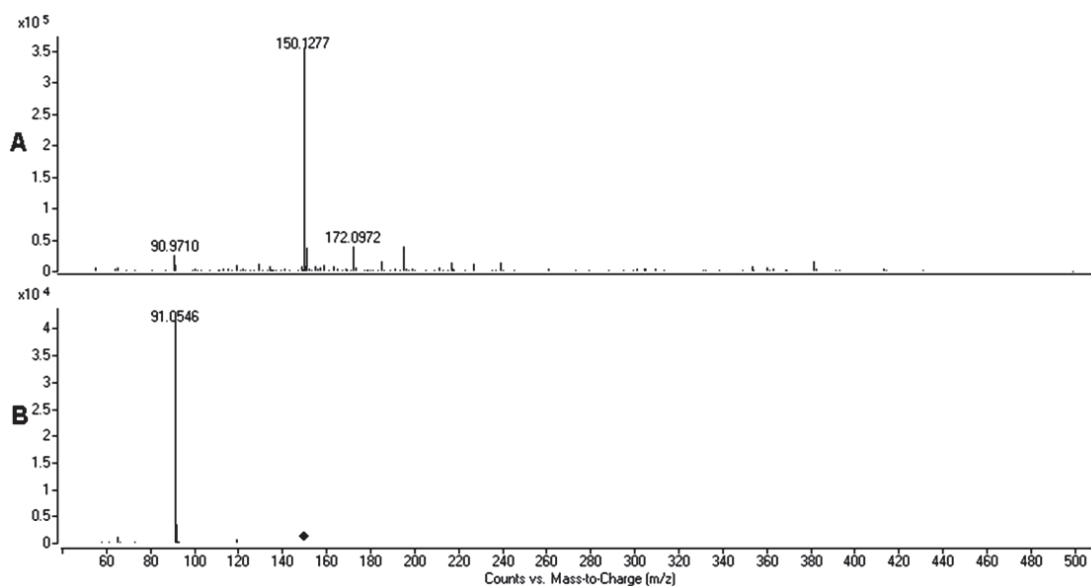


Figure 4-5 A: DESI-MS of MA, B: MS/MS of MA at 20 eV.

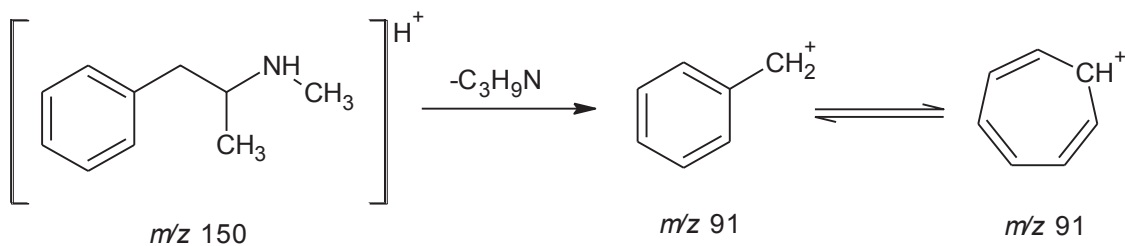


Figure 4-6 Proposed collision induced dissociation of the $[M+H]^+$ ion of MA.

4.3.1.2 4-Methoxyamphetamine

A PMA standard was adulterated with various amounts of caffeine. Based on the data obtained, it was determined that the LOD for PMA using DESI-MS was $1.65 \mu\text{g}$ (equivalent to $0.24 \mu\text{g}/\text{mm}^2$). The average signal response (peak height) of PMA at this concentration (with 0 % caffeine) was 13987 cps which was greater than the LOD determined from the solvent blank plus $3 \times \text{SD}$ (i.e. average + $3\text{SD} = 5862 \text{ cps}$, m/z 100 - 200), allowing PMA to be distinguished unambiguously amongst the background noise peaks. At $1.65 \mu\text{g}$ of PMA, the signal response for subsequent increasing amounts of caffeine produced ion suppression effects at 90 % and 95 % w/w ($p < 0.05$, Figure 4-7). Despite the signal response of PMA being relatively larger than the calculated solvent blank, this concentration was chosen as the LOD due to some suppression effects observed with the addition of caffeine which may render the analyte undetectable at concentrations close to the LOD in routine analyses. The presence of PMA in these samples was supported by MS/MS data¹²³ (Figure 4-8); the proposed collision induced dissociation of the $[\text{M}+\text{H}]^+$ ion is illustrated in Figure 4-9.

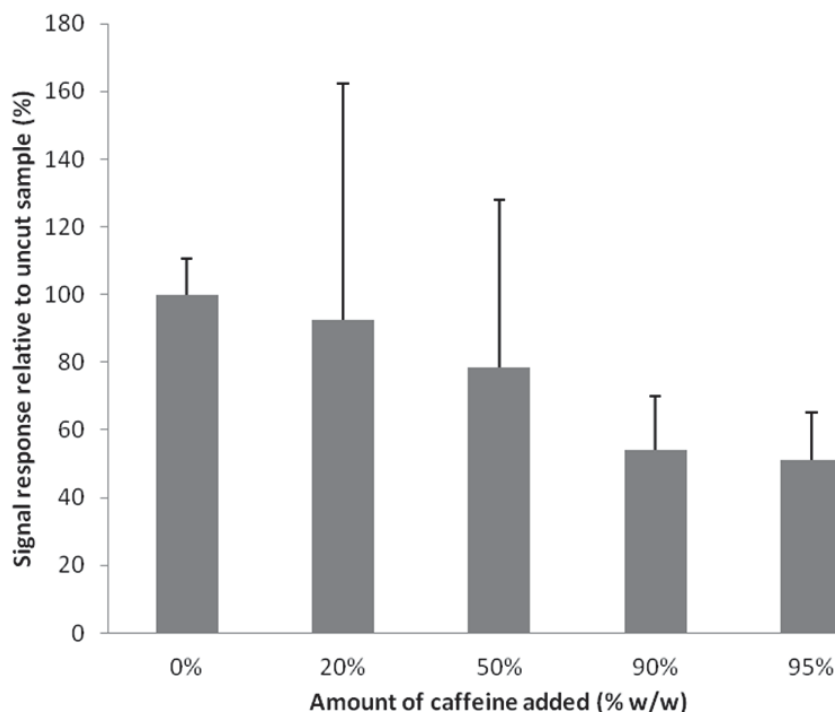


Figure 4-7 Adulterating PMA standard with caffeine at varying amounts of caffeine added (0 %, 20 %, 50 %, 90 %, 95 % w/w), $n=3$, $2 \mu\text{L}$ $826 \mu\text{g}/\text{mL}$, equivalent to $1.65 \mu\text{g}$ PMA.

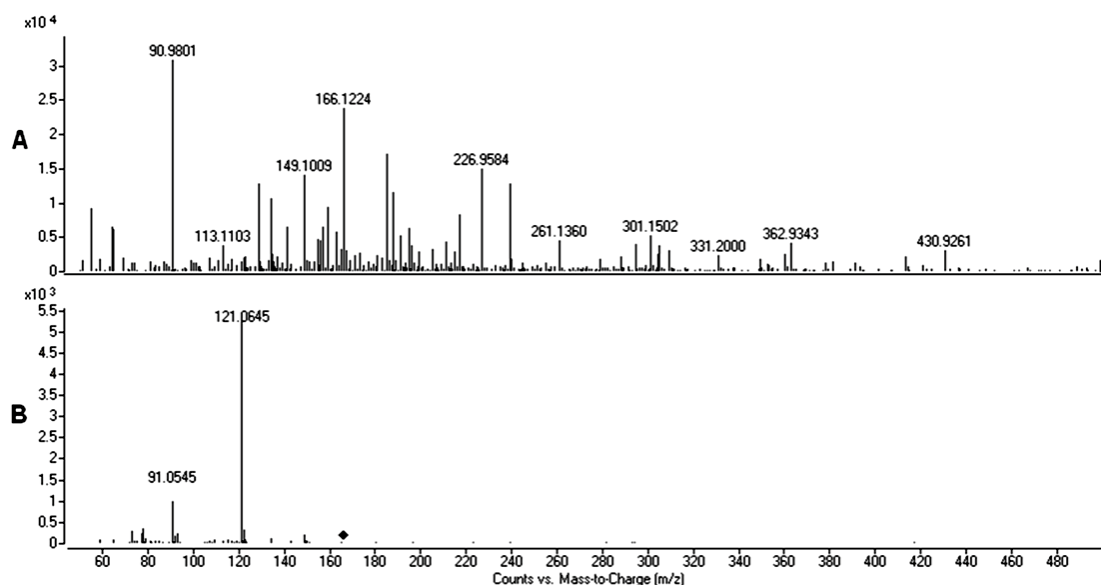


Figure 4-8 A: DESI-MS of PMA, B: MS/MS of PMA at 20 eV.

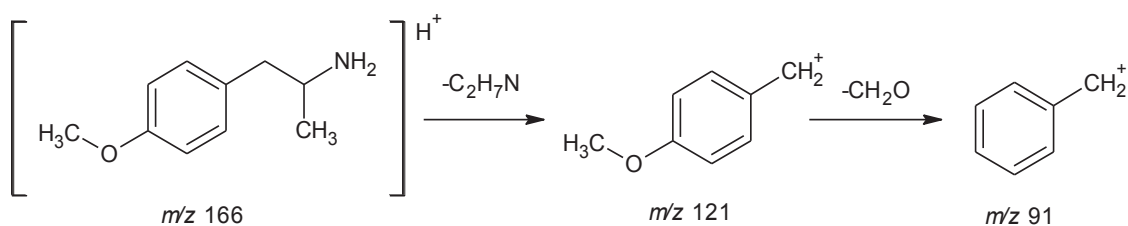


Figure 4-9 Proposed collision induced dissociation of the $[M+H]^+$ ion of PMA.

4.3.1.3 Amphetamine

An AP standard was adulterated with various amounts of caffeine. Based on the data obtained, it was determined that the LOD for AP using DESI-MS was 0.14 μg (equivalent to 0.02 $\mu\text{g}/\text{mm}^2$). The average signal response (peak height) of AP at this concentration (with 0 % caffeine) was 10593 cps which was greater than the LOD determined from the solvent blank plus 3 x SD (i.e. average + 3SD = 3682 cps, m/z 100 - 200), allowing AP to be distinguished unambiguously amongst the background noise peaks. It was evident that at 0.14 μg of AP, increasing the amount of caffeine (20 % to 95 % w/w) had little effect on the AP being detected in the DESI source ($p > 0.05$, Figure 4-10). Despite the signal response of AP being relatively larger than the calculated solvent blank, this concentration was chosen as the LOD to avoid false negative results at concentrations close to the LOD in routine analyses. The presence of AP in these samples was supported by MS/MS data¹²³ (Figure 4-11); the proposed collision induced dissociation of the $[M+H]^+$ ion is illustrated in Figure 4-12.

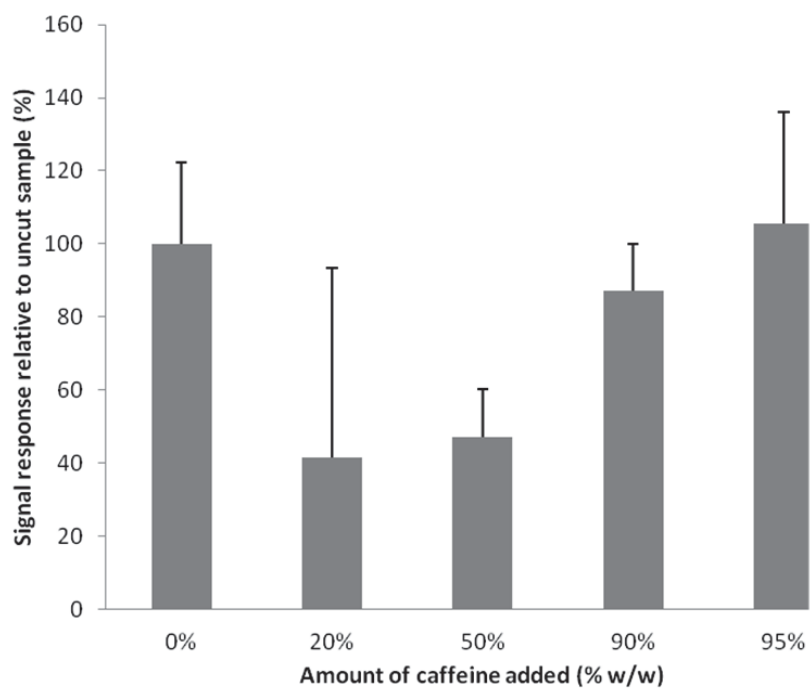


Figure 4-10 Adulterating AP standard with caffeine at varying amounts of caffeine added (0 %, 20 %, 50 %, 90 %, 95 % w/w), $n=3$, $2 \mu\text{L}$ of $67.6 \mu\text{g/mL}$, equivalent to $0.14 \mu\text{g AP}$.

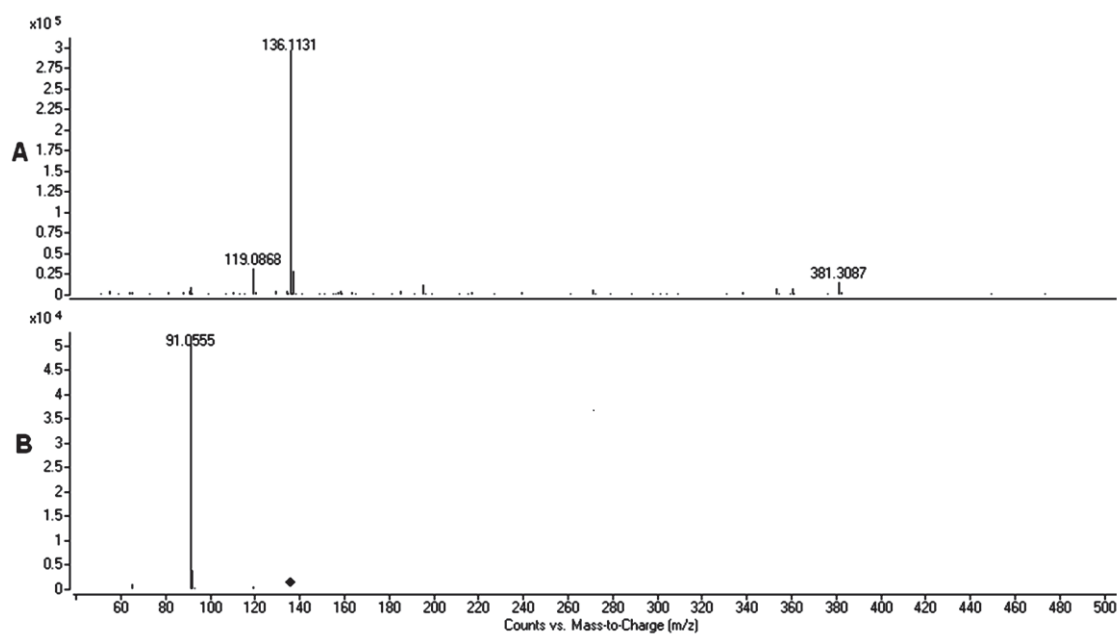


Figure 4-11 A: DESI-MS of AP, B: MS/MS of AP at 20 eV.

0 % caffeine) was 4057 cps which was greater than the LOD determined from the solvent blank plus 3 x SD (i.e. average + 3SD = 3052 cps, m/z 100 - 200), allowing DMA to be distinguished unambiguously amongst the background noise peaks. It was evident that at 0.16 μg of DMA, 50 % w/w caffeine added produced ion enhancement effects ($p < 0.05$, Figure 4-14). Despite the signal response of DMA being slightly larger than the calculated solvent blank, this concentration was chosen as the LOD in order to prevent false negative results at concentrations close to the LOD in routine analyses. The presence of DMA in these samples was supported by MS/MS data¹²³ (Figure 4-15); the proposed collision induced dissociation of the $[\text{M}+\text{H}]^+$ ion is illustrated in Figure 4-16.

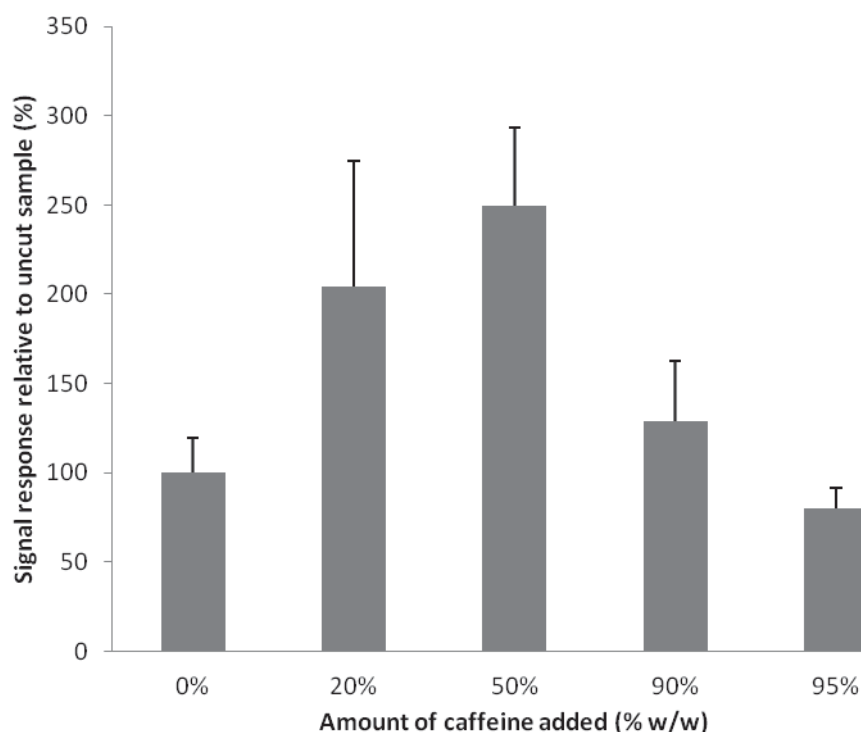


Figure 4-14 Adulterating DMA standard with caffeine at varying amounts of caffeine added (0 %, 20 %, 50 %, 90 %, 95 % w/w), $n=3$, 2 μL of 80 $\mu\text{g}/\text{mL}$, equivalent to 0.16 μg DMA.

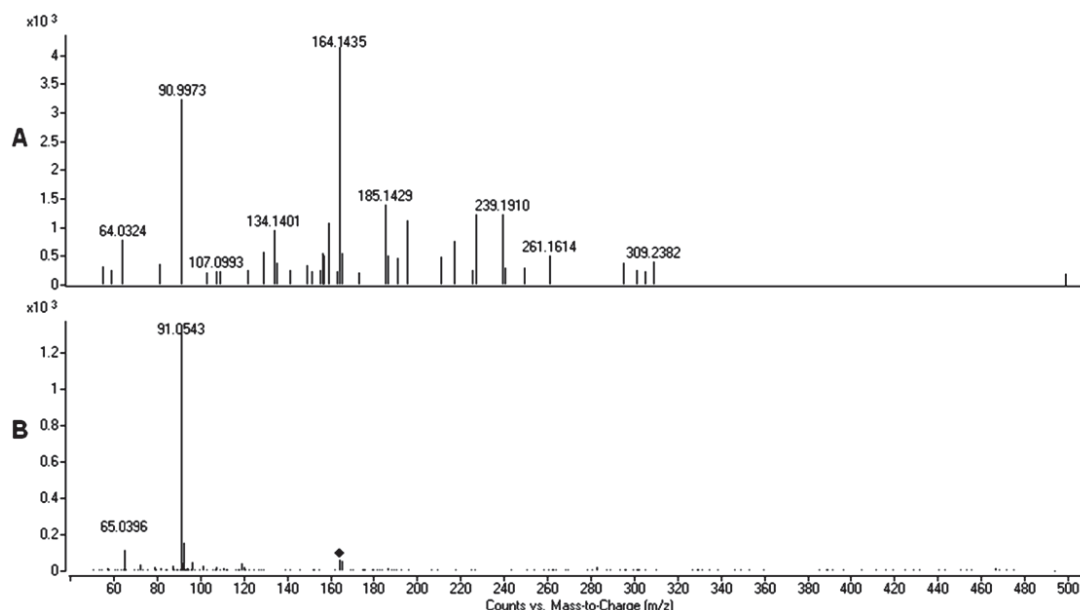


Figure 4-15 A: DESI-MS of DMA, B: MS/MS of DMA at 20 eV.

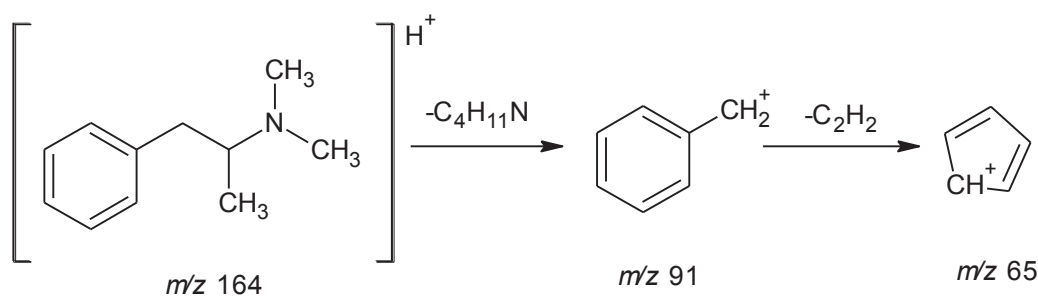


Figure 4-16 Proposed collision induced dissociation of the $[M+H]^+$ ion of DMA.

4.3.1.5 3,4-Methylenedioxymethylamphetamine

A MDMA standard was adulterated with various amounts of caffeine. Based on the data obtained, it was determined that the LOD for MDMA using DESI-MS was 19.4 μg (equivalent to 2.80 $\mu\text{g}/\text{mm}^2$). The average signal response (peak height) of MDMA at this concentration (with 0 % caffeine) was 4648 cps which was greater than the LOD determined from the solvent blank plus 3 x SD (i.e. average + 3SD = 2028 cps, m/z 100 - 200), allowing MDMA to be distinguished unambiguously amongst the background noise peaks. At 19.38 μg , the presence of caffeine did not affect the signal response significantly ($p > 0.05$, Figure 4-17).

The presence of MDMA in these samples was supported by MS/MS data (Figure 4-18); the proposed collision induced dissociation of the $[M+H]^+$ ion is illustrated in Figure 4-19.

However, some limitations arose due to the simultaneous detection of MDMA and caffeine. The protonated molecular ions for MDMA and caffeine are m/z 194 and m/z 195, respectively. This poses an issue when fragmentation data is taken since the detection of these two compounds interferes with one another. The MS/MS data collected exhibited mixed fragments of each compound. The limitation in resolving power of the quadrupole in the QTOF instrument utilized is hypothesised to be due to hardware limitations. This may be rectified by new technology where the resolving power is much higher. However, this was not a recurring issue and was only encountered in the MDMA and caffeine samples as these two compounds were within 1 m/z unit. The fragments in each MS/MS spectra which are shown with a box or oval are characteristic fragments to MDMA and caffeine, respectively. The fragments at m/z 105 and 163 corresponding to MDMA were also present in the caffeine spectra. Despite this, a majority of the characteristic fragments for MDMA were present allowing for a preliminary identification of the compound of interest.

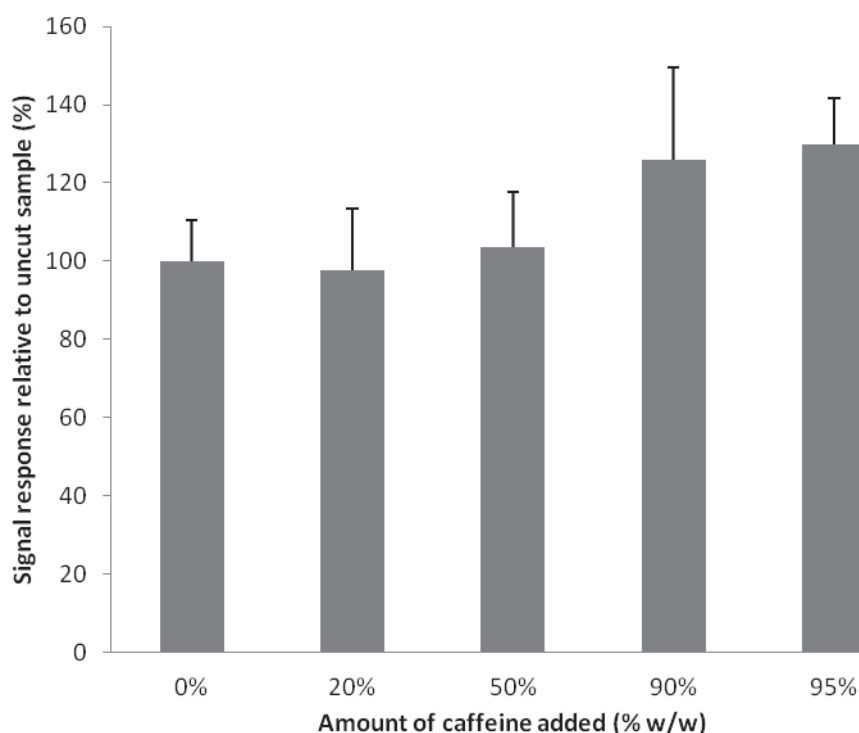


Figure 4-17 Adulterating MDMA standard with caffeine at varying amounts of caffeine added (0 %, 20 %, 50 %, 90 %, 95 % w/w), $n=3$, 2 μL of 9660 $\mu\text{g}/\text{mL}$, equivalent to 19.4 μg MDMA.

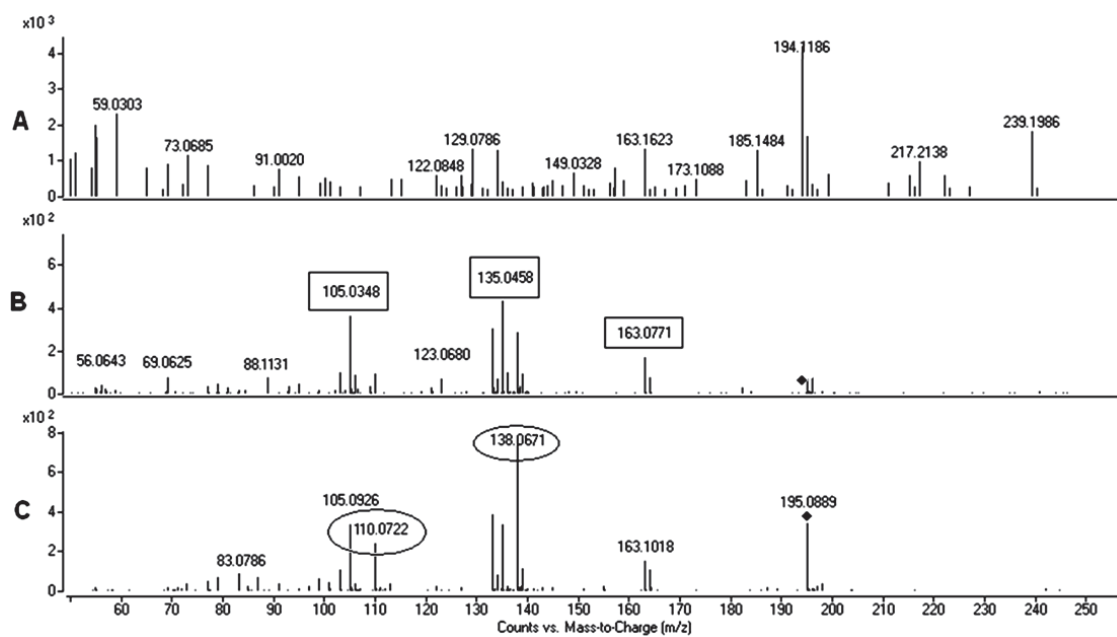


Figure 4-18 A: DESI-MS of MDMA; B: MS/MS of MDMA; C: MS/MS of caffeine at 20 eV.

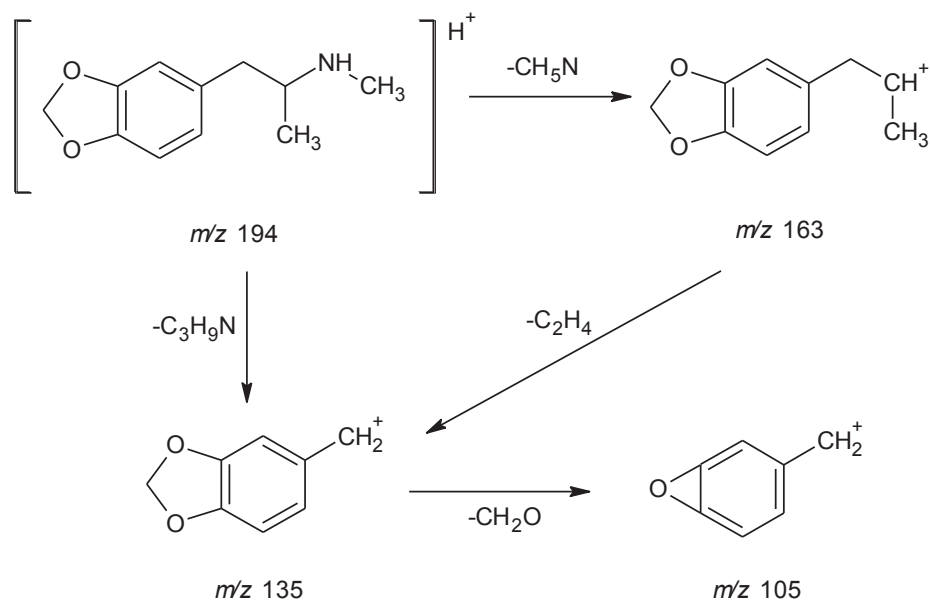


Figure 4-19 Proposed collision induced dissociation of the $[M+H]^+$ ion of MDMA.

4.3.1.6 Limit of Detection summary

The LOD determined for MA, PMA, AP, MDMA and DMA are presented in Table 4-1. In addition, the intra-day precision (n=3) of the technique for the analysis of ATS was found to be <25 % (RSD).

Table 4-1 Limit of detection of different ATS, n=3.

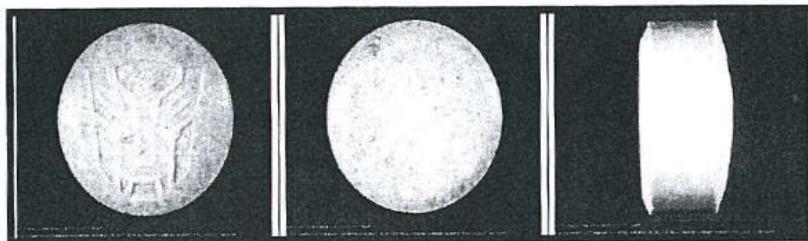
Sample	LOD ^a (µg/mm ²)
MA	0.02
PMA	0.24
AP	0.02
MDMA	2.80
DMA	0.02

^a sample well size 7 mm².

4.3.2 Analysis of 3,4-methylenedioxyamphetamine

4.3.2.1 Desorption electrospray ionisation – mass spectrometry

Prior to DESI-MS analysis, an MDMA tablet was analysed by NMI and was found to contain 25.7 % MDMA.HCl and three impurities 3,4-methylenedioxyphenyl-2-propanol (MDP-2-POH, 90.6 % peak normalised), 3,4-methylenedioxydimethylamphetamine (MDDMA, 3.7 % peak normalised), and 3,4-methylenedioxyphenyl-2-propanone (MDP-2-P, 2.2 % peak normalised) (Figure 4-20).

MDMA**PS3122183 TT1 (Items 1 and 2)**

Analysis: MDMA HCl 25.7%

Synthetic Route: Reductive Amination – Borohydride

Major Impurities/By-products Detected (% peak normalised)¹:

- 3,4-methylenedioxy-2-propanol (90.6)
- 3,4-methylenedioxy-dimethylamphetamine (3.7)
- 3,4-methylenedioxy-2-propanone (2.2)

Elemental Analysis (mg/kg)

- Aluminium (1660.0)
- Boron (49.0)
- Phosphorus (12.0)
- Nickel (1.5)
- Platinum (0.01)
- Sulphur (860.0)
- Zinc (1.8)

Figure 4-20 Data on MDMA sample provided by AFP (analysis conducted by NMI).

Using DESI-MS, MDMA was detected as the protonated molecular ion at m/z 194 (Figure 4-21). The impurities MDP-2-POH and MDDMA were detected at m/z 181 and m/z 208 (in trace amounts), respectively as the protonated molecular ion peaks. The presence of MDMA and the by-products/impurities were supported by their MS/MS spectra¹²³ (Figure 4-22 and Figure 4-23). The third impurity MDP-2-P remained undetected due to a low concentration present and also due to possible ion suppression in the mixture. The identification of these compounds agree with the route of manufacture utilised, i.e. reductive amination of MDP-2-P to MDMA¹²⁴.

The precursor ions in the DESI-MS spectra below (i.e. MDP-2-POH and MDDMA) appear to be below the SNR; however, on inspection of the MS/MS spectra, lower LOD are achievable resulting in higher SNR in the collision induced dissociation spectra (Figure 4-22 C and D). This

suggests that the use of MS/MS data can provide increased sensitivity to a detection technique such as DESI-MS⁷².

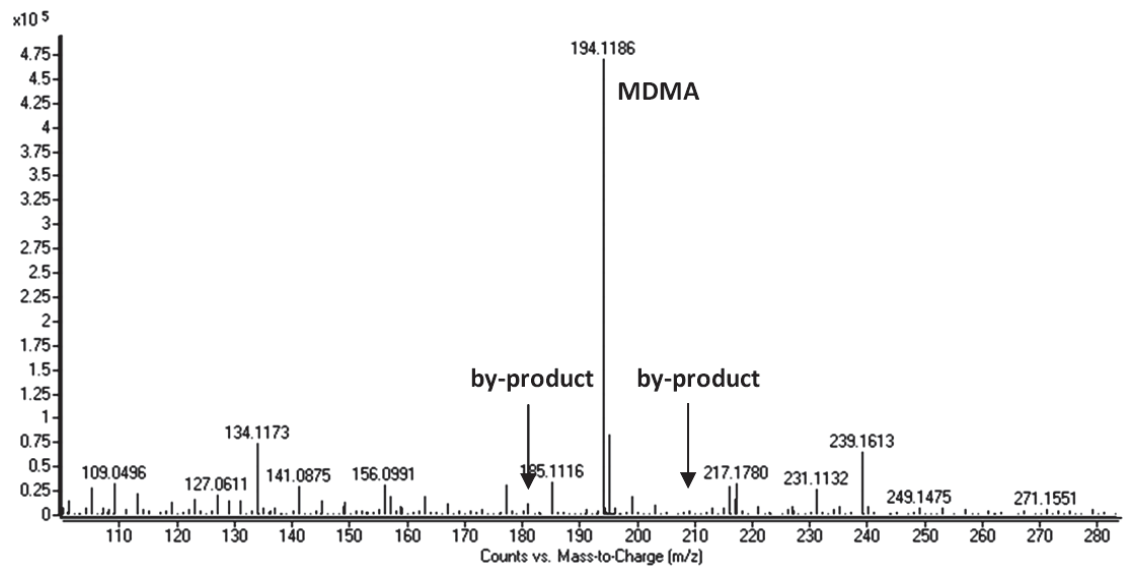


Figure 4-21 DESI-MS spectra of MDMA tablet.

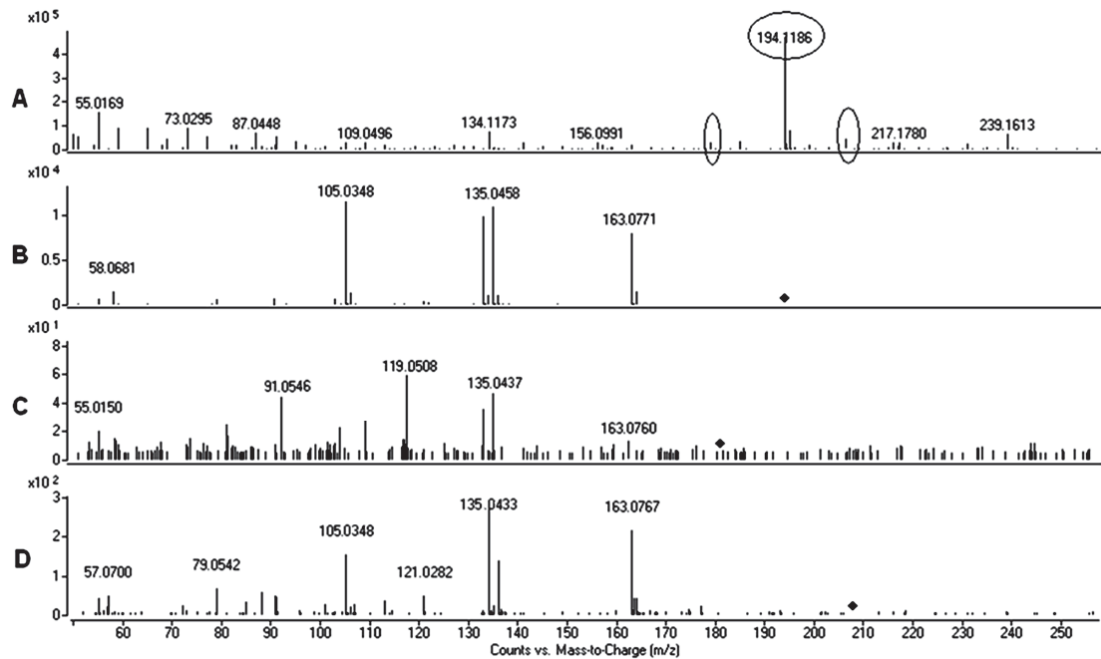


Figure 4-22 A: DESI-MS of MDMA tablet, B: MS/MS of MDMA, C: MS/MS of 3,4-methylenedioxyphenyl-2-propanol (MDP-2-POH), D: MS/MS of 3,4-methylenedioxymethylamphetamine (MDDMA).

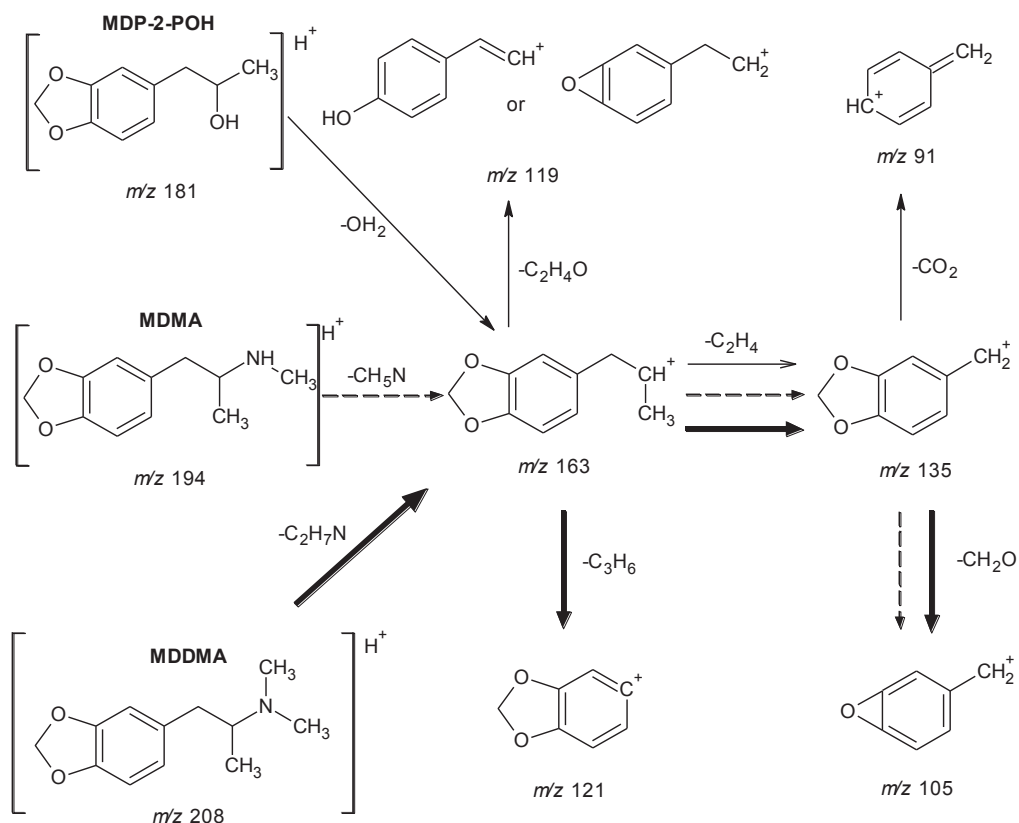


Figure 4-23 Proposed collision induced dissociation of the $[M+H]^+$ ion of MDMA (---), MDP-2-POH (→) and MDDMA (⇒).

The synthesised MDMA base was analysed using DESI-MS and was found to contain MDMA as the protonated molecular ion at m/z 194 (Figure 4-24 - Figure 4-26). PCDL software was used in all instances where compound confirmation was required. The PCDL library match is based on a score calculated on the similarity of the ions present and their relative abundances as compared to the reference spectra. In the current research a match score above 60 was deemed acceptable since differences in fragment ion abundances would significantly decrease a match score, thus enabling a high differentiating power in the matches obtained. The library match score obtained using the PCDL software was 86.84 for the MDMA tablet.

One major by-product of reaction was detected at m/z 179 which was determined to be MDP-2-P and supported by MS/MS spectra (Figure 4-24 C and Figure 4-25). Piperonyl nitrile (PN) was also identified as being present in the illicit MDMA sample (Figure 4-24 D). The presence of this by-product confirms that MDMA was synthesised via MDP-2-P using piperonal as the main precursor, consistent with the method utilised¹²⁴.

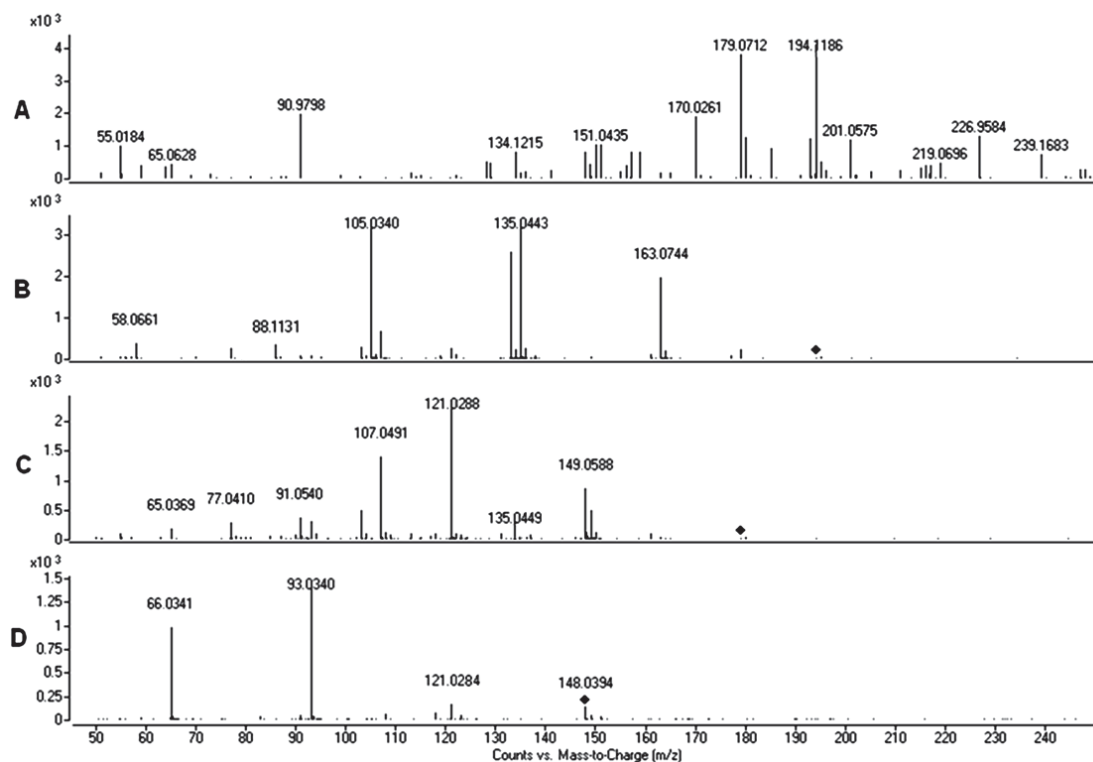


Figure 4-24 A: DESI-MS of MDMA sample, B: MS/MS of MDMA, C: MS/MS of MDP-2-P, D: MS/MS of PN.

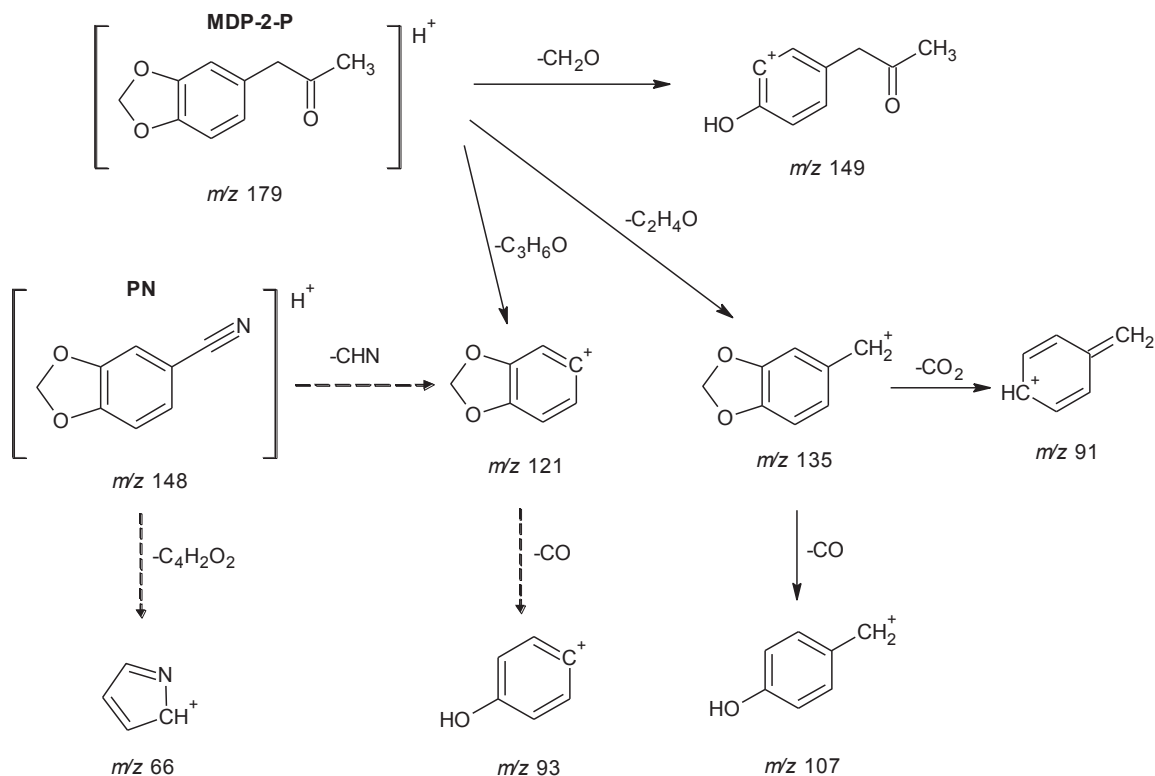


Figure 4-25 Proposed collision induced dissociation of the $[M+H]^+$ ion of MDP-2-P (- - >) and PN (→).

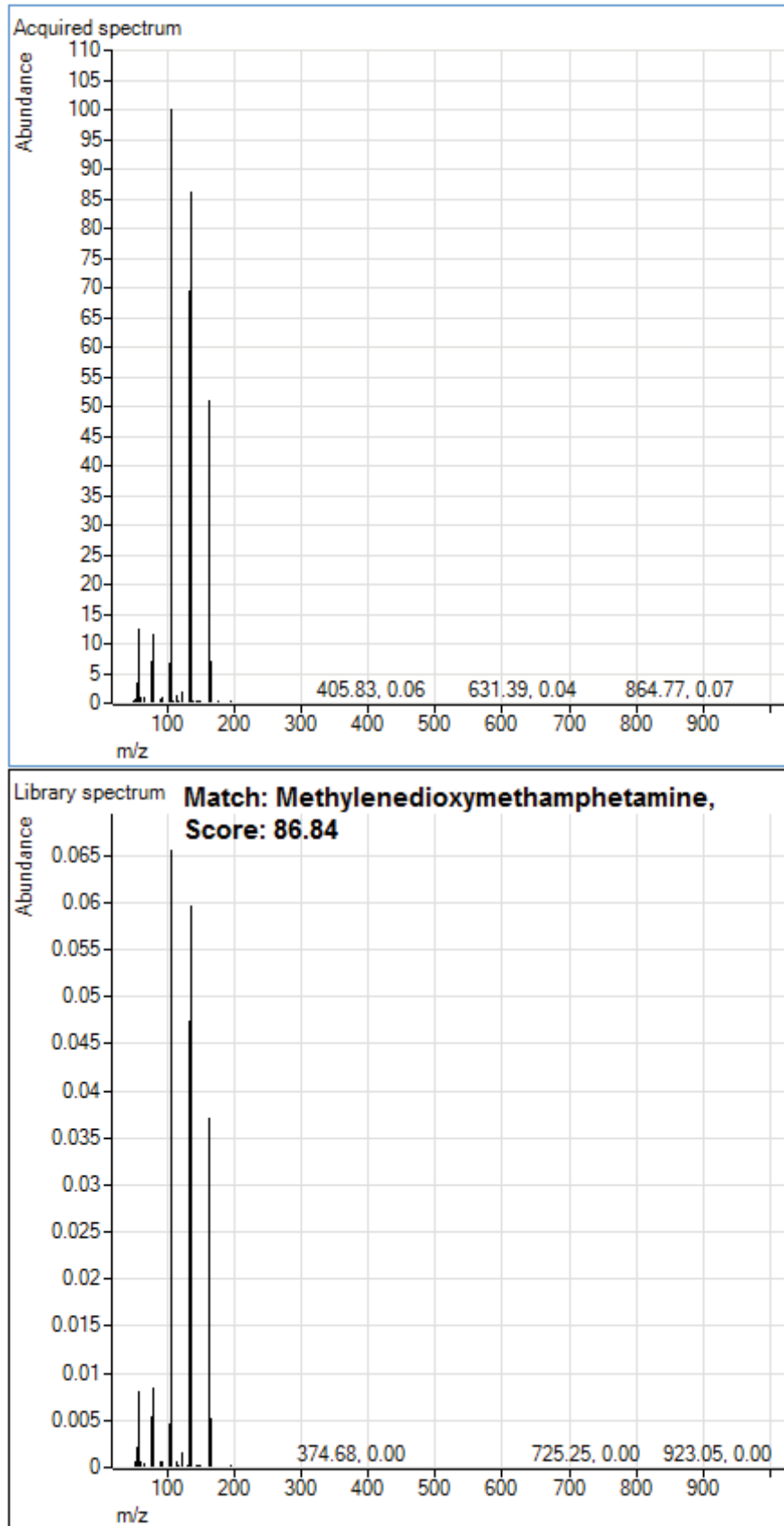


Figure 4-26 PCDL library match to MDMA.

4.3.2.2 Gas chromatography – mass spectrometry

Based on the GC-MS chromatogram obtained for the MDMA tablet, three compounds of interest were identified. The presence of MDMA can be seen at a retention time of 6.3 minutes (Figure 4-27 - Figure 4-31). The relative amount of MDMA in this sample was reported to be 25.7 %. The peak at 6.1 minutes is representative of the by-product MDP-2-POH. Another by-product, MDDMA was also detected at 6.5 minutes.

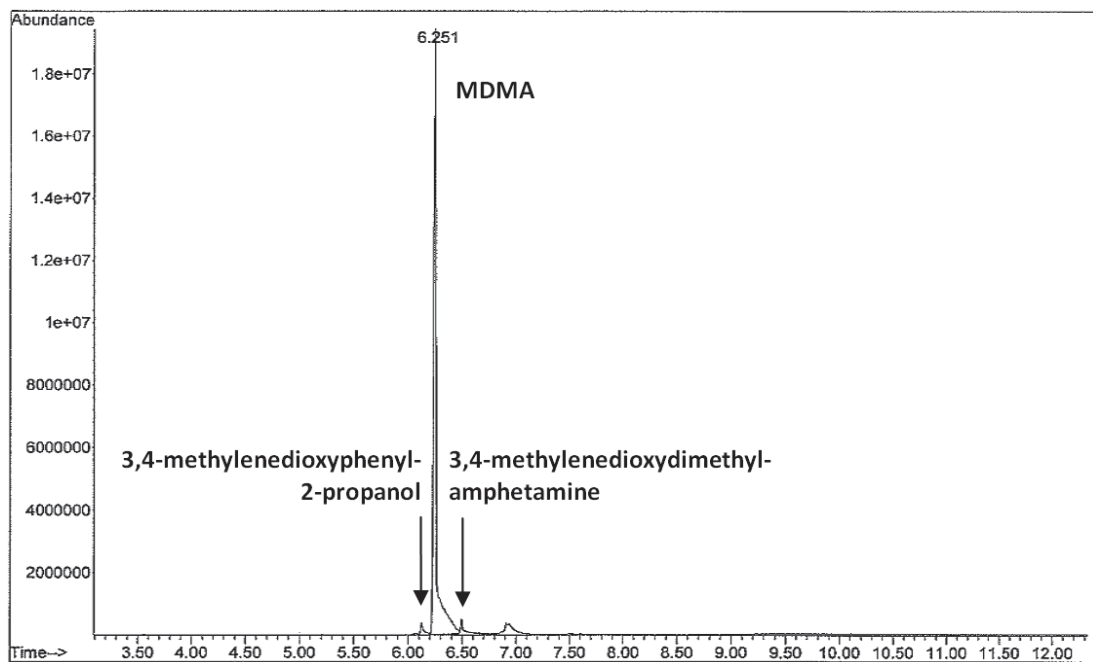


Figure 4-27 GC-MS chromatogram of MDMA tablet; MDP-2-POH at 6.1 minutes, MDMA at 6.3 minutes, MDDMA at 6.5 minutes (GC method 2).

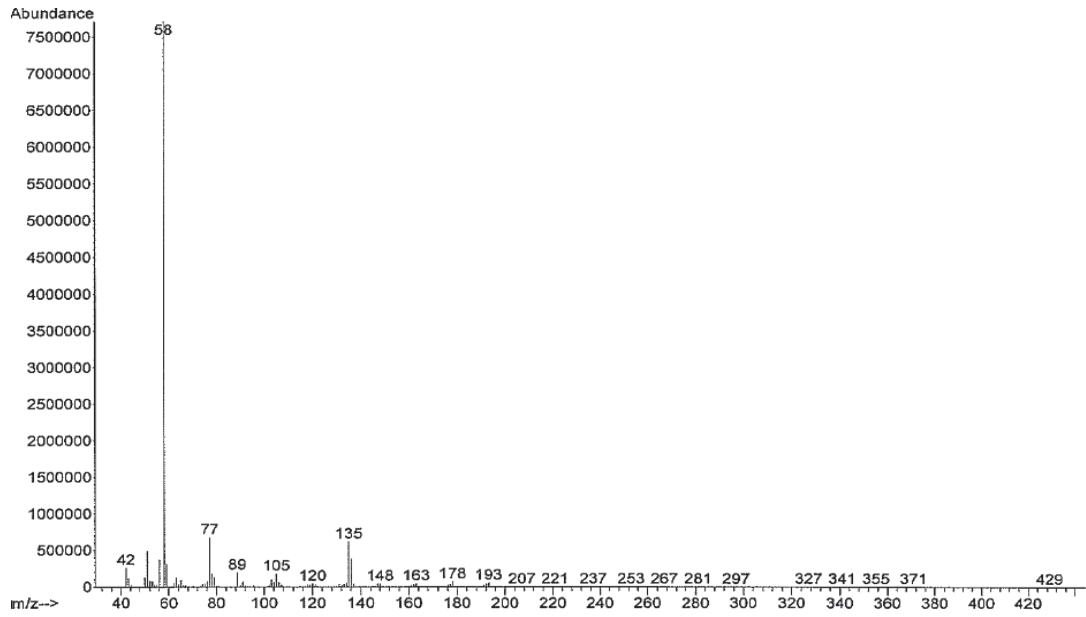


Figure 4-28 EI mass spectrum of MDMA (GC method 2).

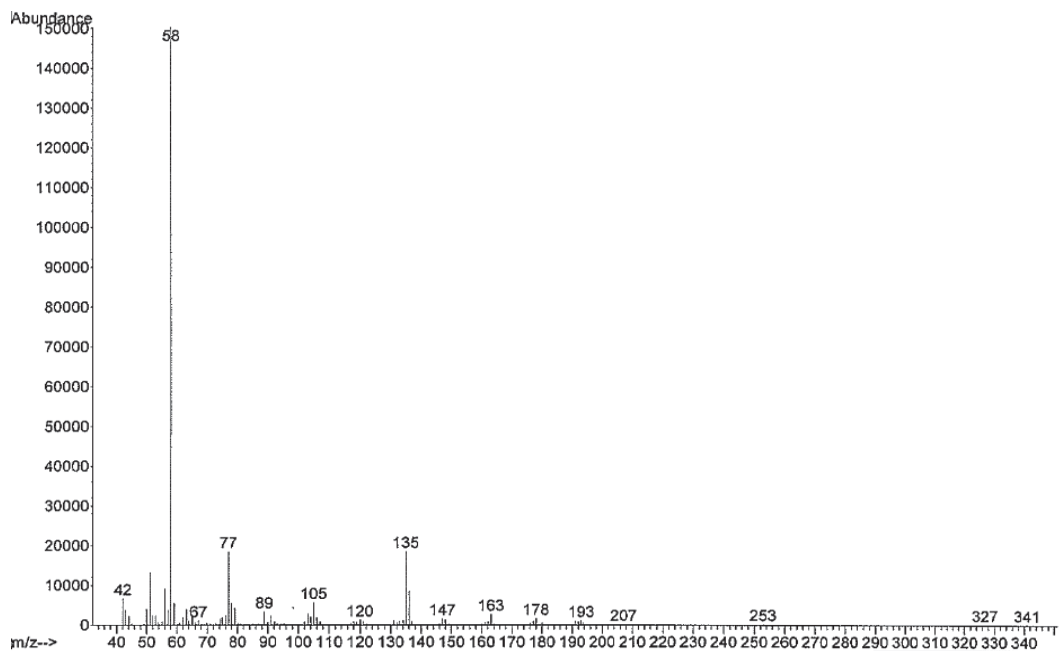


Figure 4-29 EI mass spectrum of MDP-2-POH (GC method 2).

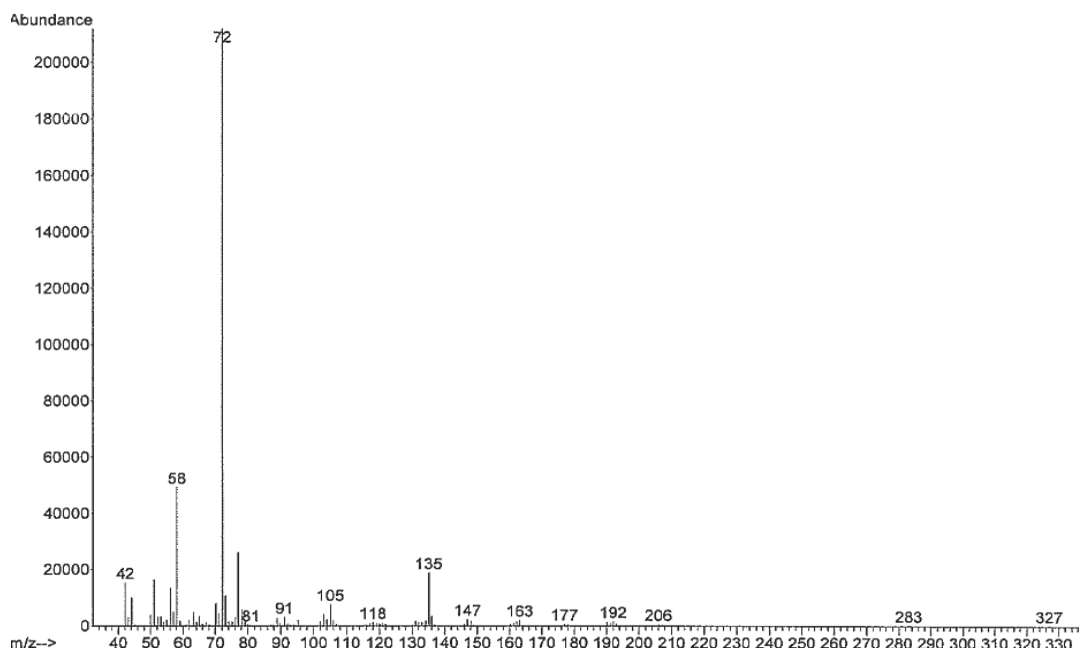


Figure 4-30 EI mass spectrum of MDMA (GC method 2).

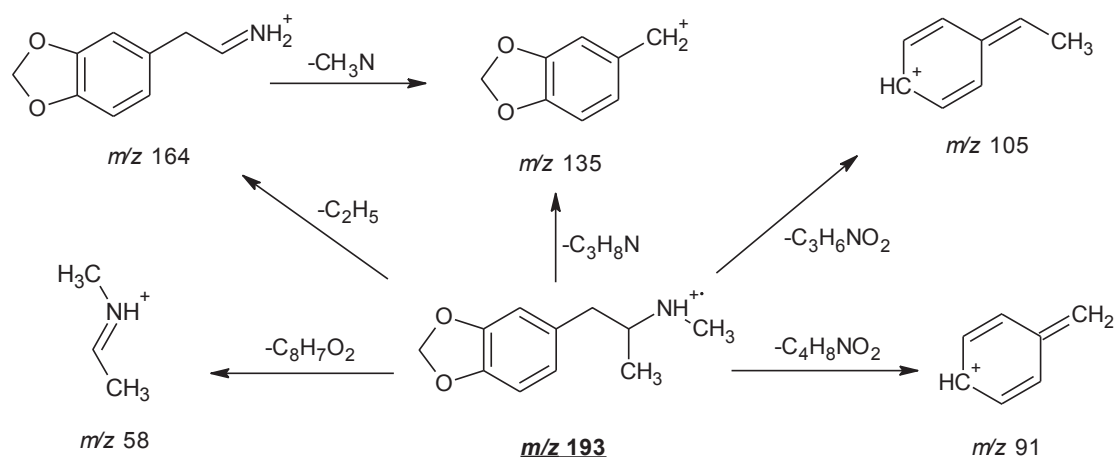


Figure 4-31 Proposed EI fragmentation of MDMA tablet.

Gas chromatography – mass spectrometry was conducted on the MDMA base synthesised using piperonal as starting material. The compounds detected included MDMA (6.2 minutes), PN (5.4 minutes), MDP-2-P (6.6 minutes) and *N*-formyl-MDMA (7.7 minutes, Figure 4-32 - Figure 4-35). The detection of these compounds in this sample supports the method utilised, i.e. Leuckart route using piperonal as the starting material. The broad peak observed for MDMA in this instance is most likely due to the high concentration of sample utilised. This was necessary to detect the trace compounds present.

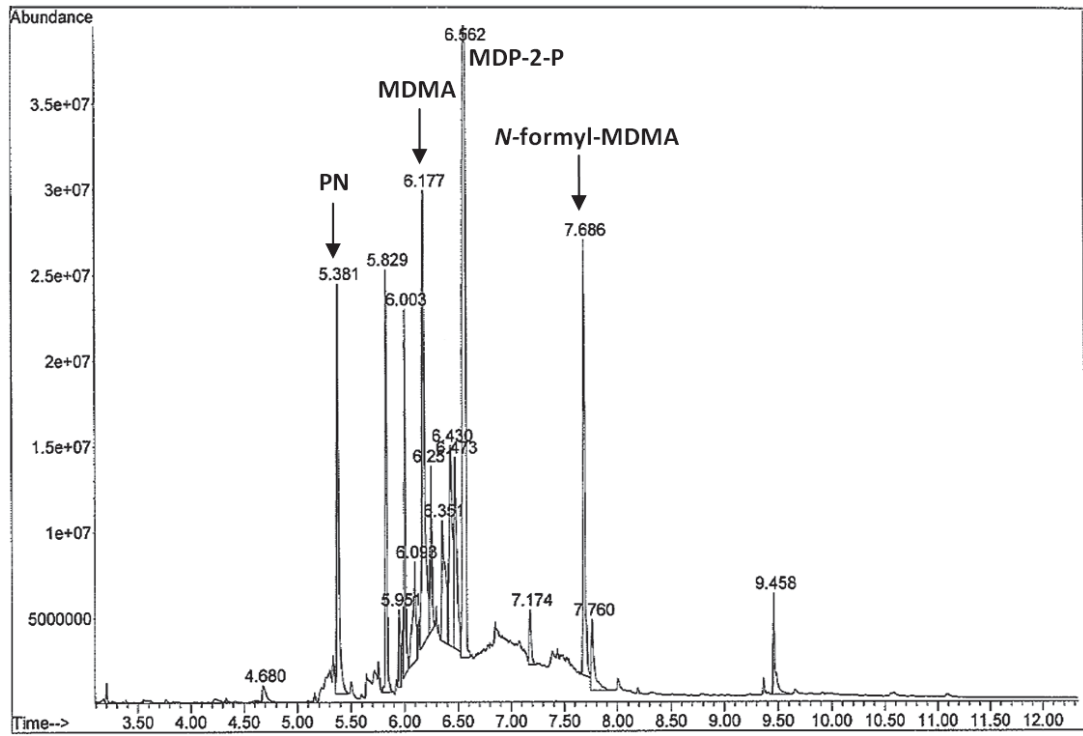


Figure 4-32 GC-MS chromatogram of synthesised MDMA base; PN at 5.4 minutes, MDMA at 6.2 minutes, MDP-2-P at 6.6 minutes, N-formyl-MDMA at 7.7 minutes (GC method 2).

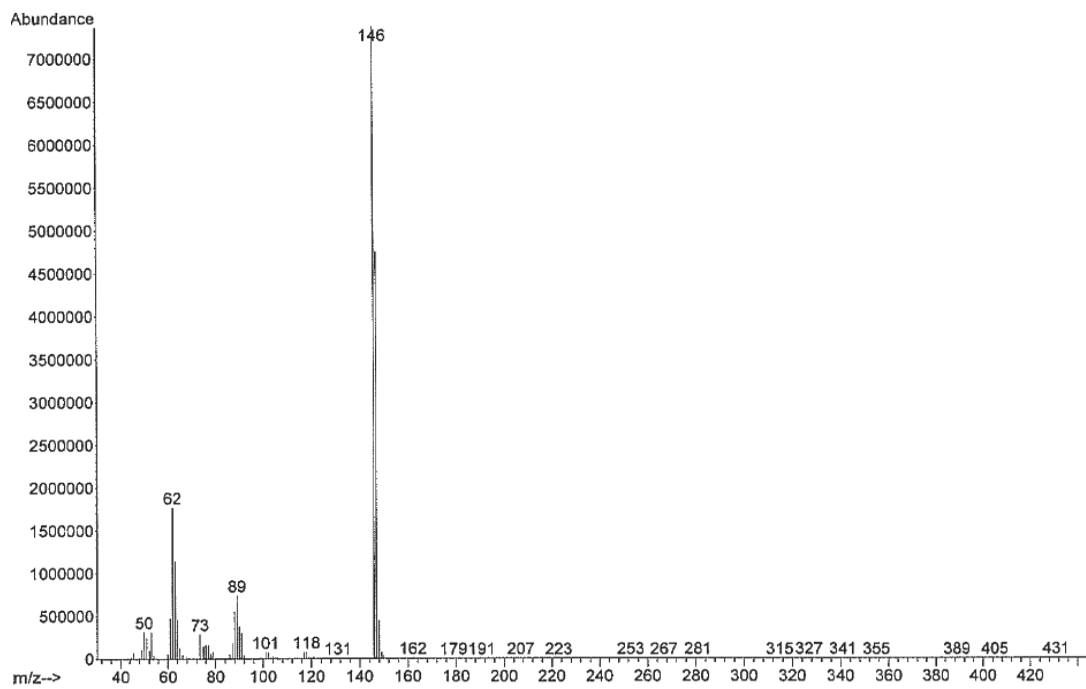


Figure 4-33 EI mass spectrum of PN (GC method 2).

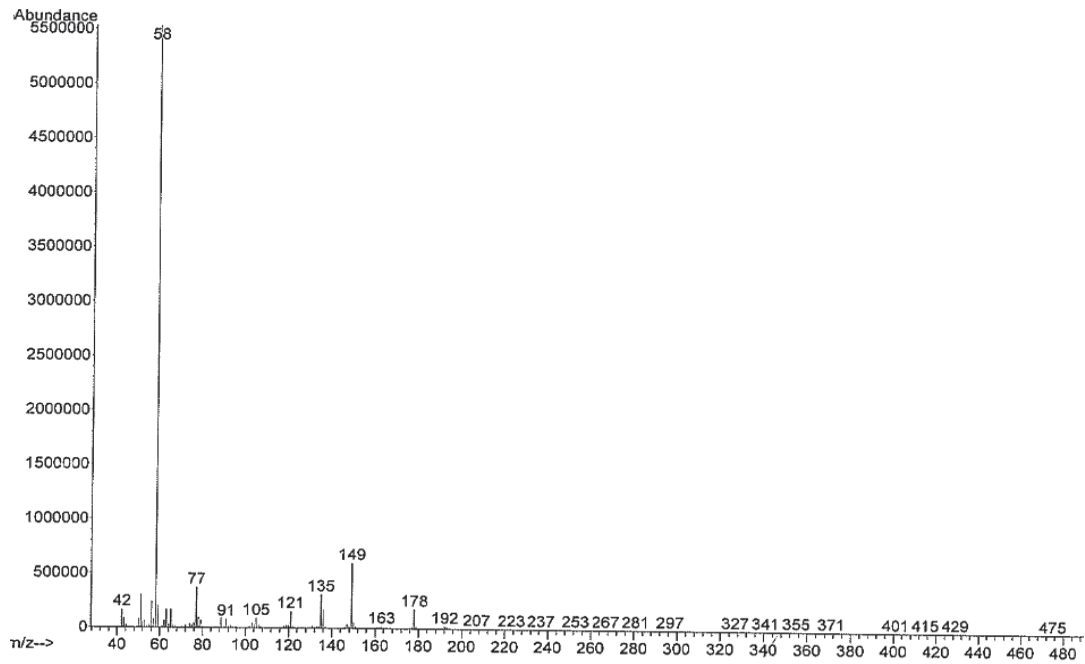


Figure 4-34 EI mass spectrum of MDP-2-P (GC method 2).

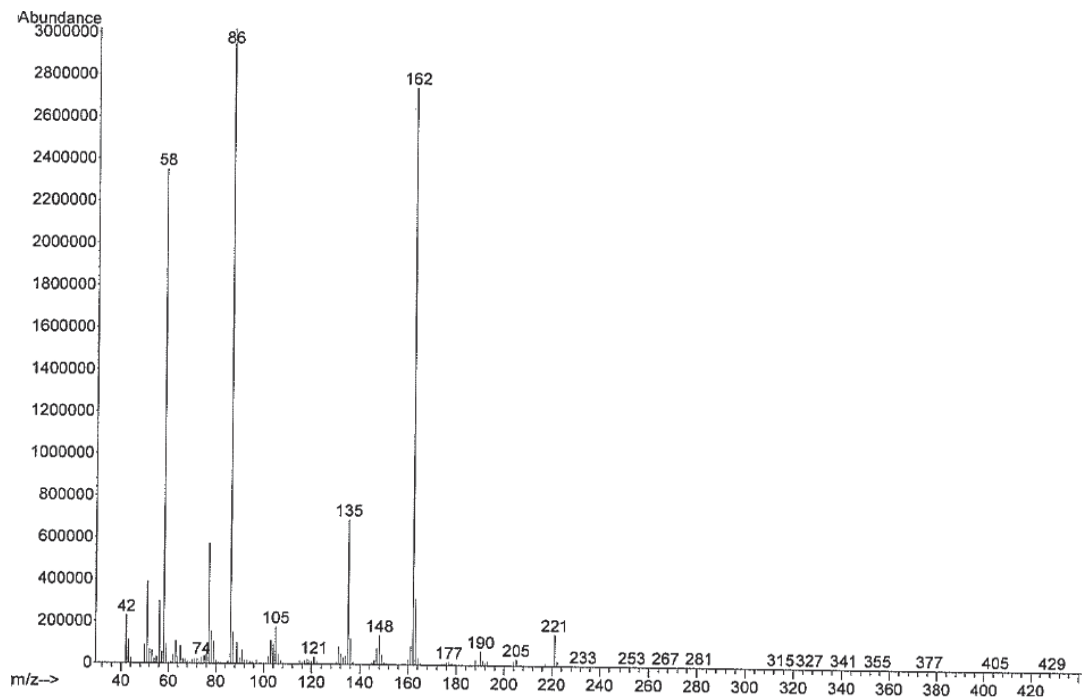


Figure 4-35 EI mass spectrum of N-formyl-MDMA (GC method 2).

4.3.2.3 Liquid chromatography – mass spectrometry

The LC-MS chromatogram obtained from the MDMA tablet exhibited the presence of MDMA, and the by-product MDDMA. MDP-2-POH was also detected; however, this compound

possessed the lowest ionisation efficiency and thus a smaller peak resulted (Figure 4-36 and Figure 4-37). The by-product MDP-2-P was not detected due to trace amounts being present in the sample (2.2 % normalised peak ratios based on NMI analysis). The NMI analysis report (Figure 4-20) indicated that MDP-2-POH was present as 90.6 % (normalised peak ratio) of the by-products which is inconsistent with the relatively small abundance observed in the LC-MS data. The sample was run in positive ion mode which is ideal for basic samples; however, MDP-2-POH is slightly acidic and therefore does not ionise efficiently in positive ion mode suggesting that detection of this compound was hindered.

The synthesised MDMA base was also analysed using LC-MS. The analysis indicated the presence of MDMA in highest proportions (Figure 4-38). In addition, two other by-products were detected; MDP-2-P and *N*-formyl-MDMA. PN was absent in the LC-MS chromatogram. The lack of detection using LC-MS may suggest that it was present in trace amounts and/or due to inefficient ionisation in positive ion mode. The presence of all compounds detected were supported by MS/MS spectra by comparison to reference spectra (Figure 4-39).

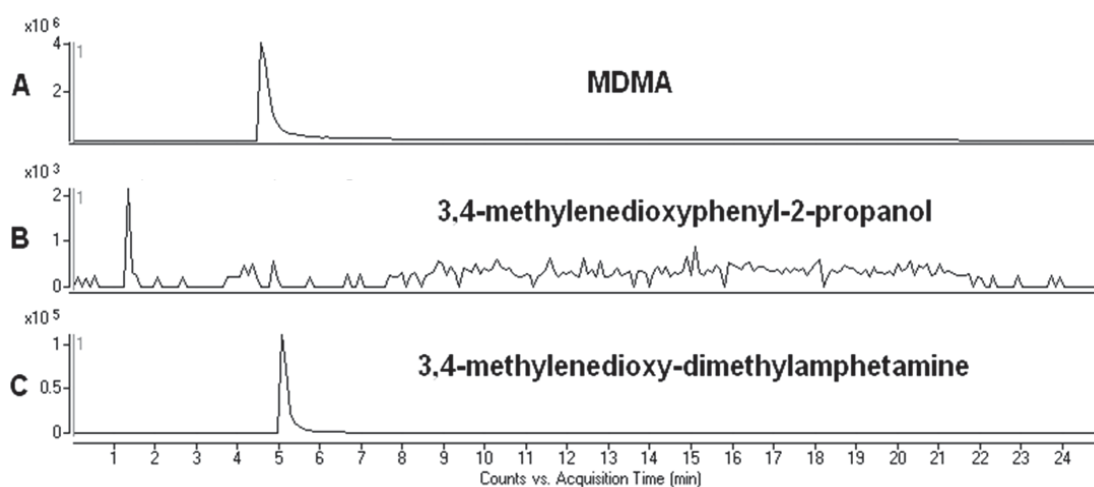


Figure 4-36 LC-MS chromatogram of MDMA tablet; A: EIC of MDMA at 4.9 minutes, m/z 194; B: EIC of MDP-2-POH (trace) at 1.3 minutes, m/z 181; C: EIC of MDDMA at 5.1 minutes, m/z 208.

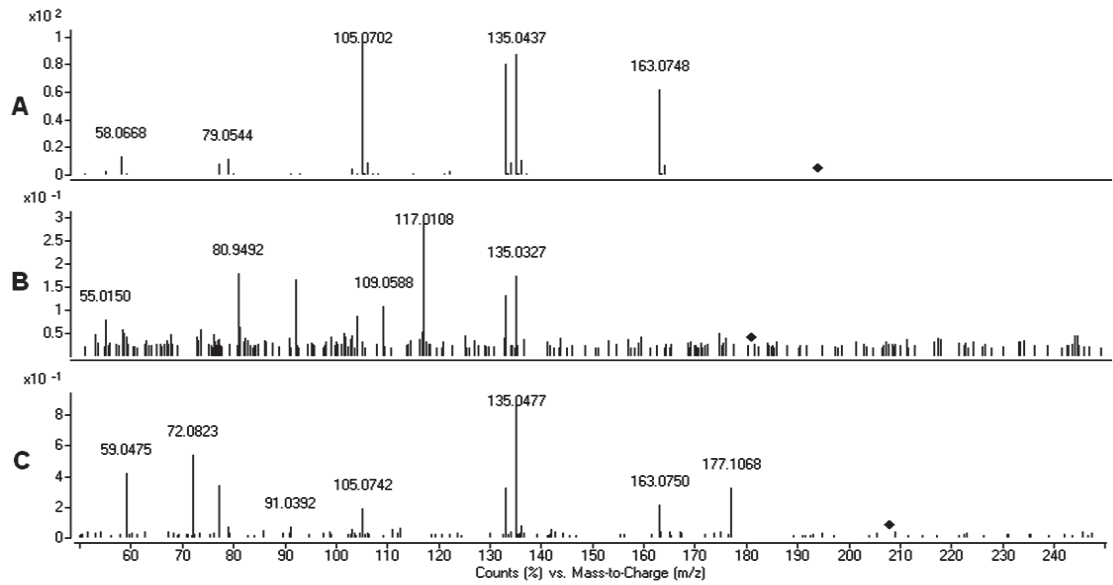


Figure 4-37 LC-MS spectra of MDMA tablet; A: MDMA, B: MDP-2-POH, C: MDDMA.

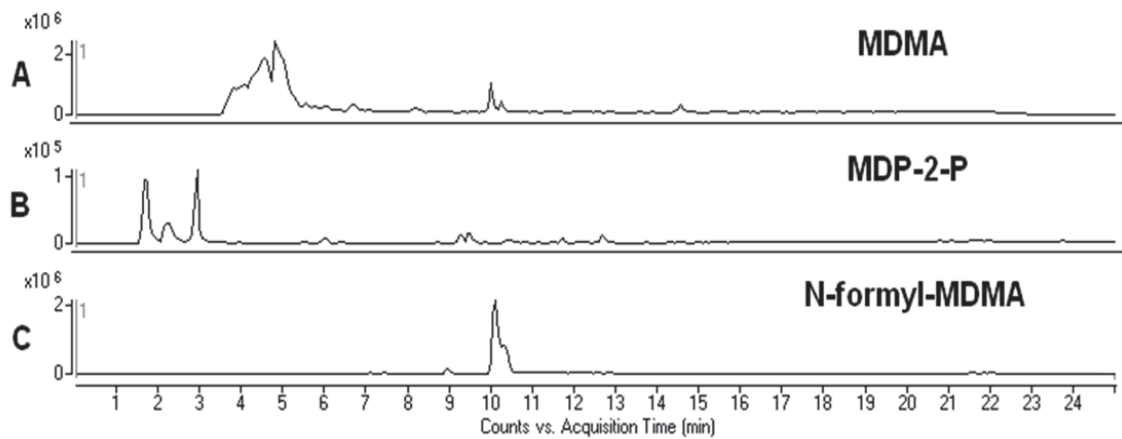


Figure 4-38 LC-MS chromatogram of MDMA base; A: EIC of MDMA at 4.8 minutes, m/z 194; B: EIC of MDP-2-P at 1.8 minutes, m/z 179; C: EIC of N-formylMDMA at 10.2 minutes, m/z 222.

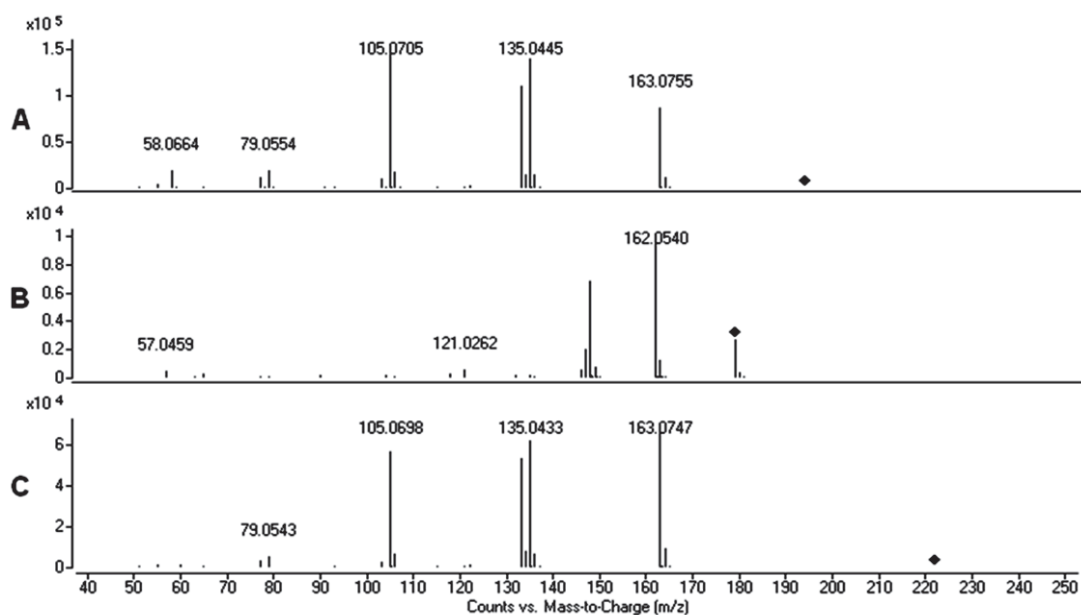


Figure 4-39 LC-MS/MS spectra of MDMA base; A: MDMA; B: MDP-2-P; C: N-formyl-MDMA.

4.3.3 Analysis of 4-methoxymethylamphetamine

4.3.3.1 Desorption electrospray ionisation – mass spectrometry

The synthesised PMMA base was also analysed using DESI-MS. PMMA was detected as the protonated molecular ion at m/z 180 (Figure 4-40) and supported by MS/MS spectra (Figure 4-40 - Figure 4-42). A possible impurity at m/z 149 was thought to correspond to anethole. In the synthesis, peracid oxidation was utilised in the conversion of anethole, originated from star anise (the starting material used in this synthesis), to the intermediate 4-methoxyphenyl-2-propanone (PMP-2-P), followed by its conversion to the end product PMMA (via Leuckart route). PMP-2-P was not detected using DESI-MS, therefore, it is difficult to ascertain the exact method of synthesis based on DESI-MS spectra alone; however, the presence of anethole is a good indicator of the method employed.

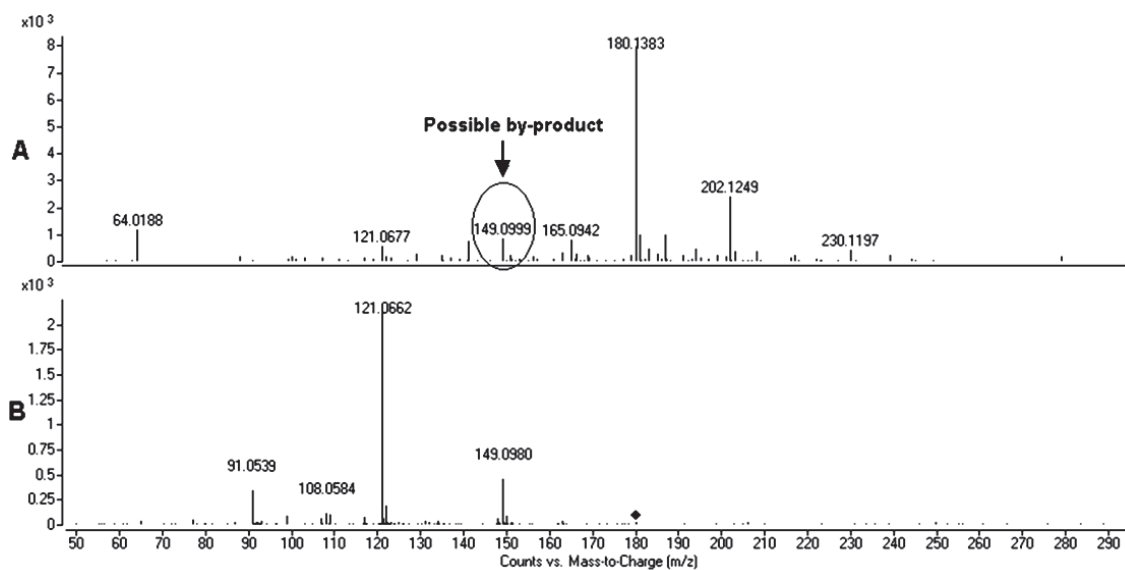


Figure 4-40 A: DESI-MS spectra of PMMA; B: MS/MS of PMMA.

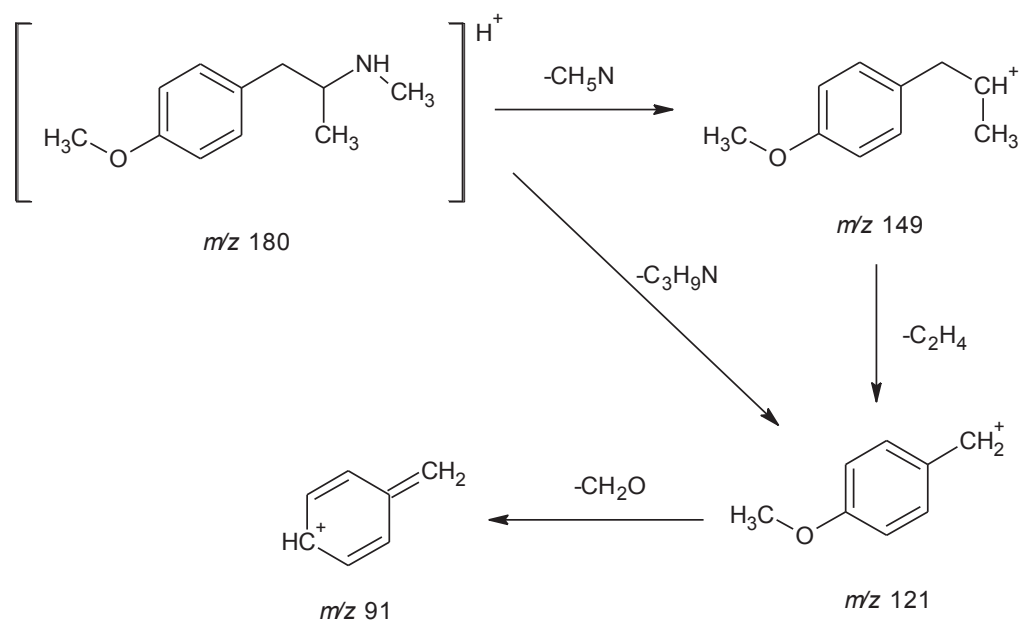


Figure 4-41 Proposed collision induced dissociation of the $[M+H]^+$ ion of PMMA.

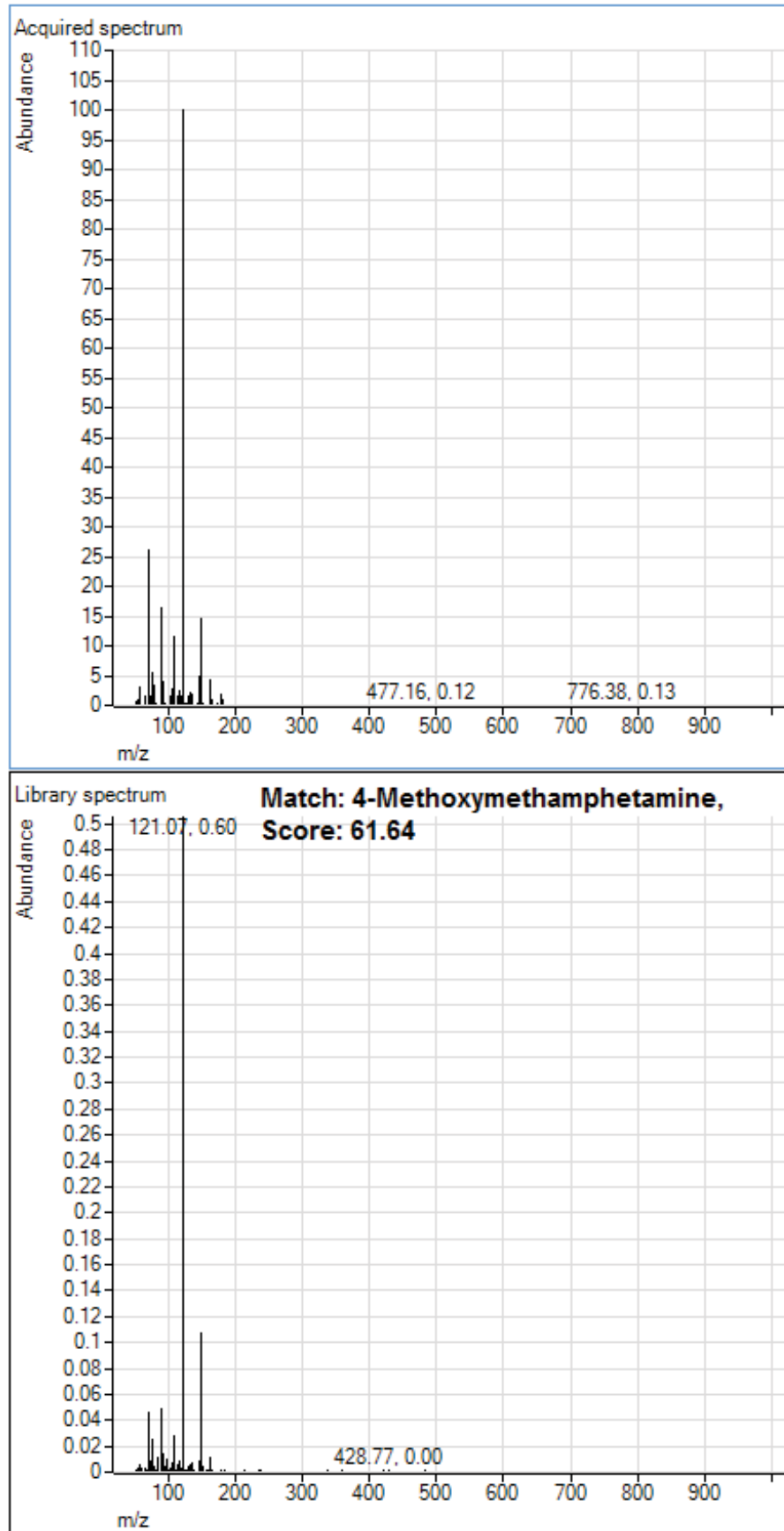


Figure 4-42 PCDL library match to PMMA.

4.3.3.2 Gas chromatography – mass spectrometry

The PMMA base was also analysed using GC-MS and three main compounds were identified; PMMA, anethole and PMP-2-P as the intermediate. PMMA was supported by EI mass spectra and comparison to a reference library (Figure 4-43 - Figure 4-46). The presence of these by-products and impurities suggest that anethole was used in the synthesis of PMMA via the Leuckart method, which is consistent with the method utilised⁹⁸. The broad peak observed for PMMA is due to the high concentration of sample utilised. Other compounds that were detected using GC-MS in lower amounts include *p*-allylanisole, 2-methoxy-*N,N*-dimethylaniline and *p*-hydroxymethylamphetamine which are also consistent with the method employing anethole as precursor.

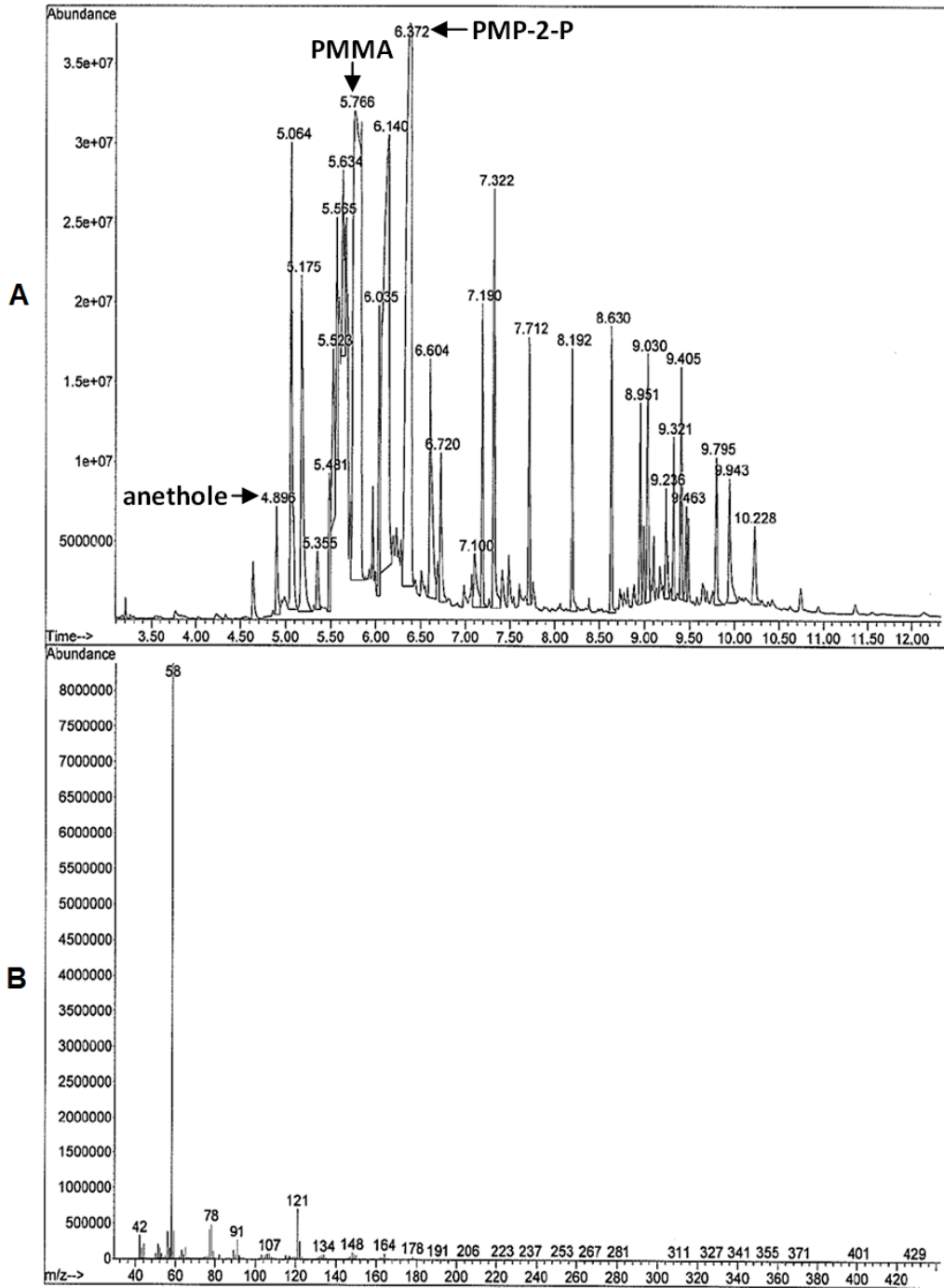


Figure 4-43 A: GC-MS chromatogram of synthesised PMMA, anethole at 4.9 minutes, PMMA at 5.8 minutes, PMP-2-P at 6.4 minutes; B: EI mass spectrum of PMMA (GC method 2).

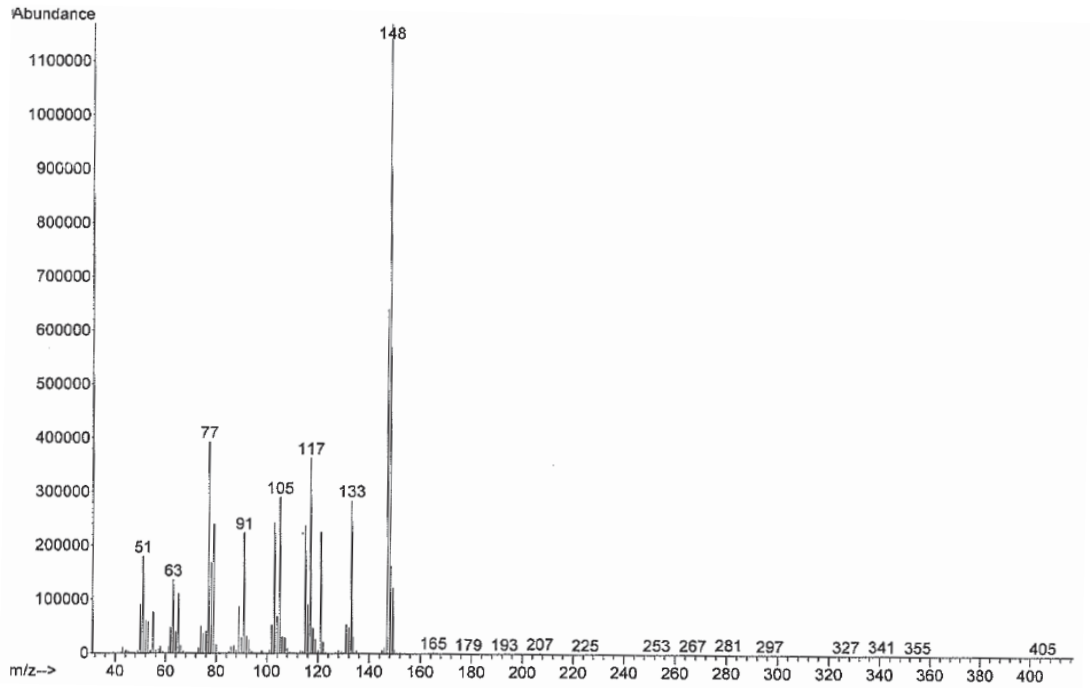


Figure 4-44 EI mass spectrum of anethole (GC method 2).

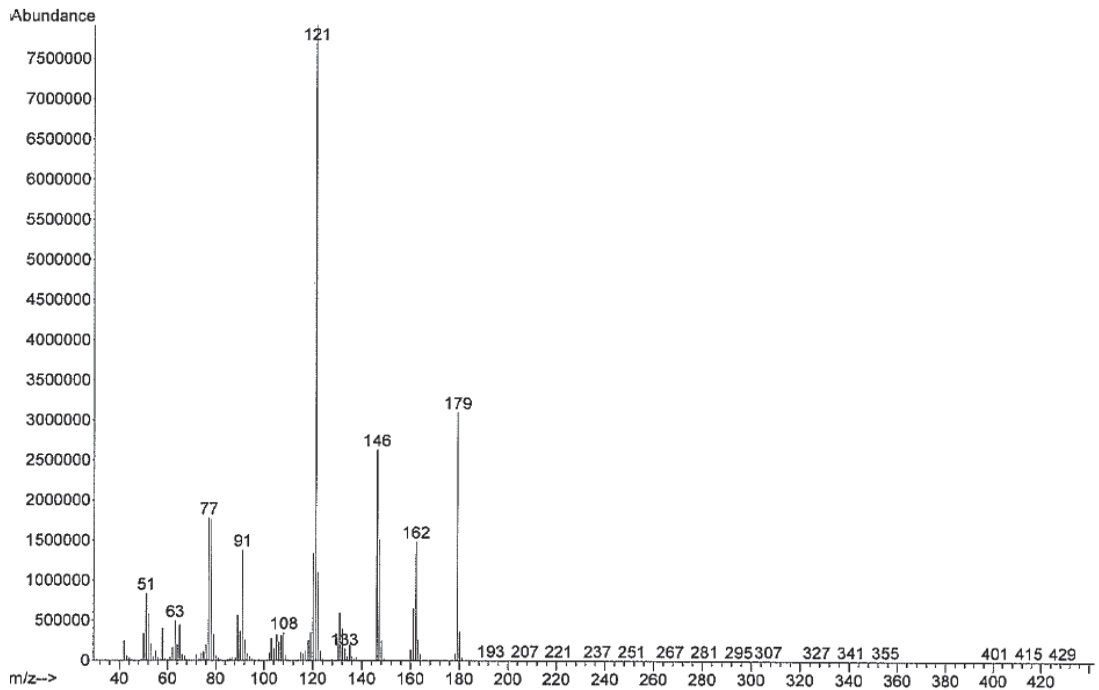


Figure 4-45 EI mass spectrum of PMP-2-P (GC method 2).

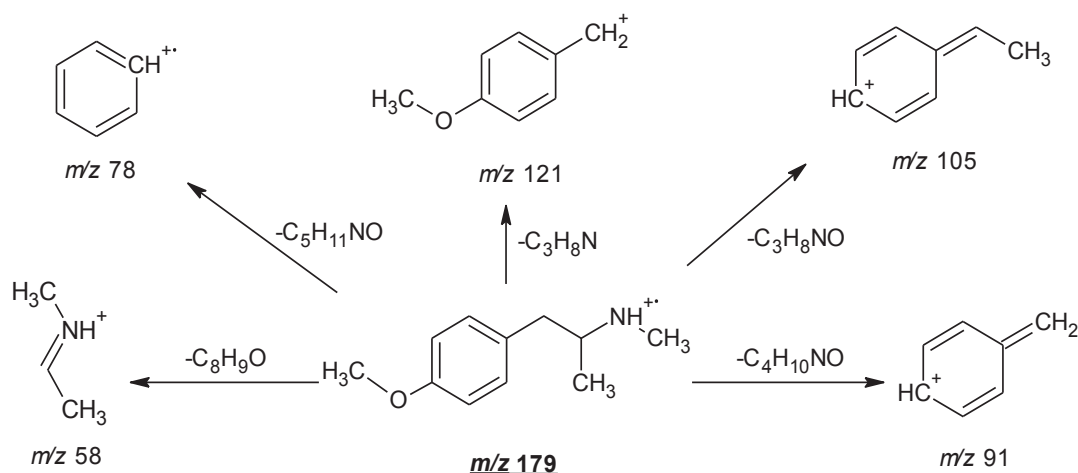


Figure 4-46 Proposed EI fragmentation of PMMA base.

4.3.3.3 Liquid chromatography – mass spectrometry

The PMMA base was analysed using LC-MS and three compounds (PMMA, anethole and PMP-2-P as the intermediate) were detected and supported by MS/MS spectra (Figure 4-47 and Figure 4-48). The presence of these by-products/impurities reiterates that anethole was used in the synthesis of PMMA via the Leuckart method.

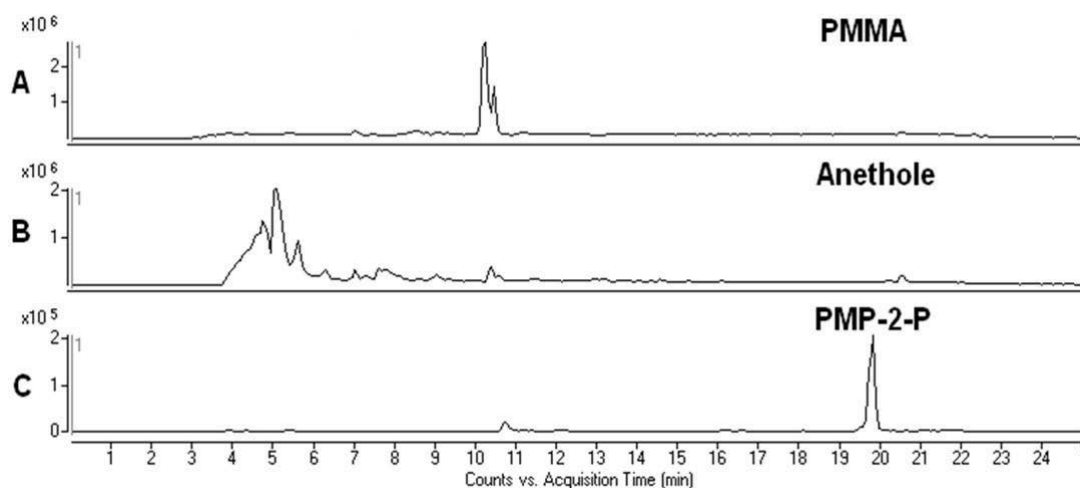


Figure 4-47 LC-MS chromatogram of PMMA base; A: EIC of PMMA at 10.3 minutes, m/z 180; B: EIC of anethole at 5.1 minutes, m/z 149; C: EIC of PMP-2-P at 19.8 minutes, m/z 165.

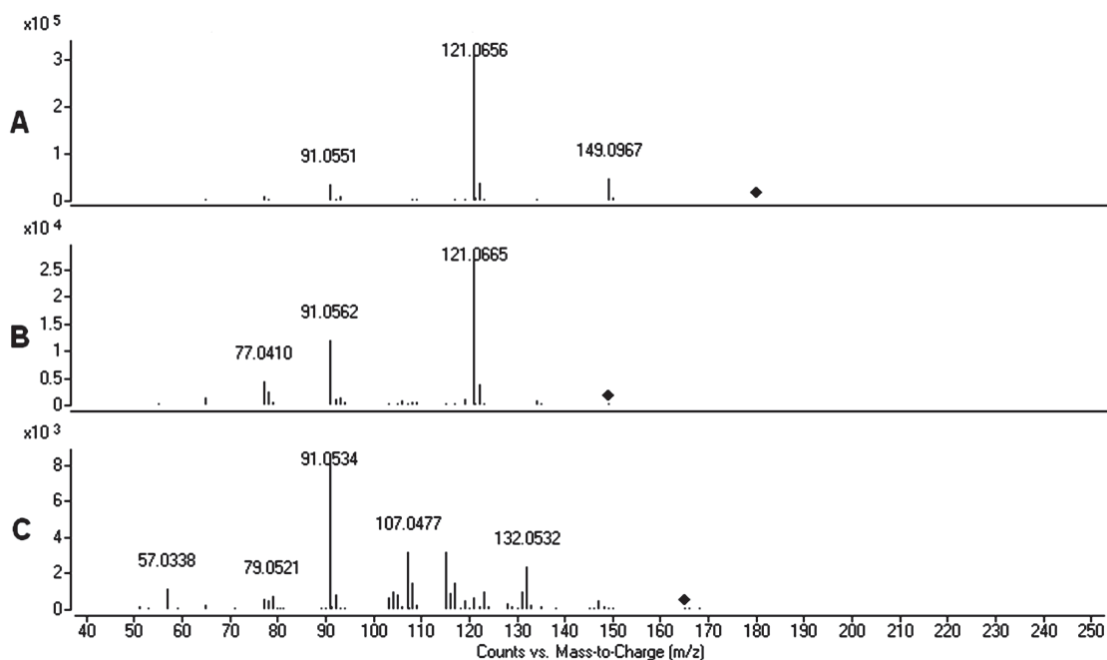


Figure 4-48 LC-MS/MS of PMMA base; A: PMMA; B: anethole; C: PMP-2-P.

4.3.4 Analysis of dimethylamylamine

4.3.4.1 Desorption electrospray ionisation – mass spectrometry

“Jack3d” is a pre-workout supplement drink that has been available over the counter and is used to aid body-building. The main active ingredients in this product include creatine monohydrate, caffeine and DMAA amongst others. These compounds are common in pre-workout supplements as they facilitate body-building due to their stimulant effects. In addition, creatine aids in supplying energy to the body’s cells for a more efficient work-out.

Dimethylamylamine was detected using DESI-MS in trace amounts at m/z 116 (Figure 4-49). In addition, caffeine was also detected in the sample. The presence of DMAA and caffeine were supported by MS/MS experiments (Figure 4-50 - Figure 4-52). Creatine monohydrate was not detected using DESI-MS (possibly due to trace amounts present).

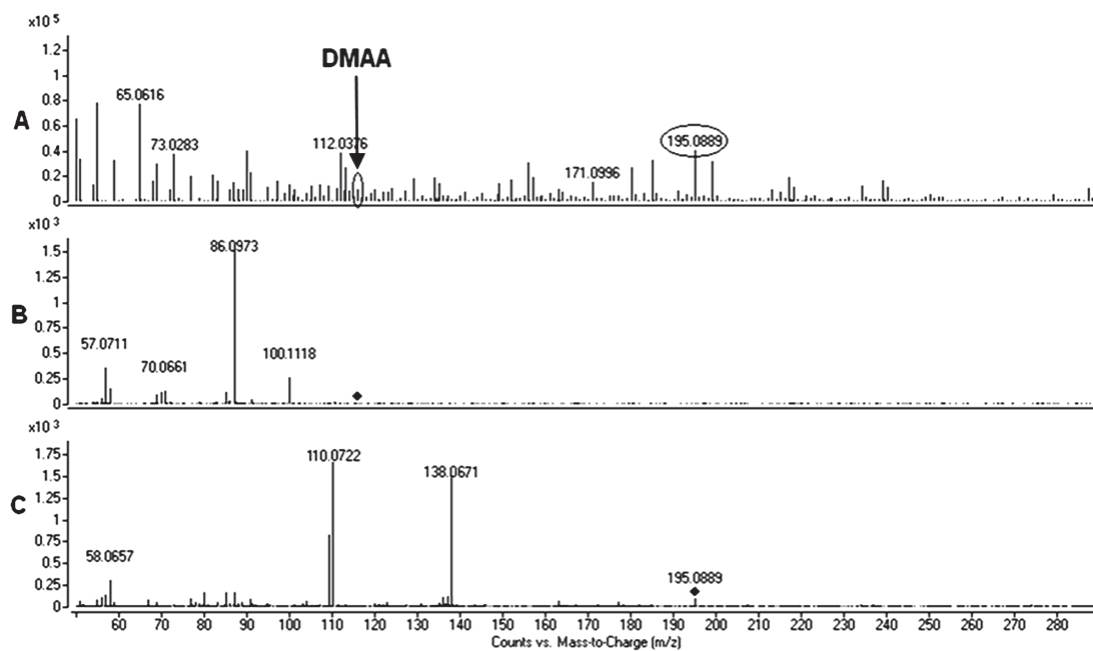


Figure 4-49 A: DESI-MS spectra of "Jack3d" containing DMAA and caffeine, B: MS/MS of DMAA, C: MS/MS of caffeine.

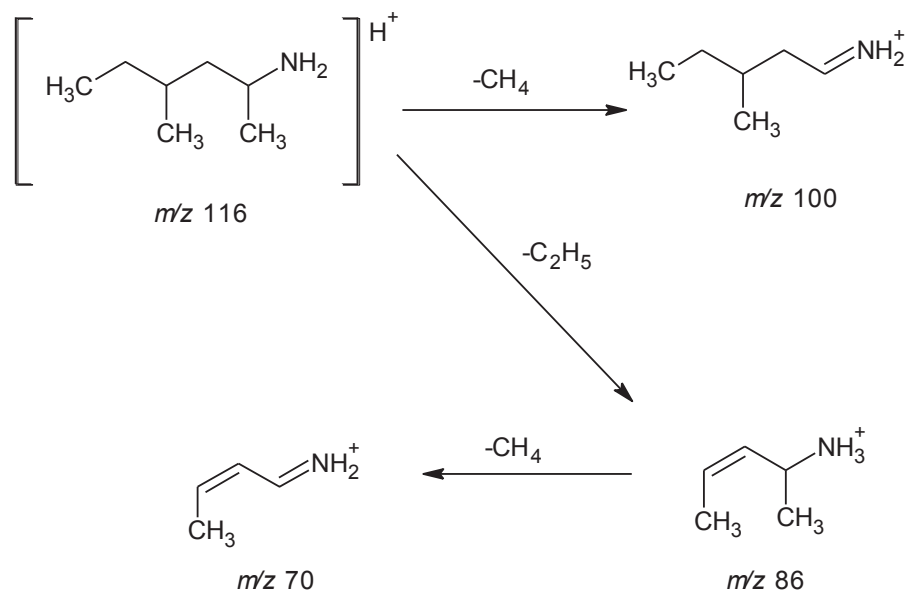


Figure 4-50 Proposed collision induced dissociation of the $[M+H]^+$ ion of DMAA.

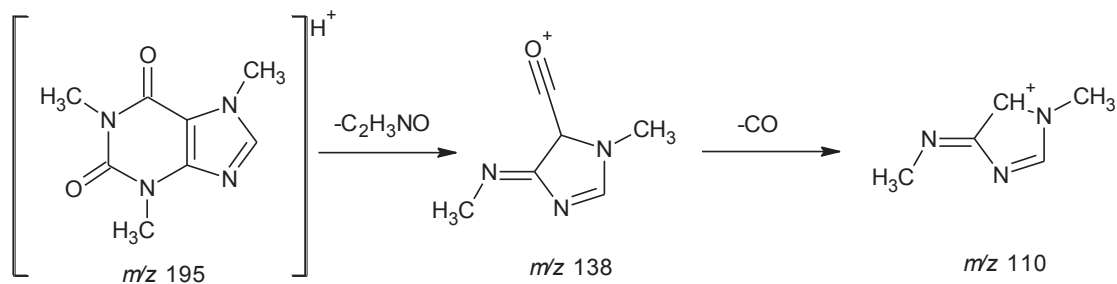


Figure 4-51 Proposed collision induced dissociation of the $[M+H]^+$ ion of caffeine.

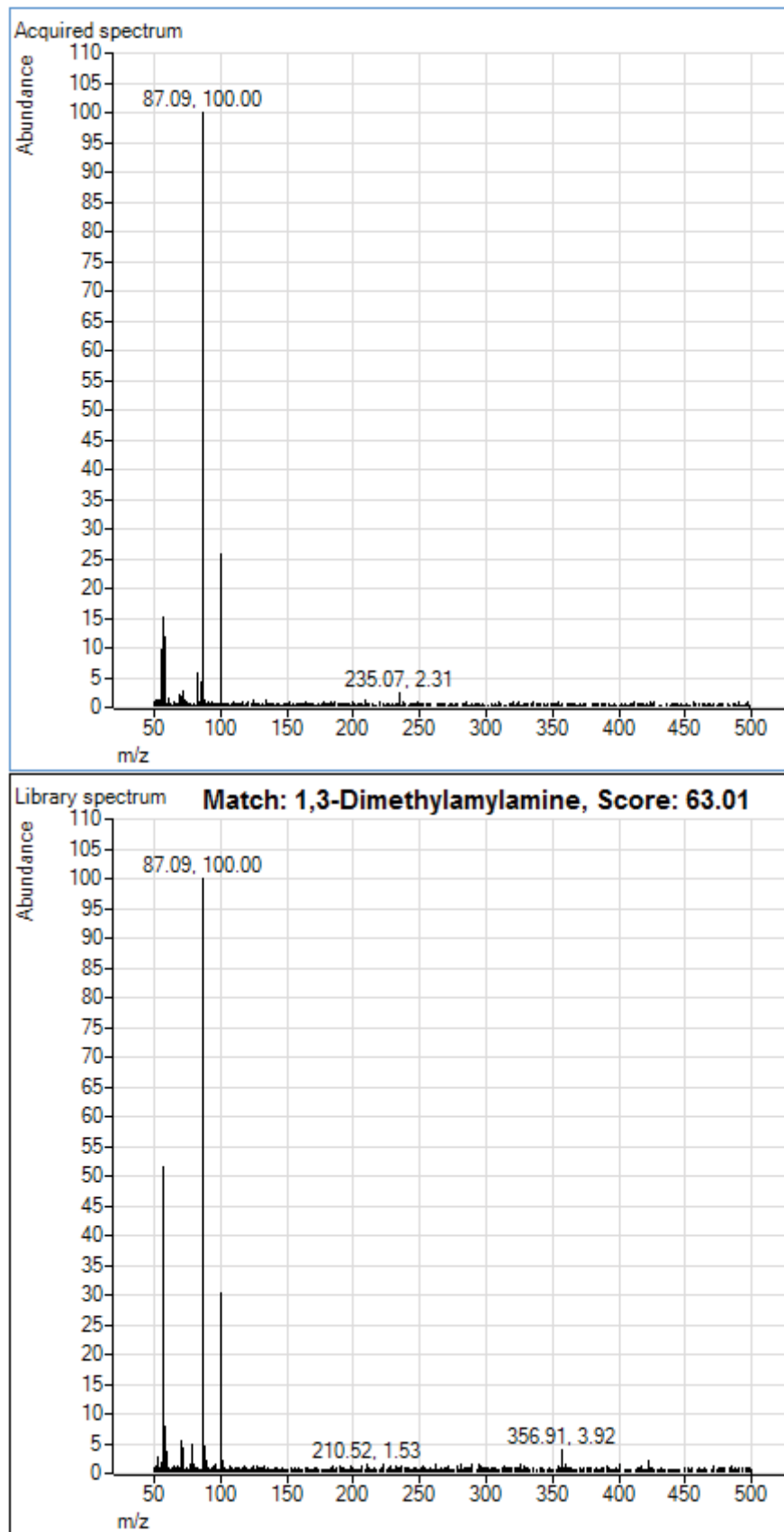


Figure 4-52 PCDL library match to DMAA.

4.3.4.2 Gas chromatography – mass spectrometry

Using GC-MS, a large amount of caffeine was detected in this sample (Figure 4-53). This may suggest that this ingredient was present in the highest concentration in this supplement drink. Creatine monohydrate was undetected using GC-MS possibly due insufficient volatility. DMAA may be present in trace amounts attributing to its lack of detection, alternatively, the temperature program utilised in the GC-MS method may be obscuring the detection of this compound (starting at 100 °C) as it may elute much earlier in the run.

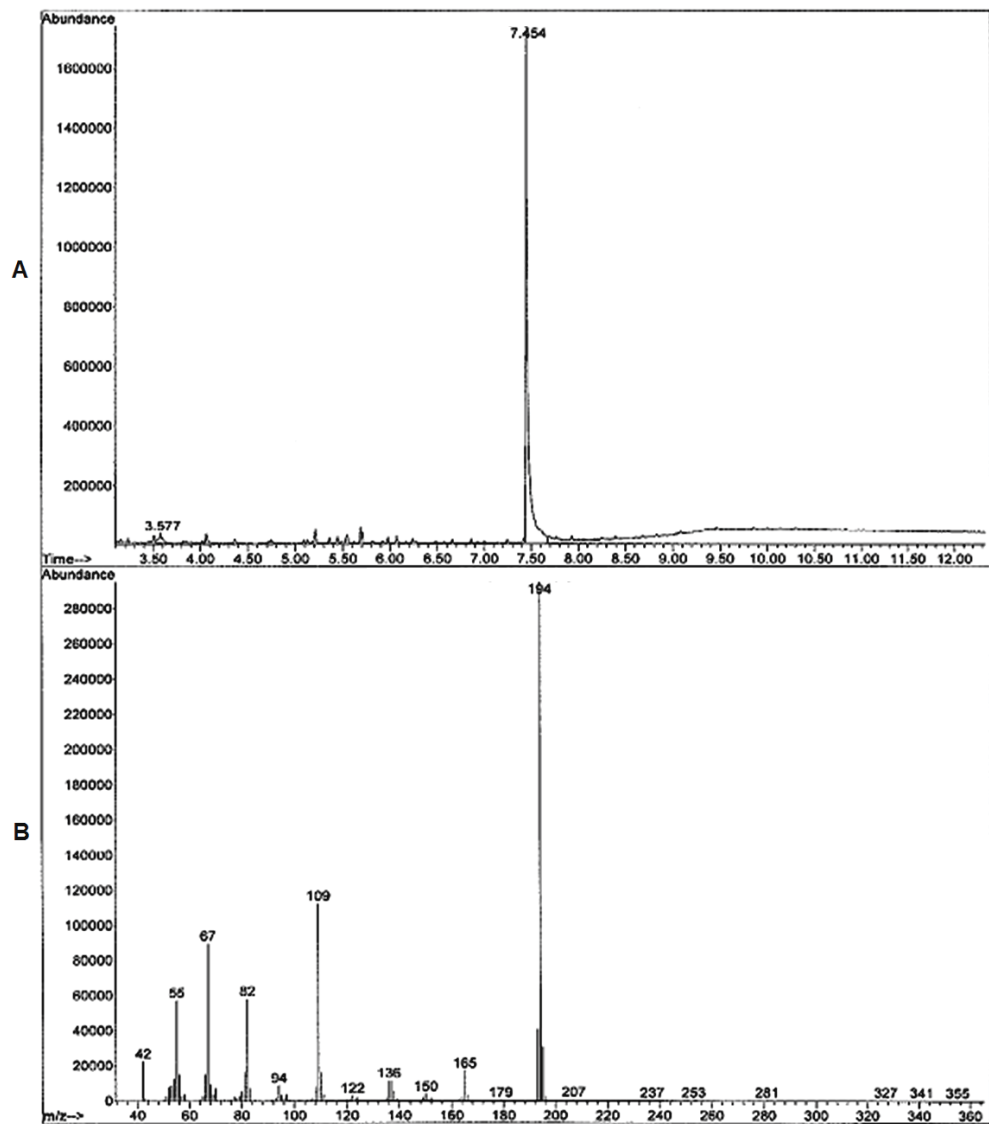


Figure 4-53 A: GC-MS chromatogram of "Jack3d", caffeine at 7.5 minutes; B: EI mass spectrum of caffeine (GC method 2).

4.3.4.3 Liquid chromatography – mass spectrometry

The LC-MS analysis exhibited the most compounds in the analysis of “Jack3d”. Caffeine was detected with highest abundance for the protonated molecular ion peak at m/z 195. DMAA was detected with lower abundance at m/z 116 and creatine monohydrate was also detected at m/z 132 (Figure 4-54 and Figure 4-55). Other ingredients in this product remain undetected due to presence in trace amounts.

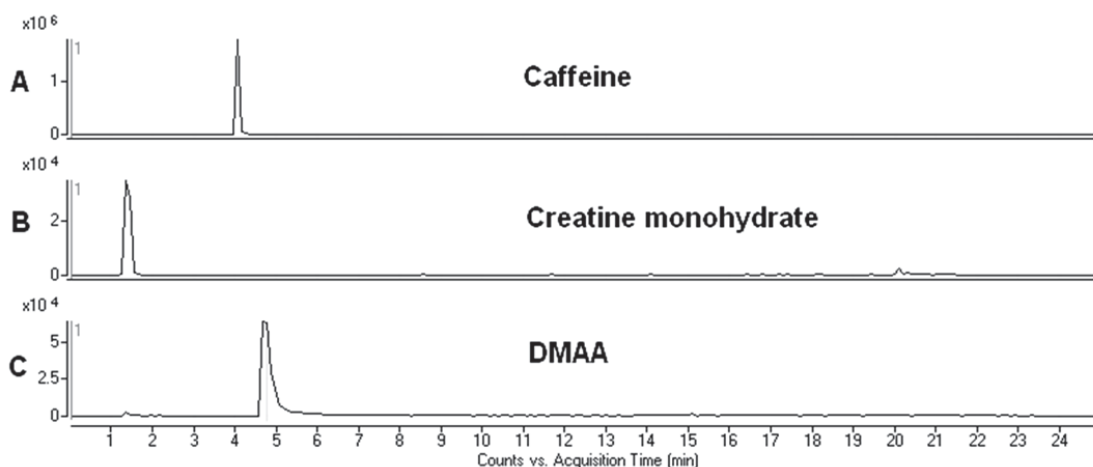


Figure 4-54 LC-MS chromatogram of “Jack3d”; A: EIC of caffeine at 4.1 minutes, m/z 195; B: EIC of creatine monohydrate at 1.2 minutes, m/z 132; C: EIC of DMAA at 4.9 minutes, m/z 116.

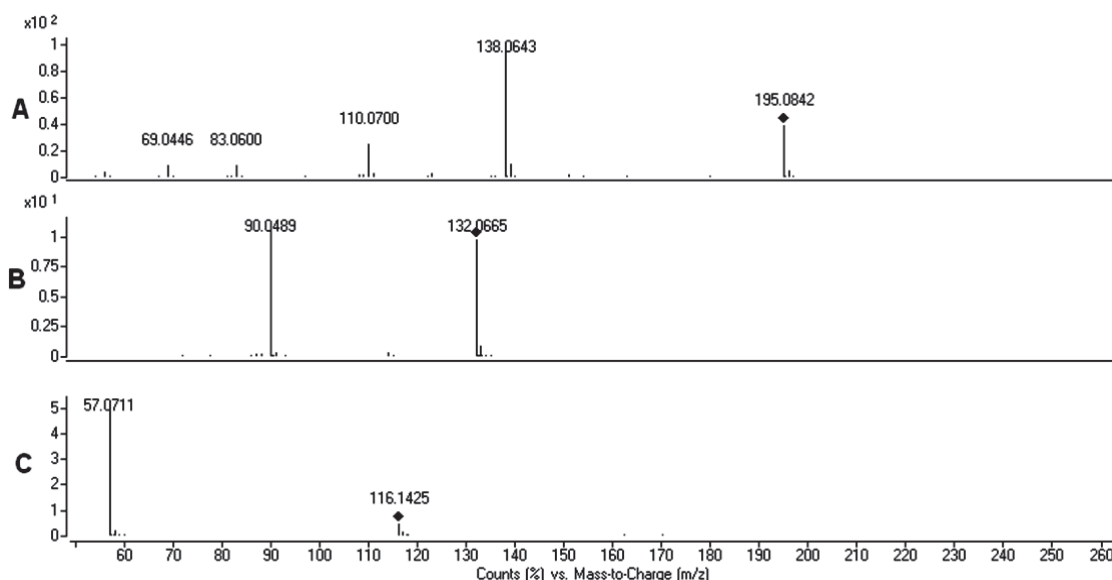


Figure 4-55 LC-MS/MS spectra of “Jack3d”; A: caffeine, B: creatine monohydrate, C: DMAA.

4.3.5 Mass accuracy

In all the compounds tested, a MS/MS match score greater than 60 was obtained using the PCDL software with the exception of some compounds present in trace amounts where MS/MS data was poor. Compounds were further supported by MS/MS data in which all MS spectra were at best within 5 ppm and all MS/MS spectra were at best within 10 ppm (Table 4-2 and Table 4-3).

Table 4-2 Mass accuracy of ATS, using positive ion mode.

Compound	Formula [M+H] ⁺	Accurate Mass [M+H] ⁺	Acquired Mass [M+H] ⁺	Mass Accuracy (ppm)
MA	C ₁₀ H ₁₆ N	150.1283	150.1277	-4.0
PMA	C ₁₀ H ₁₆ NO	166.1232	166.1224	-4.8
AP	C ₉ H ₁₄ N	136.1126	136.1131	3.7
DMA	C ₁₁ H ₁₈ N	164.1439	164.1435	-2.4
MDMA	C ₁₁ H ₁₆ NO ₂	194.1181	194.1186	2.6
MDP-2-POH	C ₁₀ H ₁₃ O ₃	181.0865	181.0871	3.3
MDDMA	C ₁₂ H ₁₈ NO ₂	208.1338	208.1329	-4.3
MDP-2-P	C ₁₀ H ₁₁ O ₃	179.0708	179.0712	2.2
PN	C ₈ H ₆ NO ₂	148.0399	148.0394	3.4
PMMA	C ₁₁ H ₁₈ NO	180.1388	180.1383	-2.8
DMAA	C ₇ H ₁₈ N	116.1439	116.1434	-4.3
caffeine	C ₈ H ₁₁ N ₄ O ₂	195.0882	195.0889	3.6

MA = methylamphetamine, PMA = 4-methoxyamphetamine, AP = amphetamine, DMA = N,N-dimethylamphetamine, MDMA = 3,4-methylenedioxyamphetamine, MDP-2-POH = 3,4-methylenedioxyphenyl-2-propanol, MDDMA = 3,4-methylenedioxydimethylamphetamine, MDP-2-P = 3,4-methylenedioxyphenyl-2-propanone, PN = piperonyl nitrile, PMMA = 4-methoxymethylamphetamine, DMAA = dimethylamine.

Table 4-3 Mass accuracy of MS/MS ions using positive ion mode at 20 eV.

Compound	Chemical Formula	Accurate Mass	Acquired Mass	Mass Accuracy (ppm)
MA	$C_{10}H_{16}N [M+H]^+$	150.1283	150.1277	-4.0
	C_7H_7	91.0548	91.0546	-2.2
PMA	$C_{10}H_{16}NO [M+H]^+$	166.1232	166.1224	-4.8
	C_8H_9O	121.0653	121.0645	-6.6
	C_7H_7	91.0548	91.0545	-3.3
AP	$C_9H_{14}N [M+H]^+$	136.1126	136.1131	3.7
	C_9H_{11}	119.0861	119.0868	5.9
	C_7H_7	91.0548	91.0555	7.7
DMA	$C_{11}H_{18}N [M+H]^+$	164.1439	164.1435	-2.4
	C_7H_7	91.0548	91.0543	-5.5
	C_5H_5	65.0391	65.0396	7.7
MDMA	$C_{11}H_{16}NO_2 [M+H]^+$	194.1181	194.1186	2.6
	$C_{10}H_{11}O_2$	163.0759	163.0771	7.4
	$C_8H_7O_2$	135.0446	135.0458	8.9
	C_7H_5O	105.0340	105.0348	7.6
MDP-2-POH	$C_{10}H_{13}O_3 [M+H]^+$	181.0865	181.0871	3.3
	$C_{10}H_{11}O_2$	163.0759	163.0760	0.6
	$C_8H_7O_2$	135.0446	135.0437	-6.7
	C_8H_7O	119.0497	119.0508	9.2
	C_7H_9O	109.0653	109.0655	1.8
	C_7H_7	91.0548	91.0546	1.2
MDDMA	$C_{12}H_{18}NO_2 [M+H]^+$	208.1338	208.1329	-4.3
	$C_{10}H_{11}O_2$	163.0759	163.0767	4.9
	$C_8H_7O_2$	135.0446	135.0433	-9.6
	$C_7H_5O_2$	121.0290	121.0282	-6.6
	C_7H_5O	105.0340	105.0348	7.6
MDP-2-P	$C_{10}H_{11}O_3 [M+H]^+$	179.0708	179.0712	2.2
	$C_9H_9O_2$	149.0603	149.0588	-10
	$C_8H_7O_2$	135.0446	135.0449	2.2
	$C_7H_5O_2$	121.0290	121.0288	-1.7
	C_7H_7O	107.0497	107.0491	-5.6
	C_7H_7	91.0548	91.0540	-8.8
PN	$C_8H_6NO_2 [M+H]^+$	148.0399	148.0394	3.4
	$C_7H_5O_2$	121.0290	121.0284	-5.0
	C_6H_5O	93.0340	93.0340	0.0
	C_4H_4N	66.0344	66.0341	-4.5
PMMA	$C_{11}H_{18}NO [M+H]^+$	180.1388	180.1383	-2.8
	$C_{10}H_{13}O$	149.0966	149.0980	9.4
	C_8H_9O	121.0653	121.0662	7.4
	C_7H_7	91.0548	91.0539	-9.9

Table 4-3 continued.

Compound	Chemical Formula	Accurate Mass	Acquired Mass	Mass Accuracy (ppm)
DMAA	C ₇ H ₁₈ N [M+H] ⁺	116.1439	116.1434	-4.3
	C ₆ H ₁₄ N	100.1126	100.1118	-8.0
	C ₅ H ₁₂ N	86.0970	86.0973	3.5
	C ₄ H ₈ N	70.0657	70.0661	5.7
caffeine	C ₈ H ₁₁ N ₄ O ₂ [M+H] ⁺	195.0882	195.0889	3.6
	C ₆ H ₈ N ₃ O	138.0667	138.0671	2.9
	C ₅ H ₈ N ₃	110.0718	110.0722	3.6

The compounds identified in the ATS using DESI-MS, GC-MS and LC-MS have been summarised in Table 4-4.

Table 4-4 Compounds detected in "Jack3d", MDMA (tablet and synthesised base), and PMMA (synthesised base) using DESI-MS, GC-MS, and LC-MS.

Sample	Compound	MW (Da)	DESI-MS	GC-MS	LC-MS
MDMA tablet	MDMA	193	✓	✓	✓
	MDP-2-POH	180	✓	✓	✓
	MDDMA	207	✓	✓	✓
	MDP-2-P	178	X	X	X
MDMA base	MDMA	193	✓	✓	✓
	MDP-2-P	178	✓	✓	✓ (trace)
	PN	147	✓	✓	X
	N-formylMDMA	221	X	✓	✓
PMMA base	PMMA	179	✓	✓	✓
	anethole	148	✓ (trace)	✓	✓
	PMP-2-P	164	X	✓	✓
"Jack3d"	DMAA	115	✓ (trace)	X	✓
	caffeine	194	✓	✓	✓
	creatine monohydrate	132	X	X	✓

✓ = detected, X = not detected

Note: Where listed as being detected in "trace" amounts, MS/MS data was not obtained due to very low signal responses.

The collision induced dissociation of the ATS in this chapter share some common fragmentation pathways. Typical of any collision induced dissociation experiment is the formation of precursor ions, i.e. [M+H]⁺ in positive ion mode. The presence of the ion at *m/z* 91 (i.e. C₇H₇) was consistent in the MS/MS spectra of a number of ATS in this study including

MA, PMA, AP, DMA, MDP-2-POH, MDP-2-P and PMMA. Some general rules that have been applied in the interpretation of the spectra include common product ions such as $[M+H-NH_3]^+$ for primary amines, $[M+H-HCN]^+$, $[M+H-H_2O]^+$, $[M+H-CO_2]^+$ and $[M+H-CH_2O]^+$ for methoxy substituted compounds. In the positive ion mode, adduct ions are also commonly seen and are indicative of certain molecules, i.e. sodiated $[M+Na]^+$, potassiated $[M+K]^+$ and ammonium ion $[M+NH_3]^+$ ¹²⁵. Furthermore, knowledge of the nitrogen rule, i.e. an odd value of molecular mass (M^+) means an odd number of nitrogen atoms, aided in the elucidation of unknown compounds and their respective MS/MS fragment ions.

4.4 Conclusions

Dimethylamylamine present in the “Jack3d” sample was detectable in trace amounts using DESI-MS and LC-MS; however, it remained undetectable using GC-MS. The ingredient which was seemingly present in the largest amount was caffeine and this was detectable using all three techniques. All the by-products in the MDMA samples were detectable using all three techniques with the exception of MDP-2-P in the MDMA tablet, confirming that reductive amination was used in the synthesis of MDMA. The detection of anethole in PMMA suggested that anethole was used as a starting material in the synthesis of this compound (Table 4-4).

Chapter 5: Analysis of cocaine

Chapter 5: Analysis of cocaine

5.1 Introduction

The DESI-MS analysis of illicit cocaine samples is detailed in this chapter. Three batches of seized cocaine were obtained from the AFP for analysis using DESI-MS. The LOD of cocaine and the effect of common adulterants were also evaluated. The impurities/by-products present in the cocaine samples was found to be indicative of the geographical origin of the coca leaf used to manufacture the samples. The impurities/by-products identified were also compared to those identified using GC-MS and LC-MS.

5.2 Materials and methods

The methods developed using DESI-MS, GC-MS and LC-MS in section 3.3.1 - 3.3.4 were applied to the analysis of seized cocaine samples in this chapter. The DESI-MS operating parameters were as previously optimised with experiments run in full scan mode (m/z 50 - 1000) and MS/MS experiments conducted in the targeted product ion scan mode with collision energy of 20 eV. Samples were dissolved in methanol (12 mg/mL) unless otherwise specified. Aliquots of solution (2 μ L) were deposited onto the PTFE sample plate. Analyte identity was supported by MS/MS experiments and compared to reference spectra. Data analysis was conducted using Agilent MassHunter Workstation software, Qualitative Analysis, Version B.03.01 (Agilent Technologies). GC-MS was conducted in full scan mode (m/z 50 - 1000). Samples were dissolved in methanol (3 mg/mL). Injection was done in splitless mode and injection volume was 2 μ L. LC-MS was conducted in full scan mode (m/z 50 - 1000) and MS/MS experiments were conducted in the product ion scan mode (auto MS/MS) with collision energy of 20 eV. LC-MS samples were dissolved in methanol (1 mg/mL). See section 2.2 for more method details.

A cocaine standard was cut with adulterants such as caffeine, paracetamol, procaine, atropine, levamisole, and lignocaine in order to evaluate the effects of adulterating the compound of interest. Adulteration involving caffeine was conducted at varying amounts of caffeine added to the cocaine standard (i.e. 20 %, 50 %, 90 %, 95 % w/w, respectively).

In DESI-MS analysis, the LOD was defined to be the lowest concentration required to give a signal equal or greater than the average intensity of the blank signal plus three times the SD of the blank⁹. In GC-MS and LC-MS analysis, the LOD was defined to be the lowest peak concentration to exhibit a peak height three times the noise level (SNR 3:1). The ANOVA test was utilised as a means to determine whether the observed ion enhancement or suppression in adulteration experiments was significantly different to the unadulterated signal response (i.e. $p < 0.05$).

5.3 Results and discussion

5.3.1 Adulteration and LOD

A study assessing the effects of common adulterants on the detectability of cocaine was conducted. The adulterants used were atropine, paracetamol (acetaminophen), procaine, lignocaine, levamisole and caffeine as these are the most prevalent adulterants used in cocaine preparations¹⁰. The chemical structures of these adulterants are illustrated in Figure 5-1. Solutions containing cocaine and adulterant were prepared (1:1 mole ratios) to approximately 12 mg/mL, and 2 μ L aliquots of these solutions were spotted onto a PTFE plate prior to DESI-MS analysis. It was found that the addition of paracetamol, procaine and lignocaine resulted in enhancement of the cocaine signal response (approximately double the unadulterated signal response, $p < 0.05$). There are many factors which can contribute to ion suppression and enhancement in a mixture of compounds, basicity of the analytes being one of them. Procaine and lignocaine are relatively basic and will easily be detectable in the DESI source in positive ion mode (Figure 5-2). On the contrary, atropine, levamisole and caffeine did not result in a significant difference in signal response to the unadulterated sample ($p > 0.05$). Overall, the adulterants tested using DESI-MS resulted in some enhancement effects of the analyte signal suggesting that despite the presence of these compounds as adulterants in illicit cocaine seizures, the analyte will, in most cases, remain detectable. However, caution must be taken when interpreting the effects of an adulterant on the detectability of an analyte using this technique. Due to the transient signal response observed using DESI-MS, the relative enhancement effects of these adulterants may change in subsequent analyses (evident in large SDs), thus the trends reported here should only be taken as a guide as to the effects of certain adulterants on the detectability of cocaine.

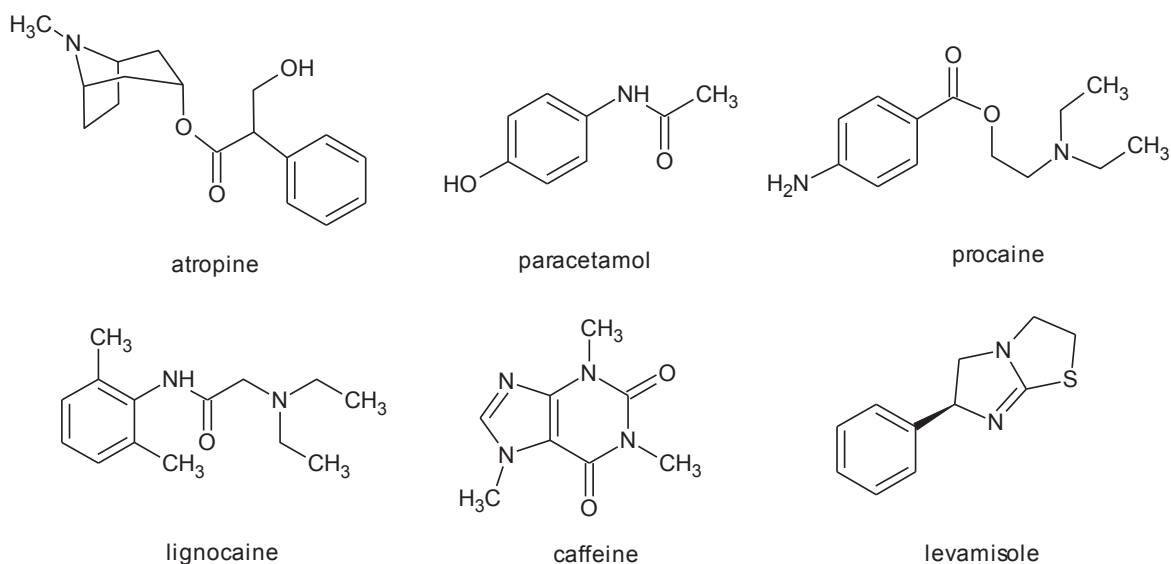


Figure 5-1 Chemical structures of common adulterants in illicit cocaine preparations.

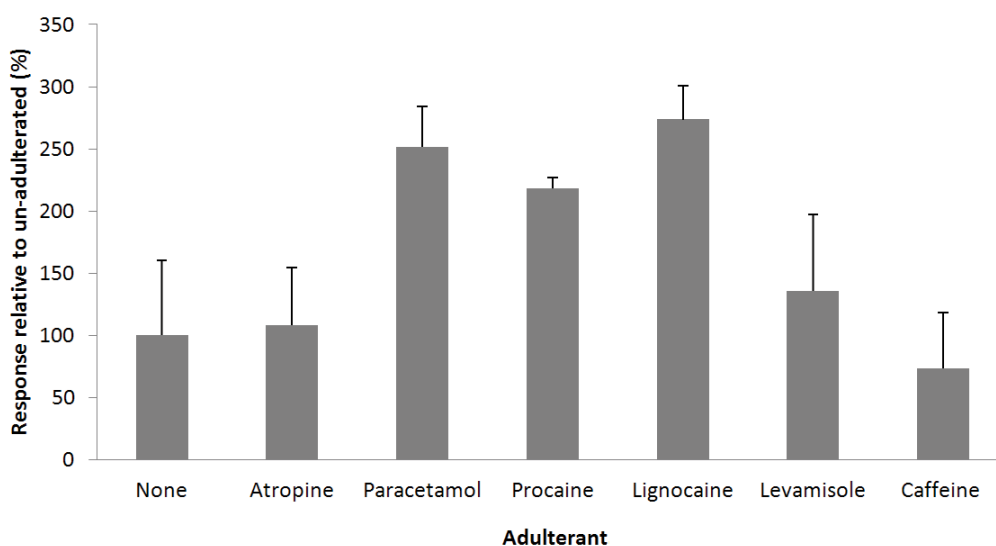


Figure 5-2 Intra-day study of the effects of different adulterants on the detection of cocaine, n=3.

This experiment was repeated over three days (n=3) in order to evaluate whether the adulterant effects were consistent over time. The same trend was observed over the three days tested (Figure 5-3). The intra-day and inter-day precision were found to be 35 % RSD and 42 % RSD, n=3 respectively. The change in instrument response over time and also the variation in desorption of the analyte from the sampling surface all contribute to the precision value obtained.

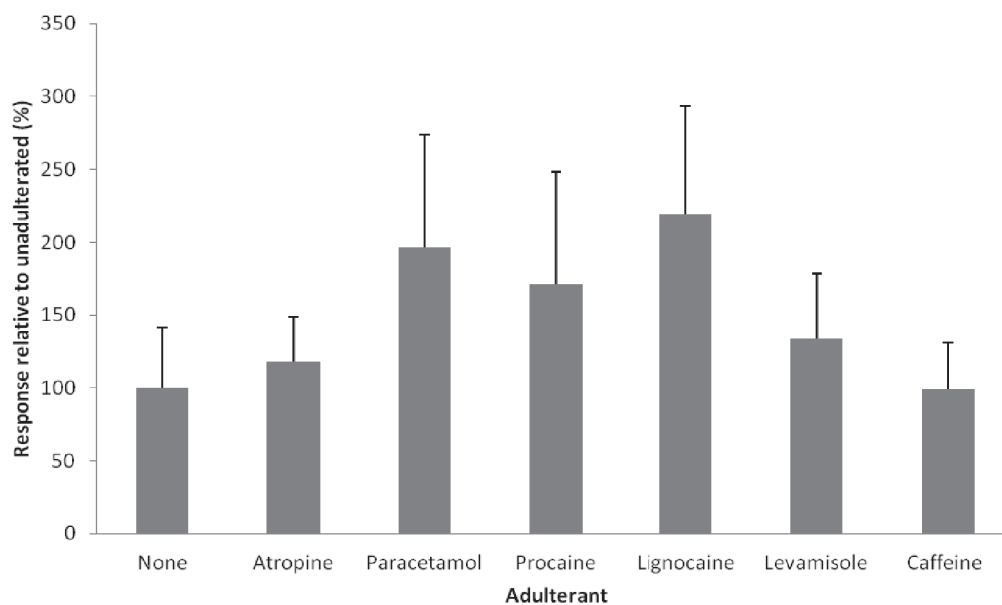


Figure 5-3 Inter-day study of the effect of different adulterants on the detection of cocaine, $n=3$.

A cocaine hydrochloride standard was adulterated with varying amounts of caffeine. The presence of caffeine did not affect the signal response significantly ($p>0.05$ for 20 % to 95 % w/w caffeine added, Figure 5-4). Based on the data obtained, the LOD for cocaine using DESI-MS was found to be $24.3 \mu\text{g}$ (equivalent to $3.47 \mu\text{g}/\text{mm}^2$). The average signal response (peak height) of cocaine at this concentration (with 0 % caffeine) was 10708 cps which was greater than the LOD determined from the average of the solvent blank plus $3 \times \text{SD}$ (i.e. 5216 cps, m/z 250 - 350), allowing the analyte to be distinguished unambiguously amongst the background noise peaks.

The presence of cocaine in these samples was supported by MS/MS data (Figure 5-5); the proposed collision induced dissociation of the $[\text{M}+\text{H}]^+$ ion is illustrated in Figure 5-6. The intra-day and inter-day precision of the technique for the detection of cocaine was less than 11 % and 42 % RSD, respectively (Table 5-1).

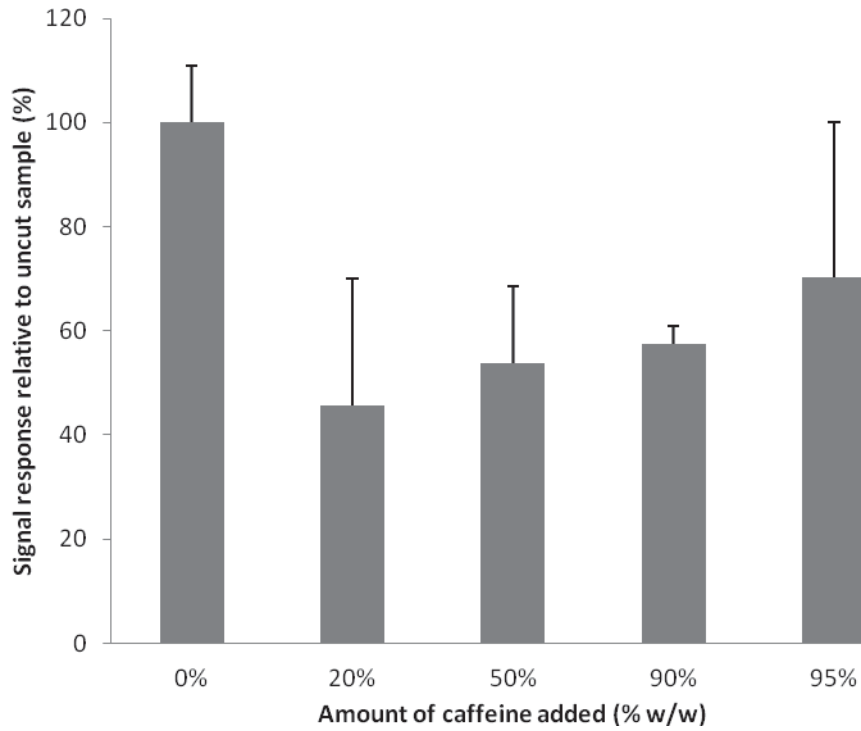


Figure 5-4 Adulterating cocaine standard with varying amounts of caffeine added (i.e. 0 %, 20 %, 50 %, 90 %, 95 % w/w), $n=3$, $2 \mu\text{L}$ of $12130 \mu\text{g/mL}$, equivalent to $24.3 \mu\text{g}$ cocaine.

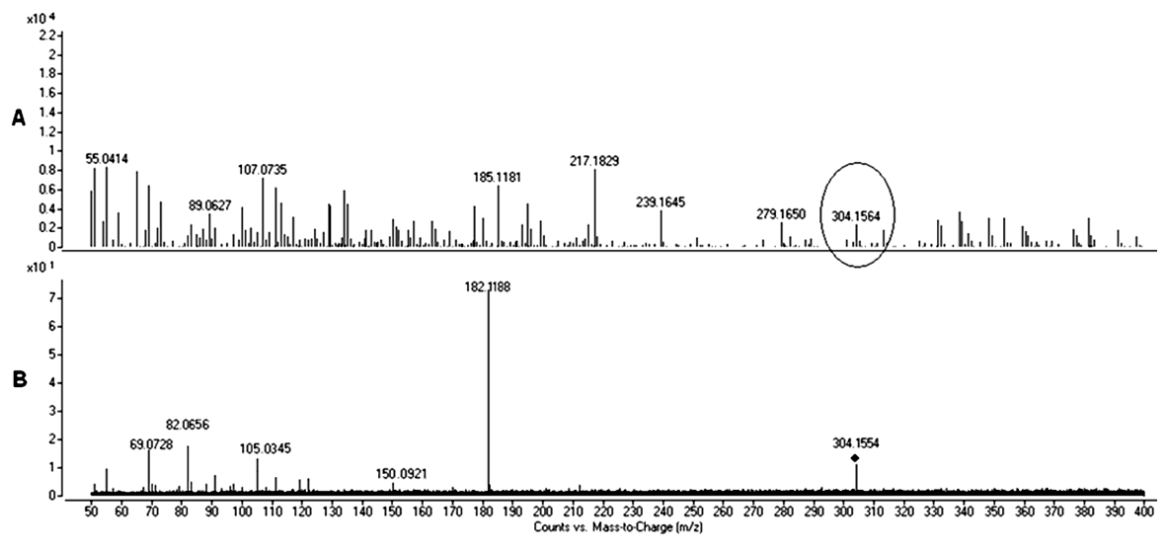


Figure 5-5 A: DESI-MS spectra of cocaine; B: MS/MS spectra of cocaine at 20 eV.

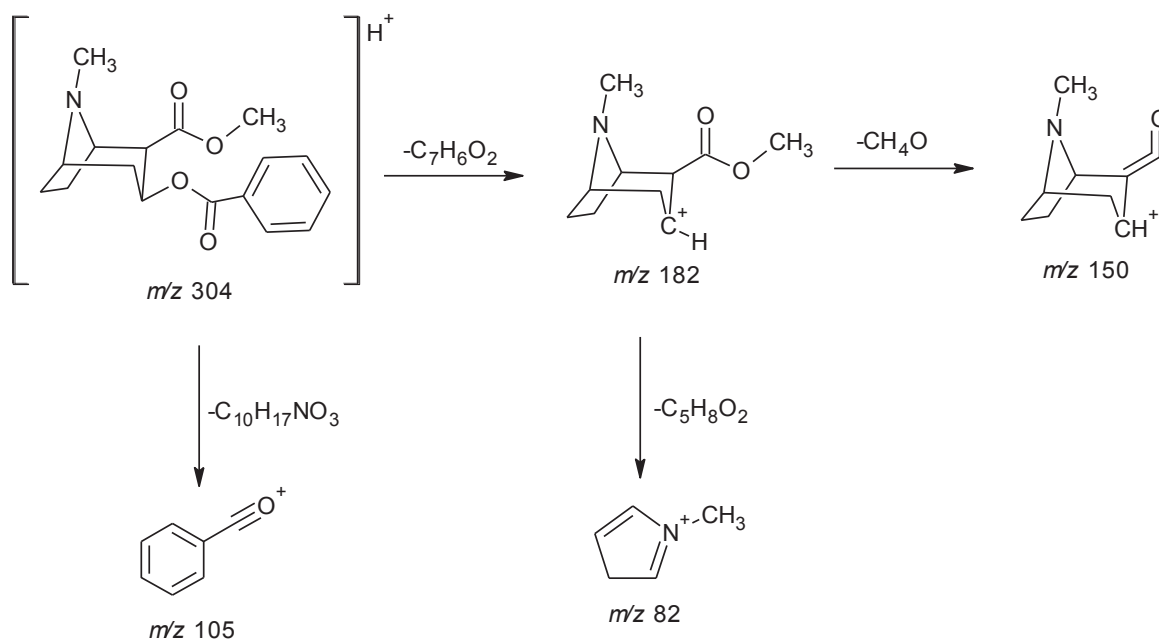


Figure 5-6 Proposed collision induced dissociation of the $[M+H]^+$ ion of cocaine¹²⁶.

A comparison was conducted using three techniques, i.e. DESI-MS, GC-MS and LC-MS on the detectability of cocaine. The LOD obtained for DESI-MS is relatively large when compared to GC-MS and LC-MS; however, in the current context, most drug seizures have sufficient sample for analysis by multiple detection techniques; therefore, this is not a limiting factor in the current context (Table 5-1). The intra-day and inter-day precision using DESI-MS was also larger than that obtained with GC-MS and LC-MS.

Table 5-1 Limit of detection, intra-day and inter-day precision of cocaine, $n=3$.

Technique	LOD ($\mu\text{g}/\text{mL}$)	Intra-day	Inter-day
		RSD (%) ^b	RSD (%)
DESI-MS	12×10^3 ($3.47 \mu\text{g}/\text{mm}^2$) ^a	11	42
GC-MS	12	12	15
LC-MS	0.12	8	14

^a sample well size 7 mm^2 .

^b RSD = relative SD.

It was found that different concentrations of adulterant have differing effects on the signal responses in DESI-MS. Large SDs, transient signal responses, matrix effects from background signals and from caffeine itself, and differences in the desorption of analytes from sampling surfaces all contributed to fluctuations in the signal intensity observed.

5.3.2 Analysis of seized cocaine samples

5.3.2.1 Desorption electrospray ionisation – mass spectrometry

Natural alkaloids and impurities that have been found in significant levels in illicit natural cocaine include *N*-acetylnorcocaine, 2,3-didehydroecgonine, 2,3-didehydroecgonine methyl ester, benzoic acid, benzoyl ecgonine, *N*-benzoyl norecgonine methyl ester, *trans*-cinnamic acid, *cis*- and *trans*-cinnamoylcocaine, *cis*- and *trans*-cinnamoylecgonine, ecgonine, methyl ecgonine, *N*-formylcocaine, *N*-norcocaine, *N*-norecgonine, tropacocaine, all five diastereomeric truxillic acids, all eleven diastereomeric truxillines, and all six diastereomeric truxinic acids^{117, 120, 121, 127-157}. Cocaine samples from three different cocaine seizures, i.e. Item 1, Item 1/2, and Item 5/2 were obtained from the AFP. All three cocaine samples were previously analysed by NMI, using GC-MS, gas chromatography - flame ionisation detection (GC-FID) and stable isotope ratio – mass spectrometry analysis (IRMS). Following the NMI analysis, an analysis report was provided indicating the compounds present in each sample (Figure 5-7).

Cocaine and truxilline were detected as the protonated molecular ions at m/z 304 and 659 in all three samples using DESI-MS, respectively (Figure 5-8). The truxillines detected in DESI-MS analysis may represent a mixture of diastereoisomers, i.e. *epsilon*-, *delta*-, *beta*-, *peri*-, *neo*-, *epi*-, *alpha*-, *omega*-, *gamma*-, *mu*-, and *zeta*-truxilline due to lack of chromatographic separation. Trace amounts of 3,4,5-trimethoxycocaine, tropacocaine, caffeine and ecgonine methyl ester (EME) were identified in Item 1 as protonated molecular ions at m/z 394, 246, 195 and 200, respectively. In our results, where specified as trace amounts, MS data was obtained; however, MS/MS was unable to be exploited due to such low quantities of molecular ion present. EME was found in trace amounts in all three samples. During the manufacture of illicit cocaine from coca leaves, manufacturing by-products are created and carried through to the end-product. One of the most common chemical processes that occur is hydrolysis (of ester linkages) in the parent drug. This process can occur during manufacture/synthesis or while in storage giving rise to the presence of alkaloids such as benzoylecgonine (BE), EME, ecgonine and benzoic acid¹⁵⁸. Another compound which was detected in all three samples using DESI-MS was cinnamoyl cocaine (CC) at m/z 330. The presence of this compound in cocaine samples is not unusual as is a natural tropane alkaloid originating from the coca plant (*Erythroxylum coca* Lam.)¹. Trace amounts of caffeine were

also detected in Item 1/2 and Item 5/2. Two additional adulterants at m/z 205 and m/z 375 which correspond to the protonated molecular ions of levamisole and hydroxyzine respectively were found in cocaine Item 5/2. Both peaks are significantly smaller than cocaine due to much lower concentrations in the mixture (Figure 5-8 C). The identification of these two additional adulterants clearly discriminates cocaine Item 5/2 from Item 1 and Item 1/2 (Table 4-4). The presence of cocaine and the impurities in each of the samples were supported by MS/MS spectra where possible (Figure 5-9, Figure 5-10 -Figure 5-16).

Analysis of residual solvents by head space – gas chromatography (HS-GC), stable isotope ratios, tropane alkaloids analysis by GC-MS, GC-MS analysis of derivitised truxillines and physical data (five signatures) are used in routine analysis to distinguish cocaine samples (e.g. Peruvian and Bolivian cocaine)¹⁵⁷. It has been well established that Colombian cocaine commonly possesses the highest amount of truxilline content¹⁵⁹. In the current work, we were able to detect truxillines in all three samples. The signal response (peak height) of truxillines in the three samples tested (i.e. Item 1, Item 1/2 and Item 5/2) was 363, 257, 3345 counts, respectively. The large response found in Item 5/2 may indicate that a higher amount of truxillines are present in this cocaine sample alluding to the fact that this may be Colombian cocaine (as was indicated in the AFP analysis report). However, certain caution should be taken in interpreting total truxilline content since cocaine originating from Ecuador has also been reported to contain high amounts of truxillines¹⁶⁰. Research has shown that the lowest truxilline content is commonly associated with Peruvian cocaine, while a slightly higher level of truxillines can be associated with Bolivian cocaine¹⁶⁰. This may suggest that Item 1/2 contains Peruvian cocaine and Item 1 is Bolivian in origin. In order to confirm the origin of these samples quantitative analysis of the total truxilline content is essential (derivitisation required prior to GC-MS analysis)¹⁵⁹. Further work involving a larger selection of samples would be required in order to confirm the validity of geographical origin determination using DESI-MS; however, the current work demonstrates great potential in this area. As previously mentioned, there can be up to eleven diastereomeric truxillines, present in varying amounts depending on the geographical origin of each cocaine sample. Despite having detected truxillines in these cocaine samples using DESI-MS, the analysis does not provide an indication of how many or which truxilline stereoisomers are present in these samples as they are all simultaneously detected using this technique (all at m/z 659). However, the advantage of applying DESI-MS to the analysis of seized cocaine samples is in

the speed of preliminary identification/screening of compounds which may differentiate cocaine samples at a very early stage in the investigative process.

COCAINE**PS3125333 Item 1**

Analysis: Cocaine HCl 81.5%
 Coca Leaf Origin: Bolivian
 Solvent A: Ethyl Acetate
 Solvent B: None
 Cocaine Processing Classification: Colombian
 Adulterants: Caffeine (not quantified)
 Alkaloid Analysis:

	% relative to cocaine
Total Truxilline	1.47
3',4',5'-Trimethoxycocaine	0.16
Tropacocaine	0.07

Stable Isotope Ratio Analysis

15N / 14 N: -11.5

13C / 12C: -34.8

PS3179907 Item 1/2

Analysis: Cocaine HCl 83.0%
 Coca Leaf Origin: Peruvian
 Solvent A: Acetone
 Solvent B: Acetone
 Cocaine Processing Classification: Peruvian
 Adulterants: Caffeine (not quantified)
 Alkaloid Analysis:

	% relative to cocaine
Total Truxilline	0.35
3',4',5'-Trimethoxycocaine	0.01
Tropacocaine	-

PS3179907 Item 5/2

Analysis: Cocaine HCl 64.1%
 Coca Leaf Origin: Colombian
 Solvent A: Ethyl Acetate
 Solvent B: None
 Cocaine Processing Classification: Colombian
 Adulterants: Caffeine (not quantified), Levamisole (15.11% as base), Hydroxyzine (2.30% as base)
 Diluents: monosaccharide sugar
 Alkaloid Analysis:

	% relative to cocaine
Total Truxilline	6.17
3',4',5'-Trimethoxycocaine	0.20
Tropacocaine	-

Figure 5-7 Data on cocaine samples provided by AFP (analysis conducted by NMI).

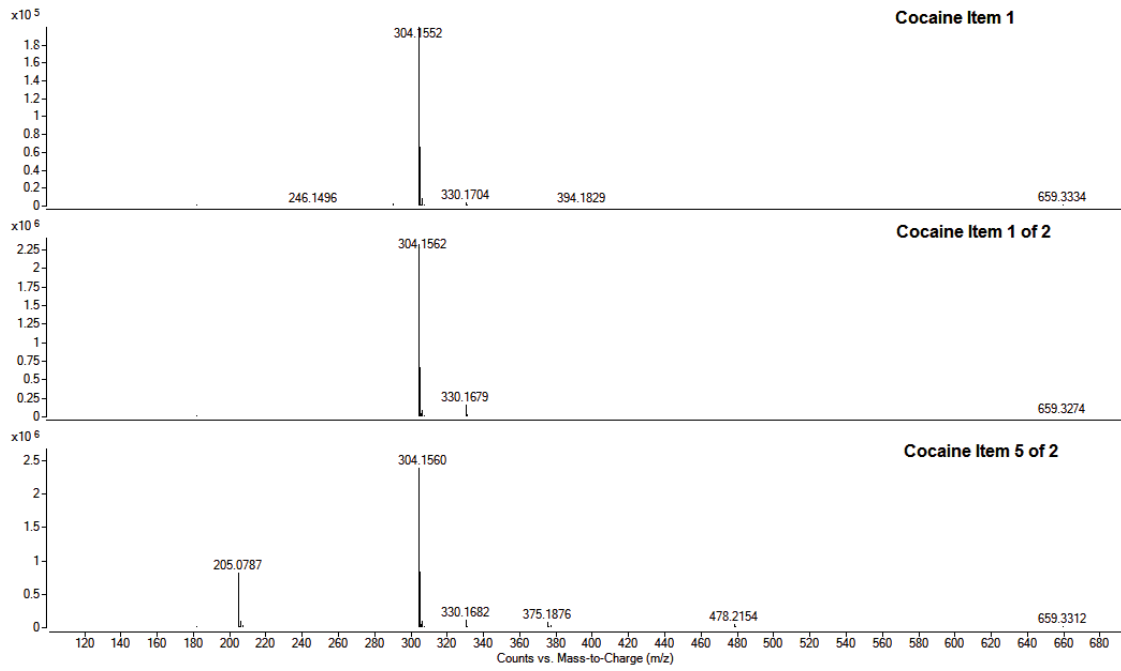


Figure 5-8 DESI-MS spectra of AFP cocaine samples; A: Item 1, B: Item 1/2, C: Item 5/2.

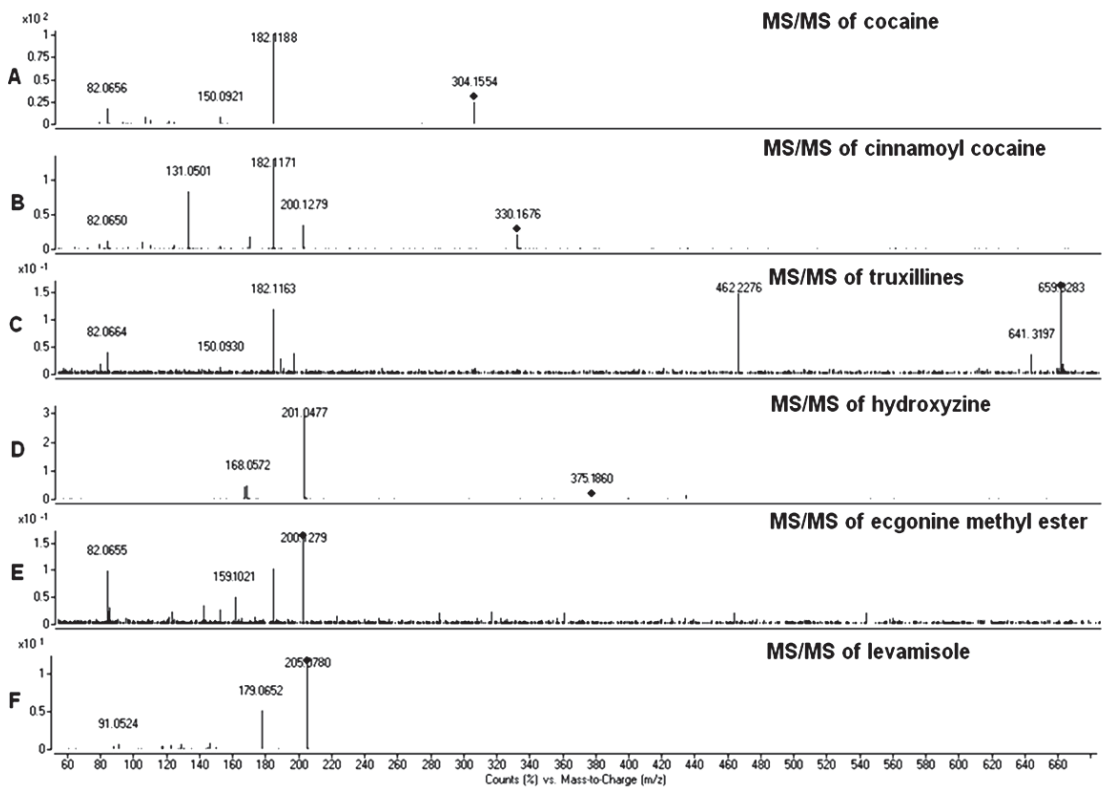


Figure 5-9 DESI-MS/MS spectra of cocaine item 5/2; A: cocaine, B: CC, C: truxilline, D: hydroxyzine, E: EME, F: levamisole.

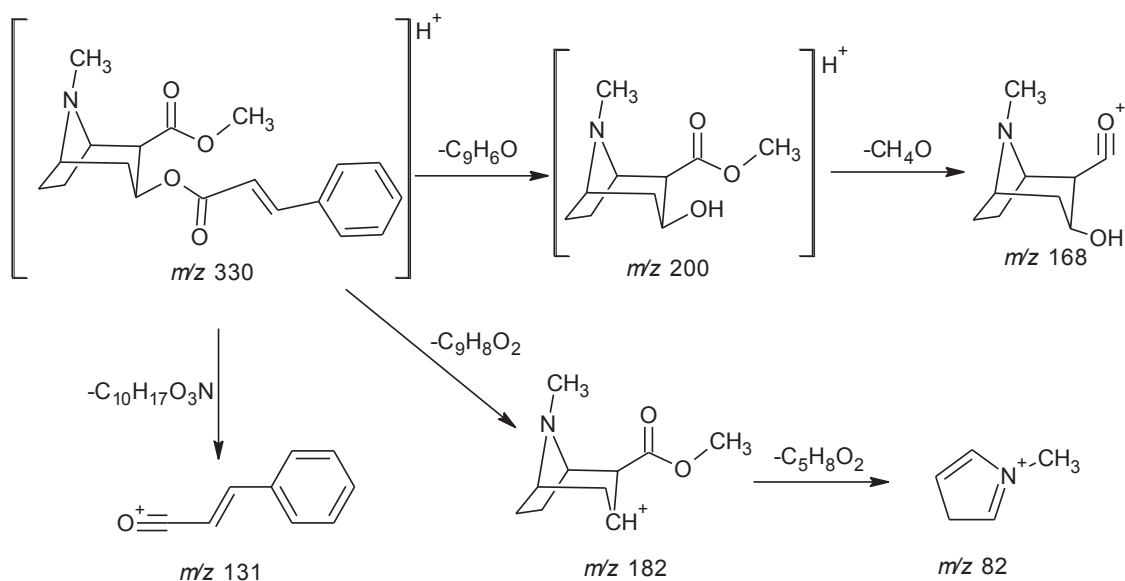


Figure 5-10 Proposed collision induced dissociation of the $[M+H]^+$ ion of CC.

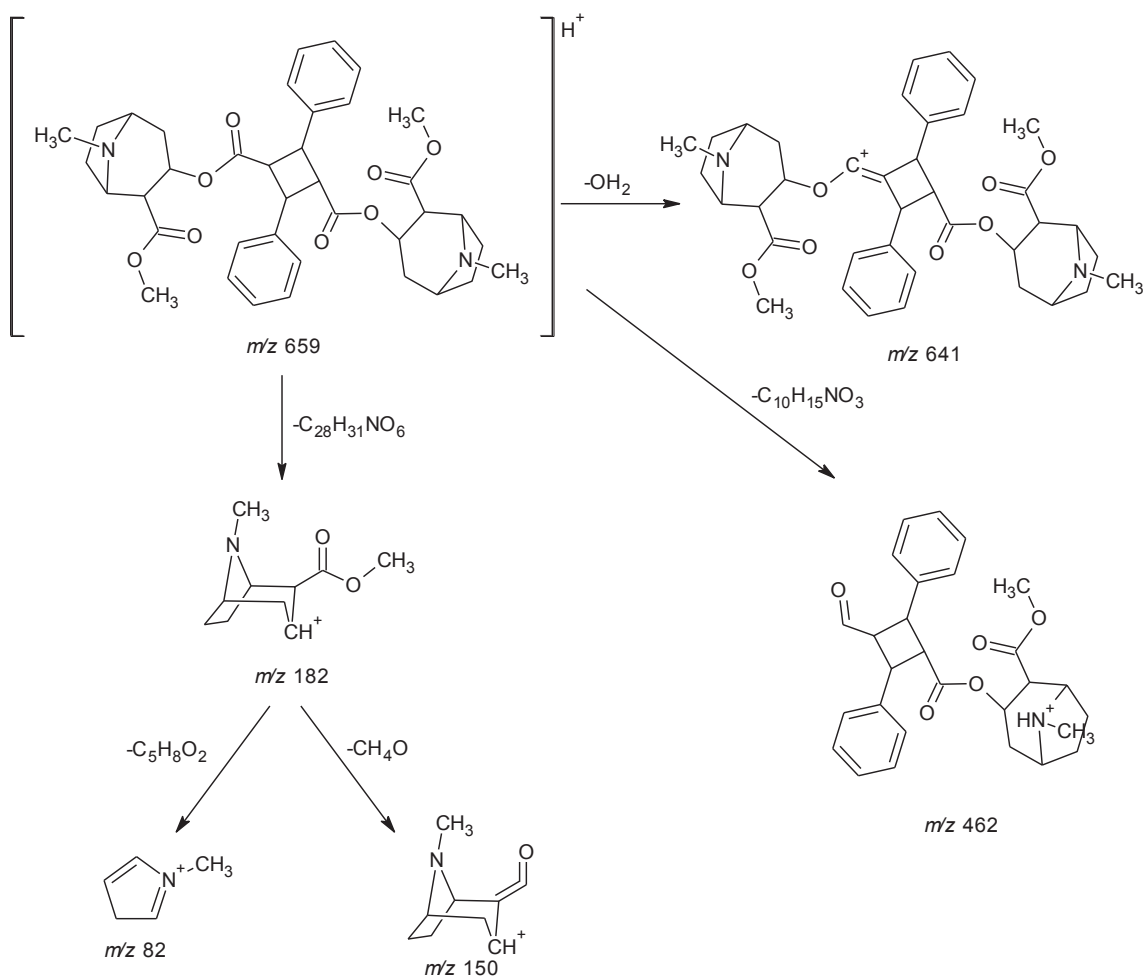


Figure 5-11 Proposed collision induced dissociation of the $[M+H]^+$ ion of α -truxilline.

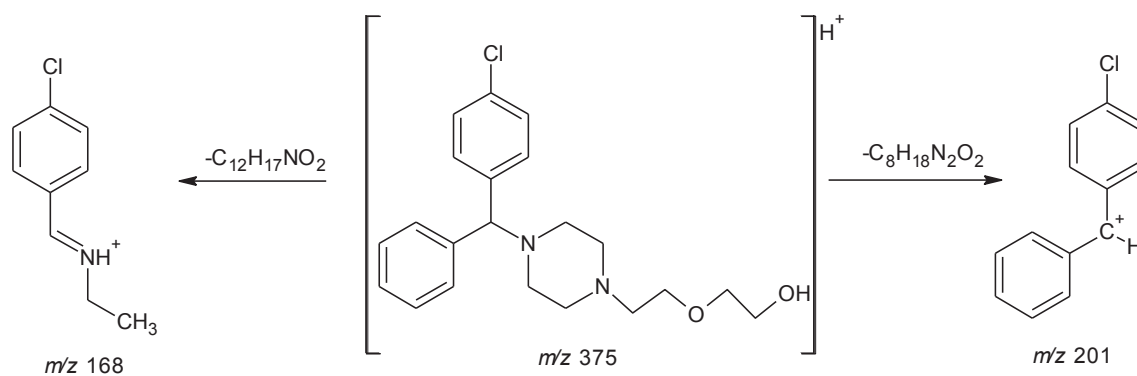


Figure 5-12 Proposed collision induced dissociation of the $[M+H]^+$ ion of hydroxyzine.

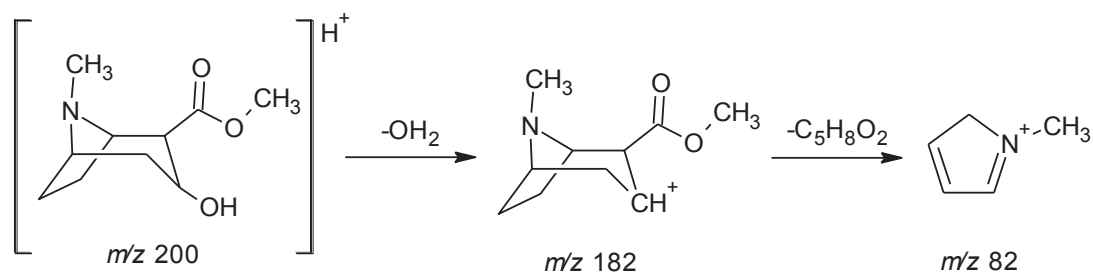


Figure 5-13 Proposed collision induced dissociation of the $[M+H]^+$ ion of EME.

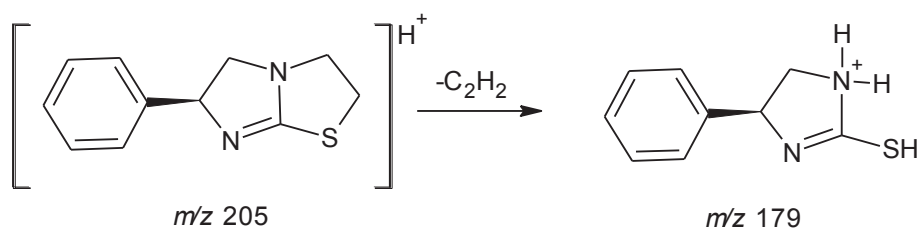


Figure 5-14 Proposed collision induced dissociation of the $[M+H]^+$ ion of levamisole.

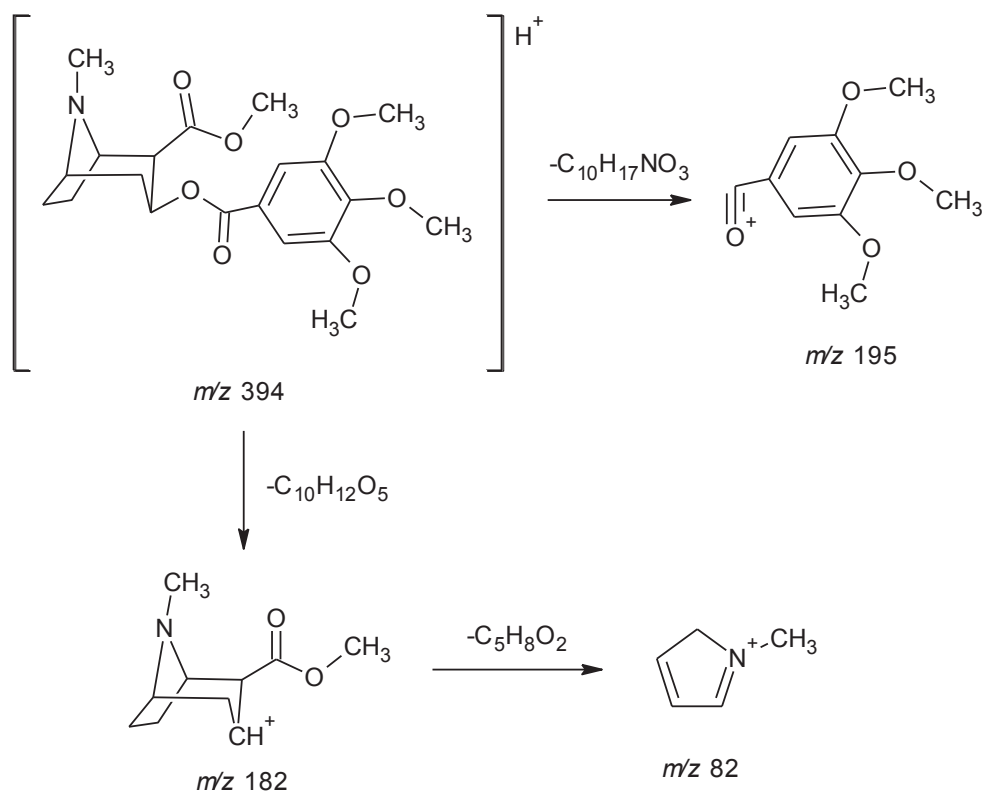


Figure 5-15 Proposed collision induced dissociation of the $[M+H]^+$ ion of 3,4,5-trimethoxycocaine.

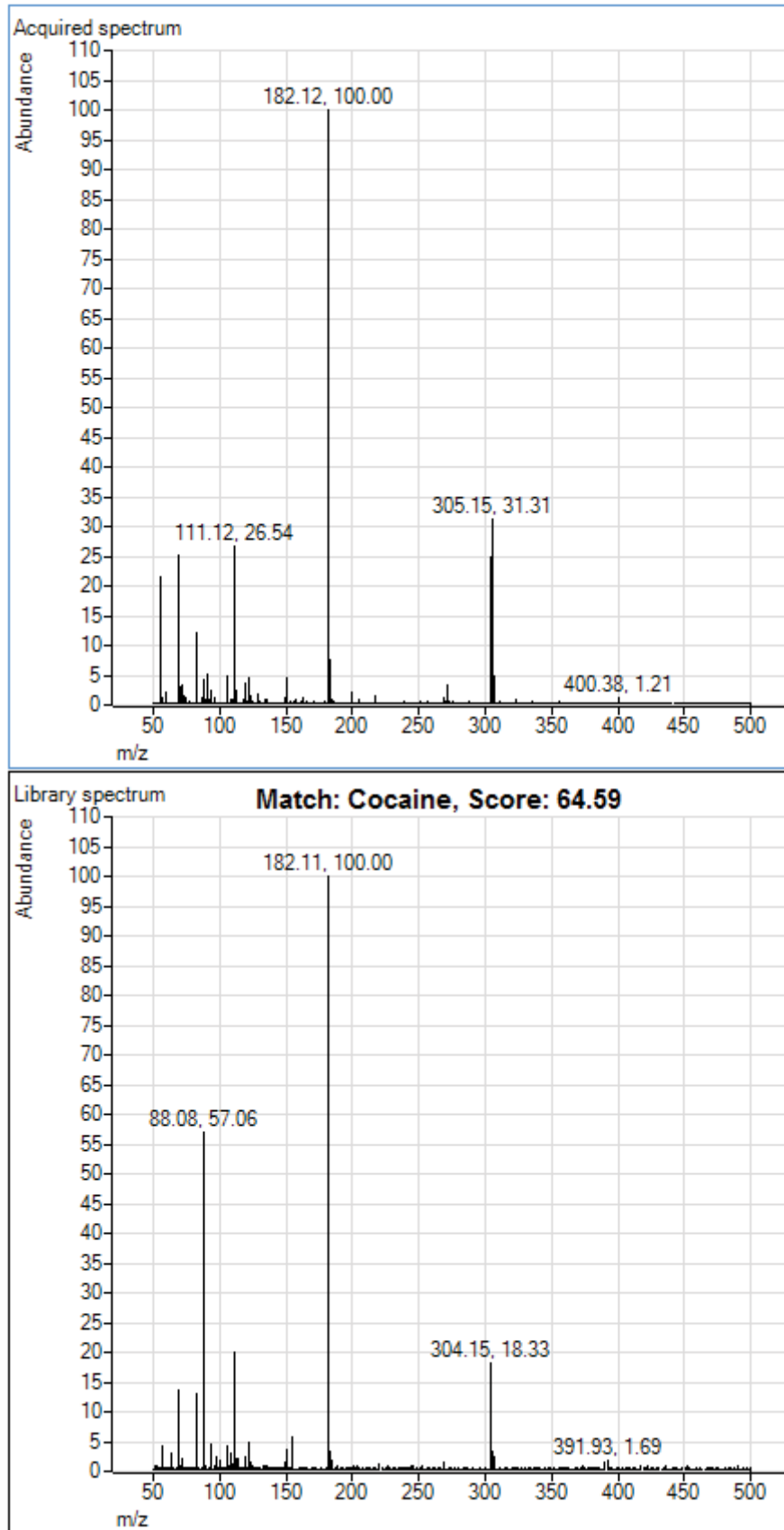


Figure 5-16 PCDL library match to cocaine.

5.3.2.2 Gas chromatography – mass spectrometry

From the GC-MS chromatogram obtained for cocaine Item 1, eight compounds were identified. This included benzoic acid at 4.6 minutes, ecgonidine methyl ester at 5.7 minutes, EME at 6.1 minutes, caffeine at 7.6 minutes, tropacocaine at 7.9 minutes, cocaine at 8.8 minutes, 3,4,5-trimethoxycocaine at 9.1 minutes and cinammoyl cocaine (CC) at 9.7 minutes (Figure 5-17 - Figure 5-23). The presence of benzoic acid and ecgonidine methyl ester are hypothesised to be degradation products due to the high temperatures used in the GC-MS causing hydrolysis of the cocaine¹⁶¹. The presence of hydrolysis products were supported by analysing a pure cocaine standard using GC-MS (Figure 5-24).

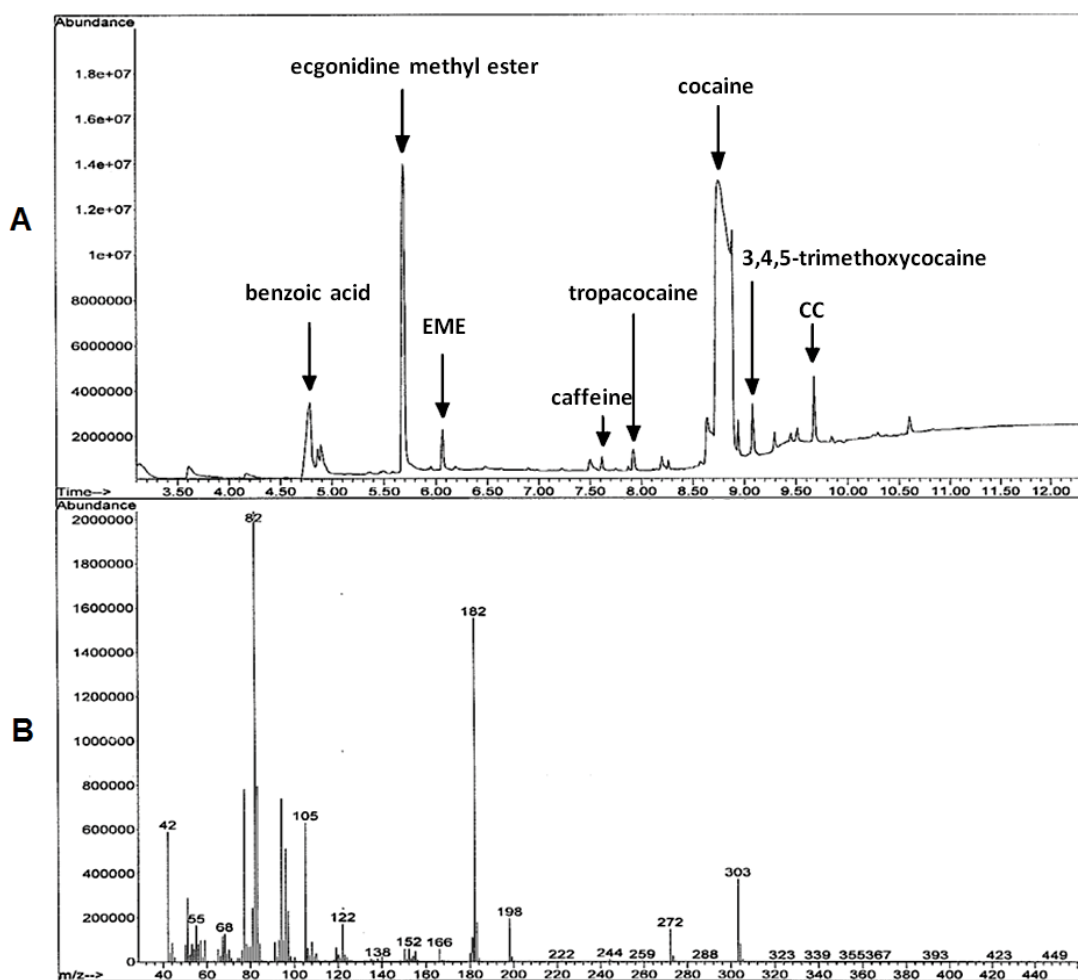


Figure 5-17 A: GC-MS chromatogram of cocaine Item 1, benzoic acid at 4.6 minutes, ecgonidine methyl ester at 5.7 minutes, EME at 6.1 minutes, caffeine at 7.6 minutes, tropacocaine at 7.9 minutes, cocaine at 8.8 minutes, 3,4,5-trimethoxycocaine at 9.1 minutes, CC at 9.7 minutes; B: EI mass spectrum of cocaine (GC method 2).

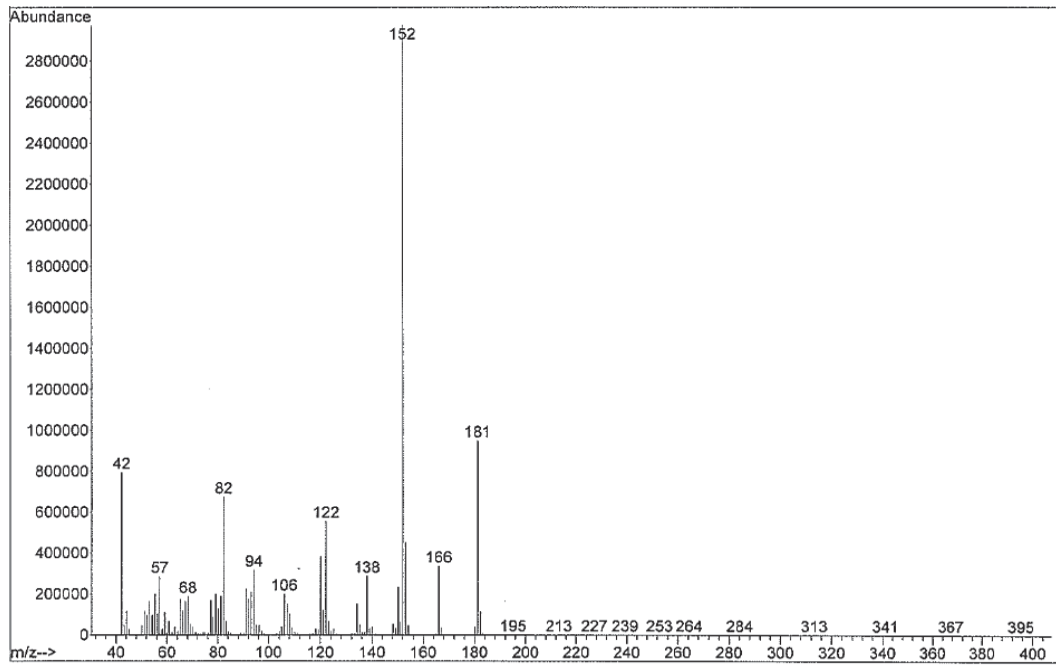


Figure 5-18 EI mass spectrum of ecgonidine methyl ester (GC method 2).

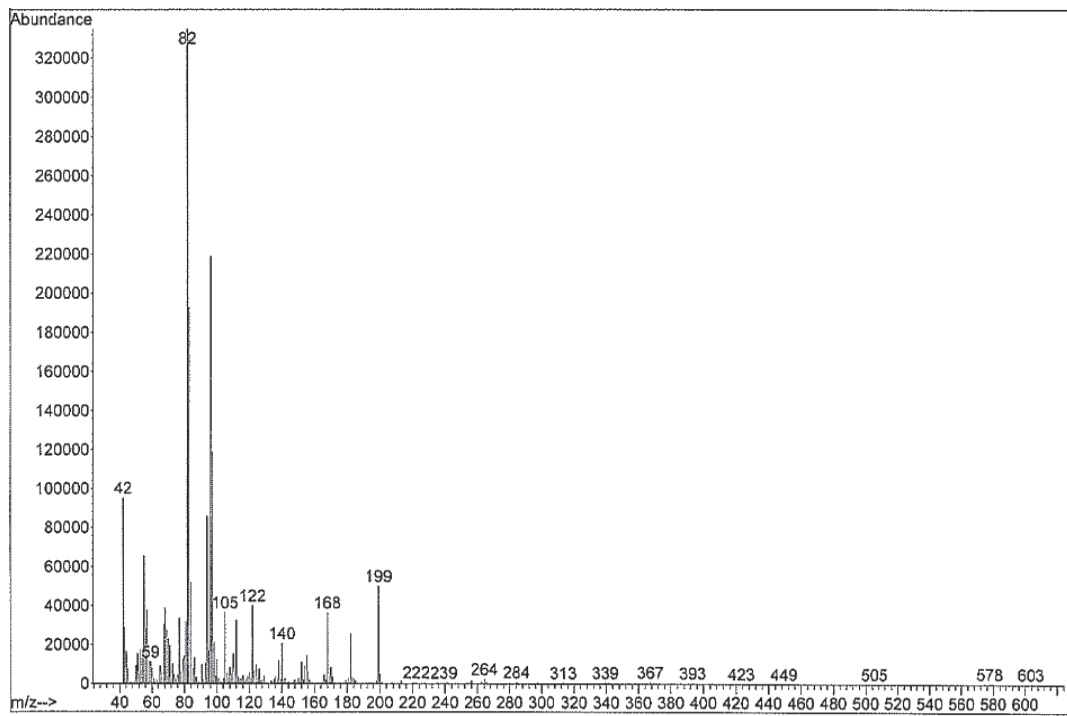


Figure 5-19 EI mass spectrum of EME (GC method 2).

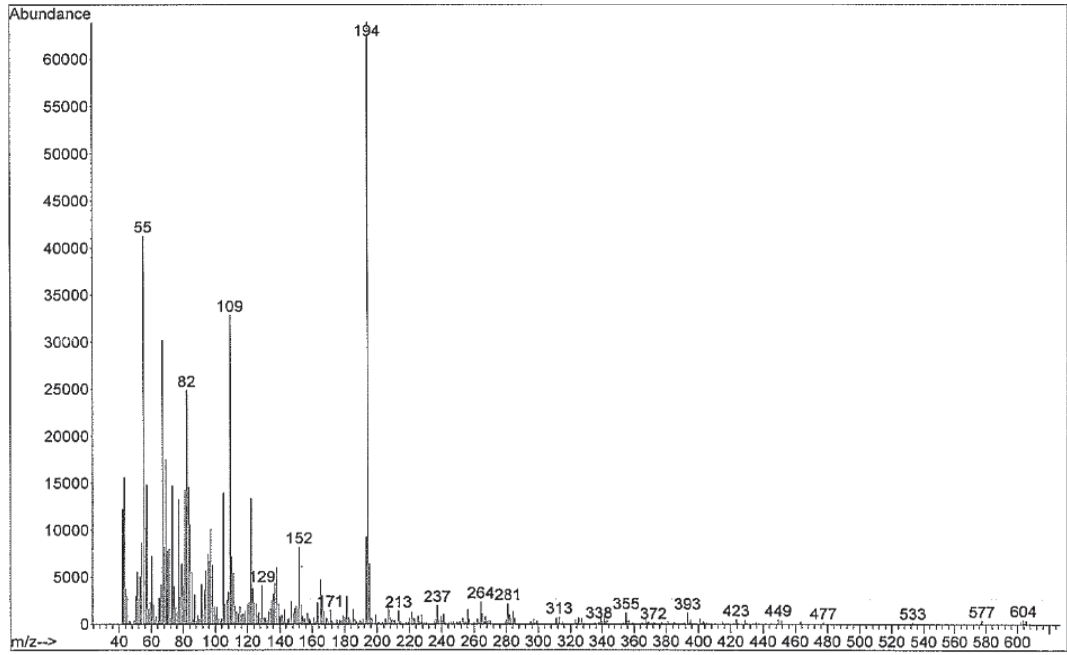


Figure 5-20 EI mass spectrum of caffeine (GC method 2).

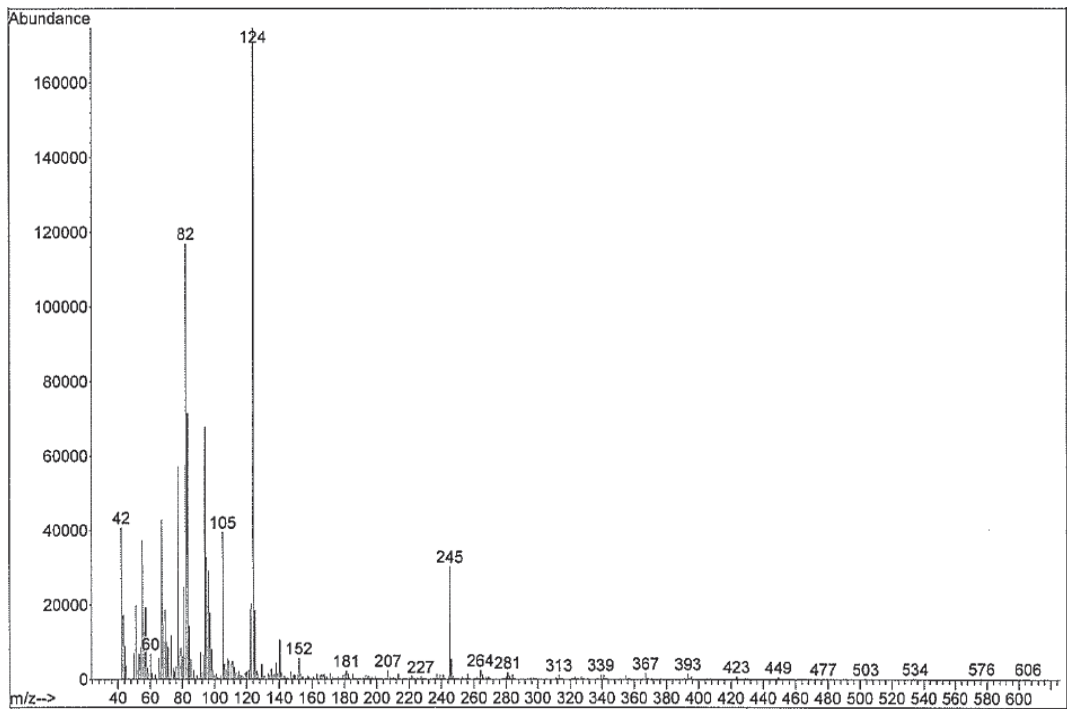


Figure 5-21 EI mass spectrum of tropacocaine (GC method 2).

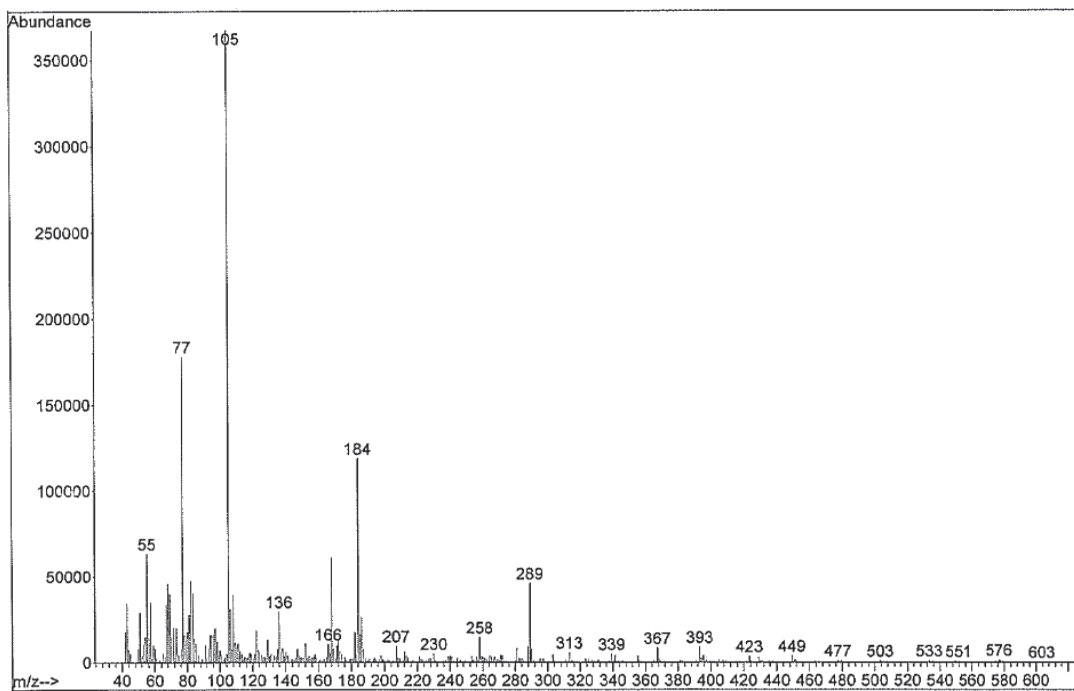


Figure 5-22 EI mass spectrum of 3,4,5-trimethoxycocaine (GC method 2).

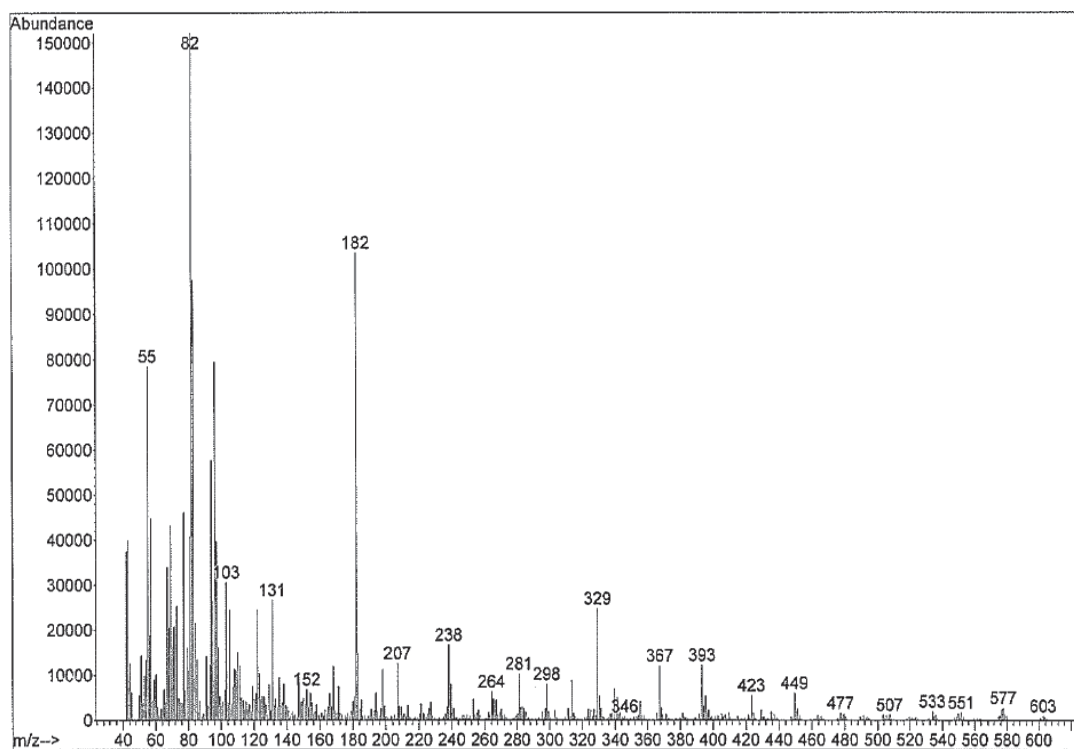


Figure 5-23 EI mass spectrum of CC (GC method 2).

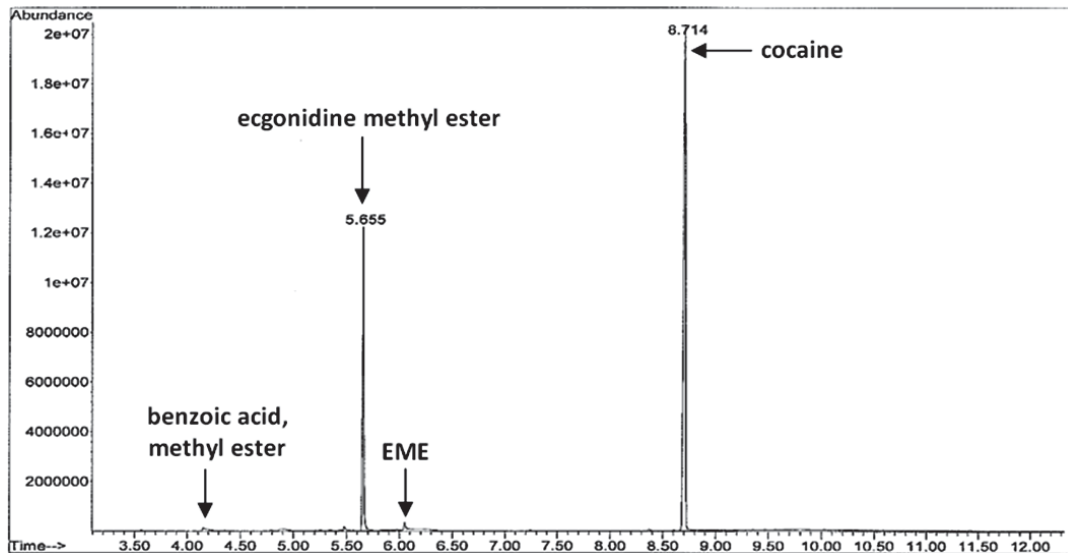


Figure 5-24 GC-MS chromatogram of cocaine standard; benzoic acid methyl ester at 4.2 minutes, ecgonidine methyl ester at 5.7 minutes, EME at 6.1 minutes, cocaine at 8.7 minutes (GC method 2).

The GC-MS chromatogram obtained for cocaine Item 1/2 exhibited peaks corresponding to benzoic acid at 4.7 minutes, ecgonidine methyl ester at 5.7 minutes, EME at 6.2 minutes, caffeine at 7.6 minutes, cocaine at 8.8 minutes, CC at 9.4 minutes and BE at 10.1 minutes (Figure 5-25, Figure 5-18 - Figure 5-20, Figure 5-23, Figure 5-26). The presence of benzoic acid, ecgonidine methyl ester and BE are hypothesised to be hydrolysis products present due to degradation of cocaine at high temperatures (Figure 5-27)¹⁶¹.

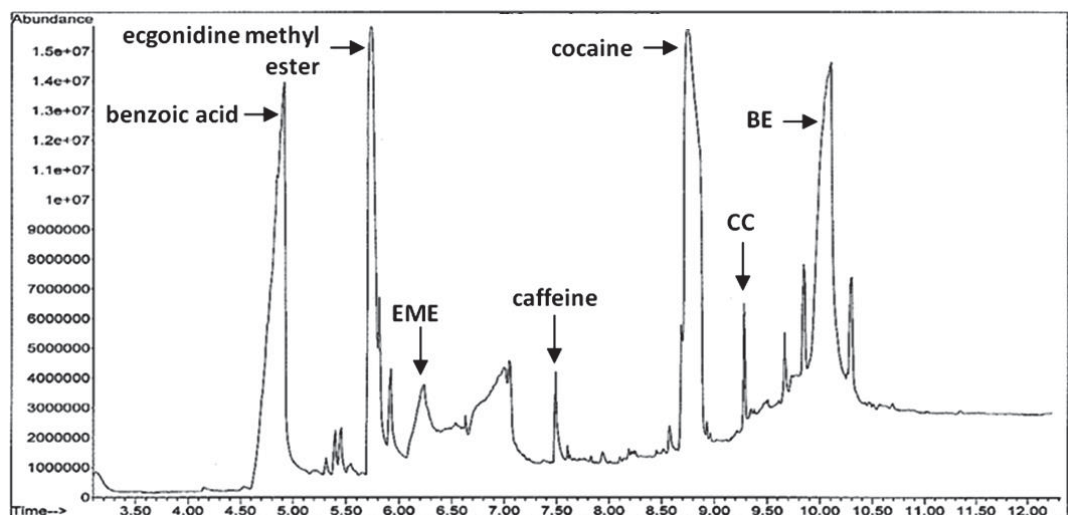


Figure 5-25 GC-MS chromatogram of cocaine Item 1/2; benzoic acid at 4.7 minutes, ecgonidine methyl ester at 5.7 minutes, EME at 6.2 minutes, caffeine at 7.6 minutes, cocaine at 8.8 minutes, CC at 9.4 minutes, BE at 10.1 minutes (GC method 2).

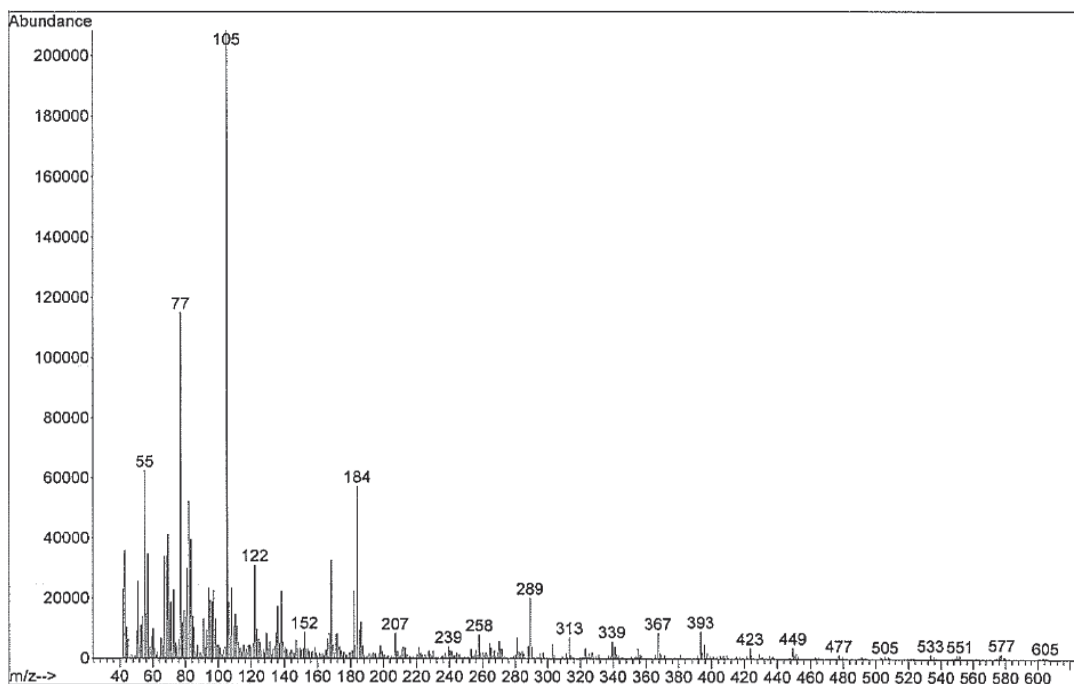


Figure 5-26 EI mass spectrum of BE (GC method 2).

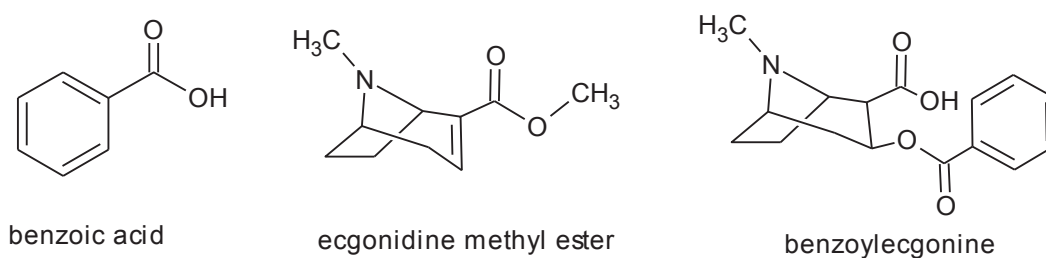


Figure 5-27 Chemical structures of benzoic acid, ecgonidine methyl ester and benzoylecgonine.

Cocaine Item 5/2 also exhibits peaks corresponding to benzoic acid at 4.7 minutes, ecgonidine methyl ester at 5.7 minutes, EME at 6.1 minutes, caffeine at 7.6 minutes, levamisole at 8.1 minutes, cocaine at 8.8 minutes, CC at 9.7 minutes, BE at 10.1 minutes (Figure 5-28, Figure 5-18 - Figure 5-20, Figure 5-23, Figure 5-26, Figure 5-29). Levamisole was identified as an additional adulterant in this sample. Hydroxyzine was also reported to be present in this sample (Figure 5-7); however, it remained undetectable using GC-MS. Truxillines remained undetectable in all three cocaine samples tested, this was hypothesised to be due to the requirement for derivitisation prior to GC-MS analysis (as in routine analysis). The presence of each compound in GC-MS was supported by library match based on their fragmentation spectra.

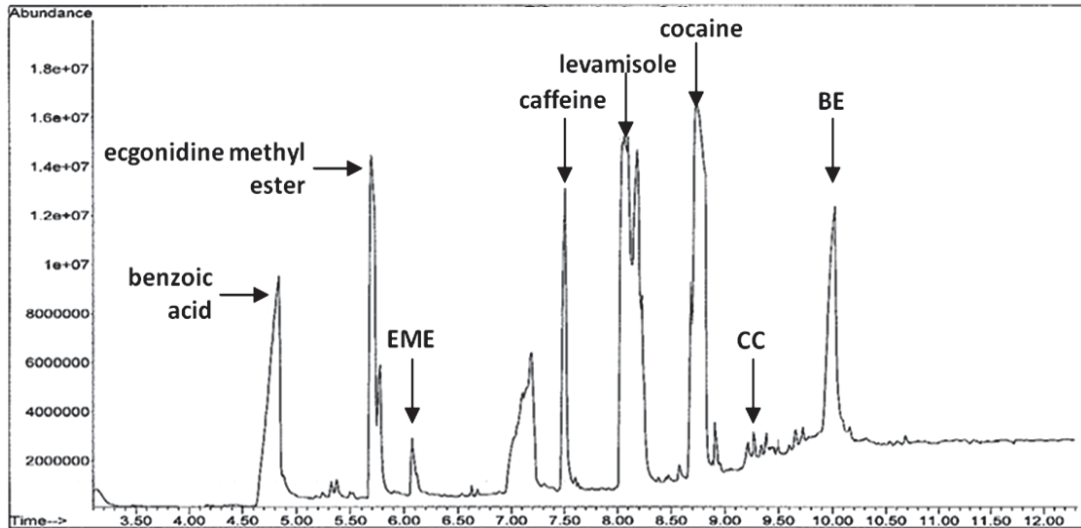


Figure 5-28 GC-MS chromatogram of cocaine Item 5/2; benzoic acid at 4.7 minutes, ecgonidine methyl ester at 5.7 minutes, EME at 6.1 minutes, caffeine at 7.6 minutes, levamisole at 8.1 minutes, cocaine at 8.8 minutes, CC at 9.7 minutes, BE at 10.1 minutes (GC method 2).

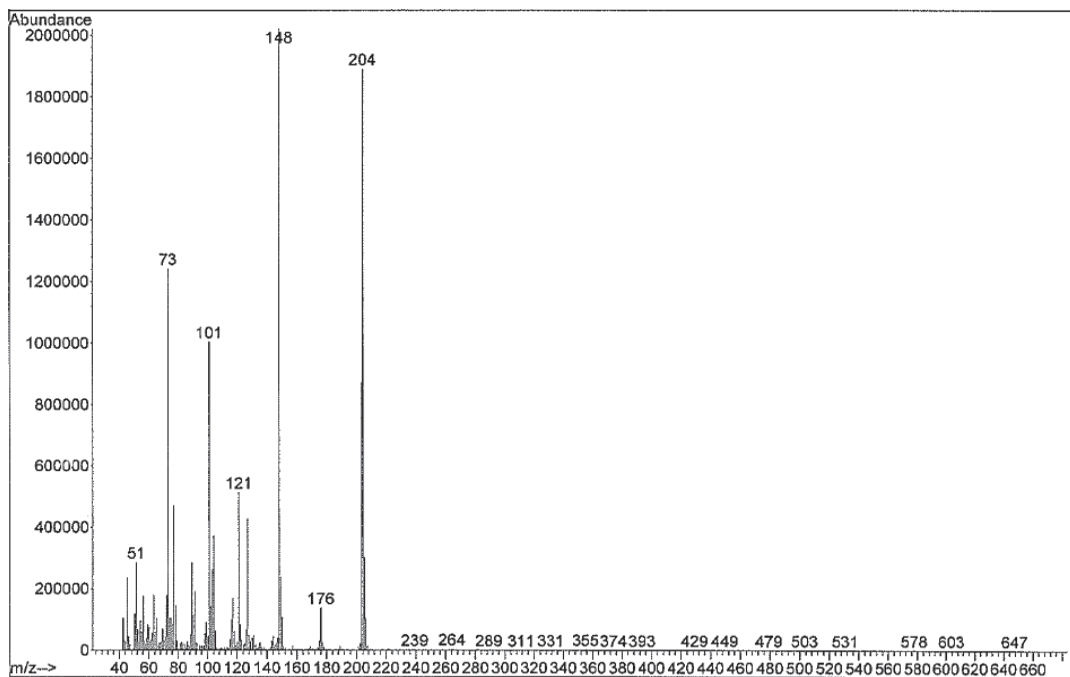


Figure 5-29 EI mass spectrum of levamisole (GC method 2).

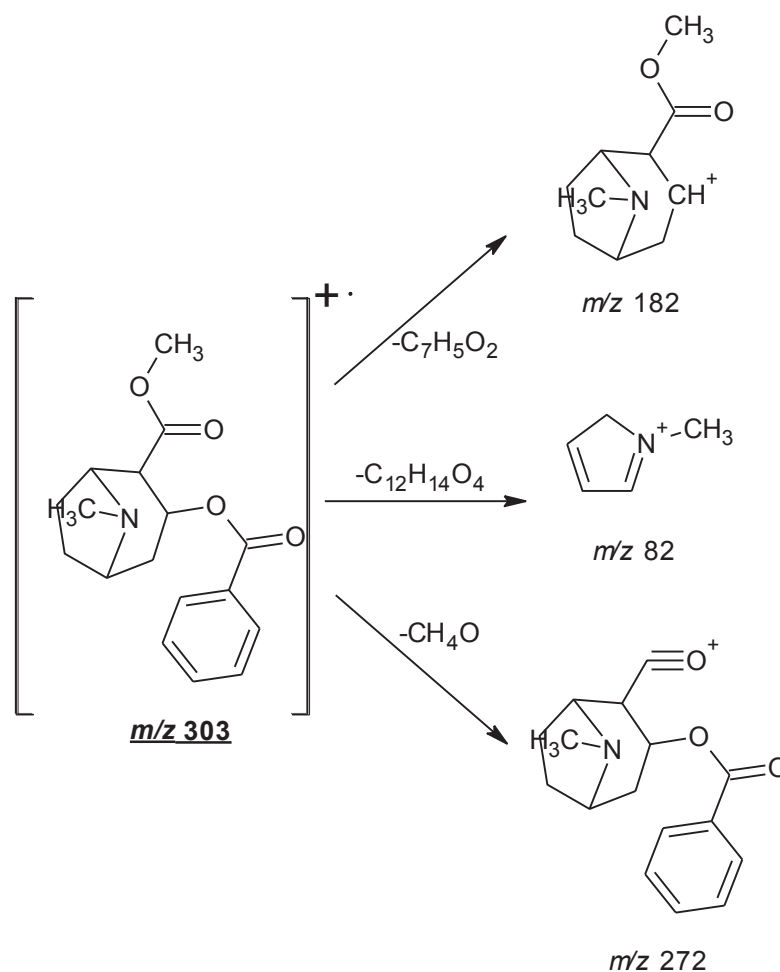


Figure 5-30 Proposed EI fragmentation pathway for cocaine.

5.3.2.3 Liquid chromatography – mass spectrometry

The LC-MS spectra obtained for cocaine Item 1 exhibited the protonated cocaine molecular ion at m/z 304. Other protonated compounds detected using LC-MS included truxilline at m/z 659, 3,4,5-trimethoxycocaine at m/z 394, tropacocaine at m/z 246, caffeine at m/z 195, EME at m/z 200 and CC at m/z 330 (Figure 5-31 and Figure 5-32). Truxillines are a coca leaf alkaloid which are carried through the manufacturing process of cocaine and are very useful in profiling and determining the geographical origin of illicit cocaine samples¹⁵⁹. The multiple peaks present for truxillines may suggest the presence of stereoisomers that are being resolved on the LC-MS column. Similarly, the unresolved multi-peak present for CC may indicate the presence of *-cis* and *-trans* cinnamoyl cocaine. The presence of these compounds was supported by MS/MS data (Figure 5-32). The peak shape of cocaine in particular was not ideal due to the large concentration of sample (1 mg/mL); however, a high

concentration of sample was required in order to detect the trace compounds present in the illicit sample (tropacocaine, caffeine, etc.) for profiling purposes.

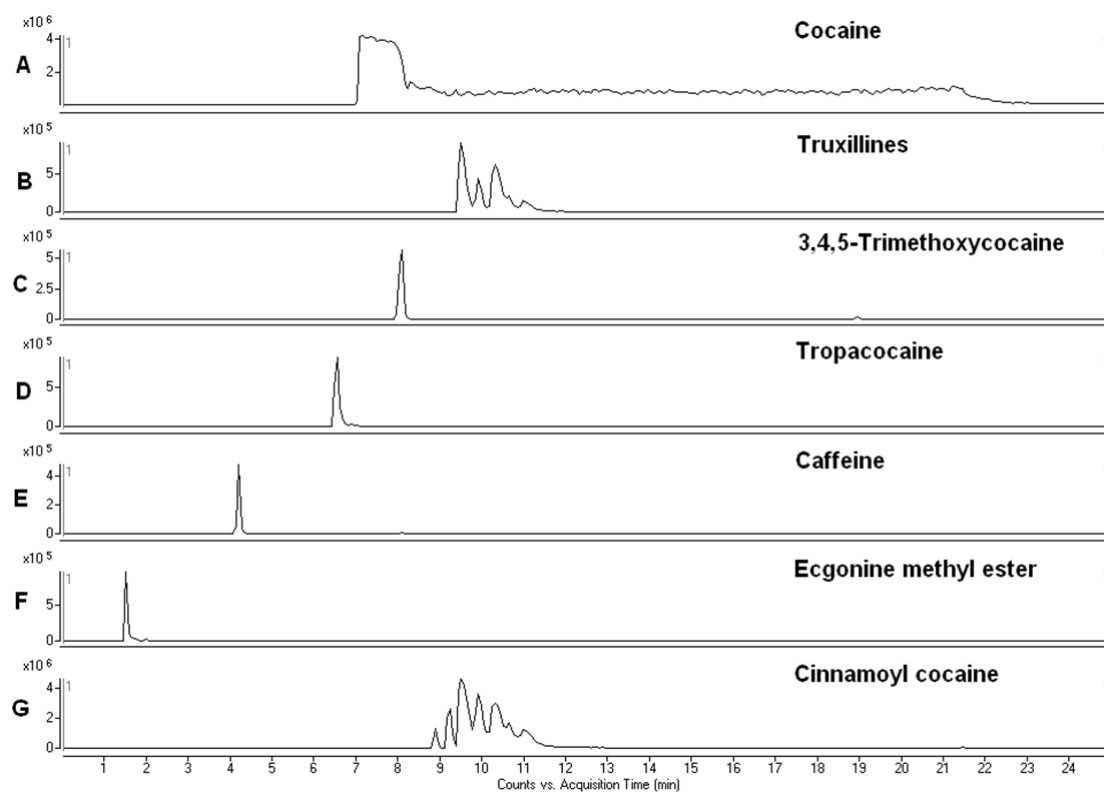


Figure 5-31 LC-MS chromatogram of cocaine Item 1; A: EIC of cocaine at 7.2 minutes, m/z 304; B: EIC of truxillines at 9.2 minutes, m/z 659; C: EIC of 3,4,5-trimethoxycocaine at 8.1 minutes, m/z 394; D: EIC of tropacocaine at 6.3 minutes, m/z 246; E: EIC of caffeine at 4.2 minutes, m/z 195; F: EIC of EME at 1.5 minutes, m/z 200; G: EIC of CC at 9.6 minutes, m/z 330.

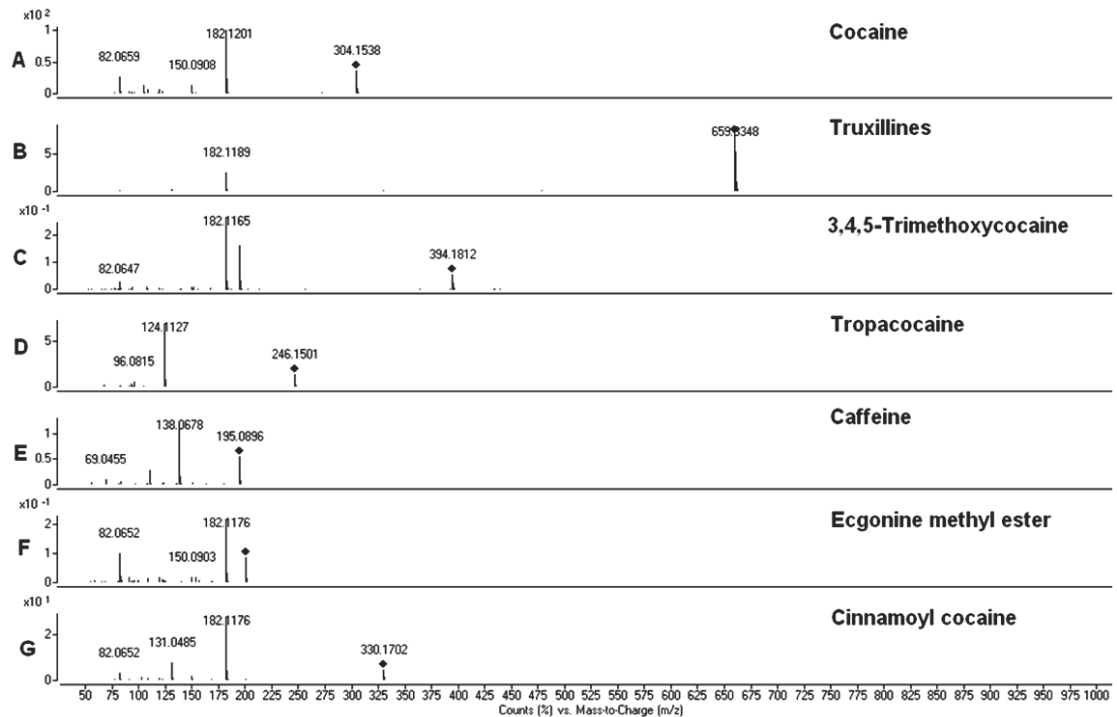


Figure 5-32 LC-MS/MS spectra of cocaine Item 1; A: cocaine, B: truxilline, C: 3,4,5-trimethoxycocaine, D: tropacocaine, E: caffeine, F: EME, G: CC at 20 eV.

The LC-MS results for cocaine Item 1/2 exhibits the same compounds as Item 1 above although cocaine Item 1/2 did not contain tropacocaine at m/z 246 (Figure 5-33 and Figure 5-34). The presence of all compounds were supported by MS/MS data and compared to reference spectra.

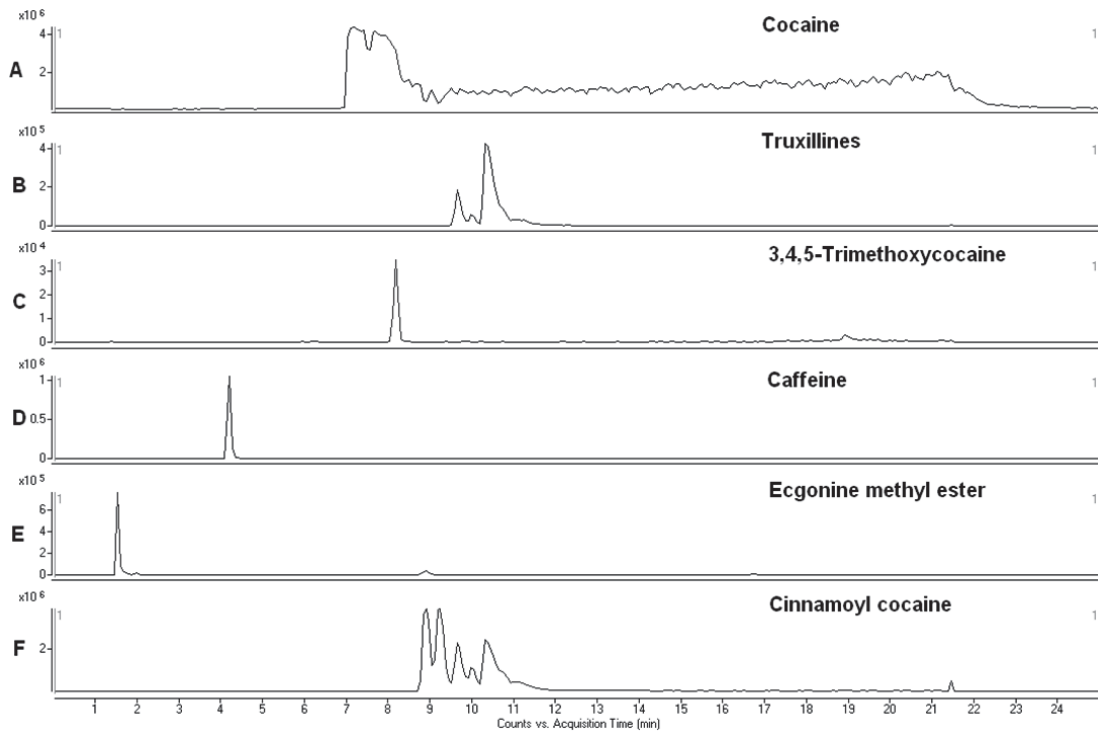


Figure 5-33 LC-MS chromatogram of cocaine Item 1/2; A: EIC of cocaine at 7.2 minutes, m/z 304; B: EIC of truxillines at 10.2 minutes, m/z 659; C: EIC of 3,4,5-trimethoxycocaine at 8.1 minutes, m/z 394; D: EIC of caffeine at 4.2 minutes, m/z 195; E: EIC of EME at 1.5 minutes, m/z 200; F: EIC of CC at 9.4 minutes, m/z 330.

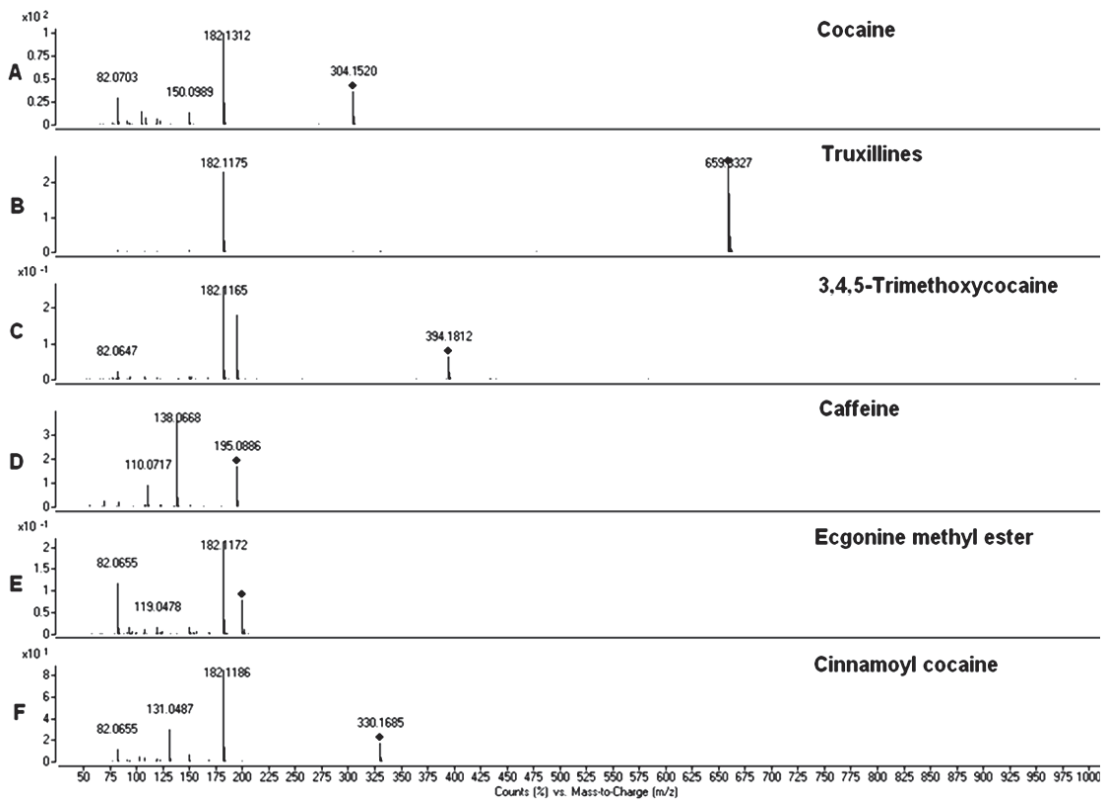


Figure 5-34 LC-MS/MS spectra of cocaine Item 1/2; A: cocaine, B: truxilline, C: 3,4,5-trimethoxycocaine, D: caffeine, E: EME, F: CC at 20 eV.

The LC-MS spectra obtained for cocaine Item 5/2 exhibits cocaine, truxillines, 3,4,5-trimethoxycocaine, levamisole, hydroxyzine, caffeine, EME and CC. The two additional adulterants levamisole (m/z 205 $[M+H]^+$) and hydroxyzine (m/z 375 $[M+H]^+$) are distinguishing compounds for this sample (Figure 5-35 and Figure 5-36). The presence of each compound was further supported by MS/MS data (Figure 5-10 - Figure 5-15).

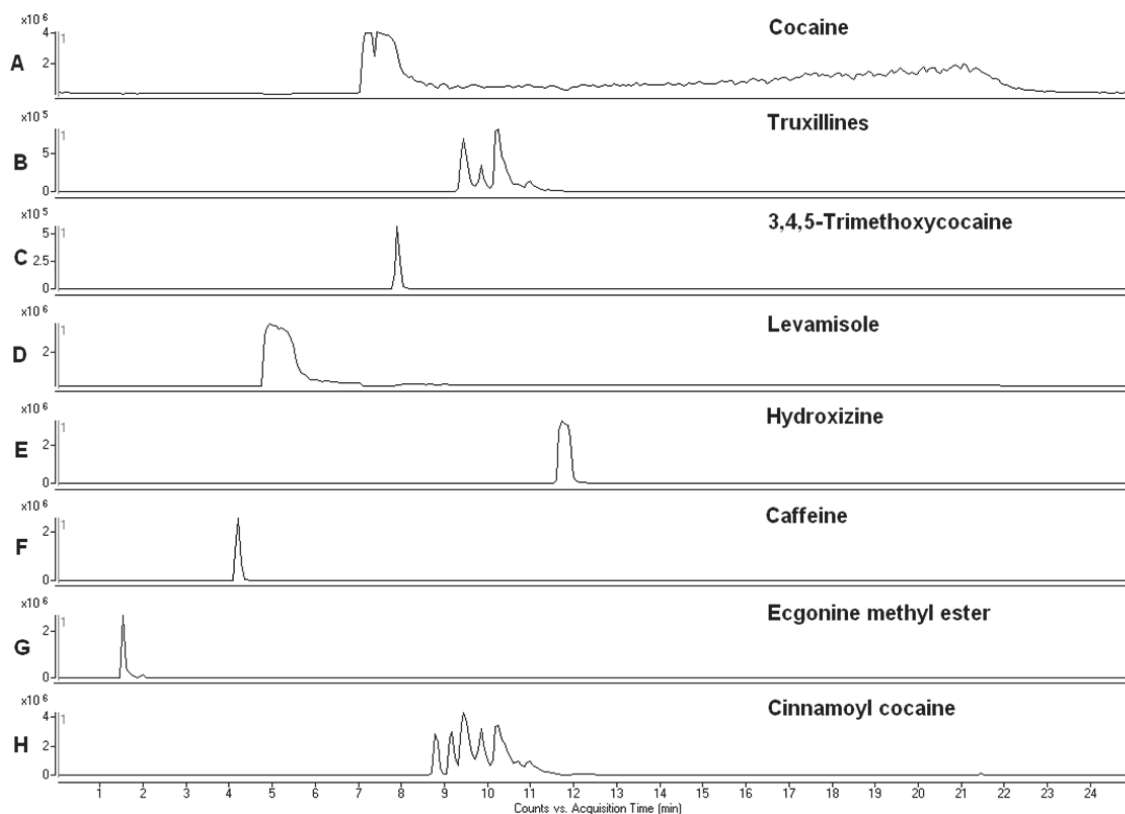


Figure 5-35 LC-MS chromatogram of cocaine Item 5/2; A: EIC of cocaine at 7.3 minutes, m/z 304; B: EIC of truxillines at 9.2 minutes, m/z 659; C: EIC of 3,4,5-trimethoxycocaine at 8.1 minutes, m/z 394; D: EIC of levamisole at 5.0 minutes, m/z 205; E: EIC of hydroxyzine at 12.1 minutes, m/z 375; F: EIC of caffeine at 4.2 minutes, m/z 195; G: EIC of EME at 1.5 minutes, m/z 200; H: EIC of CC at 9.6 minutes, m/z 330.

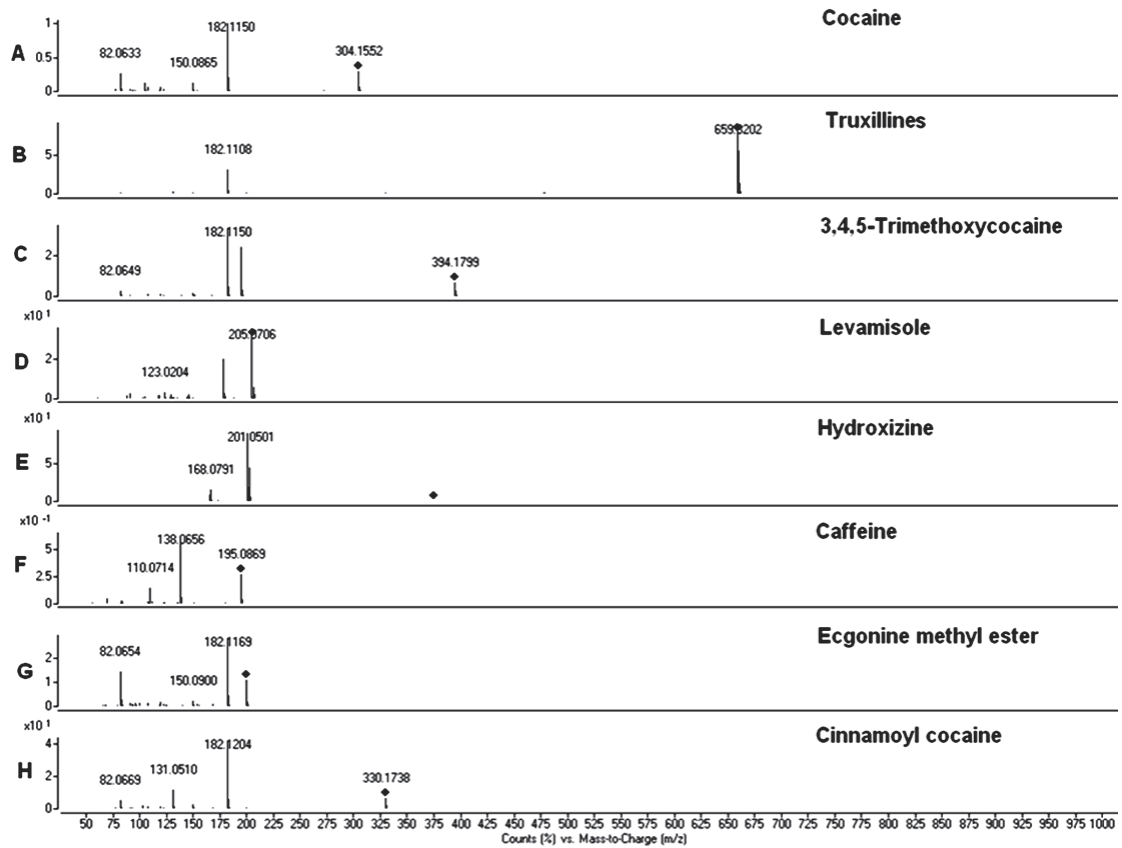


Figure 5-36 LC-MS/MS spectra of cocaine Item 5/2; A: cocaine, B: truxilline, C: 3,4,5-trimethoxycocaine, D: levamisole, E: hydroxyzine, F: caffeine, G: EME, H: CC at 20 eV.

A cocaine standard was analysed using LC-MS (Figure 5-37). This supported the presence of EME at m/z 200 as being a trace degradation product of cocaine. The absence of a peak at m/z 330 representative of CC suggests that this standard was prepared synthetically as opposed to naturally derived from the Coca plant.

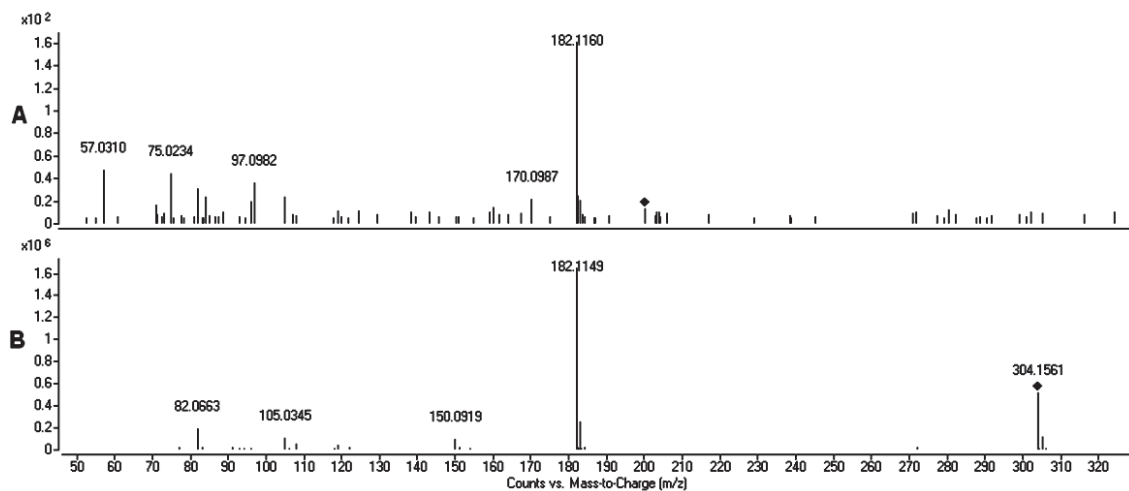


Figure 5-37 LC-MS/MS spectra of cocaine standard; A: EME at m/z 200, B: cocaine at m/z 304.

5.3.3 Mass accuracy

A MS/MS match score exceeding 60 was obtained for all compounds tested using PCDL software, with the exception of some compounds present in trace amounts where MS/MS data was poor. Compounds were further supported by MS/MS data in which all MS spectra were at best within 5 ppm and all MS/MS spectra were at best within 10 ppm (Table 5-2 and Table 5-3).

Table 5-2 Mass accuracy of cocaine and related compounds using positive ion mode.

Compound	Formula [M+H] ⁺	Accurate Mass [M+H] ⁺	Acquired Mass [M+H] ⁺	Mass Accuracy (ppm)
cocaine	C ₁₇ H ₂₂ NO ₄	304.1549	304.1552	1.0
truxilline	C ₃₈ H ₄₇ N ₂ O ₈	659.3332	659.3334	0.3
3,4,5-TMC ^a	C ₂₀ H ₂₈ NO ₇	394.1866	394.1829	-9.4
tropacocaine	C ₁₅ H ₂₀ NO ₂	246.1494	246.1496	0.8
caffeine	C ₈ H ₁₁ N ₄ O ₂	195.0882	195.0888	3.1
EME	C ₁₀ H ₁₈ NO ₃	200.1287	200.1288	0.5
CC	C ₁₉ H ₂₄ NO ₄	330.1705	330.1704	-0.3
hydroxyzine	C ₂₁ H ₂₈ ClN ₂ O ₂	375.1839	375.1876	9.9
levamisole	C ₁₁ H ₁₃ N ₂ S	205.0799	205.0787	-5.9

^a 3,4,5-TMC = 3,4,5-trimethoxycocaine, EME = ecgonine methyl ester, CC = cinnamoyl cocaine.

Table 5-3 Mass accuracy of MS/MS ions using positive ion mode at 20 eV.

Compound	Chemical Formula	Accurate Mass	Acquired Mass	Mass Accuracy (ppm)
cocaine	$C_{17}H_{22}NO_4 [M+H]^+$	304.1549	304.1554	1.6
	$C_{10}H_{16}NO_2$	182.1181	182.1188	3.8
	$C_9H_{12}NO$	150.0919	150.0921	1.3
	C_7H_5O	105.0340	105.0345	4.8
	C_5H_8N	82.0657	82.0656	-1.2
truxilline	$C_{38}H_{47}N_2O_8 [M+H]^+$	659.3332	659.3283	-7.4
	$C_{38}H_{45}N_2O_7$	641.3227	641.3197	-4.7
	$C_{28}H_{32}NO_5$	462.2280	462.2276	-0.9
	$C_{10}H_{16}NO_2$	182.1181	182.1163	-9.9
	$C_9H_{12}NO$	150.0919	150.0930	7.3
	C_5H_8N	82.0657	82.0664	8.5
EME	$C_{10}H_{18}NO_3 [M+H]^+$	200.1287	200.1279	-4.0
	$C_{10}H_{16}NO_2$	182.1181	182.1173	-4.4
	C_5H_8N	82.0657	82.0655	-2.4
CC	$C_{19}H_{24}NO_4 [M+H]^+$	330.1705	330.1676	-8.8
	$C_{10}H_{18}NO_3$	200.1287	200.1279	-4.0
	$C_{10}H_{16}NO_2$	182.1181	182.1171	-5.5
	$C_9H_{14}NO_2$	168.1025	168.1033	4.8
	C_9H_7O	131.0497	131.0501	3.1
	C_5H_8N	82.0657	82.0650	-8.5
hydroxyzine	$C_{21}H_{28}ClN_2O_2 [M+H]^+$	375.1839	375.1860	5.6
	$C_{13}H_{10}Cl$	201.0471	201.0477	3.0
	$C_9H_{11}ClN$	168.058	168.0572	-4.8
levamisole	$C_{10}H_{13}N_2S [M+H]^+$	205.0799	205.0780	-9.3
	$C_9H_{11}N_2S$	179.0643	167.0652	5.0

The compounds identified in the cocaine samples using DESI-MS, GC-MS and LC-MS have been summarised in Table 5-4.

Table 5-4 Compounds detected in cocaine samples using DESI-MS, GC-MS, and LC-MS.

Sample	Compound	Composition (%)	MW (Da)	DESI-MS	GC-MS	LC-MS
Item 1	cocaine	81.5	303	✓	✓	✓
	truxillines	1.47	658	✓	X	✓
	3,4,5-trimethoxycocaine	0.16	393	✓	✓	✓
	tropacocaine	0.07	245	✓ (trace)	✓	✓
	caffeine	NQ	194	✓ (trace)	✓	✓
	EME*	NQ	199	✓ (trace)	✓	✓
	CC*	NQ	329	✓	✓	✓
Item 1/2	cocaine	83.0	303	✓	✓	✓
	truxillines	0.35	658	✓	X	✓
	3,4,5-trimethoxycocaine	0.01	393	X	X	✓
	caffeine	NQ	194	✓ (trace)	✓	✓
	EME	NQ	199	✓ (trace)	✓	✓
	CC	NQ	329	✓	✓	✓
Item 5/2	cocaine	64.1	303	✓	✓	✓
	truxillines	6.17	658	✓	X	✓
	3,4,5-trimethoxycocaine	0.20	393	X	X	✓
	levamisole (as base)	15.11	204	✓	✓	✓
	hydroxyzine (as base)	2.30	374	✓	X	✓
	caffeine	NQ	194	✓ (trace)	✓	✓
	EME	NQ	199	✓ (trace)	✓	✓
	CC	NQ	329	✓	✓	✓

✓ = detected, X = not detected. Percentages shown above are obtained from the NMI analysis report.

* EME and CC were not listed on the AFP analysis report; however, these compounds were detected in the analysis using DESI-MS

Note: Where listed as being detected in "trace" amounts, MS/MS data was not obtained due to very low signal responses.

The collision induced dissociation of cocaine and related compounds in this chapter share some common fragmentation pathways. The ions at m/z 182 (i.e. $C_{10}H_{16}NO_2$) and m/z 82 (i.e. C_5H_8N) were consistent in the MS/MS spectra of a number of compounds including cocaine, truxillines, EME and CC. Some general rules that have been applied in the interpretation of the spectra include common product ions such as $[M+H-H_2O]^+$, and $[M+H-CH_3OH]^+$ ¹²⁵.

5.4 Conclusions

In all three cocaine samples, truxillines were detectable using DESI-MS and LC-MS (Table 4-4). Adulterants such as levamisole and hydroxyzine were detected using all three techniques in cocaine Item 5/2 with the exception of hydroxyzine in GC-MS analysis. The presence of truxillines in each sample indicated the geographical origin of the seized cocaine samples. The largest amount of truxilline found in cocaine item 5/2 was indicative of Colombian cocaine, while the lowest truxilline content was associated with Peruvian cocaine, i.e. Item 1/2, and a slightly higher level of truxilines was associated with Bolivian cocaine, i.e. Item 1.

Chapter 6: Analysis of piperazine analogues

Chapter 6: Analysis of piperazine analogues

6.1 Introduction

This chapter describes the application of the developed DESI-MS method to the chemical analysis of piperazine analogues. The LOD and effects of common adulterants on the detectability of piperazines is evaluated. The synthesised BZP, TFMPP, mCPP and MeOPP samples (section 2.2.2 - 2.2.5) were analysed using DESI-MS and the by-products/impurities were identified (confirming synthetic route of manufacture). The compounds detected using DESI-MS were also compared to those identified using GC-MS and LC-MS.

6.2 Materials and methods

The methods developed using DESI-MS, GC-MS and LC-MS in section 3.3.1 - 3.3.4 were applied to the analysis of piperazine analogues. The DESI-MS operating parameters were optimised with experiments run in full scan mode (m/z 50 - 500) and MS/MS experiments conducted in the targeted product ion scan mode with collision energy of 20 eV. DESI-MS samples were dissolved in methanol (10 mg/mL) unless otherwise specified. Two microlitres aliquots of solution were deposited onto the PTFE sample plate. Analyte identity was supported by MS/MS experiments. Data analysis was conducted using Agilent MassHunter Workstation software, Qualitative Analysis, Version B.03.01 (Agilent Technologies). GC-MS was conducted in full scan mode (m/z 50 - 500). GC-MS samples were dissolved in methanol (1 mg/mL), with an injection volume of 2 μ L in splitless mode. LC-MS was conducted in full scan mode (m/z 50 - 500) and MS/MS experiments were conducted in the product ion scan mode (auto MS/MS) with collision energy of 20 eV. LC-MS samples were dissolved in methanol (0.1 mg/mL), with an injection volume of 10 μ L. See section 2.2 for more method details.

The piperazine standards were adulterated with varying amounts of caffeine (i.e. 0 %, 20 %, 50 %, 90 %, 95 % w/w caffeine added, respectively) in order to evaluate the effects of this adulterant on the detectability of the compound of interest. Mixtures of piperazine compounds were also tested to evaluate the matrix effects resulting from mixed samples.

In DESI-MS analysis, the LOD was defined to be the lowest concentration required to give a signal equal or greater than the average intensity of the blank signal plus three times the SD of the blank⁹. In the GC-MS and LC-MS analysis, the LOD was defined to be the lowest peak concentration to exhibit a peak height three times the noise level (SNR 3:1). The ANOVA test was utilised as a means to determine whether the observed ion enhancement or suppression in adulteration experiments was significantly different to the unadulterated signal response (i.e. $p < 0.05$).

6.3 Results and discussion

6.3.1 Adulteration and LOD

6.3.1.1 1-Benzylpiperazine

1-Benzylpiperazine 2 was recrystallised from isopropanol and adulterated with various amounts of caffeine. Based on the data obtained, it was determined that the LOD for BZP using DESI-MS was 14.1 μg (equivalent to 2.00 $\mu\text{g}/\text{mm}^2$). The average signal response (peak height) of BZP at this concentration (with 0 % caffeine) was 11812 cps which was greater than the LOD determined from the solvent blank plus 3 x SD (i.e. average + 3SD = 3877 cps, m/z 100 - 200), allowing the analyte to be distinguished unambiguously amongst the background noise peaks. At 14.1 μg , the presence of 20 % to 95 % caffeine w/w did not affect the signal response significantly ($p > 0.05$, Figure 6-1). Despite the signal response of BZP 2 being relatively larger than the calculated solvent blank, this concentration was chosen as the LOD in order to avoid false negative results at concentrations close to the LOD in routine analyses. The presence of BZP in these samples was supported by MS/MS data¹⁶² (Figure 6-2); the proposed collision induced dissociation of the $[\text{M}+\text{H}]^+$ ion is illustrated in Figure 6-3.

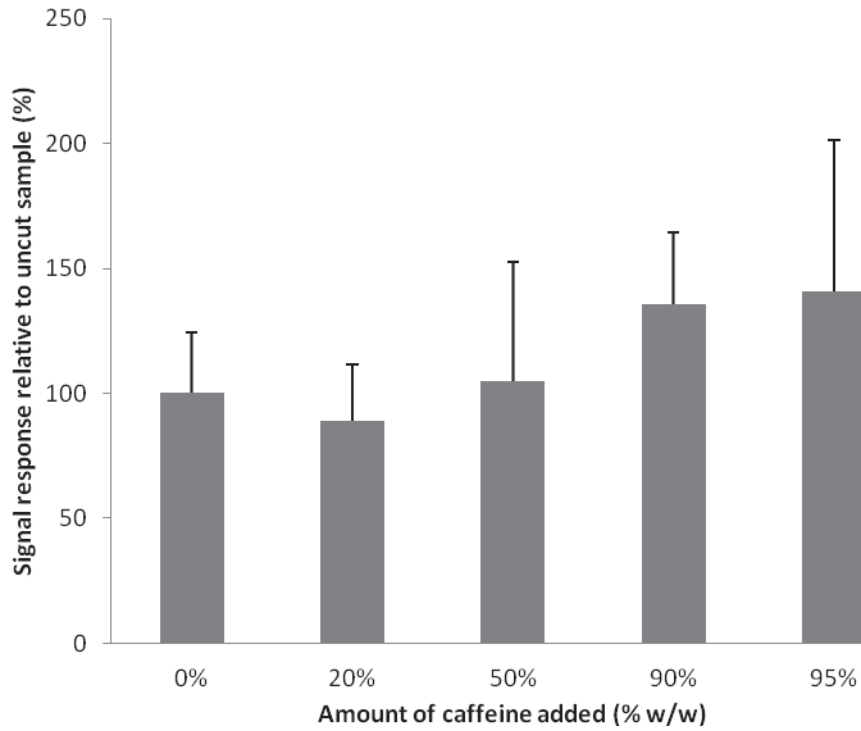


Figure 6-1 Adulterating BZP 2 with caffeine at varying amounts of caffeine added (0 %, 20 %, 50 %, 90 %, 95 % w/w), n=3, 2 μ L of 7050 μ g/mL, equivalent to 14.10 μ g BZP.

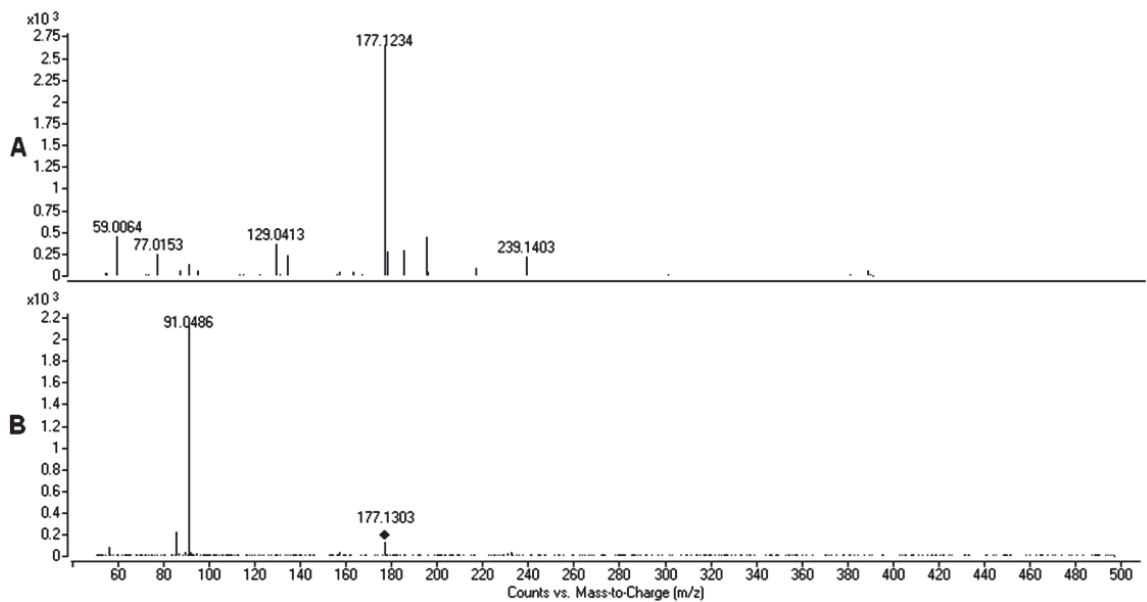


Figure 6-2 A: DESI-MS spectra of BZP 2; B: MS/MS spectra of BZP at 20 eV.

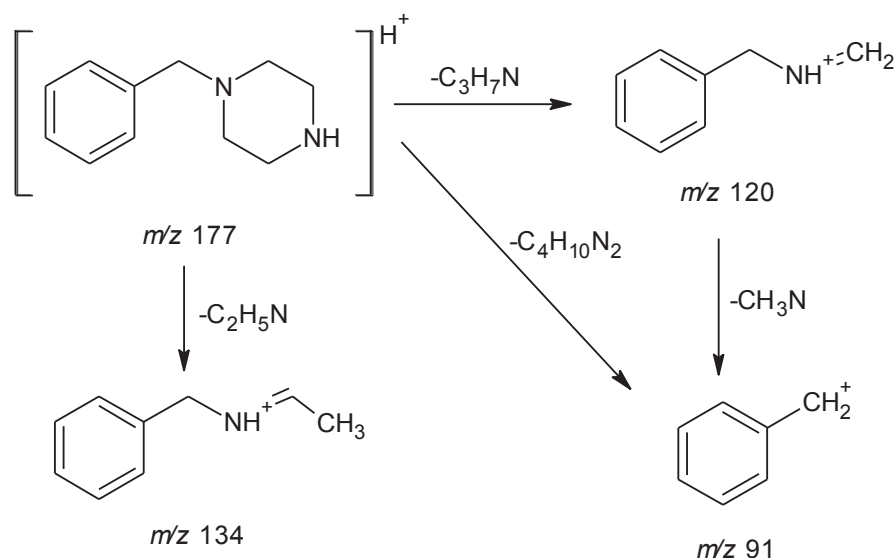


Figure 6-3 Proposed collision induced dissociation of the $[M+H]^+$ ion of BZP.

When repeating the experiment over three days using DESI-MS, it was found that the signal response and LOD determination were repeatable (Figure 6-4). The trend was generally observed to be consistent over the three days tested (Figure 6-4). The intra-day and inter-day precision (% RSD) for BZP at $2.00 \mu\text{g}/\text{mm}^2$ was found to be 24 % and 33 %, respectively, $n=3$ (Figure 6-1).

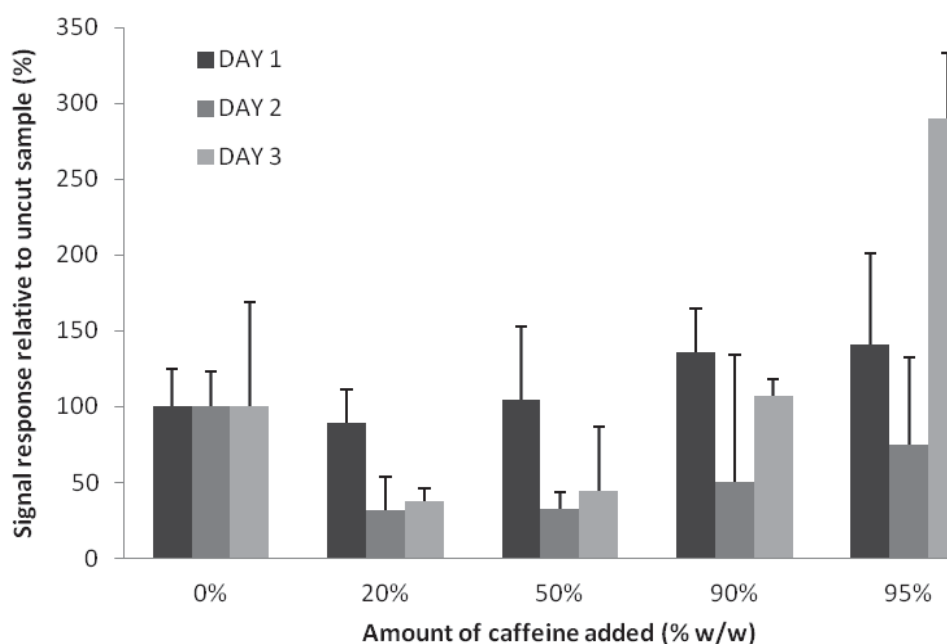


Figure 6-4 Inter-day study of BZP adulterated with caffeine (0 %, 20 %, 50 %, 90 %, 95 % w/w); $n=3$, ($2 \mu\text{L}$ of $7050 \mu\text{g}/\text{mL}$, equivalent to $14.10 \mu\text{g}$ BZP).

6.3.1.2 3-Trifluoromethylphenylpiperazine

A TFMPP standard was adulterated with various amounts of caffeine. Based on the data obtained, it was determined that the LOD for TFMPP using DESI-MS was 1.84 μg (equivalent to 0.26 $\mu\text{g}/\text{mm}^2$). The average signal response (peak height) of TFMPP at this concentration (with 0 % caffeine) was 10772 cps which was greater than the LOD determined from the solvent blank plus 3 x SD (i.e. average + 3SD = 2713 cps, m/z 150 - 250), allowing the analyte to be distinguished unambiguously amongst the background noise peaks. At 1.84 μg , 50 % to 95 % w/w caffeine added produced ion enhancement effects ($p < 0.05$, Figure 6-5). Despite the signal response of TFMPP being relatively larger than the calculated solvent blank, this concentration was chosen as the LOD in order to avoid false negative results at concentrations close to the LOD in routine analyses. The presence of TFMPP in these samples was supported by MS/MS data¹⁶² (Figure 6-6); the proposed collision induced dissociation of the $[\text{M}+\text{H}]^+$ ion is illustrated in Figure 6-7.

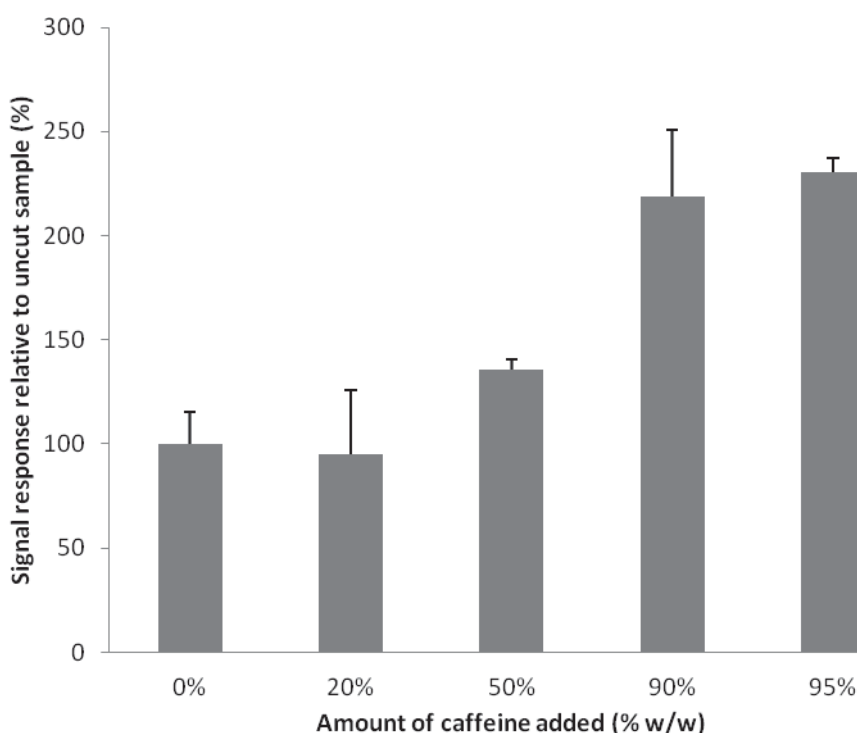


Figure 6-5 Adulterating TFMPP standard with caffeine at varying amounts of caffeine added (0 %, 20 %, 50 %, 90 %, 95 % w/w), $n=3$, 2 μL of 920 $\mu\text{g}/\text{mL}$, equivalent to 1.84 μg TFMPP.

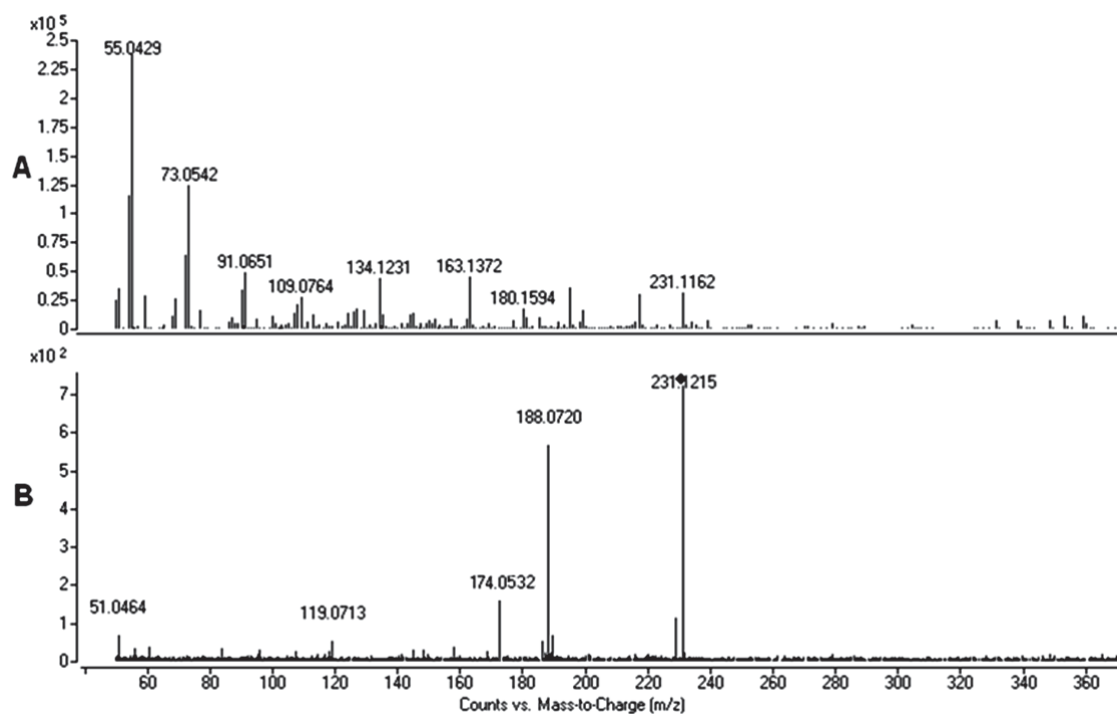


Figure 6-6 A: DESI-MS spectra of TFMP; B: MS/MS spectra of TFMP at 20 eV.

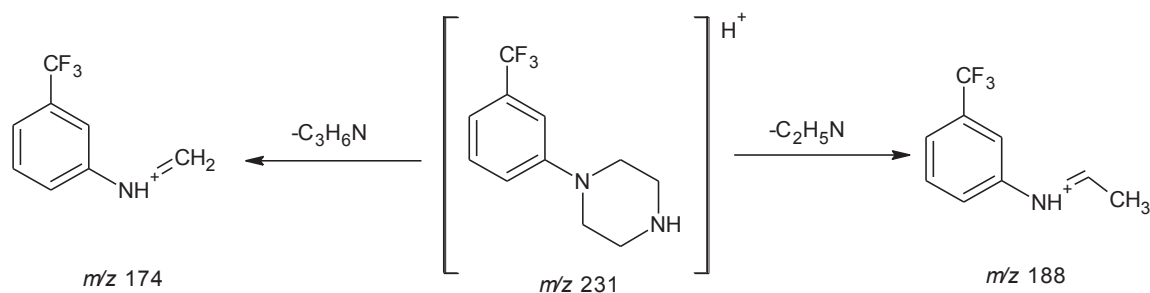


Figure 6-7 Proposed collision induced dissociation of the $[M+H]^+$ ion of TFMP.

6.3.1.3 3-Chlorophenylpiperazine

A mCPP standard was adulterated with various amounts of caffeine (Figure 6-8). Based on the data obtained, it was determined that the LOD for mCPP using DESI-MS was 16.0 μg (equivalent to 2.30 $\mu\text{g}/\text{mm}^2$). The average signal response (peak height) of mCPP at this concentration (with 0 % caffeine) was 4173 cps which was greater than the LOD determined from the solvent blank plus 3 x SD (i.e. average + 3SD = 2283 cps, m/z 150 - 250), allowing the

analyte to be distinguished unambiguously amongst the background noise peaks. At 16.0 μg , 95 % w/w caffeine added produced ion enhancement effects ($p < 0.05$). Despite the signal response of mCPP being slightly larger than the calculated solvent blank, this concentration was chosen as the LOD in order to prevent false negative results at concentrations close to the LOD in routine analyses. The presence of mCPP in these samples was supported by MS/MS data¹⁶² (Figure 6-9); the proposed collision induced dissociation of the $[\text{M}+\text{H}]^+$ ion is illustrated in Figure 6-10.

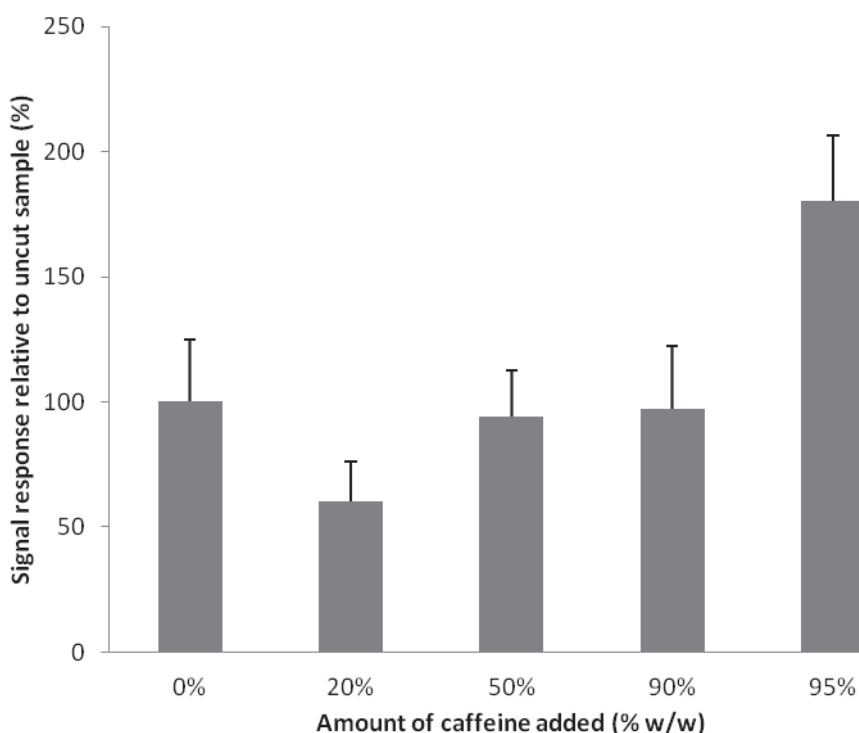


Figure 6-8 Adulterating mCPP standard with caffeine at varying amounts of caffeine added (0 %, 20 %, 50 %, 90 %, 95 % w/w), $n=3$, 2 μL of 8000 $\mu\text{g}/\text{mL}$, equivalent to 16.0 μg mCPP.

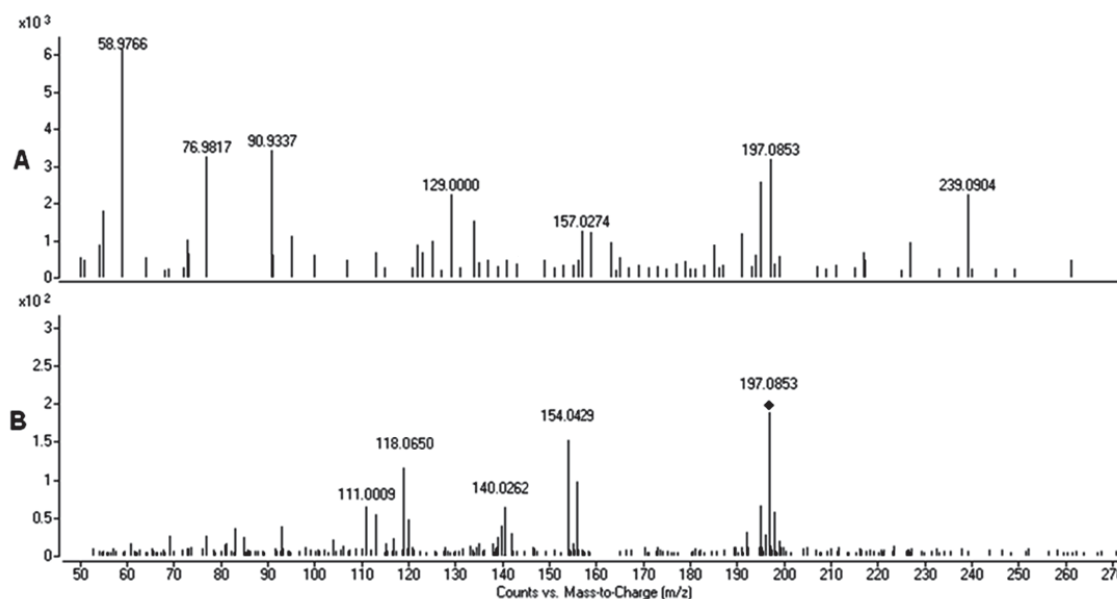


Figure 6-9 A: DESI-MS spectra of mCPP; B: MS/MS spectra of mCPP at 20 eV.

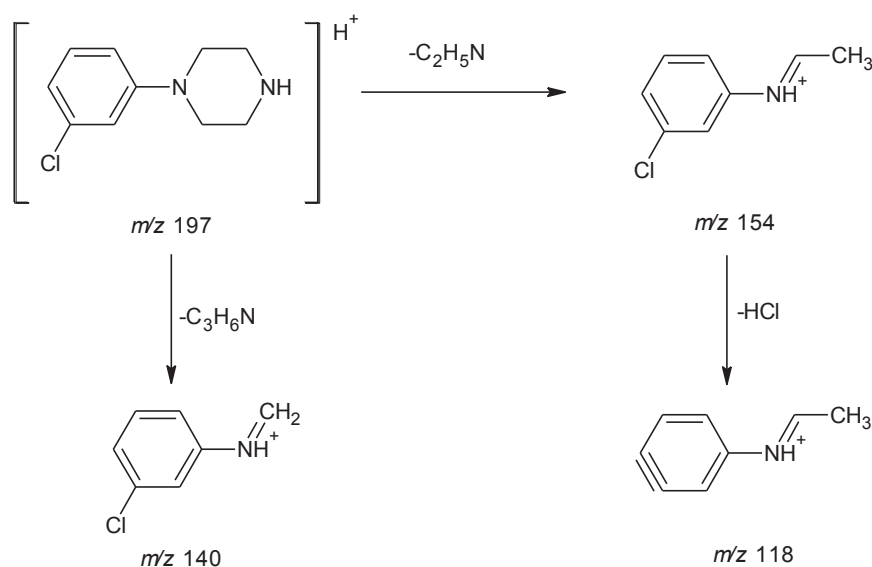


Figure 6-10 Proposed collision induced dissociation of the $[M+H]^+$ ion of mCPP.

6.3.1.4 4-Methoxyphenylpiperazine

4-Methoxyphenylpiperazine **1** was adulterated with various amounts of caffeine (Figure 6-11). Based on the data obtained, it was determined that the LOD for MeOPP using DESI-MS was 3.10 μg (equivalent to 0.44 $\mu\text{g}/\text{mm}^2$). The average signal response (peak height) of MeOPP at this concentration (with 0 % caffeine) was 7513 cps which was greater than the LOD determined from the solvent blank plus 3 x SD (i.e. average + 3SD = 4650 cps, m/z 100 -

200), allowing the analyte to be distinguished unambiguously amongst the background noise peaks. At 3.10 μg , the presence of 20 % to 95 % w/w caffeine did not have a significant effect on the MeOPP signal response ($p > 0.05$). Despite the signal response of MeOPP being slightly larger than the calculated solvent blank, this concentration was chosen as the LOD in order to prevent false negative results at concentrations close to the LOD in routine analyses. The presence of MeOPP in these samples was supported by MS/MS data¹⁶² (Figure 6-12); the collision induced dissociation of the $[\text{M}+\text{H}]^+$ ion is illustrated in Figure 6-13.

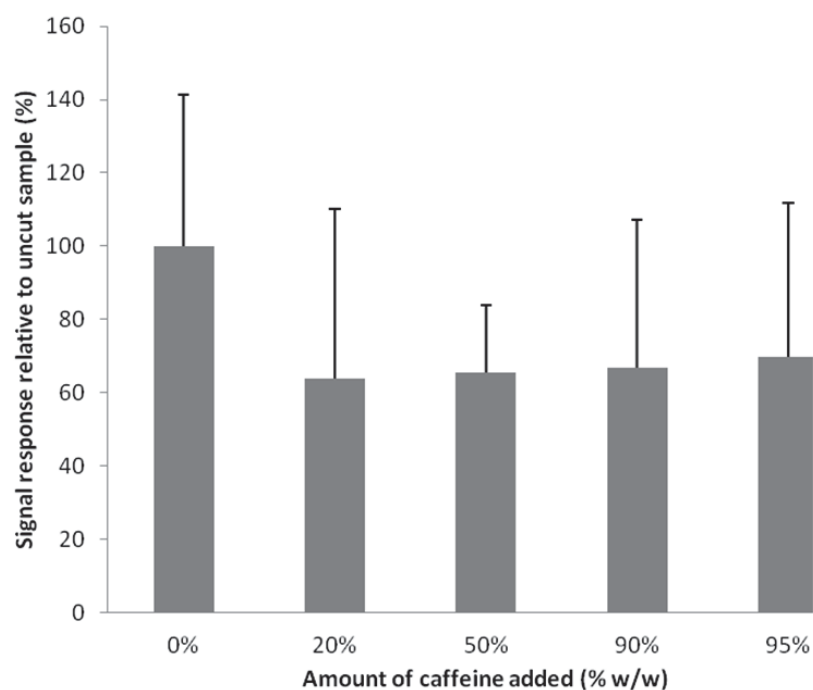


Figure 6-11 Adulterating MeOPP 1 with caffeine at varying amounts of caffeine added (0 %, 20 %, 50 %, 90 %, 95 % w/w), $n=3$, 2 μL of 1560 $\mu\text{g}/\text{mL}$, equivalent to 3.10 μg MeOPP.

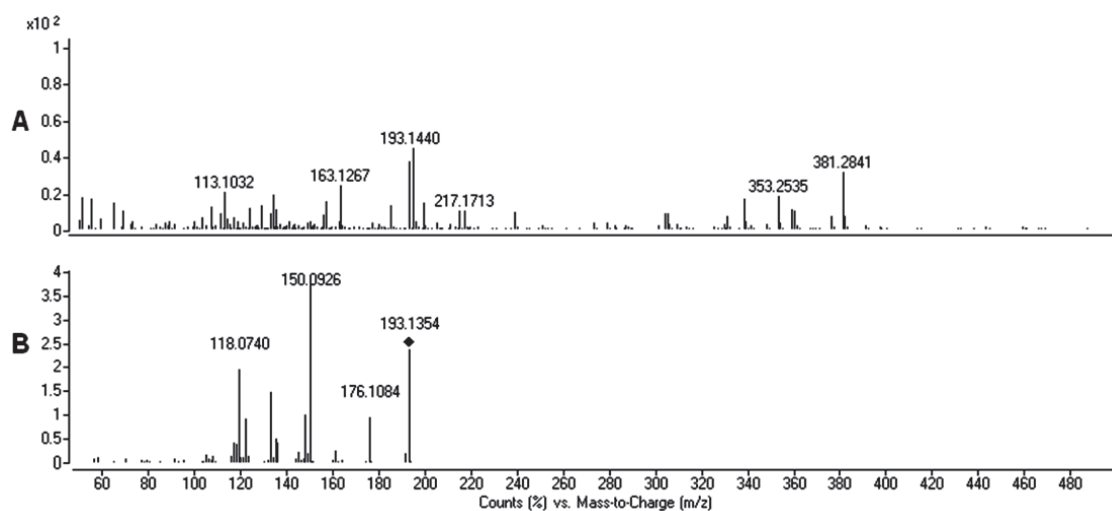


Figure 6-12 A: DESI-MS spectra of MeOPP 1; B: MS/MS spectra of MeOPP at 20 eV.

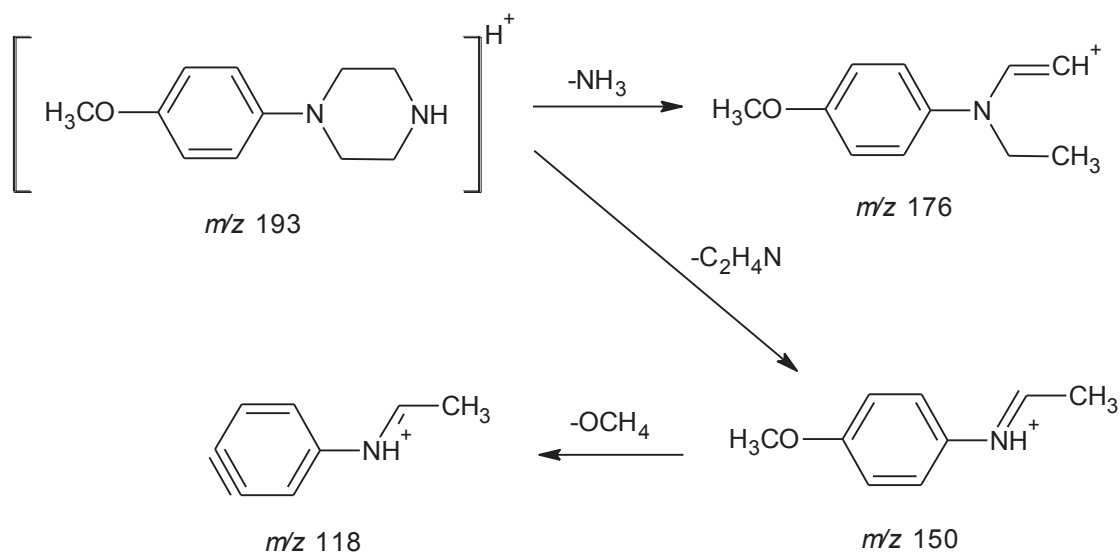


Figure 6-13 Proposed collision induced dissociation of the $[M+H]^+$ ion of MeOPP.

6.3.1.5 Piperazine mixtures

A mixture containing BZP 1 and TFMP 2 was analysed using DESI-MS with varying amounts of caffeine added (Figure 6-14). The large amount of ion suppression observed ($p < 0.05$) may be attributed to the presence of multiple by-products in the samples tested (also competing for ionisation in the DESI source). There are obvious limitations with analysing more than three of four compounds in a single mixture, mainly due to suppression effects as some analytes will be preferentially ionised over other. Caution should be taken when interpreting these results since the adulterated sample signal response (i.e. 50 % - 99 % caffeine) falls

below the determined LOD for BZP and TFMPP (14.1 and 1.84 μg , respectively). This demonstrates the increased matrix effects observed with an increase in the number of compounds per sample. This may indicate a potential for false negative results to occur in mixed samples and for this reason routine analysis of samples should be conducted using more concentrated sample. Alternatively, MS/MS may aid in increasing LOD of these compounds when present in mixtures.

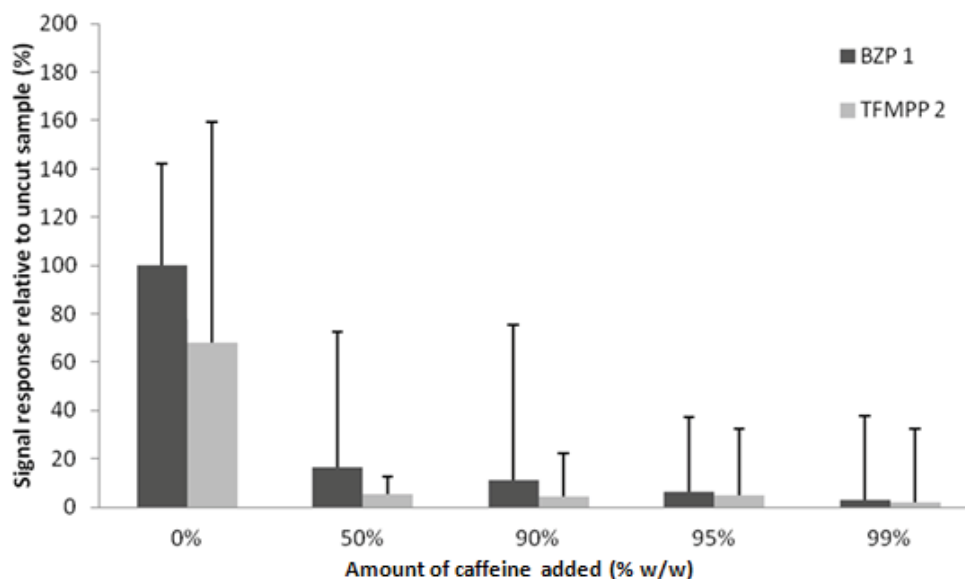


Figure 6-14 Adulterating a mixture of BZP 1 HCl and TFMPP 2 base (1:1) with varying amounts of caffeine, n=3.

The LOD determined for BZP, TFMPP, mCPP and MeOPP are presented in Table 6-1. In addition, the intra-day precision (n=3) of the technique for the analysis of piperazine analogues was found to be <25 % RSD.

Table 6-1 Limit of detection of piperazine analogues, n=3.

Sample	LOD ^a ($\mu\text{g}/\text{mm}^2$)
BZP	2.00
TFMPP	0.26
mCPP	2.30
MeOPP	0.44

^a sample well size 7 mm².

6.3.2 Analysis of 1-benzylpiperazine

6.3.2.1 Desorption electrospray ionisation – mass spectrometry

Benzylpiperazine 1 was synthesised according to the method detailed in section 2.2.2. The by-product of reaction was identified as DBZP via GC-MS and NMR (section 2.3.2). The product was analysed using DESI-MS in an attempt to identify the by-products present and link the by-product to the synthetic route of manufacture.

It was evident in the DESI-MS spectra below that the product BZP 1 was present at m/z 177 as the protonated molecular ion $[M+H]^+$ (Figure 6-15 A). In addition, another peak was present at m/z 267 corresponding to the by-product DBZP, also present as the protonated molecular ion. For further discrimination and confirmation of these products, MS/MS spectra of the two compounds were taken (Figure 6-16) and both exhibit characteristic fragmentation patterns corresponding to BZP and DBZP respectively (Figure 6-3 and Figure 6-17, Figure 6-18).

In addition, another two samples (i.e. BZP 2 and BZP 3), which were synthesised in order to alter the amount of by-product, were also analysed using DESI-MS. BZP 2 contained the smallest amount of DBZP and BZP 3 contained a larger amount of DBZP relative to BZP (Figure 6-15 B). The peak response for DBZP is comparable in all three samples, despite there being a higher concentration of DBZP in BZP 3 (Figure 6-15 C). The responses observed may be due to ion suppression as a result of matrix effects.

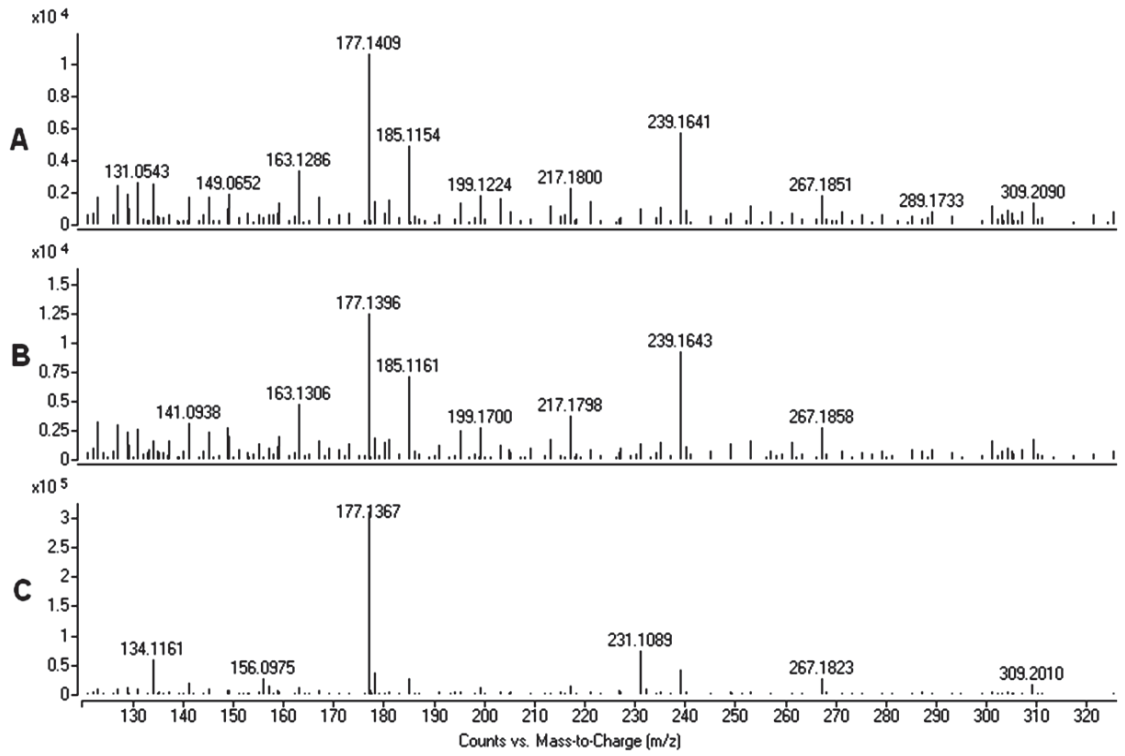


Figure 6-15 DESI-MS spectra of A: BZP 1, B: BZP 2, C: BZP 3.

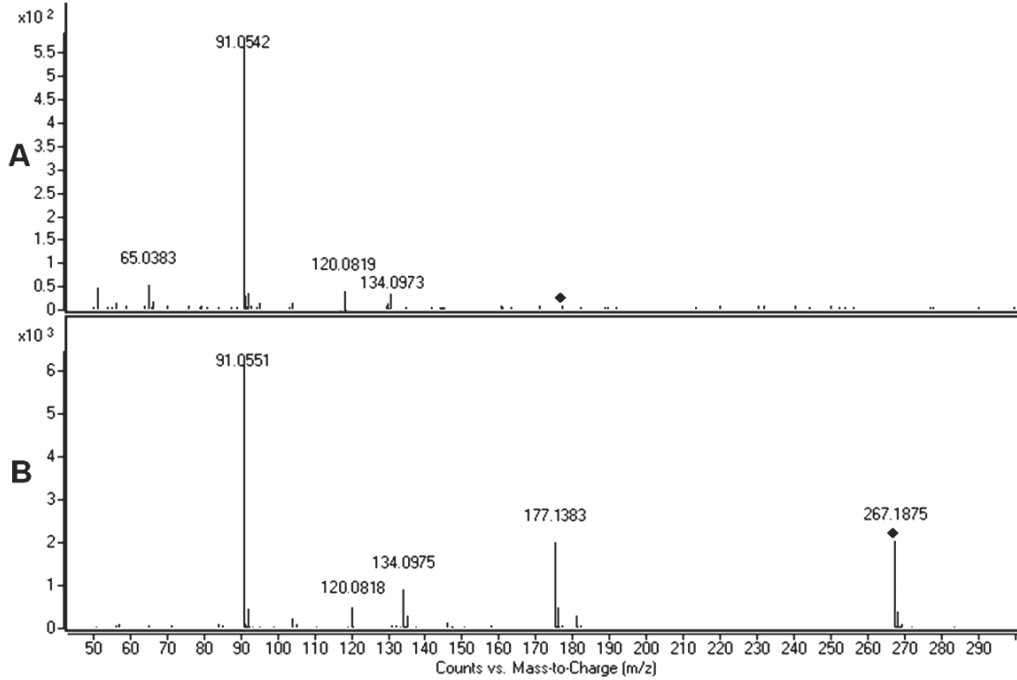


Figure 6-16 DESI-MS/MS of A: BZP 1 and B: DBZP.

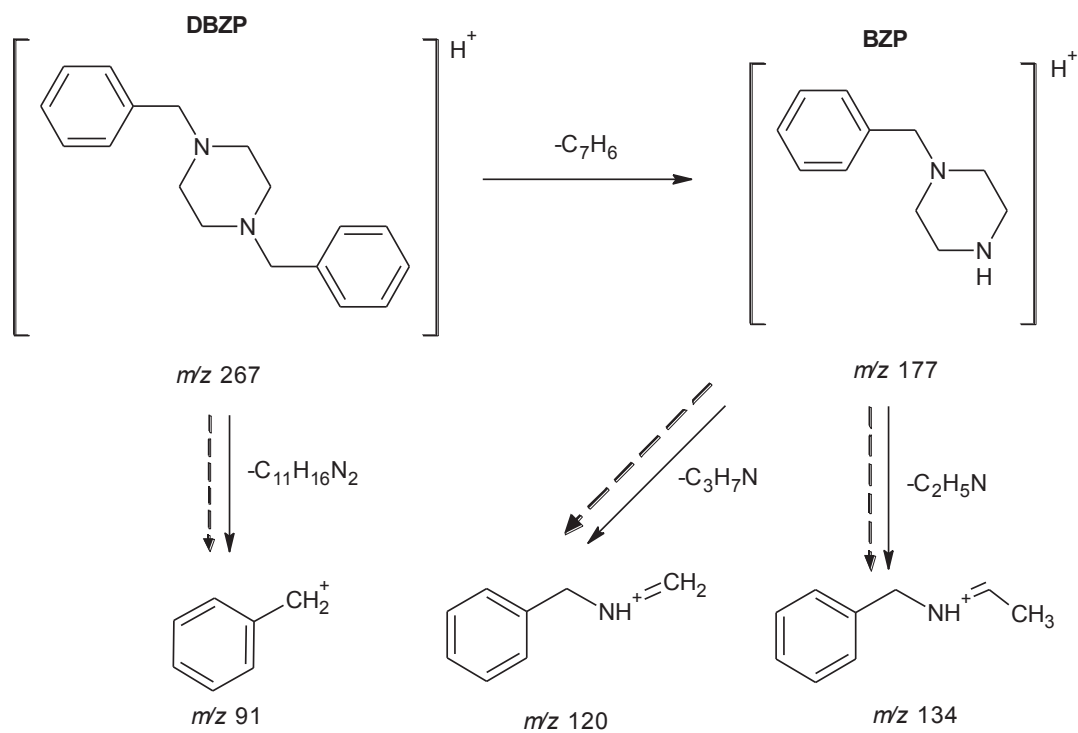


Figure 6-17 Proposed collision induced dissociation of the $[M+H]^+$ ion of BZP (---) and DBZP (→).

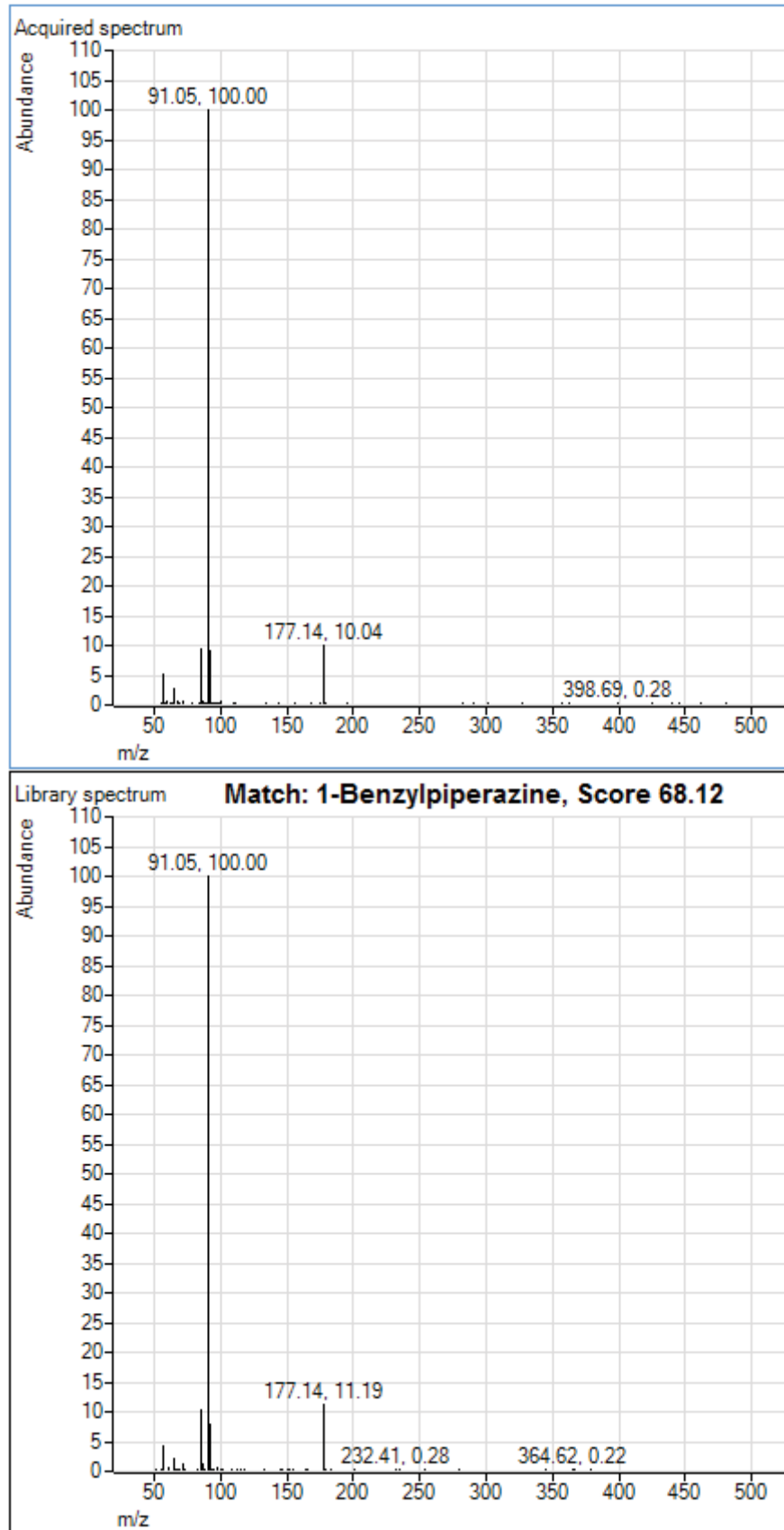


Figure 6-18 PCDL library match to BZP.

Benzylpiperazine 4 was synthesised via a different reaction pathway (section 2.2.2). The product BZP was detected at m/z 177 and further supported by MS/MS as before. DBZP was detected in trace amounts as well as benzyl chloride (Figure 6-19). The intermediate for this synthesis was also detected at m/z 249 and further supported by MS/MS as being EBCP (Figure 6-19 E). In addition, another by-product was found at m/z 235 and was thought to be MBCP, based on similar MS/MS spectra to EBCP. This by-product was hypothesised to have originated due to the transesterification reaction between EBCP and the solvent methanol in the synthesis, resulting in MBCP¹¹¹ (Figure 6-19). The proposed collision induced dissociation of the $[M+H]^+$ ions for MBCP and EBCP are shown in Figure 6-20.

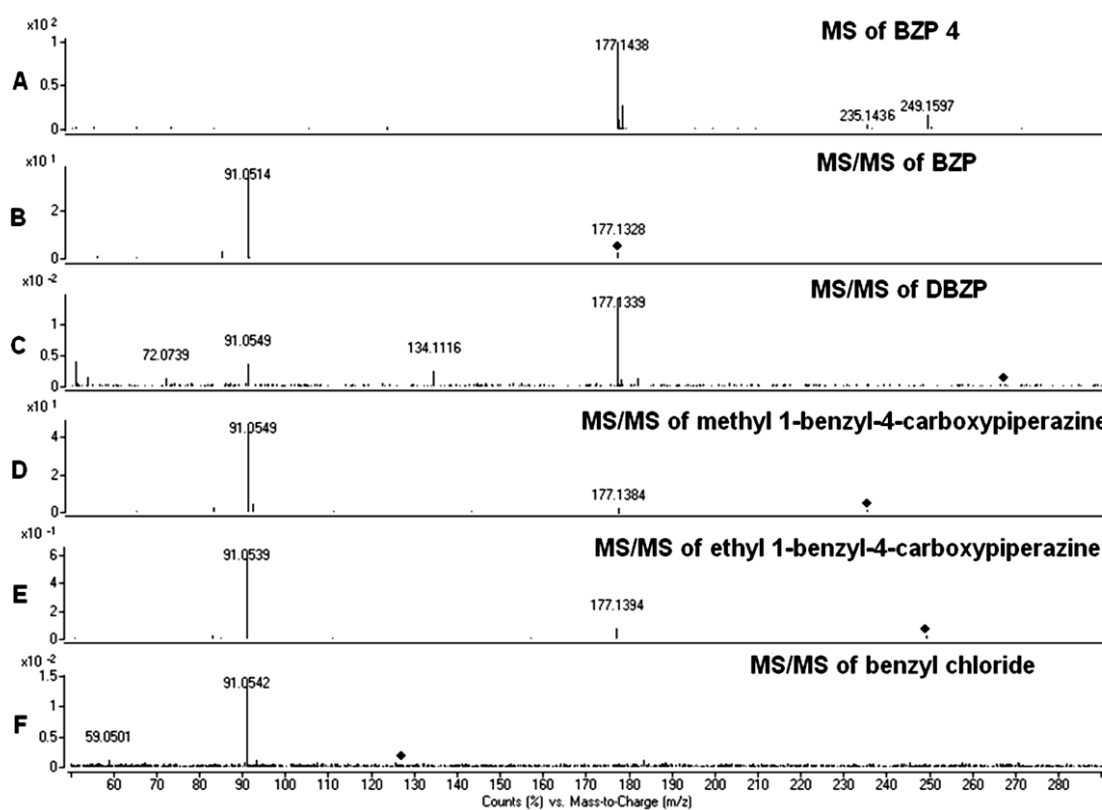


Figure 6-19 DESI-MS spectra of A: BZP 4, B: MS/MS of BZP, C: MS/MS of DBZP, D: MS/MS of MBCP, E: MS/MS of MS/MS of EBCP, F: MS/MS of benzyl chloride.

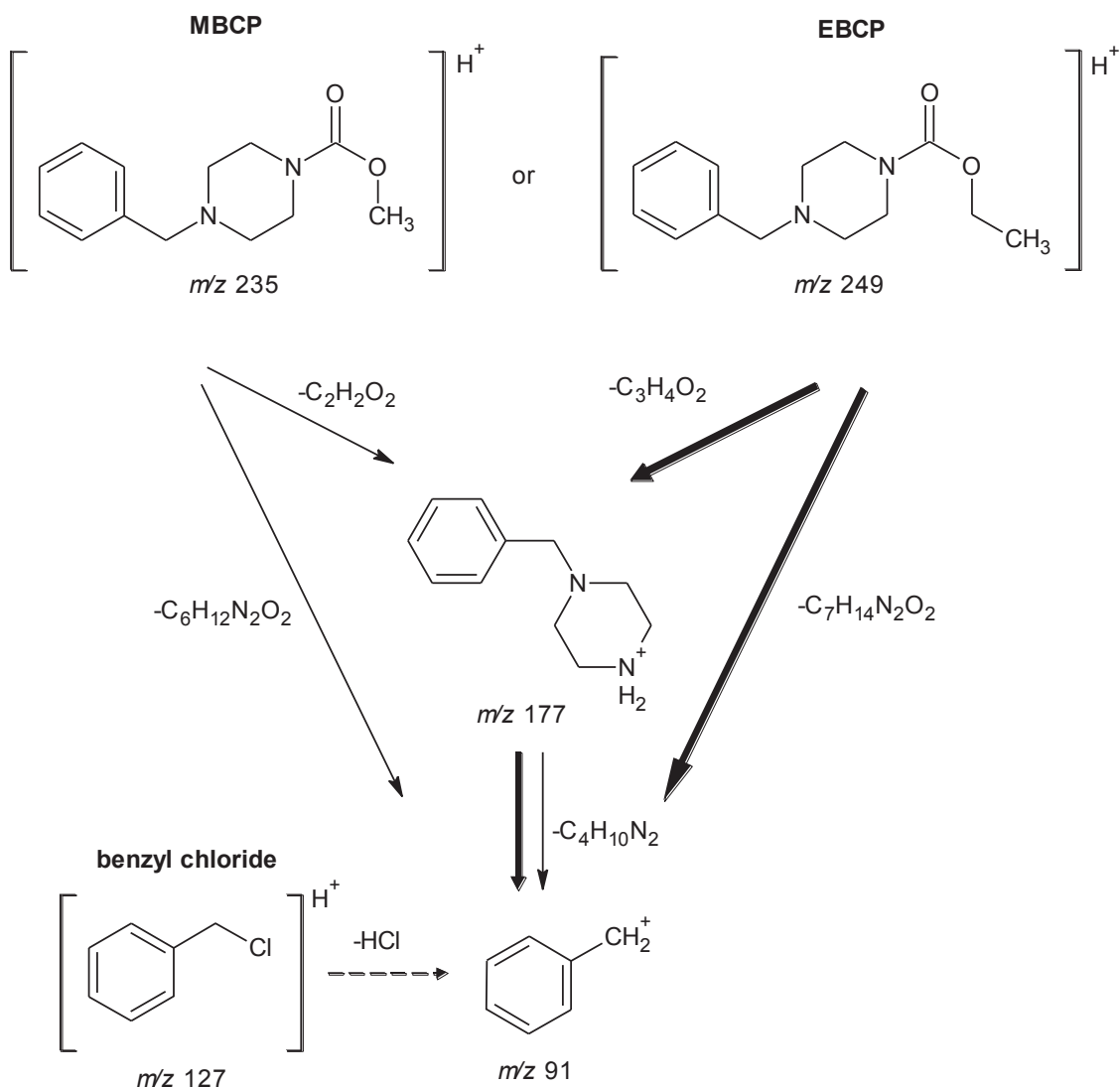


Figure 6-20 Proposed collision induced dissociation of the $[M+H]^+$ ion of MBCP (by-product, \rightarrow), EBCP (intermediate, \Rightarrow) and benzyl chloride ($--\rightarrow$).

6.3.2.2 Gas chromatography – mass spectrometry

The GC-MS data obtained for BZP 1.HCl, BZP 2.HCl, and BZP 3.HCl display three samples that contain different amounts of BZP and the by-product, DBZP. BZP 1 exhibited a 1:8 ratio of DBZP: BZP (as determined by NMR) and this was evident in the GC-MS chromatogram (Figure 6-21 - Figure 6-23, Figure 2-21). BZP 2 contains a lower amount of DBZP evident in Figure 6-24. The synthesis of BZP 3.HCl was conducted in an attempt to maximise DBZP formation and this was evident in the spectra obtained (Figure 6-25). In the synthesis of BZP 4 via the EBCP intermediate, the product and the unreacted intermediate were both detected by GC-MS as well as DBZP and MBCP (Figure 6-26, Figure 2-21, Figure 2-29, Figure 2-30).

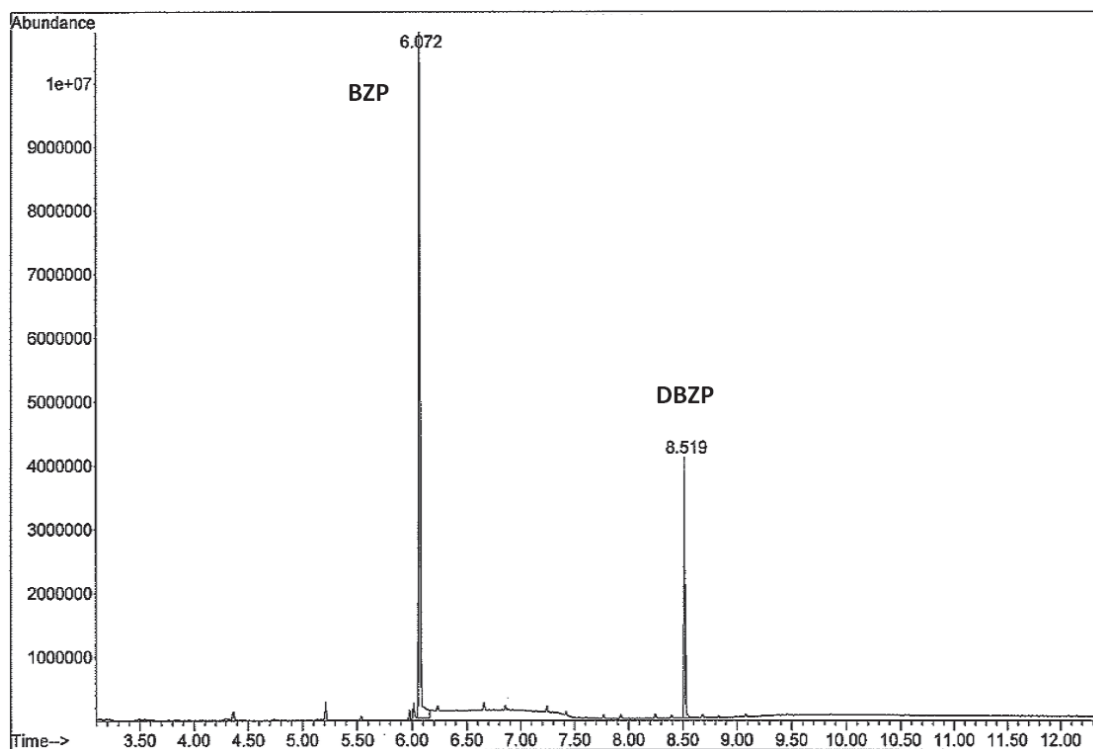


Figure 6-21 GC-MS chromatogram of BZP 1.HCl at 6.1 minutes, DBZP at 8.5 minutes (GC method 2).

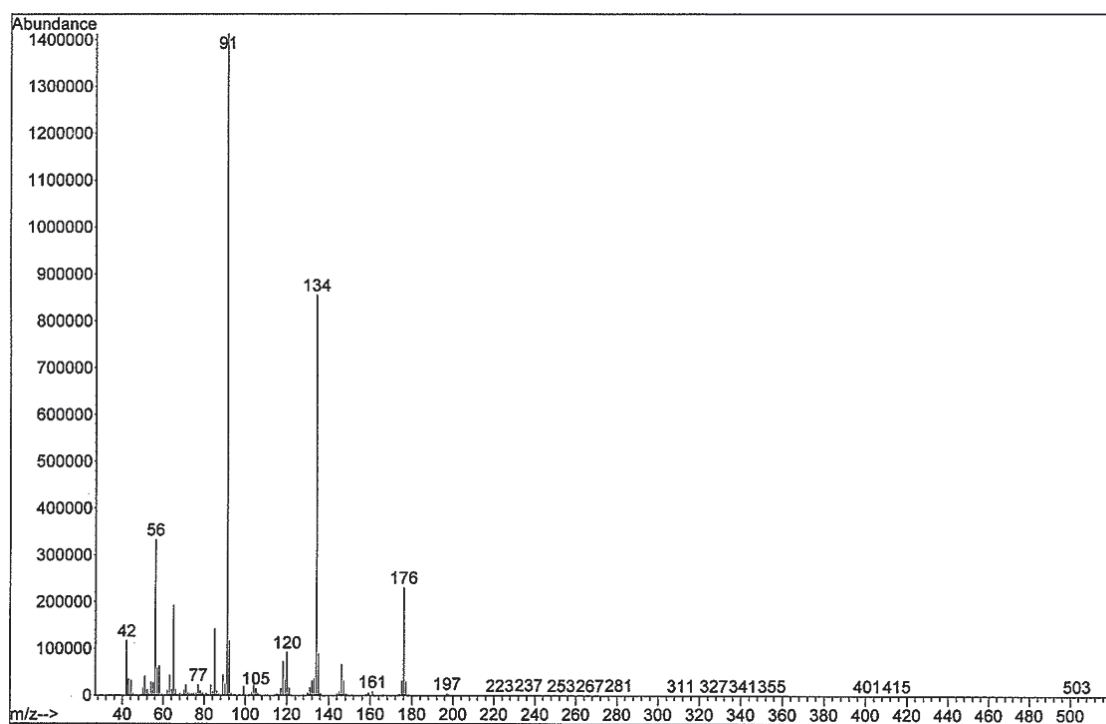


Figure 6-22 EI mass spectra of BZP 1.HCl (GC method 2).

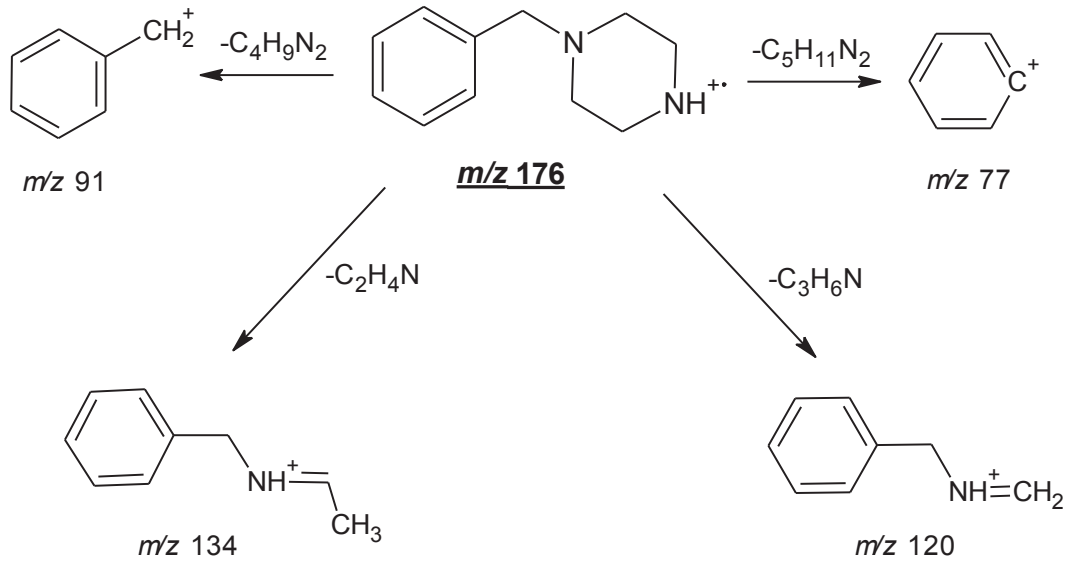


Figure 6-23 Proposed EI fragmentation pathway for BZP.

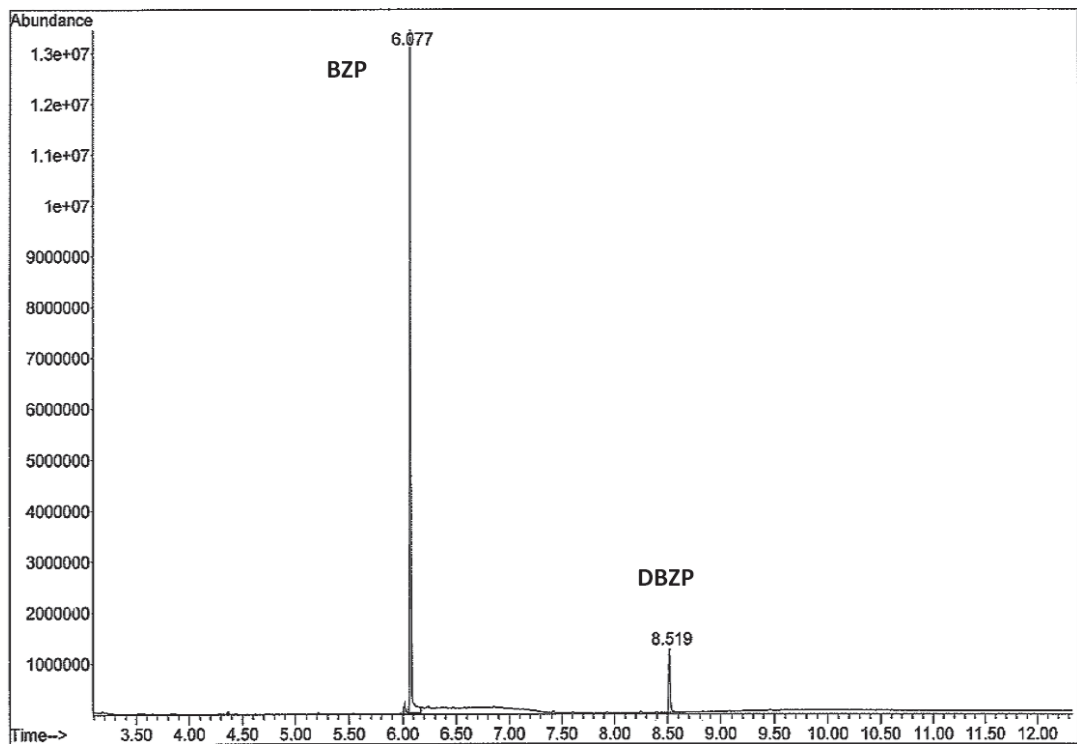


Figure 6-24 GC-MS chromatogram of BZP 2.HCl at 6.1 minutes, DBZP at 8.5 minutes (GC method 2).

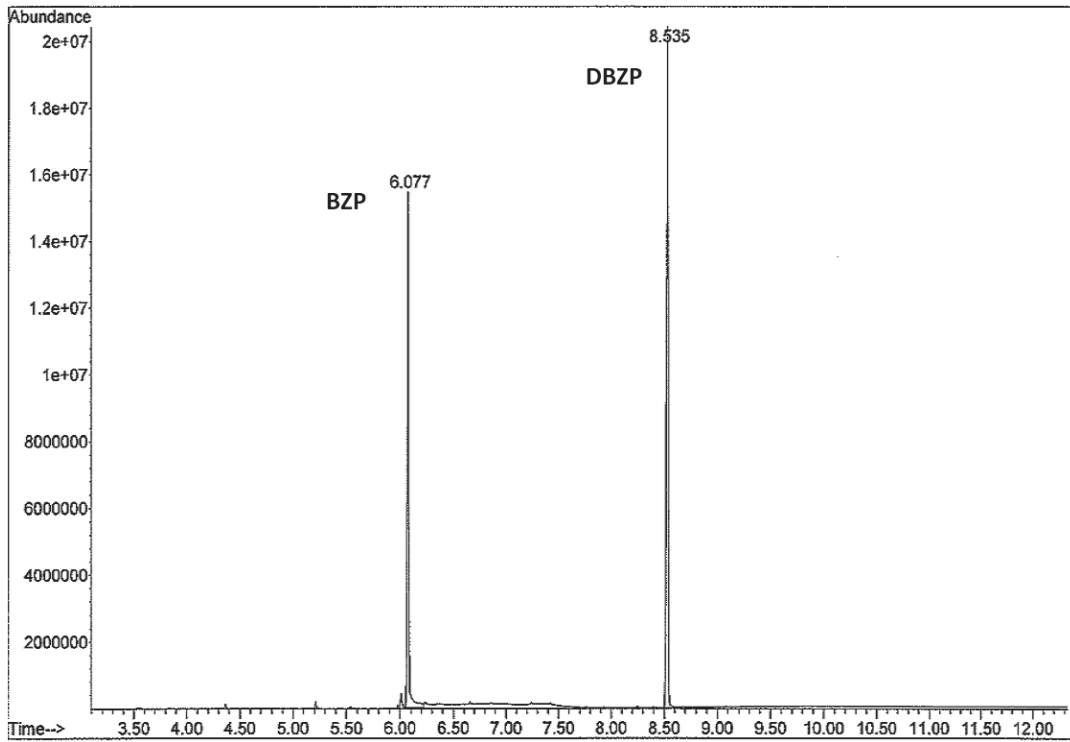


Figure 6-25 GC-MS chromatogram of BZP 3.HCl at 6.1 minutes, DBZP at 8.5 minutes (GC method 2).

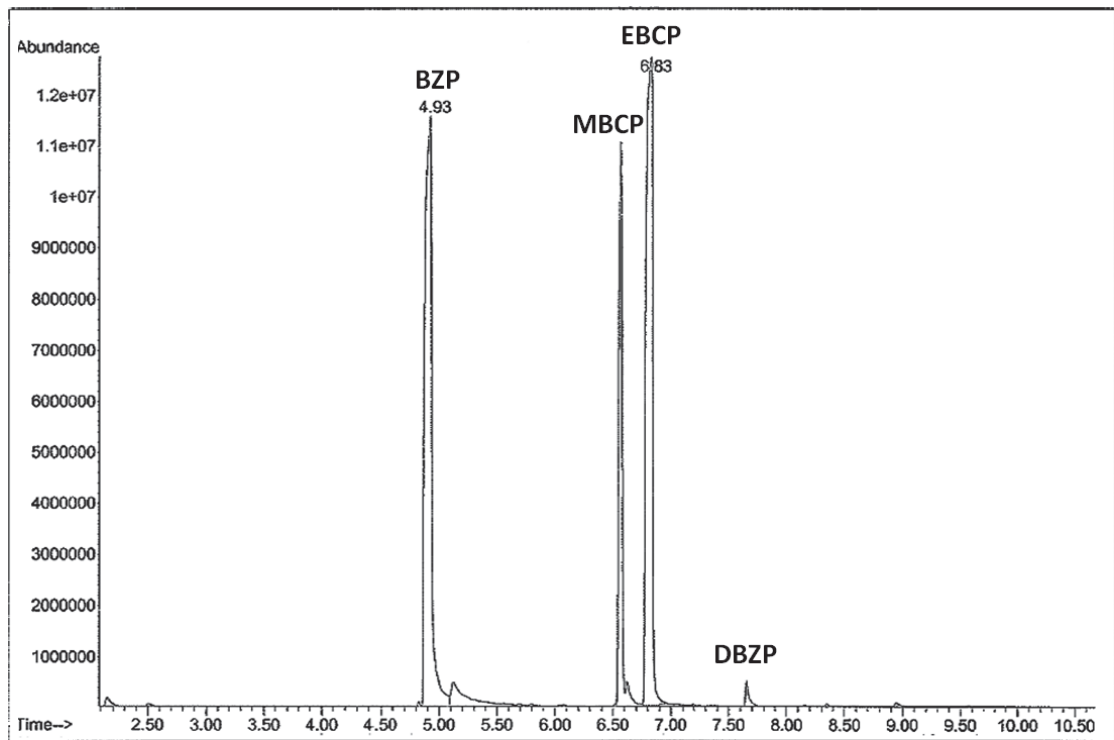


Figure 6-26 GC-MS chromatogram of BZP 4.HCl at 5.0 minutes, MDCP at 6.6 minutes, EBCP, 6.8 minutes, DBZP at 7.7 minutes (GC method 1).

6.3.2.3 Liquid chromatography – mass spectrometry

The LC-MS results obtained for the three BZP.HCl samples (BZP 1 – BZP 3) exhibit the same trend as the aforementioned GC-MS results. It was evident that all three BZP samples contain the impurity DBZP (Figure 6-27 to Figure 6-30). BZP 2 exhibits a smaller peak for DBZP as compared to BZP 1 which follows the trend observed in the GC-MS chromatogram. BZP 3 exhibits mostly DBZP and a minor amount of BZP product which was also the expected result (Figure 6-29 and Figure 6-30). Based on the detection of these by-products we can conclude that the substitution reaction (section 2.2.2: synthesis of BZP 1 – BZP 3) was the method utilised since DBZP was related to the disubstitution of the starting materials used in this reaction, i.e. benzyl chloride and piperazine.

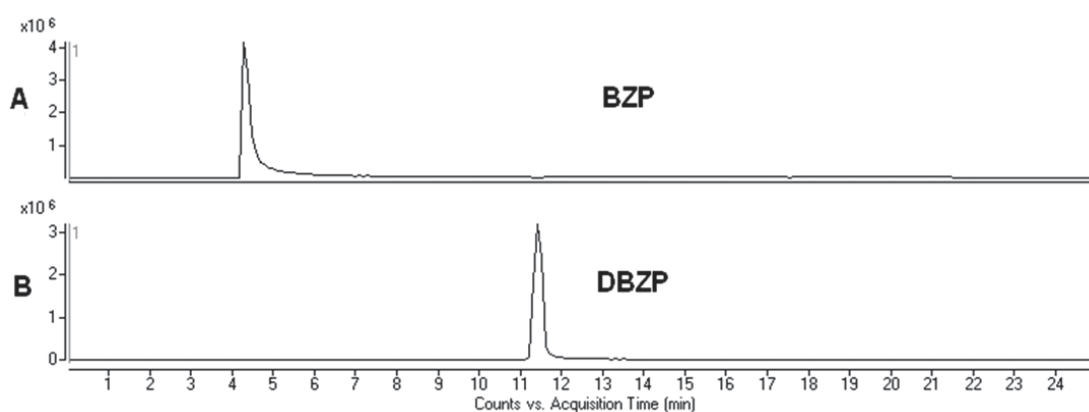


Figure 6-27 LC-MS chromatogram of BZP 1.HCl; A: EIC of BZP at 4.3 minutes, m/z 177; B: EIC of DBZP at 11.3 minutes, m/z 267.

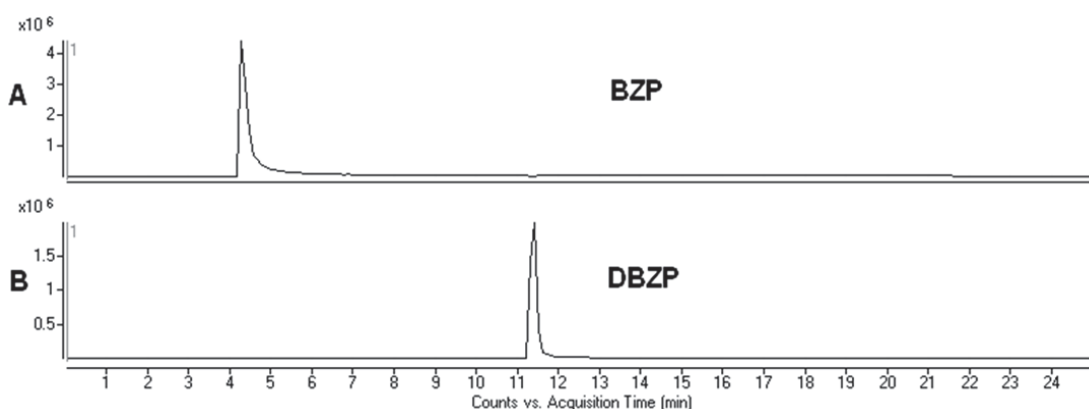


Figure 6-28 LC-MS chromatogram of BZP 2.HCl; A: EIC of BZP at 4.3 minutes, m/z 177; B: EIC of DBZP at 11.3 minutes, m/z 267.

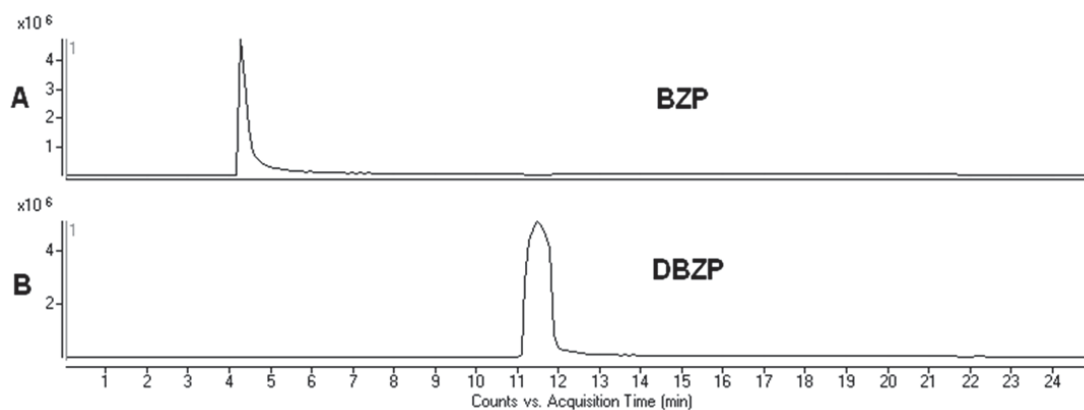


Figure 6-29 LC-MS chromatogram of BZP 3.HCl; A: EIC of BZP at 4.3 minutes, m/z 177; B: EIC of DBZP at 11.3 minutes, m/z 267.

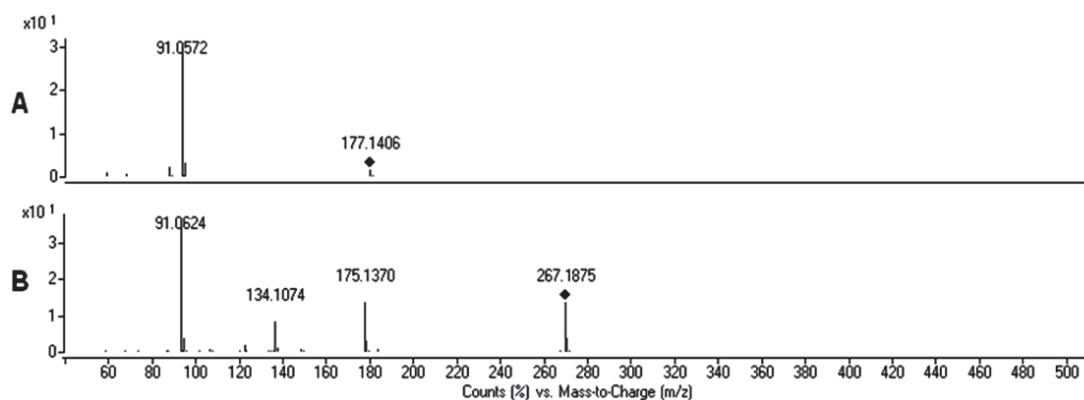


Figure 6-30 LC-MS/MS spectra of A: BZP, B: DBZP.

The LC-MS analysis of BZP 4 resulted in the detection of BZP, MBCP, EBCP and also DBZP (Figure 6-31 and Figure 6-32). The unreacted starting material benzyl chloride remained undetectable using LC-MS. Its detection using DESI-MS may be explained due to some enhancement matrix effects resulting in a larger signal than expected, allowing for its identification using DESI-MS. Co-eluting peaks may have also hindered the detection of benzyl chloride in this sample using LC-MS. The presence of EBCP and MBCP suggest a different synthetic method was utilised as compared to BZP 1 – BZP 3. The presence of these intermediates confirm that ethyl 1-piperazinecarboxylate was the precursor to this synthesis.

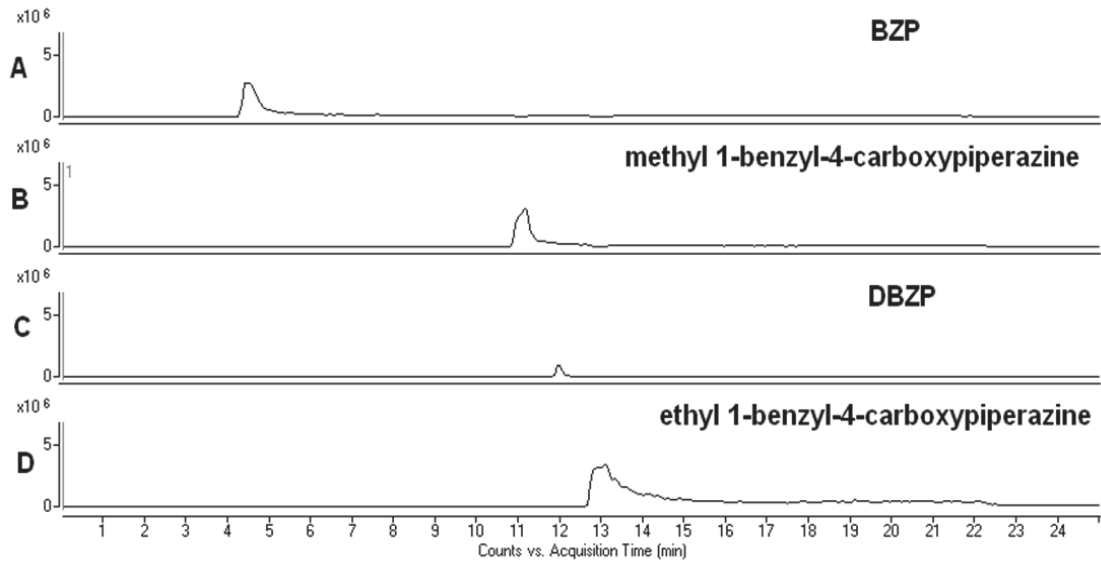


Figure 6-31 LC-MS chromatogram of BZP 4.HCl A: EIC of BZP at 4.3 minutes, m/z 177; B: EIC of MBCP at 11.1 minutes, m/z 235; C: EIC of DBZP at 11.8 minutes, m/z 267; D: EIC of EBCP at 13.0 minutes, m/z 249.

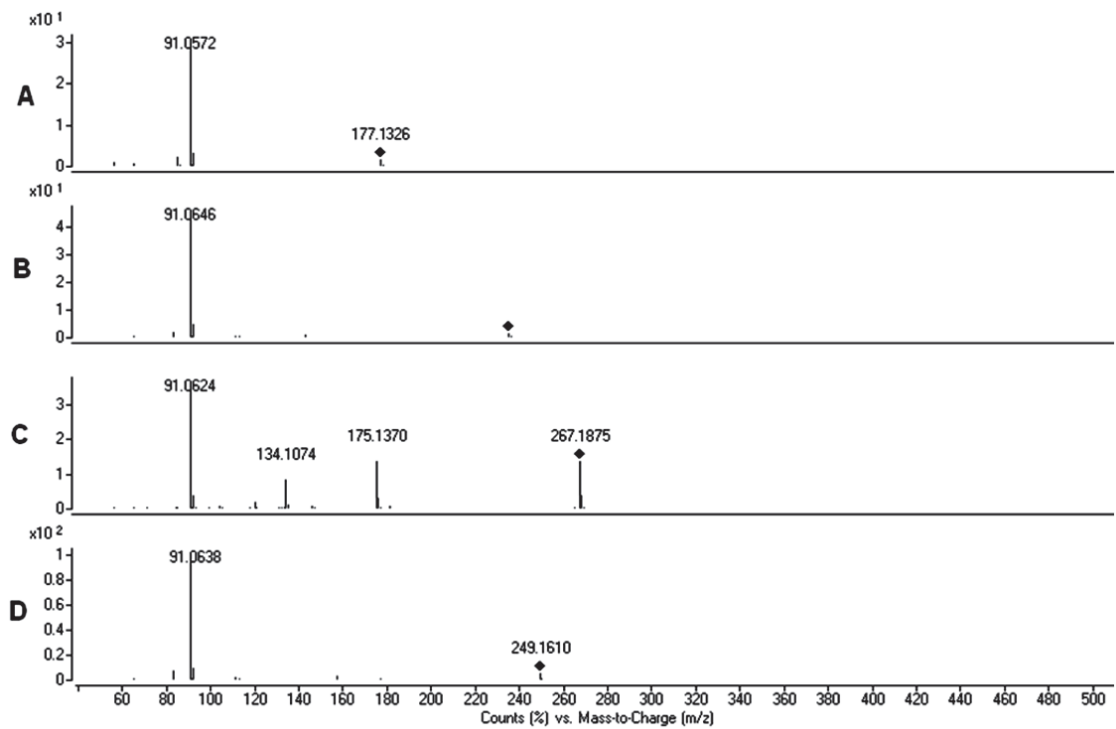


Figure 6-32 LC-MS/MS of A: BZP, B: MBCP, C: DBZP, D: EBCP.

6.3.3 Analysis of 3-trifluoromethylphenylpiperazine

6.3.3.1 Desorption electrospray ionisation – mass spectrometry

3-Trifluoromethylphenylpiperazine base was synthesised via four different synthetic reactions (section 2.2.3) all yielding different by-products/impurities of synthesis. DESI-MS analysis was conducted on all four products. The parent ion, TFMPP, exhibits a peak at m/z 231 which represents the protonated molecular ion $[M+H]^+$ in all samples and was supported by MS/MS spectra (Figure 6-33 and Figure 6-34, Figure 6-35); the proposed collision induced dissociation of the $[M+H]^+$ ion is illustrated in Figure 6-36.

The TFMPP 1.base contained the impurity 2,3-bis-(1,1-dimethylethyl)phenol in trace amounts as was determined by the GC-MS chromatogram (section 2.3.3). However, this compound was thought to be an artefact in the GC-MS chromatogram and was undetectable by DESI-MS.

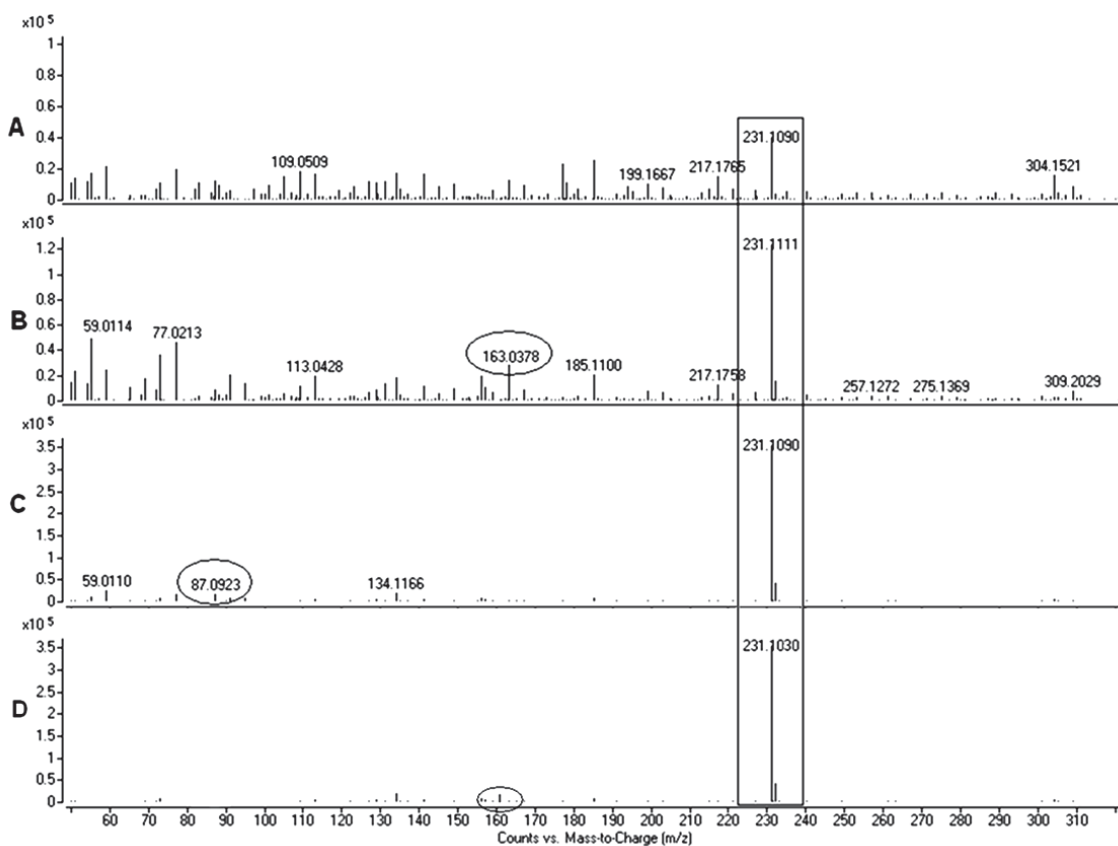


Figure 6-33 DESI-MS spectra of A: TFMPP 1, B: TFMPP 2, C: TFMPP 3, D: TFMPP 4.

The TFMPP 2.base contained the impurity 3-trifluoromethylphenol and this was shown in the DESI-MS spectra as the protonated molecular ion at m/z 163 (Figure 6-33 B). The presence of the by-product, 3-trifluoromethylphenol, was thought to be due to a minor side-reaction between 3-chlorobenzotrifluoride and water (present as moisture in solvent toluene) in which the $-Cl$ group is substituted with a $-OH$ group followed by elimination of the Cl by the strong base $K-tBuO$ to form the intermediate "benzyne" molecule (section 2.3.3). Interestingly, this side-reaction did not occur in TFMPP 1 or TFMPP 3 possibly due to lower moisture levels in these reactions suggesting that this by-product is not very characteristic to this particular reaction. Another impurity 2,3-bis-(1,1-dimethylethyl)phenol which was present in trace amounts in TFMPP 2 was undetectable by DESI-MS as it was thought to be a GC-MS artefact and not present in the synthesised sample.

The TFMPP 3.base exhibited the impurity piperazine in the DESI-MS spectra, present as the protonated molecular ion at m/z 87 (Figure 6-33 C). This piperazine was thought to be present as unreacted starting material in the synthesis of TFMPP. The DESI-MS spectra of TFMPP 4 identified the analyte of interest at m/z 231 and trace amounts of the impurity (starting material) 3-(trifluoromethyl)aniline at m/z 162 (Figure 6-34 D). The presence of these impurities were confirmed by comparison of the collision induced dissociation with relevant reference spectra¹⁶³ (Figure 6-34).

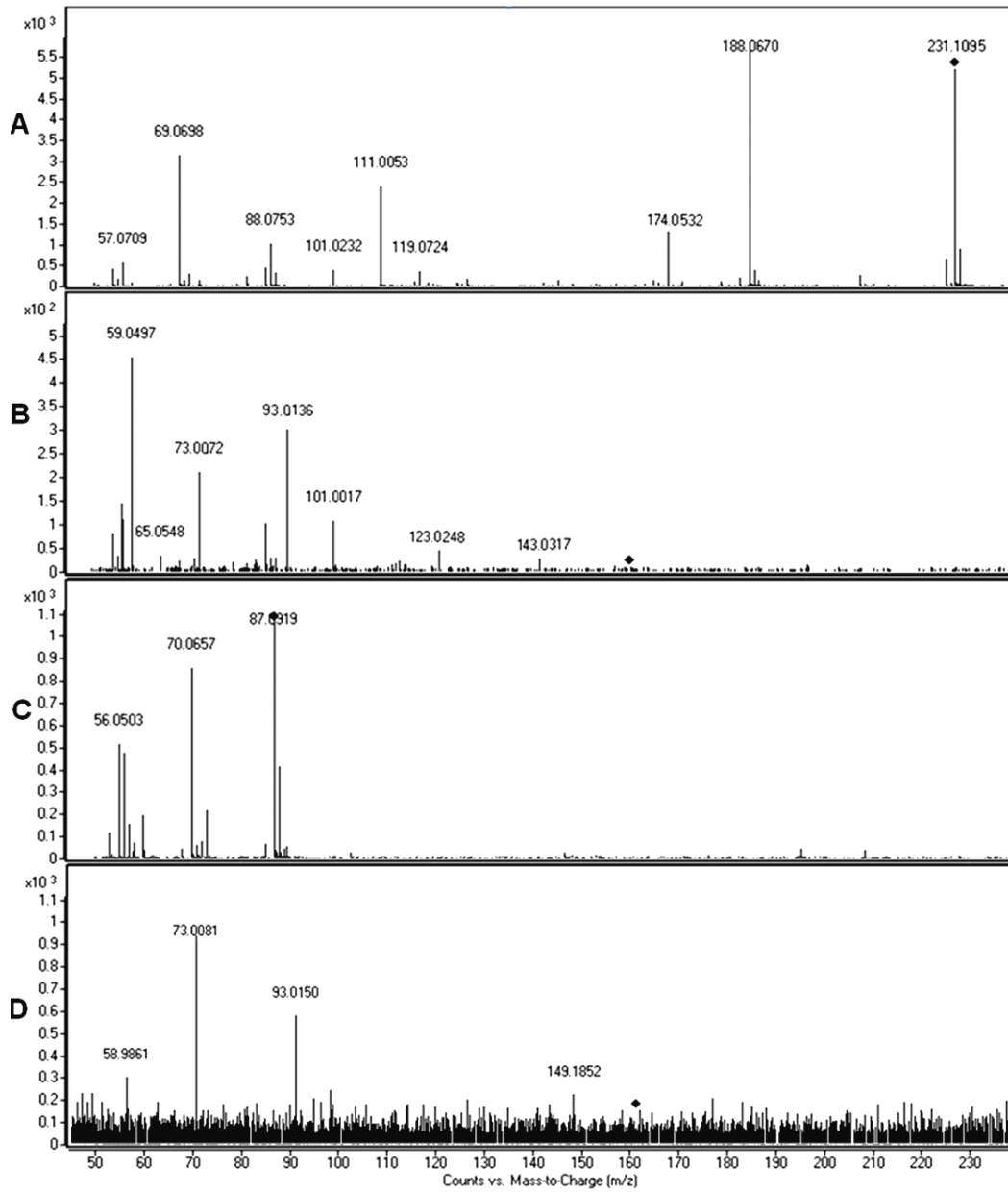


Figure 6-34 DESI-MS/MS of TFMP 2 and TFMP 3; A: TFMP, B: 3-trifluoromethylphenol, C: piperazine, D: 3-(trifluoromethyl)aniline.

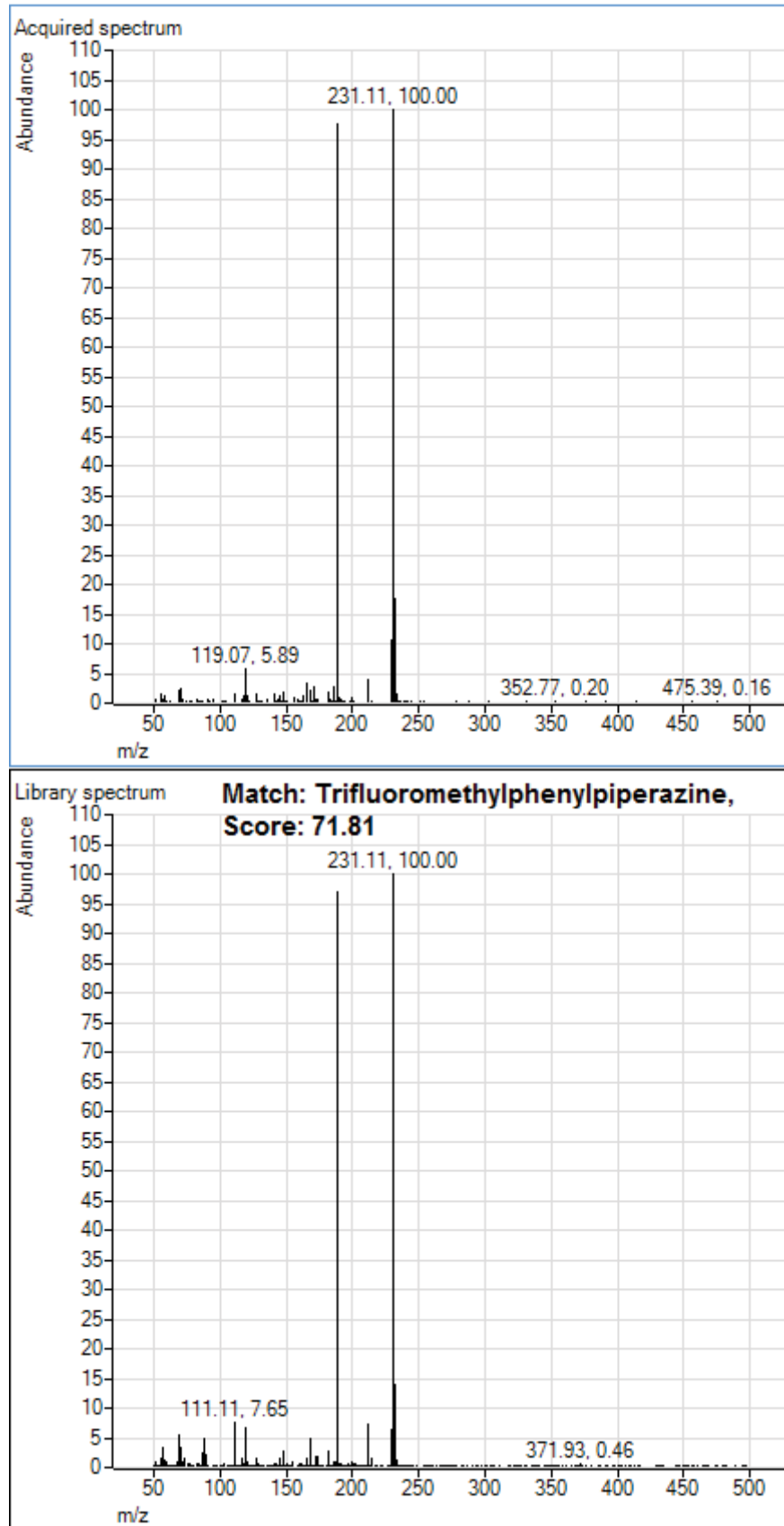


Figure 6-35 PCDL library match to TFMPP.

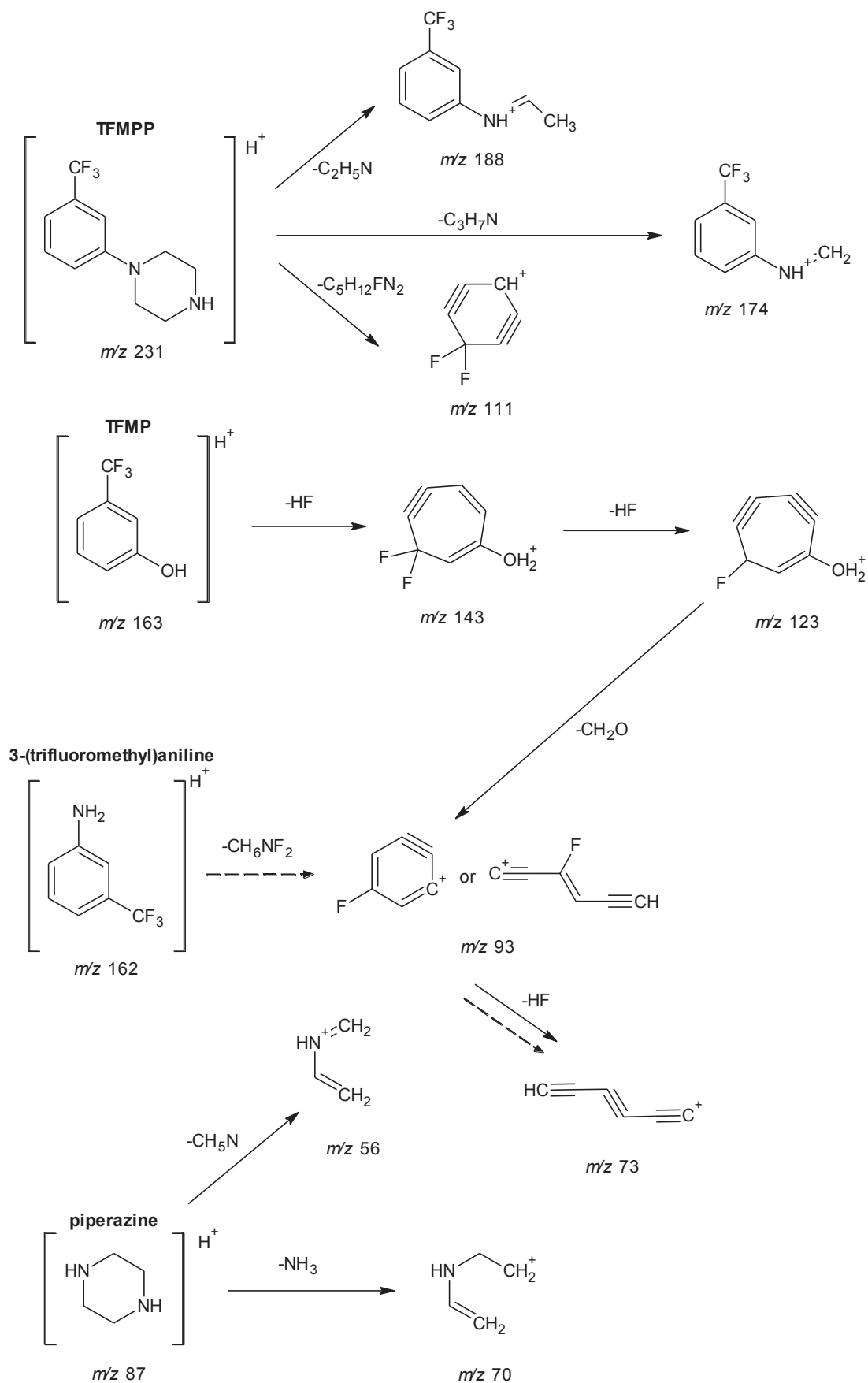


Figure 6-36 Proposed collision induced dissociation of the $[M+H]^+$ ion of TFMP, TFMP (\rightarrow), 3-(trifluoromethyl)aniline ($- - \rightarrow$) and piperazine.

6.3.3.2 Gas chromatography – mass spectrometry

The GC-MS results for TFMPP.HCl (1 - 3) all exhibit peaks for the parent compound TFMPP at m/z 231 (Figure 6-37 - Figure 6-41). TFMPP 2 exhibits an additional impurity which has been identified as 3-trifluoromethylphenol at 4.0 minutes (Figure 6-40, Figure 2-35). TFMPP 2 was also found to contain unreacted starting material, i.e. 3-chlorobenzotrifluoride which eluted at 3.3 minutes. In the GC-MS chromatogram of TFMPP 3, no other by-products or impurities were identified (Figure 6-41, Figure 2-36). TFMPP 4 was found to contain unreacted starting material, i.e. 3-(trifluoromethyl)aniline present at 3.8 minutes (Figure 6-42, Figure 2-40). The multiple peaks present in the GC-MS chromatograms of TFMPP 2 - TFMPP 3 are hypothesised to correspond to isomers of the product, i.e. 1-trifluoromethylphenylpiperazine, 2-trifluoromethylphenylpiperazine, 3-trifluoromethylphenylpiperazine; indicative of the *ortho*-, *meta*- and *para*- substituted TFMPP, respectively. The mechanism for the formation of these products has been illustrated in more detail in section 2.3.3. The major product is hypothesised to be the *meta*- substituted product corresponding to the largest TFMPP peak in each chromatogram. The *ortho*-/*para*- substituted products are minor side-products of this reaction.

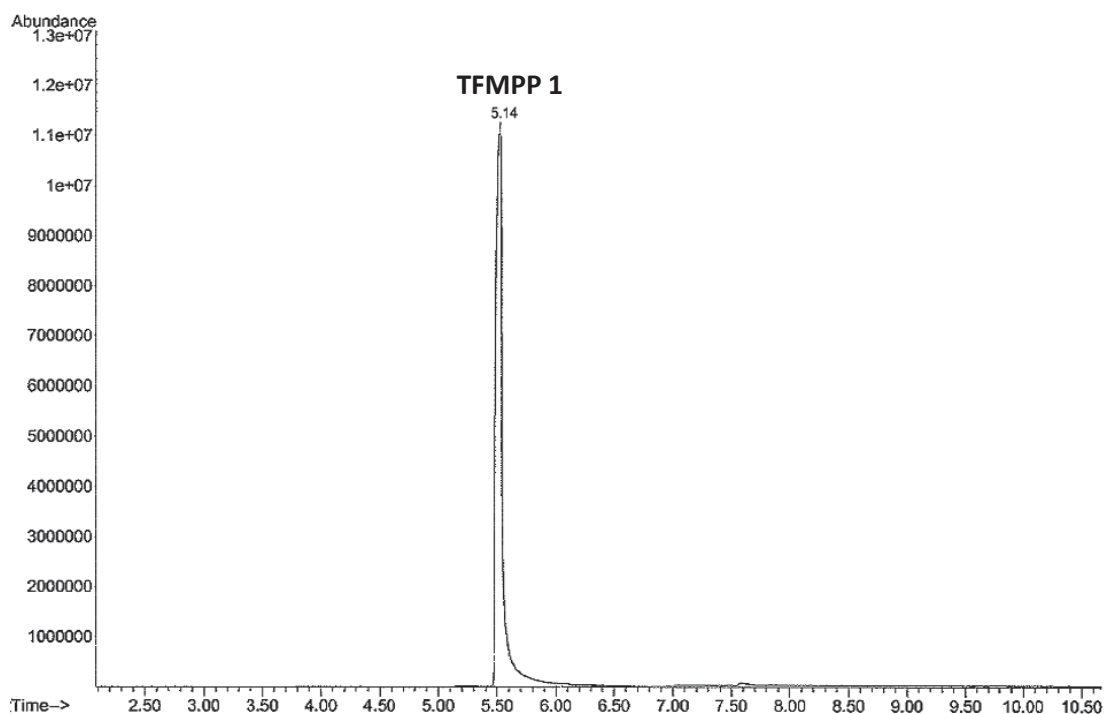


Figure 6-37 GC-MS chromatogram of TFMPP 1.HCl at 5.1 minutes (GC method 1).

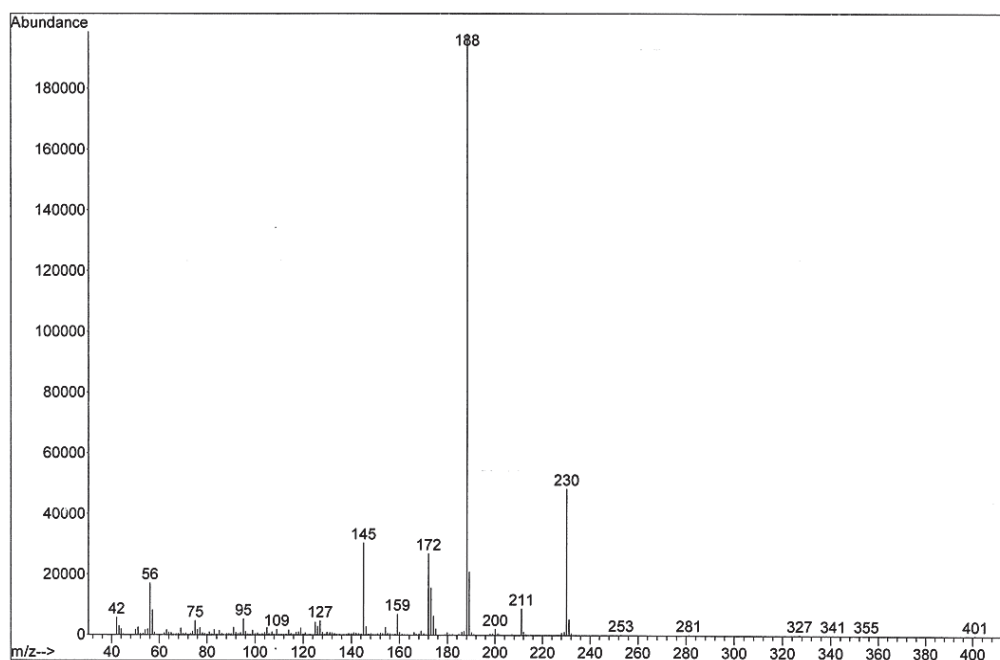


Figure 6-38 EI mass spectra for TFMP 1 (GC method 1).

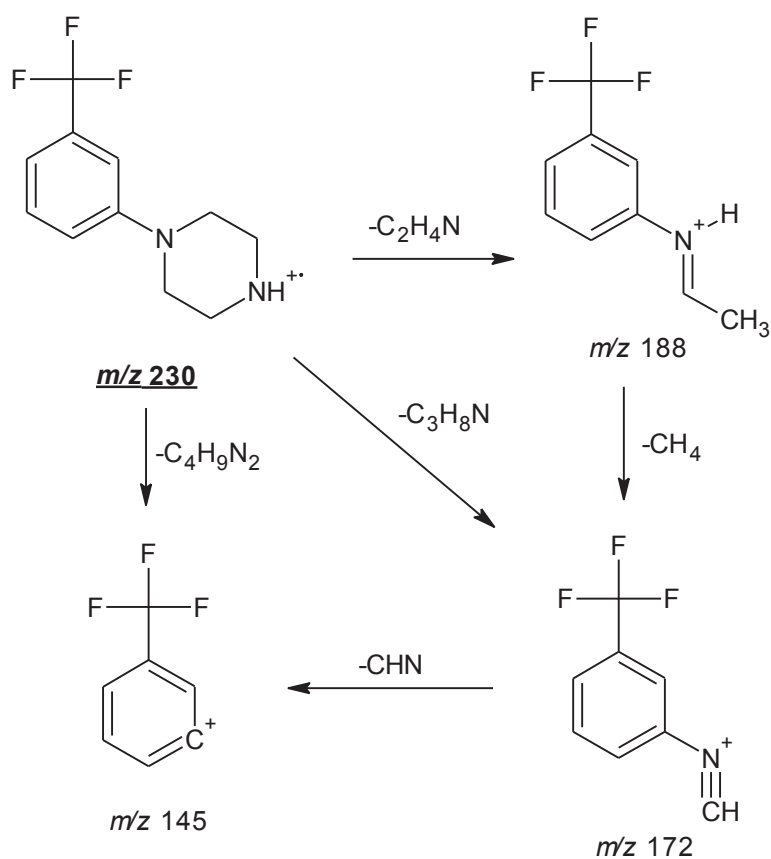


Figure 6-39 Proposed EI fragmentation pathway for TFMP.

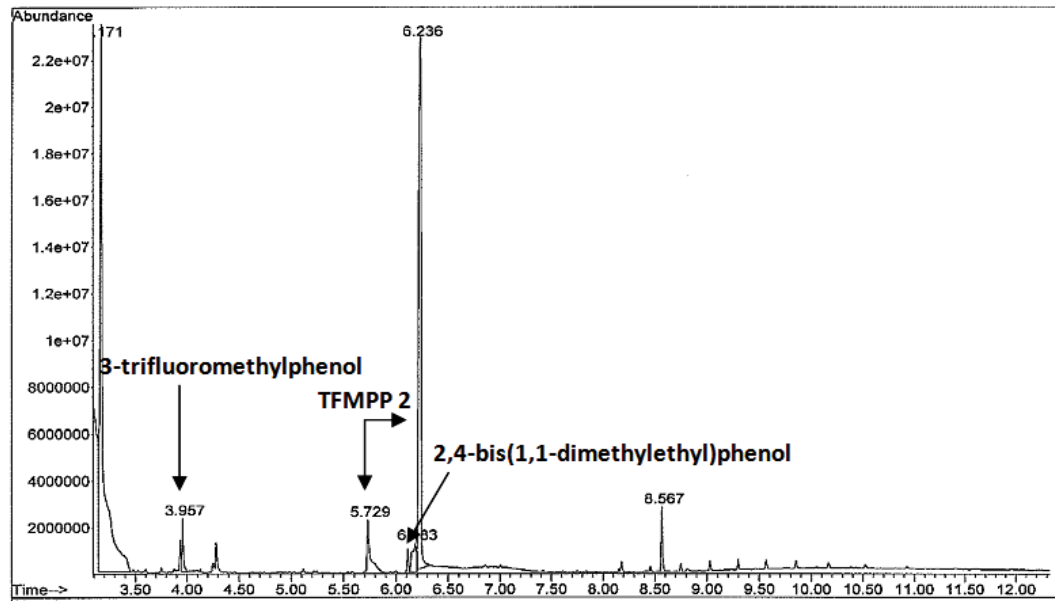


Figure 6-40 GC-MS chromatogram of TFMPP 2.HCl at 5.7 minutes and 6.2 minutes, 3-chlorobenzotrifluoride at 3.3 minutes, 3-trifluoromethylphenol at 4.0 minutes (GC method 2).

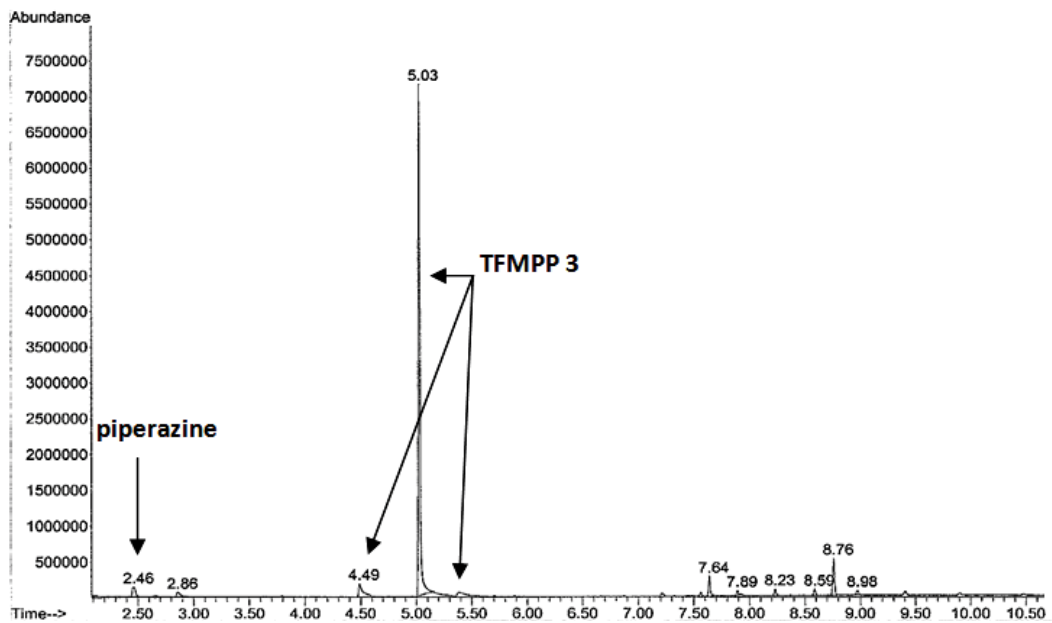


Figure 6-41 GC-MS chromatogram of TFMPP 3.HCl at 4.5 minutes, 5.0 minutes, 5.3 minutes; piperazine at 2.5 minutes (GC method 1).

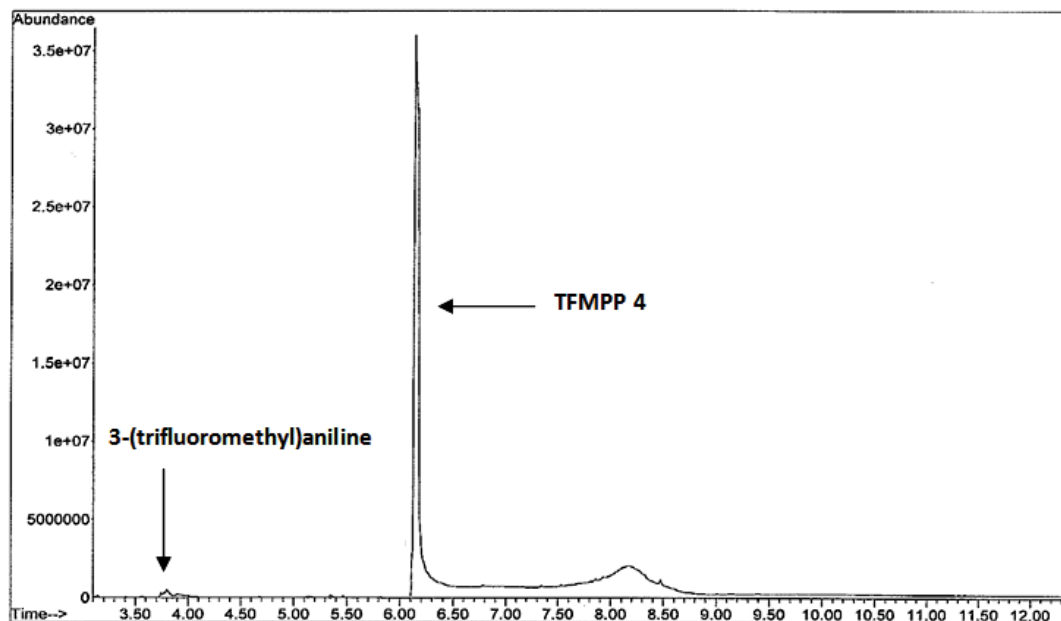


Figure 6-42 GC-MS chromatogram of TFMPP 4.HCl at 6.2 minutes, 3-(trifluoromethyl)aniline at 3.8 minutes (GC method 2).

6.3.3.3 Liquid chromatography – mass spectrometry

The TFMPP samples were subject to LC-MS analysis and in all cases TFMPP was detectable at m/z of 231 (Figure 6-43). Trace amounts of 3-(trifluoromethyl)aniline was detected in TFMPP 4. No other impurities were found using LC-MS. The detection of 3-(trifluoromethyl)aniline in TFMPP 4 clearly distinguishes this compound from TFMPP 1 – 3 and highlights the different synthetic method used to synthesise TFMPP 1 – 3 and TFMPP 4, respectively (section 2.2.3).

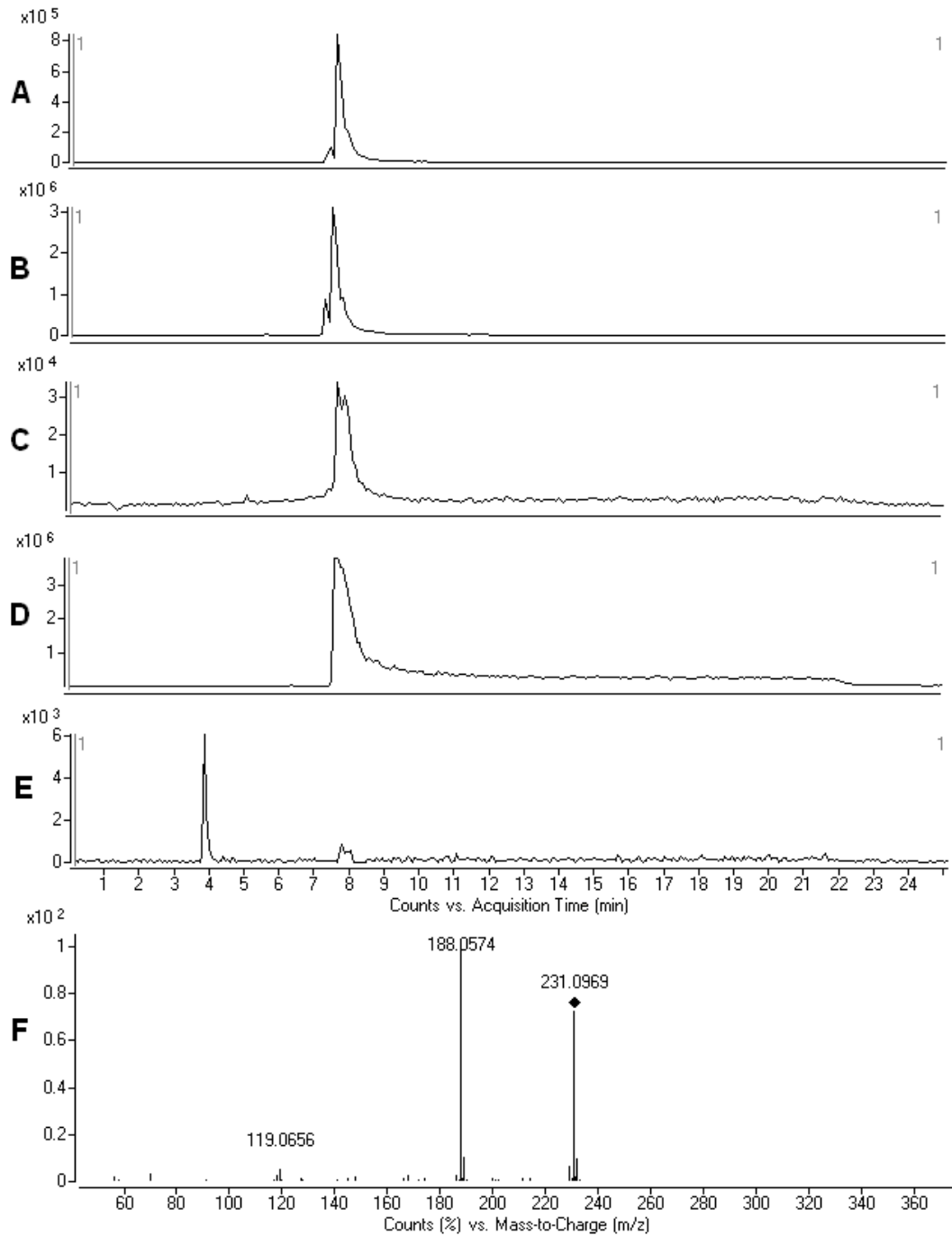


Figure 6-43 LC-MS chromatogram of TFMP; A: EIC of TFMP 1 at 8.0 minutes, m/z 231; B: EIC of TFMP 2; C: EIC of TFMP 3; D: EIC of TFMP 4; E: EIC of 3-(trifluoromethyl)aniline at 3.9 minutes, m/z 162; F: MS/MS of TFMP.

6.3.4 Analysis of 3-chlorophenylpiperazine

6.3.4.1 Desorption electrospray ionisation – mass spectrometry

The DESI-MS analysis was successful in identifying the compound mCPP at m/z 197 as the protonated molecular ion $[M+H]^+$. In addition, an impurity was found in trace amounts that corresponded to unreacted 3-chloroaniline starting material, present as the protonated molecular ion at m/z 128 (circled). The presence of these compounds was supported by MS/MS data (Figure 6-44 - Figure 6-45); the proposed collision induced dissociation of the $[M+H]^+$ ion is illustrated in Figure 6-46. The presence of 3-chloroaniline was consistent with the synthetic route of manufacture used, in which 3-chloroaniline and bis(2-chloroethyl)amine were precursors. The large SNR observed for the MS/MS data in Figure 6-44 C is due to trace amounts of the 3-chloroaniline present in this sample. A distinguishing feature in the spectra of mCPP is the presence of chlorine isotope peaks (i.e. ^{35}Cl , ^{37}Cl)¹²⁵. The protonated molecular ion at m/z 197 also exhibits and ^{37}Cl isotope peak at m/z 199 (Figure 6-44). These distinguishing features can give a strong indication of the presence of chlorine in the analysis unknown substances.

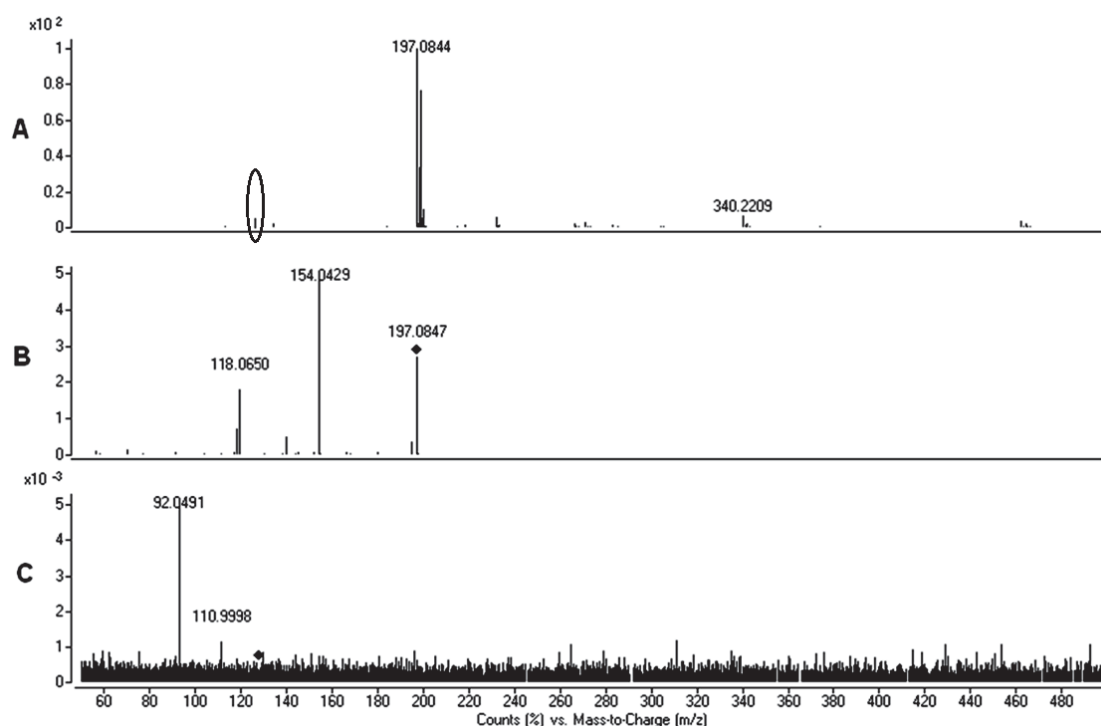


Figure 6-44 DESI-MS spectra of A: mCPP 1, B: MS/MS spectra of mCPP, C: MS/MS spectra of 3-chloroaniline.

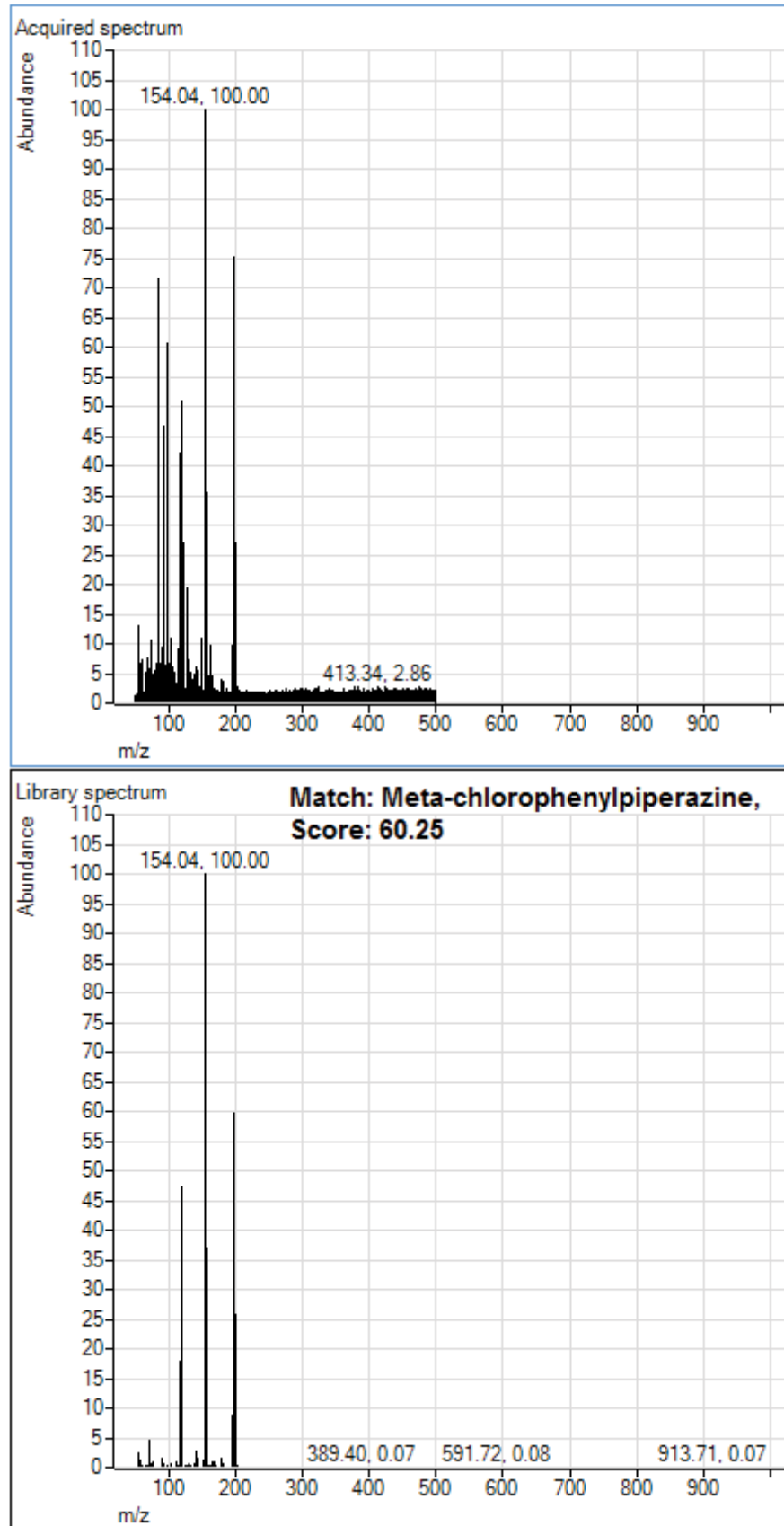


Figure 6-45 PCDL library match to mCPP.

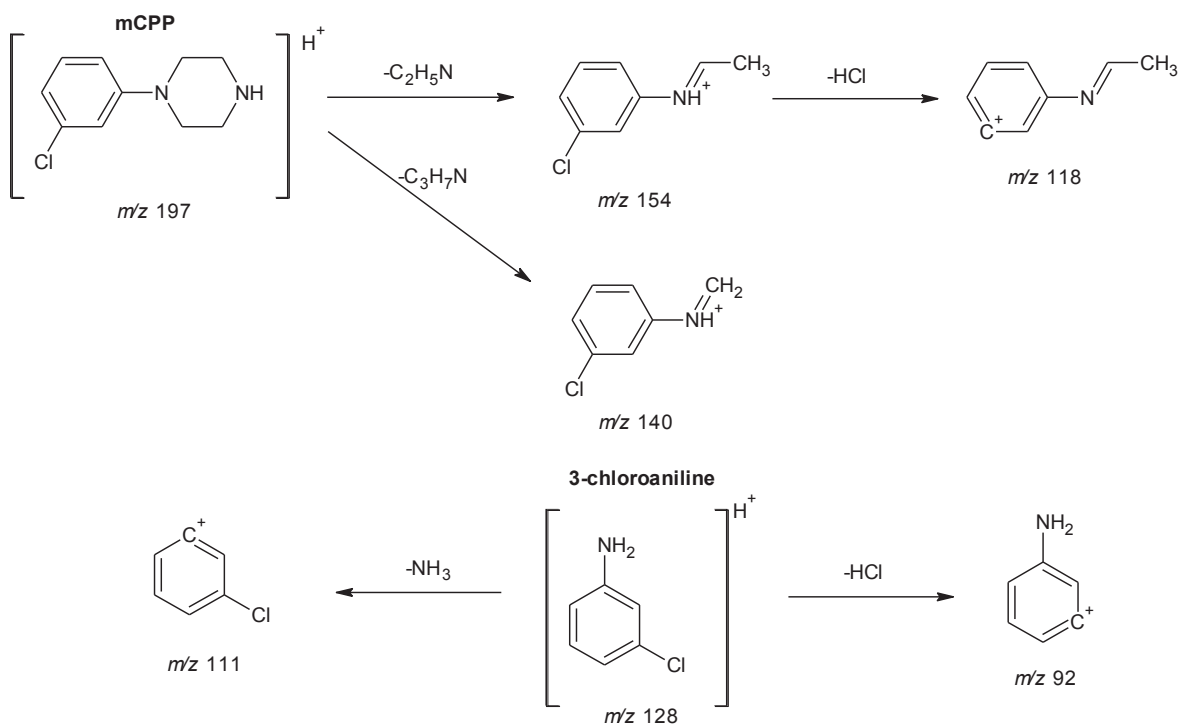


Figure 6-46 Proposed collision induced dissociation of the $[M+H]^+$ ion of mCPP and 3-chloroaniline.

6.3.4.2 Gas chromatography – mass spectrometry

Using GC-MS, mCPP was identified at 7.2 minutes and the impurity 3-chloroaniline was found in trace amounts at 4.5 minutes (unreacted starting material). No other by-products or impurities were identified using GC-MS (Figure 6-47 - Figure 6-49, Figure 2-43).

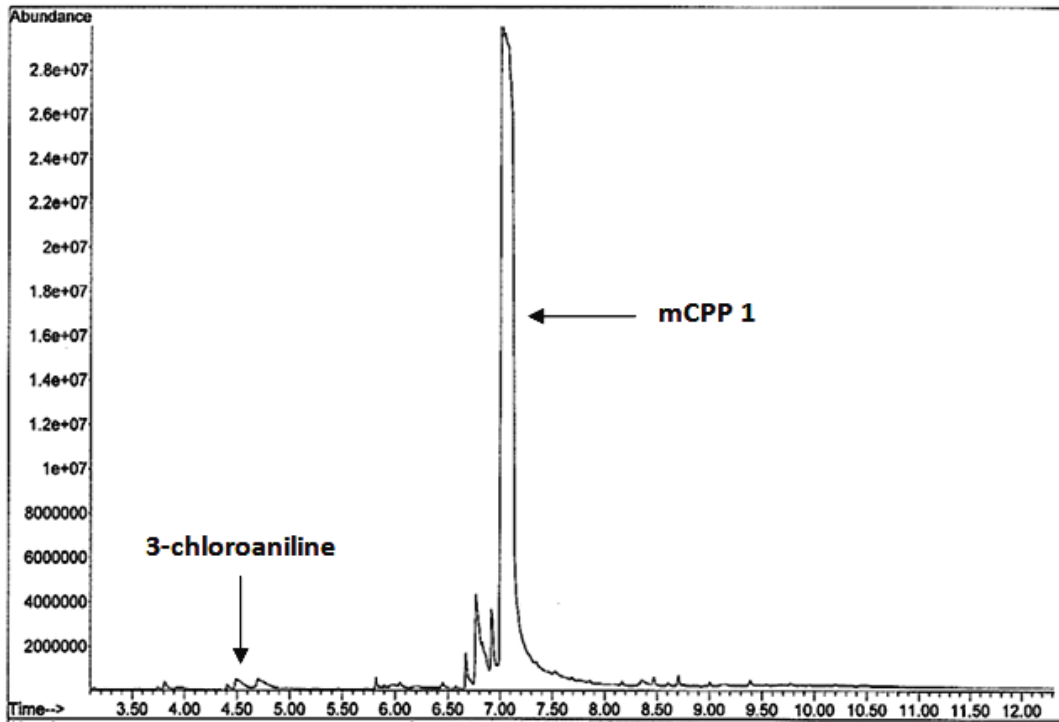


Figure 6-47 GC-MS chromatogram of mCPP 1.HCl at 7.2 minutes, 3-chloroaniline at 4.5 minutes (GC method 2).

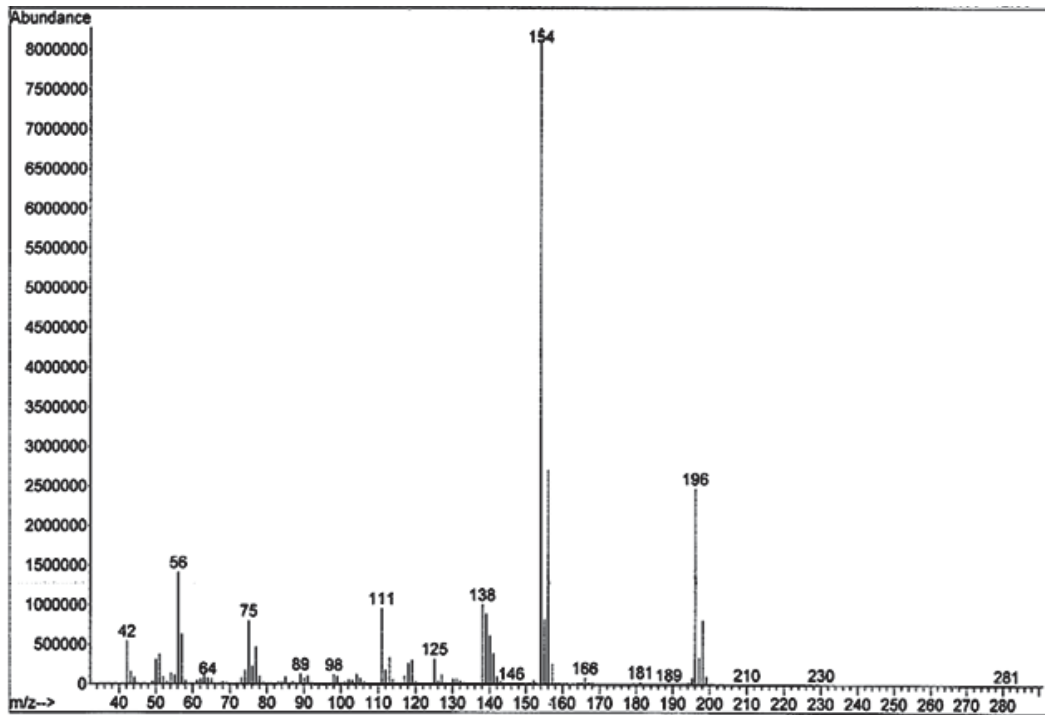


Figure 6-48 EI mass spectrum of mCPP 1 (GC method 2).

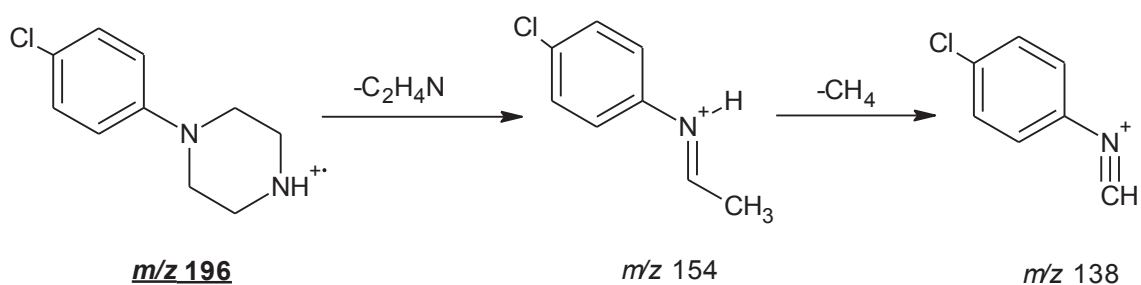


Figure 6-49 Proposed EI fragmentation pathway for mCPP.

6.3.4.3 Liquid chromatography – mass spectrometry

The LC-MS analysis was successful in detecting mCPP at m/z 197; however, the impurity 3-chloroaniline (unreacted starting material) was undetectable using this technique due to presence in trace amounts (Figure 6-50).

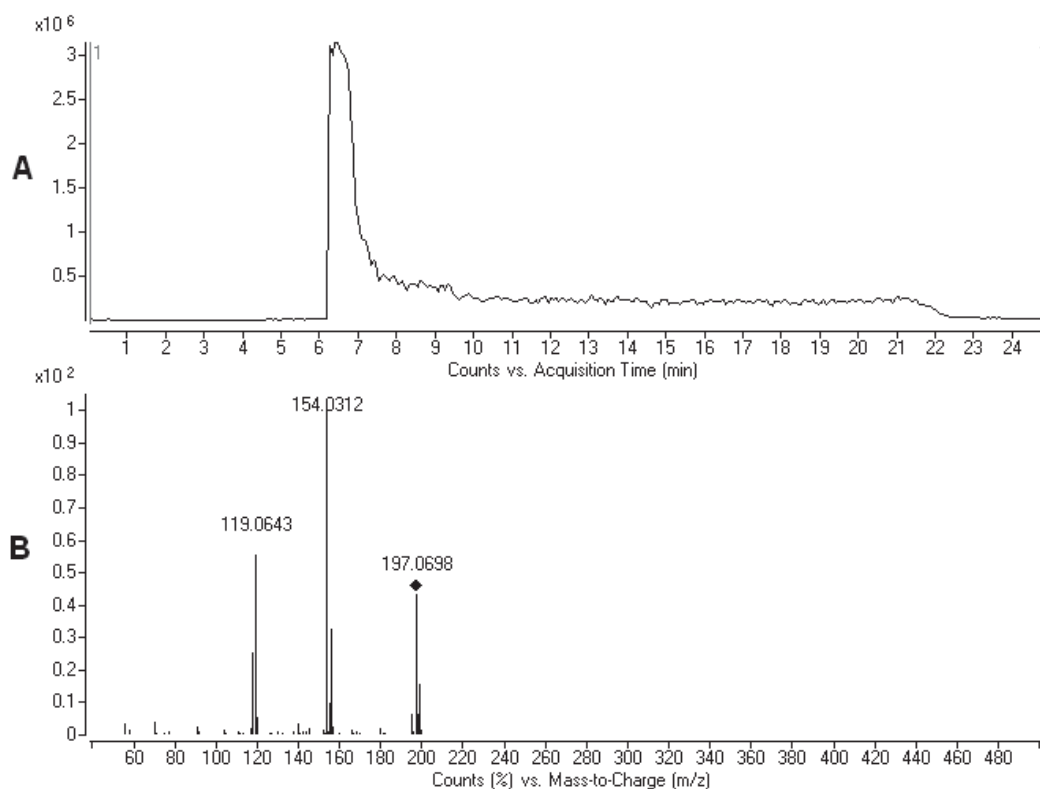


Figure 6-50 LC-MS chromatogram of mCPP 1; A: EIC of mCPP at 6.4 minutes, m/z 197; B: MS/MS of mCPP.

6.3.5 Analysis of 4-methoxyphenylpiperazine

6.3.5.1 Desorption electrospray ionisation – mass spectrometry

The DESI-MS analysis of MeOPP 1 identified the presence of MeOPP at m/z 193 (as the protonated molecular ion $[M+H]^+$) as well as the presence of the impurity 4-anisidine at m/z 124, present as unreacted starting material in trace amounts. These compounds were supported by MS/MS spectra (Figure 6-51, Figure 6-52); the proposed collision induced dissociation of the $[M+H]^+$ ion is illustrated in Figure 6-53.

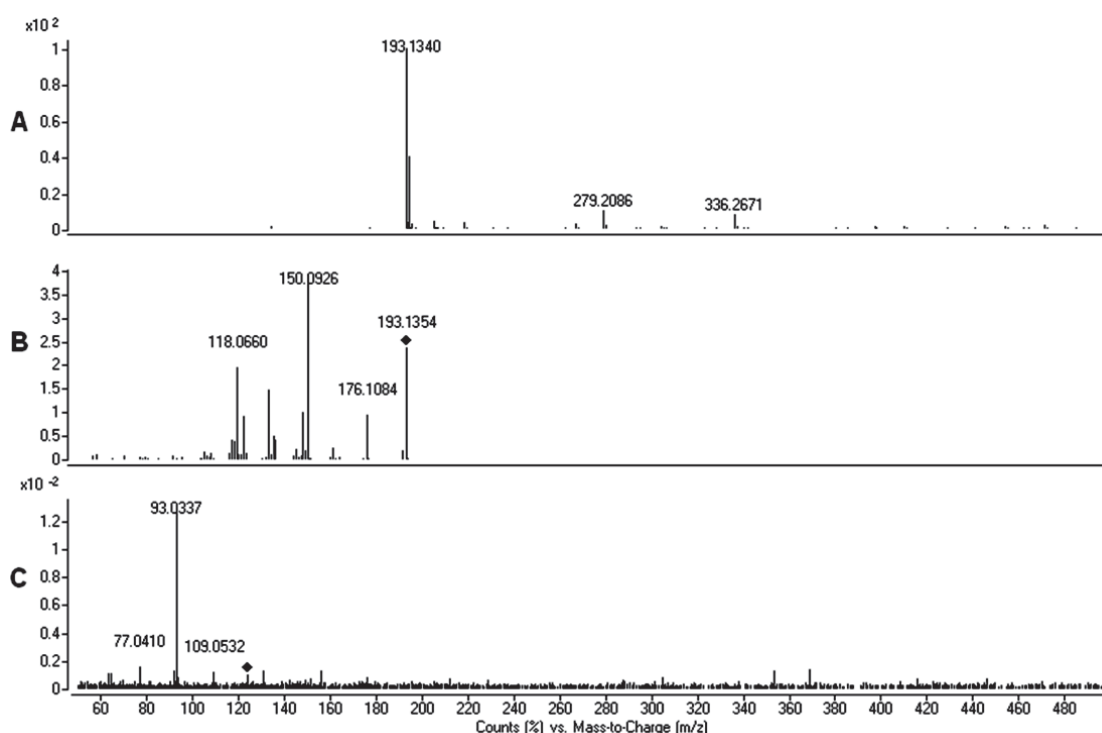


Figure 6-51 DESI-MS spectra of A: MeOPP 1, B: MS/MS spectra of MeOPP, C: MS/MS spectra of 4-anisidine.

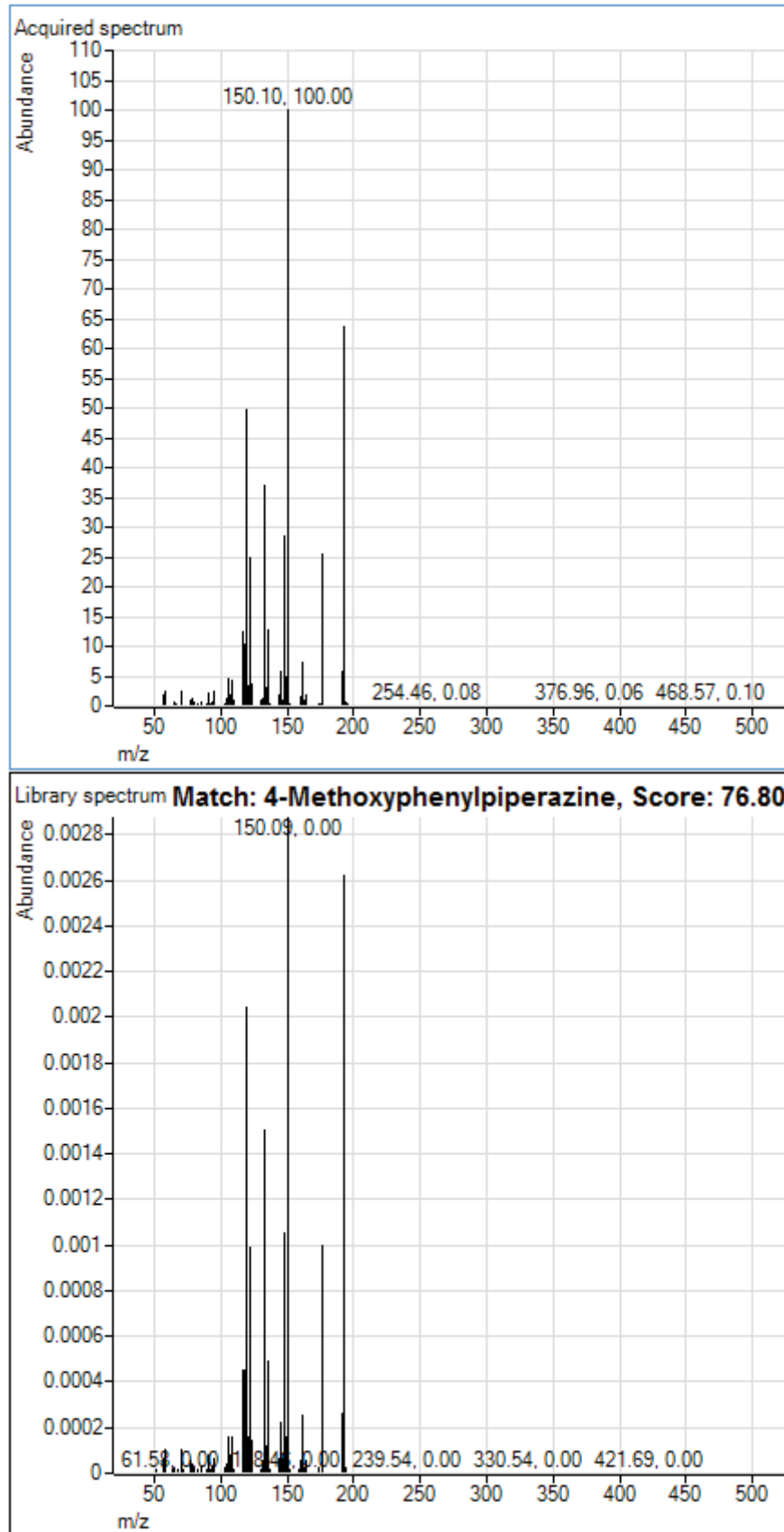


Figure 6-52 PCDL library match to MeOPP.

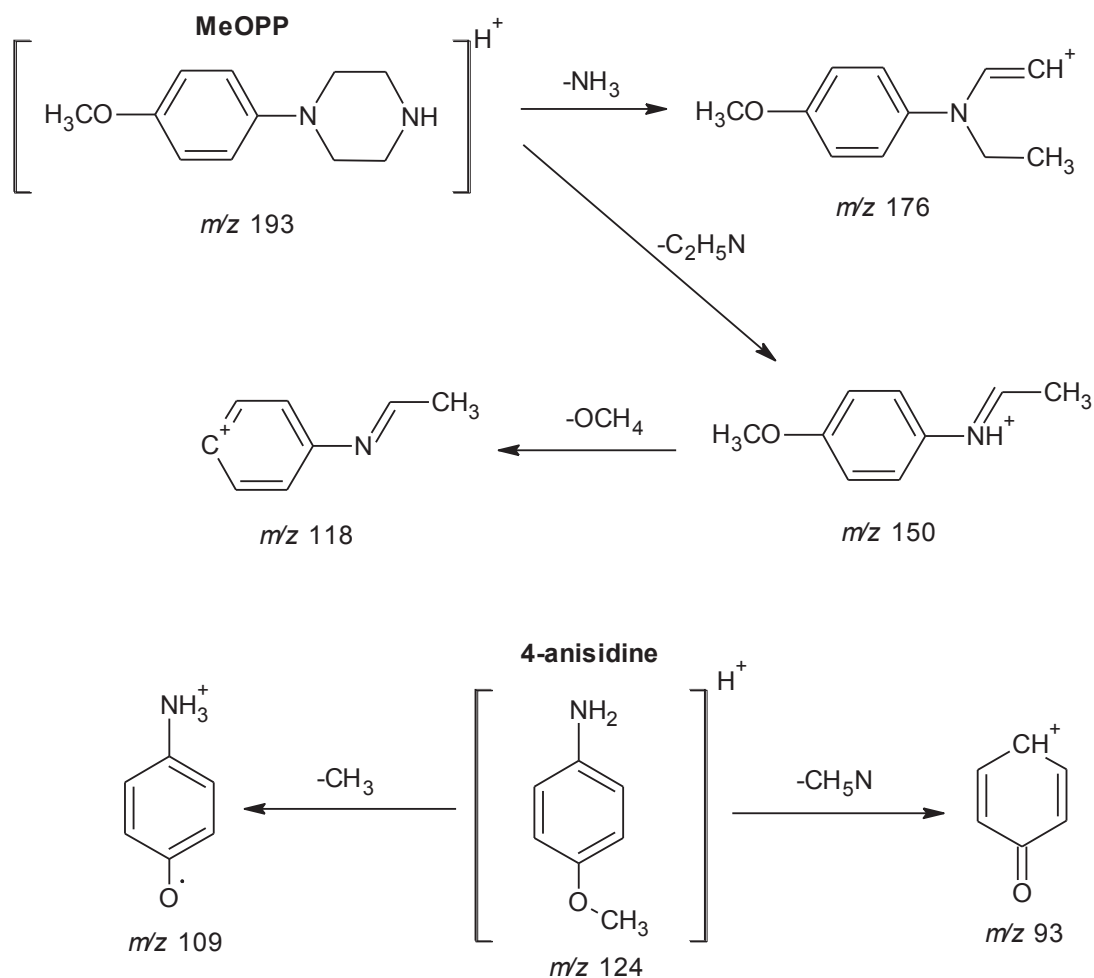


Figure 6-53 Proposed collision induced dissociation of the $[M+H]^+$ ion of MeOPP and 4-anisidine.

6.3.5.2 Gas chromatography – mass spectrometry

The GC-MS analysis identified the presence of MeOPP at approximately 7.2 minutes in the MeOPP 1 sample. In addition, two impurities were detected in trace amounts and were identified as being unreacted starting materials, i.e. bis(2-chloroethyl)amine at 3.5 minutes and 4-anisidine at 4.3 minutes (Figure 6-54 - Figure 6-56, Figure 2-47 - Figure 2-48).

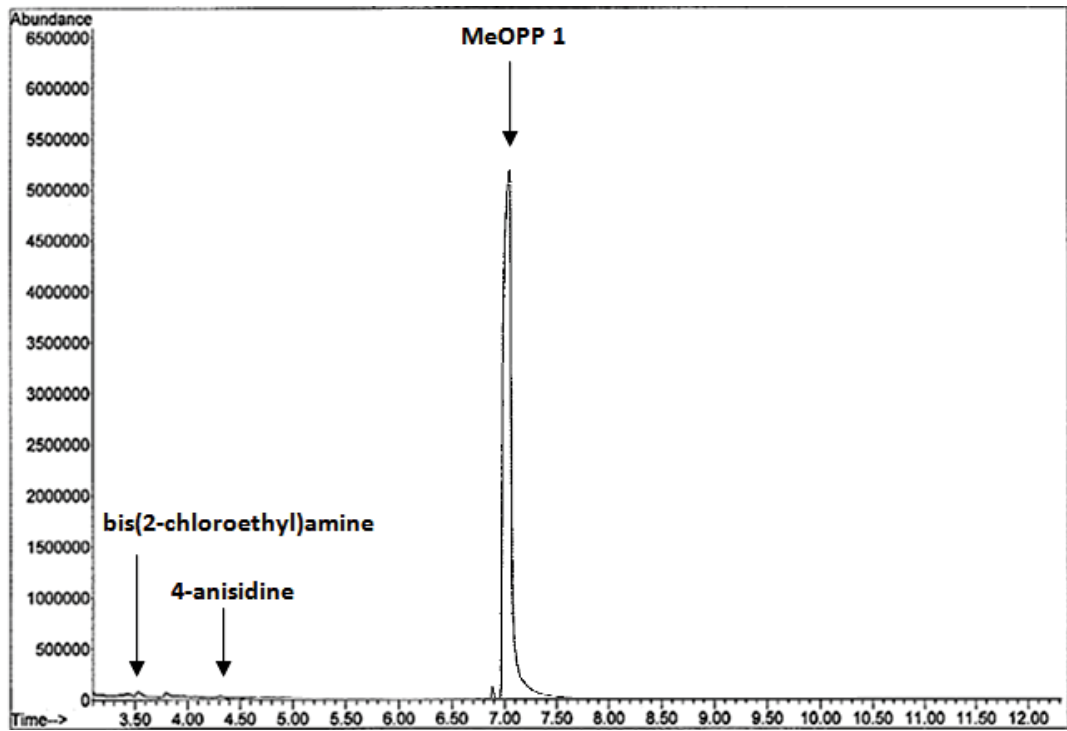


Figure 6-54 GC-MS chromatogram of MeOPP 1.HCl at 7.2 minutes, bis(2-chloroethyl)amine at 3.5 minutes, 4-anisidine at 4.3 minutes (GC method 2).

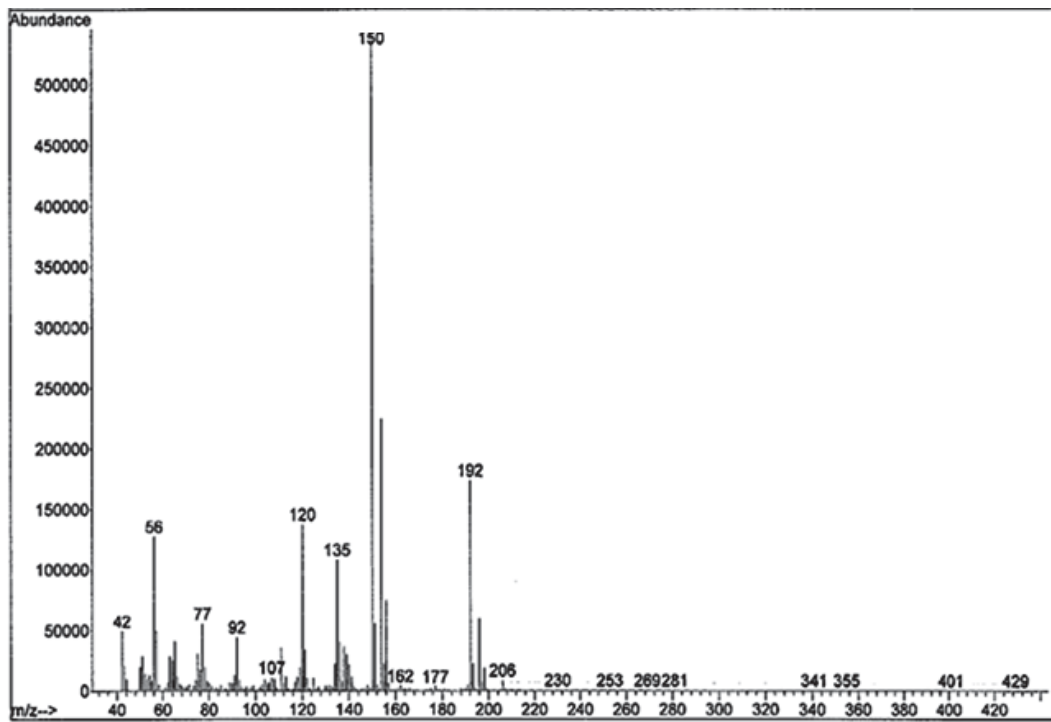


Figure 6-55 EI mass spectra of MeOPP 1 (GC method 2).

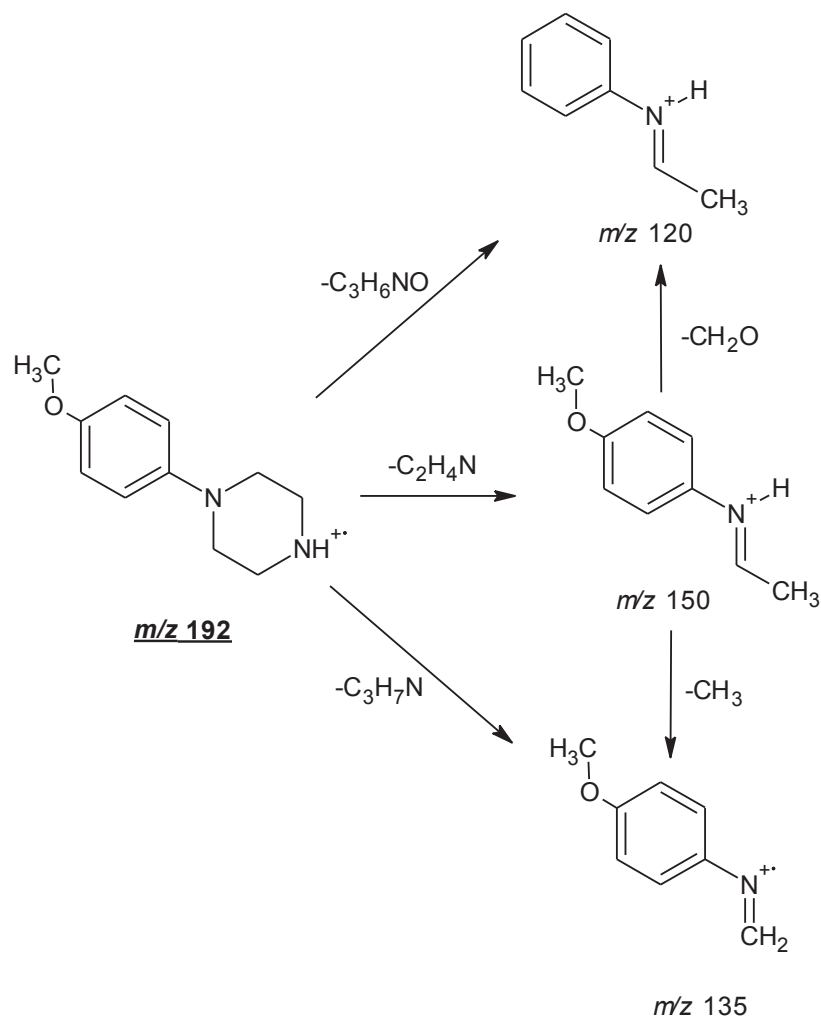


Figure 6-56 Proposed EI fragmentation pathway for MeOPP.

6.3.5.3 Liquid chromatography – mass spectrometry

The LC-MS analysis of MeOPP 1 identified the analyte of interest at m/z 193 as being MeOPP. In addition, trace amounts of the starting material 4-anisidine were detected. The presence of MeOPP was further supported based on MS/MS spectra (Figure 6-57). The presence of 4-anisidine was indicative of the synthetic route of manufacture used in which 4-anisidine and bis(2-chloroethyl)amine were precursors.

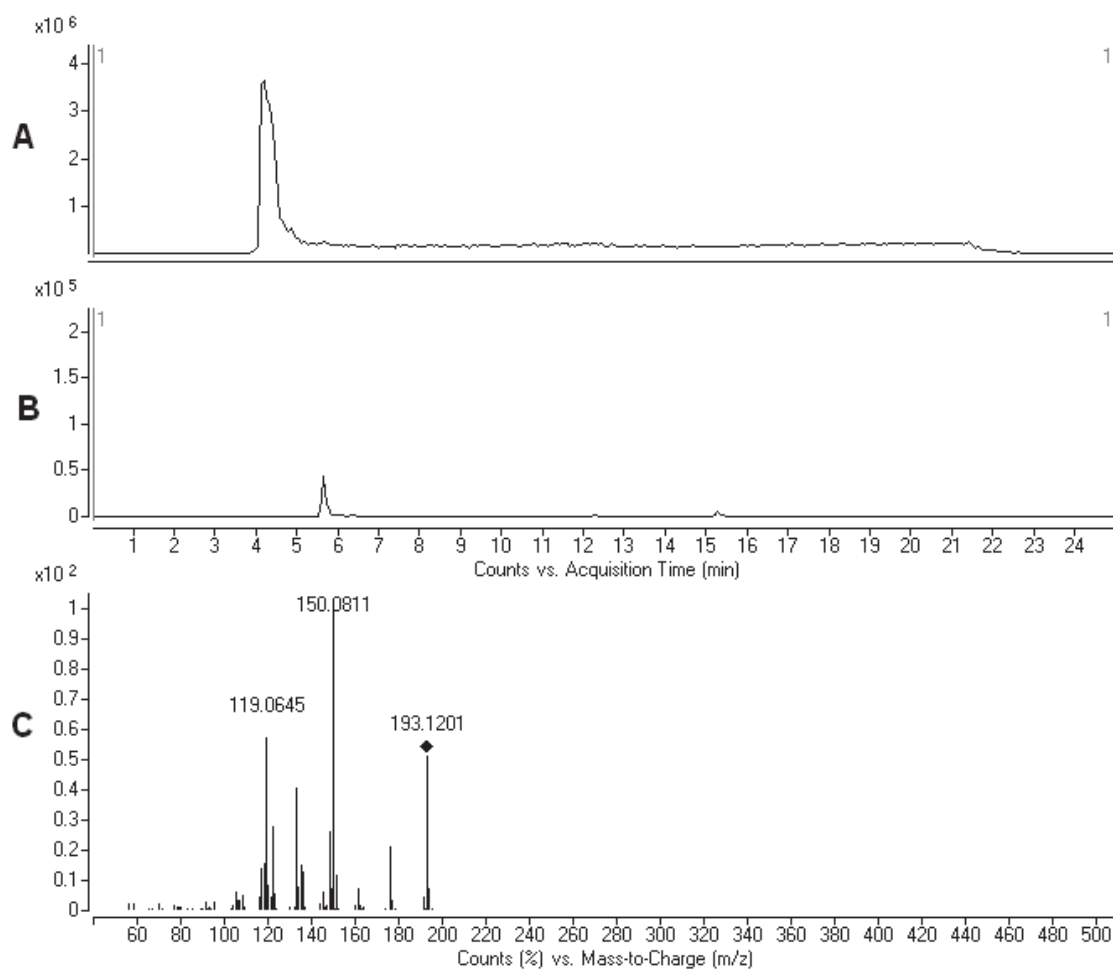


Figure 6-57 LC-MS chromatogram of MeOPP; **A:** EIC of MeOPP 1 at 4.2 minutes, m/z 193; **B:** EIC of 4-anisidine at 5.8 minutes, m/z 124; **C:** MS/MS of MeOPP 1

6.3.6 Mass accuracy

The piperazine analogues (i.e. BZP, DBZP, TFMPP, mCPP and MeOPP) were matched using the PCDL software with a minimum MS/MS score of 60. This was determined to be an adequate match to allow confirmation of the compound of interest. The accurate mass data obtained from the MS and MS/MS data were calculated to be at best within 5 ppm and 10 ppm respectively, further confirming the identity of products (Table 6-2 and Table 6-3).

Table 6-2 Mass accuracy of piperazine and related compounds using positive ion mode.

Compound	Formula [M+H] ⁺	Accurate Mass [M+H] ⁺	Acquired Mass [M+H] ⁺	Mass Accuracy (ppm)
BZP	C ₁₁ H ₁₇ N ₂	177.1392	177.1396	2.3
DBZP	C ₁₈ H ₂₃ N ₂	267.1861	267.1858	-1.1
MBCP	C ₁₃ H ₁₉ N ₂ O ₂	235.1447	235.1436	-4.7
EBCP	C ₁₄ H ₂₁ N ₂ O ₂	249.1603	249.1597	-2.4
benzyl chloride	C ₇ H ₈ Cl	127.0315	127.0319	3.1
TFMPP	C ₁₁ H ₁₄ F ₃ N ₂	231.1109	231.1111	0.9
TFMP	C ₇ H ₆ F ₃ O	163.0371	163.0378	4.3
piperazine	C ₄ H ₁₁ N ₂	87.0922	87.0923	1.1
3-(trifluoro- methyl)aniline	C ₇ H ₇ NF ₃	162.0531	162.0527	-2.5
mCPP	C ₁₀ H ₁₄ ClN ₂	197.0846	197.0844	-1.0
3-chloroaniline	C ₆ H ₇ NCl	128.0267	128.0270	2.3
MeOPP	C ₁₁ H ₁₇ N ₂ O	193.1341	193.1340	-0.5
4-anisidine	C ₇ H ₁₀ NO	124.0762	124.0759	-2.4

BZP = 1-benzylpiperazine, DBZP = 1,4-dibenzylpiperazine, MBCP = methyl 1-benzyl-4-carboxypiperazine, EBCP = ethyl 1-benzyl-4-carboxypiperazine, TFMPP = 3-trifluoromethylphenylpiperazine, TMFP = 3-trifluoromethylphenol, mCPP = 3-chlorophenylpiperazine, MeOPP = 4-methoxyphenylpiperazine.

Table 6-3 Mass accuracy of MS/MS ions using positive ion mode at 20 eV.

Compound	Chemical Formula	Accurate Mass	Acquired Mass	Mass Accuracy (ppm)
BZP	C ₁₁ H ₁₇ N ₂ [M+H] ⁺	177.1392	177.1396	2.3
	C ₉ H ₁₂ N	134.0970	134.0973	2.2
	C ₈ H ₁₀ N	120.0813	120.0819	5.0
	C ₇ H ₇	91.0548	91.0542	-6.6
DBZP	C ₁₈ H ₂₃ N ₂ [M+H] ⁺	267.1861	267.1875	5.2
	C ₁₁ H ₁₇ N ₂	177.1392	177.1383	-5.1
	C ₉ H ₁₂ N	134.0970	134.0975	3.7
	C ₈ H ₁₀ N	120.0813	120.0818	4.2
	C ₇ H ₇	91.0548	91.0551	3.3
MBCP	C ₁₃ H ₁₉ N ₂ O ₂ [M+H] ⁺	235.1447	235.1434	-5.5
	C ₁₁ H ₁₇ N ₂	177.1392	177.1384	-4.5
	C ₇ H ₇	91.0548	91.0549	1.1
EBCP	C ₁₄ H ₂₁ N ₂ O ₂ [M+H] ⁺	249.1603	249.1597	-2.4
	C ₁₁ H ₁₇ N ₂	177.1392	177.1394	1.1
	C ₇ H ₇	91.0548	91.0539	-9.9
benzyl chloride	C ₇ H ₈ Cl [M+H] ⁺	127.0315	127.0319	3.1
	C ₇ H ₇	91.0548	91.0542	-6.6

Table 6-3 continued.

Compound	Chemical Formula	Accurate Mass	Acquired Mass	Mass Accuracy (ppm)
TFMPP	$C_{11}H_{14}F_3N_2 [M+H]^+$	231.1109	231.1095	-6.1
	$C_9H_9F_3N$	188.0687	188.0670	-9.0
	$C_8H_7F_3N$	174.0531	174.0532	0.6
	C_6HF_2	111.0046	111.0053	6.3
TFMP	$C_7H_6F_3O [M+H]^+$	163.0371	163.0378	4.3
	$C_7H_5F_2O$	143.0308	143.0317	6.3
	C_7H_4FO	123.0246	123.0248	1.6
	C_6H_2F	93.0141	93.0136	-5.4
	C_6H	73.0078	73.0072	-8.2
piperazine	$C_4H_{11}N_2 [M+H]^+$	87.0922	87.0919	-3.4
	C_4H_8N	70.0657	70.0657	0.0
	C_3H_6N	56.0500	56.0503	5.4
3-(trifluoro-methyl)aniline	$C_7H_7NF_3 [M+H]^+$	162.0531	162.0527	-2.5
	C_6H_2F	93.0141	93.0150	9.7
	C_6H	73.0078	73.0081	4.1
mCPP	$C_{10}H_{14}ClN_2 [M+H]^+$	197.0846	197.0847	0.5
	C_8H_9ClN	154.0424	154.0429	3.2
	C_7H_7ClN	140.0267	140.0262	-3.6
	C_8H_8N	118.0657	118.0650	-5.9
3-chloroaniline	$C_6H_7NCl [M+H]^+$	128.0267	128.0270	2.3
	C_6H_4Cl	111.0002	110.9998	-3.6
	C_6H_6N	92.0500	92.0491	-9.8
MeOPP	$C_{11}H_{17}N_2O [M+H]^+$	193.1341	193.1354	6.7
	$C_{11}H_{14}NO$	176.1075	176.1084	5.1
	$C_9H_{12}NO$	150.0919	150.0926	4.7
	C_8H_8N	118.0657	118.0660	2.5
4-anisidine	$C_7H_{10}NO [M+H]^+$	124.0762	124.0759	-2.4
	C_6H_7NO	109.0528	109.0532	3.7
	C_6H_5O	93.0340	93.0337	-3.2

The compounds identified in the piperazine samples using DESI-MS, GC-MS and LC-MS have been summarised in Table 6-4.

Table 6-4 Compounds detected in piperazine analogues using DESI-MS, GC-MS, and LC-MS.

Sample	Compound	MW (Da)	DESI-MS	GC-MS	LC-MS
BZP 1	BZP	176	✓	✓	✓
	DBZP	266	✓	✓	✓
BZP 2	BZP	176	✓	✓	✓
	DBZP	266	✓	✓	✓
BZP 3	BZP	176	✓	✓	✓
	DBZP	266	✓	✓	✓
BZP 4	BZP	176	✓	✓	✓
	DBZP	267	✓ (trace)	✓ (trace)	✓ (trace)
	MBCP	234	✓	✓	✓
	EBCP	248	✓	✓	✓
	benzyl chloride	126	✓ (trace)	X	X
TFMPP 1	TFMPP	230	✓	✓	✓
TFMPP 2	TFMPP	230	✓	✓	✓
	3-trifluoromethylphenol	162	✓	✓	X
	3-chlorobenzotrifluoride	179	X	✓	X
TFMPP 3	TFMPP	230	✓	✓	✓
	piperazine	86	✓	X	X
TFMPP 4	TFMPP	230	✓	✓	✓
	3-(trifluoromethyl)aniline	161	✓ (trace)	✓ (trace)	✓ (trace)
mCPP 1	mCPP	196	✓	✓	✓
	3-chloroaniline	127	✓ (trace)	✓ (trace)	X
MeOPP 1	MeOPP	192	✓	✓	✓
	bis(2-chloroethyl)amine	141	X	✓ (trace)	X
	4-anisidine	123	✓ (trace)	✓ (trace)	✓ (trace)

✓ = detected, X = not detected

The collision induced dissociation of BZP and related compounds in this chapter share some common fragmentation pathways. The presence of the ion at m/z 91 (i.e. C_7H_7) was consistent in the MS/MS spectra of a number of compounds including BZP, DBZP, MBCP, EBCP and benzyl chloride. Some general rules that have been applied in the interpretation of the spectra include common product ions such as $[M+H-NH_3]^+$ for primary amines, $[M+H-HCN]^+$, $[M+H-CH_3OH]^+$, $[M+H-HF]^+$ and $[M+H-HCl]^+$ ¹²⁵.

6.4 Conclusions

In most of the piperazine sample tested, the by-products/impurities were detectable using DESI-MS. In the case of TFMPP 3, piperazine was detectable using DESI-MS and not GC-MS or LC-MS. Bis(2-chloroethyl)amine remained undetectable in MeOPP 1 using DESI-MS or LC-MS. The identification of by-products and impurities present in these samples is highly indicative of the starting materials used and also the synthetic route of manufacture.

Chapter 7: Analysis of cathinone analogues

Chapter 7: Analysis of cathinone analogues

7.1 Introduction

The DESI-MS analysis of 4-MMC and the effects of common adulterants on the detectability of 4-MMC are detailed in this chapter. The impurities/by-products identified using DESI-MS in the synthesised 4-MMC samples (section 2.2.1) are compared to the results obtained with GC-MS and LC-MS. A quantitative DESI-MS technique was applied to the purity determination of the synthesised 4-MMC samples (M1 - M4). The optimal IS (type and concentration) was determined for quantitative experiments. The quantitative nature of the developed method was used in the context of a preliminary analysis technique. These quantitative results could greatly assist in the early detection and analysis of seized 4-MMC samples in real casework. A study evaluating the selectivity of the DESI-MS technique to the detection of 4-MMC was also conducted based on differentiating compounds with the same molecular mass using MS/MS spectra.

7.2 Materials and methods

7.2.1 Selectivity study

4-Methylmethcathinone was adulterated with caffeine, paracetamol, MA, phentermine, AP, MDMA, 4-OH-AP, 4-F-AP, nordiazepam, diazepam, oxazepam, cocaine, heroin, methadone, methylone, cathine, cathinone, 4-(diethylamino)benzaldehyde (4-DEAB) and 1-benzyl-3-pyrrolidinol (1B3P) in 1:1 ratios in order to evaluate the effects of adulterants on the detectability of 4-MMC and to evaluate the selectivity of the developed DESI-MS method to 4-MMC. See section 2.2 for more method details.

7.2.2 DESI-MS method validation

For the quantitative application of the DESI-MS technique, linearity of the calibration curve (50 – 800 µg/mL, applied to PTFE wellled slide) was calculated using a line of best fit with correlation factor expected to be >0.98. The IS, codeine-D₆, was added to the solvent line for

DESI-MS analysis at a concentration of 0.25 µg/mL. Intra-day and inter-day precision and accuracy studies were carried out using quality control samples spiked with 90 and 500 µg/mL ($n = 5$ and $n = 15$, triplicate on five days, respectively). In this study, accuracy was deemed acceptable if the calculated concentration fell within 15 % relative error (% RE) of the concentration spiked. Precision was deemed acceptable if the % RSD was within 40 %. Precision was determined as the relative standard deviation (% RSD = $100(\text{SD}/\text{M})$), and accuracy as the relative error (% RE = $[(100/C_{\text{the}}) \cdot (C_{\text{the}} - \text{M})]$), where M is the mean of the experimentally determined concentrations, SD is the standard deviation and C_{the} is the theoretical concentration. The limit of detection (LOD, 8 µg/mL) was the lowest concentration of analyte that gave a SNR of 3:1. The limit of quantification (LOQ, 50 µg/mL) was the lowest concentration of analyte that gave a SNR of at least 10:1. The upper limit of quantification was 800 µg/mL (Table 7-1). A representative calibration curve is provided in Figure 7-1. For the qualitative DESI-MS experiments the LOD was defined to be the lowest concentration required to give a signal equal or greater than the average intensity of the blank signal plus three times the SD of the blank (mean + 3SD)⁸⁰.

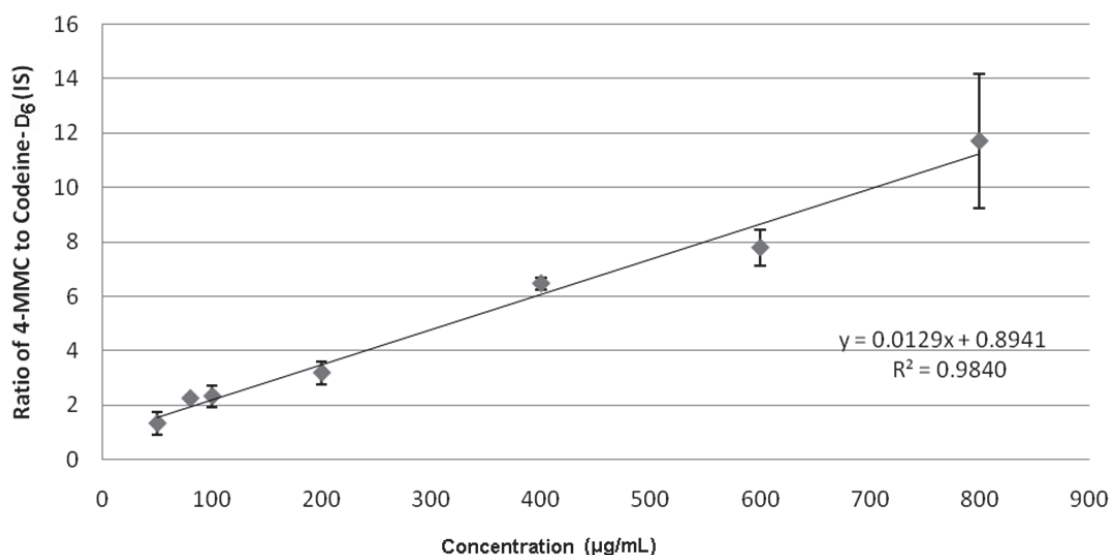


Figure 7-1 DESI-MS calibration curve for 4-MMC, $n=3$.

Technique	Analysis (mins)	Calibration Curve				QC's ($\mu\text{g/mL}$)	Intra-day, n=5		Inter-day, n=15 (triplicate, 5 days)	
		Linearity (R^2)	LOD ($\mu\text{g/mL}$)	LOQ ($\mu\text{g/mL}$)	LOL ($\mu\text{g/mL}$)		Accuracy \pm (% RE)	Precision % RSD	Accuracy \pm (% RE)	Precision % RSD
DESI-MS	1	0.9840	8	50 (12.3 % RE, 25.1 % RSD)	800	500	0.29	27.4	7.15	31.8
						90	4.88	37.3	1.68	33.2
GC-MS	11	0.9991	2	5 (11.7 % RE, 3.44 % RSD)	400	105	1.36	10.4	5.20	12.0
						25	9.99	0.37	13.0	6.56
LC-MS	25	0.9988	0.01	0.1 (8.97 % RE, 2.13 % RSD)	8	5	0.39	10.9	4.16	11.9
						0.8	5.22	12.4	10.3	13.8

Table 7-1 Statistical comparison of DESI-MS, GC-MS, and LC-MS in the analysis of 4-MMC.

7.2.3 GC-MS method validation

For the quantitative application of the GC-MS technique, linearity of the calibration curve (5 - 400 $\mu\text{g/mL}$) was calculated using a line of best fit with correlation factor expected to be >0.99 . The IS, codeine- D_6 , was spiked into the calibrators and the quality check (QC) samples at a concentration of 10 $\mu\text{g/mL}$. Intra-day and inter-day precision and accuracy studies were carried out using QC samples spiked with 25 and 105 $\mu\text{g/mL}$ ($n = 5$ and $n=15$, triplicate on five days, respectively). Accuracy was deemed acceptable if the calculated concentration fell within 20 % (% RE) of the concentration spiked. Precision was deemed acceptable if the % RSD was <15 %. The LOD was the lowest concentration of analyte that still gave a SNR ratio of 3:1. The LOQ was the lowest concentration of analyte that gave a SNR of at least 10:1. The upper limit of quantification was 400 $\mu\text{g/mL}$ (Table 7-1). A representative calibration curve is provided in Figure 7-2.

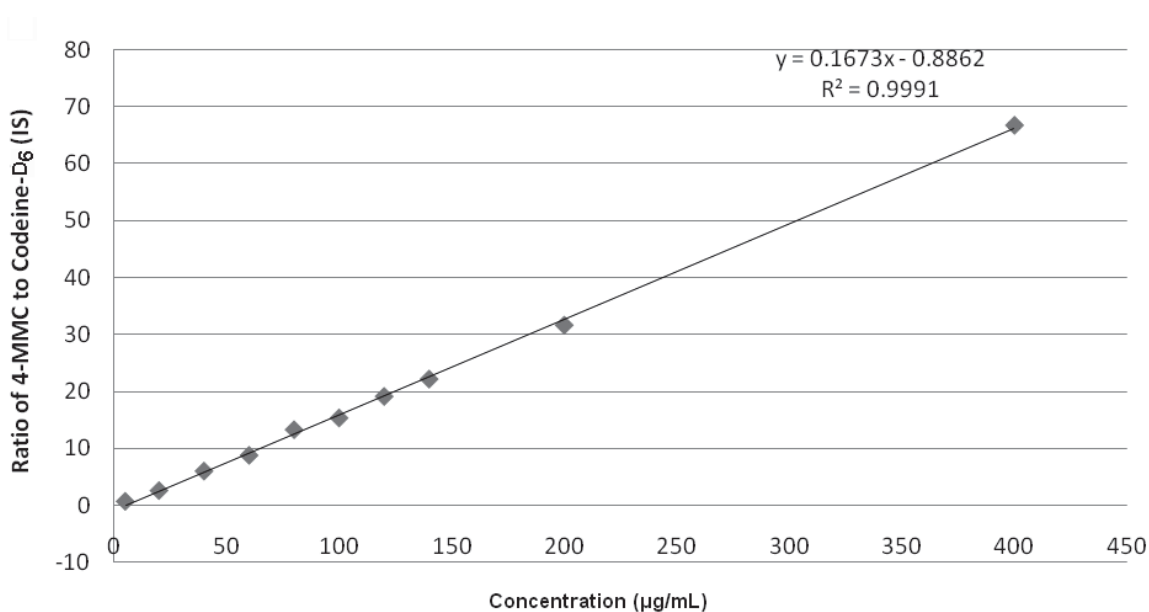


Figure 7-2 GC-MS calibration curve for 4-MMC, $n=3$ (GC method 1).

7.2.4 LC-MS method validation

For the quantitative application of the LC-MS technique, linearity of the calibration curve (0.1 - 6 µg/mL) was calculated using a line of best fit with correlation factor expected to be >0.99. The IS, codeine-D₆, was spiked into the calibrators and the QC samples at a concentration of 1 µg/mL. Intra-day and inter-day precision and accuracy studies were carried out using QC samples spiked with 0.8 and 5 µg/mL (n = 5 and n=15, triplicate on five days, respectively). Accuracy, precision, LOD and LOQ were as defined for GC-MS. The upper limit of quantification was 8 µg/mL (Table 7-1). A representative calibration curve is provided in Figure 7-3.

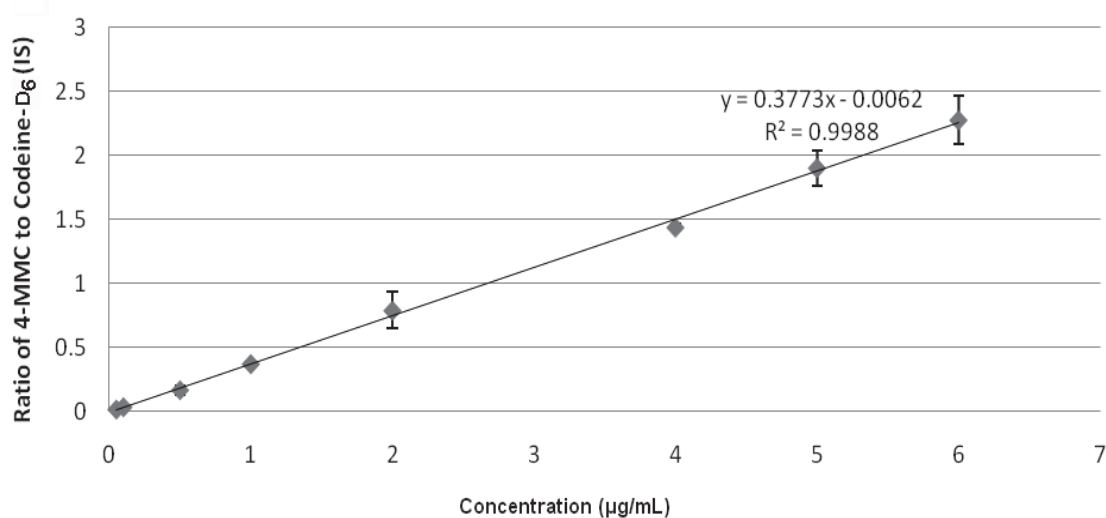


Figure 7-3 LC-MS calibration curve for 4-MMC, n=3.

7.3 Results and discussion

7.3.1 Qualitative analysis

7.3.1.1 Desorption electrospray ionisation – mass spectrometry

According to the characterisation performed on the four synthesised 4-MMC samples (section 2.2.1), a table was compiled detailing the by-products identified in each sample (Table 7-2). It was evident that the by-products and impurities that appear in M1 and M2 are the same due to the amination process utilised during synthesis (using triethylamine). Similarly, M3 and M4 also exhibit the same by-products and impurities due to a common amination reaction being conducted. The four synthesised samples were subject to DESI-MS analysis in order to identify as many by-products/impurities as possible in an attempt to profile the 4-MMC samples.

Table 7-2 List of by-products found in synthesised 4-MMC samples with corresponding m/z values.

Sample ^a	By-products of reaction	Mass to charge m/z
M1	triethylamine, 4-methylpropiofenone (trace)	101, 148
M2	triethylamine, 4-methylpropiofenone (trace)	101, 148
M3	methylamine, 4-methylpropiofenone (trace), 2-bromo-4-methylpropiofenone (trace)	31, 148, 227
M4	methylamine, 4-methylpropiofenone (trace), 2-bromo-4-methylpropiofenone (trace)	31, 148, 227

The four spectra below (Figure 7-4) all exhibit the product peak at m/z 178 $[M+H]^+$ confirming the presence of 4-MMC in these samples. The identification of this product peak was further discriminated by performing MS/MS on the target ion^{30, 164} (Figure 7-5 - Figure 7-7). A library search was performed on the MS/MS spectra and a match score of 77 supported the product as being 4-MMC (Figure 7-8). The presence of triethylamine at m/z 102 $[M+H]^+$ in M1 and M2 was further supported by MS/MS spectra (Figure 7-5).

Methylamine and 2-bromo-4-methylpropiofenone were not detected by DESI-MS in M3 and M4; this can be attributed to their presence in trace quantities and due to the lack of sensitivity of the DESI-MS technique. The presence of a large triethylamine peak in a sample of 4-MMC was highly indicative of the amination route utilising triethylamine as a catalyst in the synthetic reaction (samples M1 and M2). This information can be useful in the preliminary profiling of 4-MMC samples.

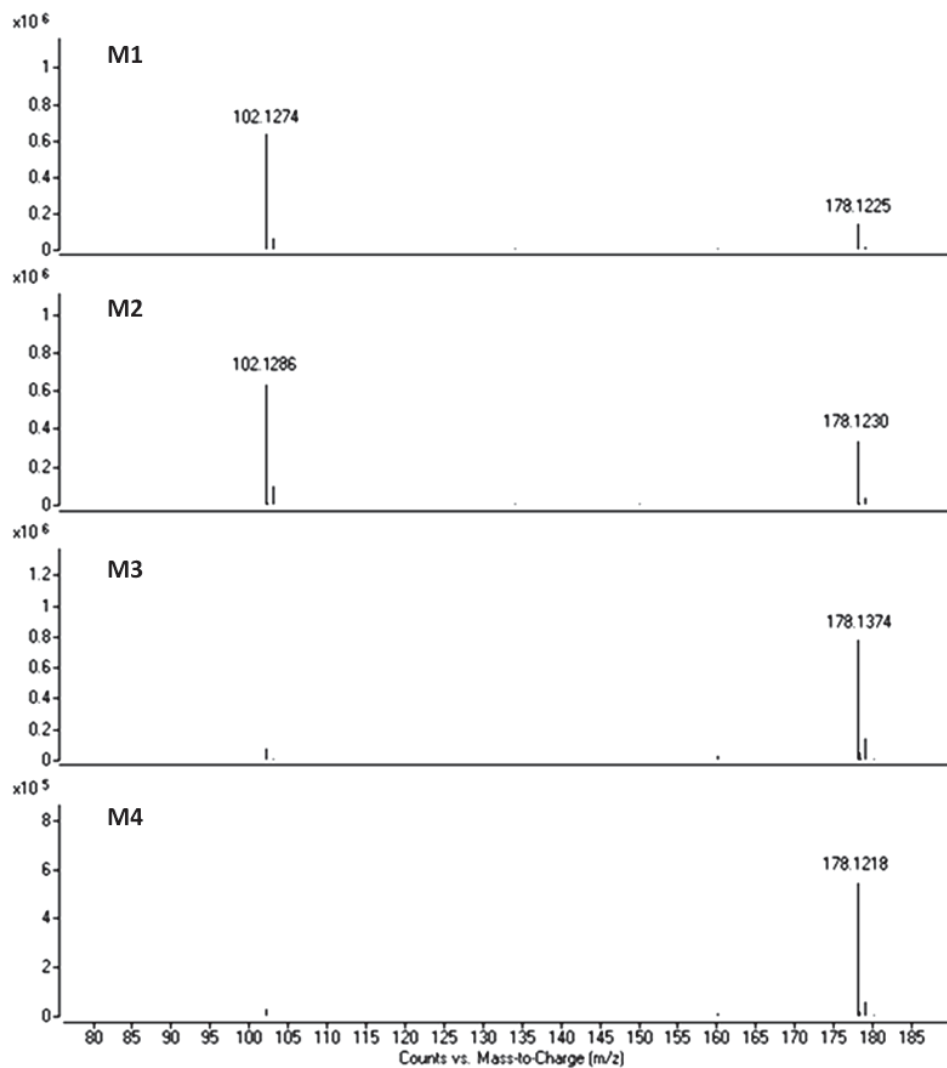


Figure 7-4 DESI-MS of 4-MMC (M1, M2, M3 and M4) in positive ion mode.

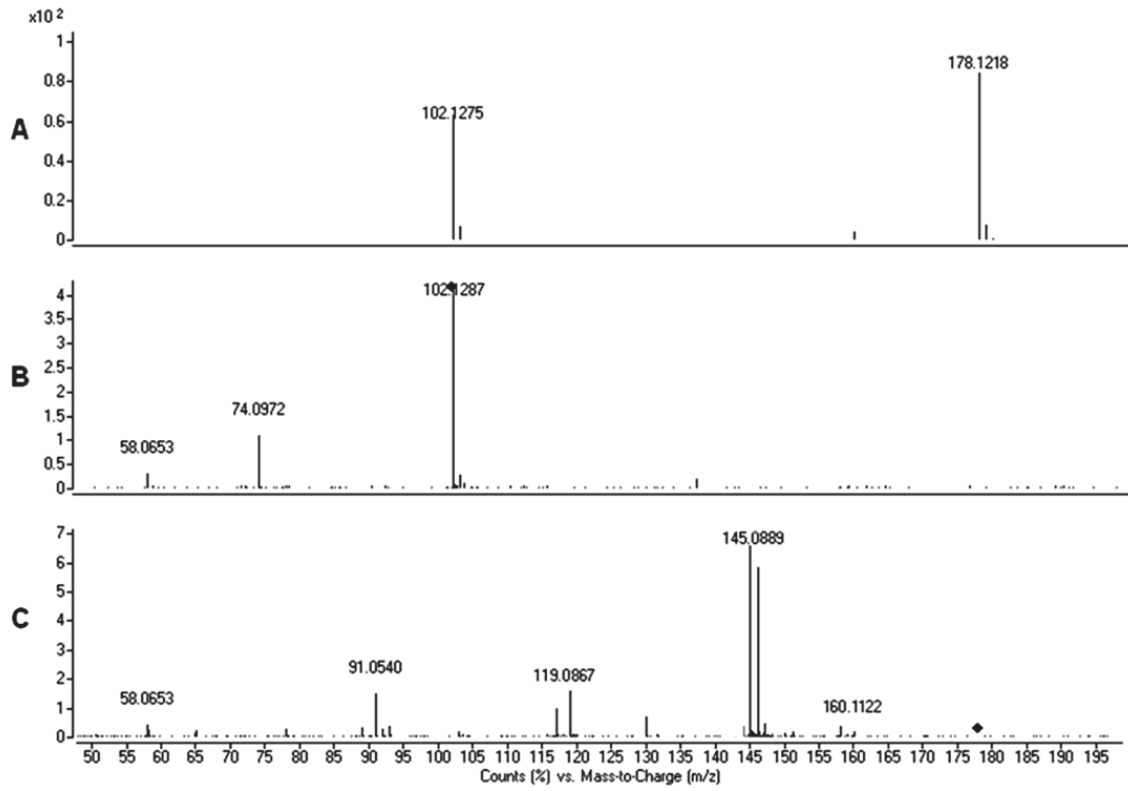


Figure 7-5 A: MS of 4-MMC, B: MS/MS spectra of triethylamine, C: MS/MS spectra of 4-MMC product ion at m/z 178 in positive ion mode at 30 eV.

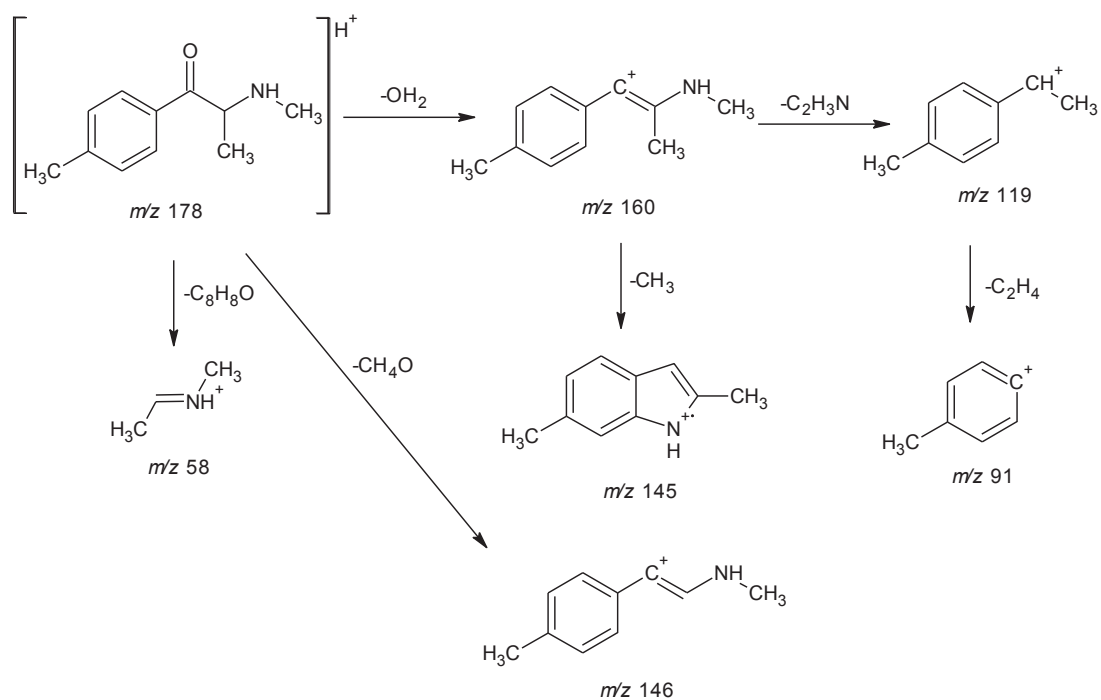


Figure 7-6 Proposed collision induced dissociation of the [M+H]⁺ ion of 4-MMC.

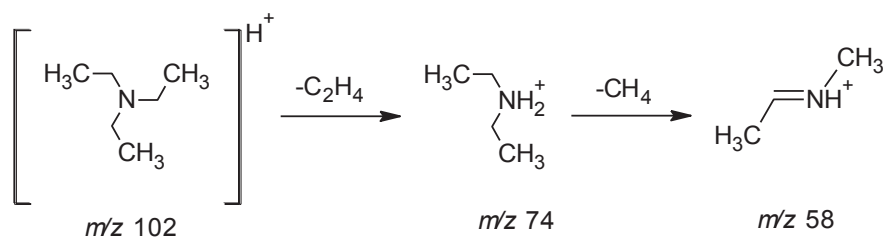


Figure 7-7 Proposed collision induced dissociation of the [M+H]⁺ ion of triethylamine.

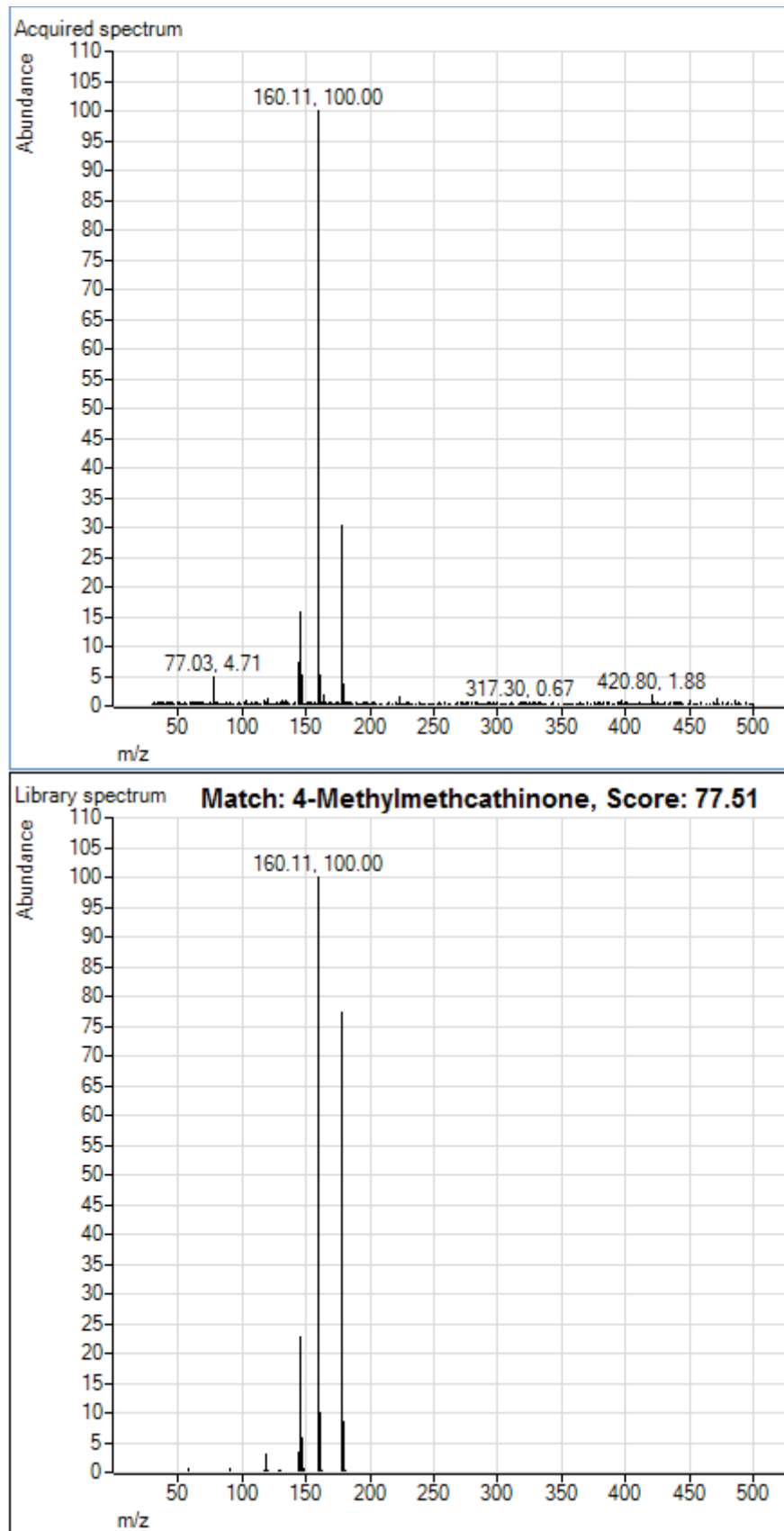


Figure 7-8 PCDL library match to 4-MMC.

7.3.1.2 Gas chromatography – mass spectrometry

The synthesised 4-MMC samples were subject to GC-MS analysis in an attempt to identify any by-products/impurities resulting from synthesis. M1, M2 and M3 did not exhibit any significant by-products/impurities in the GC-MS chromatogram obtained; however, 4-methylpropiofenone was found in trace amounts in all the samples tested as unreacted starting material. M4 was found to contain 4-methylpropiofenone (starting material) eluting at 3.6 minutes, and also 2-bromo-4-methylpropiofenone (as an intermediate) that eluted at 4.1 minutes (Figure 7-9, Figure 2-15, Figure 2-18). The presence of 4-MMC was supported by the mass spectra obtained (Figure 7-10); and the proposed EI fragmentation pathway (Figure 7-11). Triethylamine and methylamine remain undetected using GC-MS due to the high temperature program employed (starting at 100 °C) suggesting that these compounds may have eluted prior to 2 minutes.

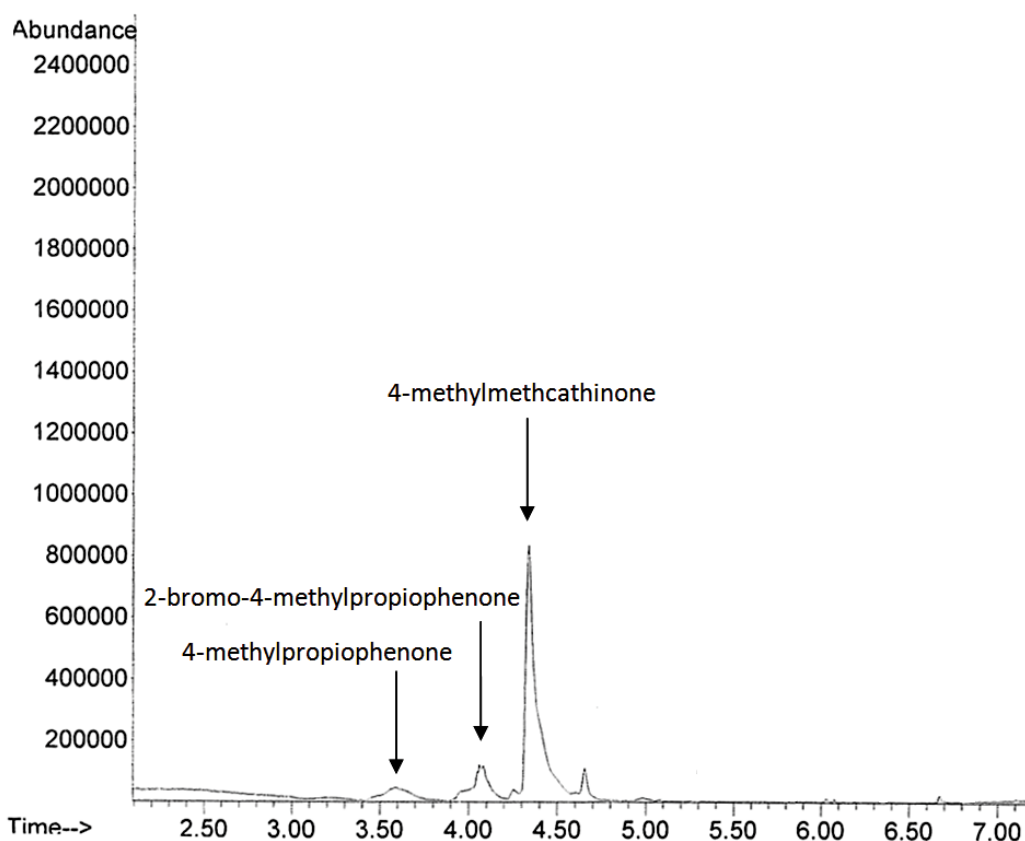


Figure 7-9 GC-MS chromatogram of 4-MMC (M4) at 4.4 minutes, 2-methylpropiofenone at 3.6 minutes, 2-bromo-4-methylpropiofenone at 4.1 minutes (GC method 1).

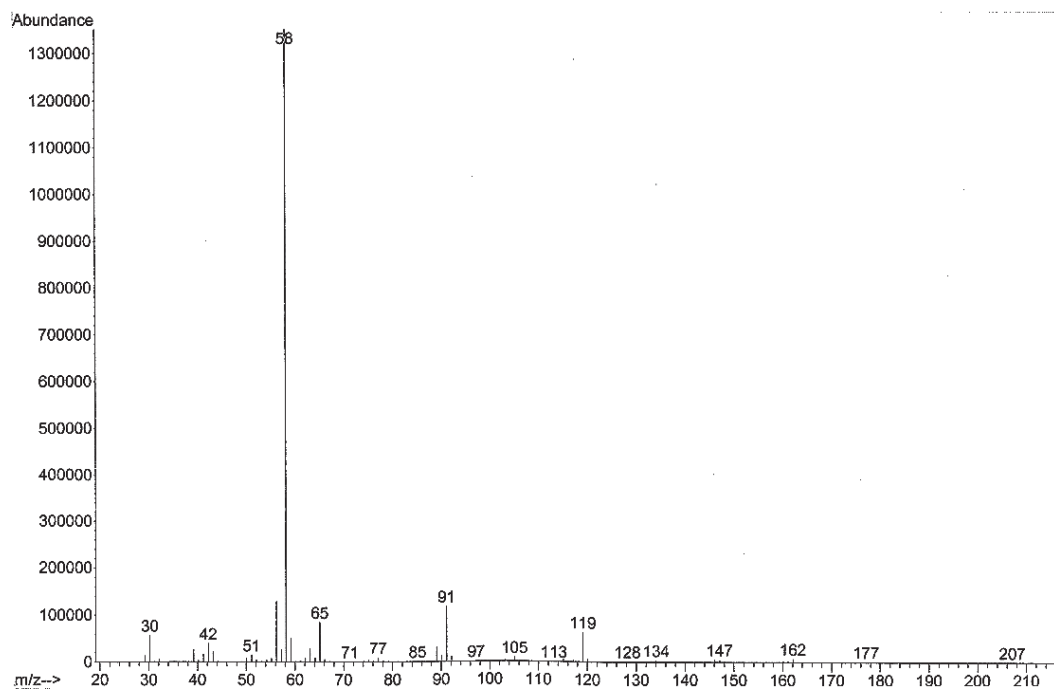


Figure 7-10 EI mass spectra of 4-MMC (GC method 1).

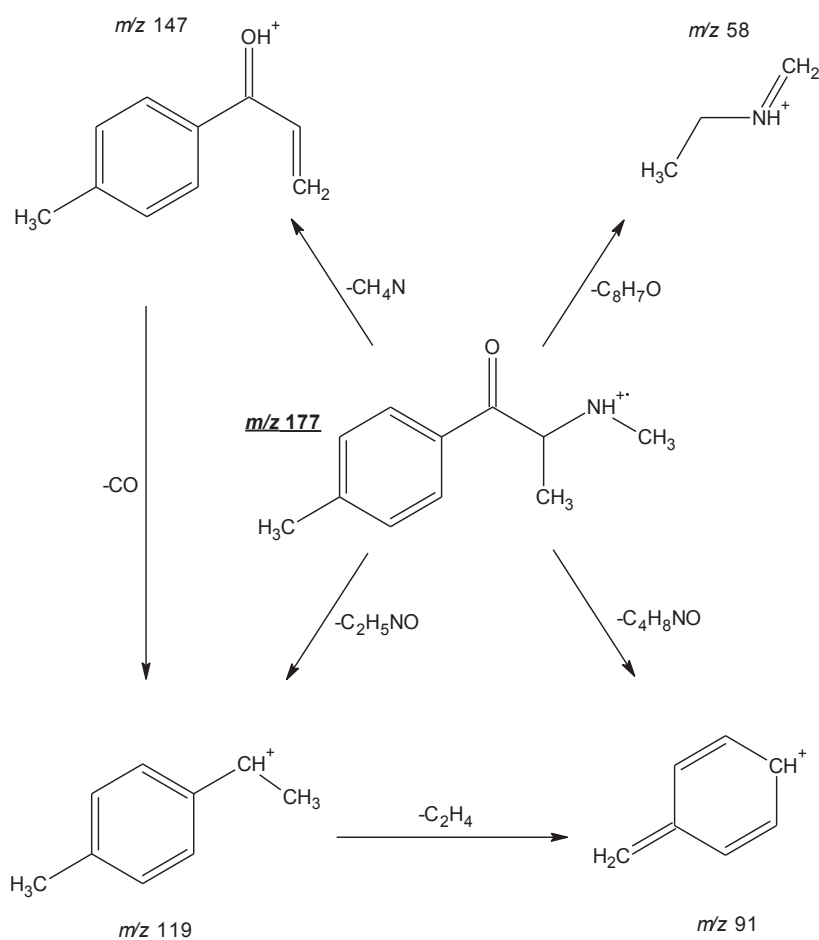


Figure 7-11 Proposed EI fragmentation pathway of 4-MMC.

7.3.1.3 Liquid chromatography – mass spectrometry

Analysis by LC-MS identified the major product 4-MMC in all four samples (M1 – M4); however, it did not reveal any by-products or impurities resulting from the synthesis reactions (Figure 7-12). This was hypothesised to be due to the gradient separation only being optimised for the parent compound 4-MMC, and the IS codeine-D₆, therefore other compounds present may have eluted later in the run or co-eluted and were not separated efficiently enough for an identification to take place.

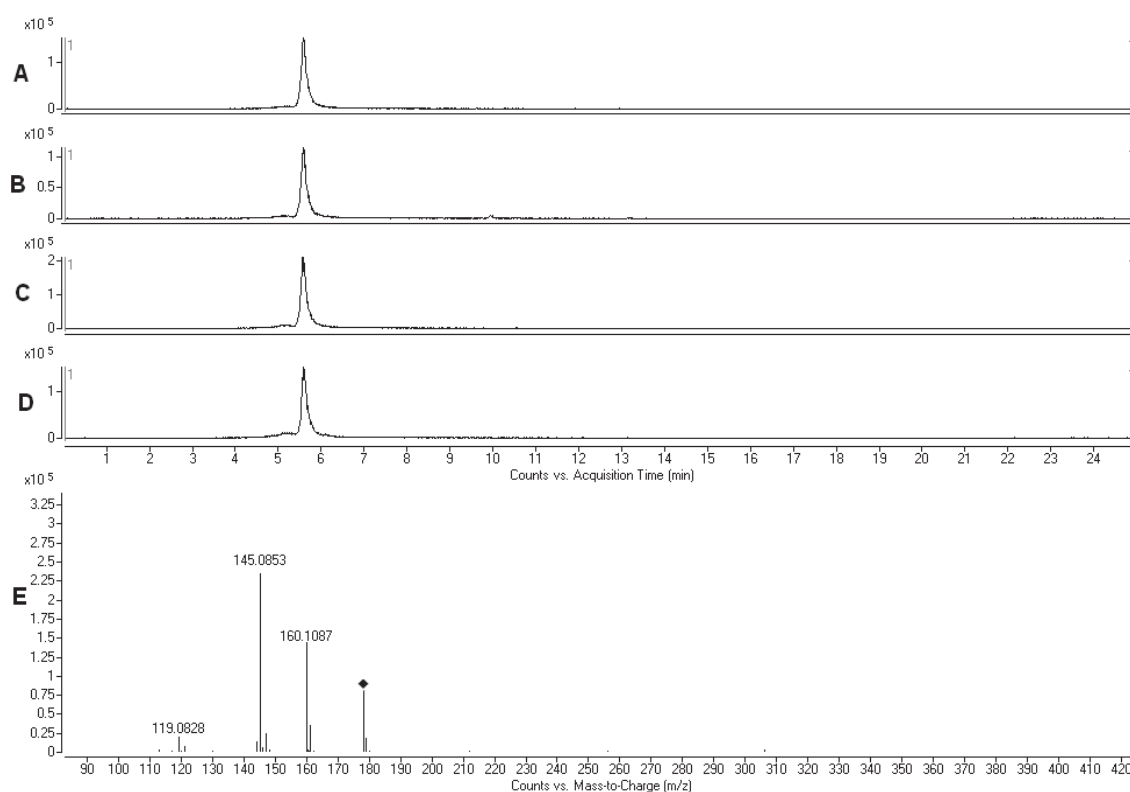


Figure 7-12 LC-MS chromatogram of 4-MMC A: EIC of M1 at 5.7 minutes, m/z 178; B: EIC of M2; C: EIC of M3; D: EIC of M4; E: LC-MS/MS of 4-MMC at 20 eV.

7.3.2 Selectivity study

It is important to consider the selectivity of a technique when developing a fast preliminary identification technique, since the compound of interest should still be detectable in a mixture of compounds. In the case of DESI-MS, one major concern is matrix effects. In multi-component samples of high concentrations, competition for either space or charge is likely to

occur and, in turn, suppression of signal is observed. Both the characteristics and concentration of an analyte determine the efficiency of its ionisation. The characteristics that decide whether a compound will out-compete others for the limited charge or space on the surface of the droplet include its surface activity and its basicity⁷⁸.

A pilot study was conducted using 4-MMC, caffeine and paracetamol, followed by a mixture of 4-MMC, caffeine, and paracetamol with codeine-D₆ in order to assess the selectivity to 4-MMC. It was apparent that the signal responses for 4-MMC, caffeine and paracetamol were reduced, due to ion suppression, when codeine-D₆ was added to the mixture (Figure 7-13).

If we consider the basicity of the samples tested, 4-MMC is a basic compound (pK_a = 8.69⁴⁶) and is easily ionisable in the ESI spray. In contrast, caffeine and paracetamol (pK_a = 14.0 and 9.9, respectively¹⁶⁵) are relatively less basic, therefore, 4-MMC will be preferentially ionised. This phenomenon was apparent in the reduced responses observed for caffeine and paracetamol (Figure 7-13 B).

In the presence of a mixture of compounds, the selectivity of 4-MMC was not compromised to a great degree, suggesting that it may still be analysed in mixtures. This pilot study was expanded to include a broad range of compounds in order to evaluate the matrix effects in different combinations of compounds with varying basicity (Figure 7-14 and Figure 7-15). These mixtures were prepared by mixing 4-MMC with equal portions of single or multiple cutting agents such as caffeine alone, caffeine and paracetamol, and a number of other licit and illicit materials.

The 4-MMC signal response was suppressed in most mixtures tested, more so when there were highly basic compounds present in the mixture such as phentermine, 4-F-AP and cathinone as these compounds compete strongly for charge/ionisation in the source (Figure 7-15).

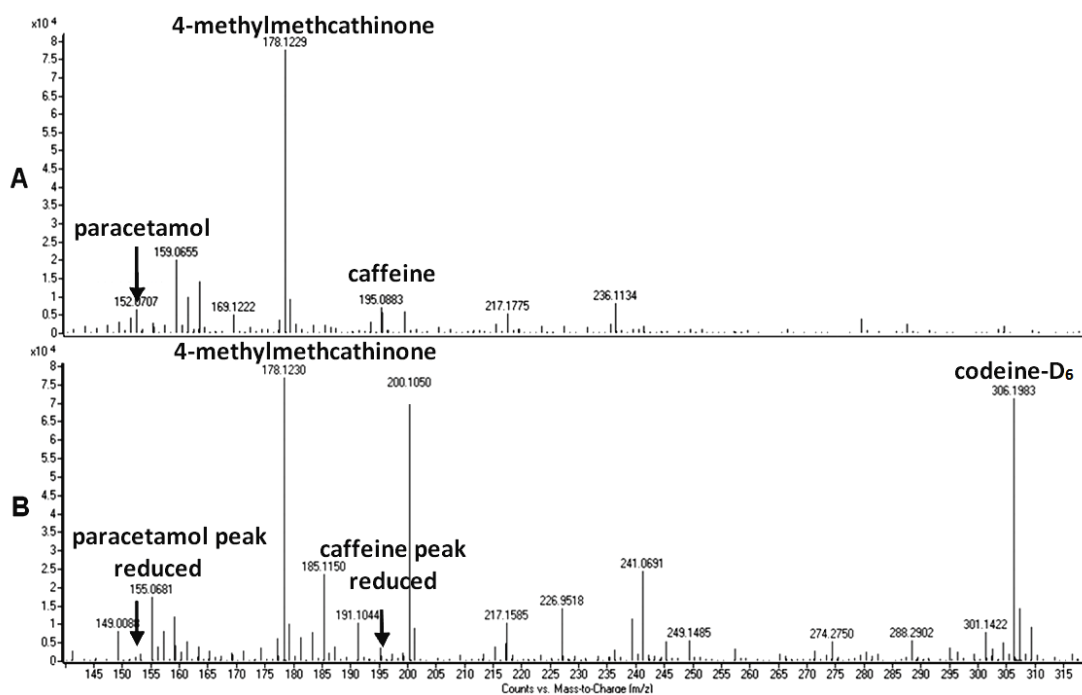


Figure 7-13 DESI-MS spectra of **A**: 4-MMC, caffeine and paracetamol as a mixture; **B**: 4-MMC, caffeine, paracetamol and codeine- D_6 as a mixture.

The least suppression was evident in mixtures of caffeine alone (14 % enhancement, mixture 1) or with caffeine and paracetamol (45 % suppression, mixture 2); with the highest level of suppression observed for mixtures of highly basic compounds such as 4-F-AP (94 % suppression, mixture 6) and cathinone (95 % suppression, mixture 10). Ion suppression was also noted for most adulterants/diluents. The ion suppression was most severe for 4-OH-AP, diazepam and oxazepam and they became undetectable in the mixtures tested (mixtures 6 and 7). Some basic compounds, such as AP and MDMA, did not fluctuate dramatically in signal response, with slight enhancement present for AP (2 %, mixture 5) and only 30 % suppression present for MDMA (mixture 5).

A general trend in the selectivity of DESI-MS is that more basic compounds are easily ionisable and in turn are easily detected, whereas the acidic compounds do not ionise as readily and are therefore suppressed in mixtures containing basic compounds. It was also evident that increasing the number of compounds in mixtures will in turn increase the amount of suppression present (i.e. increased matrix effects).

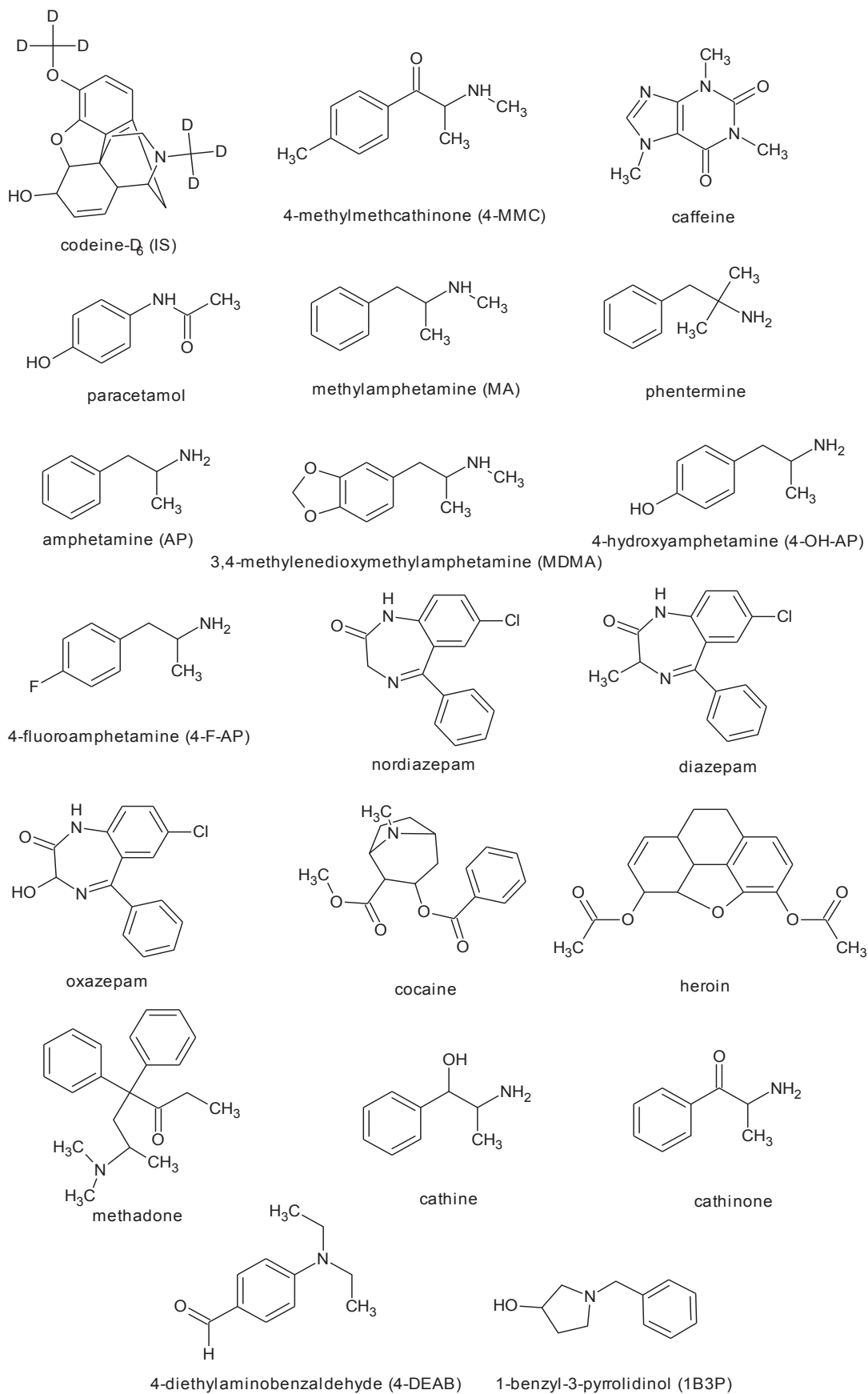
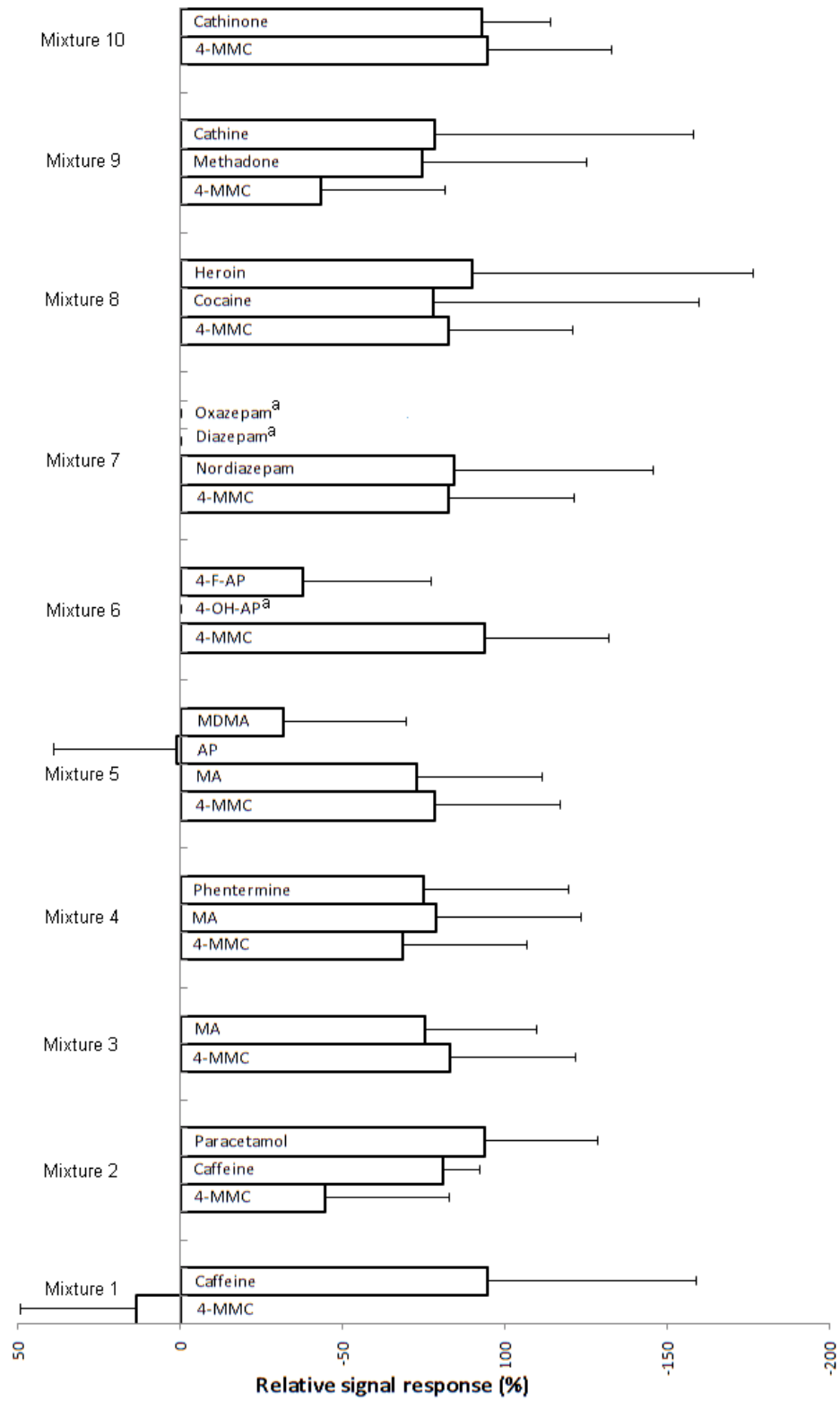


Figure 7-14 Structure of drug compounds used in selectivity study.



^a These compounds were not detected in these mixtures.

Figure 7-15 Ion suppression/enhancement present in different mixtures analysed using DESI-MS.

When using calibration curves for quantifying compounds, it is best to use a pure standard in order to obtain the highest linearity possible. The linearity obtained using DESI-MS in the calibration of a 4-MMC standard was 0.9840 (Figure 7-1). It was speculated that when 4-MMC is present in a mixture, the signal response may no longer be reproducible since multiple compounds are competing for ionisation in the DESI source. This hypothesis was tested with a mixture of 4-MMC, caffeine and MA spiked with IS. As seen in Figure 7-16 the linearity of the calibration curve in the mixture of compounds was highly compromised due to competition for charge in the source.

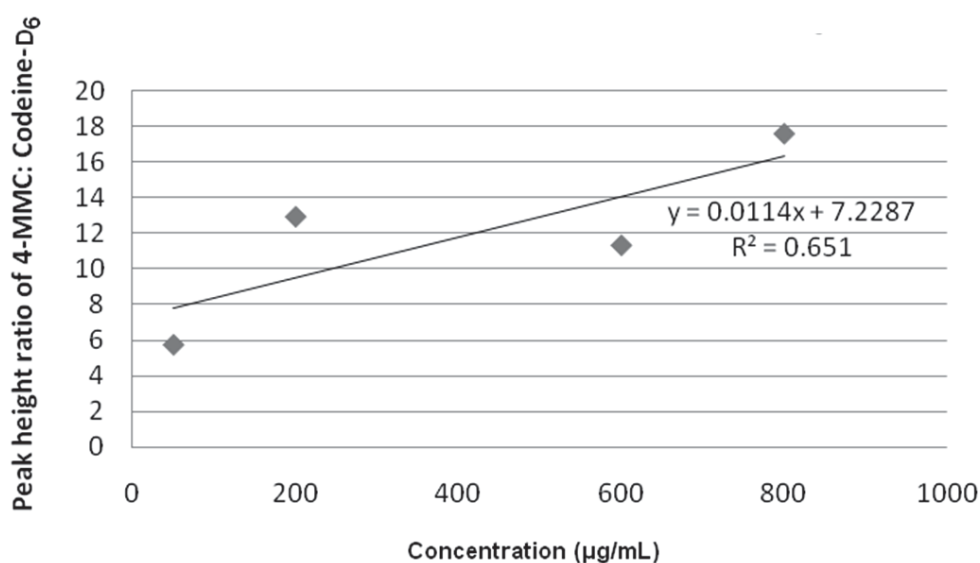


Figure 7-16 Calibration curve for 4-MMC in a mixture of caffeine and MA.

Quantification of M1 was conducted using both calibration curves. The accuracy as determined by the 'pure' calibration curve was within 4 % of the concentration tested. However, when quantifying the same sample using a calibration curve obtained from a mixture of 4-MMC, caffeine and MA, the result was inaccurate (accuracy was 62 % of the concentration tested, Table 7-3). The main contributing factor to the inaccuracy of quantifying mixtures was thought to be the ion suppression present when analysing mixtures of compounds. In the mixed sample of 4-MMC, caffeine, and MA, the 4-MMC signal was enhanced since it is a relatively basic compound.

Table 7-3 Calculated concentrations of M1 using pure and mixed calibrator calibration curves.

Sample	4-MMC ^a peak height (cps)	codeine-D ₆ ^a peak height (cps)	Ratio of peak height of 4-MMC to codeine-D ₆	Calculated concentration (µg/mL)	Accuracy (% RE)
M1	6976	1018	6.85	259.3	3.70
M1 + Caffeine + MA	26028	18595	1.40	94.6	62.2

^aTarget concentration 250 µg/mL.

7.3.2.1 4-Methylmethcathinone and methylone

Methylone is significant in this research as it has been seized in many illicit drug samples and is used as a substitute to illicit MDMA in street samples. A mixture of cathinones, namely 4-MMC and methylone (3,4-methylenedioxy-*N*-methylcathinone, bk-MDMA, Figure 7-17) was tested in order to evaluate whether both compounds would be detectable in a mixture using DESI-MS and if any significant ion suppression would be present.

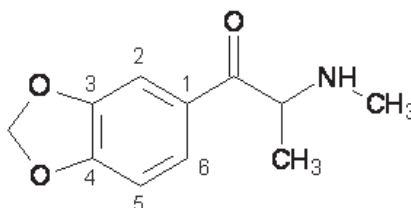


Figure 7-17 Molecular structure of methylone.

Based on the DESI-MS spectra obtained for the two cathinones (500 µg/mL) both compounds were readily detectable (Figure 7-18). 4-MMC was detected as the protonated molecular ion $[M+H]^+$ at m/z 178 and bk-MDMA at m/z 208. In addition, the IS (codeine-D₆) was present at m/z 306. 4-MMC and bk-MDMA have similar pK_a values at 8.69 and 7.74, respectively. This suggests that they will both compete strongly for ionisation in the source and this was reflected in the spectra obtained.

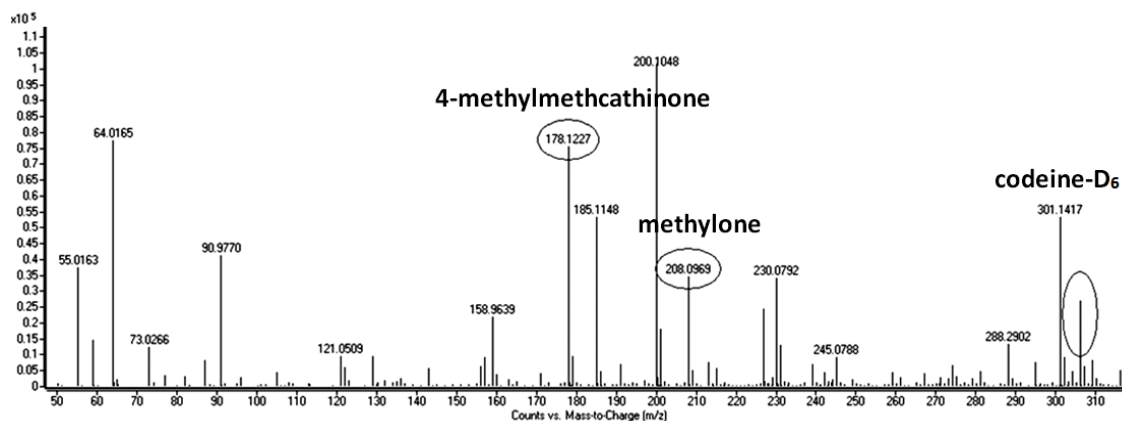


Figure 7-18 DESI-MS spectra of 4-MMC and methyldone (with codeine- D_6 IS).

Further to the MS spectrum obtained above, MS/MS experiments were conducted on 4-MMC and bk-MDMA in order to further discriminate these compounds. It was evident that there were some differences in the fragmentation data for the two compounds and this aided in identification (Figure 7-19). The proposed collision induced dissociation of the $[M+H]^+$ ion for bk-MDMA is presented in Figure 7-20.

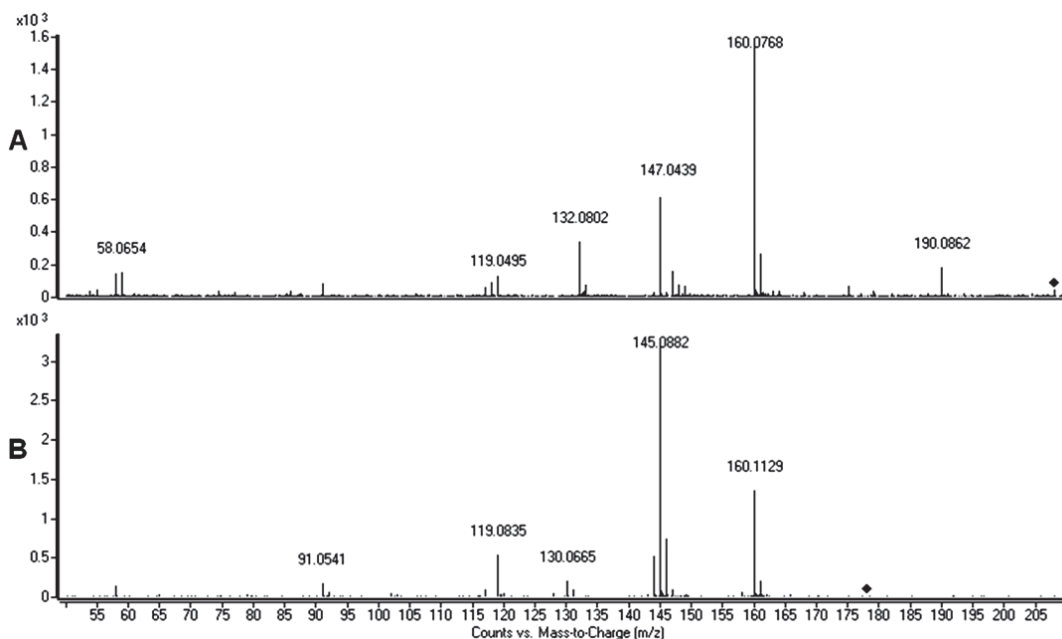


Figure 7-19 DESI-MS/MS spectra of A: methyldone, B: 4-MMC at 20 eV.

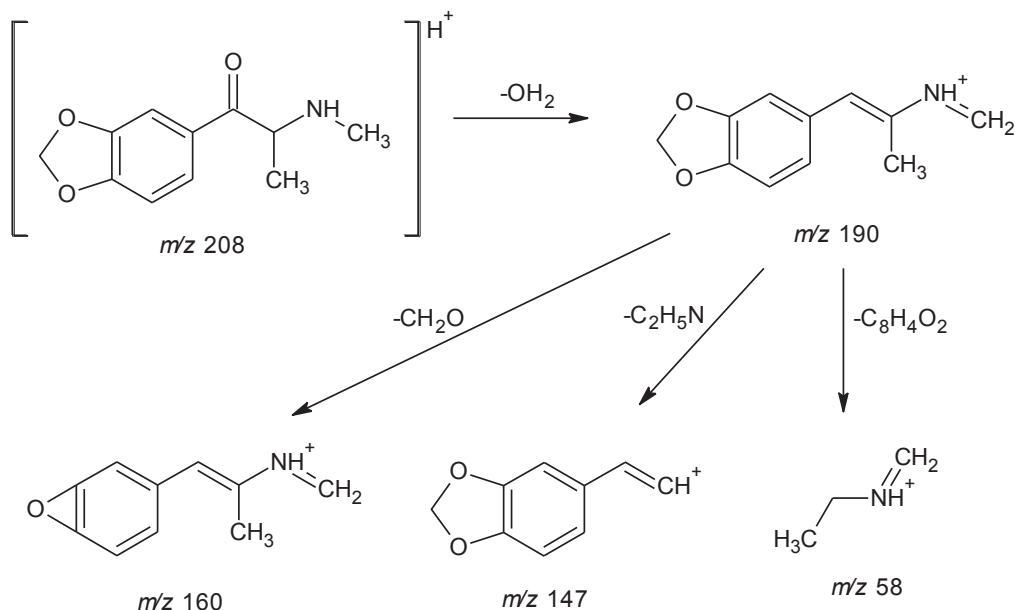


Figure 7-20 Proposed collision induced dissociation of the $[M+H]^+$ ion of methylene.

7.3.2.2 Differentiating compounds based on MS/MS spectra

Since DESI-MS is not an analytical separation technique, all of the components in a mixture are detected simultaneously, giving rise to a mixed mass spectrum. This in turn leads to matrix effects and results in compounds with the same molecular formula being indistinguishable. Fragmentation data can aid in discriminating two compounds with the same chemical formula, and thus same molecular mass.

The DESI-MS analysis was conducted on a mixture of 4-MMC and 4-DEAB; both protonated molecular ions were present at m/z 178. The compounds were detected as one peak in the DESI-MS spectrum and were indistinguishable. However, on examining the MS/MS spectrum of the individual compounds (Figure 7-21 A and B) and also a combination of the two (Figure 7-21 C), differences were apparent which may suggest that a mixture was present.

The fragmentation spectra for 4-MMC exhibited two characteristic peaks at m/z 145 and 160 which were absent in the fragmentation spectra for 4-DEAB (Figure 7-22 B). Further to this the spectra obtained for the mixture of these two compounds also exhibited peaks at m/z 145 and 160 which suggests the presence of 4-MMC. 4-DEAB exhibited two characteristic peaks at m/z 122 and 134. These two compounds pose similar fragmentation spectra and are

therefore difficult to distinguish in a mixture; however, a close assessment of the peak heights in the mixed spectra indicated a combination of the two.

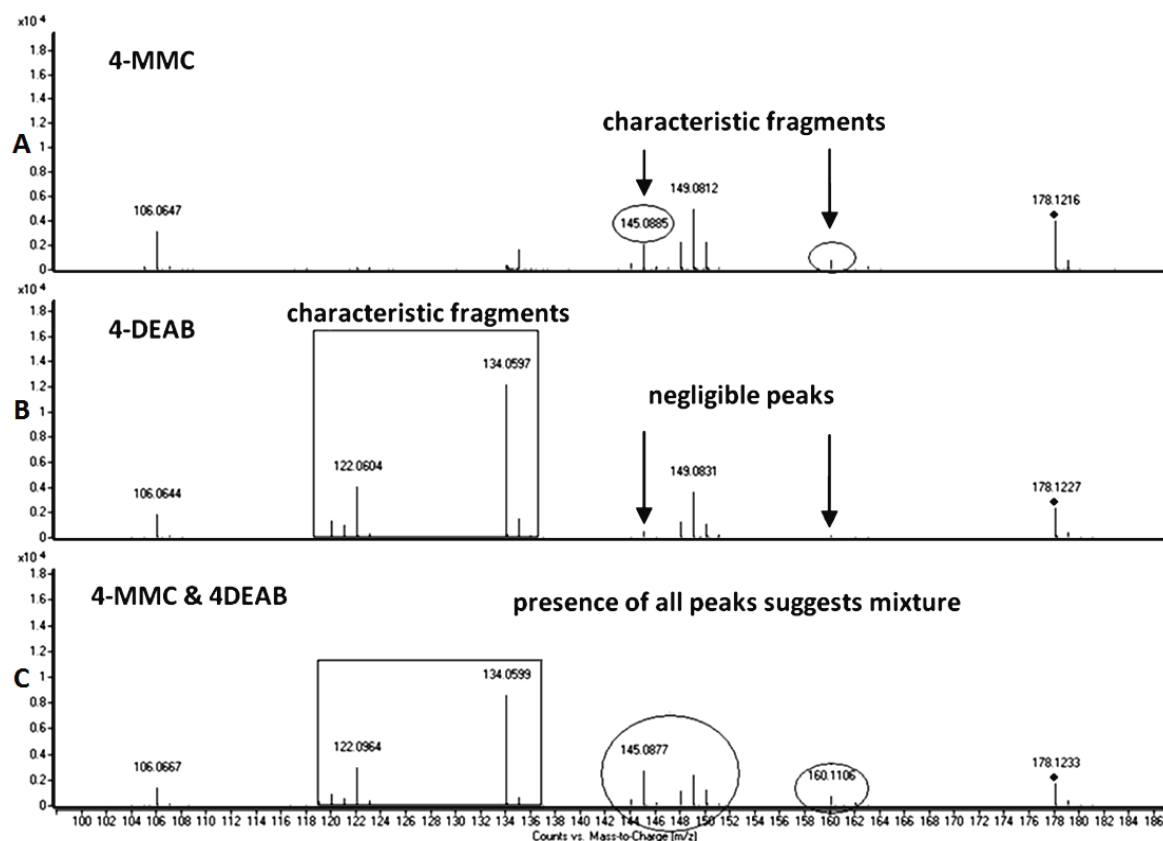


Figure 7-21 DESI-MS/MS spectra for A: 4-MMC, B: 4-DEAB, C: mixture of 4-MMC and 4-DEAB at 20 eV.

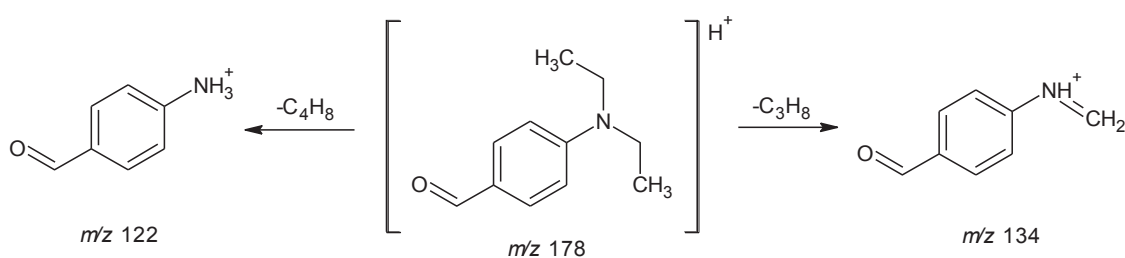


Figure 7-22 Proposed collision induced dissociation of the $[M+H]^+$ ion of 4-DEAB.

1-Benzyl-3-pyrrolidinol was also tested to evaluate whether it could be distinguished from 4-MMC based on fragmentation spectra. 1B3P has a protonated molecular mass of 178 Da. The fragmentation spectra obtained for 1B3P did not exhibit fragments at m/z 145 and 160 as were present in the 4-MMC spectra (Figure 7-23 A and B). The presence of a peak at m/z 65

may indicate 1B3P, absent in the 4-MMC spectra (Figure 7-24). The decrease in the peak height of m/z 145 and 160 relative to m/z 91 (larger in 1B3P spectra) suggested a mixture of the two compounds.

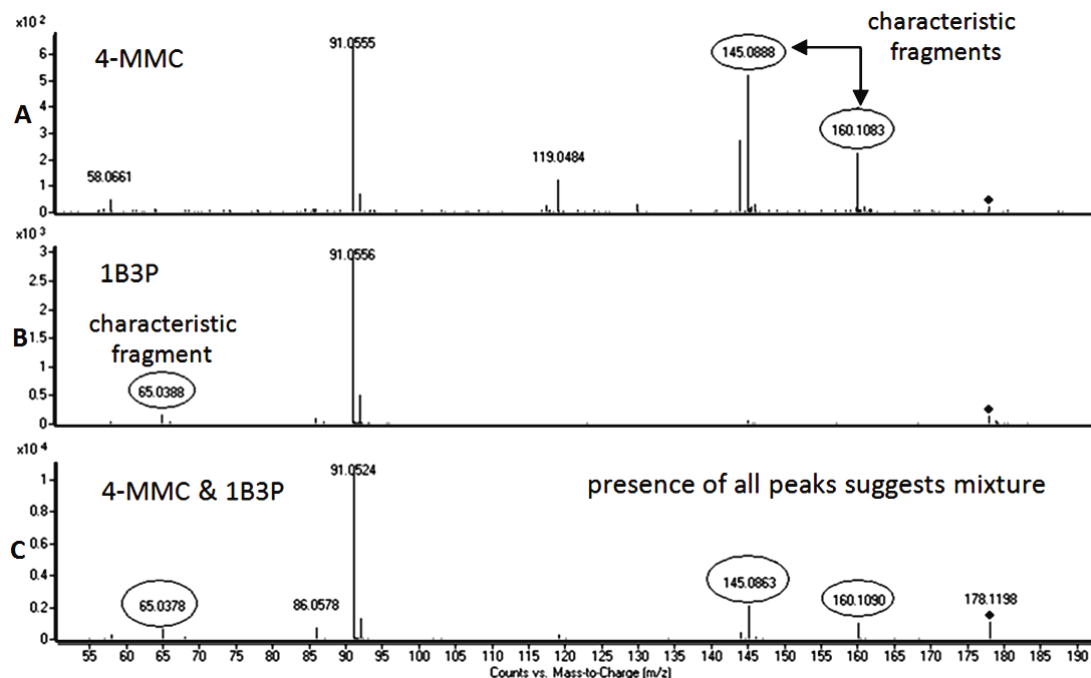


Figure 7-23 DESI-MS/MS spectra for A: 1B3P, B: 4-MMC, C: mixture of 4-MMC and 1B3P at 20 eV.

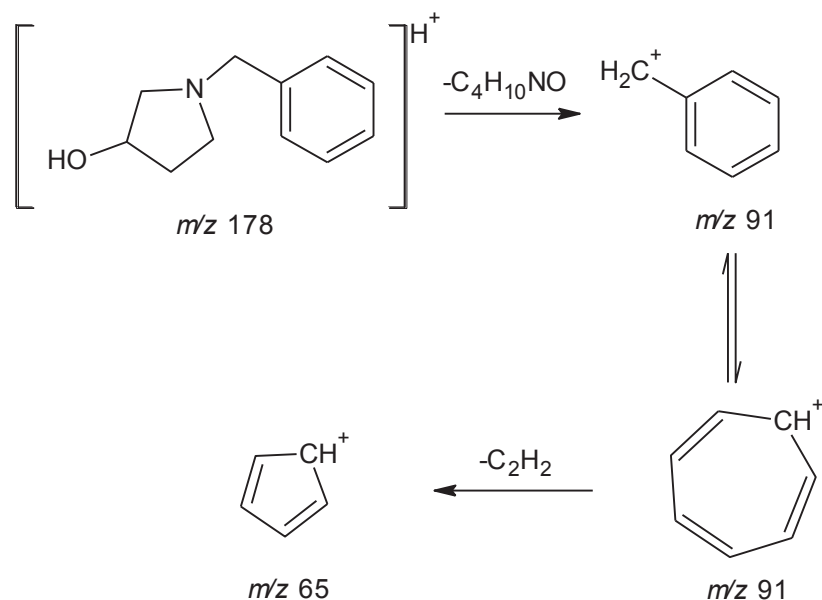


Figure 7-24 Proposed collision induced dissociation of the $[M+H]^+$ ion of 1B3P.

With the aid of MS/MS libraries, it is possible to determine whether the fragmentation spectra obtained is that of a pure compound or a mixture of compounds. The presence of characteristic fragments aid in determining which compounds are present. Some difficulties may arise when compounds with less characteristic fragments are present. For the purposes of illustrating the usefulness of fragmentation data, three compounds with the exact same molecular mass; 4-MMC, 4-DEAB and 1B3P were analysed in mixtures; however, in real drug samples it is unlikely that a mixture will contain compounds with the exact same molecular mass. Fragmentation data provides additional information and adds confidence to a compound match and should be used in all analyses to avoid false positive results.

7.3.3 Quantitative analysis

7.3.3.1 Internal standard

Codeine-D₆ and 4-MMC-D₃ were compared in order to assess the suitability of an IS for the quantitative experiments. When analysed using DESI-MS, codeine-D₆ and 4-MMC-D₃ were infused through the solvent line at a concentration of 0.25 µg/mL. The signal response for codeine-D₆ and 4-MMC-D₃ were found to be 29668 cps and 84432 cps, respectively (n=5) (Table 7-4). This may suggest that the higher response for 4-MMC-D₃ obtained will significantly suppress other compounds in a mixture. This was tested by analysing a 400 µg/mL sample of 4-MMC spotted on a plate with codeine-D₆ followed by 400 µg/mL of 4-MMC with 4-MMC-D₃. The results obtained for 4-MMC with codeine-D₆ as IS exhibited a peak ratio of 3.87 (n=5) suggesting that the response of 4-MMC was significantly larger than that of codeine-D₆. This is desirable in drug detection since the analyte of interest should always be detectable even when present in mixtures of compounds. In contrast, the results for 4-MMC using 4-MMC-D₃ as the IS revealed an average peak ratio of 0.33 (n=5), suggesting that the 4-MMC response was largely suppressed, and the IS was the dominant peak. This was undesirable, therefore codeine-D₆ was chosen as a more suitable IS and was used throughout this study. Undeuterated compounds, such as codeine, were not considered as internal standards due to the risk of the compound itself being present in seized samples, giving rise to complicated analyses.

Table 7-4 Comparison of codeine-D₆ and 4-MMC-D₃, as internal standards.

Sample	4-MMC 400 µg/mL ^a (cps)	Codeine-D ₆ 0.25 µg/mL in solvent line (cps)	4-MMC-D ₃ 0.25 µg/mL in solvent line (cps)	Ratio of 4- MMC:IS
Alone	174406	29668	84432	N/A
Mixture 1	213260	55140	N/A ^b	3.87
Mixture 2	97941	N/A	299755	0.33

^a 2 µL spotted onto PTFE plate.

^b N/A = These compounds were not included in the mixture.

The ideal concentration for the IS was one that had a minimal effect on the signal response of the analyte of interest. The expected signal response (peak height) for a 2 µL spot of 400 µg/mL, of 4-MMC was approximately 174406 cps (n=3). It can be seen in Table 7-5 that an IS concentration above 0.5 µg/mL suppressed the 4-MMC signal response and therefore concentrations were too high for the optimal IS concentration. The signal response for 4-MMC with 0.5 µg/mL IS was relatively comparable to the expected 4-MMC response; however, the signal intensity of the IS was relatively high and may suppress other analytes during analysis. Therefore, the optimal concentration was chosen to be 0.25 µg/mL since this concentration did not suppress the signal intensity of the analyte of interest (lead to slight enhancement) and the signal response of codeine-D₆ was kept at a minimum so as not to suppress other compounds in mixtures. It is important to note that the signal response of the 0.25 µg/mL codeine-D₆ IS will usually be higher than expected since it was injected through the solvent line (where no desorption occurs). The presence of 4-MMC was supported by accurate mass of the protonated parent ion [M+H]⁺ at 178.1232 and MS/MS spectra.

Table 7-5 Optimising codeine-D₆ IS concentration, n=3.

codeine-D ₆ concentration (µg/mL)	Signal intensity (peak height, cps)		
	4-MMC ^a	codeine-D ₆ ^b	ratio 4-MMC:codeine-D ₆
5	28546	400468	0.07
1	84350	278791	0.30
0.5	71957	81794	0.88
0.25	143891	45369	3.17

^a 4-MMC concentration = 400 µg/mL, 2 µL spotted onto PTFE plate; average peak height for 4-MMC alone = 62582 cps, n=3.

^b Average peak height for codeine-D₆ (0.25 µg/mL) alone = 53028, n=3.

7.3.3.2 Quantification

Analyses using DESI-MS, LC-MS and GC-MS were all applied to the purity determination of the synthesised 4-MMC samples (Table 7-6).

Table 7-6 Purity of M1, M2, M3, M4 as determined using DESI-MS, GC-MS, and LC-MS.

Sample/ Technique	M1 (% HCl)	M2 (% HCl)	M3 (% HCl)	M4 (% HCl)
DESI-MS	51.6 ± 12.9	46.4 ± 12.9	65.6 ± 19.7	53.2 ± 14.9
GC-MS	23.6 ± 5.9	19.3 ± 5.3	43.6 ± 4.2	39.4 ± 1.7
LC-MS	34.9 ± 7.2	24.7 ± 5.8	46.6 ± 1.8	35.5 ± 5.9

Quantification using DESI-MS was conducted using the molecular ion peak of 4-MMC at m/z 178.1240 (Figure 7-25). All three techniques determined the purity of the 4-MMC samples in the same trend, i.e. M3 > M4 > M1 > M2. This suggests that the synthetic reaction used in the synthesis of M3 was the most successful in producing highest yield. The purity results obtained from GC-MS and LC-MS parallel each other more closely. The observed differences in GC-MS and LC-MS could be minimised by analysing the 4-MMC base instead of the HCl salt as it would chromatograph better using both techniques. The results obtained with DESI-MS are over-estimated and this may be due to the lower linearity obtained for the calibration curve and also the higher % RSD obtained using DESI-MS (Table 7-1). Despite this, DESI-MS has shown potential in preliminary chemical analysis of 4-MMC and with these limitation in mind, the quantitative results obtained using DESI-MS could assist greatly in the early detection and analysis of seized 4-MMC samples in real casework.

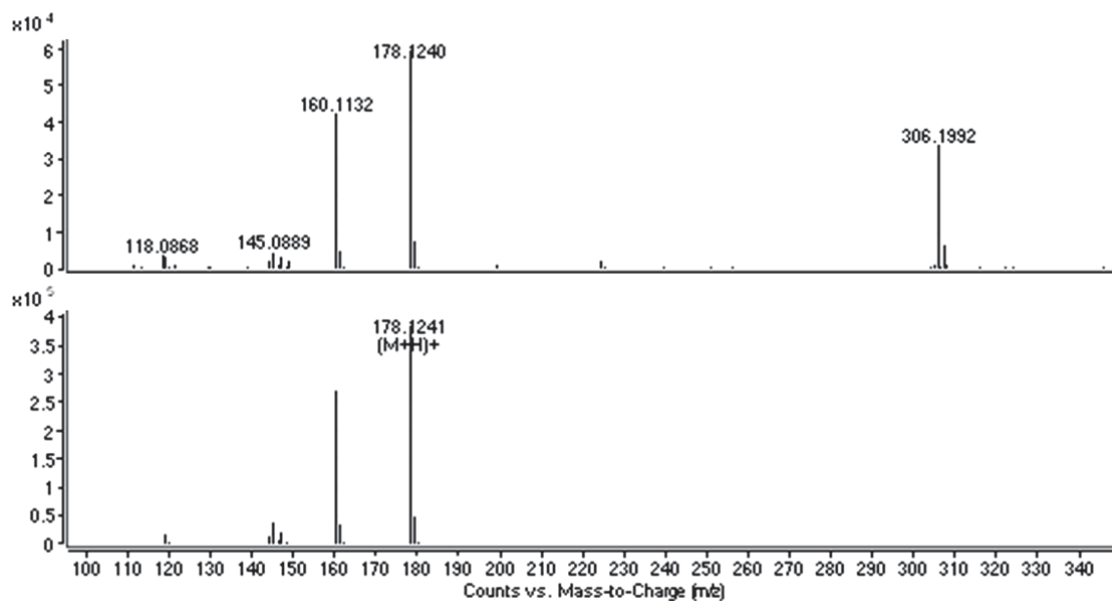


Figure 7-25 DESI-MS spectra of 4-MMC.

7.3.4 Mass accuracy

4-MMC, triethylamine, methylone, 4-DEAB, and 1B3P were all identified at best within 5 ppm of the accurate mass of the protonated molecular ion and at best within 10 ppm of the MS/MS fragment ions (Table 7-7 and Table 7-8). MS/MS match scores above 60 were achieved for all compounds using the PCDL software. It was demonstrated that there are significant differences in the fragmentation data for 4-MMC, methylone, 4-DEAB and 1B3P aiding in identification of these compounds.

Table 7-7 Mass accuracy of 4-MMC and related compounds using positive ion mode.

Compound	Formula [M+H] ⁺	Accurate Mass [M+H] ⁺	Acquired Mass [M+H] ⁺	Mass Accuracy (ppm)
4-MMC	C ₁₁ H ₁₆ NO	178.1232	178.1230	-1.1
triethylamine	C ₆ H ₁₆ N	102.1283	102.1286	3.2
methylone	C ₁₁ H ₁₄ NO ₃	208.0974	208.0969	-2.4
4-DEAB	C ₁₁ H ₁₆ NO	178.1232	178.1227	-2.8
1B3P	C ₁₁ H ₁₆ NO	178.1232	178.1233	0.6

Table 7-8 Mass accuracy of MS/MS fragments using positive ion mode at 20 eV.

Compound	Chemical formula	Accurate Mass	Acquired Mass	Mass Accuracy (ppm)
4-MMC	$C_{11}H_{16}NO [M+H]^+$	178.1232	178.1230	-1.1
	$C_{11}H_{14}N$	160.1126	160.1122	-2.5
	$C_{10}H_{12}N$	146.0970	146.0968	-1.4
	$C_{10}H_{11}N$	145.0891	145.0889	-1.4
	C_9H_{11}	119.0861	119.0867	5.0
	C_7H_7	91.0548	91.0540	-8.8
	C_3H_8N	58.0657	58.0653	-6.9
triethylamine	$C_6H_{16}N [M+H]^+$	102.1283	102.1287	3.9
	$C_4H_{12}N$	74.0970	74.0972	2.7
	C_3H_8N	58.0657	58.0653	-6.9
methylone	$C_{11}H_{14}NO_3 [M+H]^+$	208.0974	208.0979	2.4
	$C_{11}H_{12}NO_2$	190.0868	190.0862	-3.2
	$C_{10}H_{10}NO$	160.0762	160.0768	3.7
	$C_9H_7O_2$	147.0446	147.0439	-4.8
	C_3H_8N	58.0657	58.0654	-5.2
4-DEAB	$C_{11}H_{16}NO [M+H]^+$	178.1232	178.1227	-2.8
	C_8H_8NO	134.0606	134.0597	-6.7
	C_7H_8NO	122.0605	122.0604	-0.8
1B3P	$C_{11}H_{16}NO [M+H]^+$	178.1232	178.1233	0.6
	C_7H_7	91.0548	91.0556	8.8
	C_5H_5	65.0391	65.0388	-4.6

The compounds identified in the 4-MMC samples using DESI-MS, GC-MS and LC-MS have been summarised in Table 7-9.

Table 7-9 Compounds detected in 4-MMC samples using DESI-MS, GC-MS and LC-MS.

Sample	Compound	MW (Da)	DESI-MS	GC-MS	LC-MS
M1	4-MMC	177	✓	✓	✓
	triethylamine	101	✓	X	X
	4-methylpropiofenone	148	X	✓ (trace)	X
M2	4-MMC	177	✓	✓	✓
	triethylamine	101	✓	X	X
	4-methylpropiofenone	148	X	✓ (trace)	X
M3	4-MMC	177	✓	✓	✓
	methylamine	31	X	X	X
	4-methylpropiofenone	148	X	✓ (trace)	X
	2-bromo-4-methylpropiofenone	227	X	✓ (trace)	X
M4	4-MMC	177	✓	✓	✓
	methylamine	31	X	X	X
	4-methylpropiofenone	148	X	✓ (trace)	X
	2-bromo-4-methylpropiofenone	227	X	✓ (trace)	X

✓ = detected, X = not detected

The collision induced dissociation of 4-MMC and 1B3P share a common characteristic MS/MS ion at m/z 91 (i.e. C_7H_7). Some general rules that have been applied in the interpretation of the spectra include common product ions such as $[M+H-H_2O]^+$, $[M+H-CO]^+$, and $[M+H-CH_3OH]^+$ ¹²⁵.

7.4 Conclusions

4-Methylpropiofenone remained undetectable in all four samples using DESI-MS and GC-MS. Triethylamine remained undetectable in M1 and M2 using GC-MS and LC-MS. Methylamine in M3 and M4 remained undetectable using all three techniques and trace amounts of 2-bromo-4-methylpropiofenone were only detectable using GC-MS.

The quantitative method described herein has demonstrated the capabilities of the DESI-MS technique in providing preliminary purity results for 4-MMC and compounds alike. Qualitative and quantitative analyses further broaden the applicability of the DESI-MS technique. The value in obtaining a preliminary purity whilst screening for compounds is an encouraging result. With the use of the QTOF-MS, accurate mass and characteristic fragmentation patterns are achievable allowing for discrimination amongst compounds with identical chemical formulae.

***Chapter 8: Comparing DESI-MS to
current drug detection/analysis
techniques***

Chapter 8: Comparing DESI-MS to current drug detection/analysis techniques

8.1 Introduction

In this chapter, the DESI-MS technique is evaluated and compared to current preliminary identification techniques and confirmatory analysis techniques. The advantages and disadvantages are discussed and the potential for false positive and false negative results is also presented.

8.2 Marquis Reagent

The Marquis reagent was prepared by adding 50 mL of concentrated sulfuric acid to 2.5 mL of formaldehyde. Three drops of this reagent were applied to the sample and any colour change or other observation was recorded.

8.3 Confirmatory analysis techniques

The Prosofia™ DESI source was coupled to the Agilent Technologies 6500 Series Accurate Mass QTOF mass spectrometer. This instrument was compared to GC-MS and LC-MS since these are the most common confirmatory techniques currently used in drug analysis. GC-MS was performed on the Agilent Technologies 7890A gas chromatograph coupled to a 5975C MS in electron ionisation mode. The column used was an Agilent Technology HP-5MS (30 m x 0.25 mm ID x 0.25 µm). Liquid chromatography – mass spectrometry (LC-MS) was performed on an Agilent Technologies 1200 series liquid chromatograph coupled to an Agilent 6500 series QTOF mass spectrometer. The column utilised was a Phenomenex C18 column (150 x 3 mm I.D., 5 µm). The optimised parameters have been described in detail above (section 3.3.1 - 3.3.3).

8.4 Comparing DESI-MS to preliminary identification techniques

The need for a simple, rapid and reliable means of drug analysis has given rise to new research in the field of API techniques (such as DESI-MS). Traditional colour tests with specific reagents are still predominantly used as a first step for screening of suspected seizures. The Marquis and Simon's tests are widely used for on-site testing of MDMA. Although these tests are simple and inexpensive, the diversity of drugs makes it difficult to evaluate the results leading to false positive and false negative results, i.e. they lack selectivity⁵⁶. In addition, the actual colours observed by an analyst depend on many factors, such as drug concentration, the presence of contaminants in the tablets and the colour discrimination of the analyst, suggesting that the results are subjective.

Portable FTIR spectrometers have also been developed for on-site screening of hazardous materials and drugs. It has been suggested that IR spectrometry provides a higher level of discriminating power than does a colour test⁵⁷. However, built-in spectral libraries for pure compounds may not be useful for the identification of drug mixtures, which usually contain diluents and adulterants, in addition to the controlled drug(s).

Current methods for the preliminary identification of suspected border controlled substances suffer from one or more problems including a potential for false positives, poor sensitivity, poor specificity and limitations in identifying novel substances. Furthermore analysis can be time consuming and often performs poorly with samples that contain mixtures of compounds. The application of colour tests to novel drug analogues was beyond the scope of this study; however, Philp¹⁶⁶ has conducted extensive research into the application of colour tests to the detection of a variety of piperazine and cathinone analogues.

The Marquis reagent is a simple spot test used to presumptively identify compounds such as MDMA. Different compounds produce different coloured reactions and this is used to indicate the presence or absence of a compound, e.g. MDMA ('Ecstasy') reacts to form a dark purple/black colour.

Table 8-1 Results of Marquis reagent with BZP.

Compound	Colour Change	Other observations
BZP 1 HCl	No	None
BZP 1 HCl in H ₂ O	No	None
BZP 1 base	No	Vapours released, crystalline product formed (H ₂ SO ₄ salt)

The Marquis reagent was applied to the presumptive testing of BZP 1 as reports have suggested that a vigorous reaction results from this test. The lack of a coloured reaction resulting from the Marquis reagent and BZP 1 suggests that this presumptive test is not selective for piperazine drug analogues. It was found that BZP 1 base reacts vigorously with the reagent to produce vapours; however, it is a very quick reaction and may easily be overlooked. Therefore, other presumptive tests would need to be conducted in order to determine the presence or absence of these compounds.

8.5 Comparing DESI-MS to quantitative analysis techniques

In order to evaluate the quantitative abilities of DESI-MS, the technique was compared to two techniques, i.e. GC-MS and LC-MS. Intra-day and inter-day studies were conducted and precision and accuracy was evaluated for all three techniques (Table 7-1).

8.5.1 Gas chromatography – mass spectrometry

Gas chromatography – mass spectrometry has been regarded as the “gold” standard for the analysis of drug compounds in forensic samples for many years (since its development in the 1950s). Despite many new and emerging techniques, GC-MS is still widely used for a range of sample types in industry. One of the reasons as to why this technique is still in use is because it is highly reproducible and accurate. In addition, methods have been developed and validated over the years for the analysis and quantitation of various analytes.

In this study, GC-MS was applied to the quantitative analysis of 4-MMC with codeine-D₆ as IS. The linearity of the analytical run represented by the correlation co-efficient (R^2) shows a

value of 0.9991 over the linear range 5 – 400 µg/mL. This correlation co-efficient shows good linearity of the calibration range tested. The LOD was determined to be 2 µg/mL and the LOQ was determined to be 5 µg/mL with precision and accuracy within 4 % and 12 %, respectively. The limit of linearity (LOL) is the highest amount of analyte in a sample that can be quantitatively determined with acceptable precision and accuracy and was found to be 400 µg/mL.

The intra-day % RSD values were less than 11 % for the high and low concentrations tested. The inter-day % RSD values were less than 12 %. The % RE obtained for the intra-day and inter-day samples were less than 13 %, suggesting that good accuracy is achievable using this technique (Table 7-1).

8.5.2 Liquid chromatography – mass spectrometry

Liquid chromatography – mass spectrometry is a powerful technique used for many applications with a very high sensitivity and selectivity. Generally, LC-MS is used for the specific detection and identification of chemicals in the presence of other chemicals (in complex mixtures or matrices such as urine and saliva).

In this study, LC-MS was applied to the quantitative analysis of 4-MMC with codeine-D₆ as IS. The linearity of the analytical run, represented by the correlation co-efficient (R^2) shows a value of 0.9988 over the linear range 0.1 – 6 µg/mL. The LOD was determined to be 0.01 µg/mL and the LOQ determined to be 0.1 µg/mL (with accuracy and precision within 9 %). The LOL was found to be 8 µg/mL for LC-MS analysis.

The % RSD values found for the intra-day samples are less than 13 % for the high and low values tested. The % RSD values obtained for the inter-day analysis were less than 14 % (Table 7-1). The % RE obtained for the intra-day and inter-day samples were less than 11 %, suggesting that better accuracy is achievable using this technique as compared to GC-MS.

The results for the intra-day and inter-day analyses using LC-MS are slightly larger than expected. The error observed is mainly attributed by the injection efficiency of the LC-MS instrument and also the ionisation efficiency inside the ESI source. Despite the fact that there should be very minimal repeatability error during measurements, a larger error was observed

and is thought to be a result of the slight variation in the IS peak area response and also the lack of stability of 4-MMC hydrochloride in solution.

8.5.3 Desorption electrospray ionisation - mass spectrometry

The application of DESI-MS for the fast, preliminary analysis of novel drug analogues can be extended to the quantitative analysis of these compounds (as demonstrated for 4-MMC). In contrast to liquid sampling (such as in LC-MS) where the use of loops aids in preserving the volume of each individual injection with extremely low variation, controlling the amount of material sampled from surfaces using DESI-MS is a difficult task. When sampling in DESI-MS, the spray solvent is directed at the sample spot on the Teflon (PTFE) surface. This process may be thought to be quite reproducible; however, if the spray solvent is not positioned directly over the sample spot, the area in which sampling takes place is constantly changing for each spot being sampled. Even if the spots have the same size, problems during the drying/crystallisation process can still occur, producing sweet spots on the Teflon surface, all of which result in changes in the signal response and low reproducibility. The use of an appropriate IS aids in correcting the limitations mentioned. The choice of the IS is important in that it should behave in a similar manner to the analyte of interest. Codeine-D₆ was chosen as the IS in this study due to the fact that it was easily ionisable suggesting that relatively low concentrations of IS could be used whilst still maintaining a good signal response. In turn, by using low concentrations of IS (0.25 µg/mL), ion suppression was kept at a minimum favouring the analysis of 4-MMC, since signal response reflects the concentration of 4-MMC present in the sample spot.

The linearity of the analytical run, represented by the correlation co-efficient (R^2) shows a value of 0.9840 for DESI-MS analysis of 4-MMC using codeine-D₆ as IS over the linear range 50 – 800 µg/mL. This correlation co-efficient shows good linearity of the calibration range tested. The LOD was determined to be 8 µg/mL and the LOQ was determined to be 50 µg/mL (with accuracy and precision within 13 % and 25 %, respectively). The LOL was found to be 800 µg/mL for DESI-MS analysis.

The intra-day % RSD values were found to be less than 38 % for the high and low concentrations tested. The inter-day % RSD values, obtained from 15 repeat analyses

(triplicates on five days), were found to be less than 34 %. Accuracy remains below 5 % for the intra-day samples and below 8 % for the inter-day samples (Table 7-1).

In summary, accuracy and precision for both intra-day and inter-day analyses remain below 38 % suggesting that this technique can be used for the fast preliminary quantitative analysis of 4-MMC with codeine-D₆ as IS. However, other quantitative analysis techniques will still be required in order to state, with greater certainty, the amount of 4-MMC in a sample.

Desorption electrospray ionisation – mass spectrometry has some advantages over conventional quantitative analysis techniques such as LC-MS and GC-MS for quantitative analysis, one of which is that it is a very fast technique. DESI-MS analysis of a single sample spot is achievable in less than 1 minute, which is considerably faster than the 11 minutes required for a GC-MS run or the 25 minutes required for LC-MS to analyse one sample. In addition to this, sample preparation is kept to a bare minimum in DESI-MS analysis with solid samples requiring no samples preparation at all, and powder samples requiring dissolving in a suitable solvent (such as methanol) prior to analysis. GC-MS and LC-MS, on the other hand, may require lengthy extraction processes and sometimes even derivitisation if fragmentation data is insufficient for the parent compound.

Further to this, the capability of MS/MS experiments with DESI-MS allows for the differentiation between samples with the same molecular weight. MA and phentermine have the same molecular weight (protonated in positive ion mode) equal to 150.1284 Da; however, both these compounds possess very different fragmentation patterns (Figure 8-1). DESI-MS (like LC-MS) can potentially differentiate between any two compounds with the same molecular mass (assuming they exhibit different fragmentation patterns).

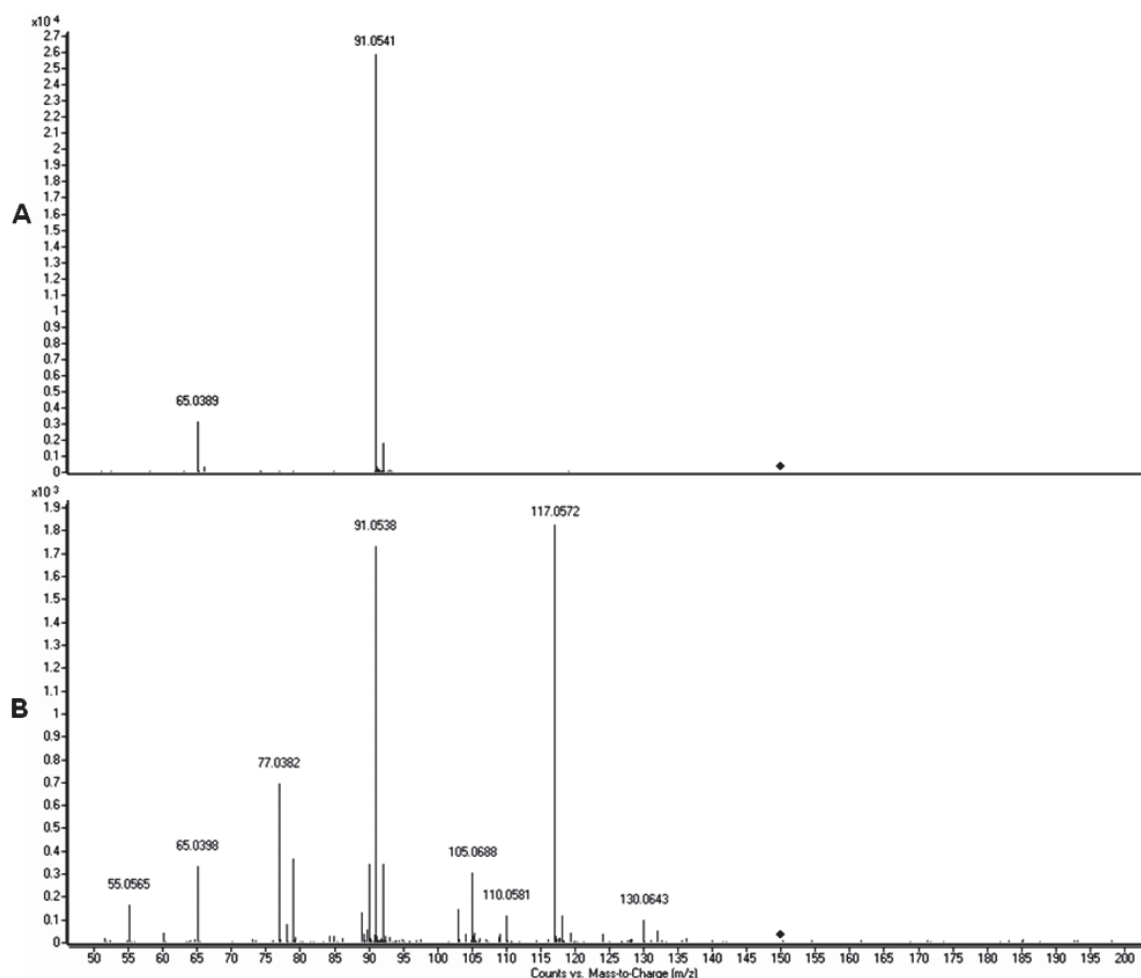


Figure 8-1 A: DESI-MS/MS spectra of MA, B: DESI-MS/MS spectra of phentermine.

One disadvantage of the technique is the lower precision (< 38 % RSD) obtained as compared to GC-MS and LC-MS (<15 % RSD). The use of an automated sample stage allowing for an increased number of repeated measurements will aid in minimising the RSD obtained using DESI-MS, this will also contribute to faster analysis times and less human error associated with manual sampling. In addition, the LOD and LOQ for DESI-MS are much higher than LC-MS and GC-MS suggesting that this technique has a lower sensitivity when compared to GC-MS and LC-MS. The accuracy of the DESI-MS technique is comparable to that of GC-MS and LC-MS as they are all within 15 % RE. The lower precision obtained using DESI-MS shows lower reproducibility as compared to GC-MS and LC-MS; however; its ability to successfully quantify novel drug analogues is highly notable since DESI-MS is largely used for qualitative measurements. The quantitative abilities of DESI-MS have been demonstrated for the preliminary quantification of novel drug analogues; however, GC-MS and LC-MS remain as the methods of choice due to higher precision and accuracy and also due to higher sensitivity.

8.6 False positive and false negative results

It is essential to address the issue of false positive and false negative identification in terms of drug detection. It is clear that false positive and false negative results should be avoided wherever possible; however, this may be limited by the technique utilised. A false positive result can be explained as the detection/identification of a compound when it is absent. A false negative result is the contrary where no compound is identified when it is present. There are certain limitations that can arise from such determinations; however, it is more important to prevent a false negative result when considering the DESI-MS technique as a screening tool in drug detection and analysis. False positive results can be rectified by compulsory confirmatory testing via other techniques.

When a compound is detected using DESI-MS, MS/MS experiments must be performed in order to prevent as many false positive results. As discussed in section 7.3.2.1, there are many compounds which possess the same chemical formula and thus the same molecular mass, therefore identification based on molecular mass alone is unreliable and can result in false positives. Using MS/MS experiments, a characteristic fragmentation pattern is obtained for each compound and is then compared to known fragmentation patterns in a library. The PCDL software can provide the user with a match score based on the similarities between the acquired spectrum and the library spectrum. A lower match score suggests that there is a reduced likelihood of a match and this should also be considered when reporting compound identification.

The LOD of various compounds using DESI-MS have been reported (section 4.3.1, 5.3.1 and 6.3.1). When compared to GC-MS and LC-MS the LOD of DESI-MS is higher. This potentially leads to more false negative results since compounds being analysed may fall below detection limits. In order to prevent these false negative results, more concentrated samples should be used. In the context of drug detection, when drugs are seized, there is usually ample sample available for analysis. This suggests that when drug screening is performed with DESI-MS, using a more concentrated sample (i.e. above the LOD) will aid in minimising the number of false negative results obtained.

8.7 Conclusions

Experiments for 2 μL spotted solutions of 4-MMC, using codeine- D_6 as an IS introduced in the desorption spray solvent, showed a linear correlation ($R^2 > 0.9840$) over the range 50 – 800 $\mu\text{g}/\text{mL}$ for quantitative experiments. The precision for triplicates analysed on five different days ($n = 15$) was less than 38 % RSD. The accuracy, expressed as relative error, was better than ± 8 %. The developed DESI-MS method was also compared to two current analysis techniques, i.e. GC-MS and LC-MS.

The DESI-MS technique has the advantage of being able to perform multiple sample analyses in a short time frame (<1 minute per sample). The use of MS and MS/MS reduces the chances of false positive and false negative results. The ability to simultaneously analyse the drug of interest and any by-products/impurities/adulterants in a sample suggests that this technique is superior to other currently used preliminary detection techniques (such as colour testing) which are best applied to the detection of pure samples. The broad detectability of DESI-MS suggests that preliminary drug “profiling” is possible with this technique. The subjectivity of colour tests is not an issue using DESI-MS. However, the presence of ion suppression or enhancement in mixtures makes quantifying analytes a difficult task (although possible with the aid of calibration curves and method validation). With the aid of simple extraction procedures, compounds can be separated prior to DESI-MS analysis allowing for a reduction in the observed ion suppression effects. Another disadvantage of the technique is the high cost involved in purchasing the DESI-interface and an accurate mass spectrometer such as the QTOF-MS used in this study. With future advances in technology and the development of portable accurate mass spectrometers, there will inevitably be a reduction in the costs associated with such instrumentation, allowing for a more streamline integration into current preliminary detection methodologies. With the use of MS and MS/MS libraries, fast screening of compounds is possible. As new compounds are detected they can be added to the database with ease for future drug detection.

Chapter 9: Conclusions and future work

Chapter 9: Conclusions and future work

9.1 Conclusions

Desorption electrospray ionisation - mass spectrometry is an ambient ionisation technique that has been applied to the analysis of illicit drugs and novel drug analogues in seized drug material. Currently used preliminary identification techniques lack sensitivity and selectivity and are prone to false positive and false negative results. Therefore, it was essential to investigate the use of DESI-MS as a novel preliminary identification technique in the analysis of a range of compounds with the potential for future automated library matching aiding in the rapid identification of unknown compounds.

The DESI-MS technique was utilised in the analysis of 4-MMC, BZP, TFMPP, MeOPP, mCPP, and other common ATS such as AP, MDMA, DMA, PMA, and PMMA. In addition, a commercially available workout supplement known as "Jack3d", containing DMAA, was successfully analysed.

A DESI-MS method was successfully developed and compared to current preliminary identification techniques such as the Marquis reagent and confirmatory analysis techniques, such as GC-MS and LC-MS. Welled, semi-porous PTFE plates have proven to provide a good surface for the analysis of small drug compounds. A method was optimised for the analysis of novel and controlled compounds. The solvent used was methanol/water (1:1) + 1 % formic acid and fragmentor voltage was set at 175 V. All mixtures were analysed at 20 eV with additional spectra recorded at 5 eV and 30 eV where required in order to obtain appropriate fragmentation data from each compound.

The LOD of the ATS were determined to be in the range 0.02 - 2.80 $\mu\text{g}/\text{mm}^2$, with a spot size of 7 mm^2 . The by-products/impurities in MDMA were detectable using all three techniques with the exception of MDP-2-P. The identification of these by-products/impurities confirm that the route of manufacture was reductive amination of MDP-2-P to form MDMA. The detection of anethole in PMMA suggests that anethole was the main precursor used in the synthesis. Caffeine and trace amounts of DMAA were detected in "Jack3d".

The DESI-MS technique was also successful in determining the impurities present in seized cocaine samples. The LOD determined for cocaine was $3.47 \mu\text{g}/\text{mm}^2$. The presence of a range of adulterants including caffeine, procaine, levamisole, lignocaine, paracetamol, and atropine did not hinder the detection of the analyte of interest which is useful in a drug detection setting since adulterants and/or diluents are commonly present in illicit seizures.

In all three cocaine samples, truxillines were detectable using DESI-MS and LC-MS along with other minor alkaloids present in the cocaine samples which were detectable using DESI-MS. The relative abundance of truxillines in these samples was indicative of the geographical origin of the cocaine. In addition, the adulterants levamisole and hydroxyzine were detected in cocaine item 5/2, differentiating it from the other two cocaine seizures.

Desorption electrospray ionisation - mass spectrometry was successful in detecting the reaction by-products (such as DBZP in BZP samples) and impurities (such as EBCP and MBCP in BZP 4) in the piperazine samples tested with the exception of some compounds present in trace amounts (i.e. below LOD). In the case of TFMPP 2 and TFMPP 3, 3-chloromethylphenol and piperazine were detected, respectively. 3-(Trifluoromethyl)aniline and 3-chloroaniline were detected in trace amounts in TFMPP 4 and mCPP 1, respectively, present as unreacted starting material.

The LOD of 4-MMC and the piperazine analogues were determined to range between $0.0023 - 2.30 \mu\text{g}/\text{mm}^2$, with a spot size of 7mm^2 . The impurity triethylamine was detected in M1 and M2 and distinguishing these two samples from M3 and M4. Triethylamine was present as the catalyst in the reaction suggesting these two samples followed a common synthetic pathway.

The detectability of ATS were evaluated by adulterating with caffeine, paracetamol, magnesium stearate, and dimethyl sulfone. Piperazine compounds were adulterated using caffeine and a mixture of piperazines was also evaluated since these are commonly found in combination. The selectivity of the DESI-MS technique was also evaluated for the detectability of 4-MMC by adulterating with caffeine, paracetamol, MA, phentermine, AP, MDMA, 4-hydroxyamphetamine, 4-fluoroamphetamine, nordiazepam, diazepam, oxazepam, cocaine, heroin, methadone, cathine, cathinone, 4-diethylaminobenzaldehyde, 1-benzyl-3-pyrrolidinol, and methylone. In most cases, despite the presence of ion enhancement or suppression due to adulterants present in mixtures, the analyte of interest remained detectable using DESI-MS.

Quantitative experiments for 2 μ L spotted solutions of 4-MMC, using codeine-D₆ as IS, introduced in the desorption spray solvent, showed a linear correlation ($R^2 > 0.9840$) over the range 50 – 800 μ g/mL. The precision for triplicates analysed on five different days ($n = 15$) was <38 % RSD. The accuracy, expressed as relative error, was <8 %. Identification based on MS/MS was also demonstrated by analysing substances with the same molecular formula as 4-MMC (i.e. 4-DEAB and 1B3P). This increases discrimination and allows identification of analytes with the exact same molecular weight. The results suggest that DESI-MS can be employed for the qualitative and preliminary quantitative analysis of 4-MMC. With the aid of other confirmatory analysis techniques such as GC-MS and LC-MS; DESI-MS can successfully be employed in the preliminary detection and analysis of novel drug analogues such as 4-MMC, BZP, TFMPP, MeOPP, mCPP, AP, MA, MDMA, DMA, PMA, PMMA and cocaine samples.

Desorption electrospray ionisation - mass spectrometry has the advantage of being able to perform multiple sample analyses in a short time frame (<1 minute per sample). The use of MS and MS/MS reduces the chances of false positive and false negative results. The ability to simultaneously analyse the drug of interest and any by-products/impurities/alkaloids/adulterants in a sample suggests that this technique is superior to other currently used preliminary detection techniques (such as colour tests) which are best applied to the detection of pure samples. The broad detectability of DESI-MS suggests that preliminary drug “profiling” is possible with this technique. The subjectivity of colour tests is not an issue using the developed DESI-MS method. However, the presence of ion suppression (matrix effects) in mixtures makes quantifying analytes a difficult task (although possible with the aid of calibration curves and method validation). With the aid of MS and MS/MS libraries, fast screening of compounds is made possible. The application of DESI-MS to the preliminary detection and analysis of novel and illicit drug compounds, presented herein, may see fast chemical profiling of samples aiding in future drug intelligence work.

9.2 Future Work

In the future, it is important to assess the usefulness of the DESI-MS technique on a larger array of compounds (including reference standards) and to add these to the PCDL spectral library in order to assist with future compound identification. Applying the developed method to a larger range of seized illicit samples will enable an evaluation of the true robustness of the DESI-MS technique. This will also allow further research into profiling by-products and impurities resulting from a larger variety of synthetic methods that have been used in clandestine laboratories in an attempt at linking batches and providing tactical intelligence.

The possibility of interfacing the DESI with a portable MS further broadens the applicability of the technique to field portable analyses of illicit and novel drug compounds. DESI-MS sample stage automation will aid greatly in increasing throughput of samples and will also increase the reproducibility of sampling, in turn resulting in better SD in qualitative and quantitative measurements. It may be beneficial to develop quantitative methods for the analysis of a larger range of compounds. Creating fully automated compound matching software will further enable high throughput of samples and will automatically generate match scores for compounds that have been detected. This significantly decreases labour time and minimises human-error.

It may also be beneficial to synthesise compounds using low grade chemicals (as is used in clandestine laboratories) as opposed to analytical grade chemicals. Low grade chemicals will contain a greater number of impurities that will be carried through to the end-product being synthesised. The additional impurities may provide further discriminating information when seized samples are analysed. The work presented in this research is envisaged to promote the application of API techniques to the fast preliminary detection of a multitude of drug analogues and other compounds (including organic and inorganic compounds) giving rise to potential future research in fields alike.

Appendix

Appendix 1

Refereed publications

Shanlin Fu, Natasha Stojanovska, *Designer Drugs*. **Encyclopaedia of Forensic Science**, Ed. 2, Elsevier, Waltham: Academic Press, 2013; p 36-44.

Natasha Stojanovska, Shanlin Fu, Mark Tahtouh, Tamsin Kelly, Alison Beavis, K. Paul Kirkbride, *A review of impurity profiling and synthetic route of manufacture of methylamphetamine, 3,4-methylenedioxymethylamphetamine, amphetamine, dimethylamphetamine and p-methoxyamphetamine*, **Forensic Science International**, 224, (2013), 8-26.

Natasha Stojanovska, Mark Tahtouh, Tamsin Kelly, Alison Beavis, Shanlin Fu, *Desorption electrospray ionisation – mass spectrometry (DESI-MS) analysis of 4-methylmethcathinone (mephedrone)*, **Australian Journal of Forensic Science**, currently being peer-reviewed.

Natasha Stojanovska, Mark Tahtouh, Tamsin Kelly, Alison Beavis, Shanlin Fu, *Presumptive analysis of seized cocaine using Desorption electrospray ionisation – mass spectrometry (DESI-MS)*, **Forensic Science International**, currently being peer-reviewed.

Natasha Stojanovska, Mark Tahtouh, Tamsin Kelly, Alison Beavis, Shanlin Fu, *Presumptive analysis of amphetamine-type substances and piperazine analogues using Desorption Electrospray Ionisation – Mass Spectrometry (DESI-MS)*, **Rapid Communications in Mass Spectrometry**, currently being peer-reviewed.

Conference proceedings

Stojanovska, Natasha; Fu, Shanlin; Tahtouh, Mark; Kelly, Tamsin; Beavis, Alison; *Qualitative and semi-quantitative analysis of novel drug analogues via Desorption Electrospray Ionisation – Mass Spectrometry*, 9th **National Conference, Safeguarding Australia Conference**, Rydges Lakeside Hotel, Canberra, 20-23 September 2010.

Stojanovska, Natasha; Fu, Shanlin; Tahtouh, Mark; Kelly, Tamsin; Beavis, Alison; *High-throughput qualitative and semi-quantitative analysis of novel drug analogues via Desorption*

Electrospray Ionisation – Mass Spectrometry, **Australasian Chemical Diversion Congress**, Burswood Convention Centre, Perth, Western Australia, 30 November – 4 December 2010.

Stojanovska, Natasha; Fu, Shanlin; Tahtouh, Mark; Kelly, Tamsin; Beavis, Alison; *Qualitative and quantitative analysis of mephedrone using Desorption Electrospray Ionisation – Mass Spectrometry*, **AFP-UTS-UC R&D Workshop**, AFP College, Barton, Canberra, 28-29 July 2011.

Stojanovska, Natasha; Fu, Shanlin; Tahtouh, Mark; Kelly, Tamsin; Beavis, Alison; *High-throughput qualitative and quantitative analysis of 4-Methylmethcathinone via Desorption Electrospray Ionisation – Mass Spectrometry*, **Forensic & Clinical Toxicology Association Conference**, Intercontinental The Rialto, Melbourne, Victoria, 31 July – 3 August 2011.

Stojanovska, Natasha; Fu, Shanlin; Tahtouh, Mark; Kelly, Tamsin; Beavis, Alison; *Qualitative and quantitative analysis of 4-Methylmethcathinone (mephedrone) by Desorption Electrospray Ionisation – Mass Spectrometry*, **The International Association of Forensic Toxicologists and the Society of Forensic Toxicologists Joint Annual Meeting**, Marriot Marquis, San Francisco, California, USA, 25-30 September 2011.

Stojanovska, Natasha; Fu, Shanlin; Tahtouh, Mark; Kelly, Tamsin; Beavis, Alison; *Synthesis of piperazine drug analogues and subsequent analysis and profiling by Desorption Electrospray Ionisation – Mass Spectrometry*, **Australian New Zealand Forensic Science Society (ANZFSS) Symposium, 21st International Symposium on the Forensic Sciences**, Hotel Grand Chancellor, Hobart, Tasmania, 23-27 September 2012.

Appendix 2

Table A-1 International seizures classified by drug type.

Compound Name	Year First Encountered	Significant Seizures Place & Quantity
Amphetamine (AP)	1930s ⁷	<p>Asia-Indonesia Over 10 kg AP sulfate (>90 % purity)¹⁶⁷</p> <p>Asia-Iraq, Al Anbar Province 9,382 tablets of AP, caffeine and theophylline seized in 2009¹⁶⁸</p> <p>Asia-Turkey, Istanbul 400 kg of AP seized in 2009¹⁶⁸</p> <p>Asia-Bahrain, Manama 14 kg of fake <i>Captagon</i> pills containing AP seized in 2010¹⁶⁹</p> <p>EU to AU-Lithuania to Sydney 28 kg of AP powder detected in granite pillar in 2008¹⁶⁹</p> <p>NA-Iceland- Reykjavik 692 g of AP seized in 2008¹⁷⁰</p> <p>EU-France-Montreuil 206 kg of AP seized in 2009¹⁶⁹</p> <p>Africa-Nigeria, Lagos 10 kg of AP seized in 2009¹⁶⁸</p> <p>CA-Nicaragua- El Carmen 760.8 g of AP seized in 2010¹⁶⁹</p>
Methamphetamine (MA)	1930s ⁷	<p>Asia-Philippines-Subic Bay 745 kg of crystal MA seized in 2008¹⁷⁰</p> <p>Asia-China-Hong Kong 10 kg of crystal MA seized in 2008¹⁷⁰</p> <p>Asia-China-Guangdong 1700 kg of liquid MA seized in 2008¹⁷⁰</p> <p>Asia-Guangdong, China to West Java, Indonesia 600 kg of crystal MA in 2008¹⁷⁰</p> <p>Asia-Japan-Kitakyushu 330 kg of MA seized in 2008¹⁷⁰</p> <p>Asia-Vietnam-Quang Binh Province 800,000 MA tablets seized in 2008¹⁷⁰</p> <p>Asia-Bangladesh, Dhaka Two seizures: 130,000 MA tablets and 1.3 million MA tablets in 2007¹⁷⁰</p> <p>Asia-India-Vadodara 1.5 kg of MA, 30 L of liquid MA and 110 L of intermediate MA seized in 2008¹⁷⁰</p> <p>Asia-India, Mumbai 7 kg of MA seized in 2008¹⁷⁰</p> <p>Asia-Kyrgyzstan, Bishkek 45 g of powdered MA seized in 2008¹⁷⁰</p> <p>Asia-Japan-Muroto 120 kg of MA seized in 2009¹⁶⁸</p> <p>Asia-Japan-Man Kam To 10 kg of crystal MA seized in 2008¹⁶⁸</p> <p>Asia-Malaysia, Johor Baru 978 kg of crystal MA seized in 2009¹⁶⁸</p>

Table A-1 continued.

Compound Name	Year First Encountered	Significant Seizures Place & Quantity
Methamphetamine (MA)	1930s	<p>Asia-Myanmar, Tachilek 3 million MA tablets, 10 kg of crystal MA, 2 million MA tablets and 340,000 MA tablets were discovered in separate seizures in 2009¹⁶⁸</p> <p>Asia-India, Patiala 28.1 kg of crystalline MA seized in 2009¹⁶⁸</p> <p>Asia-Iran, Tehran 21 kg of MA seized in 2009¹⁶⁸</p> <p>Asia-China- Hong Kong 440 g of liquid MA and 14 g of crystal methamphetamine detected in separate seizures in 2009¹⁶⁹</p> <p>Asia-China-Sichuan Province 1 kg of MA seized in 2009¹⁶⁹</p> <p>Asia-Malaysia-Jalan Batu Ferringhi 10 g of crystal MA seized in 2009¹⁶⁹</p> <p>Asia-Malaysia, Kuala Lumpur 54.5 kg of MA and 20 kg of MA seized separately in 2009¹⁶⁹</p> <p>Asia-India-Jalandhar 19 kg of MA in 2010 and 28.1 kg of crystal MA seized in 2009¹⁶⁹</p> <p>Asia-Jordan, Amman 2 kg of MA seized in 2009¹⁶⁹</p> <p>NA-Illinois 2 partial tablets containing a mixture of MA and phencyclidine (PCP)¹⁷¹</p> <p>Asia-Russia White powder (total 1.3 g) containing 44.7 % <i>d,l</i>-MA sulfate and 46.0 % lactose¹⁷²</p> <p>NA-Alaska Crystalline off-white substance containing 13 % MA HCl, DMS, and urea¹⁷³</p> <p>NA-Mexico/Texas 3 seizures: Pharr-11.04 kg (99.6+ % pure), Eagle Pass-7.56 kg (99.0 % pure), Sarita-27.08 kg (99.8 % pure)¹⁷⁴</p> <p>NA-California Dark brown solid (total 176.7 g) containing 76.6 % MA HCl, 10.4 % AP HCl, 9.1 % <i>N,N</i>-DMA HCl¹⁷⁵</p> <p>NA-Texas 23 plastic-wrapped bricks (total 22.80 kg) containing 99.7 % <i>d</i>-MA HCl¹⁷⁵</p> <p>NA-New Jersey 1000 off-white/yellowish coloured tablets containing 20.6 mg/tablet of MA, adulterated with DMS, caffeine, and procaine hydrochloride¹⁷⁶</p> <p>NA- Washington DC 330 kg of MA seized in 2009¹⁶⁸</p> <p>NA-Mexico-Tamazula 15 kg of crystal MA seized in 2009¹⁶⁸</p> <p>NA to AU- Canada to Melbourne 66 kg of crystal MA detected in foot spas in 2008³</p> <p>NA to AU-Canada to Sydney 27 kg of crystal MA detected in spa baths in 2008³</p>

Table A-1 continued.

Compound Name	Year First Encountered	Significant Seizures Place & Quantity
Methamphetamine (MA)	1930s	<p>NA to AU-Canada to Sydney 20 kg of crystal MA detected in candles in 2007³</p> <p>NA to AU-Canada to Sydney 16.6 kg of crystal MA detected in marble table tops in 2007³</p> <p>NA to AU-Canada to Sydney 12.5 kg of crystal MA detected in false sides and bottoms of suitcases in 2008³</p> <p>OC-French Polynesia-Tahiti 467 g of crystalline MA discovered in trafficking operation in 2006¹⁷⁰</p> <p>OC-French Polynesia-Tahiti 107 g of crystal MA in 2004, 323.5 g seized in 2005, 467 g in 2006, and 340 g seized in 2009¹⁶⁸</p> <p>OC-New Zealand Powder containing trace MA¹⁷⁷</p> <p>OC-New Zealand Crystal MA in hair dryers¹⁷⁷</p> <p>OC-Commonwealth of the Northern Mariana Islands-Saipan 1,021 g of crystal MA seized in 2009¹⁶⁹</p> <p>Africa-Nigeria, Lagos 10 kg of crystal MA seized in 2009¹⁶⁸</p> <p>AU-Sydney 50 kg of crystal MA¹⁶⁹</p> <p>Asia to AU-Hong Kong to Sydney 60 kg of MA seized from boxes of rubber gloves¹⁷⁸</p> <p>Asia to AU-Hong Kong to Sydney 26 kg of MA seized¹⁷⁸</p> <p>NA to AU-Canada to Sydney 21.7 kg of MA seized¹⁷⁸</p>
3,4-Methylenedioxy-amphetamine (MDA)	1960s ¹⁷⁹	<p>Asia-Indonesia Small quantity of MDA seized as a result of contamination¹⁶⁷</p>
N, N-dimethyl-amphetamine (DMA)	1980s ¹⁰	<p>Asia-Malaysia 200 g of <i>d</i>-DMA HCl with trace MA¹⁸⁰</p> <p>NA-Oregon 1.355 kg of suspected 'ice' was in fact a mixture of <i>d</i>-DMA, <i>d</i>-MA, and DMS¹⁸¹</p> <p>OC-New Zealand Powder DMA¹⁷⁷</p>
Para-methoxy-amphetamine (PMA)	2006	<p>EU-Italy White powder (350 mg containing 27 % PMA and 14 % <i>p</i>-methoxymethamphetamine (PMMA)¹⁸²</p>
3,4-Methylenedioxy-methamphetamine (MDMA) 'Ecstasy'	2000	<p>Asia-Indonesia Over 100 kg MDMA HCl (>90 % purity)¹⁶⁷</p> <p>Asia-Taiwan, Tainan 2.1 million Ecstasy tablets seized in 2009¹⁶⁸</p> <p>Asia-Malaysia-Jalan Batu Ferringhi 323 kg of Ecstasy powder and 42,282 pills seized in 2009¹⁶⁸</p>

Table A-1 continued.

Compound Name	Year First Encountered	Significant Seizures Place & Quantity
<p>3,4-Methylenedioxy-methamphetamine (MDMA)</p> <p>'Ecstasy'</p>	2000	<p>NA-California 6 light green tablets containing MDMA¹⁸³</p> <p>NA-California 985 tablets (440 mg each) containing a mixture of MDMA, MA and ketamine¹⁸⁴</p> <p>NA-Canada 200 000 tablets and powder which could be used to make an extra 100 000 tablets containing mixture of MDMA, MA, AP, GHB, and ketamine¹⁸⁴</p> <p>NA-Oklahoma 50 tablets (262 mg each) containing 55 mg of MDMA HCl and 49 mg of creatine per tablet¹⁸¹</p> <p>NA-Florida Two clear capsules containing dark, granular substance (0.72 g total) MDMA¹⁸⁵</p> <p>NA-New Jersey 10 white tablets (2.79 g total) containing a mixture of MDMA (major), ketamine, MA, cocaine and diphenhydramine¹⁸⁶</p> <p>NA-New York 4 round orange tablets (325 mg each) containing MDMA adulterated with procaine¹⁸⁷</p> <p>NA-Washington 30 uniformly packaged one-gallon plastic bags containing fluffy tan powder (total 29.89 kg) of MDMA HCl (96 % pure)¹⁸⁸</p> <p>NA-Wisconsin 100 round blue tablets (total 28.9 g) confirmed MDMA, MA, BZP, TFMPP, caffeine and procaine (ratio 67:11:24:10:33:100 respectively)¹⁸⁹</p> <p>NA-Texas 2 plastic packages containing a light brown powder (total 1970.3 g) containing MDMA HCl (95.9 %)¹⁹⁰</p> <p>NA-North California 15 tablets (total 5.2 g) containing MDMA (5.2 mg/tablet), MA (<1 %), caffeine and DMS¹⁹¹</p> <p>NA-North California 68 tablets (total 24.5 g) containing MDMA (5.7 mg/tablet), MA (<1 %), caffeine and DMS¹⁹¹</p> <p>NA-North California 70 tablets (total 25.2 g) containing MDMA (4.8 mg/tablet), ketamine, caffeine and DMS¹⁹¹</p> <p>NA-Oklahoma 10 blue, 10 purple, 10 pink tablets containing 6:3:1 mixture of caffeine, MDMA, MA¹⁷⁵</p> <p>NA-Texas 37954 tablets containing 86.1-95.3 mg/tablet MDMA, <5 % ketamine, and caffeine¹⁷⁶</p> <p>NA-Canada, Winnipeg 15 kg of MDMA tablets seized in 2009¹⁶⁹</p>

Table A-1 continued.

Compound Name	Year First Encountered	Significant Seizures Place & Quantity
<p>3,4-Methylenedioxy-methamphetamine (MDMA)</p> <p>'Ecstasy'</p>	2000	<p>NA-Washington DC 3 tablets containing MDMA, MA and caffeine and 1 tablet containing MDMA, caffeine and procaine¹⁹²</p> <p>NA to AU-Canada to Melbourne 121 kg of MDMA tablets found in foot spas also containing cocaine and crystal MA in 2008³</p> <p>AU-Perth 45 kg of MDMA powder detected post-border in 2008³</p> <p>Africa to AU-Mauritius to Sydney 40 kg of MDMA powder detected in 2007³</p> <p>EU to AU-Italy to Melbourne 15 million Ecstasy tablets seized by AFP weighing 4.4 tonnes in 2008¹⁷⁰</p> <p>Africa-Johannesburg 50 kg of Ecstasy seized in 2009¹⁶⁸</p> <p>SA-Brazil, Curitiba 1,050 capsules of MDMA seized in 2009¹⁶⁸</p> <p>SA-Brazil, Imarui 1,200 Ecstasy tablets seized in 2009¹⁶⁸</p> <p>NA to AU- Canada to Melbourne Three seizures: 121 kg, 89 kg and 93 kg of MDMA seized¹⁷⁸</p>
<p>3, 4-Methylenedioxy-N-(2-hydroxyethyl)-amphetamine (MDHOET)</p>	2004	<p>EU-France 1000 tablets (282 mg each) containing MDHOET, MDMA and caffeine¹⁹³</p> <p>EU-Netherlands 3 powder seizures (10 g, 20 g, 1.8 g) containing MDHOET and MDMA¹⁹³</p> <p>EU-Austria 50 tablets (190 mg each) containing MDHOET¹⁹³</p> <p>EU-Switzerland Tablets (28 mg each) containing MDHOET and MDMA¹⁹³</p> <p>EU-United Kingdom Tablet fragments containing MDHOET¹⁹³</p>
<p>4-bromo-2, 5-dimethoxy-phenethylamine (2C-B)</p>	1979	<p>NA-New York Clandestine 2C-B laboratory seized¹⁹⁴</p> <p>NA-Tennessee 2 tablets containing 2C-B¹⁹⁵</p>
<p>2, 5-dimethoxy-4-ethyl-phenethylamine (2C-E)</p>	Nov 2004	<p>NA-Michigan 3 gel-caps (0.36 g white powder total) containing 2C-E¹⁸¹</p> <p>NA-Michigan Glass vial containing white powder (1.28 g total)¹⁸¹</p> <p>NA-Iowa 13 clear capsules (<1 g total) containing white powder 2C-E¹⁸⁵</p> <p>NA-Oklahoma 100 clear gel-caps (10 mg of white powder in each cap) containing 2C-E¹⁹⁶</p> <p>NA-Kentucky 2 plastic dropper bottles (8 mL each) containing 2C-E¹⁷²</p>

Table A-1 continued.

Compound Name	Year First Encountered	Significant Seizures Place & Quantity
2, 5-dimethoxy-4-iodophenethylamine (2C-I)	Apr 2002 2003-UK ¹⁷⁹	<p>NA-Oregon 4 gel-caps (<10 mg powder each) containing 2C-I¹⁹⁷</p> <p>NA-Florida 6 capsules containing white crystalline 2C-I¹⁷¹</p> <p>NA-Iowa 6 clear capsules containing 2C-I¹⁹⁸</p> <p>NA-Arkansas 30 pink round tablets (total 4.9 g) containing 2C-I¹⁹⁹</p> <p>EU-Denmark 1 tablet, approx. 15-20 mg active ingredient²⁰⁰</p> <p>EU-Spain 43 tablets (154 mg each) containing 2C-I, 15-20 mg active ingredient²⁰¹</p> <p>OC-New Zealand Blotter acid containing 2C-I¹⁷⁷</p>
4-bromo-2, 5-dimethoxy-amphetamine (DOB)	~2006	<p>NA-Iowa Two full and two half pieces of blotter paper (6 mm squares) containing DOB²⁰²</p> <p>NA-California Blotter acid mimic DOB¹⁷⁴</p> <p>NA-Kansas 2 squares of blotter paper containing 2:1 of DOB and DOC¹⁷⁶</p>
4-chloro-2,5-dimethoxy-amphetamine (DOC)	~2007	<p>NA-Florida 8 small plastic squeeze bottles containing DOC (salt form)²⁰³</p> <p>NA-New Mexico Small bottle of breath freshening solution containing DOC²⁰⁴</p> <p>NA-California Small piece of blotter paper containing DOC¹⁷⁷</p> <p>NA-Kentucky 1 white square of blotter paper containing DOC and DOI (2.2:1 ratio)²⁰⁵</p> <p>NA-Florida Blotter paper containing DOC²⁰⁶</p> <p>NA-Georgia Tie-dyed blotter paper containing 2:1 mixture of DOC and DOB²⁰⁷</p>
4-iodo-2,5-dimethoxy-amphetamine (DOI)	-	<p>NA-Wisconsin Glass bottle containing clear, colourless liquid (total net volume 57.0 mL, 56.4 g) of DOI HCl²⁰⁸</p> <p>NA-Florida Blotter paper containing DOI²⁰⁶</p>
4-Methyl-methcathinone (Mephedrone)	UK-2008 AU-2009	<p>Dec 2009-AU AFP seized 20 kg of 4-methylmethcathinone</p> <p>NA-Oregon Two seizures: 17 plastic bags of white powder (total 15.7 g) and 2 plastic bags of white powder containing 4-methylmethcathinone¹⁹²</p>

Table A-1 continued.

Compound Name	Year First Encountered	Significant Seizures Place & Quantity
3'-Fluorometh-cathinone	UK~2008	EU-United Kingdom 250 mg of off white powder in orange and white capsules (purchased off internet as 'Lift')
'Spice'	2006 ²⁰⁹	NA-Illinois 5 foil packets (approx. 5 g each) containing 'HU-210' ((6aR, 10aR)-9-(hydroxymethyl)-6,6-dimethyl-3-(2-methyloctan-2-yl)-6a,7,10,10a-tetrahydrobenzo[c]chromen-1-ol) ²⁰⁷ NA-Virginia Light yellow powder (total 0.27 g) containing 1-butyl-3-(1-naphthoyl)indole, aka JWH-073 ²¹⁰
Ketamine	Jan 2003	Asia-China-Hong Kong 307 kg of ketamine seized in 2008 ¹⁷⁰ Asia-Japan-Man Kam To 140 kg of ketamine seized in 2009 and 307 kg of ketamine seized in 2008 ¹⁶⁸ Asia-Taiwan, Tainan 366 kg of ketamine seized in 2009 Asia-India, Chennai 9 seizures totalling 195.5 kg of ketamine in 2009 ¹⁶⁸ Asia-Malaysia-Jalan Batu Ferringhi 2.3 kg of ketamine seized in 2009 ¹⁶⁹ Asia-India-Tuticorin 440 kg of ketamine HCl seized in 2009 ¹⁶⁹ NA-Maryland 85.3 g of ketamine in the form of sugar cubes ¹⁶⁷ EU-Spain 2 small bottles seized-liquid ketamine ¹⁶⁷ NA-Michigan 68.05 g of Ketamine HCl ²¹¹ NA-California 10 mL bottle containing liquid ketamine ²¹¹ NA-Washington 50 packages (total 49.68 kg) containing ketamine HCl ²¹² NA-California 22 tablets containing 10:1 ratio of ketamine and MA ²¹³ NA-California 2 blue tablets (total 249 mg) and 2 pink tablets (total 256 mg) containing ketamine, MA and DMS in ratio 1.4 %K:0.4 %M and 1.4 %K:0.7 %M ²¹⁴ NA-California 12 round blue tablets (280 mg each) containing ketamine, procaine, MDMA (53:37:10) ¹⁸⁷ NA-Colorado Over 4 kg fine, fluffy white powder (made up of 30 100 g bottles, 56 25 g bottles, 100 g loose powder) containing ketamine HCl (>95 % pure) ²¹⁵ NA-California 98 white round tablets (total 26.95 g) containing ketamine and caffeine (5:2 ratio) ²¹⁶

Table A-1 continued.

Compound Name	Year First Encountered	Significant Seizures Place & Quantity
<p>Piperazine Mixtures:-</p> <p>1-Benzylpiperazine (BZP)</p> <p>1-(3-trifluoromethylphenyl)piperazine (TFMPP)</p> <p>Ortho-methoxyphenyl-piperazine (OMPP)</p> <p>Meta-chlorophenyl-piperazine (mCPP)</p> <p>Para-methoxyphenyl-piperazine (MeOPP)</p>	2002	<p>Asia-Indonesia</p> <p>2 seizures: 1 white tablet (total 0.56 g) and 2 red tablets (total 1.6 g) containing a mixture of BZP (155 mg/tablet and 68 mg/tablet respectively) and TFMPP²⁰⁸</p> <p>NA-Illinois</p> <p>67.5 g of tablets containing mixture of BZP, TFMPP, and OMPP¹⁶⁷</p> <p>EU-Spain</p> <p>2.296 g tablets containing mixture of BZP, TFMPP, and MeOPP¹⁶⁷</p> <p>NA-Iowa</p> <p>3 (450 mg) tablets containing mixture of BZP, TFMPP, and OMPP¹⁸³</p> <p>NA-California</p> <p>~200 tablets containing mixture of MDMA, BZP, TFMPP, OMPP, MeOPP and MDP-2-P²¹⁷</p> <p>NA-Michigan</p> <p>107 capsules containing mixture of TFMPP and BZP¹⁸⁴</p> <p>NA-Texas</p> <p>3146 g capsules containing BZP and TFMPP, 2782 g tablets containing BZP and TFMPP, 2704 g powder of 75 % BZP, 1830 g powder of TFMPP, 1609 g powder of 27-35 % BZP and TFMPP²¹⁸</p> <p>NA-Texas</p> <p>0.8 g of compressed green material containing OMPP¹⁹⁶</p> <p>NA-Missouri</p> <p>1 round green tablet (290 mg) containing BZP, MA and caffeine (300:6:85 ratio)²⁰⁴</p> <p>NA-California</p> <p>1 blue tablet containing mixture of MA, BZP, TFMPP, MDMA, 1, 4-dibenzylpiperazine and procaine¹⁸⁸</p> <p>NA-Michigan</p> <p>1432 tablets (approx. 288 mg each) containing mixture of BZP (84 mg/tablet), TFMPP and caffeine¹⁸⁸</p> <p>NA-Florida</p> <p>75 chocolates (total 1.2 kg) of TFMPP¹⁹⁰</p> <p>NA-Virginia</p> <p>705 yellow tablets (total 198.1 g) containing major BZP, TFMPP and MDMA (10.9 mg/tablet), MA (6.1mg/tablet), dibenzylpiperazine, caffeine, procaine, trace MDP-2-P and piperanol (from MDMA synthesis)²¹⁹</p> <p>NA-Texas</p> <p>1002 round yellow tablets (total 305 g) containing mixture of BZP, TFMPP and caffeine (ratio 2:3.5:1:20)²⁰⁶</p> <p>NA-Massachusetts</p> <p>12 round mottled blue tablets (total 3.2 g) containing BZP (78.7 mg/tablet), ketamine, TFMPP and caffeine²⁰⁶</p> <p>NA-Washington</p> <p>5 clear zip-lock bags of white powder (total 0.30 g) containing 4.0 % heroin, approx. 1 % BZP, caffeine, procaine and quinine¹⁷²</p>

Table A-1 continued.

Compound Name	Year First Encountered	Significant Seizures Place & Quantity
<p>Piperazine Mixtures:-</p> <p>1-Benzylpiperazine (BZP)</p> <p>1-(3-trifluoromethylphenyl)piperazine (TFMPP)</p> <p>Ortho-methoxyphenyl-piperazine (OMPP)</p> <p>Meta-chlorophenyl-piperazine (mCPP)</p> <p>Para-methoxyphenyl-piperazine (MeOPP)</p>	2002	<p>NA-North California</p> <p>17 tablets (total 4.6 g) containing ketamine (22.3 mg/tablet), BZP, TFMPP, caffeine, and DMS¹⁹¹</p> <p>NA-Oregon</p> <p>6 orange (total 1.7 g), 4 green (total 1.1 g), 4 purple (total 1.2 g), 3 pink (total 0.8 g), 1 blue (total 0.8 g) containing BZP and TFMPP. 1:1 mixture for orange, green, purple, blue and 1:2 mixture for ink tablets¹⁷⁵</p> <p>NA-Oklahoma</p> <p>17 light blue tablets containing TFMPP¹⁷⁵</p> <p>NA-Ohio</p> <p>10 yellow tablets (total 14.2 g) containing BZP, TFMPP and caffeine²²⁰</p> <p>NA-Idaho</p> <p>Two seizures: 1st containing 1:3:1 mixture of BZP, TFMPP, and caffeine. 2nd containing 3:2 mixture of BZP and TFMPP²²¹</p> <p>NA-Arizona</p> <p>5 blue, 2 orange, 91 blue, 232 red and 15 red tablets found containing 4:1 mixture of BZP and caffeine²¹⁶</p> <p>NA-Kansas</p> <p>492 tablets containing 2:1 mixture of BZP and TFMPP. The tablets also contained 1, 4-dibanzylpiperazine and caffeine²¹⁶</p> <p>NA-Ohio</p> <p>15 re tablets (total 4.3 g) containing BZP, TFMPP, and dextromethorphan²¹⁶</p> <p>NA-Louisiana</p> <p>200 tablets containing BZP, TFMPP, dextromethorphan, and caffeine²¹⁶</p> <p>NA-North Carolina</p> <p>5 tablets containing BZP, TFMPP and caffeine shaped like ninja turtles, Snoopy and Barack Obama²²²</p> <p>NA-New York</p> <p>170 purple tablets (total 49 g) containing 139 mg/tablet of BZP with TFMPP and caffeine²²²</p> <p>NA-Washington DC</p> <p>1 purple tablet containing BZP and TFMPP¹⁹²</p> <p>NA-New York</p> <p>7792 tablets (total 2345 g) containing BZP (122.2 mg/tablet), TFMPP and caffeine²²³</p> <p>NA-New York</p> <p>2 off-white tablets (Barack Obama) containing BZP, TFMPP, procaine and caffeine²²³</p> <p>NA-Alabama</p> <p>Several tablets containing TFMPP and dapoxetine²²⁴</p> <p>OC-New Zealand</p> <p>Tablets containing a mixture of diphenylprolinol and benzophenone, trace BZP and TFMPP¹⁷⁷</p> <p>OC-New Zealand</p> <p>Brown powder containing mixture of BZP, FPP and methylone¹⁷⁷</p>

Table A-1 continued.

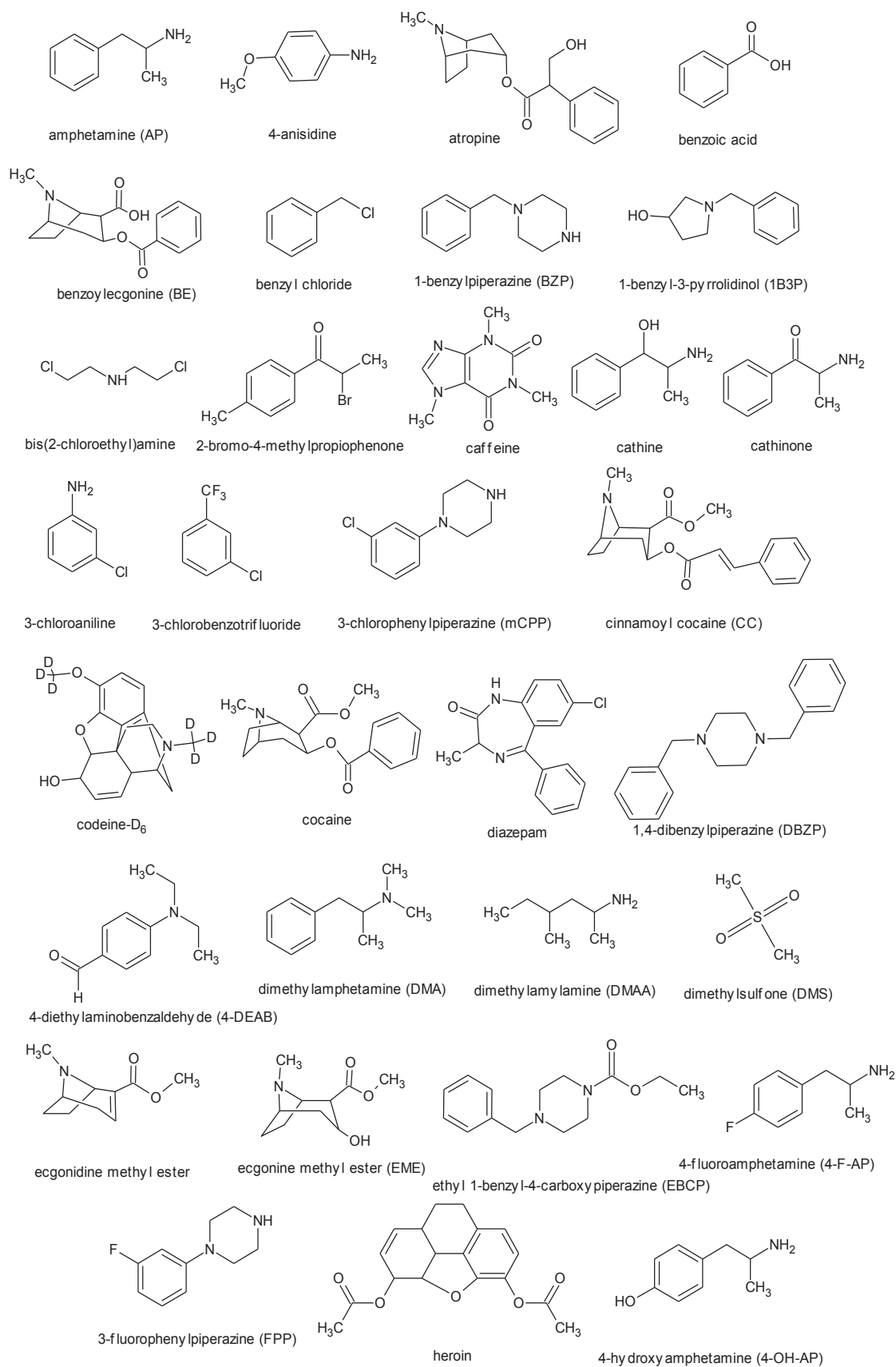
Compound Name	Year First Encountered	Significant Seizures Place & Quantity
Meta--chlorophenyl-piperazine (mCPP)	2004	<p>NA-Iowa 44 multi-coloured tablets containing mCPP¹⁹⁸</p> <p>NA-Texas 6 beige tablets (total 1.70 g) containing mCPP¹⁹⁸</p> <p>NA-Illinois 140 mottled tablets (total 42 g) containing mCPP²²⁵</p> <p>NA-Indiana 11 pink tablets (280 mg each) containing mCPP and trace MDMA¹⁹⁶</p> <p>NA-Ohio 2 round tablets (170 mg and 270 mg respectively) containing 3:2 mixture of mCPP and caffeine²⁰⁷</p> <p>NA-Texas 20 round blue tablets (150 mg each) containing mCPP²¹⁶</p> <p>EU-Spain 17 tablets containing mCPP¹⁷³</p> <p>EU-Greece Two seizures (156 and 11151 tablets respectively) (av. mass of tablet 299.6 mg) contained 6.5 % MDMA and 5.9 % mCPP²⁰²</p>
Fluorophenyl-piperazine (FPP)	2009	<p>NA-California 12 red Playboy tablets containing FPP²²³</p>
Pseudoephedrine (pEP)	-	<p>Asia to AU-Thailand to Melbourne 850 kg of pEP seized in 2008¹⁷⁰</p> <p>Asia-Bangladesh, Dhaka 55,000, 2.1 million and 409,000 pEP tablets seized separately in 2009¹⁶⁸</p> <p>CA-Guatemala, Guatemala City 10 million pEP tablets seized in 2009¹⁶⁸</p> <p>CA-Honduras, Tegucigalpa 2.1 million, 34,000 and 55,000 pEP tablets seized separately in 2009¹⁶⁸</p> <p>CA-Dominican Republic, Santa Domingo 409,000 and 800,000 pEP tablets seized separately in 2009¹⁶⁸</p> <p>Africa to AU-Cambodia to Sydney 105 kg of pEP powder detected in 212 bags of coffee in 2007³</p> <p>AU-Sydney 200 kg of pEP seized in 2009¹⁶⁸</p> <p>OC-New Zealand-Wellington 10 million pEP tablets diverted into NZ market annually in 2008¹⁷⁰</p> <p>OC-New Zealand-Auckland Over 1 tonne of pEP seized in 2010¹⁶⁹</p> <p>Asia to AU-Thailand to Sydney 848 kg of pEP seized¹⁷⁸</p> <p>Asia to AU-Thailand to Sydney 662 kg of pEP seized¹⁷⁸</p> <p>Asia to AU-India to Adelaide 6.2kg of EP/pEP seized¹⁷⁸</p> <p>AU-Sydney - 70 kg of pEP seized from storage containers¹⁷⁸</p>

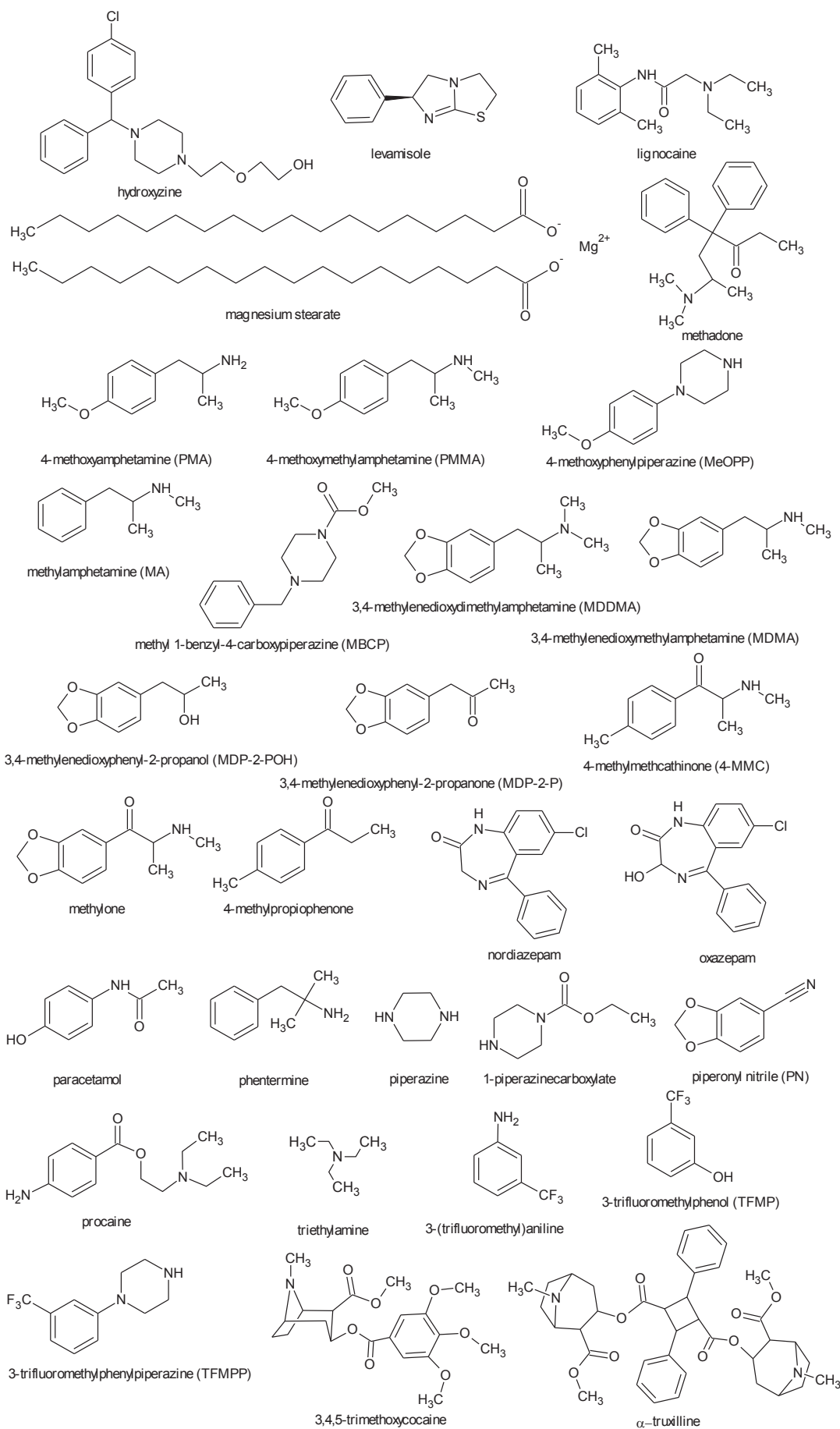
Table A-1 continued.

Compound Name	Year First Encountered	Significant Seizures Place & Quantity
Ephedrine (EP)	-	<p>Asia-China-Sichuan Province 415 kg EP seized in 2009¹⁶⁹</p> <p>NA-Mexico-Manzanillo In one seizure 3 tonnes of EP tablets and 327 kg of EP powder were seized in 2010. In 2009, an earlier seizure revealed 490 kg of EP powder¹⁶⁹</p> <p>Africa-Nigeria, Lagos 57 kg of EP seized in 2009¹⁶⁸</p> <p>SA-Chile, Santiago 850 kg of EP seized in 2009¹⁶⁸</p> <p>SA-Argentina, Buenos Aires 4.2 tonnes of EP seized in 2009¹⁶⁸</p> <p>Africa-Zambia-Lusaka 50 kg of EP seized in 2009¹⁶⁸</p>
Isosafrole and Piperonylmethylketone (PMK)	-	<p>AU-Australia 3.5 kg of isosafrole and 16 g of PMK³</p>
Sassafras Oil	-	<p>Africa-Cambodia-Veal Veng District 5.2 tonnes of sassafras oil seized in 2009¹⁶⁸</p> <p>Africa-Guinea, Conarky 5,000 L of sassafras oil seized in 2009¹⁶⁸</p>
Phenyl-2-propanone (P2P)	-	<p>EU-Turkey, Istanbul 600 kg of P2P seized in 2009¹⁶⁸</p> <p>EU-Netherlands, Rotterdam 230 L of P2P seized in 2009¹⁶⁸</p>
Methyl 3-[3',4'-(methylenedioxy)phenyl]-2-methyl glycidate (Ecstasy precursor)	2004	<p>AU-Sydney 44 gallon drums seized containing Methyl 3-[3',4'-(methylenedioxy)phenyl]-2-methyl glycidate²²⁶</p>
3,4-Methylenedioxyphenyl-2-propanone (MDP-2-P) (MDMA precursor)	<2003	<p>Asia-Indonesia Over 1.5 metric tonnes of MDP-2-P¹⁶⁷</p> <p>Africa-Guinea, Conarky 80 L of MDP-2-P seized in 2009¹⁶⁸</p>
Ephedra	-	<p>Africa-Cambodia, Kampong Cham Province 2.4 tonnes of Ephedra and 48 L of extracted liquid ephedrine were seized in 2009¹⁶⁸</p>
Piperanol	-	<p>NA-Mexico-Manzanillo 4.3 tonnes of piperanol seized in 2009¹⁶⁸</p>

Continents listed in table above: NA-North America, CA-Central America, SA-South America, EU-Europe, Asia, AU-Australia, Africa, OC-Oceania.

Appendix 2





References

References

1. UNODC, World Drug Report. *United Nations Office on Drugs and Crime* **2012**.
2. ACC, Illicit Drug Data Report 2011-12. *Australian Crime Commission* **2012**, 23-45.
3. ACC, Illicit Drug Data Report 2007-08, Amphetamine-Type Stimulants. *Australian Crime Commission* **2008**, 12-36.
4. Waumans, D.; Bruneel, N.; Hermans, B.; Tytgat, J., A rapid and simple GC/MS screening method for 4-methoxyphenol in illicitly prepared 4-methoxyamphetamine (PMA). *Microgram Journal* **2003**, 1 (3-4), 184-189.
5. Criminal Code Act 1995. *Australian Government, ComLaw* **2013**, (301.9).
6. Consideration of the cathinones. *Advisory Council on the Misuse of Drugs* **2010**, 1-50.
7. UNODCCP, Global Illicit Drug Trends *United Nations Office for Drug Control and Crime Prevention: Studies on Drugs and Crime, Statistics* **2001**.
8. Salocks, C.; Kaley, K. B., Technical support document: Toxicology clandestine drug labs: Methamphetamine. *Office of Environmental Health Hazard Assessment* **2003**, 1 (8), 1-11.
9. Glennon, R. A.; Yousif, M.; Patrick, G., Stimulus properties of 1-(3,4-methylenedioxyphenyl)-2-aminopropane (MDA) analogs. *Pharmacology Biochemistry and Behaviour* **1988**, 29 (3), 443-449.
10. Fasciano, J.; Hatzidimitriou, G.; Yuan, J.; Katz, J. L.; Ricaurte, G. A., *N*-Methylation dissociates methamphetamine's neurotoxic and behavioral pharmacologic effects. *Brain Research* **1997**, 771 (1), 115-120.
11. Witkin, J. M.; Ricaurte, G. A.; Katz, J. L., Behavioural effects of *N*-methylamphetamine and *N,N*-dimethylamphetamine in rats and squirrel monkeys. *Journal of Pharmacology and Experimental Therapeutics* **1990**, 253 (2), 466-474.
12. Lee, W. S.; Chan, M. F.; Tam, W. M.; Hung, M. Y., The application of capillary electrophoresis for enantiomeric separation of *N,N*-dimethylamphetamine and its related analogs: Intelligence study on *N,N*-dimethylamphetamine samples in crystalline and tablet forms. *Forensic Science International* **2007**, 165 (1), 71-77.
13. Waumans, D.; Bruneel, N.; Tytgat, J., Anise oil as *para*-methoxyamphetamine (PMA) precursor. *Forensic Science International* **2003**, 133 (1), 159-170.
14. Blachut, D.; Wojtasiewicz, K.; Czarnocki, Z., Some pyridine derivatives as "route specific markers" in 4-methoxyamphetamine (PMA) prepared by the Leuckart method. Studies on the role of the aminating agent in their distribution in the final product. *Forensic Science International* **2005**, 152 (2), 157-173.

15. Mortier, K. A.; Dams, R.; Lambert, W. E.; De Letter, E. A.; Van Calenbergh, S. V.; De Leenheer, A. P., Determination of paramethoxyamphetamine and other amphetamine-related designer drugs by liquid chromatography/sonic spray ionization mass spectrometry. *Rapid Communications in Mass Spectrometry* **2002**, *16* (9), 865-870.
16. Byard, R. W.; Gilbert, J.; James, R.; Lokan, R. J., Amphetamine Derivative Fatalities in South Australia-Is "Ecstasy" the Culprit? *The American Journal of Forensic Medicine and Pathology* **1998**, *19* (3), 261-265.
17. Galloway, J. H.; R., F. A., Caveat Emptor: Death involving the use of 4-methoxyamphetamine. *Journal of Clinical Forensic Medicine* **2002**, *9* (3), 160.
18. Lamberth, P. G.; Ding, G. K.; Nurmi, L. A., Fatal paramethoxy-amphetamine (PMA) poisoning in the Australian Capital Territory. *The Medical Journal of Australia* **2008**, *188* (7), 426.
19. UNODC, World Drug Report. *United Nations Office on Drugs and Crime* **2011**.
20. Blachut, D.; Wojtasiewicz, K.; Czarnocki, Z.; Szukalski, B., The analytical profile of some 4-methylthioamphetamine (4-MTA) homologues. *Forensic Science International* **2009**, *192* (1), 98-114.
21. Fu, S.; Stojanovska, N., *Encyclopedia of Forensic Science, Designer Drugs, Ed. 2*. Elsevier, Waltham: Academic Press: **2013**; p 36-44.
22. Kikura-Hanajiri, R.; Kawamura, M.; Miyajima, A.; Sunouchi, M.; Goda, Y., Determination of a new designer drug, *N*-hydroxy-3,4-methylenedioxymethamphetamine and its metabolites in rats using ultra-performance liquid chromatography-tandem mass spectrometry. *Forensic Science International* **2010**, *198* (1), 62-69.
23. Poisons List. Alphabetical List of Poisons, Restricted Substances and Drugs of Addiction. *Ministry of Health, New South Wales* **2013**, 34.
24. Antia, U.; Lee, H. S.; Hydd, R. R.; Tingle, M. D.; Russell, B. R., Pharmacokinetics of 'party pill' drug *N*-benzylpiperazine (BZP) in healthy human participants. *Forensic Science International* **2009**, *186* (1-3), 63-67.
25. Elliott, S.; Smith, C., Investigation of the first deaths in the United Kingdom involving the detection and quantitation of the piperazines BZP and 3-TFMPP. *Journal of Analytical Toxicology* **2008**, *32* (2), 172-177.
26. Gee, P.; Gilbert, M.; Richardson, S.; Moore, G.; Paterson, S., Toxicity from the recreational use of 1-benzylpiperazine. *Clinical Toxicology* **2008**, *46* (9), 802-807.
27. Baumann, M. H.; Clark, R. D.; Budzynski, A. G.; Partilla, J. S.; Blough, B. E.; Rothman, R. B., *N*-Substituted piperazines abused by humans mimic the molecular mechanism of 3,4-methylenedioxymethamphetamine (MDMA, or 'Ecstasy'). *Neuropsychopharmacology* **2005**, *30* (3), 550-560.

28. Maher, H. M.; Awad, T.; Clark, C. R., Differentiation of the regioisomeric 2-, 3-, and 4-trifluoromethylphenylpiperazines (TFMPP) by GC-IRD and GC-MS. *Forensic Science International* **2009**, *188* (1), 31-39.
29. Bossong, M. G.; Van Dijk, J. P.; Niesink, R. J. M., Methylone and mCPP, two new drugs of abuse? *Addiction Biology* **2005**, *10* (4), 321-323.
30. Fornal, E.; Stachniuk, A.; Wojtyla, A., LC-Q/TOF mass spectrometry data driven identification and spectroscopic characterisation of a new 3,4-methylenedioxy-N-benzyl cathinone (BMDP). *Journal of Pharmaceutical and Biomedical Analysis* **2013**, *72* (January 18), 139-144.
31. Swortwood, M. J.; Boland, D. M.; DeCaprio, A. P., Determination of 32 cathinone derivatives and other designer drugs in serum by comprehensive LC-QQQ-MS/MS analysis. *Analytical and Bioanalytical Chemistry* **2013**, *405* (4), 1383-1397.
32. Vardakou, I.; Pistos, C.; Spiliopoulou, C., Drugs for youth via internet and the example of mephedrone. *Toxicology Letters* **2011**, *201* (3), 191-195.
33. Brandt, S. D.; Sumnall, H. R.; Measham, F.; Cole, J., Analyses of second-generation 'legal highs' in the UK: initial findings. *Drug Testing and Analysis* **2010**, *2* (8), 377-382.
34. Brandt, S. D.; Freeman, S.; Sumnall, H. R.; Measham, F.; Cole, J., Analysis of NRG 'legal highs' in the UK: identification and formation of novel cathinones. *Drug Testing and Analysis* **2011**, *3* (9), 569-575.
35. Kelly, J. P., Cathinone derivatives: a review of their chemistry, pharmacology and toxicology. *Drug Testing and Analysis* **2011**, *3* (7-8), 439-453.
36. Zaitsev, K.; Katagi, M.; Tatsuno, M.; Soto, T.; Tsuchihashi, H.; Suzuki, K., Recently abused B(beta)-keto derivatives of 3,4-methylenedioxyphenylalkylamines: a review of their metabolism and toxicological analysis. *Forensic Toxicology* **2011**, *29* (2), 73-84.
37. Kyle, P. B.; Iverson, R. B.; Gajagowni, R. G.; Spencer, L., Illicit bath salts: not for bathing. *Journal of the Mississippi State Medical Association* **2011**, *52* (12), 375-377.
38. Khreit, O. I. G.; Irving, C.; Schmidt, E.; Parkinson, J. A.; Daeid, N. N.; Sutcliffe, O. B., Synthesis, full chemical characterisation and development of validated methods for the quantification of the components found in the evolved legal high NRG-2. *Journal of Pharmaceutical and Biomedical Analysis* **2012**, *61* (5 March), 122-135.
39. Prosser, J. M.; Nelson, L. S., The toxicology of bath salts: a review of synthetic cathinones. *Journal of Medical Toxicology* **2012**, *8* (1), 33-42.
40. Westphal, F.; Junge, T.; Girreser, U.; Greibl, W.; Doering, C., Mass, NMR and IR spectroscopic characterization of penthedrone and penthylone and identification of their isocathinone by-products. *Forensic Science International* **2012**, *217* (1-3), 157-167.

41. Westphal, F.; Junge, T.; Klein, B.; Fritschi, G.; Girreser, U., Spectroscopic characterization of 3,4-methylenedioxy-pyrrolidinobutyrophenone: a new designer drug with alpha-pyrrolidinophenone structure. *Forensic Science International* **2011**, *209* (1-3), 126-132.
42. Power, J. D.; McGlynn, P.; Clarke, K.; McDermott, S. D.; Kavanagh, P.; O'Brian, J., The analysis of substituted cathinones. Part 1: chemical analysis of 2-, 3- and 4-methylmethcathinone. *Forensic Science International* **2011**, *212* (1-3), 6-12.
43. McDermott, S. D.; Power, J. D.; Kavanagh, P.; O'Brian, J., The analysis of substituted cathinones. Part 2: an investigation into the phenylacetone based isomers of 4-methylmethcathinone and *N*-ethyl cathinone. *Forensic Science International* **2011**, *212* (1-3), 13-21.
44. Kavanagh, P.; O'Brian, J.; Fox, J.; O'Donnell, C.; Christie, R.; Power, J. D.; McDermott, S. D., The analysis of substituted cathinones. Part 3. Synthesis and characterisation of 2,3-methylenedioxy substituted cathinones. *Forensic Science International* **2012**, *216* (1), 19-28.
45. Maheux, C. R.; Copeland, C. R., Chemical analysis of two new designer drugs: buphedrone and penthedrone. *Drug Testing and Analysis* **2012**, *4* (1), 17-23.
46. Santali, E. Y.; Cadogan, A. K.; Daeid, N. N.; Savage, K. A.; Sutcliffe, O. B., Synthesis, full chemical characterisation and development of validated methods for the quantification of (\pm)-4'-methylmethcathinone (mephedrone): a new legal high. *Journal of Pharmaceutical and Biomedical Analysis* **2011**, *56* (2), 246-255.
47. Jankovics, P.; Varadi, A.; Tolgyesi, L.; Lohner, S.; Nemeth-Palotas, J.; Koszegi-Szalai, H., Identification and characterization of the new designer drug 4'-methylethcathinone (4-MEC) and elaboration of a novel liquid chromatography-tandem mass spectrometry (LC-MS/MS) screening method for seven different methcathinone analogs. *Forensic Science International* **2011**, *210* (1-3), 213-220.
48. Archer, R. P., Fluoromethcathinone, a new substance of abuse. *Forensic Science International* **2009**, *185* (1-3), 10-20.
49. Dal Cason, T. A.; Young, R.; Glennon, R. A., Cathinone: An investigation of several *N*-alkyl and methylenedioxy-substituted analogues. *Pharmacology Biochemistry and Behavior* **1997**, *58* (4), 1109-1116.
50. Esseive, P.; Ioset, S.; Anglada, F.; Gaste, L.; Ribaux, O.; P., M.; Gallusser, A.; Biedermann, A.; Specht, Y.; Ottinger, E., Forensic drug Intelligence: An important tool in law enforcement. *Forensic Science International* **2007**, *167* (2), 247-254.
51. Collins, M.; Huttunen, J.; Evans, I.; Robertson, J., Illicit drug profiling: the Australian experience. *Australian Journal of Forensic Sciences* **2007**, *39* (1), 25-32.
52. Klein, R. F. X.; Hays, P. A., Detection and analysis of drugs of interest, 1992-2001; A literature review. *Microgram Journal* **2003**, *1* (1-2), 55-71.
53. Norman, K., The synthesis of amphetamine and methamphetamine: a "big" picture. *Journal of the Clandestine Laboratory Investigating Chemists Association* **2012**, 1-30.

54. Buchanan, H. A. S.; Daeid, N. N.; Meier-Augenstein, W.; Kemp, H. F.; Kerr, W. J.; Middleditch, M., Emerging use of isotope ratio mass spectrometry as a tool for discrimination of 3,4-methylenedioxyamphetamine by synthetic route. *Analytical Chemistry* **2008**, *80* (9), 3350-3356.
55. O'Neal, C. L.; Crouch, D. J.; Fatah, A. A., Validation of twelve chemical spot tests for the detection of drugs of abuse. *Forensic Science International* **2000**, *109*, 189-201.
56. Leuthold, L. A.; Varesio, E.; Hopfgartner, G., Drug tablets instant analysis by desorption-electrospray ionisation mass spectrometry. *Spectroscopy Europe* **2006**, *18* (2), 8-12.
57. Tsujikawa, K.; Kuwayama, K.; Miyaguchi, H.; Kanamori, T.; Iwata, Y. T.; Yoshida, T.; Inoue, H., Development of an on-site screening system for amphetamine-type stimulant tablets with portable attenuated total reflection Fourier transform infrared spectrometer. *Analytica Chimica Acta* **2008**, *608* (1), 95-103.
58. Chen, H.; Talaty, N. N.; Takats, Z.; Cooks, R. G., Desorption electrospray ionization mass spectrometry for high-throughput analysis of pharmaceutical samples in the ambient environment. *Analytical Chemistry* **2005**, *77* (21), 6915-6927.
59. Balchin, E.; Malcolme-Lawes, D. J.; Poplett, J. F.; Rowe, M. D.; Smith, J. A. S.; Pearce, G. E. S.; Wren, S. A. C., Potential of Nuclear Quadrupole Resonance in Pharmaceutical Analysis. *Analytical Chemistry* **2005**, *77* (13), 3925-3930.
60. Leuthold, L. A.; Mandscheff, J. F.; Fathi, M.; Giroud, C.; Augsburg, M.; Varesio, E.; Hopfgartner, G., Desorption electrospray ionization mass spectrometry: direct toxicological screening and analysis of illicit Ecstasy tablets. *Rapid Communications in Mass Spectrometry* **2006**, *20* (2), 103-110.
61. Ifa, D. R.; Manicke, N. E.; Rusine, A. L.; Cooks, R. G., Quantitative analysis of small molecules by desorption electrospray ionization mass spectrometry from polytetrafluoroethylene surfaces. *Rapid Communications in Mass Spectrometry* **2008**, *22* (4), 503-510.
62. Kosanam, H.; Sai Prakash, P. K.; Yates, C. R.; Miller, D. D.; Ramagiri, S., Rapid screening of doping agents in human urine by vacuum MALDI-linear ion trap mass spectrometry. *Analytical Chemistry* **2007**, *79* (15), 6020-6026.
63. Hu, Q.; Talaty, N.; Noll, R. J.; Cooks, G., Desorption electrospray ionization using an orbitrap mass spectrometer: exact mass measurements on drugs and peptides. *Rapid Communications in Mass Spectrometry* **2006**, *20* (22), 3403-3408.
64. Luosujarvi, L., Analysis of street market confiscated drugs by desorption atmospheric pressure photoionization and desorption electrospray ionization coupled with mass spectrometry. *Rapid Communications in Mass Spectrometry* **2009**, *23* (9), 1401-1404.
65. Steiner, R. R.; Larson, R. L., Validation of the direct analysis in real time source for use in forensic drug screening. *Journal of Forensic Science* **2009**, *54* (3), 617-622.

66. Kauppila, T. J.; Arvola, V.; Haapala, M.; Pol, J.; Aalberg, L.; Saarela, V.; Franssila, S.; Kotiaho, T.; Kostianen, R., Direct analysis of illicit drugs by desorption atmospheric pressure photoionization. *Rapid Communications in Mass Spectrometry* **2008**, *22* (7), 979-985.
67. Pavlic, M.; Schubert, B.; Libiseller, K.; Oberacher, H., Comprehensive identification of active compounds in tablets by flow-injection data-dependent tandem mass spectrometry combined with library search. *Forensic Science International* **2010**, *197* (1-3), 40-47.
68. Weston, D. J., Ambient ionization mass spectrometry: current understanding of mechanistic theory; analytical performance and application areas: Critical Review. *Analyst* **2010**, *135* (4), 661-668.
69. Badu-Tawiah, A. K.; Eberlin, L. S.; Ouyang, Z.; Cooks, R. G., Chemical aspects of the extractive methods of ambient ionization mass spectrometry. *The Annual Review of Physical Chemistry* **2013**, *64* (16 January), 481-505.
70. Rodriguez-Cruz, S. E., Rapid analysis of controlled substances using desorption electrospray ionization mass spectrometry. *Rapid Communications in Mass Spectrometry* **2006**, *20* (1), 53-60.
71. Rodriguez-Cruz, S. E., Rapid screening of seized drug exhibits using desorption electrospray ionization mass spectrometry (DESI-MS). *Microgram Journal* **2008**, *6* (1-2), 10-25.
72. Cotte-Rodriguez, I.; Takats, Z.; Talaty, N.; Chen, H.; Cooks, R. G., Desorption electrospray ionization of explosives on surfaces: sensitivity and selectivity enhancement by reactive desorption electrospray ionization. *Analytical Chemistry* **2005**, *77* (21), 6755-6764.
73. Ifa, D. R.; Wu, C.; Ouyang, Z.; Cooks, G., Desorption electrospray ionization and other ambient ionization methods: current progress and preview. *Analyst* **2010**, *135* (4), 669-681.
74. Garcia-Reyes, J. F.; Jackson, A. U.; Molina-Diaz, A.; Cooks, R. G., Desorption electrospray ionization mass spectrometry for trace analysis of argochemicals in food. *Analytical Chemistry* **2009**, *81* (2), 820-829.
75. Badu-Tawiah, A.; Bland, C.; Campbell, D. I.; Cooks, R. G., Non-aqueous spray solvents and solubility effects in desorption electrospray ionization. *Journal of the American Society for Mass Spectrometry* **2010**, *21* (4), 572-579.
76. Kauppila, T. J.; Talaty, N.; Kuuranne, T.; Katiaho, T.; Kostianen, R.; Cooks, R. G., Rapid analysis of metabolites and drugs of abuse from urine samples by desorption electrospray ionization-mass spectrometry. *The Analyst* **2007**, *132* (9), 868-875.
77. Takats, Z.; Wiseman, J. M.; Gologan, B.; Cooks, G. R., Mass spectrometry sampling under ambient conditions with desorption electrospray ionization. *Science* **2004**, *306* (5695), 471-473.
78. Takats, Z.; Wiseman, J. M.; Cooks, R. G., Ambient mass spectrometry using desorption electrospray ionization (DESI): instrumentation, mechanisms and applications in forensics, chemistry, and biology. *Journal of Mass Spectrometry* **2005**, *40* (10), 1261-1275.

79. Green, F. M.; Stokes, P.; Hopley, C.; MSeah, M. P.; Gilmore, I. S.; O'Connor, G., Developing repeatable measurements for reliable analysis of molecules at surfaces using desorption electrospray ionization. *Analytical Chemistry* **2009**, *81* (6), 2286-2293.
80. Manicke, N. E.; Kistler, T.; Ifa, D. R.; Cooks, G.; Ouyang, Z., High-throughput qualitative analysis by desorption electrospray ionization mass spectrometry. *Journal of American Society for Mass Spectrometry* **2009**, *20* (2), 321-325.
81. Nizzia, J. L.; O'Leary, A. E.; Ton, A. T.; Mulligan, C. C., Screening of cosmetic ingredients from authentic formulations and environmental samples with desorption electrospray ionization mass spectrometry. *Analytical Methods* **2013**, *5*, 394-401.
82. Sokol, E.; Noll, R. J.; Cooks, R. G.; Beegle, L. W.; Kim, H. I.; Kanik, I., Miniature mass spectrometer equipped with electrospray and desorption electrospray ionization for direct analysis of organics from solids and solutions. *International Journal of Mass Spectrometry* **2011**, *306* (2-3), 187-195.
83. Vircks, K. E., Mulligan, C. C., Rapid screening of synthetic cathinones as trace residues and in authentic seizures using portable mass spectrometer equipped with desorption electrospray ionization. *Rapid Communications in Mass Spectrometry* **2012**, *26*, 2665-2672.
84. Nyadong, L.; Hohenstein, E. G.; Johnson, K.; Sherrill, C. D.; Green, M. D.; Fernandez, F. M., Desorption electrospray ionization reactions between host crown ethers and the influenza neuraminidase inhibitor oseltamivir for the rapid screening of Tamiflu. *The Analyst* **2008**, 1-15.
85. Griffiths, J., A mass spectrometer in every hand. *Analytical Chemistry* **2008**, *80* (21), 7904-7904.
86. Ifa, D. R.; Gumaelius, L. M.; Eberlin, L. S.; Manicke, N. E.; Cooks, R. G., Forensic analysis of inks by imaging desorption electrospray ionization (DESI) mass spectrometry. *The Analyst* **2007**, *132* (5), 461-467.
87. Van Berkel, G. J.; Kertesz, V., Automated sampling and imaging of analytes separated on thin-layer chromatography plates using desorption electrospray ionization mass spectrometry. *Analytical Chemistry* **2006**, *78* (22), 4938-4944.
88. Wiseman, J. M.; Ifa, D. R.; Song, Q.; Cook, R. G., Tissue imaging at atmospheric pressure using desorption electrospray ionization (DESI) mass spectrometry. *Angewandte Chemie International Edition* **2006**, *45* (43), 7188-7192.
89. Zhao, M.; Zhang, S.; Yang, C.; Xu, Y.; Wen, Y.; Sun, L.; Zhang, X., Desorption electrospray tandem MS (DESI-MSMS) analysis of methyl centralite and ethyl centralite as gunshot residue on skin and other surfaces. *Journal of Forensic Science* **2008**, *53* (4), 807-811.
90. Morelato, M.; Beavis, A.; Ogle, A.; Doble, P.; Kirkbride, P. K.; Roux, C., Screening of gunshot residues using desorption electrospray ionisation-mass spectrometry (DESI-MS). *Forensic Science International* **2012**, *217* (1-3), 101-106.

91. Hartmanova, L.; Ranc, V.; Papouskova, B.; Bednar, P.; Havlicek, V.; Lemr, K., Fast profiling of anthocyanins in wine by desorption nano-electrospray ionization mass spectrometry. *Journal of Chromatography A* **2010**, *1217* (25), 4223-4228.
92. Hoffman, E. d.; Stroobant, V., *Mass spectrometry: Principles and applications*. Third ed.; John Wiley & Sons, Ltd.: 2007.
93. Coumbaros, J.; Kirkbride, K. P.; G., K.; Skinner, W., Application of time of flight secondary ion mass spectrometry to the in situ analysis of ballpoint pen inks on paper. *Forensic Science International* **2009**, *193* (1-3), 42-46.
94. Ryan, T. P., *Modern experimental design*. Hoboken: John Wiley & Sons, Inc.: 2007.
95. Camilleri, A.; Johnston, M. R.; Brennan, M.; Davis, S.; Caldicott, D. G. E., Chemical analysis of four capsules containing controlled substance analogues 4-methylmethcathinone, 2-fluoromethamphetamine, α -phthalimidopropiophenone and *N*-ethylcathinone. *Forensic Science International* **2010**, *197* (1-3), 59-66.
96. Cymerman Craig, J.; Young, R. J., 1-Benzylpiperazine. *Organic Syntheses Collective* **1973**, *5*, 88.
97. Baltzly, R.; Buck, S. J.; Lorz, E.; Schon, W., The preparation of *N*-mono-substituted and unsymmetrically disubstituted piperazines - Original synthesis of Benzylpiperazine BZP 1-Benzylpiperazine *N*-Benzylpiperazine. *Journal of American Chemical Society* **1944**, *66*, 263-266.
98. Lam, B. Pathways and precursors of ether analogues of amphetamine compounds. University of Technology, Sydney, **2011**.
99. Ghallagher, R.; Shimmon, R.; McDonagh, A. M., Synthesis and impurity profiling of MDMA prepared from commonly available starting material. *Forensic Science International* **2012**, *33* (1-3), 306-313.
100. O'Neil, M. J.; Heckelman, P. E.; Koch, C. B.; Roman, K. J., *The Merk Index*. 14th ed.; Merck Research Laboratories, Merck and Co. Inc: Whitehouse Station NJ: 2006.
101. Reference Material Analysis Report. *National Measurement Institute, Department of Industry, Innovation, Science, Research and Tertiary Education, Australian Government* **2010**, 1-3.
102. Lee, C. J.; Bae, Y. H.; Chang, S. K., Efficient α -halogenation of carbonyl compounds by *N*-bromosuccinimide and *N*-chlorosuccinimide. *Bulletin of the Korean Chemical Society* **2003**, *24* (4), 407-408.
103. Craig, J. C., Preparation of 1-Benzylpiperazine. *Journal of Chemical Society* **1959**, 3634-3635.
104. Liu, K. G.; Robichaud, A. J., A general and convenient synthesis of *N*-aryl piperazines. *Tetrahedron Letter* **2005**, *46* (46), 7921-7922.

105. chemicalland21
<http://chemicalland21.com/specialtychem/nd/TRIFLUOROMETHYLPHENYLPIPERAZINE%20CHLORIDE.htm> (accessed 21/02/2013).
106. Organization, W. H., 1-(3-chlorophenyl)piperazine (mCPP) Pre-Review Report. *Expert Committee on Drug Dependence Thirty-fifth Meeting 2012, Hammamet, Tunisia, 4-8 June 2012*.
107. Mukhopadhyay, S.; Ananthkrishnan, S.; Chandalia, S. B., Oxidative bromination in a liquid-liquid two-phase system to synthesize organic intermediates: 2-Bromophenol, 2,6-dibromophenol, and 2-bromo-4-methylphenol. *Organic Process Research & Development* **1999**, *3* (6), 451-454.
108. McMurry, J., *Organic Chemistry*. 6th ed.; Brooks/Cole: **2004**.
109. Zhang, M.; Zhou, Y.-H.; Hu, L.-H.; Yang, X.-H., 1,4-Dibenzylpiperazine. *Acta Crystallographica Section E* **2010**, *66* (12), 3336.
110. Nordstrom, L. U.; Madsen, R., Iridium catalysed synthesis of piperazine from indols. *Chemical Communications* **2007**, *Electronic Supplementary Information*, 1-11.
111. Smith, M. B.; March, J., *March's Advanced Organic Chemistry: Reactions, Mechanisms, and Structures, 6th Edition*. 2007.
112. Beller, M.; Breindl, C.; Riermeier, T. H.; Tillack, A., Synthesis of 2,3-dihydroindoles, indoles, and anilines by transition metal-free amination of aryl chlorides. *Journal of Organic Chemistry* **2001**, *66* (4), 1403-1412.
113. March, J., *Advanced organic Chemistry: Reactions, mechanisms, and structures*. Fourth ed.; John Wiley & Sons: **1992**.
114. Andersson, K.; Jalava, K.; Lock, E.; Finnon, Y.; Huizer, H.; Kaa, E.; Lopes, A.; Poortman-van der Meer, A.; Cole, M. D.; Dahlen, J.; Sippola, E., Development of a harmonised method for the profiling of amphetamines III. Development of the gas chromatographic method. *Forensic Science International* **2007**, *169*, 50-63.
115. Cheng, J. Y. K.; Chan, M. F.; Chan, T. W.; Hung, M. Y., Impurity profiling of ecstasy tablets seized in Hong Kong by gas chromatography - mass spectrometry. *Forensic Science International* **2006**, *162*, 87-94.
116. Kuwayama, K.; Tsujikawa, K.; Miyaguchi, H.; Kanamori, T.; Iwata, Y.; Inoue, H.; Saitoh, S.; Kishi, T., Identification of impurities and the statistical classification of methamphetamine using headspace solid phase microextraction and gas chromatography - mass spectrometry. *Forensic Science International* **2006**, *160*, 44-52.
117. Moore, J. M.; Cooper, D. A., The application of capillary gas chromatography-electron capture detection in the comparative analyses of illicit cocaine samples *Journal of Forensic Science* **1993**, *38* (6), 1286-1304.

118. Palhol, F.; Boyer, S.; Naulet, N.; Chabrilat, M., Impurity profiling of seized MDMA tablets by capillary gas chromatography. *Analytical and Bioanalytical Chemistry* **2002**, *374*, 274-281.
119. Sanger, D. G.; Humphreys, I. J.; Patel, A. C.; Japp, M.; Osborne, R. G. L., The significance of gas chromatographic impurity patterns obtained from illicitly produced amphetamine. *Forensic Science International* **1985**, *29*, 7-11.
120. Gill, R.; Abbott, R. W.; Moffat, A. C., High-performance liquid chromatography systems for the separation of local anaesthetic drugs with applicability to the analysis of illicit cocaine samples. *Journal of Chromatography* **1984**, *301* (1), 155-163.
121. Jane, I.; Scott, A.; Sharpe, E. W. L.; C., W. P., Quantitation of cocaine in a variety of matrices by high-performance liquid chromatography. *Journal of Chromatography* **1981**, *214* (2), 243-248.
122. Niessen, W. M. A., *Liquid chromatography-mass spectrometry*. 3 ed.; CRC Taylor & Francis: **2006**; Vol. 97.
123. Steiner, W. E.; Clowers, B. H.; Fuhrer, K.; Gonin, M.; Matz, L. M.; Slems, W. F.; Schultz, A. J.; JHill, H. H. J., Electrospray ionization with ambient pressure ion mobility separation and mass analysis by orthogonal time-of-flight mass spectrometry. *Rapid Communications in Mass Spectrometry* **2001**, *15*, 2221-2226.
124. Stojanovska, N.; Fu, S.; Tahtouh, M.; Kelly, T.; Beavis, A.; Kirkbride, K. P., A review of impurity profiling and synthetic route of manufacture of methylamphetamine, 3,4-methylenedioxymethylamphetamine, amphetamine, dimethylamphetamine and *p*-methoxyamphetamine. *Forensic Science International* **2013**, *224* (1-3), 8-26.
125. Holcapek, M.; Jirasko, R.; Lisa, M., Basic rules for the interpretation of atmospheric pressure ionization mass spectra of small molecules. *Journal of Chromatography A* **2010**, *1217*, 3908-3921.
126. Sergi, M.; Napoletano, S., Analysis of Illicit Drugs in Human Biological Samples by LC-MS. *LC-MS in Drug Bioanalysis* **2012**, *8* (1 January), 349-398.
127. Allen, A. C.; Cooper, D. A.; Kiser, W. O.; Cotrell, R. C., The cocaine diastereomers. *Journal of Forensic Science* **1981**, *26* (1), 12-26.
128. Baugh, L. D.; Liu, R. H., Sample differentiation: cocaine example. *Forensic Science Review* **1991**, *3* (2), 101-115.
129. Brewer, L. M.; Allen, A. C., *N*-formyl cocaine: a study of cocaine comparison parameters. *Journal of Forensic Science* **1991**, *36* (3), 697-707.
130. By, A. W.; Lodge, B. A.; Sy, W. W., Characterization of cis-cinnamoylcocaine. *Journal of the Canadian Society of Forensic Science* **1988**, *21*, 41-45.

131. Casale, J. F., *N*-Acetylnorcocaine: a new cocaine impurity from clandestine processing. I. *Journal of the Clandestine Laboratory Investigating Chemists Association* **1991**, *1*, 23.
132. Casale, J. F., Detection of pseudoecgonine and differentiation from ecgonine in illicit cocaine. *Forensic Science International* **1990**, *47* (3), 277-287.
133. Casale, J. F., A practical total synthesis of cocaine's enantiomers. *Forensic Science International* **1987**, *33* (4), 275-298.
134. Casale, J. F.; Waggoner, R. W., A chromatographic impurity signature profile analysis for cocaine using capillary gas chromatography. *Journal of Forensic Science* **1991**, *36* (5), 1312-1330.
135. Casale, J. F.; Watterson, J. W., A computerized neural network method for pattern recognition of cocaine signatures. *Journal of Forensic Science* **1993**, *38* (2), 292-301.
136. Chiarotti, M.; Fucci, N., HPLC analysis of cocaine diastereomers by chiral stationary phase. *Forensic Science International* **1990**, *44* (1), 37-41.
137. ElSohly, M. A.; Brenneisen, R.; Jones, A. B., Coca paste: chemical analysis and smoking experiments. *Journal of Forensic Science* **1991**, *36* (1), 93-103.
138. Ensing, J. G.; de Zeeuw, R. A., Detection, isolation and identification of truxillines in illicit cocaine by means of thin-layer chromatography and mass spectrometry. *Journal of Forensic Science* **1991**, *36* (5), 1299-1311.
139. Ensing, J. G.; Hummelen, J. C., Isolation, identification and origin of three previously unknown congeners in illicit cocaine. *Journal of Forensic Science* **1991**, *36* (6), 1666-1687.
140. Ensing, J. G.; Racamy, C.; de Zeeuw, R. A., A rapid gas chromatographic method for the fingerprinting of illicit cocaine samples. *Journal of Forensic Science* **1992**, *37* (2), 446-459.
141. Janzen, K. E.; Walter, L.; Fernando, A. R., Comparison analysis of illicit cocaine samples. *Journal of Forensic Science* **1992**, *37* (2), 436-445.
142. LeBelle, M. J.; Callahan, S. A.; Latham, D. J.; Lauriault, G., Identification and determination of norcocaine in illicit cocaine and coca leaves by gas chromatography-mass spectrometry and high-performance liquid chromatography. *Analyst* **1988**, *113* (8), 1213-1215.
143. LeBelle, M. J.; Callahan, S. A.; Latham, D. J.; Lauriault, G.; Savard, C., Comparison of illicit cocaine by determination of minor components. *Journal of Forensic Science* **1991**, *36* (4), 1102-1120.
144. LeBelle, M. J.; Lauriault, G.; Callahan, S. A.; Latham, D. J.; Chiarelli, C.; Beckstead, H., The examination of illicit cocaine. *Journal of Forensic Science* **1988**, *33* (3), 662-675.

145. Lewin, A. H.; Parker, S. R.; Carroll, F. I., Positive identification and quantitation of isomeric cocaines by high-performance liquid chromatography. *Journal of Chromatography* **1980**, *193* (3), 371-381.
146. Lukaszewski, T.; Jeffery, W. K., Impurities and artefacts of illicit cocaine. *Journal of Forensic Science* **1980**, *25* (3), 499-507.
147. Lurie, I. S.; Moore, J. M.; Cooper, D. A.; Kram, T. C., Analysis of manufacturing by-products and impurities in illicit cocaine via high-performance liquid chromatography and photodiode array detection. *Journal of Chromatography* **1987**, *405*, 273-281.
148. Lurie, I. S.; Moore, J. M.; Kram, T. C.; Cooper, D. A., Isolation, identification and separation of isomeric truxillines in illicit cocaine. *Journal of Chromatography A* **1990**, *504*, 391-401.
149. Medina, F., Anhydroecgonine ester in cocaine seizures. *Microgram* **1979**, *12* (7), 139-144.
150. Moore, J. M., The application of chemical derivatization in forensic drug chemistry for gas and high performance liquid chromatographic methods of analysis *Forensic Science Review* **1990**, *2* (2), 79-124.
151. Moore, J. M., Gas chromatographic detection of ecgonine and benzoylecgonine in cocaine. *Journal of Chromatography* **1974**, *101* (1), 215-218.
152. Moore, J. M., Identification of *cis*- and *trans*- cinnamoylcocaine in illicit cocaine seizures. *Journal of the Association of Official Analytical Chemists* **1973**, *56* (5), 1199-1205.
153. Moore, J. M.; Cooper, D. A.; Lurie, I. S.; Kram, T. C.; Carr, S.; Harper, C.; Yeh, J., Capillary gas chromatographic-electron capture detection of coca-leaf-related impurities in illicit cocaine: 2,4-diphenylcyclobutane-1,3-dicarboxylic acids, 1,4-diphenylcyclobutane-2,3-dicarboxylic acids and their alkaloidal precursors, the truxillines. *Journal of Chromatography* **1987**, *410* (2), 297-318.
154. Moore, J. M.; Meyers, R. P.; Jimenez, M. D., The anatomy of a cocaine comparison case: a prosecutorial and chemistry perspective. *Journal of Forensic Science* **1993**, *38* (6), 1305-1325.
155. Noggle, F. T. J.; Clark, C. R., Liquid chromatographic analysis of samples containing cocaine, local anaesthetics, and other amines. *Journal of the Association of Official Analytical Chemists* **1983**, *66* (1), 151-157.
156. Noggle, F. T. J.; Clark, C. R., Liquid chromatographic identification of *cis*- and *trans*-cinnamoylcocaine in illicit cocaine. *Journal of the Association of Official Analytical Chemists* **1982**, *65* (3), 756-761.
157. Olieman, C.; Maat, L.; Beyerman, H. C., Analysis of cocaine, pseudococaine, allococaine and allospseudococaine by ion-pair reverse-phase high-performance liquid chromatography. *Recl. Trav. Chim. des Pays-Bas.* **1979**, *98* (10), 501-502.

158. Moore, J. M.; Casale, J. F., In-depth chromatographic analyses of illicit cocaine and its precursor, coca leaves. *Journal of Chromatography A* **1994**, *674* (1-2), 165-205.
159. Ehleringer, J. R.; Casale, J. F.; Lott, M. J.; Ford, V. L., Tracing the geographical origin of cocaine. *Brief communications, Macmillan Magazines* **2000**, *408* (6810), 311-312.
160. Moore, J. M.; Casale, J. F.; Cooper, D. A., Comparative determination of total isomeric truxillines in illicit refined, South American cocaine hydrochloride using capillary gas chromatography-electron capture detection. *Journal of Chromatography A* **1996**, *756* (1-2), 193-201.
161. UNODC, Methods for impurity profiling of heroin and cocaine. *United Nations Office on Drugs and Crime* **2005**.
162. de Boer, D.; Bosman, I. J.; Hidvegi, E.; Manzoni, C.; Benko, A. A.; deos Reys, L. J. A. L.; Maes, R. A. A., Piperazine-like compounds: a new group of designer drugs-of-abuse on the European market. *Forensic Science International* **2001**, *121*, 47-56.
163. Fromel, T.; Knepper, T. P., Mass Spectrometry as an indispensable tool for studies of biodegradation of surfactants. *Trends in Analytical Chemistry* **2008**, *27* (11), 1091-1106.
164. Zuba, D., Identification of cathinones and other active components of 'legal highs' by mass spectrometric methods. *Trends in Analytical Chemistry* **2012**, *32*, 15-30.
165. Med-Lib pKa's of drugs and reference compounds: Appendix H. http://web.squ.edu.om/med-Lib/MED_CD/E_CDs/A%20Practical%20Guide%20to%20Contemporary%20Pharmacy%20Practice/pdf/pKa-table.pdf (accessed 24/09/2013).
166. Philp, M., Development of colour tests for screening cathinone and piperazine analogues. *University of Technology, Sydney* **2012**, *Centre for Forensic Science*.
167. Department of Justice, U. S., Microgram Bulletin. **2003**, *36* (1), 1-10.
168. UNODC, Global Smart Update. *United Nations Office on Drugs and Crime* **2009**, *2* (October).
169. UNODC, Global Smart Update. *United Nations Office on Drugs and Crime* **2010**, *3* (March).
170. UNODC, Global Smart Update. *United Nations Office on Drugs and Crime* **2009**, *1* (March).
171. Department of Justice, U. S., Microgram Bulletin. **2006**, *39* (1), 3-4.
172. Department of Justice, U. S., Microgram Bulletin. **2008**, *41* (7), 60, 62.
173. Department of Justice, U. S., Microgram Bulletin. **2006**, *39* (5), 56.
174. Department of Justice, U. S., Microgram Bulletin. **2007**, *40* (2), 24.

175. Department of Justice, U. S., Microgram Bulletin. **2008**, 41 (12), 105-107.
176. Department of Justice, U. S., Microgram Bulletin. **2009**, 42 (4), 36, 39.
177. Department of Justice, U. S., Microgram Bulletin. **2007**, 40 (12), 110.
178. AFP, Statistics of illicit drug offences. *Commonwealth of Australia 2010* **2010**.
179. Drees, J. C.; Stone, J. A.; Wu, A. H. B., Morbidity involving the hallucinogenic designer amines MDA and 2C-I. *Journal of Forensic Sciences* **2009**, 54 (6), 1485-1487.
180. Chan, K. B.; Chong, Y. K.; Nazarudin, M., The Identification of *d-N,N*-dimethylamphetamine (DMA) in an exhibit in Malaysia. *Microgram Journal* **2003**, 1 (3-4), 163-168.
181. Department of Justice, U. S., Microgram Bulletin. **2004**, 37 (11), 193-196.
182. Department of Justice, U. S., Microgram Bulletin. **2006**, 39 (8), 99.
183. Department of Justice, U. S., Microgram Bulletin. **2003**, 36 (6), 118-119.
184. Department of Justice, U. S., Microgram Bulletin. **2003**, 36 (9), 203-204.
185. Department of Justice, U. S., Microgram Bulletin. **2005**, 38 (4), 59.
186. Department of Justice, U. S., Microgram Bulletin. **2006**, 39 (5), 54.
187. Department of Justice, U. S., Microgram Bulletin. **2007**, 40 (5), 50.
188. Department of Justice, U. S., Microgram Bulletin. **2008**, 41 (1), 1, 4-5.
189. Department of Justice, U. S., Microgram Bulletin. **2008**, 41 (2), 16-18.
190. Department of Justice, U. S., Microgram Bulletin. **2008**, 41 (4), 40.
191. Department of Justice, U. S., Microgram Bulletin. **2008**, 41 (11), 98.
192. Department of Justice, U. S., Microgram Bulletin. **2009**, 42 (7), 62, 64.
193. Koper, C.; Ali-Tolppa, E.; Bozenko Jr., J. S.; Dufey, V.; Puetz, M.; Weyermann, C.; Zrcek, F., Identification of a new amphetamine type stimulant: 3,4-methylenedioxy-*N*-(2-hydroxyethyl)amphetamine (MDHOET). *Microgram Journal* **2005**, 3 (3-4), 166-174.
194. Department of Justice, U. S., Microgram Bulletin. **2004**, 37 (12), 208-209.
195. Department of Justice, U. S., Microgram Bulletin. **2009**, 42 (11), 84.
196. Department of Justice, U. S., Microgram Bulletin. **2007**, 40 (4), 38-39.
197. Department of Justice, U. S., Microgram Bulletin. **2004**, XXXVII (6), 113-114.

198. Department of Justice, U. S., Microgram Bulletin. **2006**, 39 (9), 112-113.
199. Department of Justice, U. S., Microgram Bulletin. **2008**, 41 (8), 72.
200. Department of Justice, U. S., Microgram Bulletin. **2003**, 36 (5), 89-90.
201. Department of Justice, U. S., Microgram Bulletin. **2004**, 37 (3), 48-49.
202. Department of Justice, U. S., Microgram Bulletin. **2006**, 39 (12), 145, 147.
203. Department of Justice, U. S., Microgram Bulletin. **2007**, 40 (4), 42.
204. Department of Justice, U. S., Microgram Bulletin. **2007**, 40 (10), 91, 93.
205. Department of Justice, U. S., Microgram Bulletin. **2008**, 41 (3), 28.
206. Department of Justice, U. S., Microgram Bulletin. **2008**, 41 (6), 53, 56.
207. Department of Justice, U. S., Microgram Bulletin. **2009**, 42 (3), 23-26.
208. Department of Justice, U. S., Microgram Bulletin. **2007**, 40 (9), 87, 89.
209. Auwarter, V.; Dresen, S.; Weinmann, W.; Muller, M.; Putz, M.; Ferreiros, N., 'Spice' and other herbal blends: harmless incense or cannabinoid designer drug? *Journal of Mass Spectrometry* **2009**, 44 (5), 832-837.
210. Department of Justice, U. S., Microgram Bulletin. **2009**, 42 (9), 75.
211. Department of Justice, U. S., Microgram Bulletin. **2003**, 36 (11), 247, 250.
212. Department of Justice, U. S., Microgram Bulletin. **2006**, 39 (3), 29.
213. Department of Justice, U. S., Microgram Bulletin. **2007**, 40 (2), 19.
214. Department of Justice, U. S., Microgram Bulletin. **2007**, 40 (3), 32-33.
215. Department of Justice, U. S., Microgram Bulletin. **2007**, 40 (11), 102.
216. Department of Justice, U. S., Microgram Bulletin. **2009**, 42 (5), 45-49.
217. Department of Justice, U. S., Microgram Bulletin. **2003**, 36 (7), 153.
218. Department of Justice, U. S., Microgram Bulletin. **2006**, 39 (4), 45.
219. Department of Justice, U. S., Microgram Bulletin. **2008**, 41 (5), 48.
220. Department of Justice, U. S., Microgram Bulletin. **2009**, 42 (1), 3.
221. Department of Justice, U. S., Microgram Bulletin. **2009**, 42 (2), 16-17.

222. Department of Justice, U. S., Microgram Bulletin. **2009**, 42 (6), 53-54, 58.
223. Department of Justice, U. S., Microgram Bulletin. **2009**, 42 (8), 68, 70.
224. Department of Justice, U. S., Microgram Bulletin. **2009**, 42 (12), 93-94.
225. Department of Justice, U. S., Microgram Bulletin. **2006**, 39 (10), 123.
226. Collins, M.; Heagney, A.; Cordaro, F.; Odgers, D.; Tarrant, G.; Stewart, S., Methyl 3-[3',4'-(methylenedioxy)phenyl]-2-methyl glycidate: An Ecstasy Precursor Seized in Sydney, Australia. *Journal of Forensic Science* **2007**, 52 (4), 898-903.